The Atmospheric Lifetime Experiment and the Global Atmospheric Gas Experiment (ALE/GAGE).

FINAL REPORT

by

R.A.Rasmussen and M.A.K.Khalil

Global Change Research Center &
Department of Environmental Science and Engineering
Oregon Graduate Institute
P.O.Box 91,000
Portland, Oregon 97291 USA

Grant No. NAGW-1348

Period Covered: 4-1-88 to 1-31-91

January 1995

Report Submitted to:

Technical Monitor: Dr. Michael Kurylo
NASA Headquarters, Code YSM
Washington, D.C. 20546-0001

The Atmospheric Lifetime Experiment and the Global Atmospheric Gas Experiment (ALE/GAGE).

FINAL REPORT

by

R.A.Rasmussen and M.A.K.Khalil

Global Change Research Center &
Department of Environmental Science and Engineering
Oregon Graduate Institute
P.O.Box 91,000
Portland, Oregon 97291 USA

Grant No. NAGW-1348

Period Covered: 4-1-88 to 1-31-91

January 1995

Report Submitted to:

Technical Monitor: Dr. Michael Kurylo
NASA Headquarters, Code YSM
Washington, D.C. 20546-0001

The Atmospheric Lifetime Experiment and the Global Atmospheric Gas Experiment (ALE/GAGE).

R.A.Rasmussen and M.A.K.Khalil
Global Change Research Center &
Department of Environmental Science and Engineering
Oregon Graduate Institute, Portland, Oregon

CONTENTS

Note: Figures and tables for each of the main sections I - VII are at the end of the respective section.

Summary:

The ALE/GAGE project was designed to determine the global atmospheric lifetimes of the chloroflurocarbons CCl_3F and CCl_2F_2 (F-11 and F-12), which had been identified as the main gases that cause stratospheric ozone depletion. The experimental procedures also provided the concentrations of CH_3CCl_3, CCl_4 and N_2O. The extended role of the project was to evaluate the mass balances of these gases as well. Methylchloroform (CH_3CCl_3) serves as a tracer of average atmospheric OH concentrations and hence the oxidizing capacity of the atmosphere. Nitrous oxide (N_2O) is a potent greenhouse gas and can also deplete the ozone layer. Measurements of these gases were taken with optimized instruments in the field at a frequency of about 1 sample/hr. Toward the end of the present project methane measurements were added to the program.

This final report deals with the research of the Oregon Graduate Institute as part of the ALE/GAGE program between 4/1/1988 and 1/31/1991 when the project was funded by NASA (Project # NAGW 1348). This project, NAGW-1348, continued the measurements previously funded under NASA Project # NAGW-280. The report defines the scope of the OGI project, the approach, and the results. The results include: 1) A high quality data base on the concentrations of the gases mentioned earlier at four locations covering all the major latitudinal regions of the earth's atmosphere. 2) A quality assurance that has two aspects. First, the demonstration of the stability of the calibration standards so that the concentrations and trends that are observed are not affected by experimental artifacts and, second, the use of flask samples to independently verify the quality of the real time field data. 3) An assessment of the role of sampling frequency on the trends and lifetimes of trace gases. 4) The data have been used to establish the trends and lifetimes of the chloroflurocarbons and the average concentrations of OH in the atmosphere.

In this report we have provided a guide to the ALE/GAGE program and the role of the OGI group in the program. We have discussed the data and their quality, aspects of the information in the data regarding trends and lifetimes, and how to obtain the data for further research.

I. Introduction

I.1. Objectives and Methods

The chlorofluorocarbons, particularly CCl_3F (F-11) and CCl_2F_2 (F-12), have been known for more than twenty years to endanger the stratospheric ozone layer. The major objective of the ALE/GAGE project was to determine the atmospheric lifetimes of chlorofluorocarbons F-11 and F-12. The project was designed to rely entirely on global atmospheric measurements of these two gases to determine the lifetimes. It was well known, before the project started, that the lifetimes of these gases were long, perhaps between 30 - 200 years. While it seemed that stratospheric photolysis was likely to be the main removal process, there were many other possible sinks that could also remove these fluorocarbons. Many small sinks could add up to substantial total annual removal rates. But because all these sinks were small, it was practically impossible to obtain accurate estimates of the removal rates from these processes. At the same time, only the stratospheric photolysis that released Cl atoms was regarded as having the potential for environmental damage by causing ozone depletion, while any other process that could remove these gases from the environment would, in effect, prevent the destruction of the ozone layer. These other processes, known and unknown, could easily affect the calculations of stratospheric ozone depletion from these chloroflorocarbons by a factor of two. Therefore, estimates of the lifetimes of these fluorocarbons based only on their stratospheric photolysis may not represent the total atmospheric lifetimes or the role of these gases in ozone depletion. The ALE/GAGE experiment was designed to overcome the difficulty of estimating the total lifetime of the chlorofluorbcarbons without having to account for the removal by each process when the nature and removal rates of the individual process were not known, and indeed, all the removal processes were not even known.

To accomplish this task, two main theoretical ideas were formulated. First, that the trend of the concentration of a chlorofluorocarbons is a direct index of the lifetime and second, that the global atmospheric mass balance could be determined from a few sites carefully chosen to be representative of large spatial scales.

The idea that the trend was an indicator of the global lifetime is expressed by the following equation:

$$\frac{dC}{dt} = S - \frac{C}{\tau} \tag{1}$$

where C is the global burden of the gas (grams), S are the emissions (grams/yr), and τ is the lifetime (years).

The solution of this equation is, assuming that time is taken as zero when the atmospheric concentration is nearly zero:

$$C = e^{-\eta t} \int_0^t S(v) e^{\eta v} dv \tag{2}$$

By dividing both sides of equation (1) by C, it can be recast as:

$$\frac{1}{C}\frac{dC}{dt} = \frac{S}{C} - \frac{1}{\tau} \tag{3}$$

Substituting Equation (2) into Equation (3) gives:

$$\frac{1}{C}\frac{dC}{dt} = \frac{S(t)}{\int_0^t S(v)\, e^{\eta(v-t)}\, dv} - \frac{1}{\tau} \tag{4}$$

Equation (4) has two significant properties. The left hand side is "concentration scale invariant." That is to say that if the absolute concentration was in error so that the true concentration was $C_{true} = \alpha\ C_{meas}$, then $1/C_{true}\ dC_{true}/dt = 1/C_{meas}\ dC_{meas}/dt$. So the relative trend is independent of absolute calibration. Second, if the emissions were underestimated by some fraction, then on the right hand side the effect of this error would also not affect Equation (4) - "emissions scale invariance."

These two invariance properties of Equation 4 were of considerable practical importance. Absolute calibration of the chlorofluorocarbons was extremely difficult to pin down within acceptably narrow bands, and to some extent this still remains a problem today. Secondly, the estimate of the emissions was uncertain on two grounds. First, it was not clear how much emission may occur from countries that did not report their production of the CFCs, most notably the former Soviet Union and China. And second, because the release of the CFCs occurred many years after they were used in many applications. For example, when the CFCs were used in spray cans, the release could occur within a year or so since consumer goods are sold during this time. But releases from refrigerators, air conditioners, and foams could have mean release time lags of decades to a hundred years. Thus systematic under-estimates (most likely) or overestimates (less likely) would not affect the calculations based on Equation (4) because the errors appear both in the numerator and the denominator of the right hand side. These were the main arguments for using Equation 4. This has been called the "Trend Method" for calculating lifetimes.

An alternative is to use the mass balance (Eqn. 1) directly and calculate the lifetime that best fits the observed concentrations C (from which the trends dC/dt can be estimated) and the industrial emissions S. This is sometimes called the "Overburden Method" or the "Global Mass Balance." This method is sensitive to errors in absolute calibration and our knowledge of the emissions. In practice, more complex versions of Equation (1) or (4) are used to take into account atmospheric mixing processes that cause differences of concentrations by latitude, height, and, to a lesser degree, with longitude.

II. The Project

II.1 Site Selection, Sampling Frequency, and the Transport Model

Four sites were chosen, one in each of the four latitudinal semi-hemispheres of the earth. First, the choices for ALE/GAGE sites were Adrigole, Ireland (52° N); Barbados (13° N); Samoa (14° S); and Cape Grim, Tasmania (42° S), covering the middle and tropical latitudes of both the northern and southern hemispheres. Soon afterwards Cape Meares, Oregon, was added, mostly as a replacement for Adrigole, which was heavily influenced by emissions from Europe. Adrigole did not represent the northern semi-hemispheric mean concentrations, while the geography of Cape Meares, Oregon, made it an ideal mid-northern latitude station. At the time Cape Meares became an ALE/GAGE station, it was already operational, and automated measurements were being taken for our other projects (with R.A.Rasmussen, M.A.K.Khalil, and D.Pierotti as principal investigators). The conversion of the site to an ALE/GAGE station was therefore relatively straightforward. At the same time it remained a primary station for other funded projects of the Global Change Research Center. When the present NASA contract expired, the Cape Meares station continued to operate in support of other projects although it has not been a GAGE or AGAGE site.

In summary, then, the expectation was that real-time or high frequency measurements of the chlorofluorocarbons, at these four sites, would provide a complete understanding of the global distribution, which would, by the use of a model based on Equation 4, yield an estimate of the lifetime of these gases. The lifetime would not depend on absolute calibration or the lack of knowledge of emissions from certain parts of the world.

II.2 Frequency of Measurements

The trend is highly variable, being a derivative of the measured concentrations. Therefore, high frequency measurements were proposed to reduce the uncertainties in the mean trends on a monthly average basis. Gas chromotographs with electron capture detectors were selected

for the measurements (see Appendix IV for details). These instruments measured not only F-11 and F-12 but also measured CH_3CCl_3, CCl_4 and N_2O. Since these gases are also important to global change science, they were included in the program, although for CCl_4 and N_2O Eqn. 4 cannot be used since the emissions are not known. During the 1980s, Khalil and Rasmussen showed that methane was increasing in the atmosphere. With funding from various sources, unrelated to the ALE/GAGE program, they developed the budgets and trends of methane. As the research program on methane (CH_4) became established, its measurements were added to the ALE/GAGE program.

Since there was no theoretical guide, the initial frequency of measurements was made 1/hr, which was the highest frequency that could be achieved with the instrumentation available at the time when the project was set up. This frequency was chosen because of the highly variable nature of the short-term trends from which the lifetime was to be calculated. High frequency measurements reduced the uncertainty of the monthly mean approximately as 1/sqrt N where N is the number of measurements per month. A high frequency of measurements also allows for detecting and eliminating pollution events that cause high concentrations, or intrusions of stratospheric air that on rare occasions cause low observed concentrations. These pollution events became more frequent as the experiment progressed and the usage, or the emissions, of the chlorocarbons, chlorofluorocarbons, and other gases continued to increase.

II.3 The Mass Balance Model

The model to estimate the lifetimes was designed as a nine-box mass balance with latitudinal variations represented by the four semi-hemispheres (with one site in each) and with two vertical layers in the troposphere and one layer representing the stratosphere. This was a compact model, tightly coupled to the experimental data at the four main ALE/GAGE sites. It was also the smallest model that could incorporate the mean motion of the atmosphere by Hadley circulation. It included the four main latitudinal regions across each of which the atmospheric circulation is slowed by rising or subsiding air movements (Figure 1).

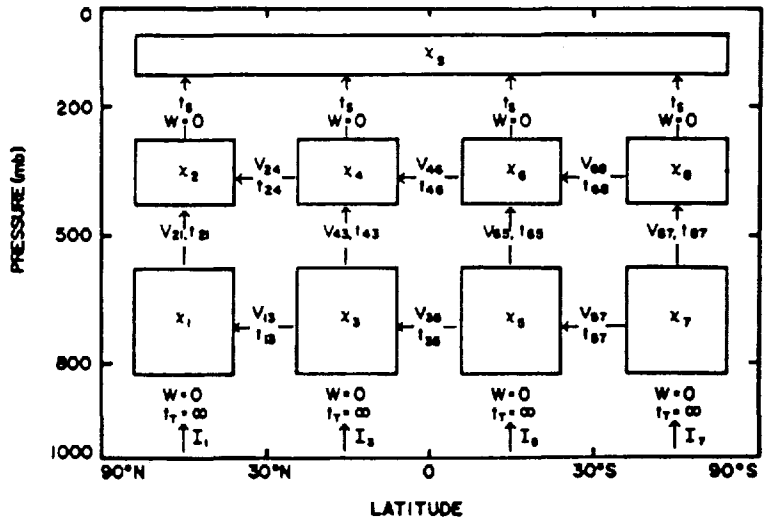

Figure 1. Schematic of nine-box two-dimensional model of the atmosphere. Values of the diffusion coefficients t_{ij} and inverse advection times V_{ij} are given in Table 1 in Cunnold et al., 1983, page 8380 (see Appendix V). Atmospheric release of halocarbons is assumed to occur directly into boxes 1, 3, 5, and 7.

This model is written as follows:

$$\frac{d\chi_i}{dt} = \sum_j V_{ij}\,\overline{\chi_{ij}} + \sum_j \frac{\Delta\chi_{ij}}{t_{ij}} + \frac{I_i}{M_i} + \frac{\chi_i}{\tau_i}$$

$$\overline{\chi_{ij}} = \frac{1}{2}(\chi_i + \chi_j) \qquad (5)$$

$$(\Delta\chi)_{ij} = \chi_i - \chi_j$$

Here the first term is the transfer of gases by the mean motions of the atmosphere for box i. The box gains CFCs or other trace gases from the winds that blow material in from boxes j and loses gases by winds blowing materials from box i to boxes j. j is an index representing all the boxes with which box i shares a boundary. Similarly, the second term is the effect of "turbulent" processes that transfer gas by the gradient of the mean concentrations between the boxes ($\Delta\chi_{ij}$). I_i is the "Input" or source of gases into box i. (It is zero for boxes that do not include the surface of the earth.) M_i is the mass of air in box i, and τ_i = the lifetime of the gas in box i. The lifetime may be infinite in some boxes, in which case this last term is zero.

An example of a mass balance for a box according to Eqn. (5) is (Cunnold et al., 1983):

$$\frac{d\chi_2}{dt} = \frac{5}{3}V_{24}\overline{\chi_{24}} + \frac{5}{3}V_{21}\overline{\chi_{21}} - \frac{(\Delta\chi)_{24}}{t_{24}} - \frac{5}{3}\frac{(\Delta\chi)_{21}}{t_{21}} - \frac{2}{3}\frac{\chi_u - \chi_2}{\tau_s} - \frac{\chi_2}{\tau_2}$$

It shows the factor 5/3 and 2/3 required to convert for the different masses of air in the boxes at the surface compared to those above.

II.4 OGC's Role in the Project

This project was a collaboration between principal investigators at several institutions. Each group had its separate primary role. The groups and principal investigators were Dr. R.A. Rasmussen from OGC, and when methane was added to the ALE/GAGE program Dr. M.A.K. Khalil, also at OGC, joined the research team; Dr. R. Prinn of MIT; Drs. D. Cunnold and F. Alyea of Georgia Institute of Technology; Dr. P. Simmonds of University of Bristol; Dr. P. Fraser of CSIRO in Australia; and Dr. R. Rosen of AER, Inc. Many technical staff members participated from each of these institutions.

The Oregon Graduate Institute, then called the Oregon Graduate Center, had four main roles and responsibilities in the overall ALE/GAGE project.

Part 1) Dr. R.A. Rasmussen was the chief experimentalist for the ALE/GAGE program and was responsible for maintaining all stations and ensuring uniformity of data quality.

Part 2) The OGI group was responsible for all calibration standards. This was a major task which included :

a) Making the primary absolute standards.

b) Making and calibrating secondary standards that were used at all sites.

c) Determining the stability of the primary (and secondary) calibration standards.

Part 3) The OGI group maintained the Cape Meares and the Samoa stations (two of 4-5 stations of the network). Moreover, the field technician in-charge (Mr. A.J. Crawford) maintained instruments at the other stations as well.

Part 4) Quality Assurance by collection and of flask samples for the measurements of the chloroflorocarbons. The flask sampling provides an independent check for the accuracy of the ALE/GAGE data sets. The flask samples are measured on laboratory instruments, not the ones that took the automated measurements, and were calibrated against primary laboratory standards instead of the secondary standards that were used in the field. The flask samples also provide data on other gases that were not measured by the field instruments, and thus represented an exploratory component of the project. The ALE/GAGE program had an intent to add with high frequency field measurements any other gas that was found by the flask sampling program to be potentially important in global change science.

It is noteworthy that before the NASA funding was provided (for which this report is being written) the ALE/GAGE program was fully operational and Dr. R.A. Rasmussen was the chief experimentalist. He had fulfilled the following responsibilities that have a direct bearing on the present report:

a) Design and selection of automated instruments for all sites. All instruments were of the same brand and number and the same experimental methods were applied to all sites.
b) Set up instrumentation and refine the operations to produce data of precision acceptable to the ALE/GAGE program.
c) Provide training for principal investigators in the program who ran the stations namely Dr. Simmonds who managed Barbados (and Adrigole) and Dr. Fraser who managed Cape Grim, Tasmania.

The accomplishment of these tasks is a matter of record, since high frequency and high precision data were produced during the time that OGI was involved in the project. These

data have been reported in the peer-reviewed scientific literature including the publications that are attached in Appendix V and listed in Appendix III.

In the rest of this report, we discuss three areas that complete the documentation of the accomplishments of the project. These areas are:

a) A review of the preparation and stability of the calibration standards. (Relates primarily to Part 2 above on the role of OGI, secondarily to Part 1.)

b) The data at the two sites: Cape Meares and Samoa and some features of the data. (Relates primarily to Part 3, secondarily to Part 1.)

c) An analysis of the information content of high frequency ALE/GAGE measurements compared to flask samples. (Relates primarily to parts 4 and 3, secondarily to Part 1.)

III. A Review of the Stability of the Calibration Standards.

The atmospheric concentration is measured using a calibration standard. A sample from the calibration standard is analyzed before and after the analysis of each ambient sample. The concentration of the trace gas in the atmosphere is determined as:

$$C(\text{Atmosphere}) = \frac{M(\text{Atmosphere})}{M(\text{Standard})} \times C(\text{Standard})$$

where M(Atmosphere) is the "area under the (usually Gaussian) peak" representing the trace on the output of the gas chromatograph for the ambient sample, or M could be the "peak height." The areas are measured by an electronic integrator. C(Standard) is the "Absolute Concentration" assigned to the standard from which the sample is drawn.

The calibration is perhaps the single most important aspect of ensuring a high quality of data and is therefore a fundamental part of the quality assurance program. It has two aspects - absolute calibration and stability. Absolute calibration refers to the how close the assigned concentration of a gas in a tank is to the real concentration of the gas in that tank. Stability refers to the potential changes that may occur in the concentrations of a gas in a calibration tank over time. If the absolute calibration has a positive error (assigned value greater than the real value), it will lead to an underestimate of the atmospheric concentration, and similarly if the assigned value is too low, it will lead to an overestimate of the atmospheric concentration. For long-lived gases, small errors of the absolute calibration can result in large errors of lifetime. The "Trend Method" for estimating lifetimes was chosen to avoid this problem (unfortunately, there is a cost for the insensitivity of the lifetime based on the trend to absolute calibration - a brief discussion will be provided later in Section V). If a calibration standard is found to be too high or too low, all existing data can be easily corrected by multiplying it by the appropriate "calibration correction factor." These corrections had to be made at certain times during the course of the ALE/GAGE project.

For the success of any long-term measurement project, the stability is much more important

than the absolute calibration. If standard concentrations drift during the course of the experiment, it is difficult to correct the data, since such changes are not linear or systematic. Moreover, drifts in the standard concentrations cause errors in the measured trend. Since the lifetime is sensitive to the trend, drifts in the standards can lead to large errors in the lifetimes estimated by the trend method. Much time was spent, therefore, to ensure that there were no drifts in the calibration standards. If any tank is found to have a drift, it is immediately discarded.

The results of periodic analysis of the calibration standards are shown in a set of Figures 2, 3, and 4 and are given in Tables 1, 2 and 3. The results show that the main calibration tanks had no significant drifts. These data also establish the limits and uncertainties associated with the long-term stability of the calibration standards.

The absolute calibration has to be modified by a multiplicative factors as new and more refined methods become available. The original standards were made nearly 20 years ago. Since then, there have been improvements in the available instrumentation for precise analysis and in the purity of the materials available for the making of standards. Recently NIST (National Institute for Standards and Technology), formerly the National Bureau of Standards (NBS), has released standard reference materials (SRMs) for halocarbons. No such materials were available at the start of the project, so all standards used for ALE/GAGE were prepared by R.A. Rasmussen. These original primary standards, from 1976-1978, were recently compared to the NIST SRMs with the following results: x(F-11) = 0.92; x(F-113) = 0.75 $x(CCl_4)$ = 0.72; $x(CH_3CCl_3)$ = 0.71 where x(gas) is the factor by which the original concentrations should be multiplied to arrive at the concentrations that would be consistent with the latest NIST SRM. (See also Rasmussen and Khalil, 1986, and Khalil and Rasmussen, 1984.)

Section III. A Review of the Stability of the Calibration Standards.

Figure 1. Schematic of nine-box two-dimensional model of the atmosphere. Values of the diffusion coefficients t_{ij} and inverse advection times V_{ij} are given in Table 1 in Cunnold et al., 1983, page 8380 (see Appendix V). Atmospheric release of halocarbons is assumed to occur directly into boxes 1, 3, 5, and 7.

Figure 2. The stability of trace gases measured in the GAGE program over a 14-year period. The graph shows the change relative to the original calibration value as Percent Deviation = [1 - C(t)/C(0)]100%, where C(t) is the concentration in the tank at time t and C(0) was the original assigned concentration.

Figure 3. The trends in the calibration for all gases. The trends are calculated as 1/C dC/dt x 100%.

Table 1. Concentrations of trace gases in the calibration tanks during the last 14 years. Note that these concentrations are on the original calibration scale and must be multiplied by the appropriate factors in Section III to convert to current scales.

Table 2. Changes in the concentrations of trace gases in the calibration tanks. The percent deviations are shown relative to the original calibration values. Data plotted in Figure 2.

Table 3. Trends in the concentrations of trace gases in the calibration tanks during the last 14 years. Data plotted in Figure 3.

Figure 2

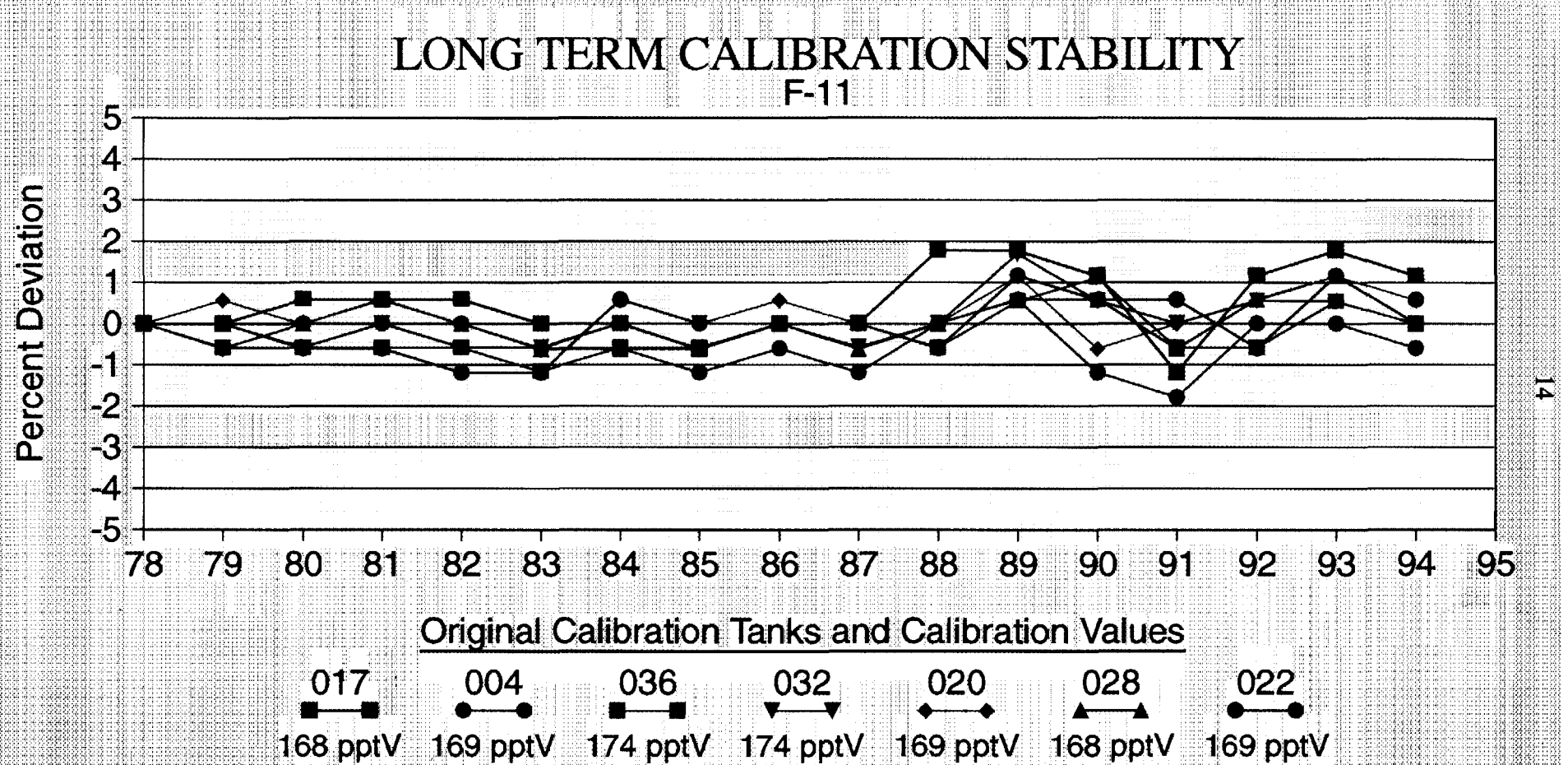

R A Rasmussen

Global Change Research Center
(503) 690-1077 FAX (503) 690-1669

M A K Khalil

Figure 2

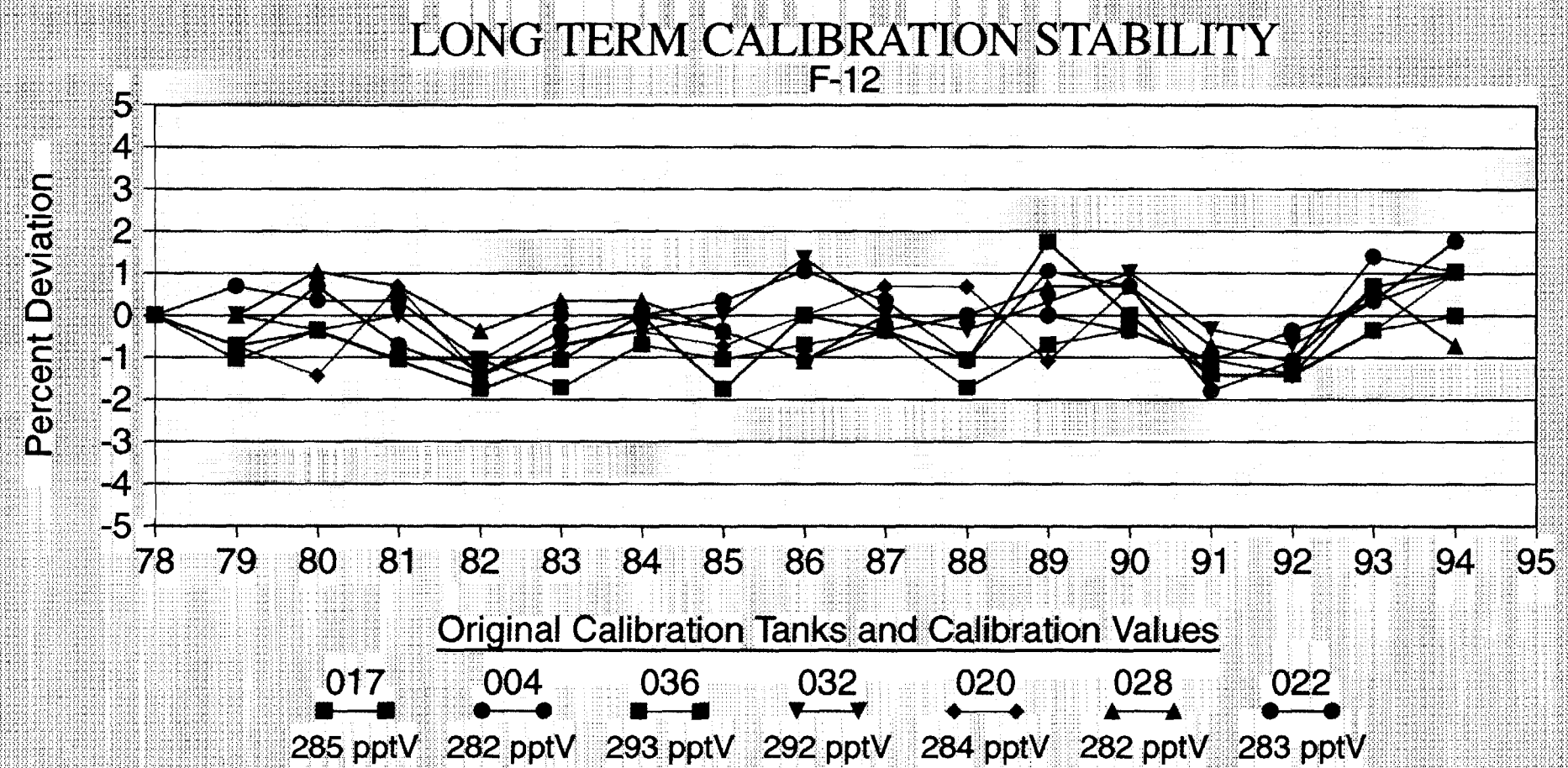

R A Rasmussen

Global Change Research Center
(503) 690-1077 FAX (503) 690-1669

M A K Khalil

Figure 2

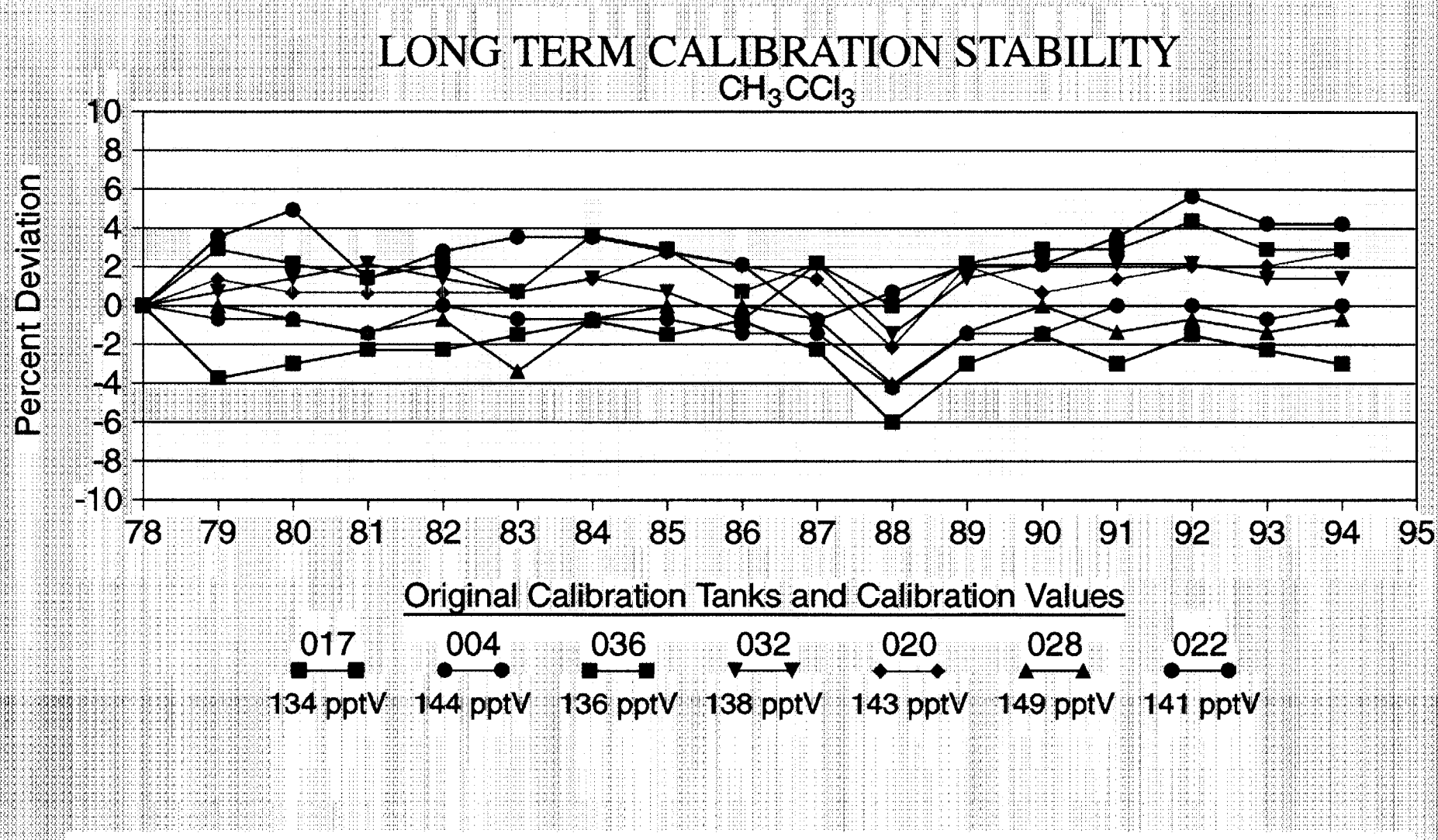

R A Rasmussen

Global Change Research Center
(503) 690-1077 FAX (503) 690-1669

M A K Khalil

Figure 2

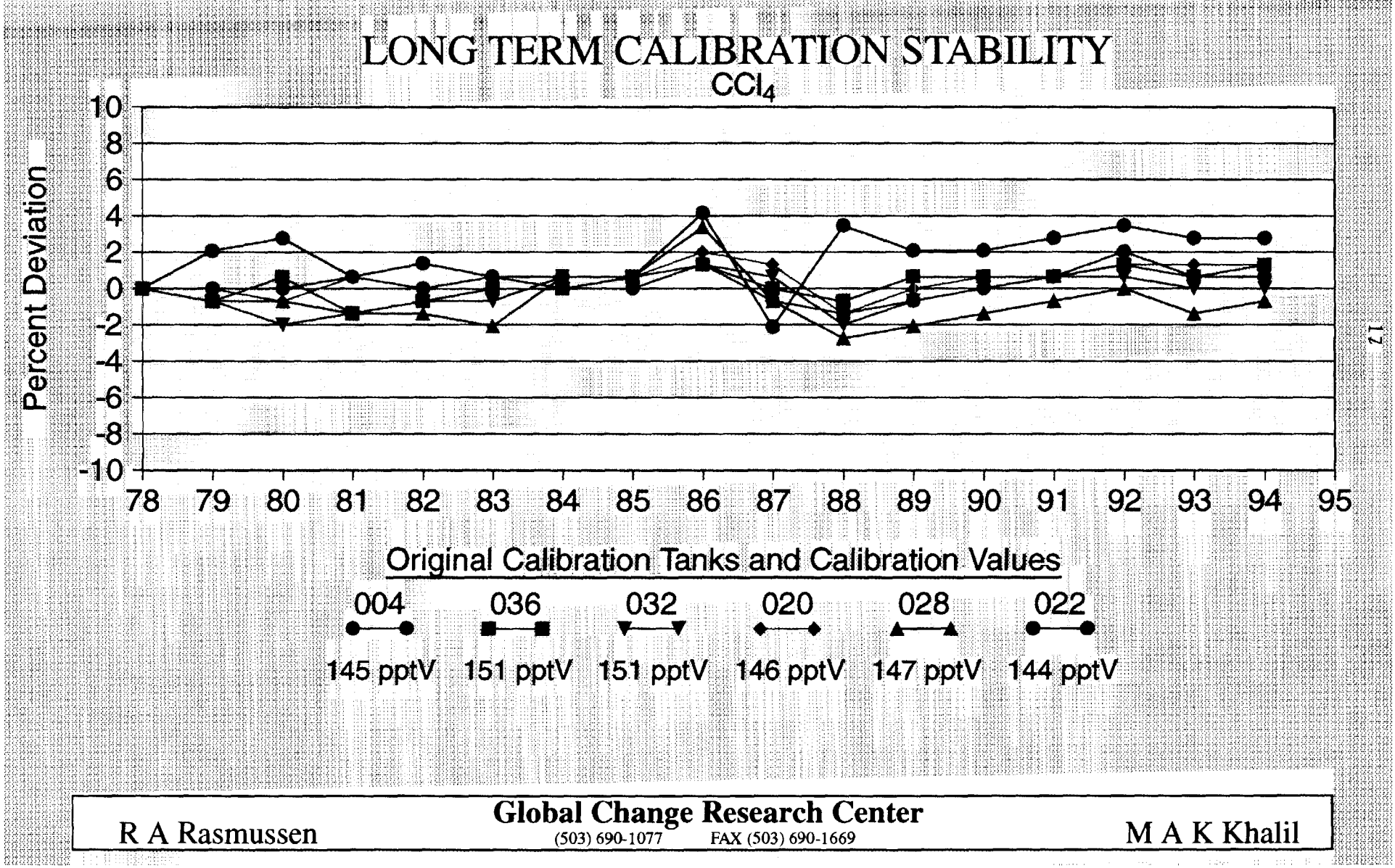

R A Rasmussen

Global Change Research Center
(503) 690-1077 FAX (503) 690-1669

M A K Khalil

Figure 2

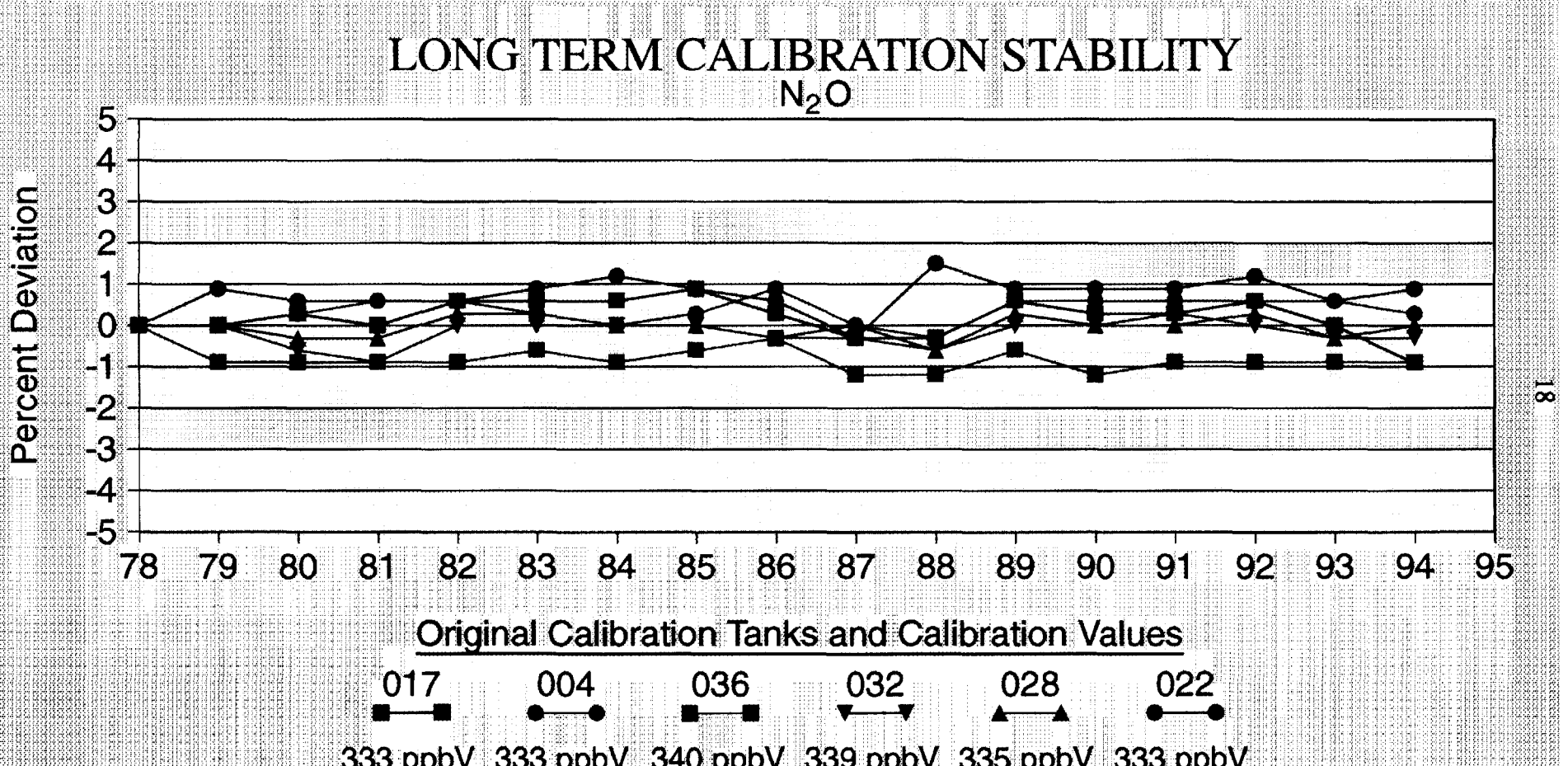

R A Rasmussen

Global Change Research Center
(503) 690-1077 FAX (503) 690-1669

M A K Khalil

Figure 3

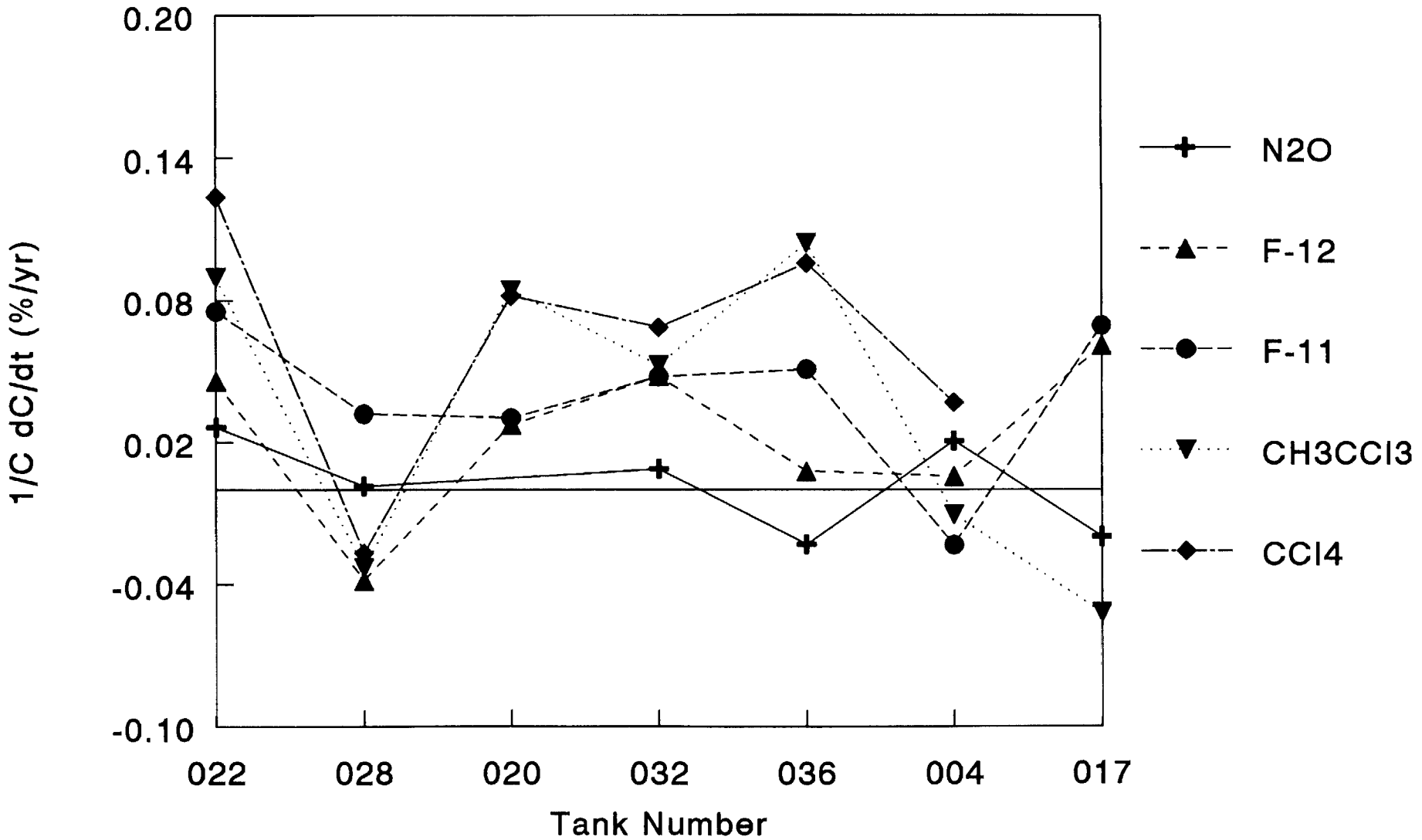
0.20
0.14
0.08
0.02
-0.04
-0.10
1/C dC/dt (%/yr)
022
028
020
032
036
004
017
Tank Number
N2O
F-12
F-11
CH3CCl3
CCl4

Table 1 (1)

ALE - GAGE Long Term Standards
2/9/95

		022	028	020	032	036	004	017
N2O	**1978**	**333**	**335**	**334**	**339**	**340**	**333**	**333**
N2O	1979	336	335	337	339	337	333	333
N2O	1980	335	334	342	337	337	334	334
N2O	1981	335	334	345	336	337	335	333
N2O	1982	335	336	345	339	337	335	335
N2O	1983	336	336	348	339	338	334	335
N2O	1984	337	335	337	339	337	333	335
N2O	1985	336	335	336	339	338	334	336
N2O	1986	335	334	355	338	339	336	334
N2O	1987	332	335	359	338	336	333	332
N2O	1988	338	333	357	337	336	332	332
N2O	1989	336	336	367	339	338	335	335
N2O	1990	336	335	368	339	336	335	334
N2O	1991	336	335	370	340	337	335	334
N2O	1992	337	336	370	339	337	335	335
N2O	1993	335	334	368	338	337	335	333
N2O	1994	336	335	369	338	337	334	330
F12	**1978**	**283**	**282**	**284**	**292**	**293**	**282**	**285**
F12	1979	281	282	282	292	290	284	283
F12	1980	285	285	280	291	292	283	284
F12	1981	281	284	286	292	290	283	282
F12	1982	279	281	280	288	290	279	280
F12	1983	282	283	282	290	288	282	282
F12	1984	283	283	283	291	291	282	285
F12	1985	282	281	282	292	290	283	280
F12	1986	280	279	284	296	291	285	285
F12	1987	282	282	286	292	292	283	284
F12	1988	283	282	286	291	288	279	282
F12	1989	283	284	281	293	291	285	290
F12	1990	282	284	286	295	292	284	285
F12	1991	280	280	280	291	290	277	281
F12	1992	282	279	280	290	289	279	281
F12	1993	284	284	283	293	292	286	287
F12	1994	288	280	287	295	293	285	288
F11	**1978**	**169**	**168**	**169**	**174**	**174**	**169**	**168**
F11	1979	169	168	170	174	173	168	168
F11	1980	168	168	169	173	173	169	169
F11	1981	168	169	170	174	173	169	169
F11	1982	167	168	169	174	173	169	169
F11	1983	167	167	168	173	172	168	168
F11	1984	170	167	169	174	173	168	168
F11	1985	169	167	169	174	173	167	167
F11	1986	169	168	170	174	174	168	168
F11	1987	169	167	169	173	174	167	168
F11	1988	168	168	169	174	173	169	171
F11	1989	171	169	171	177	175	170	171
F11	1990	170	169	168	175	176	167	170
F11	1991	170	167	169	174	173	166	166
F11	1992	168	169	170	175	173	169	170
F11	1993	171	170	171	175	175	169	171
F11	1994	170	168	170	174	174	168	170

Table 1 (2)

ALE - GAGE Long Term Standards
2/9/95

METC	**1978**	**141**	**149**	**143**	**138**	**136**	**144**	**134**
METC	1979	146	149	145	139	140	143	129
METC	1980	148	148	144	140	139	143	130
METC	1981	143	147	144	141	138	142	131
METC	1982	145	148	144	140	139	144	131
METC	1983	146	144	144	139	137	143	132
METC	1984	146	148	145	140	141	143	133
METC	1985	145	149	147	139	140	143	132
METC	1986	144	149	146	137	137	142	133
METC	1987	140	148	145	141	139	142	131
METC	1988	142	143	140	136	136	138	126
METC	1989	144	147	146	140	139	142	130
METC	1990	144	149	144	141	140	142	132
METC	1991	146	147	145	141	140	144	130
METC	1992	149	148	146	141	142	144	132
METC	1993	147	147	146	140	140	143	131
METC	1994	147	148	147	140	140	144	130
CCl4	**1978**	**144**	**147**	**146**	**151**	**151**	**145**	**146**
CCl4	1979	147	146	146	150	150	145	144
CCl4	1980	148	146	145	148	152	145	143
CCl4	1981	145	145	147	149	149	146	141
CCl4	1982	146	145	146	150	150	145	139
CCl4	1983	145	144	146	150	151	146	138
CCl4	1984	145	148	146	152	151	145	136
CCl4	1985	145	148	147	152	152	145	135
CCl4	1986	150	152	149	153	153	147	133
CCl4	1987	141	146	148	152	151	144	127
CCl4	1988	149	143	144	148	150	143	125
CCl4	1989	147	144	146	150	152	144	125
CCl4	1990	147	145	147	151	152	145	123
CCl4	1991	148	146	147	152	152	146	122
CCl4	1992	149	147	148	152	153	148	122
CCl4	1993	148	145	148	151	152	146	119
CCl4	1994	148	146	148	151	153	146	117

Table 2 (1)

ALE - GAGE Long Term Standards
% Deviation from 1978 values
2/9/95

		022	028	020	032	036	004	017
N2O	1978	0.00	0.00	0.00	0.00	0.00	0.00	0.00
N2O	1979	0.90	0.00	0.90	0.00	-0.88	0.00	0.00
N2O	1980	0.60	-0.30	2.40	-0.59	-0.88	0.30	0.30
N2O	1981	0.60	-0.30	3.29	-0.88	-0.88	0.60	0.00
N2O	1982	0.60	0.30	3.29	0.00	-0.88	0.60	0.60
N2O	1983	0.90	0.30	4.19	0.00	-0.59	0.30	0.60
N2O	1984	1.20	0.00	0.90	0.00	-0.88	0.00	0.60
N2O	1985	0.90	0.00	0.60	0.00	-0.59	0.30	0.90
N2O	1986	0.60	-0.30	6.29	-0.29	-0.29	0.90	0.30
N2O	1987	-0.30	0.00	7.49	-0.29	-1.18	0.00	-0.30
N2O	1988	1.50	-0.60	6.89	-0.59	-1.18	-0.30	-0.30
N2O	1989	0.90	0.30	9.88	0.00	-0.59	0.60	0.60
N2O	1990	0.90	0.00	10.18	0.00	-1.18	0.60	0.30
N2O	1991	0.90	0.00	10.78	0.29	-0.88	0.60	0.30
N2O	1992	1.20	0.30	10.78	0.00	-0.88	0.60	0.60
N2O	1993	0.60	-0.30	10.18	-0.29	-0.88	0.60	0.00
N2O	1994	0.90	0.00	10.48	-0.29	-0.88	0.30	-0.90
F12	1978	0.00	0.00	0.00	0.00	0.00	0.00	0.00
F12	1979	-0.71	0.00	-0.70	0.00	-1.02	0.71	-0.70
F12	1980	0.71	1.06	-1.41	-0.34	-0.34	0.35	-0.35
F12	1981	-0.71	0.71	0.70	0.00	-1.02	0.35	-1.05
F12	1982	-1.41	-0.35	-1.41	-1.37	-1.02	-1.06	-1.75
F12	1983	-0.35	0.35	-0.70	-0.68	-1.71	0.00	-1.05
F12	1984	0.00	0.35	-0.35	-0.34	-0.68	0.00	0.00
F12	1985	-0.35	-0.35	-0.70	0.00	-1.02	0.35	-1.75
F12	1986	-1.06	-1.06	0.00	1.37	-0.68	1.06	0.00
F12	1987	-0.35	0.00	0.70	0.00	-0.34	0.35	-0.35
F12	1988	0.00	0.00	0.70	-0.34	-1.71	-1.06	-1.05
F12	1989	0.00	0.71	-1.06	0.34	-0.68	1.06	1.75
F12	1990	-0.35	0.71	0.70	1.03	-0.34	0.71	0.00
F12	1991	-1.06	-0.71	-1.41	-0.34	-1.02	-1.77	-1.40
F12	1992	-0.35	-1.06	-1.41	-0.68	-1.37	-1.06	-1.40
F12	1993	0.35	0.71	-0.35	0.34	-0.34	1.42	0.70
F12	1994	1.77	-0.71	1.06	1.03	0.00	1.06	1.05
F11	1978	0.00	0.00	0.00	0.00	0.00	0.00	0.00
F11	1979	0.00	0.00	0.59	0.00	-0.57	-0.59	0.00
F11	1980	-0.59	0.00	0.00	-0.57	-0.57	0.00	0.60
F11	1981	-0.59	0.60	0.59	0.00	-0.57	0.00	0.60
F11	1982	-1.18	0.00	0.00	-0.57	-0.57	0.00	0.60
F11	1983	-1.18	-0.60	-0.59	-0.57	-1.15	-0.59	0.00
F11	1984	0.59	-0.60	0.00	0.00	-0.57	-0.59	0.00
F11	1985	0.00	-0.60	0.00	0.00	-0.57	-1.18	-0.60
F11	1986	0.00	0.00	0.59	0.00	0.00	-0.59	0.00
F11	1987	0.00	-0.60	0.00	-0.57	0.00	-1.18	0.00
F11	1988	-0.59	0.00	0.00	0.00	-0.57	0.00	1.79
F11	1989	1.18	0.60	1.18	1.72	0.57	0.59	1.79
F11	1990	0.59	0.60	-0.59	0.57	1.15	-1.18	1.19
F11	1991	0.59	-0.60	0.00	0.00	-0.57	-1.78	-1.19
F11	1992	-0.59	0.60	0.59	0.57	-0.57	0.00	1.19
F11	1993	1.18	1.19	1.18	0.57	0.57	0.00	1.79
F11	1994	0.59	0.00	0.59	0.00	0.00	-0.59	1.19

Table 2 (2)

ALE - GAGE Long Term Standards
% Deviation from 1978 values
2/9/95

METC	1978	0.00	0.00	0.00	0.00	0.00	0.00	0.00
METC	1979	3.55	0.00	1.40	0.72	2.94	-0.69	-3.73
METC	1980	4.96	-0.67	0.70	1.45	2.21	-0.69	-2.99
METC	1981	1.42	-1.34	0.70	2.17	1.47	-1.39	-2.24
METC	1982	2.84	-0.67	0.70	1.45	2.21	0.00	-2.24
METC	1983	3.55	-3.36	0.70	0.72	0.74	-0.69	-1.49
METC	1984	3.55	-0.67	1.40	1.45	3.68	-0.69	-0.75
METC	1985	2.84	0.00	2.80	0.72	2.94	-0.69	-1.49
METC	1986	2.13	0.00	2.10	-0.72	0.74	-1.39	-0.75
METC	1987	-0.71	-0.67	1.40	2.17	2.21	-1.39	-2.24
METC	1988	0.71	-4.03	-2.10	-1.45	0.00	-4.17	-5.97
METC	1989	2.13	-1.34	2.10	1.45	2.21	-1.39	-2.99
METC	1990	2.13	0.00	0.70	2.17	2.94	-1.39	-1.49
METC	1991	3.55	-1.34	1.40	2.17	2.94	0.00	-2.99
METC	1992	5.67	-0.67	2.10	2.17	4.41	0.00	-1.49
METC	1993	4.26	-1.34	2.10	1.45	2.94	-0.69	-2.24
METC	1994	4.26	-0.67	2.80	1.45	2.94	0.00	-2.99
CCl4	1978	0.00	0.00	0.00	0.00	0.00	0.00	0.00
CCl4	1979	2.08	-0.68	0.00	-0.66	-0.66	0.00	-1.37
CCl4	1980	2.78	-0.68	-0.68	-1.99	0.66	0.00	-2.05
CCl4	1981	0.69	-1.36	0.68	-1.32	-1.32	0.69	-3.42
CCl4	1982	1.39	-1.36	0.00	-0.66	-0.66	0.00	-4.79
CCl4	1983	0.69	-2.04	0.00	-0.66	0.00	0.69	-5.48
CCl4	1984	0.69	0.68	0.00	0.66	0.00	0.00	-6.85
CCl4	1985	0.69	0.68	0.68	0.66	0.66	0.00	-7.53
CCl4	1986	4.17	3.40	2.05	1.32	1.32	1.38	-8.90
CCl4	1987	-2.08	-0.68	1.37	0.66	0.00	-0.69	-13.01
CCl4	1988	3.47	-2.72	-1.37	-1.99	-0.66	-1.38	-14.38
CCl4	1989	2.08	-2.04	0.00	-0.66	0.66	-0.69	-14.38
CCl4	1990	2.08	-1.36	0.68	0.00	0.66	0.00	-15.75
CCl4	1991	2.78	-0.68	0.68	0.66	0.66	0.69	-16.44
CCl4	1992	3.47	0.00	1.37	0.66	1.32	2.07	-16.44
CCl4	1993	2.78	-1.36	1.37	0.00	0.66	0.69	-18.49
CCl4	1994	2.78	-0.68	1.37	0.00	1.32	0.69	-19.86

Table 3: The stability of primary calibration standards over 16 years

Tank #		022	028	020	032	036	004	017
N2O	Trend	0.026	0.001		0.009	-0.023	0.021	-0.020
	90% CL	0.036	0.023		0.026	0.026	0.027	0.039
F-12	Trend	0.046	-0.038	0.027	0.048	0.008	0.006	0.061
	90% CL	0.063	0.057	0.077	0.058	0.047	0.081	0.085
F-11	Trend	0.075	0.032	0.030	0.048	0.051	-0.023	0.069
	90% CL	0.056	0.046	0.044	0.044	0.047	0.054	0.071
CH3CCl3	Trend	0.090	-0.033	0.084	0.053	0.104	-0.011	-0.052
	90% CL	0.145	0.104	0.098	0.092	0.099	0.092	0.125
CCl4	Trend	0.124	-0.027	0.082	0.068	0.096	0.037	
	90% CL	0.126	0.124	0.068	0.081	0.055	0.070	0.090

IV. The Data at the Two Sites: Cape Meares and Samoa

The data are displayed in the sets of Figures 5 and 6. These figures represent clean air concentrations (that is to say, without the pollution events) for the period of this project and beyond at the two sites we were responsible for. Similar data were obtained at the other two (or three) sites, namely Barbados and Cape Grim, Tasmania (and for some periods at Adrigole). Data for the other sites are included in the papers in Appendix V and have also been reported extensively in other documents produced by the U.S. agencies and international organizations dealing with the assessment of Atmospheric Ozone (see, for instance, WMO, 1985; 1988; 1990; 1991).

The main points of these figures are:

1. They demonstrate the success of the experimental program in producing a very high precision data set for the main chlorofluorocarbons of interest in the issue of ozone depletion, namely F-11 and F-12. And a similarly high quality of data for the secondary compounds for the ALE/GAGE project, namely CH_3CCl_3, CCl_4, N_2O, F-113, and CH_4.

2. The graphs show the rates of change and the changes in the trends. These features can be explained by the available emissions data and global mass balance models. The data have been used in numerous publications (see Khalil and Rasmussen, 1993).

3. Since we have demonstrated the high stability of the calibration standards in the last section, these data represent accurate trends of the chlorocarbons and the other gases we measured. The absolute calibration may still need revisions, but it is not likely to change by more than $\pm$ 5% for any of the gases.

The data plotted are on the original Rasmussen scale and should be adjusted according to the factors given in Section III.

Section IV. The Data from Cape Meares and Samoa and Some Features of the Data

Figure 4. The trends in the calibration for each gas and associated 90% confidence limits.

Figure 5. The concentrations of F-11, F-12, CH_3CCl_3, CCl_4, F-113, N_2O, and CH_4 at Cape Meares, including the period covered by the project discussed here. The data are shown for both the flask samples and the real-time instruments. Note that these concentrations are on the original calibration scale and must be multiplied by the appropriate factors in Section III to convert to current scales.

Figure 6. The concentrations of trace gases as in Figure 5, but for Samoa.

Figure 4

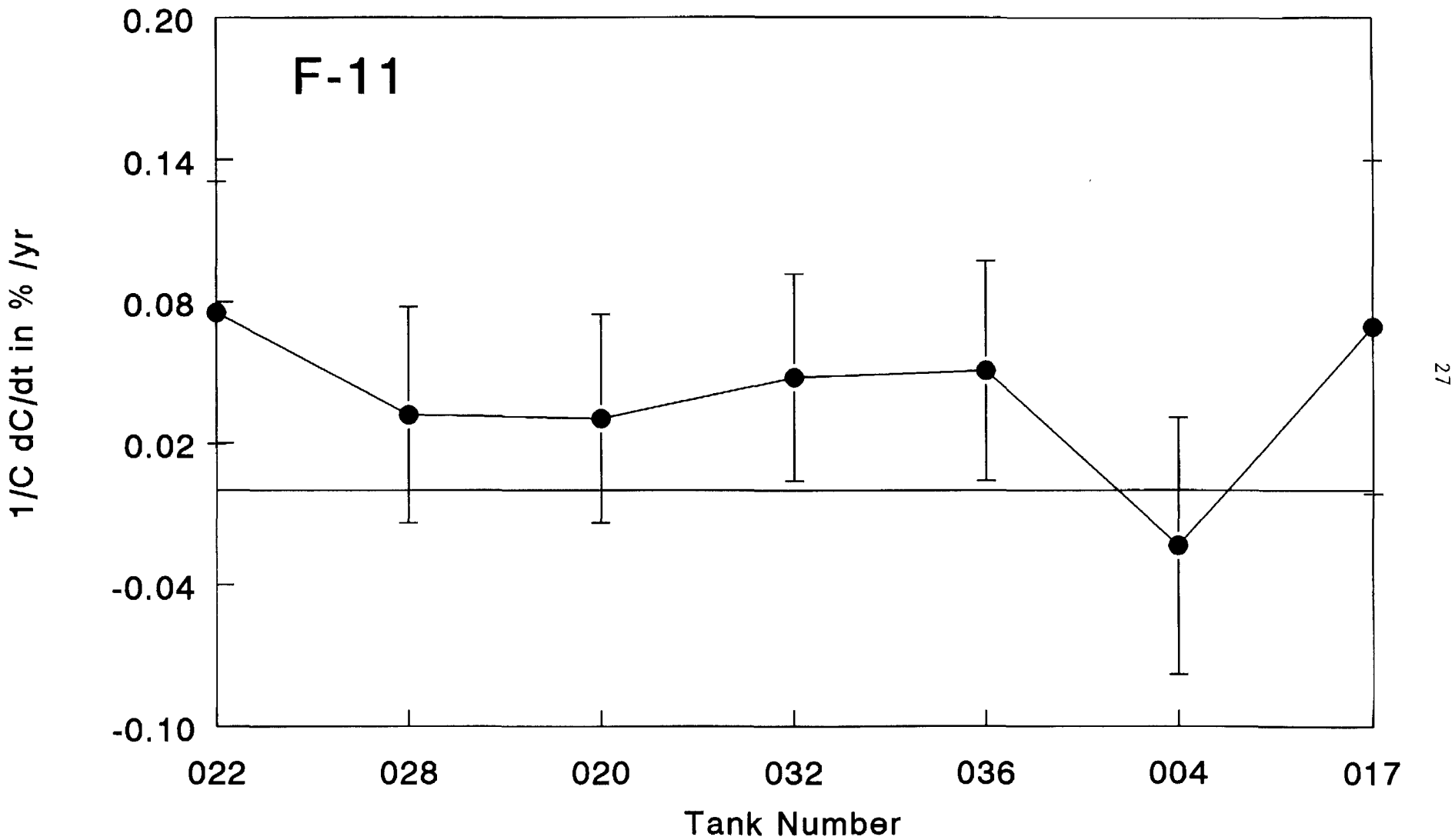
F-11
0.20
0.14
0.08
0.02
-0.04
-0.10
1/C dC/dt in % /yr
022
028
020
032
036
004
017
Tank Number

Figure 4

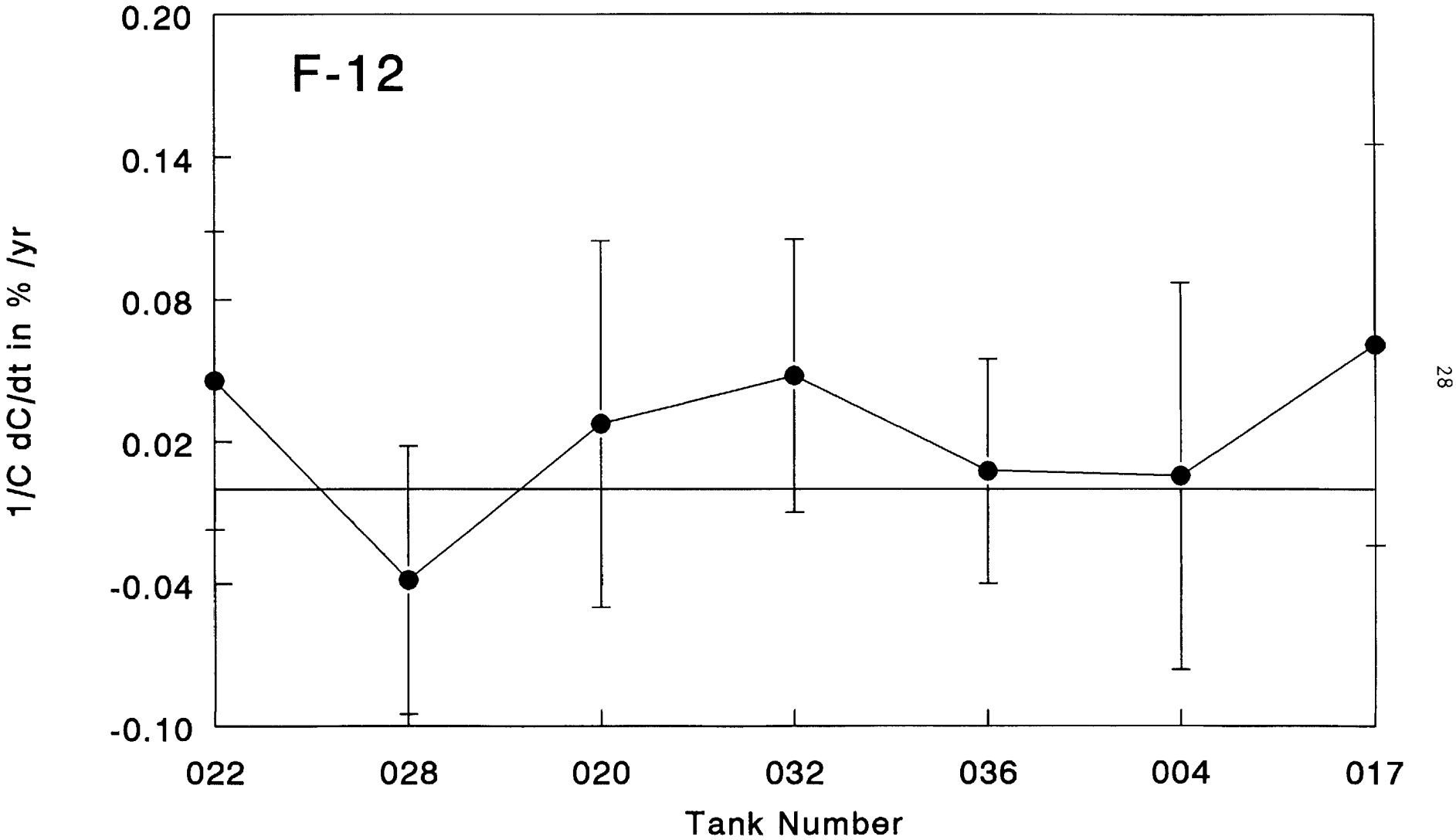
F-12
0.20
0.14
0.08
0.02
-0.04
-0.10
1/C dC/dt in % /yr
022
028
020
032
036
004
017
Tank Number

Figure 4

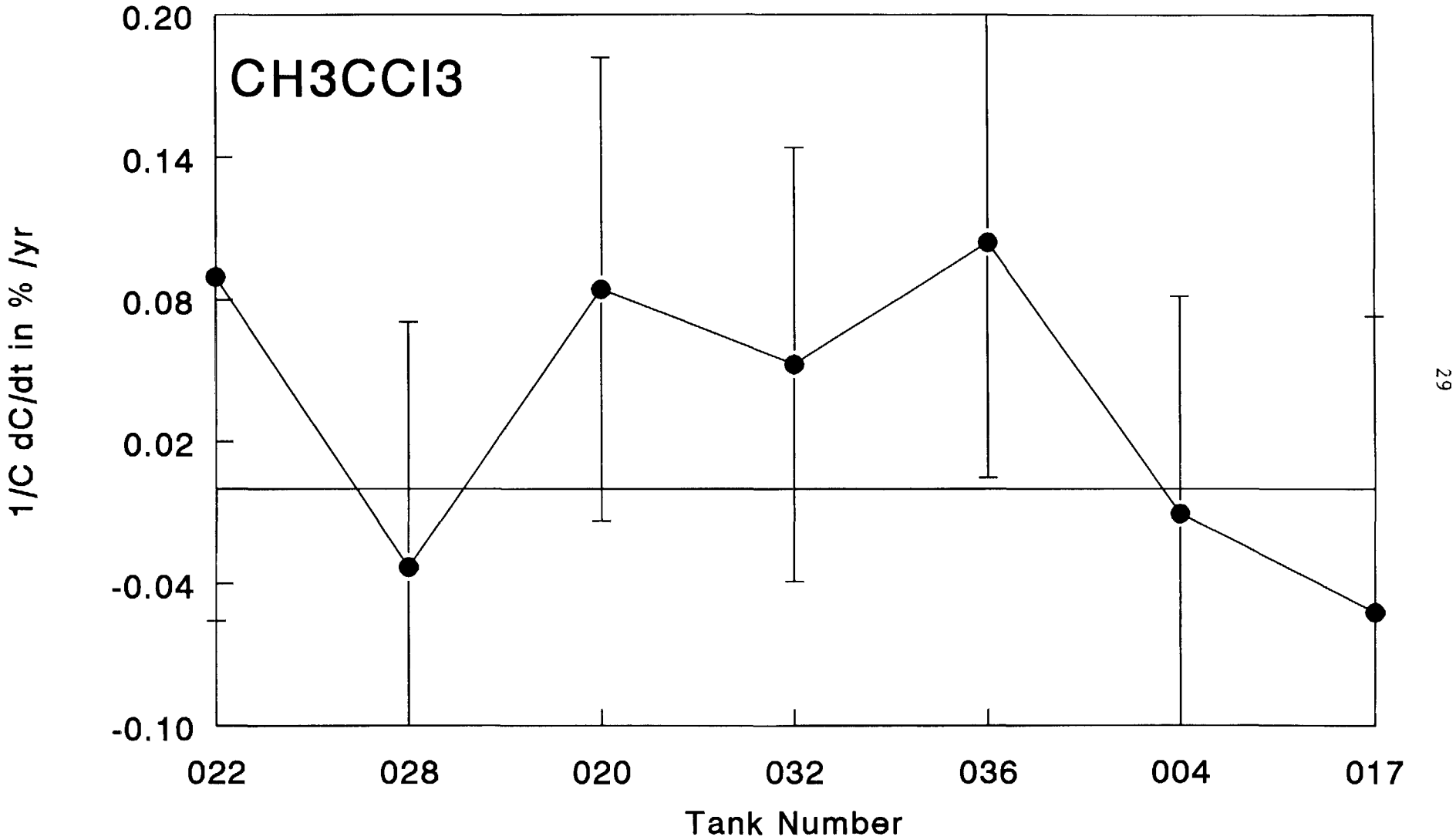
CH3CCl3
0.20
0.14
0.08
0.02
-0.04
-0.10
1/C dC/dt in % /yr
022
028
020
032
036
004
017
Tank Number

Figure 4

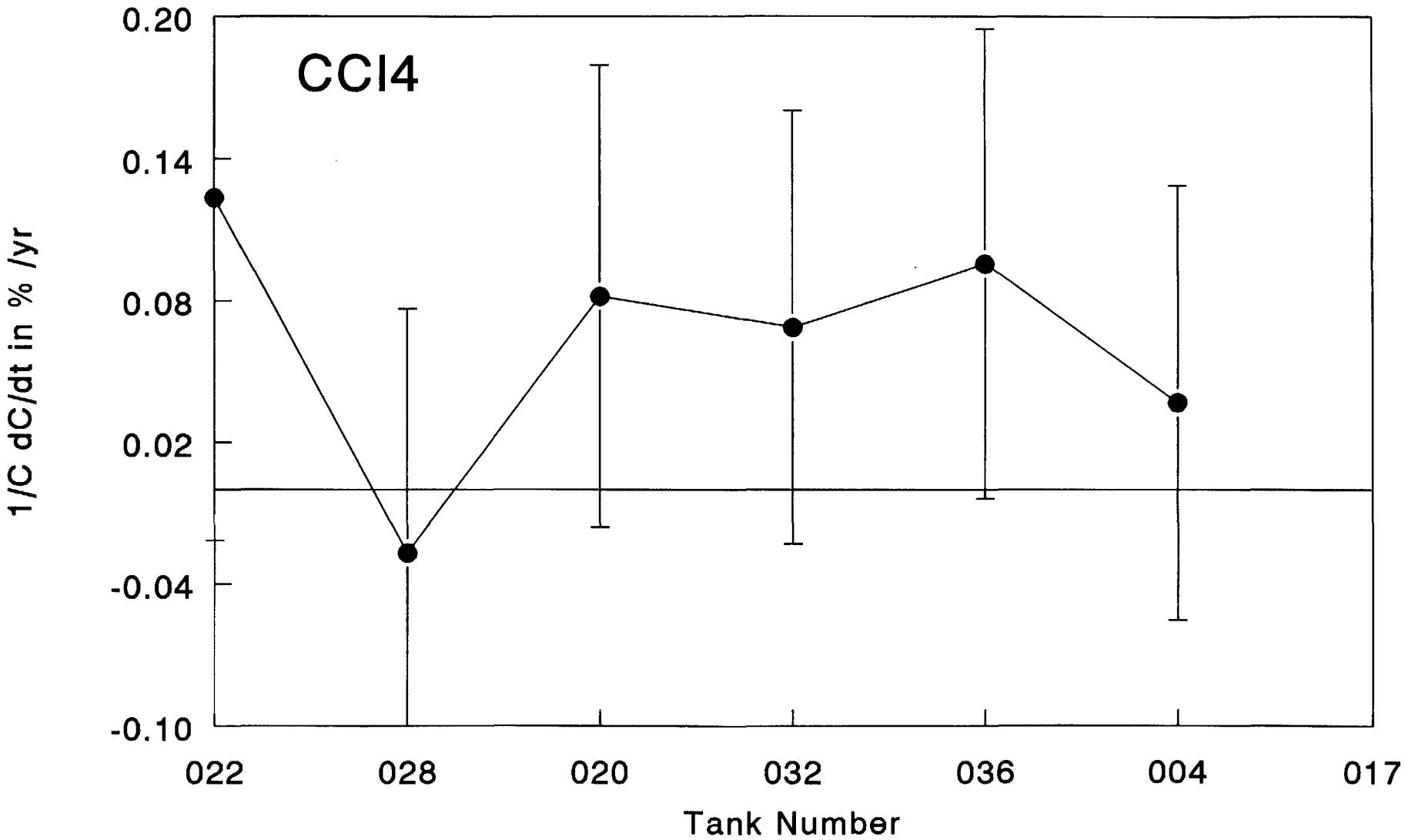
CCl4
0.20
0.14
0.08
0.02
-0.04
-0.10
1/C dC/dt in % /yr
022
028
020
032
036
004
017
Tank Number

Figure 4

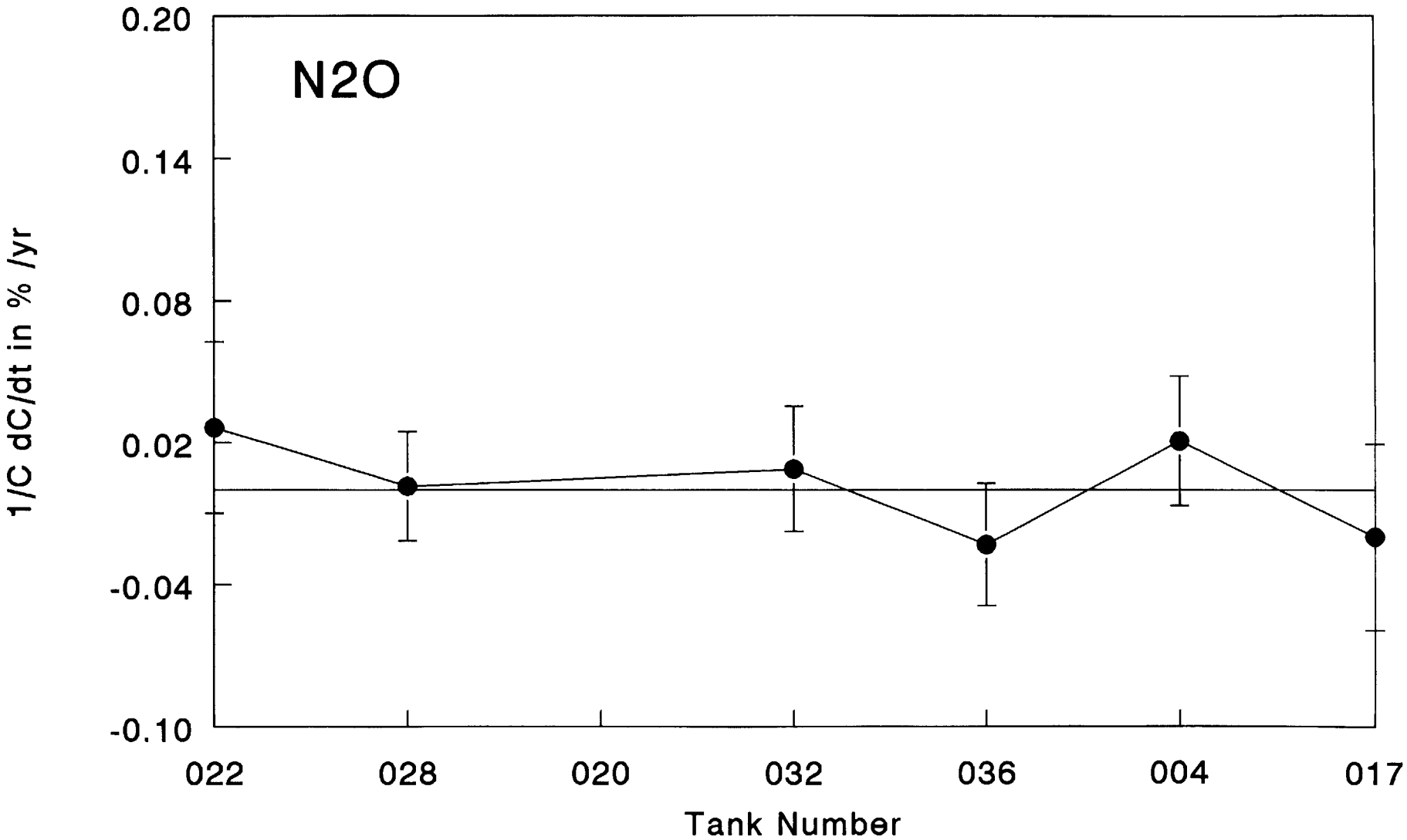
N2O
0.20
0.14
0.08
0.02
-0.04
-0.10
1/C dC/dt in % /yr
022
028
020
032
036
004
017
Tank Number

Figure 5

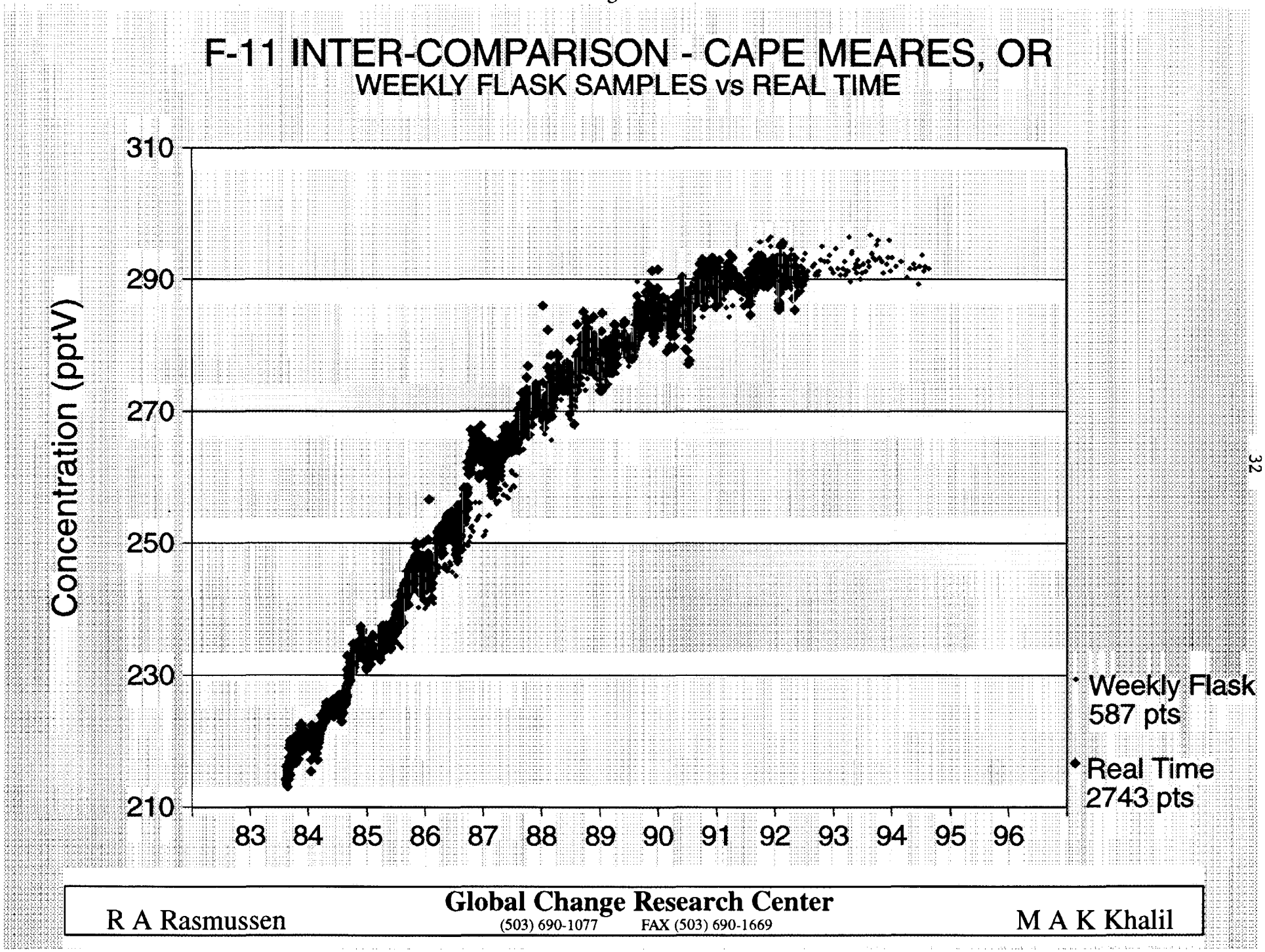
F-11 INTER-COMPARISON - CAPE MEARES, OR
WEEKLY FLASK SAMPLES vs REAL TIME
Concentration (pptV)
310
290
270
250
230
210
83
84
85
86
87
88
89
90
91
92
93
94
95
96
Weekly Flask
587 pts
Real Time
2743 pts
Global Change Research Center
R A Rasmussen
(503) 690-1077
FAX (503) 690-1669
M A K Khalil

Figure 5

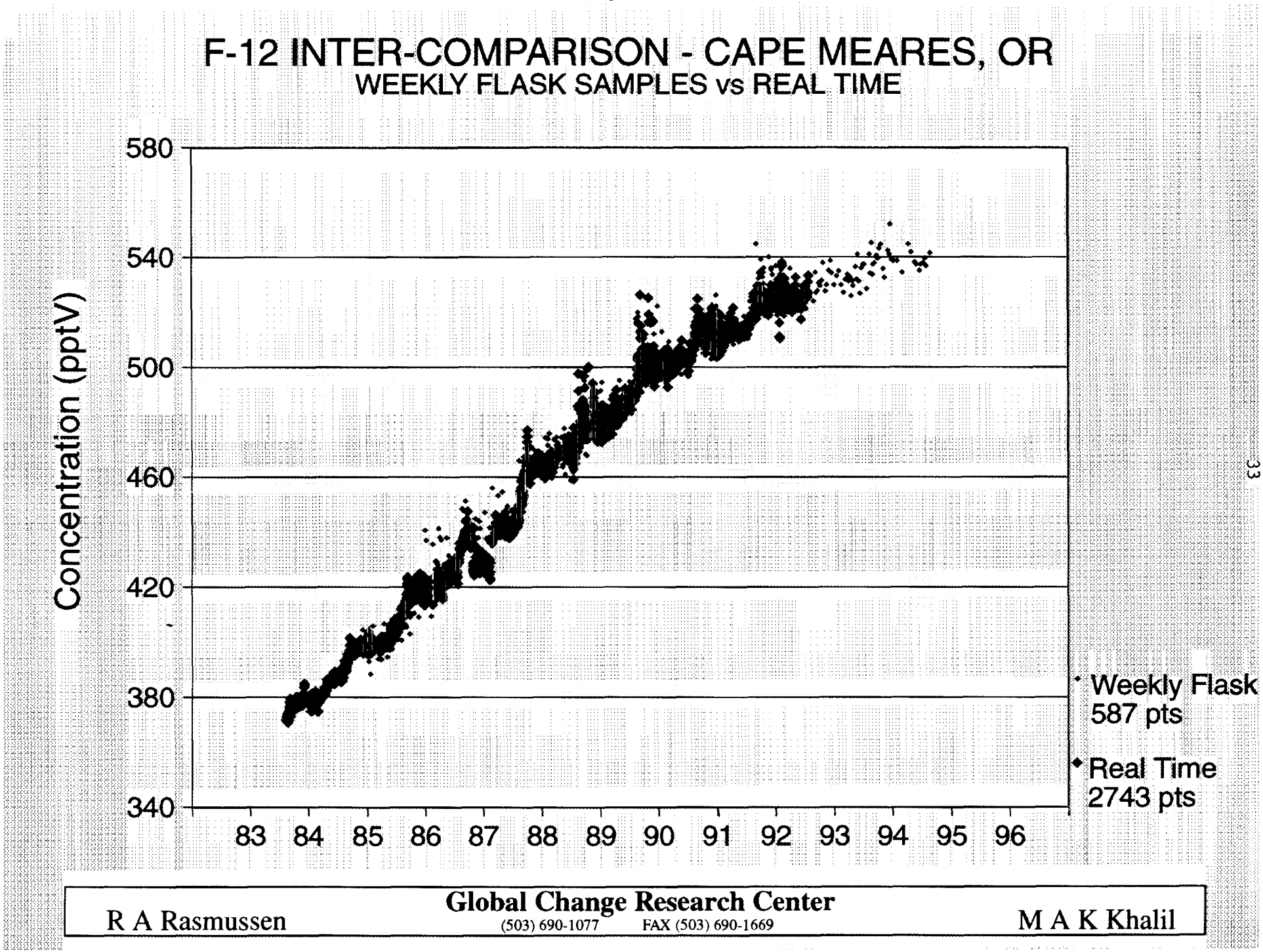
F-12 INTER-COMPARISON - CAPE MEARES, OR
WEEKLY FLASK SAMPLES vs REAL TIME
Concentration (pptV)
580
540
500
460
420
380
340
83
84
85
86
87
88
89
90
91
92
93
94
95
96
Weekly Flask
587 pts
Real Time
2743 pts
Global Change Research Center
R A Rasmussen
(503) 690-1077 FAX (503) 690-1669
M A K Khalil

Figure 5

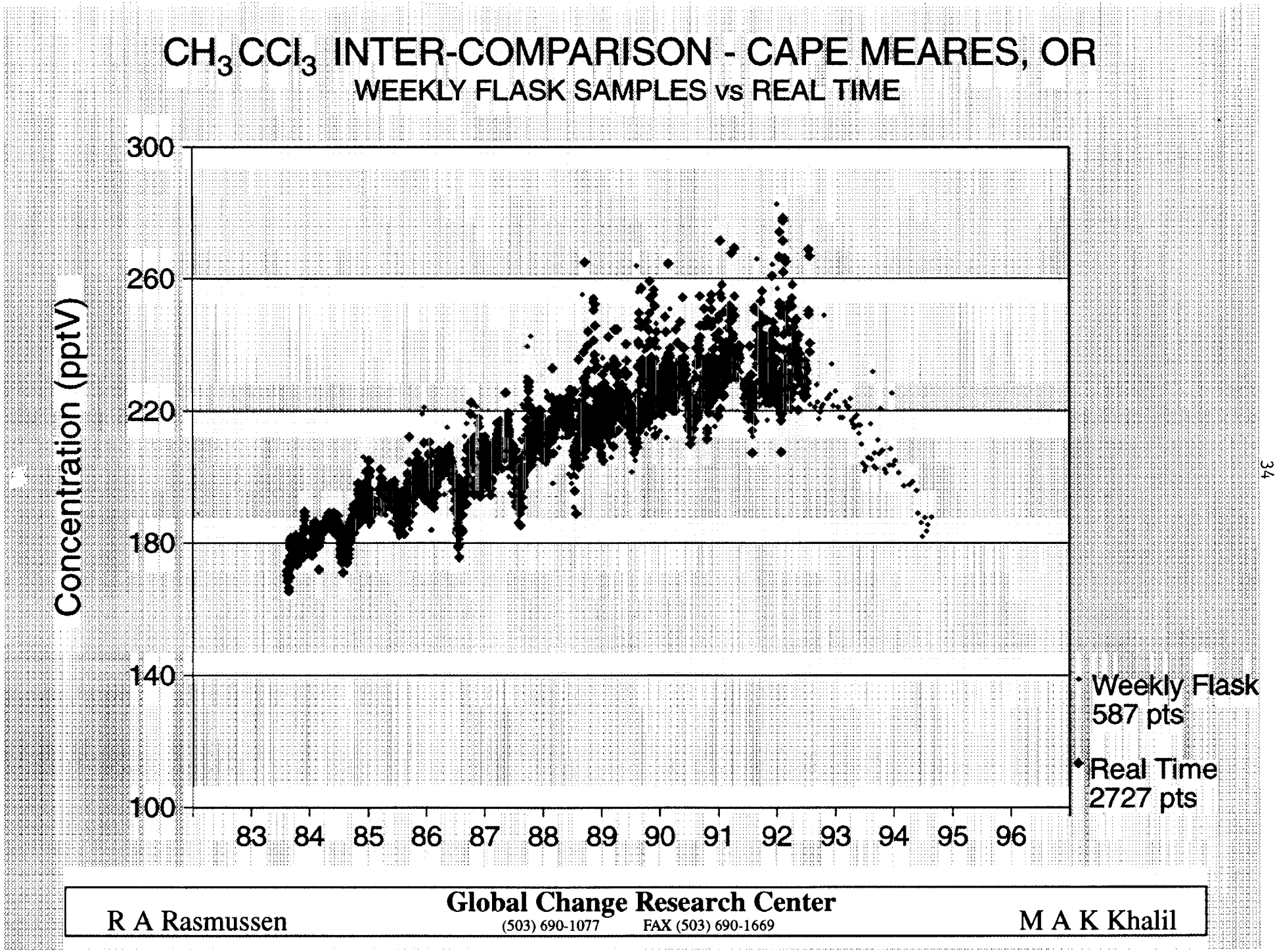
CH3CCl3 INTER-COMPARISON - CAPE MEARES, OR
WEEKLY FLASK SAMPLES vs REAL TIME
Concentration (pptV)
300
260
220
180
140
100
83
84
85
86
87
88
89
90
91
92
93
94
95
96
Weekly Flask
587 pts
Real Time
2727 pts
Global Change Research Center
R A Rasmussen
(503) 690-1077 FAX (503) 690-1669
M A K Khalil

Figure 5

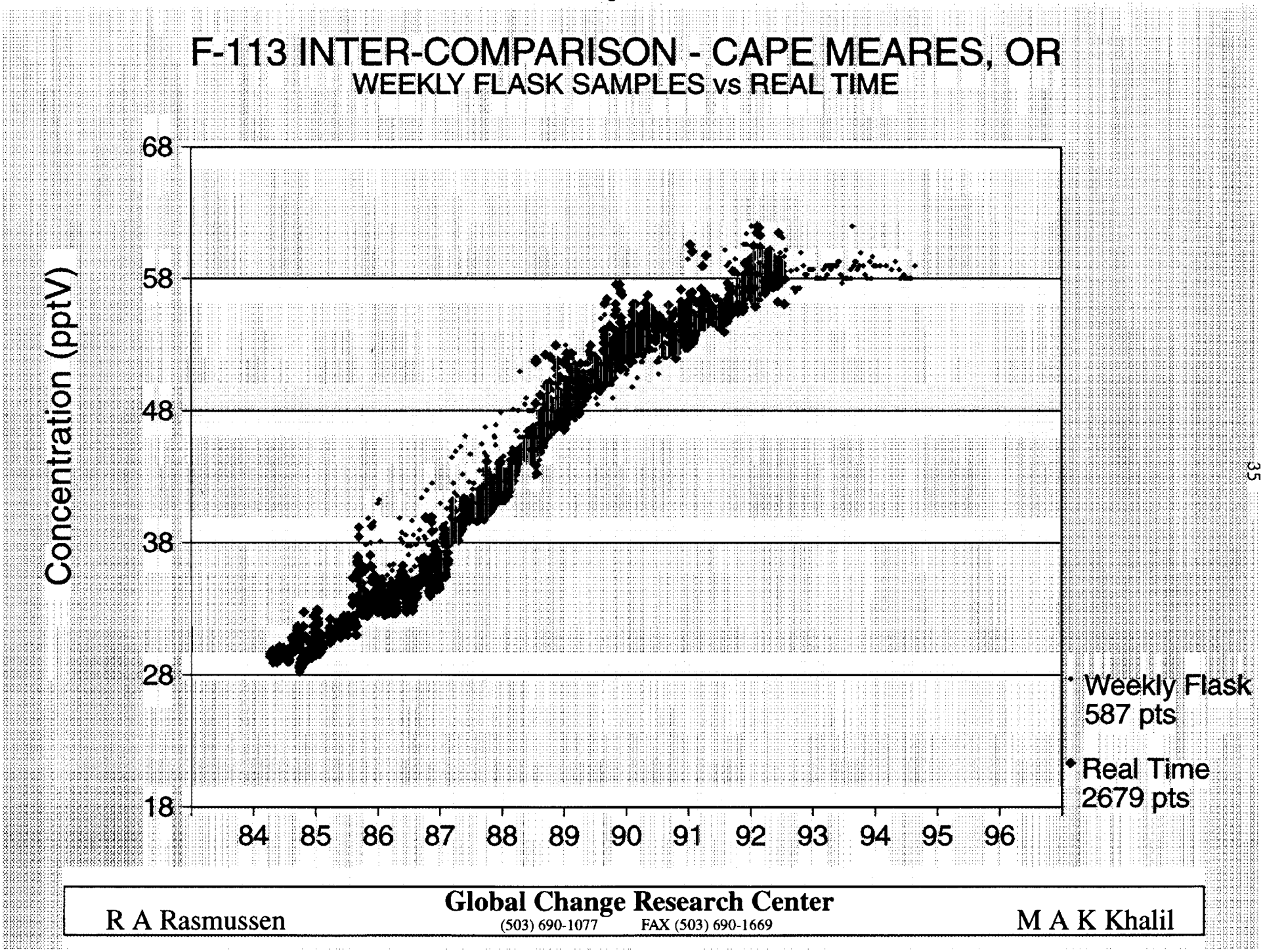
F-113 INTER-COMPARISON - CAPE MEARES, OR
WEEKLY FLASK SAMPLES vs REAL TIME
Concentration (pptV)
68
58
48
38
28
18
84
85
86
87
88
89
90
91
92
93
94
95
96
Weekly Flask
587 pts
Real Time
2679 pts
Global Change Research Center
R A Rasmussen
(503) 690-1077 FAX (503) 690-1669
M A K Khalil

Figure 5

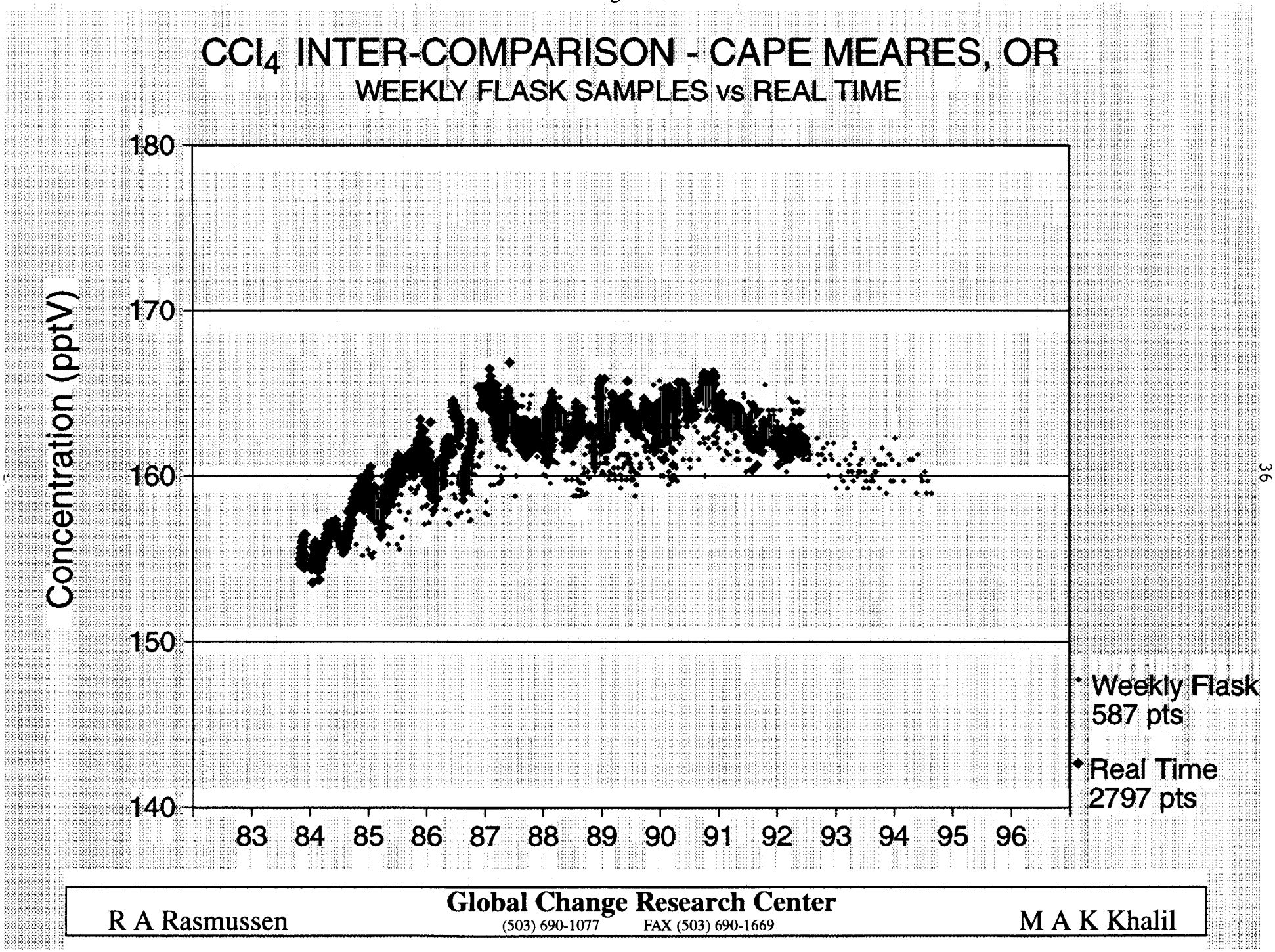
CCl4 INTER-COMPARISON - CAPE MEARES, OR
WEEKLY FLASK SAMPLES vs REAL TIME
Concentration (pptV)
180
170
160
150
140
83
84
85
86
87
88
89
90
91
92
93
94
95
96
Weekly Flask
587 pts
Real Time
2797 pts
Global Change Research Center
R A Rasmussen
(503) 690-1077 FAX (503) 690-1669
M A K Khalil

Figure 5

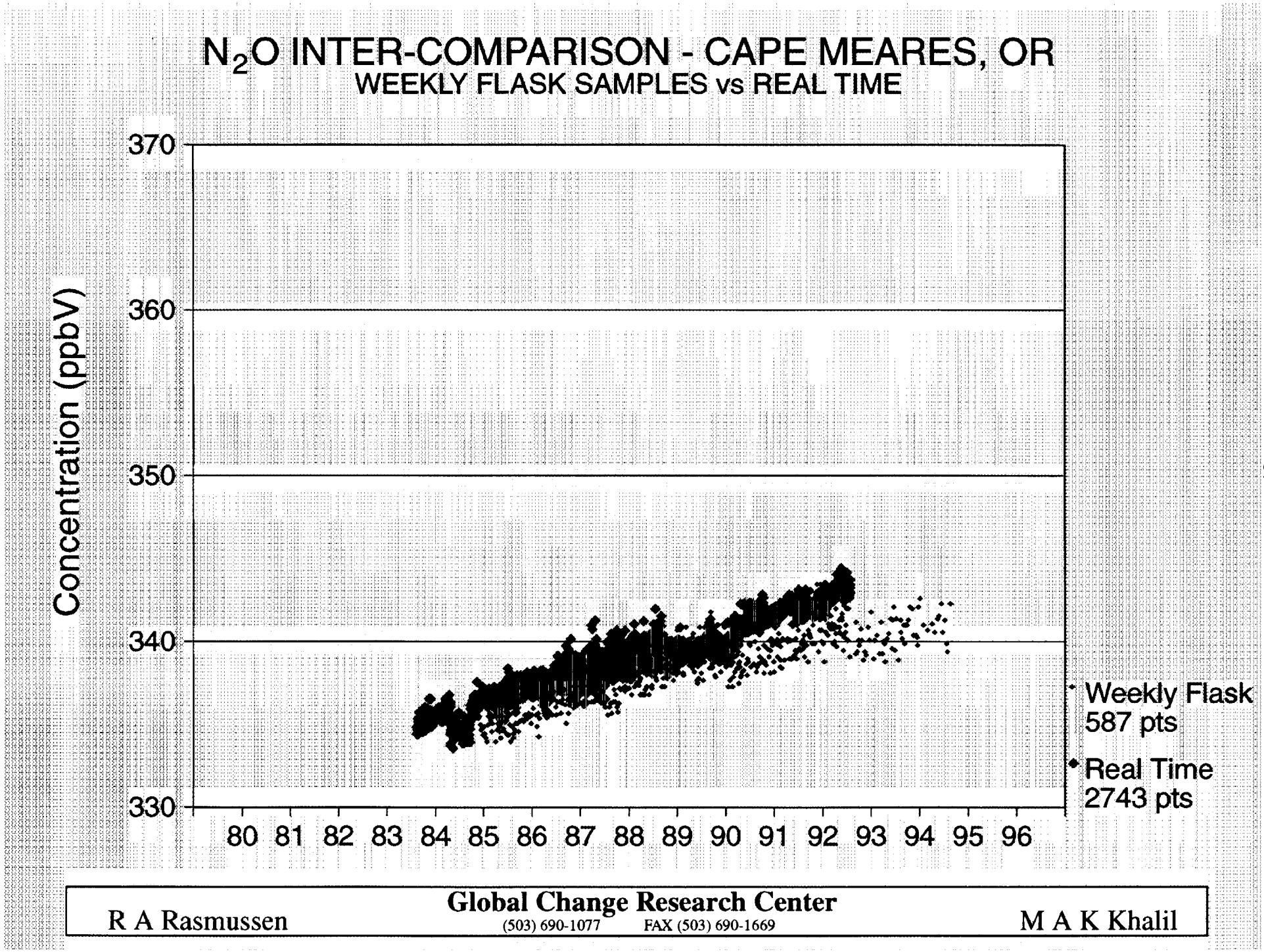
N_2O INTER-COMPARISON - CAPE MEARES, OR
WEEKLY FLASK SAMPLES vs REAL TIME
Concentration (ppbV)
370
360
350
340
330
80 81 82 83 84 85 86 87 88 89 90 91 92 93 94 95 96
Weekly Flask
587 pts
Real Time
2743 pts
Global Change Research Center
R A Rasmussen
(503) 690-1077 FAX (503) 690-1669
M A K Khalil

Figure 5

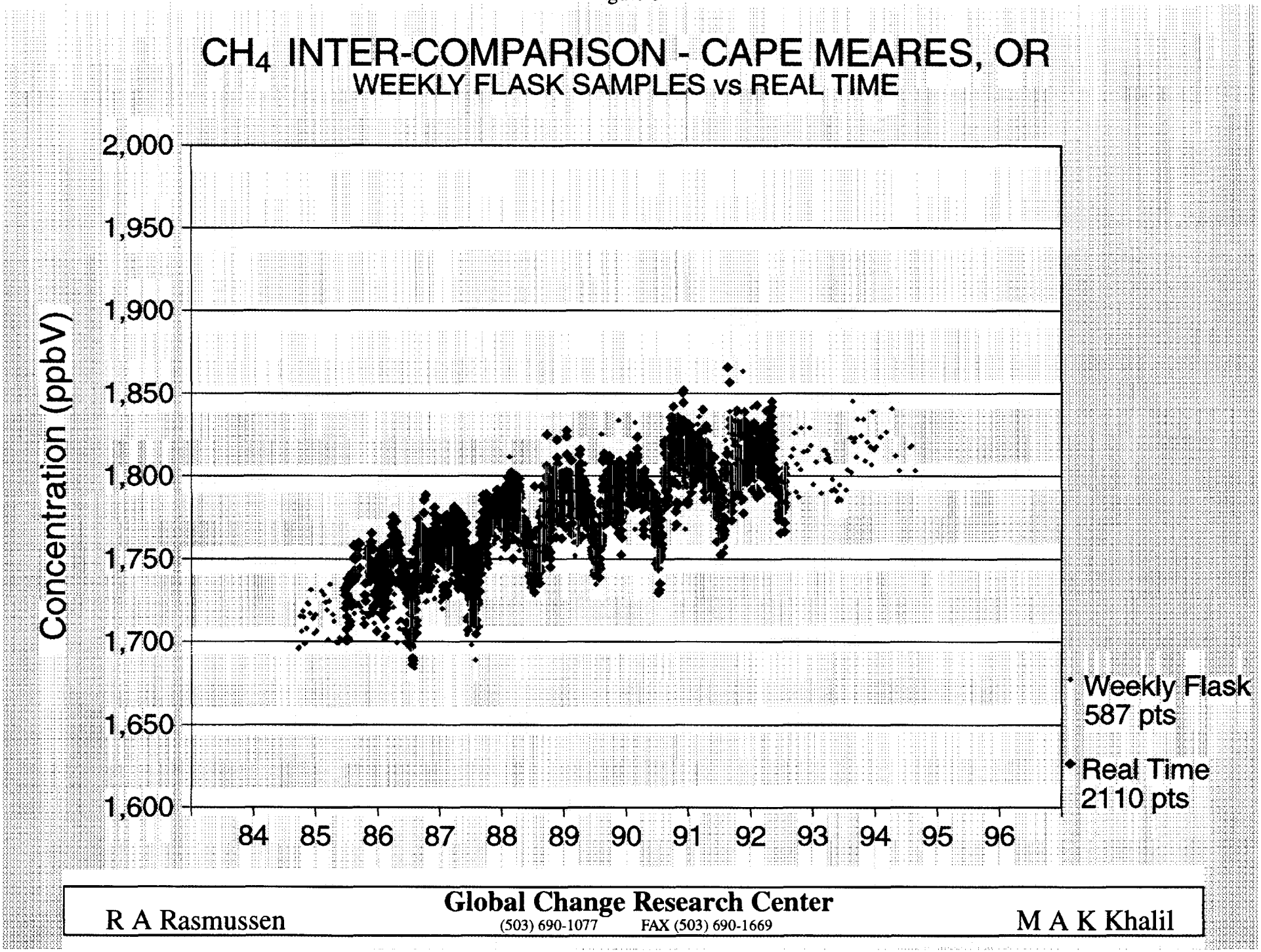
CH4 INTER-COMPARISON - CAPE MEARES, OR
WEEKLY FLASK SAMPLES vs REAL TIME
Concentration (ppbV)
2,000
1,950
1,900
1,850
1,800
1,750
1,700
1,650
1,600
84
85
86
87
88
89
90
91
92
93
94
95
96
Weekly Flask
587 pts
Real Time
2110 pts
Global Change Research Center
R A Rasmussen
(503) 690-1077 FAX (503) 690-1669
M A K Khalil

Figure 6

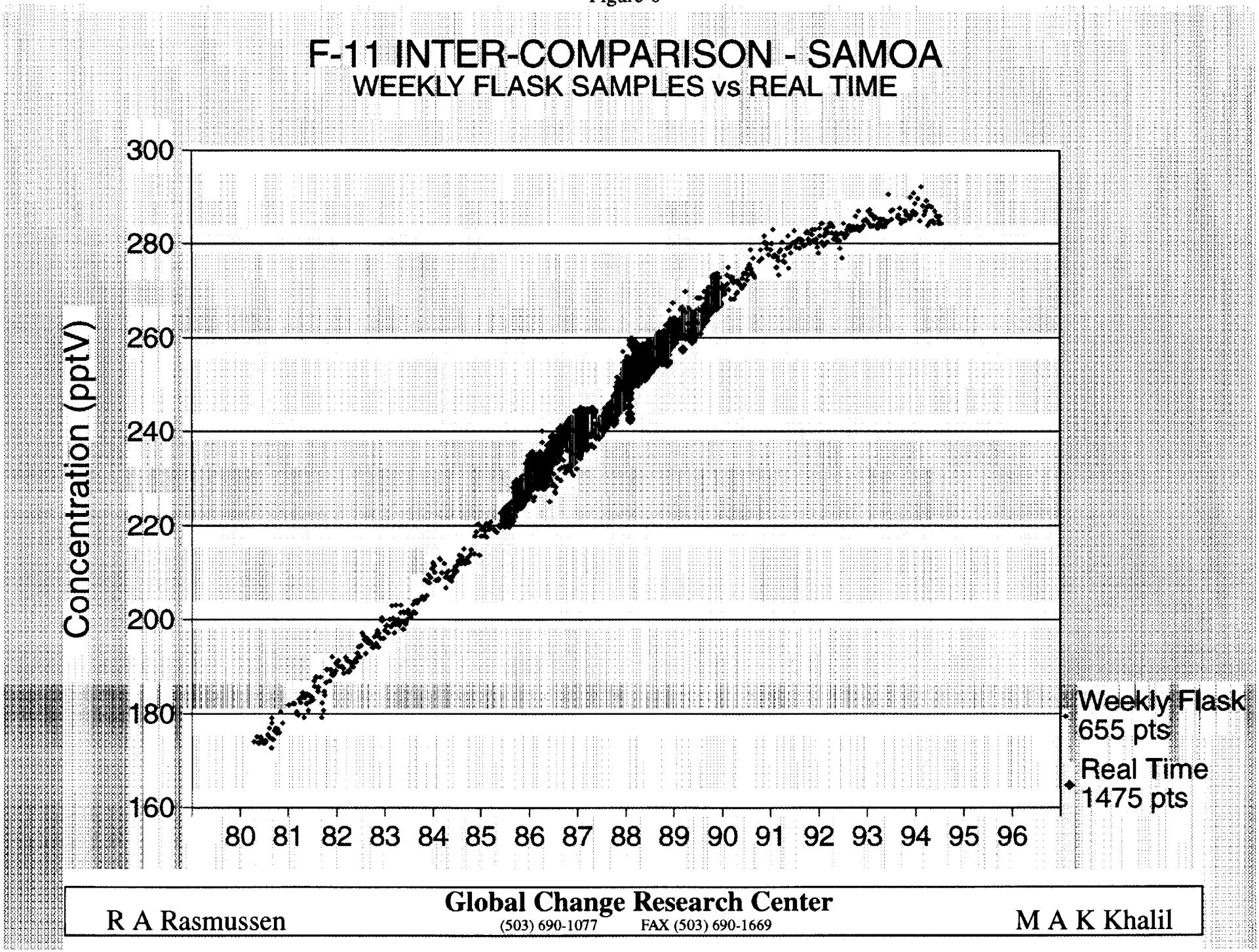
F-11 INTER-COMPARISON - SAMOA
WEEKLY FLASK SAMPLES vs REAL TIME
Concentration (pptV)
300
280
260
240
220
200
180
160
80 81 82 83 84 85 86 87 88 89 90 91 92 93 94 95 96
Weekly Flask
655 pts
Real Time
1475 pts
Global Change Research Center
R A Rasmussen
(503) 690-1077 FAX (503) 690-1669
M A K Khalil

Figure 6

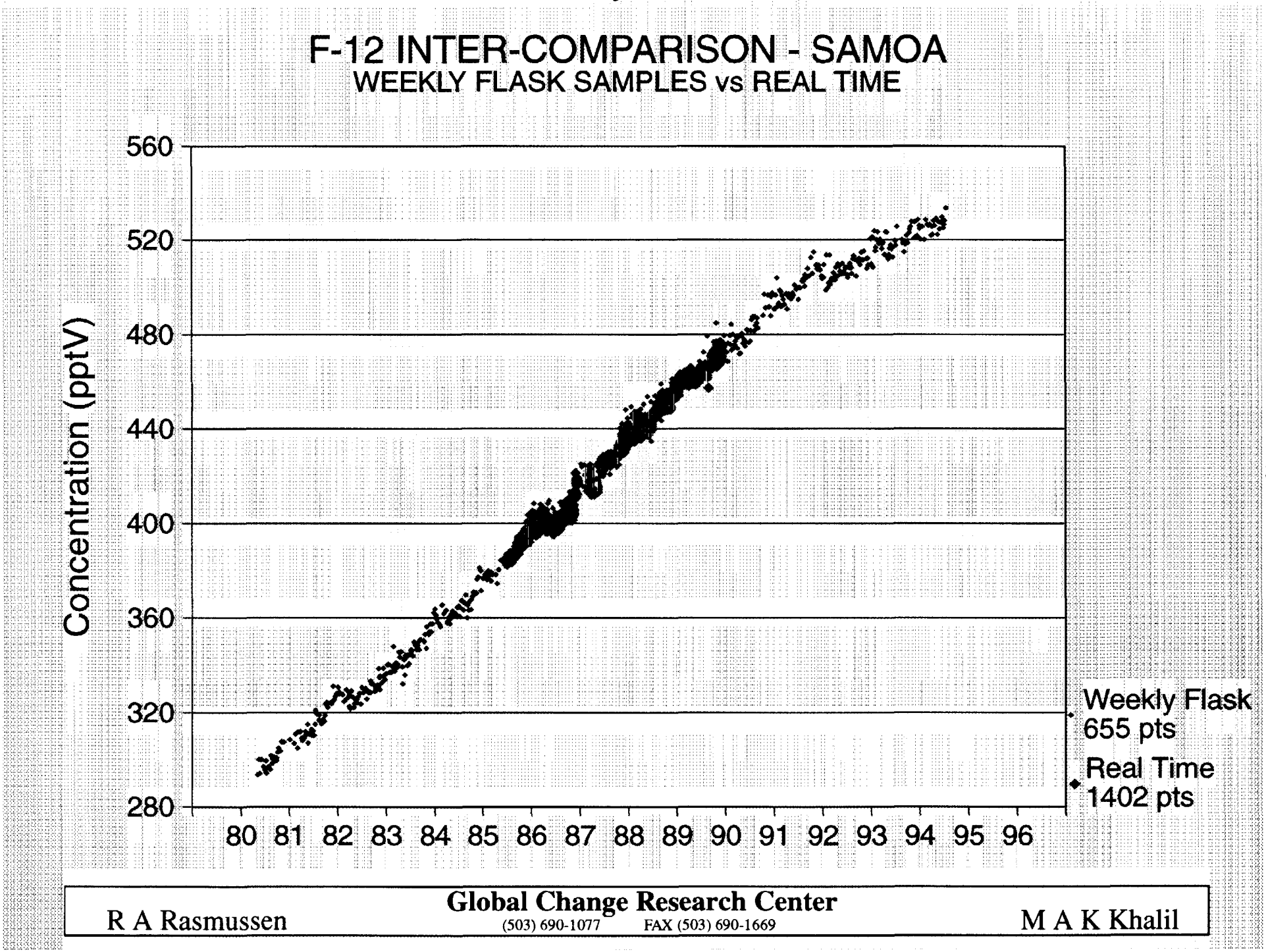
F-12 INTER-COMPARISON - SAMOA
WEEKLY FLASK SAMPLES vs REAL TIME
Concentration (pptV)
560
520
480
440
400
360
320
280
80 81 82 83 84 85 86 87 88 89 90 91 92 93 94 95 96
Weekly Flask
655 pts
Real Time
1402 pts
Global Change Research Center
R A Rasmussen
(503) 690-1077 FAX (503) 690-1669
M A K Khalil

Figure 6

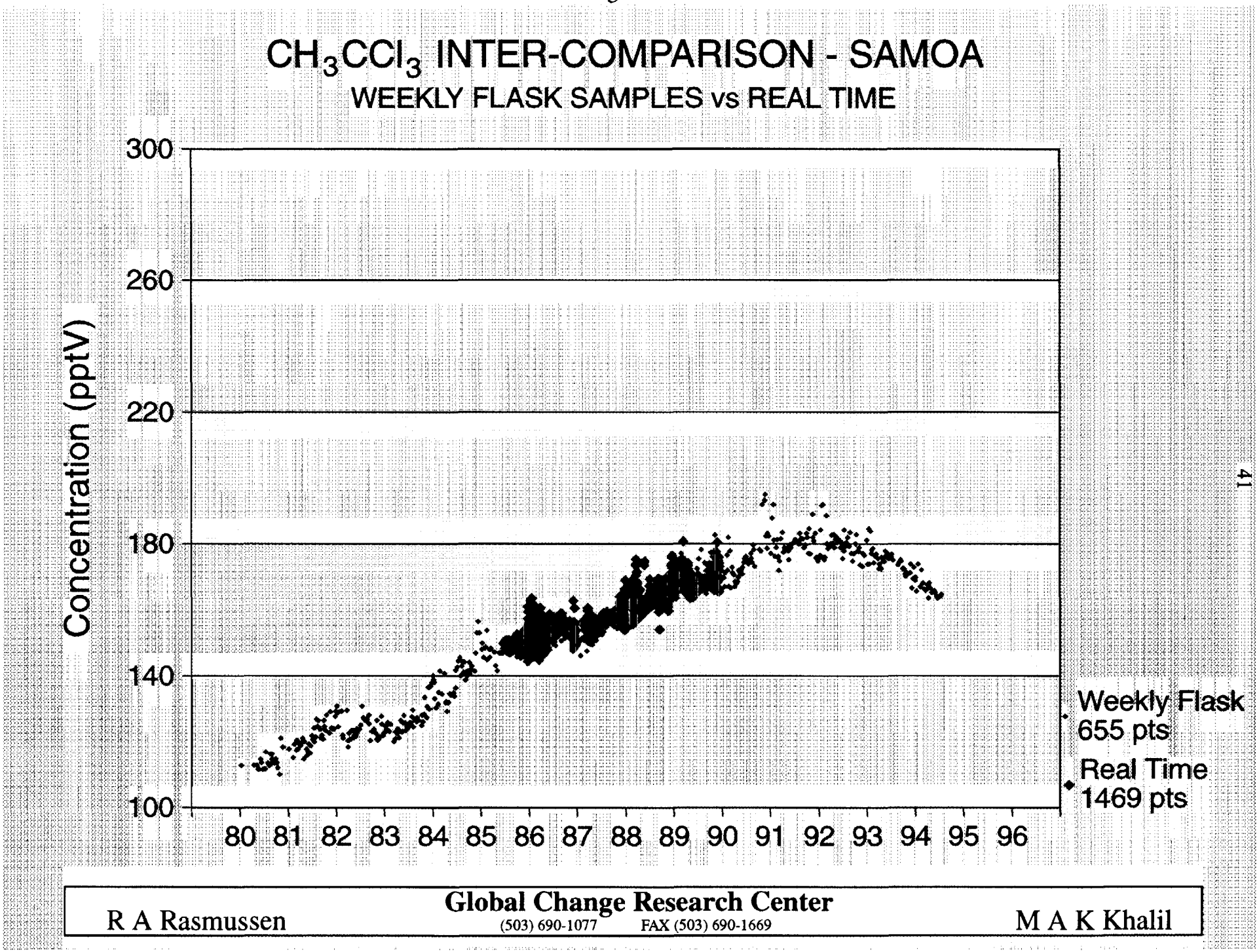
CH3CCl3 INTER-COMPARISON - SAMOA
WEEKLY FLASK SAMPLES vs REAL TIME
Concentration (pptV)
300
260
220
180
140
100
80 81 82 83 84 85 86 87 88 89 90 91 92 93 94 95 96
Weekly Flask
655 pts
Real Time
1469 pts
Global Change Research Center
R A Rasmussen
(503) 690-1077 FAX (503) 690-1669
M A K Khalil

Figure 6

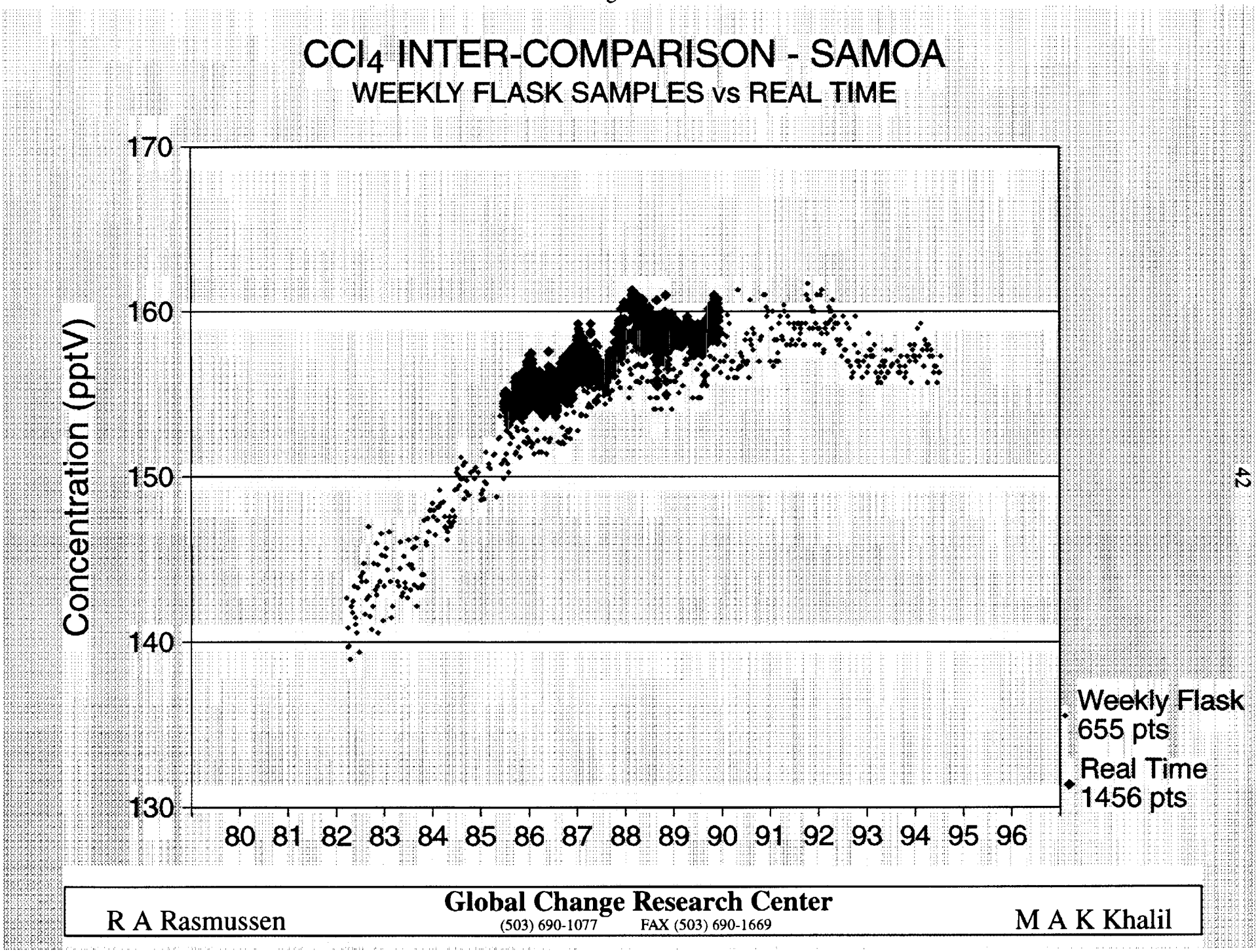
CCl_4 INTER-COMPARISON - SAMOA
WEEKLY FLASK SAMPLES vs REAL TIME
Concentration (pptV)
170
160
150
140
130
80 81 82 83 84 85 86 87 88 89 90 91 92 93 94 95 96
Weekly Flask
655 pts
Real Time
1456 pts
42
Global Change Research Center
R A Rasmussen
(503) 690-1077 FAX (503) 690-1669
M A K Khalil

Figure 6

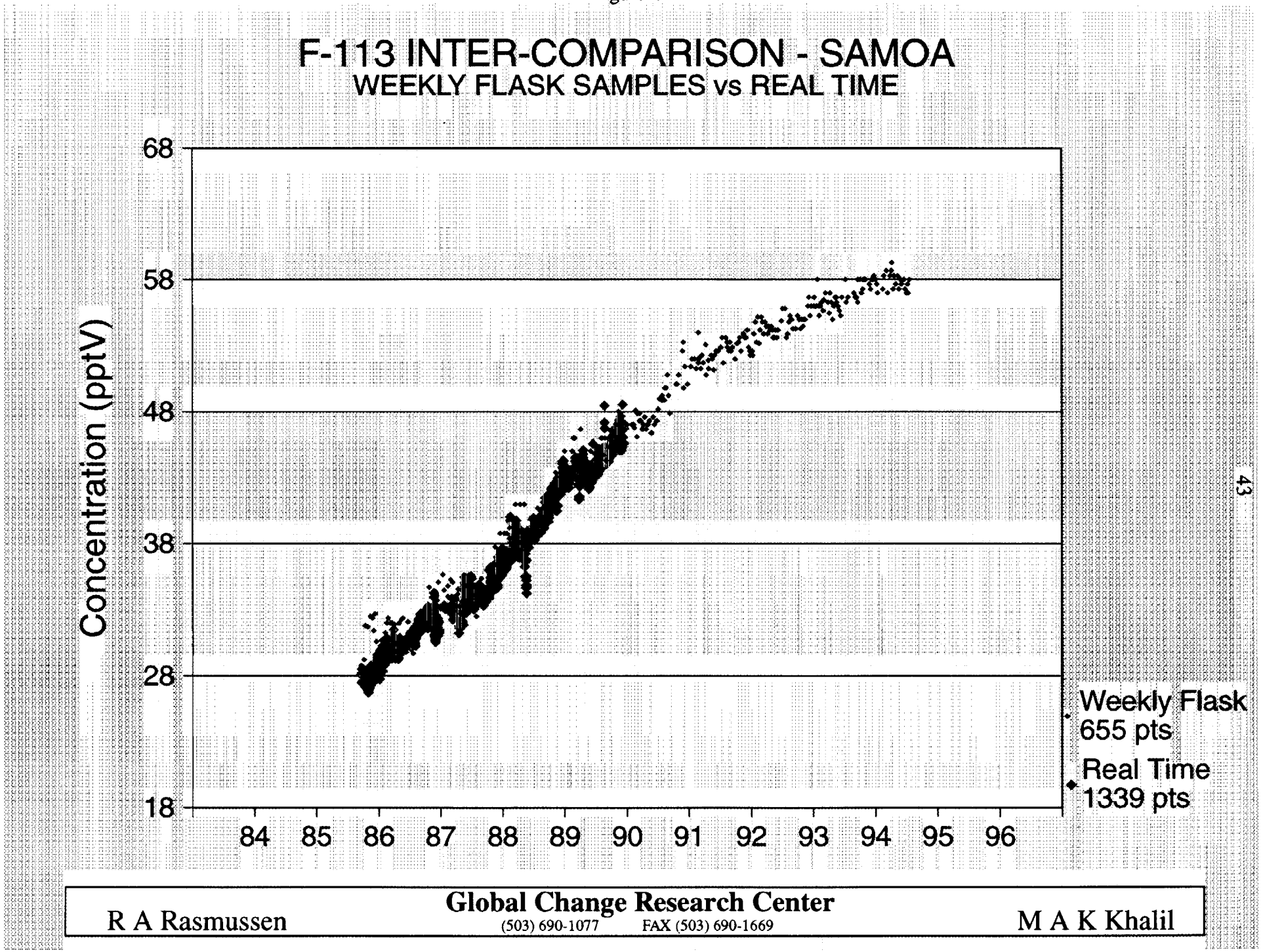
F-113 INTER-COMPARISON - SAMOA
WEEKLY FLASK SAMPLES vs REAL TIME
Concentration (pptV)
68
58
48
38
28
18
84
85
86
87
88
89
90
91
92
93
94
95
96
Weekly Flask
655 pts
Real Time
1339 pts
43
Global Change Research Center
R A Rasmussen
(503) 690-1077 FAX (503) 690-1669
M A K Khalil

Figure 6

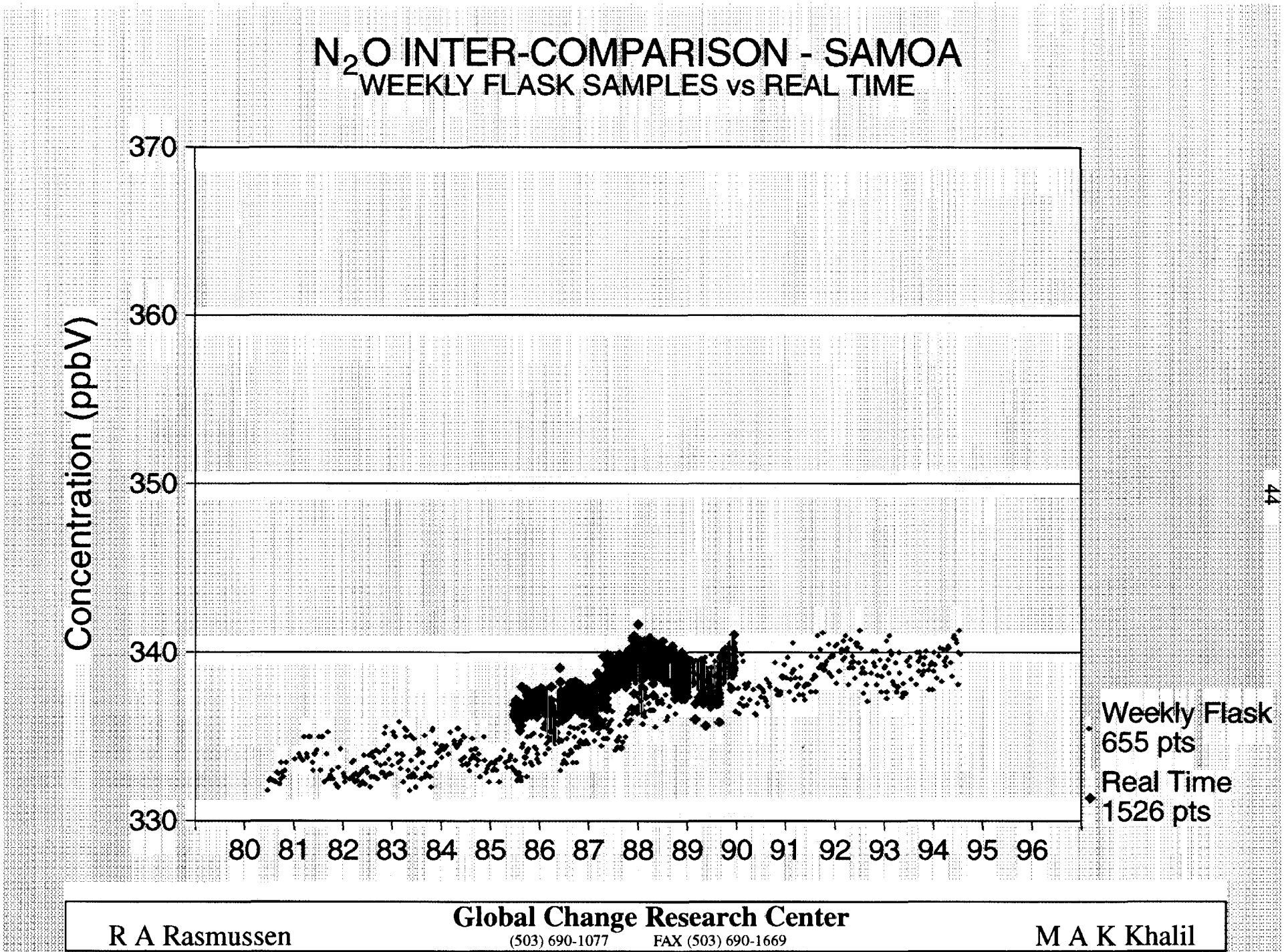
N2O INTER-COMPARISON - SAMOA
WEEKLY FLASK SAMPLES vs REAL TIME
Concentration (ppbV)
370
360
350
340
330
80 81 82 83 84 85 86 87 88 89 90 91 92 93 94 95 96
Weekly Flask
655 pts
Real Time
1526 pts
Global Change Research Center
R A Rasmussen
(503) 690-1077 FAX (503) 690-1669
M A K Khalil

Figure 6

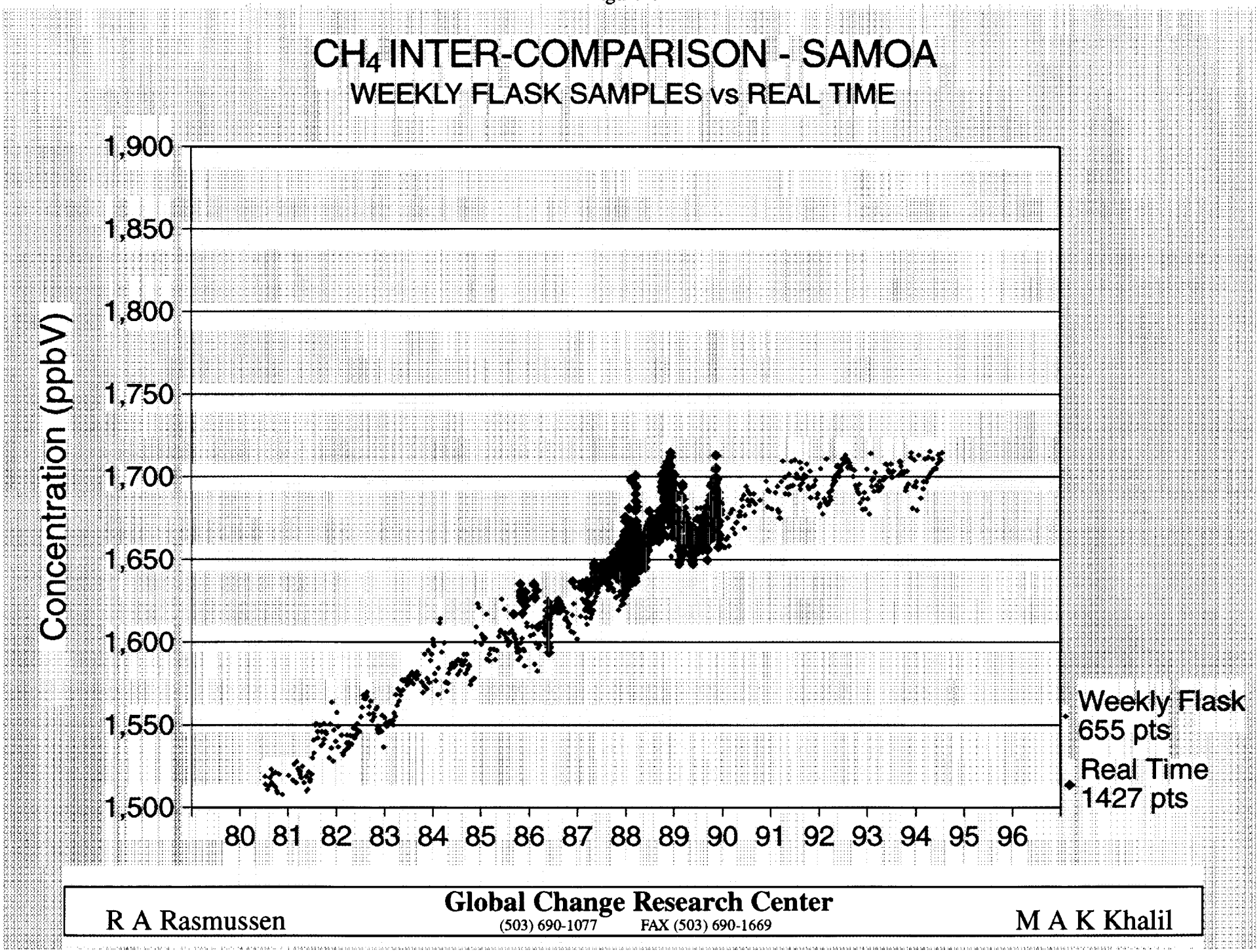
CH4 INTER-COMPARISON - SAMOA
WEEKLY FLASK SAMPLES vs REAL TIME
Concentration (ppbV)
1,900
1,850
1,800
1,750
1,700
1,650
1,600
1,550
1,500
80 81 82 83 84 85 86 87 88 89 90 91 92 93 94 95 96
Weekly Flask
655 pts
Real Time
1427 pts
Global Change Research Center
R A Rasmussen
(503) 690-1077 FAX (503) 690-1669
M A K Khalil

V. The Atmospheric Lifetimes and Results on Global Average OH.

V.1 Lifetimes by the Trend and Mass Balance Methods

The atmospheric lifetimes are obtained by using the ALE/GAGE nine-box model described earlier in Eqn. 5. In the published papers, Kalman Filtering techniques were used to obtain the optimal lifetime consistent with the measured concentrations at all four ALE/GAGE sites. These methods are described in detail in the papers by Cunnold et al. (1983) in Appendix V. The results of these calculations are summarized in Table 4 at the end of this section.

To gain a deeper insight into the nature of the lifetime calculations, we performed additional calculations (see Khalil, 1994). A simpler model was used, consisting of four latitudinal regions (the semi-hemispheres) that is very closely tied to the data with measurements in each cell. This model can be derived from the ALE/GAGE model. In this model we defined the variance between measured and calculated values as a weighted average over all four sites:

We then used a computer program to search for the value of the lifetime that would lead to the minimum variance of either the concentration (global mass balance) or the trend (trend method). That is to say, the best fit between theory and experiment for the trend or the concentration. The main findings of these calculations, relevant to this report, are shown in Figures 7a and b, and are summarized as follows:

1) If the trend method is used, the minimum of the variance is not well defined. The value of the variance decreases slowly as the lifetime is changed towards the optimal value. But the variance changes extremely slowly as the lifetime is increased beyond the minimum. This means that while the method may provide an estimate of the lifetime, and it may provide a reasonable lower limit, it cannot provide a reasonable upper limit. While these limits can be improved by longer time of measurements, the time it would take to reduce the uncertainty of the upper limit of the lifetime is extremely long, and therefore is not practical.

2) The overburden method, on the other hand, establishes a well defined lifetime with relatively narrow uncertaines based on the variability of the data. It is, however, sensitive to to absolute calibration that, if in error, would cause an systematic error in the optimal lifetime and in the uncertainties associated with the calculated lifetime.

3) The uncertainty of the estimated lifetime is dependent on the lifetime itself. For shorter-lived gases such as methylchloroform, the trend method can establish narrow limits of uncertainty, but for longer-lived gases the uncertainties are too large to estimate.

The main implication of this result for the OGI ALE/GAGE project is that the trend method is not likely to produce a narrowing of uncertainties in the lifetimes for a long time to come. In fact, it may well be that if we continue to rely on the trend method, the estimated lifetime will continue to have very large uncertainties, no matter how precise the atmospheric measurements and how long the measurements are taken. The longer the measurements are taken the less the uncertainty in the estimated lifetime; however, this reduction in the uncertainty is very slow for the trend method and other limits to maintaining the accuracy and precision of the calibration standards may increase the uncertainties in the estimated lifetime during the same time (for additional details see Khalil, 1994).

V.2 Estimating Global OH.

Hydroxyl radicals (OH) are a highly reactive gaseous species in the atmosphere. Many man-made and natural gases are removed from the atmosphere primarily by reacting with OH. Yet because of its low concentrations and high reactivity, it is extremely difficult to directly measure OH in the atmosphere. The measured concentrations of methylchloroform have been used for a long time to estimate the effective globally averaged concentrations of OH. The idea is that if we know the emissions of methylchloroform and its concentrations and trends, then the only unknown in Eqn. 1 is the lifetime, which can be estimated from this equation. Assuming that the only process for removing methylchloroform from the atmosphere is the reaction with OH, we can write:

$$[OH] \sim \frac{1}{(K_{eff}\,\tau)} \qquad (10)$$

where K_{eff} is the effective rate constant for the reaction of OH with methylchloroform, which is measured in laboratory experiments, and τ is the atmospheric lifetime determined as just described by using Eqn. 1, Eqn. 4, or similar more refined equations such as Eqn. 5.

The ALE/GAGE measurements of methylchloroform have been instrumental in determining the average OH concentrations to a greater accuracy than was possible before. The average OH turns out to be about 8×10^5 molecules/cm^3. These results are also reported in the papers in Appendix V.

Section V. Atmospheric Lifetimes and Results on Global Average OH

Figure 7. The variances as a function of atmospheric lifetime. The variance is the sum of the squared differences between measured and calculated concentrations (from Khalil, 1994).

Table 4. A summary of the lifetimes of halocarbons and other gases estimated from the GAGE measurements.

Figure 7

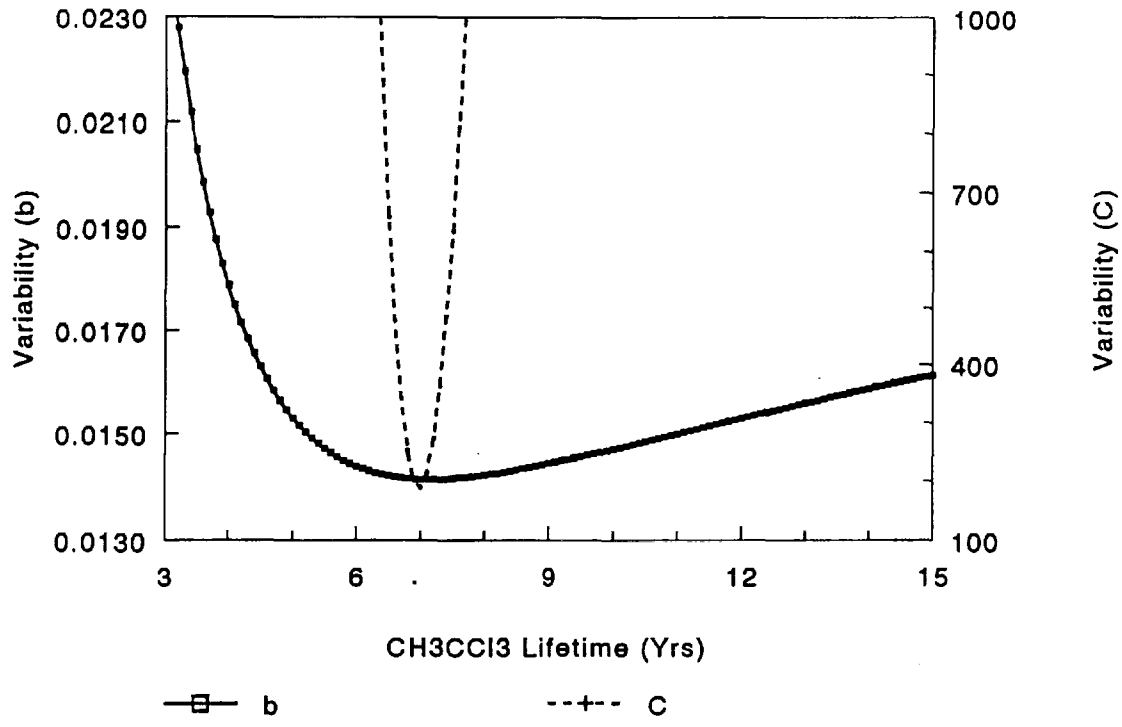
0.0230
0.0210
0.0190
0.0170
0.0150
0.0130
Variability (b)
1000
700
400
100
Variability (C)
3
6
9
12
15
CH3CCl3 Lifetime (Yrs)
b
C

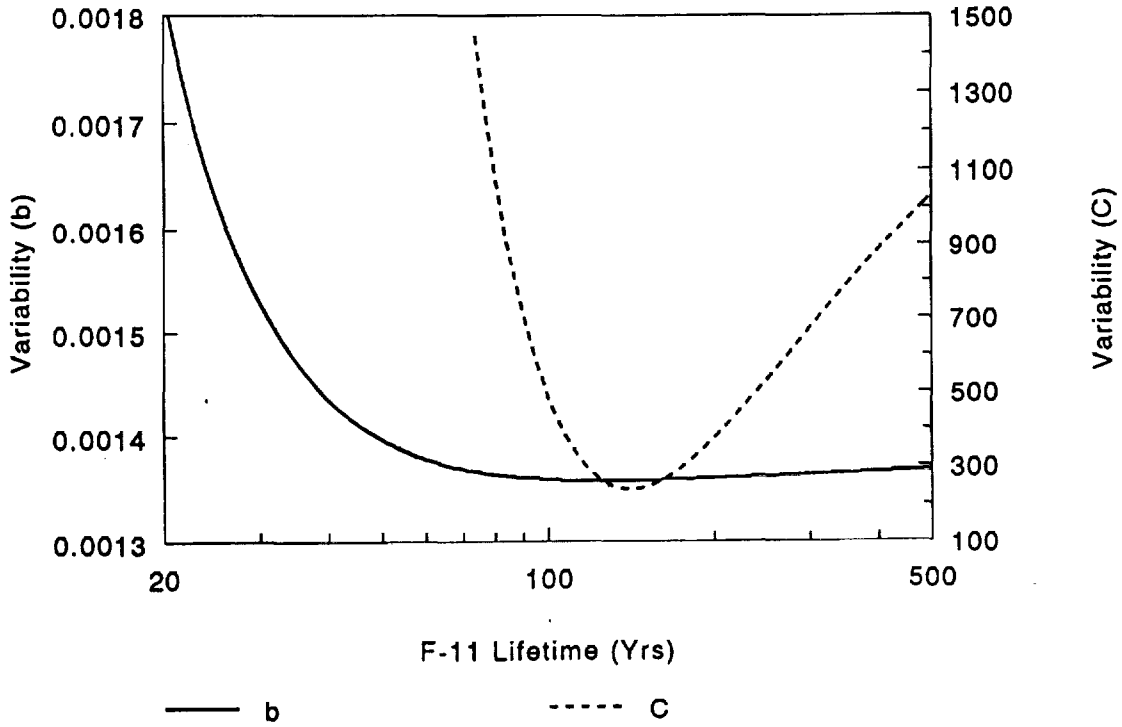
0.0018
0.0017
0.0016
0.0015
0.0014
0.0013
Variability (b)
1500
1300
1100
900
700
500
300
100
Variability (C)
20
100
500
F-11 Lifetime (Yrs)
b
C

Table 4. Estimates of trace gas lifetimes made throughout the ALE/GAGE program.

Trace Gas	Lifetime years (*)	Calculation Technique†	Reference
$CFCl_3$	83 (-27, +73) 70 (-25, +89)	Trend Inventory	Cunnold et al. (1983a)
CF_2Cl_2	769 (-688, +∞) 69 (-18, +36)	Trend Inventory	Cunnold et al. (1983b)
CH_3CCl_3	10.5 (-2.8, +6.2) 9.8 (-2.3, +4.5)	Trend Inventory‡	Prinn et al. (1983)
CCl_4	50 (-8, +12) 57 (-28, +∞)	Trend Inventory	Simmonds et al. (1983)
$CFCl_3$	74 (-17, +31) 68 ± ?	Trend Inventory	Cunnold et al. (1986)
CF_2Cl_2	111 (-44, +222) 69 ± ?	Trend Inventory	
CH_3CCl3	6.9 (-0.9, +1.2) 6.0 (-0.8, +1.1) 6.0 (-1.0, +1.4)	Trend Inventory Gradient	Prinn et al. (1987)
N_2O	185 ± 7 to 137 ± 4 179 to 164 (± 16)	Trend Inventory	Prinn et al. (1990)
CH_3CCl3	4.8 (-0.7, +0.5) 6.1 (-1.0, +1.4) 6.0 ± 0.4	Trend Inventory‡ Gradient	Prinn et al. (1992)
$CFCl_3$	55 (-11, +17) 44 (-10, +21)	Trend Inventory	Cunnold et al. (1994)§
CF_2Cl_2	256 (-107, +653) 161 (-72, +672)	Trend Inventory	

* 1σ confidence limit

† "Trend" method: the lifetime is estimated using an optimal allocation scheme based on the trends at the measurement sites; "Inventory" method: the lifetime is estimated by making a total inventory of the trace gas in the atmosphere, and its destruction rates; (see Cunnold et al., 1983a, for original discussion of these two techniques) "Gradient" method: the lifetime is estimated by comparing observed and model generated interhemispheric gradients (see Prinn et al., 1986).

‡ Called "content" method in this paper.

§ With new calibration scale SIO 1993 (co-author R.F. Weiss)

VI. An Analysis of the High Frequency Measurements Compared to Flask Samples

An alternative to the in situ automated measurements is to obtain samples of air in stainless steel (or glass) flasks and analyze them in the laboratory. The advantages of the flask sampling program are: 1) significantly lower cost, 2) the ability to measure many more gases simultaneously and therefore address new and emerging issues in global change science, and 3) the ability to maintain a stringent control on the stability of the absolute calibration and hence the quality of the data.

There are two ways of looking at the information that the ALE/GAGE type of measurements provide relative to the flask sampling programs. The first is to compare the trends and concentrations from the flask samples that are taken at the same sites as the "real time" automated instruments, and the second is to simulate what the data would be like for various types of flask sampling strategies. This simulation is done by selecting small subsets of data from the full ALE/GAGE data sets. Such an analysis has been done in detail by Khalil (1994) and is briefly summarized here as it relates to this project.

First we have shown the results of the flask samples collected at the same sites where the ALE/GAGE measurements were taken (see Figures 5 and 6 in Section IV). The agreement between the two types of data is extremely good for most gases and times. There are occasional differences that are being analyzed. For CCl_4 and N_2O there seem to be some systematic differences between the flask samples and the ALE/GAGE real time data. We believe that the flask samples are correct and may require a readjustment of the "real time" data. This establishes a high degree of confidence in the quality of the ALE/GAGE data set. As mentioned earlier, the flask sampling provides a "Quality Assurance" for the ALE/GAGE data sets. The flask samples are measured on laboratory instruments, not the ones that take the automated measurements and are calibrated against primary laboratory standards instead of the secondary standards that are used in the field.

The second set of figures (Figure 8) is based on the simulated flask sampling analysis based on the ALE/GAGE 5-year data set that has been released to the scientific community. The project investigated the effect of reducing the sampling frequency on the amount of information in the time series as it affects the estimates of trends and lifetimes. The results are reported in a series of graphs only for F-12 - but similar results were obtained for all the gases. The first graph (Figure 8a) shows the trends of F-12 as the number of data used was reduced from all to one set of 3 back to back measurements/year. The graph shows that sampling frequencies as low as once per month give nearly the same trends as the full data set. As expected, the uncertainty in the estimate of the trend increases as fewer and fewer data are used. The statistical theory is discussed in the full report. The nature of the trends and uncertainties is shown in Figure 6b for Cape Meares F-12 (similar results are obtained for other gases and sites).

The effects of reducing the sampling frequency on the estimated lifetime of F-12 is shown in Figures 9a and 9b. The first is for the trend method (represented by Eqn. 4) and the second is for the mass balance method (represented by Eqn. 1). The results show that there is very little difference in the lifetimes estimated by using all the data or reduced amounts of data, up to about one sample per two weeks. The uncertainties increase as less data are used. For sampling frequencies of less than one sample per 2 days, no upper limit for the lifetime could be calculated by the trend method. But the lower limit for the lifetime can be calculated for much reduced sampling frequencies. This reflects the nature of the trend method as previously shown in Figure 4.

The consequence of these results for the present project are that:

1) High frequency measurements such as in the ALE/GAGE program, no matter how precisely they are made, will not rapidly reduce the uncertainties in the lifetime because of the nature of the trend method for estimating lifetimes.

2) The length of the time series will also produce a slow reduction of uncertainties in the trend method. During the time it takes to reduce uncertainties, other factors may tend to increase the uncertainties.

Section VI. Analysis of High Frequency Measurements Compared to Flask Samples.

Figure 8. The effect of sampling frequency on the trends of F-12 (from Khalil, 1994).

Figure 9. The effect of sampling frequency on the estimated lifetimes of F-12 (from Khalil, 1994).

Figure 8

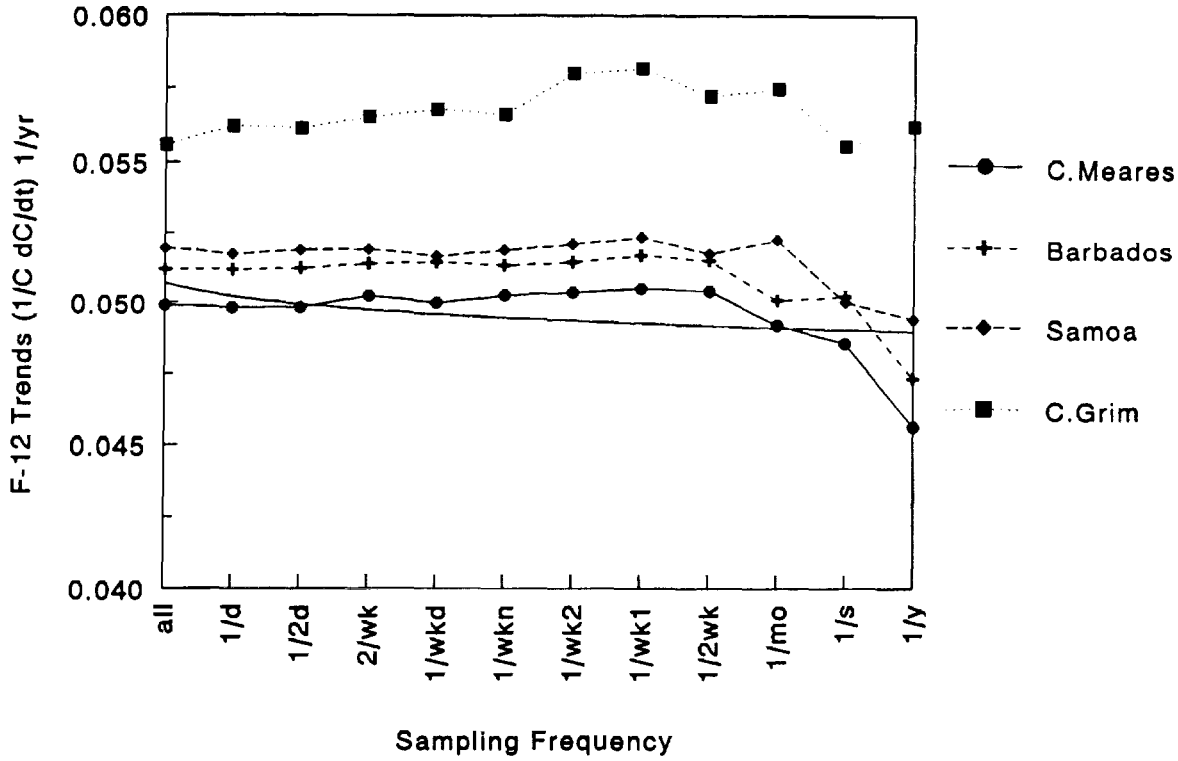
0.060
0.055
0.050
0.045
0.040
F-12 Trends (1/C dC/dt) 1/yr
all
1/d
1/2d
2/wk
1/wkd
1/wkn
1/wk2
1/wk1
1/2wk
1/mo
1/s
1/y
Sampling Frequency
C.Meares
Barbados
Samoa
C.Grim

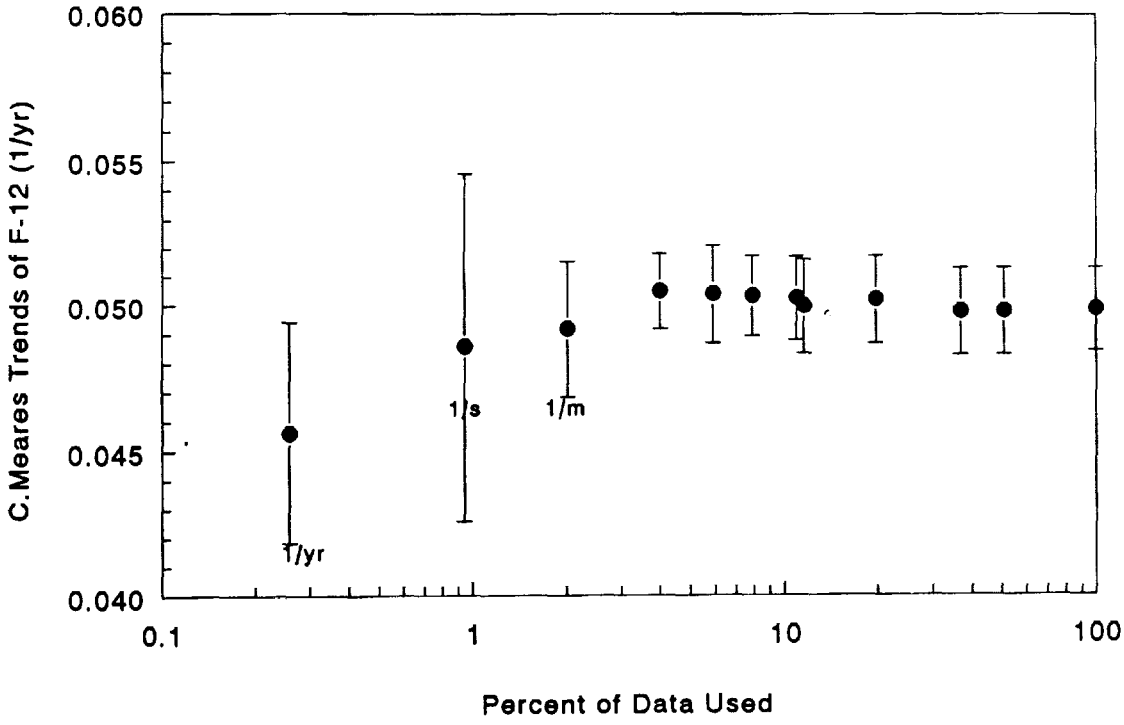
0.060
0.055
0.050
0.045
0.040
C.Meares Trends of F-12 (1/yr)
1/yr
1/s
1/m
0.1
1
10
100
Percent of Data Used

Fig 6

Fig 7

Figure 9

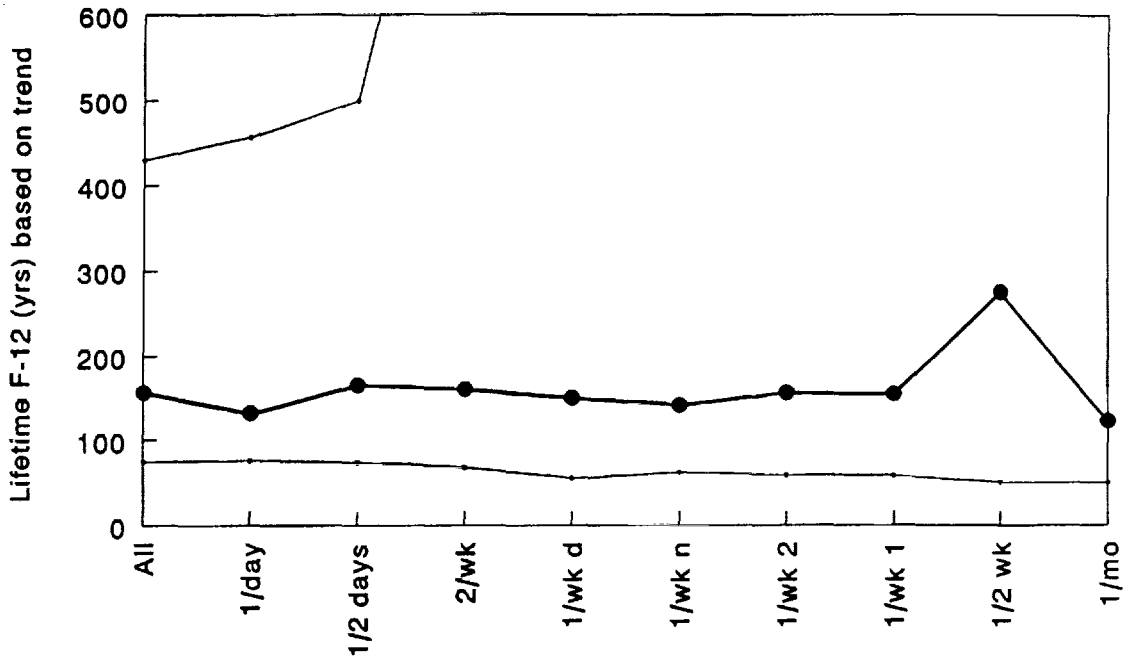

Fig 20d

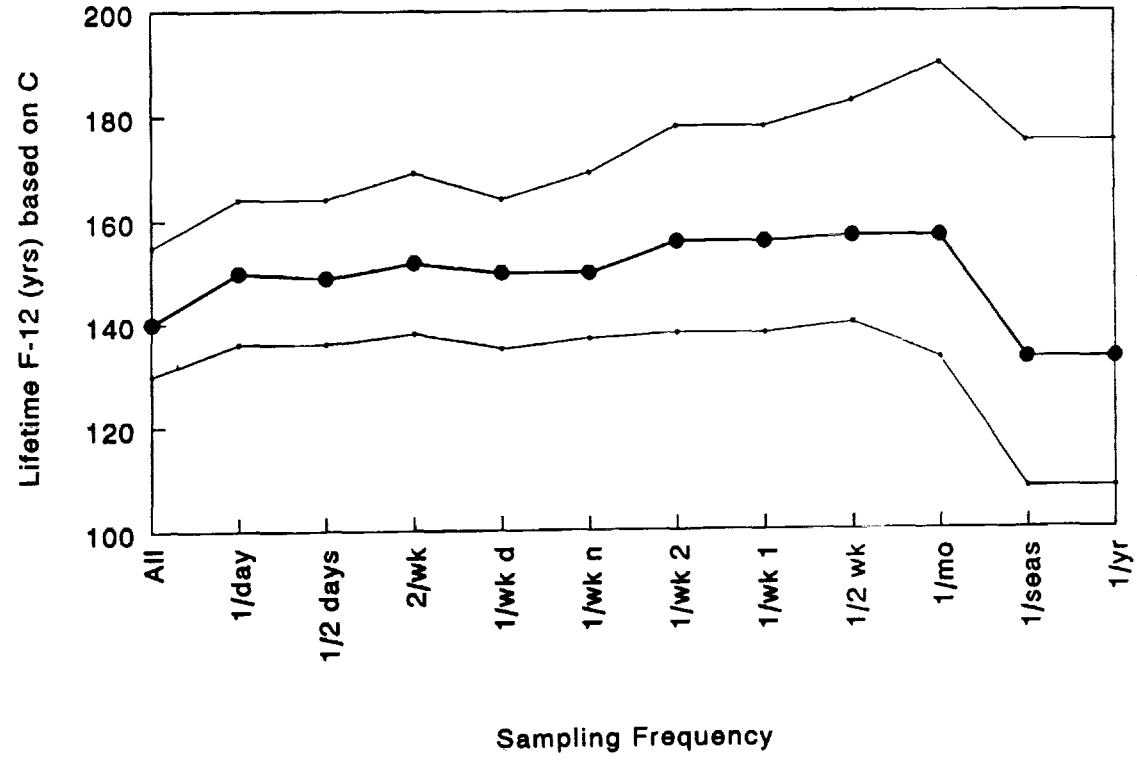

VII. Conclusions

In this final report we have provided a guide to the ALE/GAGE program and the role of the OGI group in the program. We have shown that our role has produced the following results:

1) A high quality, high frequency data base on the time series of CCl_3F, CCl_2F_2, CH_3CCl_3, CCl_4, and N_2O. These gases play important roles in the global environment (see summary and references). Although our specific responsibility was to maintain two of four stations (Cape Meares and Samoa), we were also responsible for the uniformity of quality of data from all sites.

2) We have shown the high level of stability of the calibration standards on which the quality of the data is based. We have also shown an independent verification of the high frequency field data by using flask samples.

3) We have used the data to show that for most practical applications, the frequency of sampling can be reduced substantially without significant loss of information.

4) Finally, the data have been used for determining the lifetimes and budgets of these gases. The use of the data is fully documented in the scientific literature, and we have summarized the salient points and attached the relevant publications for completeness.

Appendix II shows where readers may be obtain the data for their own research and what data are included in the archive.

References:

Cunnold, D.M., et al. Global Trends and Annual Releases of CCl_3F and CCl_2F_2 Estimated from ALE/GAGE and Other Measurements from July 1978 to June 1991. *Journal of Geophysical Research 99* (D1), 1,107-1,126, 1994.

Cunnold, D.M., et al. Atmospheric Lifetime and Annual Release Estimates for $CFCl_3$ and CF_2Cl_2 from 5 Years of ALE Data. *Journal of Geophysical Research 91* (D10), 10,797-10,817, 1986.

Cunnold, D.M., et al. The Atmospheric Lifetime Experiment. 3. Lifetime Methodology and Application to Three Years of $CFCl_3$ Data. *Journal of Geophysical Research 88* (C13), 8,379-8,400, 1983a.

Cunnold, D.M., et al. The Atmospheric Lifetime Experiment. 4. Results for CF_2Cl_2 Based on Three Years Data. *Journal of Geophysical Research 88* (C13), 8,401-8,414, 1983b.

Khalil, M.A.K. The Effects of Sampling Frequency and Locations on the Trends and Budgets of Greenhouse Gases and Ozone Depletors. (Final Report to the U.S. EPA contract 2D3333NASA, Andarz Co., Portland, 1994)

Khalil, M.A.K., and R.A. Rasmussen. The Environmental History and Probable Future of fluorocarbon 11. *Journal of Geophysical Research 98* (D12), 23,091-23,106, 1993.

Khalil, M.A.K., and R.A. Rasmussen. The Atmospheric Lifetime of Methylchloroform (CH_3CCl_3). *Tellus B36*, 317-332, 1984.

Prinn, R., et al. Atmospheric Trends in Methylchloroform and the Global Average for the Hydroxyl Radical. *Science 238*, 945-950, 1987.

Prinn, R.G., et al. The Atmospheric Lifetime Experiment, 1: Introduction, Instrumentation, and Overview. *Journal of Geophysical Research 88* (C13), 8,353-8,367, 1983.

Prinn, R., et al. Atmospheric Emissions and Trends of Nitrous Oxide Deduced from 10 Years of ALE-GAGE Data. *Journal of Geophysical Research 95* (D11), 18,369-18,385, 1990.

Prinn, R., et al. Global Average Concentration and Trend for Hydroxyl Radicals Deduced from ALE/GAGE Trichloroethane (Methyl Chloroform) Data for 1978-1990. *Journal of Geophysical Research 97* (D2), 2,445-2,461, 1992.

Rasmussen, R.A., and M.A.K. Khalil. Atmospheric Trace Gases: Trends and Distributions Over the Last Decade. *Science 232*, 1,623-1,624, 1986.

Simmonds, P.G., et al. The Atmospheric Lifetime Experiment, 6: Results for Carbon Tetrachloride Based on 3 Years Data. *Journal of Geophysical Research 88* (C13), 8,427-8,441, 1983.

World Meteorological Organization (WMO). *Global Ozone Research and Monitoring Project.* Reports No. 16 (3 volumes), 1985; No. 18 (2 volumes), 1988; No. 20 (2 volumes), 1989; No. 25 (1 volume), 1991.

CURRICULUM VITAE

MOHAMMAD ASLAM KHAN KHALIL, Professor Born January 7, 1950

Global Change Research Center and
Department of Environmental Science & Engineering
Oregon Graduate Institute
P.O.Box 91,000
Portland, Oregon 97291, U.S.A.

EDUCATION

B.Phys.	University of Minnesota-Minneapolis	Physics, 1970
B.A.	University of Minnesota-Minneapolis	Mathematics, 1970
B.A.	University of Minnesota-Minneapolis	Psychology, 1970
M.S.	Virginia Polytechnic Institute	Physics, 1972
Ph.D.	University of Texas (Center for Particle Theory) - Austin	Physics, 1976
M.S.	Oregon Graduate Center-Beaverton	Environmental Science, 1979
Ph.D.	Oregon Graduate Center-Beaverton	Environmental Science, 1979

EXPERIENCE

Professor	Department of Environmental Science & Engineering (OGI)	1990-Present
	and Director, Global Change Research Center at OGI	1991-Present
Professor	Institute of Atmospheric Sciences, Oregon Graduate Center (OGC)	1986-1990
Professor	Dept. of Chemical, Biological, and Environmental Sciences, OGC	1984-1986
Assoc. Professor	Dept. of Environmental Science, OGC	1982-1984
Assist. Professor	Dept. of Environmental Science, OGC	1980-1982
Senior Research Assoc.	Dept. of Environmental Science, OGC	1979-1980
Research Assistant	Dept. of Environmental Science, OGC	1977-1979
Instructor	Dept. of Physics, Pacific University, Forest Grove, OR	1978
Research Scientist Assistant	Center for Particle Theory, University of Texas-Austin	1972-1976
Teaching Assistant	Dept. of Physics, University of Texas-Austin	1972-1973, 1976
Graduate Assistant	Dept. of Mathematics & Dept. of Physics, University of Texas-Austin	1971-1972
Teaching Assistant	Dept. of Physics, Virginia Polytechnic Institute and State University	1970-1971
Undergraduate Assistant	Dept. of Mathematics & Dept. of Physics, University of Minnesota-Minneapolis	1968-1970

PROFESSIONAL ACTIVITIES:

Editor: Atmospheric Chemistry and Global Change Section, *Chemosphere*, Pergamon Press, Oxford, England.

Editorial Board: *Handbook of Environmental Chemistry* (Springer-Verlag, Berlin). *Environmental Science and Pollution Research International*, a new environmental magazine beginning publication in 1993 (EcoMed Verlagsgesellschaft, Landsberg Germany).

Author: Author of more than 150 published papers on physics, atmospheric trace gases, global change, atmospheric chemistry and physics. Editor (book), *Atmospheric Methane* (Springer-Verlag, New York, 1993).

Owner: Andarz Co. 9961 N.W.Kaiser Rd. Portland, Oregon 97231, USA.

Member: American Geophysical Union; American Physical Society; American Chemical Society; Air and Waste Management Association; Nature Conservancy, Sigma Xi.

CURRICULUM VITAE

Reinhold A. Rasmussen, Professor
Global Change Research Center
Department of Environmental Science and Engineering
Oregon Graduate Institute for Science & Technology
19600 N.W. Von Neumann Drive, Beaverton, Oregon 97006

Date of Birth: [redacted]
Place of Birth: [redacted]

I. Educational Background

B.S., Geology and Botany, University of Massachusetts, 1958
M.Ed., Biology, University of Massachusetts, 1960
Ph.D., Botany-Plant Physiology, Washington University, 1964

II. Professional Career

Plant Biochemist, Ag. Div., Monsanto Co., St. Louis, MO, 1962-1963.
Captain, Medical Service Corps, U.S.A. (Clinical Biochemist), Walter Reed Army Medical Center, Washington, D.C., and Consultant to the U.S. Army Tropical Test Center, Canal Zone, Panama, 1964-1967.
Research Project Chemist, Plant Science Section (Head), Biomedical Research Laboratory, Dow-Corning Corp., Midland, MI, 1967-1969.
Associate Plant Physiologist, Air Pollution Research Section, College of Engineering Research Division, Washington State University, Pullman, WA, 1969-June 1974.
Professor, Air Pollution Research Section, College of Engineering Research Division, Washington State University, Pullman, WA, July 1974-September 1977.
Section Head, Air Resources Section, Chemical Engineering Branch, Washington State University, Pullman, WA, May 1975-August 1976.
Affiliate Professor to Institute for Environmental Studies, University of Washington, Seattle, WA, March 1975-present.
Professor, Department of Environmental Science, Oregon Graduate Center, Beaverton, OR, September 1977-1986.
Professor, Institute of Atmospheric Sciences, Oregon Graduate Center, Beaverton, OR, 1986-1989.
Professor, Center for Atmospheric Studies, Dept. of Environmental Science and Engineering, Oregon Graduate Institute, Beaverton, OR, 1989-present.

III. Other Professional Activities

Member, National Academy of Science-National Research Council panels:
Vapor Phase Organic Air Pollutants from Hydrocarbons
Ammonia
Low-Molecular-Weight Halogenated Hydrocarbons
Air Pollution Physics and Chemistry Advisory Committee, EPA, 1972-1975.
Environmental Pollutant Movement and Transformation Advisory Committee, EPA, 1975-1978.
Member, Intersociety Committee D-5, Hydrocarbon Analyses, 1973-1978; Substance Subcommittee #4/5, Carbon and Hydrocarbon Compounds, 1979-1984.
American Meteorological Society Committee on Atmospheric Chemistry and Radioactivity, 1975-1979.
Polar Ice Core Office Advisory Committee for Greenland Ice Sheet Program, NSF, 1976-79, 1986-1988.
Review Board on Halogenated Alkanes/Alkenes, International Agency for Research on Cancer, WHO, 1982-1985.
American Chemical Society, Instructor, Air Toxics: Short Course, 1990-present

IV. Professional Societies

American Chemical Society, Air and Waste Management Association
The Explorers Club.

Appendix II: Where to Obtain the Data and What Is in the Archive

The data that are currently available from the archives are described here. These data may be obtained from the following address:

Carbon Dioxide Information Analysis Center
Oak Ridge National Laboratory
Building 1000, MS-6335
P.O. Box 2008
Oak Ridge, Tennessee 37831-6335, U.S.A.

(615) 574-0390
(615) 574-2232 (FAX)

BITNET: CDP@ORNLSTC
OMNET: CDIAC
INTERNET: CDP@ORNL.GOV

Data for the other ALE/GAGE sites are also available from the same source and are described by Boden et al.

Reference: Boden et al., Editors. Trends '93. A compendium of data on global change. U.S. Department of Energy, Environmental Sciences Division, Publication No. ORNL/CDIAC-65, ESD Publication No. 4195.

Atmospheric CFC-11 (CCl_3F), CFC-12 (CCl_2F_2), and N_2O from the ALE/GAGE network

R.G. Prinn, R.F. Weiss, F.N. Alyea, D.M. Cunnold, P.J. Fraser, P.G. Simmonds, A.J. Crawford, R.A. Rasmussen, and R.D. Rosen (continued)

Cape Meares

Period of Record

1979–89 (CFC-11); 1980–89 (CFC-12 and N_2O)

Trends

The ALE/GAGE site at Cape Meares, Oregon, U.S.A., was operated under the supervision of R.A. Rasmussen and A.J. Crawford of the Oregon Graduate Institute of Science and Technology. The site is located on the Pacific coast of Oregon, immediately overlooking the ocean ~30 m above mean sea level. The site initially appeared to receive largely unpolluted Pacific air, but pollution episodes increased in more recent years. Measurements for CFC-11 began as part of ALE in December 1979. Due to start-up problems, reliable measurements for N_2O began in March 1980 and for CFC-12 in November 1980. These measurements continued as part of ALE through July 1984 and as part of GAGE from September 1983 through June 1989.

The monthly mean mixing ratio of CFC-11 increased from 169.4 parts per trillion (ppt) in December 1979 to 253.9 ppt in June 1989. Cunnold et al. (1994) reported that the average rate of increase of CFC-11 was 8.8 ± 0.1 ppt/year from July 1978 to June 1988. The mixing ratio of CFC-12 increased from 326.2 ppt in November 1980 to 481.8 ppt in June 1989. For the period July 1978 to June 1988, Cunnold et al. (1994) determined that the average rate of increase of CFC-12 was 16.7 ± 0.2 ppt/year. For both CFC-11 and CFC-12, the trends are highly significant ($P < 0.0001$).

The time series of the monthly mean mixing ratios of N_2O shows little evidence of an upward trend until about mid-1981, after which the mixing ratio begins to increase in a generally linear fashion. During 1980–89, the monthly values show a highly significant ($P < 0.0001$) trend. The monthly mixing ratio increased from 301.1 parts per billion (ppb) in March 1980 to a high of 309.1 ppb in December 1988 and then dropped slightly to 307.2 ppb in June 1989. For 1980–88, Prinn et al. (1990) calculated that the mixing ratio of N_2O increased by an average of 0.94 ± 0.07 ppb/year. No significant periodic oscillation is evident. Throughout the period of record, the daily N_2O variability is generally larger than at equatorial and Southern Hemisphere sites.

CITE AS: Prinn, R.G., R.F. Weiss, F.N. Alyea, D.M. Cunnold, P.J. Fraser, P.G. Simmonds, A.J. Crawford, R.A. Rasmussen, and R.D. Rosen. 1994. Atmospheric CFC-11 (CCl_3F), CFC-12 (CCl_2F_2), and N_2O from the ALE/GAGE network. pp. 396–420. In T.A. Boden, D.P. Kaiser, R.J. Sepanski, and F.W. Stoss (eds.), *Trends '93: A Compendium of Data on Global Change.* ORNL/CDIAC-65. Carbon Dioxide Information Analysis Center, Oak Ridge National Laboratory, Oak Ridge, Tenn., U.S.A.

Other Trace Gases and Atmospheric Aerosols

Atmospheric CFC-11 (CCl_3F), CFC-12 (CCl_2F_2), and N_2O from the ALE/GAGE network

R.G. Prinn, R.F. Weiss, F.N. Alyea, D.M. Cunnold, P.J. Fraser, P.G. Simmonds, A.J. Crawford, R.A. Rasmussen, and R.D. Rosen (continued)

SAMOA

Period of Record

1978–89

Trends

The ALE/GAGE monitoring site in Samoa is located at the National Oceanic and Atmospheric Administration (NOAA) station at Cape Matatula, on a rocky promontory overlooking the Pacific ocean ~30 m above mean sea level. The ALE/GAGE operation at Samoa through 1989 was carried out under the supervision of R.A. Rasmussen and A.J. Crawford of the Oregon Graduate Institute of Science and Technology. The site is now supervised by R.F. Weiss of the Scripps Institution of Oceanography (SIO). The site receives unpolluted oceanic air almost exclusively; during the southern summer, however, conditions during the Northern Hemisphere winter often allow air from the Northern Hemisphere to reach Samoa. Measurements at the site began in July 1978 and continued as part of ALE through May 1986. Beginning in July 1985, measurements were also collected as part of GAGE. After the conclusion of ALE, measurements at Samoa continued as part of GAGE through June 1989 and then began again in late 1990.

The monthly mean mixing ratio of CFC-11 increased from 138.9 parts per trillion (ppt) in July 1978 to 240.8 ppt in June 1989. The mixing ratio of CFC-12 increased from 251.1 to 457.8 ppt during the same period. Cunnold et al. (1994) determined that the average rate of increase in atmospheric mixing ratios at Samoa from July 1978 to June 1988 was 9.2 ± 0.1 ppt/year for CFC-11 and 17.3 ± 0.2 ppt/year for CFC-12. For both CFC-11 and CFC-12, the trends are highly significant ($P < 0.0001$). In addition, annual cycles are evident for both CFC-11 and CFC-12; maximum mixing ratios are observed in late summer and minima in late winter (Prinn et al. 1983; Cunnold et al. 1994).

The time series of the monthly mean mixing ratios of N_2O is generally linear, except for an anomalously large increase during the first 4 months of record. The values show a highly significant ($P < 0.0001$) trend over the period of record. The monthly mixing ratio increased from 293.8 parts per billion (ppb) in July 1978 to a high of 307.6 ppb in January 1989 to 306.1 ppb in June 1989. For January 1979 to June 1988, Prinn et al. (1990) calculated that the mixing ratio of N_2O increased by an average of 0.91 ± 0.04 ppb/year. No significant periodic oscillation is evident.

CITE AS: Prinn, R.G., R.F. Weiss, F.N. Alyea, D.M. Cunnold, P.J. Fraser, P.G. Simmonds, A.J. Crawford, R.A. Rasmussen, and R.D. Rosen. 1994. Atmospheric CFC-11 (CCl_3F), CFC-12 (CCl_2F_2), and N_2O from the ALE/GAGE network. pp. 396–420. In T.A. Boden, D.P. Kaiser, R.J. Sepanski, and F.W. Stoss (eds.), *Trends '93: A Compendium of Data on Global Change*. ORNL/CDIAC-65. Carbon Dioxide Information Analysis Center, Oak Ridge National Laboratory, Oak Ridge, Tenn., U.S.A.

APPENDIX III

Publications: ALE-GAGE Program NASA Grant #NAGW-1348
4-1-88 to 1-31-91

The Atmospheric Lifetime Experiment, 1: Introduction, Instrumentation, and Overview. R.G. Prinn, P.G. Simmonds, R.A. Rasmussen, R.D. Rosen, F.N. Alyea, C.A. Cardelino, A.J. Crawford, D.M. Cunnold, P.J. Fraser, and J.E. Lovelock. *J. Geophys. Res. 88*, 8353-8367, 1983.

The Atmospheric Lifetime Experiment, 2: Calibration. R.A. Rasmussen and J.E. Lovelock. *J. Geophys. Res. 88*, 8369-8378, 1983.

The Atmospheric Lifetime Experiment, 3: Lifetime Methodology and Application to Three Years of $CFCl_3$ Data. D.M. Cunnold, R.G. Prinn, R.A. Rasmussen, P.G. Simmonds, F.N. Alyea, C.A. Cardelino, A.J. Crawford, P.J. Fraser, and R.D. Rosen. *J. Geophys. Res. 88*, 8379-8400, 1983.

The Atmospheric Lifetime Experiment, 4: Results for CF_2Cl_2 Based on Three Years Data. D.M. Cunnold, R.G. Prinn, R.A. Rasmussen, P.G. Simmonds, F.N. Alyea, C.A. Cardelino, and A.J. Crawford. *J. Geophys. Res. 88*, 8401-8414, 1983.

The Atmospheric Lifetime Experiment, 5: Results for CH_3CCl_3 Based on Three Years of Data. R.G. Prinn, R.A. Rasmussen, P.G. Simmonds, F.N. Alyea, D.M. Cunnold, B.C. Lane, C.A. Cardelino, and A.J. Crawford. *J. Geophys. Res. 88*, 8415-8426, 1983.

The Atmospheric Lifetime Experiment, 6: Results for Carbon Tetrachloride Based on 3 Years Data. P.G. Simmonds, F.N. Alyea, C.A. Cardelino, A.J. Crawford, D.M. Cunnold, B.C. Lane, J.E. Lovelock, R.G. Prinn, and R.A. Rasmussen. *J. Geophys. Res. 88*, 8427-8441, 1983.

Atmospheric Lifetime and Annual Release Estimates for $CFCl_3$ and CF_2Cl_2 from 5 Years of ALE Data. D.M. Cunnold, R.G. Prinn, R.A. Rasmussen, P.G. Simmonds, F.N. Alyea, C.A. Cardelino, A.J. Crawford, P.J. Fraser, and R.D. Rosen. *J. Geophys. Res. 91*, 10797-10817, 1986.

Atmospheric Trends in Methylchloroform and the Global Average for the Hydroxyl Radical. R. Prinn, D. Cunnold, R. Rasmussen, P. Simmonds, F. Alyea, A. Crawford, P. Fraser, R. Rosen. *Science 238*, 945-950, 1987.

Atmospheric Emissions and Trends of Nitrous Oxide Deduced from 10 Years of ALE-GAGE Data. R. Prinn, D. Cunnold, R. Rasmussen, P. Simmonds, F. Alyea, A. Crawford, P. Fraser, and R. Rosen. *J. Geophys. Res. 95*, 18369-18385, 1990.

Global Average Concentration and Trend for Hydroxyl Radicals Deduced from ALE/GAGE Trichloroethane (Methyl Chloroform) Data for 1978-1990. R. Prinn, D. Cunnold, P. Simmonds, F. Alyea, R. Boldi, A. Crawford, P. Fraser, D. Gutzler, D. Hartley, R. Rosen, and R. Rasmussen. *J. Geophys. Res. 97*, 2,445-2,461, 1992.

Khalil, M.A.K, R.A. Rasmussen, and F. Moraes. Atmospheric Methane at Cape Meares: Analysis of a High-Resolution Data Base and Its Environmental Implications. *Journal of Geophysical Research 98* (D8), 14,753-14,770, 1993

Cunnold, D.M., et al. Global Trends and Annual Releases of CCl_3F and CCl_2F_2 Estimated from ALE/GAGE and Other Measurements from July 1978 to June 1991. *Journal of Geophysical Research 99* (D1), 1,107-1,126, 1994.

Cited in Acknowledgements:

Atmospheric Methane at Cape Meares: Analysis of a High Resolution Data Base and Its Environmental Implications. M.A.K. Khalil, R.A. Rasmussen, and F. Moraes. *J. Geophys. Res.*, 14,753-14,770, 1993.

Atmospheric Methane at Cape Meares, Oregon. M.A.K. Khalil and R.A. Rasmussen. *Climate Monitoring and Diagnostics Laboratory, No. 21, Summary Report 1992*, J.T. Peterson and R.M. Rosson, Editors, NOAA, Boulder, Colorado, December 1993, pp. 100-101.

APPENDIX IV

Instrumentation

HP 5840 Gas Chromatograph

Cape Meares, December 11,1979 - August 1984
Samoa, July 1, 1978 - May 22,1986

HP 5880A Gas Chromatograph

Cape Meares, January 18, 1983 - Present
Samoa, July 6, 1985 - January 1, 1990

Enhancements to Instrumentation

July 1990 - added an analog output board and analog input board to Cape Meares HP5880a system. The effect of this change was approximately a 10 fold increase in signal response to the integrator. The signal from the SP2100 column and mol sieve column are enhanced in this manner.

Columns

Porasil D 8' x 1/4"
10% SP2100 on Supelcoport 8' x 1/4"
Washed Mol Sieve 5a 6' x 1/8"

Detectors

2 Electron Capture Detectors (ECD)

Frequency Modulated 15 mCi Ni-63 detector

1 Flame Ionization Detector (FID)

Flow Rates

ECD Detectors

Make up Gas 95% Ar, 5% CH_4 ~ 50 ml/min

FID Detector (on HP 5880A GC only)

Carrier gas N_2 ~ 30 ml/min
H_2 ~ 25 ml/min
60/40 ~ 300 ml/min

Operating Conditions

Isothermal Mode - Oven Temp 50°C
10% SP2100 Channel Detector Temp 350°C, Injection Port Temp 270°C
Porasil channel Detector Temp 200°C, Injection Port Temp 270°C
Mol Sieve Channel Detector Temp 75°C
Chart Speed 0.3 cm/min

Retention Times

10% SP2100 Channel

F-11	4.01 min
F-113	5.10 min
CH_3CCl_3	10.23 min
CCl_4	11.83 min

Porasil channel

N_2O	2.51 min
F-12	3.57 min
F-11	8.07 min

Mol Sieve Channel

CH_4 - Calibration	18.96 min
CH_4 - Ambient	24.16 min

Data Acquisition System

IBM PC XT computer

Custom software written to interrogate HP5880A, download data and store to floppy disk.

SP2100 COLUMN

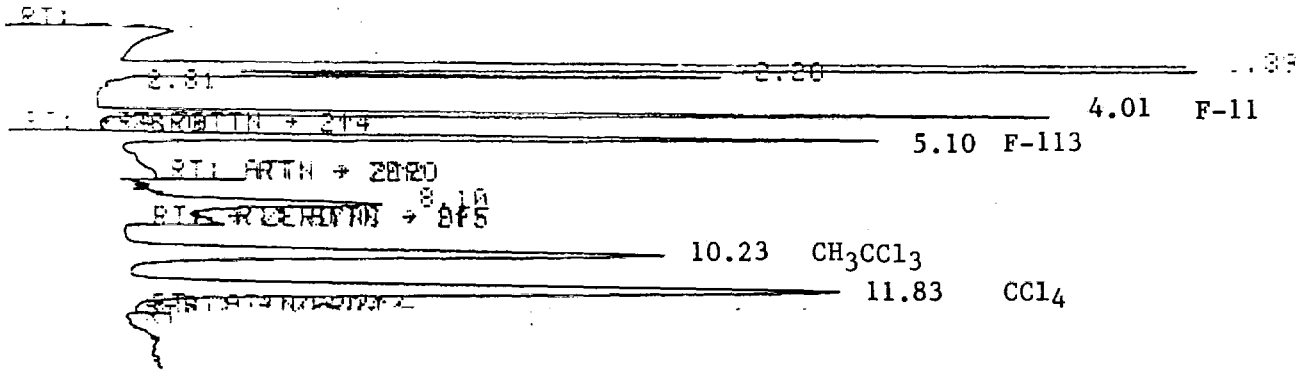

PORASIL D COLUMN

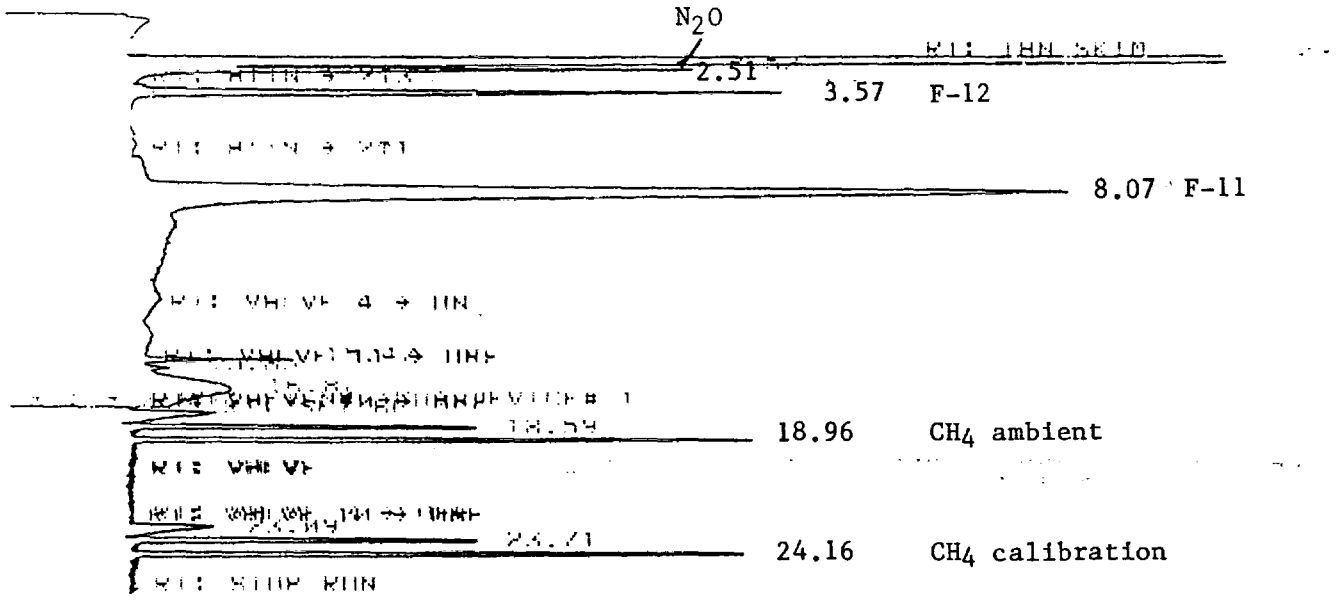

Appendix V: Technical Publications

Cunnold, D.M., et al. Global Trends and Annual Releases of CCl_3F and CCl_2F_2 Estimated from ALE/GAGE and Other Measurements from July 1978 to June 1991. *Journal of Geophysical Research 99* (D1), 1,107-1,126, 1994. 95A 62832

Khalil, M.A.K, R.A. Rasmussen, and F. Moraes. Atmospheric Methane at Cape Meares: Analysis of a High-Resolution Data Base and Its Environmental Implications. *Journal of Geophysical Research 98* (D8), 14,753-14,770, 1993 93A 56126

Prinn, R., et al. Global Average Concentration and Trend for Hydroxyl Radicals Deduced from ALE/GAGE Trichloroethane (Methyl Chloroform) Data for 1978-1990. *Journal of Geophysical Research 97* (D2), 2,445-2,461, 1992. 92A 26104

Prinn, R., et al. Atmospheric Emissions and Trends of Nitrous Oxide Deduced from 10 Years of ALE-GAGE Data. *Journal of Geophysical Research 95* (D11), 18,369-18,385, 1990. 91A 13109

Cunnold, D.M., et al. Atmospheric Lifetime and Annual Release Estimates for $CFCl_3$ and CF_2Cl_2 from 5 Years of ALE Data. *Journal of Geophysical Research 91* (D10), 10,797-10,817, 1986. 87A 19077

Prinn, R.G., et al. The Atmospheric Lifetime Experiment, 1: Introduction, Instrumentation, and Overview. *Journal of Geophysical Research 88* (C13), 8,353-8,367, 1983. 83A 49328

Rasmussen, R.A., and J.E. Lovelock. The Atmospheric Lifetime Experiment, 1: Introduction, Instrumentation, and Overview. *Journal of Geophysical Research 88* (C13), 8,369-8,378, 1983. 83A 49328

Cunnold, D.M., et al. The Atmospheric Lifetime Experiment. 3. Lifetime Methodology and Application to Three Years of $CFCl_3$ Data. *Journal of Geophysical Research 88* (C13), 8,379-8,400, 1983a. 83A 49330

Cunnold, D.M., et al. The Atmospheric Lifetime Experiment. 4. Results for CF_2Cl_2 Based on Three Years Data. *Journal of Geophysical Research 88* (C13), 8,401-8,414, 1983b. 83A 49331

Prinn, R.G., et al. The Atmospheric Lifetime Experiment, 5: Results for CH_3CCl_3 Based on Three Years of Data. *Journal of Geophysical Research 88* (C13), 8,353-8,367, 1983. NDB

Simmonds, P.G., et al. The Atmospheric Lifetime Experiment, 6: Results for Carbon Tetrachloride Based on 3 Years Data. *Journal of Geophysical Research 88* (C13), 8,427-8,441, 1983. 83A 49332

Atmospheric Trends in Methylchloroform and the Global Average for the Hydroxyl Radical

R. PRINN, D. CUNNOLD, R. RASMUSSEN, P. SIMMONDS, F. ALYEA, A. CRAWFORD, P. FRASER, R. ROSEN

Frequent atmospheric measurements of the anthropogenic compound methylchloroform that were made between 1978 and 1985 indicate that this species is continuing to increase significantly around the world. Reaction with the major atmospheric oxidant, the hydroxyl radical (OH), is the principal sink for this species. The observed mean trends for methylchloroform are 4.8, 5.4, 6.4, and 6.9 percent per year at Aldrigole (Ireland) and Cape Meares (Oregon), Ragged Point (Barbados), Point Matatula (American Samoa), and Cape Grim (Tasmania), respectively, from July 1978 to June 1985. These measured trends, combined with knowledge of industrial emissions, were used in an optimal estimation inversion scheme to deduce a globally averaged methylchloroform atmospheric lifetime of 6.3 (+1.2, −0.9) years (1σ uncertainty) and a globally averaged tropospheric hydroxyl radical concentration of (7.7 ± 1.4) × 10^5 radicals per cubic centimeter (1σ uncertainty). These 7 years of gas chromatographic measurements, which comprise about 60,000 individual calibrated real-time air analyses, provide the most accurate estimates yet of the trends and lifetime of methylchloroform and of the global average for tropospheric hydroxyl radical levels. Accurate determination of hydroxyl radical levels is crucial to understanding global atmospheric chemical cycles and trends in the levels of trace gases such as methane.

METHYLCHLOROFORM IS A LONG-lived atmospheric species whose only known sources are anthropogenic. It is widely used in industry as a solvent for degreasing and in other applications; its global production and use accelerated significantly in the mid-1970s as it replaced the increasingly regulated solvent trichloroethylene (*1*). Its concentration has rapidly increased worldwide (*1–3*). This increase is of considerable concern because methylchloroform is a significant stratospheric source of atomic chlorine and chlorine monoxide (*4*) that can catalytically destroy stratospheric ozone (*5*), and because it is one of the greenhouse gases that may contribute to future climate change (*6*).

The principal recognized atmospheric sink for methylchloroform (CH_3CCl_3) is the reaction (*7, 8*)

$$CH_3CCl_3 + OH \rightarrow CH_2CCl_3 + H_2O \quad (1)$$

The global rate of loss of CH_3CCl_3, which can be deduced from its known industrial emissions and observed global trends, can be used to deduce accurately an appropriately weighted globally averaged tropospheric concentration for the hydroxyl radical (OH) (*1–3, 8*). Knowledge of precise OH concentrations is crucial because OH is widely recognized as the major gas-phase oxidant in clean tropospheric air. Thus it plays a central role in tropospheric chemistry, including chemical destruction of a wide range of species of anthropogenic and natural origin that are important radiatively or chemically or both (for example, CO, CH_4, NO_x, and SO_2) (*9*).

Since 1978 we have performed frequent (4 to 12 measurements per day) real-time gas chromatographic measurements of methylchloroform at stations throughout the world, first as part of the Atmospheric Lifetime Experiment (ALE) and (since late 1984) as part of the Global Atmospheric Gases Experiment (GAGE) (*1, 10*). The surface measurement stations are located at coastal sites remote from industrial and urban sources and are designed to measure accurately the tropospheric trends of trace gases whose lifetimes are long compared to global tropospheric mixing times (*11*). In this report we present and interpret ALE-GAGE data obtained over the 7-year period from July 1978 to June 1985 which, primarily because of the greater number of measurements, provide much more accurate determinations than previously possible (*1–3, 8*) of the global trend and atmospheric destruction time for methylchloroform and for the globally averaged OH concentration.

Monthly mean volume mixing ratios for methylchloroform were computed from the approximately 100 to 400 measurements made each month at each of the five ALE-

R. Prinn, Department of Earth, Atmospheric, and Planetary Sciences, Massachusetts Institute of Technology, Cambridge, MA 02139.
D. Cunnold and F. Alyea, School of Geophysical Sciences, Georgia Institute of Technology, Atlanta, GA 30332.
R. Rasmussen and A. Crawford, Institute of Atmospheric Sciences, Oregon Graduate Center, Beaverton, OR 97005.
P. Simmonds, Department of Geochemistry, University of Bristol, Bristol, BF8-1TS, United Kingdom.
P. Fraser, Division of Atmospheric Research, Commonwealth Scientific and Industrial Research Organization, Aspendale, 3195 Victoria, Australia.
R. Rosen, Atmospheric and Environmental Research, Inc., Cambridge, MA 02139.

GAGE stations (Table 1). The data are calibrated with a more accurate absolute standard than was used previously (*12*). Each station (or combination of stations in the case of Ireland and Oregon) is intended to be indicative of the air between the surface and a pressure of 500 mbar in the semihemisphere in which it lies. Objective techniques were used therefore to recognize periods (typically less than a few days in duration) of local air pollution (*1, 10, 13*). These time periods are not represented in the data reported here but have been archived (*14*) and used to deduce information on local sources (*15*).

Greater variability in methylchloroform levels is observed at Northern Hemisphere sites than at Southern Hemisphere sites even after removal of local pollution effects in the data. This variability is expected on theoretical grounds because of the presence of continental-scale methylchloroform source regions (North America, Europe, eastern Asia, and Japan) in the northern mid-latitudes that have no Southern Hemisphere analog (*16*). After removal of pollution effects, methylchloroform levels were still slightly greater at Adrigole than at Cape Meares, probably reflecting higher methylchloroform concentrations in Atlantic air compared to Pacific air, which is also expected theoretically (*16*). Although most of the variance in the monthly mean data is associated with real atmospheric variability, there are also instrumental contributions associated with detector signal processing and calibration tank changes (*1, 10*).

The long-term components of variability in the monthly-mean mixing ratios χ_i measured at station i can be described by an empirical model

$$\chi_i = a_i + b_i t + d_i t^2 + e_i t^3 + c_i \cos(2\pi t) + s_i \sin(2\pi t) \quad (2)$$

in which t is time (in years) measured from the midpoint of the record (1 January 1982 unless otherwise noted). Maximum likelihood estimates of the coefficients in Eq. 2 and their uncertainties (Table 2) are computed with techniques described elsewhere (*17*). Approximating Eq. 2 by using zero-order and first-order Legendre polynomials, the mean concentration is $a_i + 4.08\ d_i$, and the mean linear trend is $b_i + 7.35\ e_i$ over the 7-year period of the observations. From the mean concentrations it is evident that a strong north-to-south gradient exists. Statistically significant negative values for d_i at the stations indicate that the trends decrease with time in a manner consistent with a slow approach to a steady state. Significant seasonal cycles (described by c_i and s_i) are evident in the Northern Hemisphere sites and in Tasmania but not at Samoa. These seasonal cycles differ from those observed for the Freons or chlorofluoromethanes (*17*). In particular, Adrigole and Cape Meares are out of phase for methylchloroform but in phase for the Freons; there is a significant cycle for the Freons at Point Matatula but not at Ragged Point (*17*). These differences must be due to differences in space and time in the emissions of methylchloroform and the Freons. The seasonal cycle of methylchloroform at Tasmania has been attributed to seasonal cycles either in OH (*3*) or in interhemispheric circulation (*1*).

Detailed information on annual production $P(t)$ and sales $S(t)$ of methylchloroform worldwide in year t are available from industry sources (*18*). Global emissions $E(t)$ are computed from these data with the formula

$$E(t) = (1 - a)fS(t) + afS(t - 1)$$
$$= (1 - a - b + ab)fP(t) + (a + b - 2ab)fP(t - 1) + abfP(t - 2$$

Here a is the fraction of annual sales enters the user's inventory, b is the fra of annual production entering the pr er's inventory, and f is the fraction of a sales to the users that is released (the rer der is destroyed or incarcerated). By assessments of a, b, and f and their uncertainties, which were based on ind information (*19*), we computed $E(t)$ v with 2σ uncertainties (Table 3).

To deduce the chemical destruction of methylchloroform in the atmos from the observed concentrations an above emissions, we used an optimal es tion inversion technique (*17, 20*). The nique includes the use of a two-dimens model (eight tropospheric boxes, one u atmospheric box) of the global atmos

Table 1. Monthly mean mixing ratios (χ) and standard deviations (σ) observed at ALE-GAGE over the period July 1978 to June 1985. Units are parts per trillion by volume. For Oregon (begir September 1983) and Tasmania (beginning July 1981), ALE (HP 5840) and GAGE (HP 5

Year	Month	Ireland		Oregon		Barbados		Samoa		Tasma
		χ	σ	χ	σ	χ	σ	χ	σ	χ
1978	7	112.1	4.6	0.0	0.0	99.6	5.8	71.1	2.9	68.8
1978	8	109.8	3.8	0.0	0.0	99.5	6.2	72.1	3.4	66.6
1978	9	105.8	3.9	0.0	0.0	94.2	8.2	72.4	2.9	68.5
1978	10	107.4	3.8	0.0	0.0	94.6	8.2	74.2	2.9	70.8
1978	11	107.7	3.3	0.0	0.0	92.7	7.1	74.6	4.2	74.9
1978	12	0.0	0.0	0.0	0.0	99.3	6.7	75.0	5.1	74.2
1979	1	111.4	4.6	0.0	0.0	100.2	7.4	78.0	3.3	73.1
1979	2	112.7	3.1	0.0	0.0	99.8	7.0	75.8	3.6	73.1
1979	3	112.2	5.0	0.0	0.0	100.9	6.9	76.6	3.0	75.1
1979	4	115.4	4.9	0.0	0.0	0.0	0.0	76.2	3.4	76.5
1979	5	117.2	4.6	0.0	0.0	101.7	3.3	77.9	2.0	76.6
1979	6	117.7	5.1	0.0	0.0	99.9	4.6	78.5	0.7	78.1
1979	7	115.1	5.6	0.0	0.0	102.8	6.6	79.7	1.1	77.3
1979	8	115.8	5.0	0.0	0.0	105.7	4.2	81.2	1.7	78.7
1979	9	116.9	5.1	0.0	0.0	99.0	7.4	81.3	1.9	79.8
1979	10	120.3	4.1	0.0	0.0	98.9	5.9	83.0	1.8	80.8
1979	11	119.7	5.8	0.0	0.0	102.8	5.8	85.1	1.7	81.5
1979	12	122.5	5.6	125.4	7.0	105.2	4.1	79.1	4.6	81.0
1980	1	121.8	6.4	127.7	4.8	107.8	5.0	84.0	2.4	80.6
1980	2	123.0	5.4	0.0	0.0	108.5	5.2	86.2	2.6	81.0
1980	3	126.6	5.7	123.9	1.9	112.5	3.8	86.7	2.6	82.4
1980	4	130.1	6.0	126.4	2.4	110.1	3.1	87.1	3.1	82.0
1980	5	132.1	5.9	126.3	1.8	111.0	3.8	88.2	1.8	85.9
1980	6	130.6	6.6	124.1	2.4	113.8	3.4	89.2	1.2	86.8
1980	7	130.7	5.0	120.8	2.9	112.9	4.6	90.5	0.8	87.6
1980	8	127.0	4.7	121.5	2.4	111.3	3.4	91.6	1.0	88.7
1980	9	124.8	4.2	125.4	6.2	109.6	6.6	92.1	1.6	89.9
1980	10	127.4	4.4	132.1	6.6	109.9	6.3	92.5	1.0	90.8
1980	11	129.0	3.8	130.1	5.4	114.9	4.6	94.2	1.8	90.6
1980	12	129.2	4.0	128.2	4.6	115.4	6.2	96.1	3.0	89.4
1981	1	128.5	5.8	129.4	4.2	114.8	4.4	96.7	3.2	89.4
1981	2	129.4	4.2	133.0	7.8	116.8	4.2	0.0	0.0	89.7
1981	3	130.2	4.9	128.6	2.9	112.6	3.8	97.8	1.6	91.2
1981	4	131.9	3.3	128.9	2.2	117.4	5.3	96.2	1.9	92.1
1981	5	135.0	4.0	129.8	2.9	119.1	3.6	95.9	2.3	92.8
1981	6	135.3	4.7	130.6	2.2	117.5	3.4	97.4	1.5	93.4
1981	7	131.4	6.3	126.4	3.5	120.4	3.7	97.4	1.8	93.2
1981	8	131.9	5.1	126.2	3.0	116.4	7.2	99.4	1.0	0.0
1981	9	134.2	6.5	128.9	2.8	115.9	6.2	100.2	1.8	93.7
1981	10	134.2	5.4	131.0	3.1	116.6	5.4	97.8	1.4	96.2
1981	11	134.7	5.4	134.3	2.4	116.3	4.8	97.9	1.7	96.5
1981	12	137.2	5.4	135.8	2.5	115.4	4.2	98.8	2.2	97.2

ith horizontal surfaces at 1000, 500, 200, id 0 mbar and tropospheric vertical surces at latitudes 30°N, 0°, and 30°S. Mean dvective and eddy diffusive transports in ie model are specified from meteorological bservations and an optimal fit to global ata for the Freons fluorotrichloromethane id dichlorodifluoromethane (*17*). The ove methylchloroform emissions are input ito the four lower tropospheric boxes in ie model. The chemical lifetime for methlchloroform in the upper atmospheric box 6 years) is specified from detailed calculaions in a global three-dimensional circulaion model (*16*). The lifetime τ_i in the ith ropospheric box is given by

$$\tau_i^{-1} = k_i A[\mathrm{OH}]_i^* \quad (4)$$

here k_i is the temperature-dependent rate onstant for reaction 1 in box i, $[\mathrm{OH}]_i^*$ is a heoretical estimate of the OH concentration in box i (*21*), and A is an unknown dimensionless coefficient by which the theoretical estimates are to be multiplied to provide an optimal fit between the model and observed methylchloroform concentrations and trends (*1*). There is also sufficient information in the observations to permit an estimate of the factor α by which our current absolute concentrations should be multiplied to provide the best fit to the emission and station data. Because the two-dimensional model is not capable of accurately simulating oscillations associated with the measurement technique (for example, periodic renewal of on-site calibration gases) or natural meteorological oscillations on interannual, seasonal, and shorter term time scales, the 12-month running mean model predictions are used. The model is then augmented by two empirical models that are designed to describe the spectrum of the differences between the observations and the two-dimensional model predictions [that is, the residuals that for methylchloroform have a mean standard deviation of 2.4 parts per trillion by volume (pptv)]. Lower frequencies in this spectrum of residuals were fit with a first-order auto-regressive model common to all sites with a correlation of 0.5 after 1 month; higher frequencies were modeled by assuming that the spectra at each site were the same as those found in the residuals between the observations and the empirical model (Eq. 2). Because both the Adrigole and Cape Meares stations lie in the region from 30° to 90°N, the concentrations observed at these sites were combined into a single time series in which they overlap in time by adding 0.493 times the Adrigole concentrations to 0.507 times the Cape Meares concentrations (this slightly unequal weighting avoids producing spurious trends because of the different mean concentrations and observational time periods at the two sites).

The optimal estimation scheme we used (*17*, *20*) was designed to minimize the squares of the deviations between the logarithms of the observed (χ) and model-calculated (χ_c) mixing ratios at time t (months)

$$\ln \chi(t) - \ln \chi_c(t) = -\ln \alpha - [A(t) - A(t - \Delta t)] \left\{ \frac{\partial \ln \chi_c(t - \Delta t)}{\partial A} + \frac{d}{dt}\left[\frac{\partial \ln \chi_c(t - \Delta t)}{\partial A} \right] \Delta t \right\} \quad (5)$$

by continuously updating the values of α, A, and thus $\partial \ln \chi_c/\partial A$ in the model. Because A and the inverse atmospheric lifetime $1/\tau$ of methylchloroform are equivalent variables (*1*), A in Eq. 5 can also be replaced by $1/\tau$.

Estimates of $1/\tau$ (or A) can be obtained with each station data set alone or all station data sets simultaneously (Table 4). The estimate of lifetime obtained by using all station data and including emission trend uncertainty (Table 3) is 6.9 (+1.2, −0.9) years (1σ). The estimate for α is 1.09, which is in satisfactory agreement with our absolute calibration uncertainty of ±10% (1σ). Relative to the lifetime estimates for 3 years of data (*1*), there is substantially closer agreement between the individual site lifetime estimates because of the much better definition of long-term variability in methylchloroform with 7 years of data. Moreover, all the individual site lifetime estimates are shorter in this report because of increases of 5 to 10% in the estimates of global sales between 1979 and 1983 (*18*). This sensitivity of the lifetime estimates to the emissions during this period was emphasized in our

onthly data were combined by weighting equally ALE and GAGE monthly means to determine χ, id ALE and GAGE individual measurements to determine σ. An absolute calibration factor of 0.8 is cluded.

Year	Month	Ireland		Oregon		Barbados		Samoa		Tasmania	
		χ	σ	χ	σ	χ	σ	χ	σ	χ	σ
982	1	132.4	5.8	134.6	1.4	120.3	3.1	99.4	2.4	96.7	1.6
1982	2	133.8	4.9	135.3	2.9	120.5	3.0	101.8	2.7	96.6	1.5
1982	3	138.9	6.6	136.4	2.3	120.1	3.0	100.0	1.0	97.0	1.4
1982	4	140.9	5.1	139.6	2.1	126.0	3.3	0.0	0.0	98.3	1.6
1982	5	138.5	5.2	139.0	1.8	123.8	3.8	0.0	0.0	100.1	0.9
1982	6	138.8	3.7	136.9	2.2	124.1	3.0	101.3	1.4	101.4	0.7
1982	7	138.3	5.5	134.4	2.5	125.6	2.8	100.9	1.6	102.2	0.9
1982	8	134.5	4.6	131.0	2.8	125.0	3.8	102.2	1.7	103.1	0.9
1982	9	135.5	5.6	130.6	3.9	121.3	4.9	102.1	1.3	103.3	0.5
1982	10	139.8	5.0	134.5	2.6	119.3	5.2	102.1	1.0	103.9	0.7
1982	11	142.8	4.2	135.9	2.3	123.1	4.5	101.4	0.9	103.8	0.7
1982	12	141.4	5.2	138.9	2.2	130.1	3.6	100.9	1.0	103.0	0.5
1983	1	138.2	4.6	137.4	3.6	128.9	3.8	100.2	0.9	102.4	0.5
1983	2	140.5	4.3	137.5	2.0	127.4	3.8	101.8	1.2	102.7	0.9
1983	3	141.8	3.4	141.6	3.4	125.4	3.0	102.9	1.1	103.2	0.7
1983	4	145.1	4.1	143.1	3.8	130.4	3.0	103.4	1.2	103.7	0.9
1983	5	150.2	5.5	141.7	2.3	129.0	2.2	104.6	1.2	104.8	0.8
1983	6	146.4	6.2	141.4	2.2	128.4	3.7	105.9	1.0	105.4	0.7
1983	7	142.4	3.0	139.4	1.8	130.3	5.2	106.6	1.0	106.6	0.9
1983	8	142.3	3.3	137.1	3.2	129.7	6.0	106.8	1.0	107.2	0.9
1983	9	139.3	3.7	138.1	3.4	127.0	4.2	108.2	1.0	107.0	0.7
1983	10	141.8	4.6	141.6	2.4	124.7	4.2	107.6	1.0	107.3	0.5
1983	11	146.2	4.9	143.5	2.1	125.4	5.2	106.6	1.3	107.1	0.6
1983	12	147.1	4.6	147.0	3.2	132.1	4.1	109.1	1.8	106.3	0.7
1984	1	0.0	0.0	143.0	0.5	132.6	2.5	111.6	2.4	105.6	0.6
1984	2	0.0	0.0	147.3	2.7	132.3	3.4	112.6	2.5	105.4	0.6
1984	3	0.0	0.0	147.2	2.5	135.5	3.1	114.5	5.4	106.0	0.7
1984	4	0.0	0.0	149.3	1.2	131.6	2.3	111.9	3.6	106.5	0.8
1984	5	0.0	0.0	150.4	1.6	135.8	3.0	109.0	1.4	107.2	1.0
1984	6	0.0	0.0	150.4	1.7	136.5	3.4	110.0	0.9	108.4	1.0
1984	7	0.0	0.0	147.3	2.9	137.7	4.9	111.0	1.4	109.4	1.0
1984	8	0.0	0.0	143.4	2.5	139.6	3.8	112.2	1.0	110.5	1.2
1984	9	0.0	0.0	144.8	3.1	135.4	4.9	113.2	1.6	110.8	0.6
1984	10	0.0	0.0	149.8	2.1	134.2	3.8	112.6	1.4	112.2	1.9
1984	11	0.0	0.0	152.0	2.4	132.0	7.0	113.5	2.4	111.8	1.6
1984	12	0.0	0.0	154.1	2.2	139.6	3.4	115.6	3.0	112.1	1.6
1985	1	0.0	0.0	158.4	5.2	140.5	4.3	116.5	5.6	112.3	1.4
1985	2	0.0	0.0	153.0	1.9	140.8	5.7	117.2	2.3	112.0	1.1
1985	3	0.0	0.0	155.4	1.7	142.6	3.2	116.4	2.9	112.8	1.4
1985	4	0.0	0.0	155.8	2.3	140.1	3.1	115.8	1.9	114.6	1.3
1985	5	0.0	0.0	155.7	1.0	144.0	3.1	116.7	2.9	115.6	1.2
1985	6	0.0	0.0	155.8	1.6	137.4	2.5	116.5	1.8	116.2	1.2

report (*1*), which noted that hypothetical changes of up to 8% in the emissions could reduce the estimated lifetime deduced from 3 years of data on trends in methylchloroform from 10 to 6.5 years.

The above method for determining τ makes maximum use of the fractional trends in the concentration at each site that are more accurately measured than the tc atmospheric content (which requires kno edge of absolute calibration). An alternat method for determining τ that invol matching model and observed contents *17, 20*) yields $\tau = 6.0$ (+1.1, −0.8) ye (1σ) based on the 7 years of data a includes emission uncertainties. The c crease in the τ estimate by this method fr that obtained from 3 years of data (*1*) almost entirely due to the revision of abs lute calibration for methylchloroform (*1*. The calculated atmospheric content w 2400×10^9 g on 1 January 1982, which the midpoint of the 7-year data period; tl result is sensitive to our specified time of years for mixing between the upper trop spheric boxes and the stratospheric box our model.

A third method for determining τ cor pares observed and model-calculated latit dinal gradients. If we take into account tl uncertainty in the observed latitudinal grac ent that results from uncertainties in the 3 to 90°N average concentration (exemplifie by the difference between Adrigole ar Cape Meares a_i values) and in the concentr tions at the other three stations (Table 2 we calculate that $\tau = 6.0$ (+1.4, −1.0) yea (1σ). Uncertainties in the latitudinal distr bution of emissions are not included he but are not expected to be a significar source of error.

By combining all three of the above way of analyzing the data, the best estimate of τ is 0.159 ± 0.026 year^{-1} (1σ); that is, th atmospheric lifetime of methylchloroform i 6.3 (+1.2, −0.9) years (1σ). If we assum that 6.3 years is the precise methylchloro form lifetime, an alternative inversion prob lem can be solved in which the emission $E(t)$ are the unknowns rather than $1/\tau$ (*17*) In this way, for the seven successive 12 month intervals beginning July 1978, w predict emissions (in units of 10^9 g/year) o 497 ± 41, 553 ± 24, 509 ± 20, 519 ± 42 520 ± 50, 574 ± 61, and 583 ± 26. These generally compare well with emissions fo these intervals deduced from industry data (Table 3).

Our best estimate for $1/\tau = 0.159 \pm 0.026$ year^{-1} (or, equivalently, $A = 0.661 \pm 0.121$) corresponds to a globally averaged tropospheric OH concentration of $(7.7 \pm 1.4) \times 10^5$ radicals cm^{-3} (1σ uncertainties). This estimate is much more accurate than that derived from the much smaller data sets previously available (*1–3, 8*). Since methylchloroform concentrations are proportional to total air density and since the rate of reaction 1 increases with air temperature, this average OH concentration must be interpreted as an appropriate density- and temperature-weighted average. On the basis

Table 2. Optimally determined coefficients (with 1σ uncertainties) in empirical model (Eq. 2) fit to data in Table 1. The mean fractional trends for the 7-year time intervals are given by $(b_i + 7.35\ e_i)/(a_i + 4.08\ d_i)$.

Site	a_i (pptv)	b_i (pptv year^{-1})	d_i (pptv year^{-2})	e_i (pptv year^{-3})	c_i (pptv)	s_i (pptv)
Adrigole, Ireland*	135.6 ± 0.6	5.1 ± 0.8	0.0 ± 0.3	0.1 ± 0.3	1.3 ± 0.7	−1.4 ± 0.7
Cape Meares, Oregon*	132.9 ± 0.5	4.8 ± 0.8	0.2 ± 0.4	0.2 ± 0.4	−1.0 ± 0.6	−2.6 ± 0.7
Adrigole and Cape Meares†	134.3 ± 0.4	5.1 ± 0.3	−0.2 ± 0.1	0.17 ± 0.04	0.2 ± 0.5	−1.8 ± 0.5
Ragged Point, Barbados†	120.0 ± 0.4	6.1 ± 0.3	−0.2 ± 0.1	0.04 ± 0.04	1.2 ± 0.4	−1.4 ± 0.4
Point Matatula, American Samoa†	99.0 ± 0.6	5.1 ± 0.5	−0.4 ± 0.1	0.16 ± 0.06	−0.2 ± 0.5	0.1 ± 0.5
Cape Grim, Tasmania†	97.0 ± 0.3	6.0 ± 0.3	−0.5 ± 0.1	0.07 ± 0.03	0.2 ± 0.3	1.0 ± 0.3

*From December 1979 through December 1983. †From July 1978 through June 1985.

Table 3. Global emissions $E(t)$ computed with Eq. 3 and industry data (*18, 19*). Units are 10^9 g/year and uncertainties are 2σ. Also shown are modified emissions computed by adding or subtracting the quantity 4.353 times t (where t is time in years measured from 1 July 1980) for the years 1976 to 1985, which represents the maximum and minimum trends in emissions in the period from 1976 to 1985 consistent with the 2σ uncertainties.

Year	Emission	Uncertainty	Emissions	
			Maximum trend	Minimum trend
1951	0.09	0.01	0.09	0.09
1952	0.18	0.01	0.18	0.18
1953	0.88	0.09	0.88	0.88
1954	0.58	0.23	2.58	2.58
1955	7.47	0.67	7.47	7.47
1956	12.55	0.95	12.55	12.55
1957	18.83	1.37	18.83	18.83
1958	20.40	1.35	20.40	20.40
1959	29.11	2.11	29.11	29.11
1960	35.23	2.39	35.23	35.23
1961	37.36	2.46	37.36	37.36
1962	54.22	3.95	54.22	54.22
1963	54.62	3.58	54.62	54.62
1964	57.45	4.54	57.45	57.45
1965	75.37	5.08	75.37	75.37
1966	105.14	7.39	105.14	105.14
1967	133.21	8.92	133.21	133.21
1968	147.07	9.38	147.07	147.07
1969	156.42	9.90	156.42	156.42
1970	168.74	10.73	168.74	168.74
1971	178.54	11.29	178.54	178.54
1972	242.12	16.89	242.12	242.12
1973	319.00	21.76	319.00	319.00
1974	360.98	23.18	360.98	360.98
1975	352.58	22.04	352.58	352.58
1976	419.31	19.59	399.72	438.98
1977	455.50	21.24	440.27	470.74
1978	476.21	22.17	465.33	487.10
1979	540.59	25.39	534.06	547.12
1980	544.91	25.28	542.73	547.08
1981	538.68	24.97	540.85	536.50
1982	510.91	23.65	517.44	504.38
1983	515.97	23.97	526.85	505.09
1984	550.03	37.71	565.26	534.79
1985	581.22	39.84	600.81	561.63

Table 4. Lifetime estimates for methylchloroform derived from trends in 7 years of ALE-GAGE data at each site and for all sites combined. Uncertainties are 1σ and, in contrast to uncertainties given in Prinn *et al.* (*1*), include allowance for potential biases of the time series inferred from the variance of the individual site lifetime estimates. Also given are lifetimes derived from global atmospheric content and from latitudinal gradients.

Case	Reciprocal lifetime ($year^{-1}$)	Lifetime (years)	Weight given to site in optimal estimation of lifetime
Adrigole, Ireland and Cape Meares, Oregon	0.162 ± 0.016	6.2 (+0.7, −0.6)	0.26
Ragged Point, Barbados	0.156 ± 0.016	6.4 (+0.7, −0.6)	0.26
Point Matatula, Samoa	0.138 ± 0.017	7.2 (+1.1, −0.7)	0.22
Cape Grim, Tasmania	0.131 ± 0.016	7.6 (+1.1, −0.8)	0.26
All sites from trend	0.145 ± 0.008	6.9 (+0.4, −0.4)	
All sites from trend (with emission trend uncertainty included)	0.145 ± 0.021	6.9 (+1.2, −0.9)	
Global atmospheric content (with emission uncertainty included)	0.167 ± 0.025	6.0 (+1.1, −0.8)	
Latitudinal gradient	0.167 ± 0.031	6.0 (+1.4, −1.0)	

Table 5. Optimally determined tropospheric OH concentrations (units are 10^5 radicals per cubic centimeter and uncertainties are 1σ). Global average tropospheric OH concentration is $(7.7 \pm 1.4) \times 10^5$ radicals per cubic centimeter.

Pressure (mbar)	OH concentration			
	90° to 30°N	30°N to 0°	0° to 30°S	30° to 90°S
200 to 500	4.8 ± 0.9	9.9 ± 1.8	10.4 ± 1.9	6.0 ± 1.1
500 to 1000	4.9 ± 0.9	10.4 ± 1.9	9.8 ± 1.8	5.4 ± 1.0

of the spatial pattern in the theoretical OH concentration $[OH]_i^*$ we can also compute the average OH concentration in each box (which equals $A[OH]_i^*$) (Table 5).

The sensitivity of these results to the assumed theoretical spatial distribution of OH may be evaluated by repeating the calculations with a tropospherically uniform distribution of OH (that is, OH is reduced in the tropics and increased in higher latitudes relative to the theoretical values). A comparison of the two-dimensional model results for nonuniform and uniform distributions shows a decrease in the model Northern Hemisphere mid-latitude methylchloroform concentrations by 2.3% because of the substantially increased OH levels there. The increase in the model tropical lower troposphere is less (only 0.4%) because of the reduction in the OH concentrations there. There is thus a small overall decrease in globally averaged model methylchloroform concentrations of 1.4% for the case of uniform OH concentrations. The sensitivity of the globally averaged lifetime estimates to the distribution of OH within the troposphere is negligible (a decrease in the estimated lifetime τ of only 0.1 year is obtained with uniform OH) except for the lifetime that would be inferred from the latitudinal distribution of methylchloroform, which would decrease by approximately 0.3 year).

Methane is observed to be increasing throughout the world and its global tropospheric distribution has been measured (*22*). The major tropospheric sink for methane is reaction with the hydroxyl radical with a rate constant similar to that for methylchloroform (*23*). Therefore, the average hydroxyl radical concentrations deduced from methylchloroform (Table 5) have been used together with observed atmospheric temperatures and the global distribution and rate data for methane (*22, 23*) to calculate an average tropospheric lifetime for methane of 9.6 (+2.2, −1.5) years (1σ). The uncertainty in this lifetime does not include uncertainty in the rate constants.

REFERENCES AND NOTES

1. R. Prinn *et al.*, *J. Geophys. Res.* **88**, 8415 (1983).
2. A. Khalil and R. Rasmussen, *Tellus* **36B**, 317 (1984).
3. P. Fraser, P. Hyson, R. Rasmussen, A. Crawford, A. Khalil, *J. Atmos. Chem.* **4**, 3 (1986).
4. J. C. McConnell and H. I. Schiff, *Science* **199**, 174 (1978); P. Crutzen, I. Isaksen, J. McAfee, *J. Geophys. Res.* **83**, 345 (1978).
5. M. Molina and F. Rowland, *Nature (London)* **249**, 810 (1974); R. Stolarski and R. Cicerone, *Can. J. Chem.* **52**, 1610 (1974).
6. R. Ramanathan, R. Cicerone, H. Singh, J. Kiehl, *J. Geophys. Res.* **90**, 5547 (1985).
7. Y. Yung, M. McElroy, S. Wofsy, *Geophys. Res. Lett.* **2**, 397 (1975); R. Cox, R. Derwent, A. Eggleton, J. Lovelock, *Atmos. Environ.* **1**, 305 (1976).
8. Pioneering studies were done by H. Singh [*Geophys. Res. Lett.* **4**, 453 (1977)], J. E. Lovelock [*Nature (London)* **267**, 32 (1977)], and Y. Makide and S. Rowland [*Proc. Natl. Acad. Sci. U.S.A.* **78**, 5933 (1981)].
9. H. Levy II, *Science* **173**, 141 (1971); Global Tropospheric Chemistry Panel, *Global Tropospheric Chemistry: A Plan for Action* (National Academy Press, Washington, DC, 1984).
10. ALE is described by R. Prinn *et al.* [*J. Geophys. Res.* **88**, 8353 (1983)] and in five reports that immediately follow. GAGE is a follow-on to ALE in which the ALE HP 5840 instruments (Hewlett-Packard) (4 measurements per day) were first run together with and then replaced by HP 5880 instruments (12 measurements per day). Agreement between ALE and GAGE instruments for methylchloroform was excellent during the overlap period.
11. The stations are located at Adrigole, Ireland (52°N, 10°W), Cape Meares, Oregon (45°N, 124°W), Ragged Point, Barbados (13°N, 59°W), Point Matatula, American Samoa (14°S, 171°W), and Cape Grim, Tasmania (41°S, 145°E). The Cape Meares station was opened in January 1980 and the Adrigole station was closed in December 1983. All of the other stations opened in July 1978.
12. Our new calibration, which is based on A. Khalil and R. Rasmussen [*Chemosphere* **13**, 789 (1984)], is specifically 0.80 ± 0.08 (1σ) times our old calibration standard, which was based on R. Rasmussen and J. Lovelock [*J. Geophys. Res.* **88**, 8369 (1983)]. This means that the so-called ALE-GAGE calibration factor for methylchloroform is 0.80 ± 0.08 in the present report compared to 1.0 ± 0.15 in our previous report (*1*). In (*1*) we noted that multiplying our old calibration standard by 0.82 yielded a better fit to observations and a lifetime estimate of 6.5 years [similar conclusions were made in (*2*) and (*3*)].
13. The techniques involved identifying large, highly coherent short-term increases in several anthropogenic halocarbons and detection of the anthropogenic species trichloroethylene and perchloroethylene, which have atmospheric lifetimes of only a few days (*1, 10*). Episodes of pollution are fairly common at Adrigole (about one-third of the time) and, although much rarer, are becoming more common at the other sites. Autocovariances computed by using the complete data record at Adrigole indicate that these techniques are indeed effective in identifying polluted air at this site (M. Prather, personal communication).
14. A tape that contains every calibrated measurement taken from 1978 to 1985 including the polluted periods can be obtained from F. Alyea, Georgia Institute of Technology, Atlanta, GA 30332.
15. M. J. Prather, *Nature (London)* **317**, 221 (1985).
16. A. Golombek and R. Prinn, *J. Geophys. Res.* **91**, 3985 (1986).
17. D. Cunnold *et al.*, *ibid.*, p. 10797.
18. Global production data are from W. Neely and J. Plonka [*Environ. Sci. Technol.* **12**, 317 (1978)] for 1951 through 1976, and P. Midgley [in *Atmospheric Ozone 1985* (World Meteorological Organization, Geneva, 1985), p. 72], for 1976 through 1983. Global and semihemispheric sales data are from Prinn *et al.* (*1*) for 1977 through 1981, and P. Midgley (ICI Americas, Inc., letter, 18 April 1986) for 1979 to 1985. Uncertainty (2σ) in these production and sales data is ±5%. The percentages sold in each semihemisphere (90° to 30°N, 30°N to 0°, 0° to 30°S, and 30° to 90°S) are 96.67, 1.36, 0.47, and 1.50 in 1977; 96.38, 1.41, 0.55, and 1.66 in 1978; 95.70, 1.6, 0.9, and 1.8 in 1979; 95.5, 1.8, 0.9, and 1.8 in 1980; 95.1, 2.0, 1.0, and 1.9 in 1981; 94.7, 2.2, 1.1, and 2.0 in 1982; 94.50, 2.5, 1.1, and 1.9 in

1983; 94.4, 2.8, 1.1, and 1.7 in 1984; and 94.4, 2.9, 1.1, and 1.6 in 1985. We assumed the percentages before 1977 varied linearly from their 1951 values (100, 0, 0, and 0) to their 1977 values.
19. Specifically, we assumed that $a = 1/24 \pm 1/24$ after 1964 and $0 \pm 1/24$ before 1964, $b = 1/12 \pm 1/12$, and $f = 0.94 \pm 0.02$, based on industry evaluations (*1*). Uncertainties are 2σ.
20. D. Cunnold *et al.*, *J. Geophys. Res.* **88**, 8379 (1983).
21. Values for [OH], and k_i are given in Prinn *et al.* (*1*) and are based, respectively, on the theoretical model of J. Logan *et al.* [*J. Geophys. Res.* **86**, 7210 (1981)] and the kinetic studies of K. Jeong and F. Kaufman [*Geophys. Res. Lett.* **6**, 757 (1979)] and others. Theoretical OH concentrations are a sensitive function of ultraviolet irradiance and O_3, H_2O, CO, NO, and NO_2 concentrations.
22. L. Steele *et al.*, *J. Atmos. Chem.* **5**, 125 (1987).
23. D. Davis, S. Fischer, R. Schiff, *J. Chem. Phys.* **61**, 2213 (1974).
24. We thank M. Prather for constructive comments. Supported by NASA (grants NAGW-732, NAGW-729, NASW-4057, and NAGW-280); Chemical Manufacturers Association (contract FC-85-567); NOAA (contract NA85-RACO5103); Commonwealth Scientific and Industrial Research Organization, Victoria, Australia; and Bureau of Meteorology, Melbourne, Australia.

2 June 1987; accepted 1 September 1987

JOURNAL OF GEOPHYSICAL RESEARCH, VOL. 99, NO. D1, PAGES 1107–1126, JANUARY 20, 1994

Global trends and annual releases of CCl_3F and CCl_2F_2 estimated from ALE/GAGE and other measurements from July 1978 to June 1991

D. M. Cunnold,[1] P. J. Fraser,[2] R. F. Weiss,[3] R. G. Prinn,[4] P. G. Simmonds,[5] B. R. Miller,[3] F. N. Alyea,[1] and A. J. Crawford[6]

Abstract. Thirteen years of Atmospheric Lifetime Experiment/Global Atmospheric Gases Experiment CCl_3F and CCl_2F_2 measurements at five remote, surface, globally distributed sites are analyzed. Comparisons are made against shipboard measurements by the Scripps Institution of Oceanography group and archived air samples collected at Cape Grim, Tasmania, since 1978. CCl_3F in the lower troposphere was increasing at an average rate of 9.2 ppt/yr over the period July 1978 to June 1988. CCl_2F_2 was increasing at an average 17.3 ppt/yr in the lower troposphere over the same period. However, between July 1988 and June 1991 the increases of CCl_3F and CCl_2F_2 in this region have averaged just 7.0 ppt/yr and 15.7 ppt/yr, respectively. The rate of increase has been decreasing 2.4 ppt/yr^2 and 2.9 ppt/yr^2 over this 3-year period. Based on a recent scenario of the global releases of these compounds and using the new calibration scale SIO 1993, the equilibrium lifetimes are estimated to be 44^{+17}_{-10} and 180^{+820}_{-81} years for CCl_3F and CCl_2F_2, respectively. Using these lifetime estimates and a two-dimensional model, it is estimated that global releases of these two chlorofluorocarbons in 1990 were 249 ± 28 × 10^6 kg for CCl_3F and 366 ± 30 × 10^6 kg for CCl_2F_2. It is also estimated that combined releases of these chlorofluorocarbons in 1990 were 21 ± 5% less than those in 1986.

1. Introduction

Observed changes in atmospheric ozone, in particular in the Antarctic stratosphere, have been established to be primarily the result of the long-term accumulation of chlorofluorocarbons (CFCs) in the atmosphere [*Solomon*, 1990; *Anderson et al.*, 1991]. As a result, a worldwide effort was made to limit the production of chlorofluorocarbons [*United Nations Environmental Programme* (*UNEP*), 1987; *World Meteorological Organization* (WMO), 1988]. By this agreement, participating nations were required to limit their consumption (defined as production plus imports minus exports) in 1989 to 1986 levels. Moreover, by 1994, emissions are to be reduced to 80% of 1986 levels [*Albritton*, 1989]. This paper discusses 13 years of gas chromatographic observations of the chlorofluorocarbons CCl_3F (CFC-11) and CCl_2F_2 (CFC-12) at Ragged Point, Barbados (13°N, 59°W), and Cape Grim, Tasmania (41°S, 145°E), for the period July 1978 to June 1991. The data set also includes observations at Cape Matatula, American Samoa (14°S, 171°W), at Cape Meares, Oregon (45°N, 124°W), for the period December 1979 to June 1989, at Adrigole, Ireland (52°N, 10°W), from July 1978 to December 1983, and at Mace Head, Ireland (53°N, 10°W), from February 1987 to June 1991.

As a result of small changes in absolute calibration based on changing to the Scripps Institution of Oceanography (SIO 1993 scale) standards and new estimates of worldwide releases [*Alternative Fluorocarbons Environmental Acceptability Study* (*AFEAS*), 1992] which are supported by a compilation for 1986 by *UNEP* [1990], the atmospheric lifetimes of CCl_3F and CCl_2F_2 have been recalculated [cf. *Cunnold et al.*, 1986]. Annual releases derived from the measurements are then compared against the new worldwide production and release estimates. The atmospheric lifetimes of these gases are critical parameters for estimating how long the chlorofluorocarbons remain in the atmosphere after the emissions cease. The annual release estimates are important for assessing worldwide conformity to the Montreal Protocol.

There is strong evidence that a small (<2%) shift in Atmospheric Lifetime Experiment (ALE)/Global Atmospheric Gases Experiment (GAGE) secondary calibration occurred during the analysis period. Moreover, because there has been a factor of approximately 2 increase in the atmospheric concentrations of the chlorofluorocarbons over this period, nonlinearities in instrumental response can have important effects on long-term trends. The principal concern in this regard is possible nonlinearity in the response of the Oregon Graduate Institute (OGI) instrument used to assign

[1]School of Earth and Atmospheric Sciences, Georgia Institute of Technology, Atlanta.
[2]Division of Atmospheric Research, CSIRO, Aspendale, Victoria, Australia.
[3]Scripps Institution of Oceanography, University of California, La Jolla.
[4]Center for Global Change Science, MIT, Cambridge, Massachusetts.
[5]Department of Biogeochemistry, University of Bristol, Bristol, England.
[6]Center for Atmospheric Studies, Oregon Graduate Institute, Beaverton.

Paper number 93JD02715.
0148-0227/94/93JD-02715$05.00

values to the calibration tanks. Based on a limited set of measurements of the nonlinearity of the HP5880A instruments, some corrections to the values assigned to the calibration tanks used at the ALE/GAGE sites were made by the OGI team. However, the resulting long-term data set contained some inconsistencies. An incremental adjustment in calibration in 1987 has been made to both the CCl_3F and the CCl_2F_2 time series. These adjustments are discussed and it is shown that the data set presented here is consistent with two sets of independent measurements.

2. Absolute Calibration for CCl_3F and CCl_2F_2

The Advanced Global Atmospheric Gases Experiment (AGAGE) team is presently engaged in the development of new primary calibration scales for all its measurements by extending the "bootstrap" technique used previously at the SIO to calibrate measurements of N_2O, CCl_3F, and CCl_2F_2. This method uses accurately known mixtures of atmospheric trace gases at roughly their ambient molecular ratios to extend the calibration scales to successively lower concentrations and emphasizes the use of large volumes of gas to minimize measurement and handling errors. The N_2O calibration scale [*Weiss et al.*, 1981] is based on the preparation of accurate mixtures of N_2O in CO_2 at ambient ratios of about 9×10^{-4} and on accurate measurement of CO_2 at ambient levels [*Keeling et al.*, 1976]. Thus CO_2 is the bootstrap gas for N_2O. In turn, the CCl_3F and CCl_2F_2 calibrations [*Bullister*, 1984; *Bullister and Weiss*, 1988] are based on accurate mixtures of CFCs in N_2O at their ambient ratios, diluted in CFC- and N_2O-free "zero air" to near-ambient N_2O levels and calibrated by measuring the resulting N_2O concentrations. Thus N_2O is the bootstrap gas for the CFCs. In this way standards in the 10^{-11} concentration range can be prepared from mixtures with minor/major component ratios greater than 10^{-4}. Because the errors in the determination of CO_2 are much less than for N_2O and the errors in the determination of N_2O are much less than for the CFCs, the calibration results are not significantly penalized by the additional steps used in this method.

Measurements of CCl_3F and CCl_2F_2 by the SIO group have been reported on the SIO 1984 [*Weiss et al.*, 1985] and SIO 1986 [*Bullister and Weiss*, 1988] calibration scales. These scales are based on CFC/N_2O mixtures prepared volumetrically (using the virial equation of state for nonideality corrections) and diluted to near-ambient concentration levels by introducing aliquots of these mixtures into silanized aluminum high-pressure cylinders using an all-metal high vacuum system.

At the beginning of AGAGE an effort was made to use the same apparatus to prepare ambient-level standards for the less volatile CCl_2FCClF_2 (CFC-113), but the results showed unacceptably poor precision (order 5%) which we have since demonstrated to be due to the adsorption of small amounts of this compound (order 10^{-5} cm^3 STP) onto the walls of the high vacuum system during the introduction of aliquots of the CFC/N_2O mixtures. To solve this problem, we constructed a separate system to introduce aliquots of the CFC/N_2O mixtures directly into the primary standard cylinders using a high-pressure gas chromatography sampling valve which reduces the surface area exposed to the injected aliquots by about 2 orders of magnitude, has no unflushed "dead volumes," and is never exposed to pure CFCs. Using this system, we are able to obtain highly reproducible results for all the AGAGE halocarbons, including the three least volatile compounds CCl_2FCClF_2, CH_3CCl_3 (methyl chloroform), and CCl_4 (carbon tetrachloride).

The least volatile AGAGE halocarbons are also not suitable for gas phase volumetric calibration because their vapor pressures are low and their nonidealities have not been determined with sufficient accuracy. We have therefore developed a gravimetric method for preparing halocarbon/N_2O mixtures, in which roughly 10^{-2} to 10^{-1} g quantities of the pure halocarbon components are weighed in sealed glass microcapillary tubes and roughly 10 g quantities of the diluent N_2O are determined by weighing the prepared mixtures in 0.8-L stainless steel canisters. The AGAGE primary standards are then prepared in 35-L electroplished stainless steel high-pressure cylinders, to which 10 torr of water vapor are added to inhibit the degradation of CCl_4 and CH_3CCl_3 which we and others [cf. *Yokohata et al.*, 1985] have observed in dry containers. For CCl_3F and CCl_2F_2 we have observed no measurable drifts in SIO primary or secondary standards stored in either silanized aluminum or electropolished stainless steel cylinders.

The AGAGE primary calibrations are still in progress, and the details of these techniques and their results will be discussed in a separate publication. However, we are sufficiently confident that our progress to date constitutes a significant improvement over our previous methods to release a new SIO 1993 calibration scale for CCl_3F and CCl_2F_2. The atmospheric CCl_3F and CCl_2F_2 results in this paper are therefore reported on the SIO 1993 calibration scale. The units are dry air mole fractions.

The SIO 1993 scale for CCl_3F and CCl_2F_2 is based on seven independent primary standards prepared using gravimetric CFC/N_2O mixtures. The gases used in these standards had quoted purities of 99.9% for CCl_3F, 99.97% for CCl_2F_2 (both Aldrich Chemical), and 99.99% for N_2O (Matheson). The diluent zero air (Air Products) was further purified of all detectable traces of these CFCs and N_2O using a molecular sieve 13X trap at −78°C. Chromatographic comparisons among these standards showed precisions of standard preparation (expressed as relative standard deviation (rsd)) of 0.20% for CCl_3F and 0.14% for CCl_2F_2. Comparisons between standards prepared using gravimetric CFC/N_2O mixtures and standards prepared using volumetric CFC/N_2O mixtures showed no significant differences, but the SIO 1993 scale is based only on the gravimetric values because this method gives higher precisions.

The SIO 1993 scale has been compared to the SIO 1986 and SIO 1984 scales for these compounds by the direct chromatographic comparison of primary standards. Values reported on the SIO 1986 scale may be converted to the SIO 1993 scale (see Table 1) by dividing by 1.0251 for CCl_3F and 0.9874 for CCl_2F_2. To convert from the SIO 1984 scale to the SIO 1993 scale, divide by 1.021 for CCl_3F and 0.984 for CCl_2F_2.

We expected better agreement between the SIO 1993 and the SIO 1986 calibration scales. For both CCl_3F and CCl_2F_2 these shifts are somewhat greater than our combined estimates of systematic uncertainties (see Table 1). We have invested considerable effort to understand these discrepancies. For CCl_3F, comparisons between new standards prepared with the same canister of Linde pure CCl_3F used for the earlier SIO standards and those prepared with the new

Table 1. Comparisons of Oregon Graduate Institute (OGI) and Scripps Institution of Oceanography (SIO) Calibration Standards for CCl_3F and CCL_2F_2

			CCl_3F			CCL_2F_2			
Standard	Reference	Basis of Comparison	Systematic Uncertainty of Standard	Ratio of Standard to SIO 1993	Standard Error of Comparison	Systematic Uncertainty of Standard	Ratio of Standard to SIO 1993	Standard Error of Comparison	ALE/GAGE Publications Using This Standard As Reference
SIO 1993	In preparation, 1993	...	0.008	1.000	...	0.005	1.000	...	this paper
SIO 1986	*Bullister and Weiss* [1988]	direct primary standard comparisons (1993)	0.013	1.0251	0.001	0.005	0.9874	0.001	*Cunnold* [1992], but see section 3
OGI 1987*	this paper, no standard made; see text	five GAGE calibration gases *S*-001, *S*-003, *G*-006, *G*-008, and *G*-013 (1991–1992)	0.02	1.036	0.003	0.02	0.977	0.004	not used; see text
OGI 1980	*Rasmussen and Lovelock* [1983]	three OGI calibration gases (1984)	0.02	1.055	0.004	0.02	0.962	0.005	*Cunnold et al.* [1983*a*, *b*, 1986]

Measurements were performed at SIO and are reported as the mean ratios to the SIO 1993 calibration scale values (see text). Comparisons between OGI and SIO scales were carried out with three OGI calibration standards in 1984 (*Weiss et al.* [1985], the values reported here differ slightly from those published in 1985 because of improved data fitting procedures and use of the SIO 1993 scale) and with five Global Atmospheric Gases Experiment (GAGE) calibration standards in 1991–1992 (see text). ALE, Atmospheric Lifetime Experiment.

*The OGI 1987 scale refers to the measurements after August 1987 prior to the adjustments discussed in section 4.

Aldrich pure CCl_3F show that the Linde-based standards are systematically 0.8% lower in CCl_3F concentration. This difference is well outside the 0.2% precision of the standard preparations and strongly suggests that the Linde CCl_3F is contaminated below its quoted purity of 99.9%. We attribute the remaining CCl_3F discrepancy of about 1.7% to the adsorption of CCl_3F in the high vacuum system, as was found for CCl_2FCClF_2. CCl_3F is more volatile than CCl_2FCClF_2 and less volatile than CCl_2F_2, and the precision obtained for CCl_3F in the older calibrations (1.9% rsd) is significantly poorer than for CCl_2F_2 (0.7% rsd), so the sign and magnitude of this discrepancy and the improvements in precision are all consistent with this explanation. While there are several possible explanations for the smaller and opposite-sign discrepancy in the CCl_2F_2 calibration, we have not yet identified its cause. In view of the marked improvements in our primary calibration procedures, we estimate the systematic uncertainties of the SIO 1993 scale as 0.8% for CCl_3F and 0.5% for CCl_2F_2.

All of the SIO chromatographic standard comparisons and SIO atmospheric CCl_3F and CCl_2F_2 measurements reported here have been corrected for instrumental nonlinearities as determined at the time of the measurements [*Bullister and Weiss*, 1988]. We have also confirmed the accuracy of these corrections by injecting and trapping fixed-volume aliquots of standard gas at variable pressure as determined by a high-precision Paroscientific quartz pressure gauge. CCl_3F sensitivity tends to increase with increasing concentration, while CCl_2F_2 sensitivity tends to decrease with increasing concentration. Typical calibration curves are shown by *Bullister and Weiss* [1988].

The relationships between CCl_3F and CCl_2F_2 calibration gases used in the ALE/GAGE program and the SIO 1993 calibration scale are summarized in Table 1. The original ALE calibration paper [*Rasmussen and Lovelock*, 1983] describes an ALE working standard (based on earlier calibration work at OGI) and an absolute calibration scale (based on exponential dilution and coulometry) which we shall refer to as the OGI 1980 scale. To obtain OGI 1980 values, ALE working standard values are multiplied by 0.96 for CCl_3F and by 0.95 for CCl_2F_2. ALE/GAGE databases have traditionally been maintained on the ALE working standard scale, while previous ALE/GAGE CCl_3F and CCl_2F_2 papers [*Cunnold et al.*, 1983*a*, *b*, 1986] have been based on the OGI 1980 scale. Table 1 also shows the results of a comparison of CCl_3F and CCl_2F_2 in subsamples of three OGI primary standards measured at SIO in 1991–1992. It is evident that between 1984 and 1991 the calibration standards, against which the ALE/GAGE measurements have been referenced, have shifted downward by about 1.8% in CCl_3F and upward by about 1.6% in CCl_2F_2. We shall refer to the post-1987 data as having been measured on the OGI 1987 scale. These shifts have been removed from the ALE/GAGE data reported in this paper (the procedure used to remove them is described in section 4).

The SIO 1993 scale is approximately equal to the University of Tokyo scale for CCl_3F [cf. *Fraser et al.*, 1993] but gives approximately 1% larger concentrations of CCl_2F_2.

3. Atmospheric Lifetime Experiment (ALE)/ Global Atmospheric Gases Experiment (GAGE) Data From July 1983 to June 1991

The first five years (1978–1983) of CCl_3F and CCl_2F_2 measurements have been discussed by *Cunnold et al.* [1983*a*, *b*, 1986]. Over the next several years the aging of the gas chromatographs necessitated a change in instrumentation with the Hewlett Packard HP5840A instruments being replaced by HP5880As. The date of this change varied from site to site, but in each case, a minimum of 3 months of simultaneous measurements with both instruments was collected to ensure a smooth transition. This transition from the ALE program to the GAGE program included a change from four to twelve atmospheric samples analyzed per day. CCl_3F measurements continued to be made on both the silicone (S) and the Porasil (*P*) columns of each instrument and the CCl_2F_2 measurements were obtained, as before, on the Porasil channel.

The only extended period of missing GAGE data occurred at Cape Grim and was the result of a faulty Nafion drier which allowed water containing local contamination to enter the instrument from February 19 to May 4, 1987. The affected data have been removed from the data set. As in previous analyses, data which have been influenced by local pollution and identified by simultaneous increases of several gases, particularly CCl_3F, CCl_2F_2, and CH_3CCl_3, have been filtered out of the data set prior to analysis. This filter was responsible for removing approximately one third of the data collected at Adrigole and Mace Head and occasional periods at the other sites.

Because of a lack of availability of new calibration gases between 1985 and 1987 (calibration tanks have since been obtained from a new supplier) a number of old calibration tanks were recycled to the field sites without being refilled. As a result, and because of the steady increase in ambient concentrations, around 1987 there were a number of periods of observation during which substantial concentration differences existed between the calibration tank and the ambient air samples. During these periods, systematic differences between CCl_3F-derived air concentrations on the two columns were obtained, with the differences (up to 15 ppt) being found to be approximately proportional to the ambient/calibration tank concentration differences between the calibration gases and the ambient air. Different sensitivities to these differences were noted at each observing site. This problem was identified as a nonlinearity in the response of the electron capture detectors (ECD) of the HP5880A to different CCl_3F concentrations.

The nonlinearity was approximately evaluated for the HP5880A at each site by measurements using eight flasks with a range of a factor between 2 and 3 in the dilutions of CCl_3F and other GAGE gases. Under the assumption that the nonlinearity in instrument response (R) is expressed in the form $R = ax^{1-\varepsilon}$, where x is the concentration of the gas sample, values of ε (and a) were determined. It was found that the HP5880As were quite nonlinear in their responses to CCl_3F variations, with the degree of nonlinearity varying from one instrument/ECD to another. The measured values of ε were found to be consistent with the GAGE ambient CCl_3F measurement differences on the silicone (S) and Porasil (P) columns at each site. For the other GAGE gases the ε values were small (≤ 0.05) and for CCl_2F_2, in particular, the average ε for all the instruments equaled 0.03 ± 0.02 (where the error bar is the standard deviation of ε differences between the sites).

The systematic differences between the CCl_3F S and P column measurements on each instrument and during each calibration tank usage period have been removed in the reported GAGE data by the following procedure: at sites where one column was measured to be substantially more linear than the other, an adjustment factor, which was constant over each calibration tank usage period, was applied to the measurements on the more nonlinear column. This factor was equal to the mean ratio of the CCl_3F measurements on the two columns over the individual period. This procedure was used at Cape Grim (where ε for the S and P columns had measured values of -0.19 and 0.02, respectively) and Ragged Point (for which the ε values were uncertain but were clearly larger on the Porasil column). At Cape Meares and Cape Matatula the measured ε for the two columns were slightly larger than 0.1 but, fortuitously, were approximately equal and of opposite sign. Equal and opposite adjustment factors over individual calibration tank periods were applied with each factor being equal to one-half the mean ratio between the two column measurements over the period. At Mace Head the CCl_3F responses were found to be approximately linear and no adjustments were made to the data. Because of these adjustments the two columns of GAGE CCl_3F measurements are less independent than they were during the ALE measurements.

Following these adjustments, the average nonlinearity in the GAGE measurements of CCl_3F is $\varepsilon = 0.01 \pm 0.03$. No adjustments for this residual nonlinearity or the small nonlinearity in the CCl_2F_2 have been made in the ALE/GAGE data. Since the identification of nonlinearity effects in 1988, efforts have been made to ensure that the contents of calibration tanks are within 10% of the mean local ambient air concentrations during the measurement period at each site.

Possible nonlinearity in the OGI instrument used to assign the values to the calibration tank contents is particularly critical for assessing long-term trends. This instrument was included in the nonlinearity tests made in 1988 and yielded $\varepsilon = -0.03$ for the s column for CCl_3F and $\varepsilon = 0.02$ for CCl_2F_2. Because these ε values are small and the estimates are only approximate, the possible uncorrected nonlinearity effects inherent in the reported ALE/GAGE measurements is considered to be the average of those for all the instruments, i.e., $\varepsilon = 0.01 \pm 0.03$ for CCl_3F and $\varepsilon = 0.03 \pm 0.02$ for CCl_2F_2 (all uncertainities given in this paper are $\pm 1\sigma$).

4. Long-Term Trend Uncertainties

The success of any long-term measurement depends upon the investigators' ability to consistently reference the measurements against calibrated standards. As has already been indicated, based on Table 1, a change or shift in the secondary (or tertiary) standards occurred sometime between 1984 and 1991. A number of calibration tanks used in the field were reused several times between 1978 and 1987 without being refilled. Before each reuse, the concentrations of CCl_3F and CCl_2F_2 in each tank were reassigned at OGI based upon comparisons against the secondary and tertiary standards. The history of these assigned concentrations provides a test of the consistency of the calibration proce-

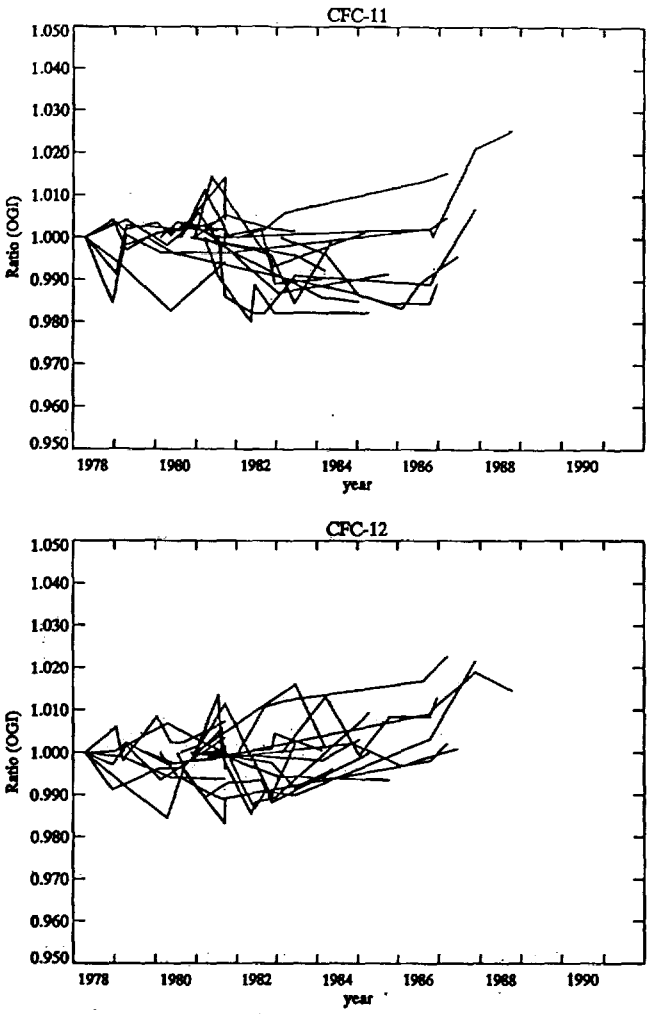

Figure 1. The ratios of different Oregon Graduate Institute measurements of the same air samples to the first measurements over the period 1978–1987. Succeeding measurements of the air in the same Atmospheric Lifetime Experiment/Global Atmospheric Gases Experiment (ALE/GAGE) calibration tanks have been joined by straight lines. (Top) CCl_3F and (bottom) CCl_2F_2.

dure between 1978 and 1987. Figure 1 shows temporal variations in the assigned concentrations divided by the concentration assigned at the time of the first measurement for a number of gases. While small drifts (≤1%) may have occurred before 1987, larger upward drifts are seen in 1987 and obvious problems (not shown) are evident in the OGI GAGE calibration records after this time.

The problem of drifting secondary and/or tertiary standards was recognized by the GAGE team in 1987 and 1988. The available calibration records prior to 1989 have been analyzed and one of us (A.J.C.) undertook an investigation of the CCl_3F- and CCl_2F_2-assigned values and the standards against which they were referenced. Corrected concentrations were obtained and A.J.C. assumed responsibility for providing gas concentrations for the tanks used in 1988 and 1989. Despite the efforts made, it appears that these gas concentrations were not on the same calibration scale. This problem probably arose from changes in the working relationship that existed between the GAGE team and OGI in 1987–1989, and we are consequently less sure of the consistency of the calibration in this period than at other times. Since 1989, the OGI responsibility for providing calibration gases to the GAGE team has been taken over by CSIRO (P.J.F.) and the tanks have been filled at Cape Grim under "baseline" conditions, when the wind was from the southwestern quadrant. Continuity of calibration since 1989 has been maintained by using three calibration gases, which were assigned values on the OGI 1987 scale, as reference standards.

We interpret Table 1 as indicating that the OGI 1987 scale and the original OGI 1980 scale are different, with the OGI 1987 scale being approximately 1.8% lower for CCl_3F and 1.6% higher for CCl_2F_2. Based on the secondary calibration history illustrated in Figure 1 and the available calibration records, prior to September 1, 1987, the ALE/GAGE CCl_3F and CCl_2F_2 values reported here are based on the calibration gas concentrations assigned by OGI. However, after September 1, 1987, the OGI 1987 values multiplied by 1.018 for CCl_3F and divided by 1.016 for CCl_2F_2 are used. (Actually the final values assigned to the gases in a calibration tank are a mean of the values measured at OGI just prior and just after its use at a field site. For those tanks whose field stay included September 1, 1987, an average of the OGI 1980 and the OGI 1987 value has been used.) This procedure obviously removes the discrepancy shown in Table 1. (The time series reported by *Cunnold* [1992] consist of the original CCl_2F_2 series divided by 1.017 after September 1, 1987, and the CCl_3F series without the 1.8% adjustment.) We shall now show that these adjustments produce time series without any obvious discontinuities and which agree with available independent measurements.

Table 2 shows a comparison of the mean values of CCl_3F and CCl_2F_2 during the ALE to GAGE overlap periods when both the HP5840A and the HP5880A were being used. At Cape Grim, Tasmania, this period of common measurements lasted 42 months; the differences in mean, trend, and curvature are shown for this period (see equation (1)). At the other sites the overlap period is short and only the mean values are compared. The error bars are based on typical standard deviations when the 13-year time series are fitted by this type of model. The only difference which is significant at the 95% confidence level is in CCl_3F at Cape Meares. Overall, however, the differences are consistent with the error bars, except perhaps for the curvture terms.

Figures 2 and 3 show the results of repeating the calculations used in generating Figure 1 but now using the adjusted data. Only calibration gases which were remeasured over an interval exceeding 3 years have been included in these figures. The bottom halves of each figure show the means of the curves contained in the top parts of the figures. To allow for the possibility that drifts over the first few years have been masked by the different times of initial calibration, separate curves are also shown for those gases which were first measured before July 1980 and those gases first measured after this time. These curves suggest that the reported CCl_3F and CCl_2F_2 time series contain no drifts in calibration exceeding approximately 0.5% before 1987.

Unfortunately, there were no tanks used prior to 1987 that were reused after 1987. However, many calibration gases were assigned calibrations on both the OGI 1980 and the OGI 1987 scales. Our supposition that there exists an offset between the two OGI scales on September 1, 1987, may be tested by comparing the values assigned before and after this

Table 2. ALE (HP5840A) and GAGE (HP5880A) Overlap Periods and Mean Ratios (ALE/GAGE) of the Measured Concentrations during These Periods

Site	Period	ALE/GAGE Means CCL_3F	ALE/GAGE Means CCl_2F_2
Adrigole/Mace Head	9/87–1/88	1.002 ± 0.007	1.009 ± 0.009
Cape Meares, Oregon	9/83–7/84	1.013 ± 0.005	1.005 ± 0.006
Ragged Point, Barbados	8/85–4/86	0.998 ± 0.005	1.004 ± 0.006
Cape Matatula, American Samoa	7/85–5/86	0.995 ± 0.005	0.997 ± 0.006
Cape Grim, Tasmania	12/81–6/85	1.001 ± 0.002	0.998 ± 0.003
Empirical Model Coefficients (See Equation (1)) for Cape Grim for December 1981 to June 1985	a_1, ppt	b_1, ppt/yr	d_1, ppt/yr^2
CCl_3F(S)			
ALE	185.9 ± 0.3	8.6 ± 0.3	−0.8 ± 0.7
GAGE	185.7 ± 0.3	8.3 ± 0.3	1.4 ± 0.7
CCl_3F(P)			
ALE	185.7 ± 0.3	8.5 ± 0.4	0.0 ± 0.9
GAGE	185.7 ± 0.4	8.3 ± 0.4	1.4 ± 0.9
CCl_2F_2			
ALE	341.8 ± 0.9	17.6 ± 0.9	−0.8 ± 1.7
GAGE	342.4 ± 0.9	16.1 ± 0.9	−1.7 ± 1.7

For Cape Grim, Tasmania, the empirical model (centered on month 63) coefficients over the 3.5-year data period are also given. Since the ALE and GAGE measurements used different calibration tanks, the error bars are based on noise variances for the 13-year data set, which include the effect of tank changes.

date to the same tank, i.e., the tanks whose time in the field included September 1, 1987. This calculation indicates that after approximately September 1, 1987, the OGI 1987 scale was 2.5 ± 0.8% less than the OGI 1980 scale for CCl_3F and 0.4 ± 0.8% higher for CCl_2F_2. This result supports the adjustment made for CCl_3F but suggests that a calibration drift for CCl_2F_2 may actually have occurred over a longer time period.

5. Comparisons Against Shipboard and Archived Air Samples at Cape Grim

Since chlorofluorocarbons should be well mixed in the southern hemisphere, particularly at the latitude of Cape Grim, useful comparisons can be made against the multiyear data set of shipboard observations. In these comparisons, monthly means of the shipboard data obtained south of 30°S have been used. These measurements were made by shipboard gas chromatography with cryogenic preconcentration and nonlinearity correction [*Bullister and Weiss*, 1988]. They have been adjusted from the SIO 1986 calibration scale to the SIO 1993 scale using the Table 1 data.

Since the beginning of the ALE/GAGE program, P.J.F. has been archiving several ambient air samples per year in stainless steel tanks. These tanks are similar to those used for the calibration gases. Figures 1 and 2 provide good evidence that CCl_3F and CCl_2F_2 are stable in these tanks over many years of use (because of the discontinuous and tank-to-tank consistency of the changes in 1987, the changes in 1987 have been interpreted as a problem with the calibration standards and as not being related to drifts in these calibration gas tanks). These tanks were filled at Cape Grim during baseline conditions. These tanks, which contain samples collected as far back as April 1978, have recently been analyzed using the HP5880A at Cape Grim. The calibration gases used in these measurements were also cylinders filled at Cape Grim (*G* series gases). The assigned gas concentrations for the *G* series gases were obtained by measurements on the Cape Grim instrument against three calibration gases, *R*-363, *R*-366, and *R*-382 whose concentrations were assigned values on the OGI 1987 scale in 1988. As already indicated, these three gases are being used as interim standards for the ongoing GAGE program. The archived air concentrations, after adjustment to the SIO 1993 calibration scale based on the 1991–1992 intercomparisons shown in Talbe 1, are now compared against the ALE/GAGE data series at Cape Grim.

5.1. CCl_3F Intercomparison

The archived air concentrations were measured in 1991 and 1992 on the HP5880A at Cape Grim. Because the ambient air concentrations of CCl_3F and CCl_2F_2 in 1978 were roughly half of what they were at the time of the measurements, it is necessary to correct the measurements for the nonlinearity in the response of this instrument. The measured nonlinearity for CCl_3F on this instrument was ϵ equal to −0.19 for the *S* column and equal to 0.025 for the *P* column. To reassess the previous measurements of instrumental nonlinearity, two of the archived air samples collected in 1978 have been directly compared against the SIO 1993 standard at SIO. To the extent that the assumed model describing the nonlinearity in response is valid (and the large ϵ value for the *S* column makes this somewhat questionable), these two measurements provide an independent

estimate of ε. These give $\varepsilon = -0.13$ for the S column and $\varepsilon = 0.01$ for the P column. The averages of the two independent estimates of ε have been used in obtaining Figure 4.

Figure 4 shows the comparison of the shipboard and the archived air measurements against the ALE/GAGE measurements at Cape Grim. The previously described adjustment procedure applied to the Cape Grim data results in the ALE/GAGE measurements prior to November 1986 being based on the OGI 1980 calibrated secondary and tertiary standards, whereas after May 1988 they are from the adjusted OGI 1987 scale. The two calibration gases used between these dates were assigned values via the transition period procedure. Significantly, there are no large systematic differences evident in Figure 4 before and after this transition period. The average ratio of the shipboard data, in particular, to the ALE/GAGE data prior to November 1986 equals 1.008 ± 0.005 and is 1.000 ± 0.006 after May 1988

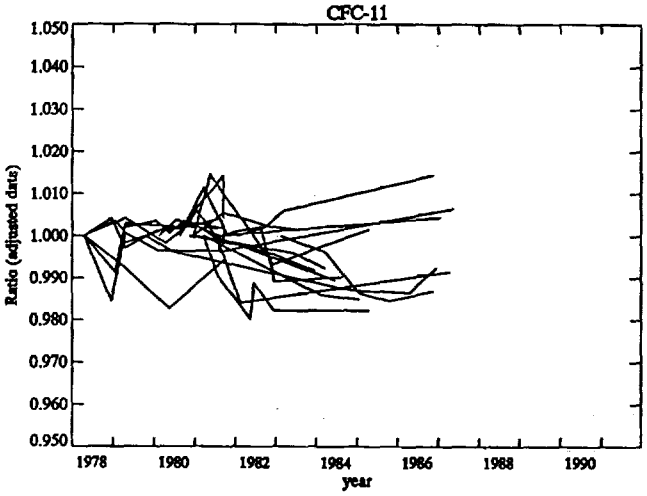

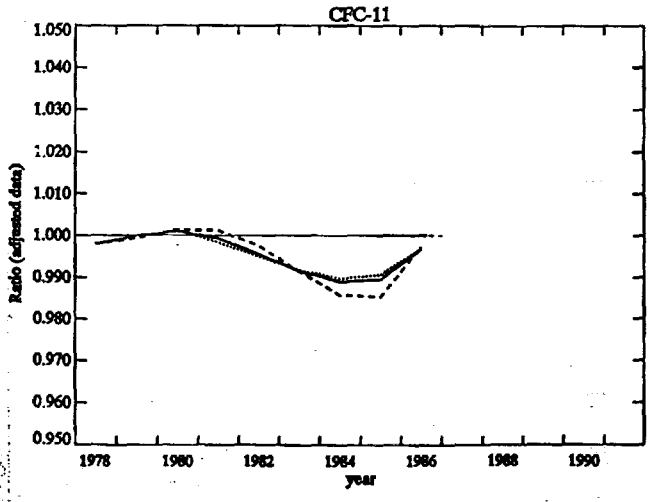

Figure 2. The ratios of different measurements of CCl_3F in the same air samples to the first measurement over the period 1978–1987 after applying the adjustments described in this paper. (Top) Succeeding measurements of the air in the same ALE/GAGE calibration tanks which have been joined by straight lines and (bottom) are polynomial fits to the results in (top) consisting of a sixth-order fit to all the data (solid line) and fourth-order fits to the data for which the first measurement was before July 1980 (dashed line) and after July 1980 (dotted line).

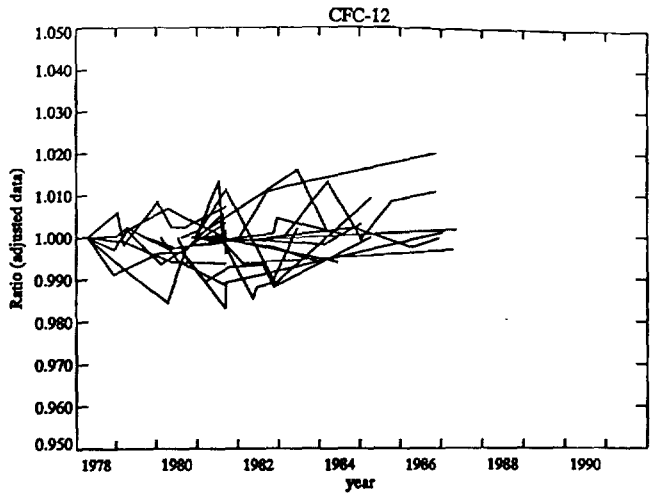

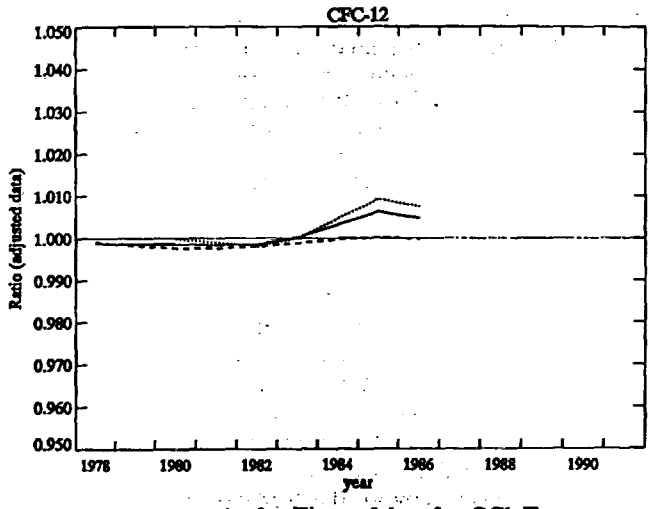

Figure 3. As for Figure 2 but for CCl_2F_2.

(where the error bars are standard deviations of the ratios). The slightly larger shipboard values in 1983–1986 might be related to a small downward drift in the relative calibration in this period suggested by Figure 2.

There is more variability in the comparisons against the archived air samples than against the shipboard measurements, but there is excellent agreement in the long-term trends of all the time series. There is better agreement with the archived air measurements on the P column than on the S column probably because of the smaller nonlinearity effects. Differences in the long-term trends between the S and the P column results and the ALE/GAGE measurements are equivalent to differences in the nonlinearity responses of $\Delta\varepsilon = 0.02$. This is consistent with the uncertainties in the measured nonlinearities. $\Delta\varepsilon = 0.02$ corresponds to an uncertainty in the trend of approximately 0.12 ppt/yr. The agreement between the long-term CCl_3F trends in the P-column-archived air measurements and the ALE/GAGE measurements also limits possible effects of residual nonlinearity in the ALE/GAGE measurements (i.e., the nonlinearity in the OGI instrumental response) to a similar value of $\Delta\varepsilon = 0.02$ (which is a similar number to that obtained earlier based on the average-measured nonlinearities in all the HP5880As).

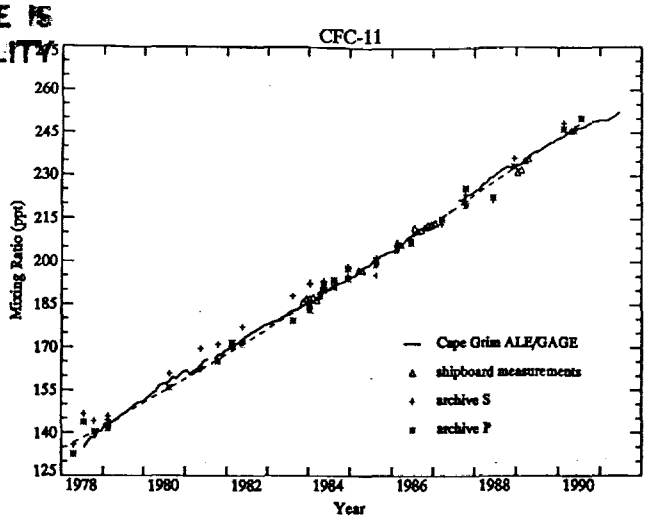

Figure 4. ALE/GAGE monthly means for CCl_3F at Cape Grim, Tasmania, compared against Scripps Institute of Oceanography (SIO) shipboard measurements south of 30°S and archived air values. The archived air measurements have been adjusted for nonlinearity using $\varepsilon = -0.16$ for the S column and $\varepsilon = 0.02$ for the P column. The dashed line is a second-order polynomial fit to the archived air measurements on the P column.

5.2. CCl_2F_2 Intercomparison

Figure 5 shows the comparison of the shipboard and the archived air measurements against the ALE/GAGE CCl_2F_2 measurements at Cape Grim. For this species both the measured nonlinearity and the measurements of two archived air samples at SIO suggest identical nonlinearity factors for the HP5880A at Cape Grim at $\varepsilon = 0.03$. Even better agreement between the time series over the period 1978 to 1990 is exhibited for CCl_2F_2 than for CCl_3F. The average ratio of the shipboard data to the ALE/GAGE data prior to November 1986 is 1.002 ± 0.006 and is an identical factor of 1.002 ± 0.006 after May 1988. Again, the 1987 transition from the OGI 1980 scale to the OGI 1987 scale appears not to have introduced any discontinuities.

The agreement between the long-term trends measured by ALE/GAGE and from the archived air samples is outstanding. The uncertainty in the trend determined from the archived air measurements is approximately 0.2 ppt/yr. This is also equivalent to a change in nonlinearity of $\Delta\varepsilon = 0.02$. Thus this suggests that uncorrected nonlinearities in the global ALE/GAGE CCl_2F_2 data set (due to a nonlinearity in the OGI instrument's response) do not exceed $\Delta\varepsilon = 0.02$. This is a slightly stronger constraint than that based on the average nonlinearity in the HP5880As.

Despite the excellent agreement between the adjusted ALE/GAGE measurements of CCl_3F and CCl_2F_2 presented here and the shipboard and archived data as well as the results presented in the previous section, there remain some uncertainties associated with the transition from the OGI 1980 to the OGI 1987 secondary scales. This is evident, for example, in the inconsistency noted for CCl_2F_2 in the transitional calibration gases. Specifically, there may have been small drifts in the secondary and tertiary standards between 1987 and 1989 which have remained undetected. The possibility of annual drifts may be bounded by examining year-to-year changes in the annual mean ratios of archived air samples to the ALE/GAGE measurements Cape Grim. The year-to-year changes in the ratios are fou to be not significantly different from zero and to vary ov the period 1987–1989 in the same way as in the other yea (provided two anomalous archived air measurements a excluded). The standard deviations in consecutive ye differences provide 1σ upper limits to the typical year-t year drifts of 0.6% for CCl_3F and 0.4% for CCl_2F_2.

6. Empirical Model Fits to the 13-Year Data Se

Plates 1 and 2 show the 13-year record of the ALE/GAG monthly means for CCl_3F and CCl_2F_2. The CCl_3F measure ments on the S and P columns have been combined into single series using the means and the root-mean-square (rms standard deviations. During the overlap periods when mea surements were being made on both the HP5840A and th HP5880A instruments, the average of the two monthl means is shown. The error bars during these periods includ both the variability during the month and the difference between the monthly means obtained by the two instru ments. From these figures it may be noted that CCl_3F an CCl_2F_2 both exhibited low concentrations at Samoa be tween November 1982 and April 1983. The simultaneous reduction in CH_3CCl_3 concentrations, associated with the strong El Nino in that year, has been discussed by *Prinn et al.* [1992]. A detailed examination of such effects in the CCl_3F and CCl_2F_2 records will appear in a future paper. The monthly means and standard deviations shown in these figures may be obtained by contacting the Carbon Dioxide Information Analysis Center at Oakridge National Laboratory.

An empirical model consisting primarily of orthogonal functions and containing an annual cycle and a 29-month oscillation has been fitted to the monthly mean data at each site over the first 10 years. Specifically,

$$\chi_i = a_i + nb_iP_1(t/n - 1) + d_iP_2(t/n - 1) + c_i \cos(2\pi t) + s_i \sin(2\pi t) + p_i \cos(2\pi t/t_0) + q_i \sin(2\pi t/t_0) \quad (1)$$

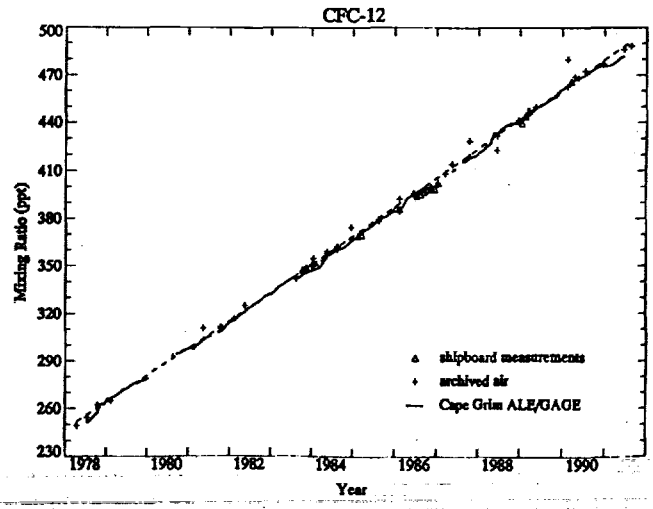

Figure 5. ALE/GAGE monthly means for CCl_2F_2 at Cape Grim, Tasmania. The measurements are compared against archived air values (adjusted for nonlinearity using $\varepsilon = 0.03$) and the SIO shipboard measurements south of 30°S. The dashed line is a second-order polynomial fit to the archived air measurements.

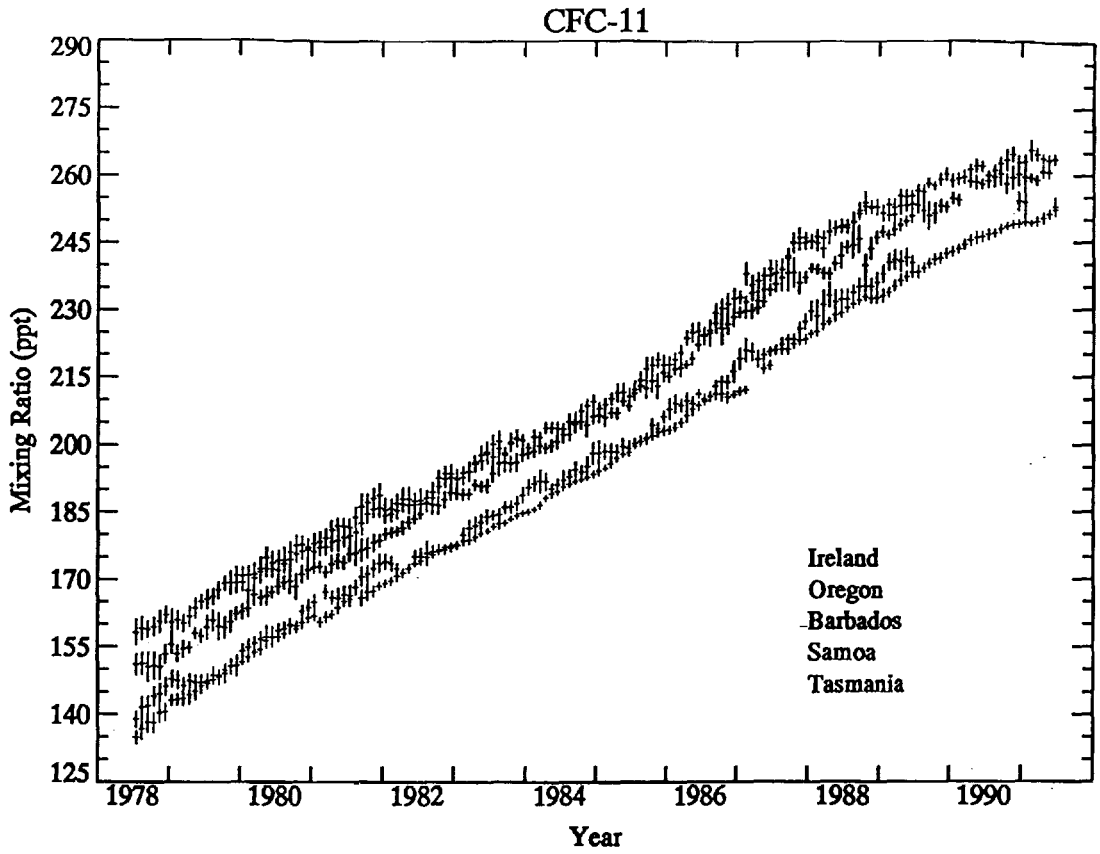

Plate 1. Monthly mean concentrations and standard deviations for CCl_3F measurements at the ALE/GAGE sites during 1978–1991. The *S* and *P* column measurements have been averaged. Units are dry air mole fractions in parts per trillion (ppt).

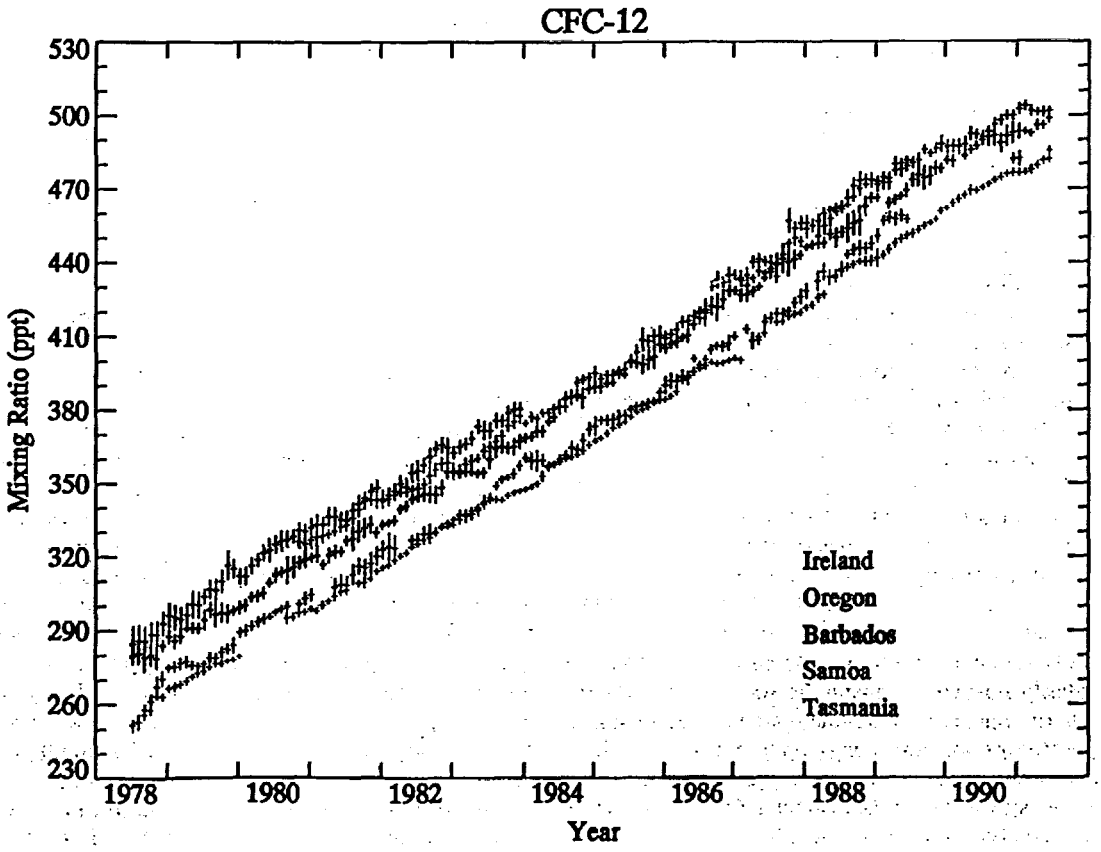

Plate 2. Monthly mean concentrations and standard deviations for CCl_2F_2 measurements at the ALE/GAGE sites during 1978–1991. Units are dry air mole fractions in ppt.

Table 3. Mean Mixing Ratios (a_i), Trends (b_i), and Curvatures for CCl_3F and CCl_2F_2 Determined From ALE/GAGE Observations for the Periods July 1, 1978, to June 30, 1988 (Using Equation (1)) and July 1, 1988, to June 30, 1991 (Using Equation (1) but Excluding the QBO Terms)

Site	July 1978–June 1988			July 1988–June 1991		
	a_i ppt	b_i ppt/yr	$3d_i/25$ ppt/yr^2	a_i ppt	b_i ppt/yr	$4d_i/3$ ppt/yr^2
			CCl_3F			
Adrigole/Mace Head, Ireland	203.0 ± 0.2	9.3 ± 0.1	0.5 ± 0.1	261.4 ± 0.2	5.3 ± 0.2	−2.6 ± 0.5
Cape Meares, Oregon	201.9 ± 0.3	8.8 ± 0.1	0.9 ± 0.1			
Ragged Point, Barbados	196.7 ± 0.2	9.4 ± 0.1	0.3 ± 0.1	256.5 ± 0.2	6.9 ± 0.3	−3.1 ± 0.8
Cape Matatula, American Samoa	187.0 ± 0.3	9.2 ± 0.1	0.2 ± 0.1			
Cape Grim, Tasmania	184.3 ± 0.3	9.0 ± 0.1	0.1 ± 0.1	244.9 ± 0.2	7.8 ± 0.2	−1.9 ± 0.4
			CCL_2F_2			
Adrigole/Mace Head, Ireland	369.8 ± 0.4	16.9 ± 0.1	−0.1 ± 0.1	483.0 ± 0.3	13.6 ± 0.4	−3.0 ± 0.8
Cape Meares, Oregon	368.0 ± 0.5	16.7 ± 0.2	1.3 ± 0.2			
Ragged Point, Barbados	359.8 ± 0.3	17.6 ± 0.1	0.4 ± 0.1	475.6 ± 0.4	15.5 ± 0.5	−4.1 ± 1.2
Cape Matatula, American Samoa	344.8 ± 0.4	17.3 ± 0.2	0.2 ± 0.1			
Cape Grim, Tasmania	339.2 ± 0.3	17.4 ± 0.1	0.1 ± 0.1	455.9 ± 0.4	16.8 ± 0.4	−2.3 ± 1.1

Results are not given for Cape Meares and Cape Matatula for the second period because data for fewer than one half of the 36 months were obtained at these locations. The error bars do not include the uncertainties in the absolute calibration factor.

where t is time (in years) measured from the beginning of the record (July 1, 1978), P_1 and P_2 are Legendre polynomials of the order of 1 and 2, respectively, $t_0 = 2.4$ years is the assumed period of the quasi-biennial oscillation (QBO), and n is one half of the number of years being analyzed. The maximum likelihood estimates of a_l, b_l, d_l, p_l, q_l, c_l, and s_l obtained by weighting each χ_l inversely by its variance are given in Tables 3 and 4. Table 3 contains d_l values multiplied by the indicated factors; this allows the adjusted d_l values to be interpreted as rates of change of the trend in ppt/yr^2.

For the last 3 of the 13 years of data, July 1988–June 1991, a separate model consisting of just the a_l, b_l, and d_l terms has been used. The coefficients in Table 3 are based on centering each analysis in its respective period. Separating the first 10 years from the last 3 years is justified by the different character of the ALE/GAGE data in these two periods. This split is fully supported both by industry estimates of the atmospheric releases of CFCs and by worldwide release estimates determined from the ALE/GAGE observations. These estimates are discussed later in this paper. During the first 10 years, CCl_3F and CCl_2F_2 releases increased fairly slowly with time; this is reflected in the positive d_l values which are associated with linear trends (b_l) which increase slowly with time. Beginning in 1988 the annual rate of increase in both CCl_3F and CCl_2F_2 became smaller and the negative d_l values indicate that the rate of increase was decreasingly rapidly as the major producers of these compounds were constrained by the Montreal Protocol. Note that the upward trend decreased first in the northernmost semihemisphere as is to be expected because of the primarily northern hemispheric source of these compounds. There appears to be an anomalously large value of d_l at Cape Meares for both compounds during the first 10 years (note, however, that the measurements of CCl_3F and CCl_2F_2 at this site started in December 1979 and November 1980, respectively). Two-dimensional model calculations (described below) of the combined data set suggest that this is associated with anomalously low concentrations at Cape Meares in 1984–1986.

The trend in CCl_2F_2 at Adrigole/Mace Head is smaller than at the sites in the other semihemispheres. This reflects higher Adrigole concentrations relative to the other sites during ALE than those observed at Mace Head during GAGE (this may be seen, for example, in Figure 7 which is discussed later). An analysis of pollution events at the Irish sites has shown a reduction in the CCl_2F_2/CCl_3F ratio in such events from the anomalous factor of 0.95 (reported by *Prather* [1988]) to the expected ratio, based on projected European emission figures, of approximately 0.8 in 1987–1989. It is not likely that this result is related to the change in the location of the Irish site because of the remarkable similarity in the pollution events at the two sites which were observed during a period of simultaneous operation [*Simmonds and Derwent*, 1990]. It suggests that European sources of CCl_2F_2 have been decreasing relative to those in the rest of the world. Additional discussion of the Mace Head data is contained by *Simmonds et al.* [1993].

Table 4 shows the seasonal cycle and the 29-month oscillation determined using the entire 13-year data set (and based on adding P_3 and P_4 terms to equation (1) in order to more accurately simulate the recent trends). Consistent seasonal cycles (CCl_2F_2 larger by a factor of approximately 1.6) are evident at Cape Matatula and Cape Grim. The phase of the Cape Matatula cycle is in agreement with that in the two-dimensional model, but the seasonal cycle in the transport rates in the original model has had to be reduced by 60% to simulate the observed amplitude. A similar seasonal cycle to that observed at Cape Grim is then also calculated, with the phase being approximately 6 months different from that at Cape Matatula. The unexpectedly weak seasonal cycles observed at Ragged Point are not easily simulated by this or other models.

The largest 29-month cycles are found at Cape Matatula. The presence of this oscillation in the CH_3CCl_3 record has been discussed by *Prinn et al.* [1992], and as already

Table 4. Seasonal Cycle and 29-Month Oscillation From 13 Years of CCl_3F and CCl_2F_2 ALE/GAGE Data

Site	c_i	s_i	p_i	q_i
		CCl_3F		
Adrigole/Mace Head, Ireland	−0.4 ± 0.3	0.5 ± 0.3	0.1 ± 0.3	0.3 ± 0.3
Cape Meares, Oregon	−0.4 ± 0.2	0.6 ± 0.2	0.4 ± 0.3	−0.1 ± 0.3
Ragged Point, Barbados	0.4 ± 0.2	0.4 ± 0.2	−0.1 ± 0.3	−0.4 ± 0.3
Cape Matatula, American Samoa	−0.8 ± 0.2	−0.6 ± 0.2	0.2 ± 0.3	0.8 ± 0.3
Cape Grim, Tasmania	0.3 ± 0.1	0.0 ± 0.1	0.4 ± 0.2	−0.1 ± 0.2
		CCl_2F_2		
Adrigole/Mace Head, Ireland	−0.9 ± 0.4	1.3 ± 0.4	0.2 ± 0.5	0.5 ± 0.5
Cape Meares, Oregon	−1.5 ± 0.4	1.4 ± 0.4	−0.5 ± 0.4	0.4 ± 0.4
Ragged Point, Barbados	0.0 ± 0.2	1.1 ± 0.2	−0.1 ± 0.3	−0.5 ± 0.3
Cape Matatula, American Samoa	−1.2 ± 0.3	−0.8 ± 0.3	−0.8 ± 0.4	1.1 ± 0.4
Cape Grim, Tasmania	0.8 ± 0.3	0.2 ± 0.3	0.6 ± 0.3	0.0 ± 0.3

Here c_i and s_i are the cosine and sine components in the annual cycle and p_i and q_i are the similar terms in the 29-month oscillation. The zero of time is July 1, 1978. The results are based on fitting the ALE/GAGE data with an expression similar to equation (1) but including P_3 and P_4 Legendre polynomials to better represent the curvature in recent years.

indicated, a simultaneous response occurred in the CCl_3F and CCl_2F_2 records in association with the 1982–1983 El Nino. A more extended discussion of this oscillation and the seasonal cycle will appear in a future paper.

In summary, the important results from Tables 3 and 4 are that steady increases of CCl_3F of 9.2 ppt/yr and of CCl_2F_2 of 17.3 ppt/yr were observed in the troposphere over the period 1978–1988. However, between mid-1988 and mid-1991 the increase of CCl_3F was observed to average 7.0 ppt/yr (assuming a trend for Samoa equal to that observed at Tasmania). Moreover, the trend was observed to have been decreasing at a rate of 2.4 ppt/yr^2 over this period. The increase of CCl_2F_2 was observed to average 15.7 ppt/yr over the same period and this trend has apparently been decreasing at a rate of 2.9 ppt/yr^2.

7. Two-Dimensional Model

The analysis reported here is primarily concerned with timescales of a year or more; therefore the analysis uses monthly mean concentrations, together with their standard errors, which probably include observations of approximately 10 different (independent) air masses per month. During the transition from the HP5840As to the HP5880As, the average of the two monthly means is used in the analysis. The standard error assigned to this monthly mean is given by

$$\sigma = (\sigma_1^{-2} + \sigma_2^{-2})^{-1/2} \quad (2)$$

where σ_1 and σ_2 are the standard errors for each instrument's data. The standard error of the monthly means is typically not a critical parameter in the optimal estimation procedure because longer timescales, such as are produced by calibration gas changes, dominate the error budget. The difference between the monthly means does not appear in equation (2) because this is assumed to be due to calibration gas and other instrumental differences which are accounted for a posteriori by adding a time-independent σ^2 to all the monthly mean error variances [see *Cunnold et al.*, 1986]. The Adrigole/Mace Head and Cape Meares data are combined in a similar manner. During months when measurements were being made at only one of the sites, the time series for the northernmost semihemisphere has been obtained by adjusting the measurements by one half of the expected differences over the observation point based on a linear interpolation of the measured differences at other times.

To interpret the observations in terms of atmospheric lifetimes and atmospheric releases, a two-dimensional model is used to extend the data globally and, in particular, to provide estimates of the chlorofluorocarbon concentrations in the upper troposphere and the stratosphere. In a previously described analysis of the GAGE nitrous oxide measurements [*Prinn et al.*, 1990], it was found that the surface latitudinal gradient of N_2O in this model is sensitive to the spatial distribution of air mass exchange between the troposphere and the stratosphere. This sensitivity exists because of the strong N_2O vertical gradient between these two regions as compared to its weak horizontal gradient in the (upper) troposphere; the horizontal gradient in the troposphere is therefore determined by where transport to the stratosphere is occurring. In order to allow for a circulation between the troposphere and the stratosphere to represent this exchange, the stratosphere in the two-dimensional model has been latitudinally subdivided into four equal parts. The two-dimensional model thus now contains 12 boxes (4 in the stratosphere and 8 in the troposphere).

For CCl_3F and CCl_2F_2 (and CH_3CCl_3, CCl_2FCClF_2 and even CCl_4) the northern hemisphere inputs are large enough to completely dominate the establishment of the horizontal gradients in the troposphere. Thus the details of transport within the stratosphere (which for the calculations reported here are represented by diffusion with a time constant of 100 days) and the locations where stratosphere/troposphere exchange occurs (this transport was here represented solely by latitudinally independent vertical diffusion) are irrelevant to the calculation of the concentrations of these gases in the

Table 5. Estimates of the World Releases of CCl_3F Derived From Production Figures and ALE/GAGE Data (Based on Equilibrium Lifetimes of 44 and 42 Years)

Year	Reporting Co., *AFEAS* [1992]	World Total, *Fisher* [1992]	Maximum Trend	Minimum Trend	ALE/GAGE, τ_e = 44	ALE/GAGE, τ_e = 42
To 1979	3769	3835	3754	3916	3746	3763
1979	264	276	266	286	276 ± 21	277 ± 21
1980	251	264	256	272	282 ± 22	284 ± 22
1981	248	264	258	270	265 ± 20	267 ± 20
1982	240	257	253	261	260 ± 22	263 ± 22
1983	253	273	271	275	296 ± 23	299 ± 23
1984	271	295	295	295	263 ± 25	266 ± 25
1985	281	308	310	306	314 ± 28	317 ± 28
1986	295	327	332	322	350 ± 28	354 ± 28
1987	311	345	353	337	364 ± 31	368 ± 31
1988	314	350	360	340	306 ± 31	310 ± 31
1989	265	305	316	294	310 ± 33	314 ± 33
1990	216	255	266	244	249 ± 28	253 ± 28
1991	188	223	239	215		

Units are 10^6 kg/yr.

lower troposphere. The global mean rate of transport between the troposphere and the stratosphere is, however, an important parameter and in these calculations this time constant (t_s) is set equal to 3.5 years. This is smaller than the 4.0 years used in previous calculations [e.g., *Cunnold et al.*, 1986] and closer to that inferred from three-dimensional model calculations by *Golombek and Prinn* [1986].

The value of t_s is based on estimates of the stratospheric content of CCl_3F and CCl_2F_2 obtained from stratospheric measurements. *Cunnold et al.* [1983*a*, *b*] suggested that the measurements indicated a stratosphere/troposphere mixing ratio ratio of 0.58 ± 0.10 for CCl_3F in 1980 and 0.67 ± 0.07 for CCl_2F_2 in 1978. If the CCl_3F lifetime were 70 years, the model required a $t_s \approx 4$ years to simulate this ratio. However, in the current paper a lifetime of roughly 50 years is inferred and there are now improved estimates of CCl_2F_2 emissions. The CCl_3F observations then suggest a $t_s \approx 3.0$ ± 1.5 years and the CCl_2F_2 observations give $t_s \approx 3.5 \pm 1$ years. A value of $t_s = 3.5$ years is used for all the calculations reported in this paper.

Some modifications to the horizontal transport rates within the troposphere have been made for these (and ongoing) calculations. Instead of the factor of 1.6 by which the horizontal diffusive transport rates in the work of *Cunnold et al.* [1983*a*] were previously multiplied, we now use factors of 2.8, 2.1, and 0.9 at northern hemisphere (NH) midlatitudes, the tropics, and southern hemisphere (SH) midlatitudes, respectively. The objective of these adjustments and of the previously mentioned 60% reduction in the seasonal cycle of diffusive transport was to improve the simulation of both the observed concentrations at each of the sites and the observed seasonal variations. Although the resulting transport rates may bear little relationship to real atmospheric transport rates on the semihemispheric scale, they provide a useful approximation for making global trend and inventory calculations and a reasonable model for interpreting the measurements of the other GAGE species at the same sites. Actually, such changes in transport rates within the troposphere have minimal effects on estimated lifetimes and emission rates. An experiment in which a tracer was injected in the NH of the model results in an interhemispheric gradient which decays by e^{-1} in 5.5 months. This implies an interhemispheric exchange time by the *Prather et al.* [1987] definition of 11 months.

8. CCl_3F and CCl_2F_2 Releases Estimates From Production Figures

Tables 5 and 6 show estimates of the annual releases of CCl_3F and CCl_2F_2 derived by the AFEAS from production figures compiled from reporting company data. The industry believes [*Gamlen et al.*, 1986] the production figures have an accuracy of ±0.5% and that the cumulative release estimates for 1980 were accurate to within 2% (1σ) for CCl_3F (the closed cell foam release time being the dominant uncertainty) and better than 1% for CCl_2F_2 (the nonhermetically sealed refrigeration release time being the most important uncertainty). These release figures, however, exclude production and release from the former USSR, Eastern Europe, and China and several smaller countries. *Borisenkov and Kazekov* [1977] reported that in 1975, USSR production amounted to 2.2% of world production for CCl_3F and 7.6% of world production for CCl_2F_2. A similarly low proportion of CCl_3F releases to CCl_2F_2 releases in Eastern Europe and the USSR relative to the rest of the world is reported in world estimates of production and release by *Chemical Manufacturers Association* (*CMA*) [1983]. *Gamlen et al.* [1986] estimate that production capability in the USSR in 1982 could have been 75×10^6 kg/yr. Thus adding possible production from Eastern Europe (15% of USSR production) and China (1% of the world total), production and release of CCl_2F_2 and CCl_3F from nonreporting companies in 1982 may have been 15% of the world total. This figure is approximately consistent with the differences between releases estimated from the first 5 years of ALE data [*Cunnold et al.*, 1986] and reporting company releases. Moreover, this figure is only slightly smaller than the sum of the CCl_2F_2 and

Table 6. Estimates of the World Releases of CCl_2F_2 Derived From Production Figures and ALE/GAGE Data (Based on Equilibrium Lifetimes of 180 and 110 Years)

Year	Reporting Co. *AFEAS* [1992]	World Total, *Fisher* [1992]	Maximum Trend	Minimum Trend	ALE/GAGE, τ_e = 180	ALE/GAGE, τ_e = 110
To 1979	5594	5897	5814	5980	5794	5887
1979	338	375	361	389	420 ± 23	432 ± 23
1980	332	373	361	385	400 ± 27	414 ± 27
1981	341	385	376	394	358 ± 28	372 ± 28
1982	337	385	379	391	388 ± 28	404 ± 28
1983	343	394	391	397	396 ± 27	414 ± 27
1984	359	414	414	414	409 ± 27	427 ± 27
1985	368	426	429	423	411 ± 28	431 ± 28
1986	376	437	443	431	460 ± 27	483 ± 27
1987	386	450	460	440	431 ± 35	452 ± 35
1988	393	459	473	445	496 ± 41	521 ± 41
1989	365	437	453	421	417 ± 43	441 ± 43
1990	310	386	403	369	366 ± 30	392 ± 30
1991	272	345	363	327		

Units are 10^6 kg/yr.

CCl_3F figures for Eastern Europe and the USSR for 1982 given by the *CMA* [1983].

As a result of the Montreal Protocol, special efforts have recently been made to compile world production levels of these gases. A compilation for 1986 has been made by *UNEP* [1990]; production figures for Eastern Europe and the (former) USSR are reported as 41 × 10^6 kg for CCl_3F and 74 × 10^6 kg for CCl_2F_2 in 1986. This indicates that in 1986 approximately 17% of world production occurred in this region. If it is assumed that releases in this region were in the same proportion to production as they were in the rest of the world, the inferred 1986 releases would be 34 × 10^6 kg for CCl_3F and 68 × 10^6 kg for CCl_2F_2. The sum of these two numbers is almost identical to the combined release of CCl_3F and CCl_2F_2 estimated for this region by the CMA for 1982 [*CMA*, 1983].

In addition to providing reporting company figures, AFEAS has provided estimates of nonreported worldwide production of the chlorofluorocarbons for 1989–1991 [*AFEAS*, 1991, 1992] together with uncertainties in the estimates. The figures for nonreported production are approximately 18 ± 2% of the world production of CCl_3F and CCl_2F_2 for 1989, 26 ± 2% for 1990, and 25 ± 3% for 1991.

Based on information such as that described above, *Fisher* [1993] has provided estimates of the global annual releases of CCl_3F and CCl_2F_2. These estimates appear in column 3 of Tables 5 and 6. Little is, however, known about the relative proportions of CCl_3F and CCl_2F_2 from the nonreporting companies since the AFEAS estimates are based on estimated production capacity (and the same plants are used to produce both gases). The UNEP figures for the consumption of CFC-113 in 1986 indicate that Eastern Europe and the USSR were consuming CFC-113 in approximately the same ratio to CCl_3F and CCl_2F_2 as the rest of the world. This suggests that the technological uses of these compounds there and in the rest of the world may have been similar in 1986. Therefore the assumption that the proportion of releases of CCl_3F in the early 1980s was significantly less in Eastern Europe and the USSR than in the rest of the world may not be justified.

To estimate the possible uncertainties in the calculated lifetimes, estimates of the uncertainties in the global release estimates are needed. Estimates for 1980 were provided by *Gamlen et al.* [1986]. They suggested that the cumulative global release figures for 1980 had an uncertainty of 2.1% (1σ) for CCl_3F and 1.4% for CCl_2F_2. In the calculations reported here, it will be assumed that similar uncertainties apply to the cumulative 1978 figures. Gamlen et al. also provide uncertainties for the ratio of the 1980 emissions to the 1980 cumulative releases. These are 2.2% for CCl_3F and 2.8% for CCl_2F_2. Combining these figures with the uncertainties in cumulative release gives rms uncertainties for the reported releases in 1980 of 3.0% for CCl_3F and 3.1% for CCl_2F_2. These uncertainties are primarily due to uncertainties in the usage patterns of the chlorofluorocarbons. Because of the significant proportion of nonreported production in recent years, the uncertainty associated with the nonreported production should be added to these release uncertainties. For the 1989–1991 period, *AFEAS* [1991 and 1992] provide estimates of this uncertainty which averages 3.1% (1σ) of production for CCl_3F and CCl_2F_2 (interpreting the AFEAS figures as $\pm 2\sigma$). Combining the production and release uncertainties (the latter have been assumed to have remained constant throughout the 13-year analysis period), rms uncertainties of 4.4% for CCl_3F and 4.5% for CCl_2F_2 are obtained for 1990. Assuming that the nonreported production uncertainty was small in 1979/1980, a linear fit was then made to (the negative of) the release uncertainty in 1979/1980 and the rms uncertainty for 1990. This linear fit was used to obtain a maximum trend in the releases based on the *Fisher* [1993] global releases. A similar procedure was used to obtain a minimum trend release scenario. These are given in columns 4 and 5 in Tables 5 and 6. To interpret the trend lifetimes, it is useful to note that these scenarios result in changes in the ratios of the annual release to the cumulative release in the middle of the analysis period of ±2.0% for CCl_3F and 1.9% for CCl_2F_2.

It is important to know the latitudinal distribution of the releases because the simulations of the observed latitudinal distributions of CCl_3F and CCl_2F_2 are regarded as an

Table 7. Proportions of CCl_3F Release (Percent) in Each Semihemisphere Calculated by D. Hartley (Private Communication, 1992)

Semihemisphere	1980	1981	1982	1983	1984	1985	1986	1986	1989	1989
30°–90°N	86.2	85.5	84.5	84.3	84.1	84.4	83.0	82.5	82.6	81.9
0°–30°N	7.3	7.8	8.4	8.6	8.9	8.8	9.5	9.8	9.4	10.0
0°–30°S	3.6	3.7	3.9	3.9	3.9	3.8	4.2	4.4	4.6	4.8
30°–90°N	2.9	3.0	3.2	3.2	3.1	2.9	3.3	3.3	3.4	3.4

The 1980 proportions are used prior to 1980 and the 1989 proportions are used for 1990 and 1991. The distribution of releases for CCl_2F_2 is assumed to be similar to that for CCl_3F.

important test of tropospheric transport representations in three-dimensional models. Transport rates inferred from the CCl_3F and CCl_2F_2 measurements can only be as accurate as the knowledge of their release distributions. Detailed spatial distributions of release have been proposed by *Prather et al.* [1987], based on electric power consumption figures, and by *Hartley and Prinn* [1993], based primarily on a combination of electric power consumption and population figures. The latter figures have been integrated by semihemisphere to yield the annual proportions shown in Table 7 (D. Hartley, private communication, 1992). Based on a comparison against independently obtained estimates given by *Cunnold et al.* [1983*a*, *b*] which were derived from chlorofluorocarbon sales and export figures, the emission proportions in the NH semihemispheres are probably accurate to ±0.05.

9. Lifetime Estimates

Based on the tabulated release figures, lifetimes of CCl_3F and CCl_2F_2 are estimated by the procedures described by *Cunnold et al.* [1983*a*] and *Cunnold and Prinn* [1991]. The trend lifetime estimates (τ) are obtained by minimizing the square of the (weighted) differences between the natural logarithm of the measured mixing ratios ($\ln \chi(t)$) and

$$\ln [\chi_c(t, 1/\tau_0)] - \ln \alpha + (1/\tau - 1/\tau_0) \frac{\partial \ln \chi_c(t_m, 1/\tau_0)}{\partial(1/\tau_0)} + \frac{d}{dt}\left[\frac{\partial \ln \chi_c(t, 1/\tau_0)}{\partial(1/\tau_0)}\right](t - t_m) \qquad (3)$$

for variations in α (a calibration factor) and $1/\tau$. Here t_m is the middle of the data period, and mean (over both time and latitude) values of the partial derivatives are used. Since in reality the partial derivatives have some dependence on $1/\tau_0$, where τ_0 is the lifetime used for the model calculation of the mixing ratios $[\chi_c(t, 1/\tau_0)]$, after a new estimate of $1/\tau$ is obtained, the entire set of calculations is repeated with the new value of τ replacing τ_0. Fortunately, the partial derivatives are relatively insensitive to the value of $1/\tau_0$ within the range of typical values of τ_0.

In this optimal estimation procedure the differences between the measured values ($\ln \chi(t)$) and the calculated values from equation (2) are weighted by σ^2 where

$$\sigma^2 = \sigma_n^2 + \sigma_i^2 + \sigma_0^2.$$

Here σ_n is the standard error of the mean of the measurements during month n (at site i) and σ_i is a measure of the difficulty in estimating a trend in time series i; σ_i is calculated by examining the smoothed spectrum of the residuals with respect to the empirical model (equation (1)) and choosing a value appropriate to wavenumber 1 (which is a reasonable proxy for the estimation of a trend in the data); σ_0 is a site-independent standard deviation which must be added in order that there is statistical agreement between the lifetime estimates obtained from the four time series.

The lifetime estimates obtained by the trend technique are shown in Tables 8 and 9. Estimates for CCl_3F on the S and P columns, which are not independent, have been averaged. To provide some feeling for the consistency of these estimates and for an approximate comparison against the estimates for the first 5 years given by *Cunnold et al.* [1986], estimates are provided for both the first and the second 6.5-year periods. Because the model simulates the seasonal cycles at most sites reasonably well and the time series extends over many years, there is almost no difference between estimates obtained before and after applying a 12-month smoother to the model data. In these calculations the unsmoothed results from the two-dimensional model are used.

Lifetime estimates based on the inventory technique are also evaluated based on minimizing optimally weighted

Table 8. Lifetime Estimates (Years) for CCl_3F in 1985 and at Equilibrium Based on 13 Years of ALE/GAGE Observations and the Emission Scenarios From *Fisher* [1993]

	Inverse Lifetime		July 1978–June 1991 Data		
	July 1978 to December 1984	January 1985 to June 1991	Inverse Lifetime	Lifetime	Equilibrium Lifetime
Trend estimate	0.0145	0.0209	0.0184 ± 0.0043	55^{+17}_{-11}	49
Inventory estimate	0.0233	0.0217	0.0225 ± 0.0072	44^{+21}_{-10}	40
Average			0.0204 ± 0.0059	49^{+19}_{-11}	44^{+17}_{-10}

Table 9. Lifetime Estimates (Years) for CCl_2F_2 Based in 1985 and at Equilibrium Based on 13 Years of ALE/GAGE Observations and the Emission Scenarios From *Fisher* [1993]

	Inverse Lifetime		July 1978–June 1991 Data		
	July 1978 to December 1984	January 1985 to June 1991	Inverse Lifetime	Lifetime	Equilibrium Lifetime
Trend estimate	0.0006	0.0063	0.0039 ± 0.0028	256^{+653}_{-107}	231
Inventory estimate	0.0064	0.0057	0.0061 ± 0.0050	161^{+672}_{-72}	145
Average			0.0050 ± 0.0041	200^{+911}_{-90}	180^{+820}_{-81}

variances of the differences in the ln $\chi(t)$ between the measurements and the calculations.

The uncertainties of the trend estimates of inverse lifetime consist of rms values of the standard deviations due to routine measurement uncertainties (resulting in 0.0005 for each species), release uncertainties as determined from the confidence limits given by the maximum and minimum release scenarios (0.0040 for CCl_3F and 0.0024 for CCl_2F_2), and possible instrument nonlinearity effects based on $\Delta\epsilon = 0.02$ (0.0015 for CCl_3F and 0.0014 for CCl_2F_2). Uncertainties in the inventory lifetime estimates are based on rms values of the standard deviations of the concentrations due to global modeling uncertainties (3.3% for CCl_3F [*Cunnold et al.*, 1983*a*] and 2.1% for CCl_2F_2 [*Cunnold et al.*, 1983*b*]), the rms calibration uncertainties (1.3% for CCl_3F and 0.9% for CCl_2F_2), and emission uncertainties equal to 2.7% for CCl_3F and 3.0% for CCl_2F_2. The latter are based on combining the uncertainties in cumulative release in 1980 [*Gamlen et al.*, 1986] with the average uncertainty due to the nonreported production in 1985 (the middle of the period being analyzed) which is proportionately derived from the nonreported production uncertainty in 1989–1991 from *AFEAS* [1991, 1992]. The absolute calibration uncertainties are a combination of the uncertainty in the SIO 1993 scale and the uncertainties associated with relating this scale to the ALE/GAGE measurements based on comparisons against only a few gas samples. Using partial derivatives from the model (6.2 for CCl_1F and 7.6 for $2CCl_2F_2$) gives uncertainties in the inverse lifetimes derived by the inventory technique of 0.0072 for CCl_3F and 0.0050 for CCl_2F_2.

The CCl_3F and CCl_2F_2 lifetime estimates given in Tables 8 and 9 differ from our previous estimates [*Cunnold et al.*, 1986] for several reasons. First, as indicated in Table 1, the SIO 1993 calibration scale is 5.2% lower for CCl_3F than the OGI 1980 scale and 3.9% higher for CCl_2F_2. The estimated systematic error in the OGI 1980 scale was ±2%, but the assessment of systematic errors in any of these calibration scales is somewhat subjective. Therefore the switch to the SIO 1993 scale represents somewhat more than a 2σ change in calibration; this accounts for almost all of the change in the inventory estimates of lifetime for CCl_3F (from 68 to 44 years) and most of the change for CCl_2F_2 (from 68 to 161 years). The rest of the changes in the inventory estimates of lifetimes are produced by the change to *Fisher* [1993] release scenario from the *CMA* [1983] scenario (the Fisher scenario assumes smaller unreported emissions in the early 1980s) and the 15% increase in the troposphere to stratosphere exchange rate in the current two-dimensional model. These changes are within the uncertainties discussed by *Cunnold et al.* [1983*a*, *b*, 1986]. It should be noted that lifetimes for the middle of the data period were quoted in those papers, not the equilibrium lifetimes which are stressed in this paper.

The trend estimates of lifetime shown in Tables 8 and 9 also differ from those given by *Cunnold et al.* [1986]. These differences are also primarily related to differences between the *Fisher* [1993] and the *CMA* [1983] scenarios as well as inconsistencies between the observed trends and these scenarios. In particular, for CCl_2F_2 the *CMA* [1983] scenario gives a larger I/C in 1981 (where I is the annual release and C is the accumulated release) by 0.0035 which leads to a change in the trend inverse lifetime based on the first 5 years data equal to roughly 0.01. This accounts for the difference between the CCl_2F_2 trend lifetime estimate for the first 6.5 years and that (111 years) given by *Cunnold et al.* [1986], and this uncertainty was recognized therein. For CCl_3F the trend lifetime estimate for the first 6.5 years given here and that given by *Cunnold et al.* [1986] (74 years) are not significantly different. In contrast to the inventory estimates of lifetime, however, there is more variation as a function of period of analysis for the trend estimates. Nevertheless, these differences are within the uncertainty limits which are larger for the shorter periods than for the longer period (e.g., *Cunnold et al.* [1986] give 0.006 for the uncertainty in the inverse lifetime of CCl_2F_2 for the first 5 years of data because of release uncertainties), but they do suggest that the *Fisher* [1993] release scenario is not entirely capturing the evolution of the releases of CCl_2F_2 over the 13-year period of analysis.

The lifetime estimates for 1985 (i.e., the middle of the analysis period) are obtained by averaging the inverse lifetime estimates by the trend and inventory techniques. The error bars are calculated as the rms of the two error bars with the differences from the mean value also being included. The corresponding equilibrium lifetimes are inferred from the two-dimensional model using

$$\tau_e = 5\tau_s + 4t_s$$

where τ_s are the lifetimes for these gases in the stratosphere and t_s is the previously discussed transport time between the troposphere and the stratosphere. The predicted equilibrium lifetime for CCl_3F is between 34 and 61 years (1σ limits) and for CCl_2F_2 is between 99 and 100 years. In comparison, the latest estimates of the equilibrium lifetimes based on three-dimensional calculations using the measured absorption cross sections are 42 years for CCl_3F and 110 years for CCl_2F_2 [*Golombek and Prinn*, 1993]. These values are not significantly different from the ALE/GAGE estimates.

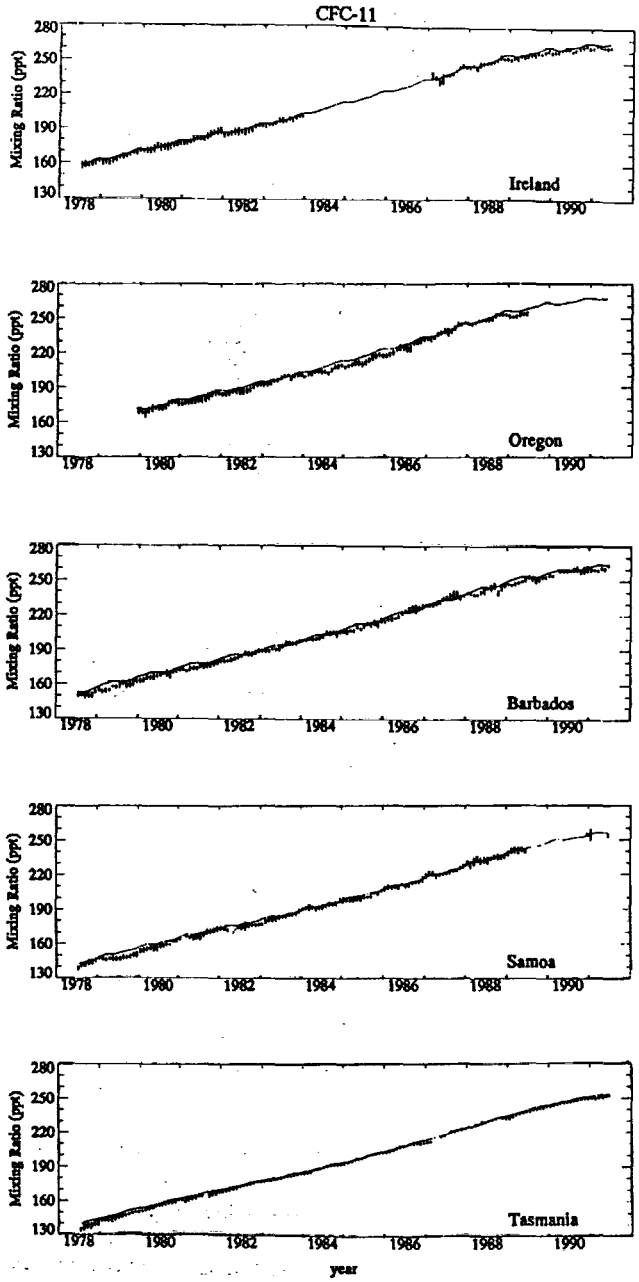

Figure 6. The fit between the model results, using the *Fisher* [1993] emissions for CFC-11 and an equilibrium lifetime of 44 years and the measurements. The fit could be improved by multiplying the ALE/GAGE measurements by approximately 1.01.

Examples of the fit of the two-dimensional model to the measurements using the *Fisher* [1993] emissions based on the ALE/GAGE estimated lifetimes (τ) are shown in Figures 6 and 7. The residual variances in the differences between the measurements and the model calculations using various combinations of τ and α are shown in Figure 8. Here for each τ which has been selected, a best fit α was chosen. The results demonstrate that well-defined minima exist and that this estimation problem is well posed. Figure 7 shows a feature of the data set for which there is no good explanation at this time: at Cape Meares the CCl_2F_2 concentrations were approximately 1% smaller between 1983 and 1986 than in the other years.

The CCl_2F_2 concentrations in Ireland are approximately 1% smaller, relative to the model calculations, at Mace Head (post-1986) than they were pre-1984 at Adrigole. A similar difference was observed during the 3 months of simultaneous measurements that were made at the two sites at the end of 1987 (no differences in CCl_3F concentrations were observed; see Table 2). This difference may therefore be characteristic of the two locations. Accordingly, in the lifetime and release rate calculations the Mace Head CCl_2F_2 concentrations have all been increased by 1%.

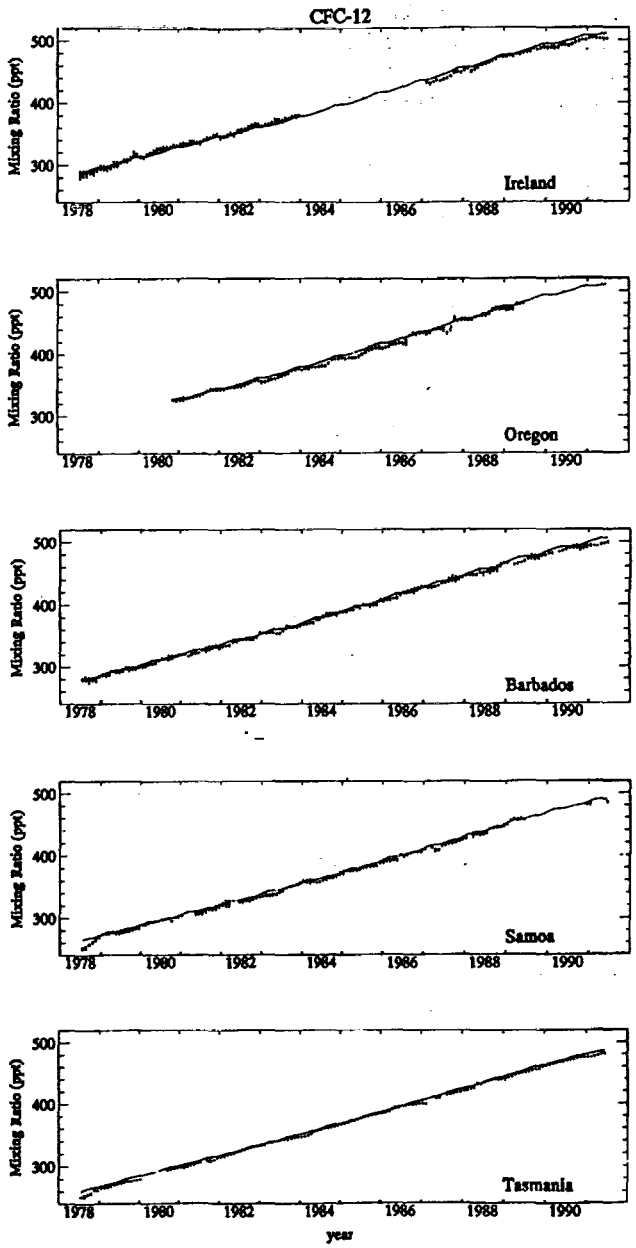

Figure 7. The fit between the model results, using the *Fisher* [1993] emissions for CFC-12 and an equilibrium lifetime of 180 years and the measurements. The fit could be improved by multiplying the ALE/GAGE measurements by approximately 1.01.

10. Release Estimates

If the optimally estimated lifetimes derived from ALE/GAGE measurements are prescribed in the two-dimensional model, estimates of the annual releases of the chlorofluorocarbons may be obtained. The procedure is to compare annual means of the measured concentrations, centered at the end of each calendar year, against annually smoothed concentrations calculated using the two-dimensional model. Annual means are used to smooth out some of the variability in the measurements. The releases are calculated iteratively by modifying the releases one year at a time so that the mean concentrations, over the sites where measurements are available, at the end of each year match the mean modeled concentrations at the same locations. The mean lifetimes deduced from the ALE/GAGE observations are used in these calculations.

The uncertainty in the estimated releases is based on the standard deviation of the differences between the measured and the modeled concentrations (typically using four sites with values at the beginning (σ_1) and end of each year (σ_2), with the uncertainty being given as $(\sigma_1^2 + \sigma_2^2)^{1/2}$). The effects of possible drifts in secondary calibration should also be included in these uncertainties. The rms variation in the year-to-year differences based on the mean curves shown in Figures 2 and 3 yield estimates of the possible effects between 1978 and 1986. These are 0.5%/yr for CCl_3F and 0.3%/yr for CCl_2F_2. Between 1987 and 1989 the only available data which can be used to provide limits on such drifts are the ratios of ALE/GAGE and the archived air measurements at Cape Grim. As discussed in section 5, these limit possible drifts to 0.6%/yr for CCl_3F and to 0.4%/yr for CCl_2F_2. From 1990 on we are confident that the network has been consistently calibrated; however, until this can be demonstrated from sufficiently long term secondary calibration records, we shall conservatively adopt the uncertainties inferred for the 1978–1986 ALE/GAGE data. The possible year-to-year variations in secondary calibration are combined in an rms sense with the differences between the measured and the modeled concentrations at each site. Both of these error sources primarily result in random errors in the releases. The conversion of these standard deviations to precisions in the release estimates is based on the model-calculated dependence of releases on variations of the observed concentrations.

The release estimates also contain possible systematic errors, the largest of which is the uncertainty in lifetime. Based on the ALE/GAGE lifetime uncertainties, the possible errors in the emissions of CCl_2F_2 increase from 3.3% in 1979 to approximately 6% in 1990. The possible errors are a factor of approximately 1.2 larger for CCl_3F. To illustrate the possible effect of this error source, the estimated emissions for the theoretically derived equilibrium lifetimes [*Golombek and Prinnn*, 1993] have been included in Table 5. The overall accuracy of the release estimates is obtained by combining the potential errors with the uncertainty in absolute calibration and the possible modeling errors (see section 9). The rms-derived accuracy ranges from 6 to 8% for CCl_3F and from 4 to 7% for CCl_2F_2 from the beginning to the end of the measurement period.

The precisions of the release estimates may be substantially improved by considering several year averages. In particular, 3-year averages may improve the precision by a factor of $3\sqrt{3}$, which increases the precision of the averages to approximately 2%. Errors due to inaccuracies in the estimates may be substantially eliminated if ratios of the emission in different periods are considered. Treated in this way, the post 1990 ALE/GAGE estimates of release may be more accurate than the future AFEAS/Fisher estimates because of the increasing proportion of nonreported production.

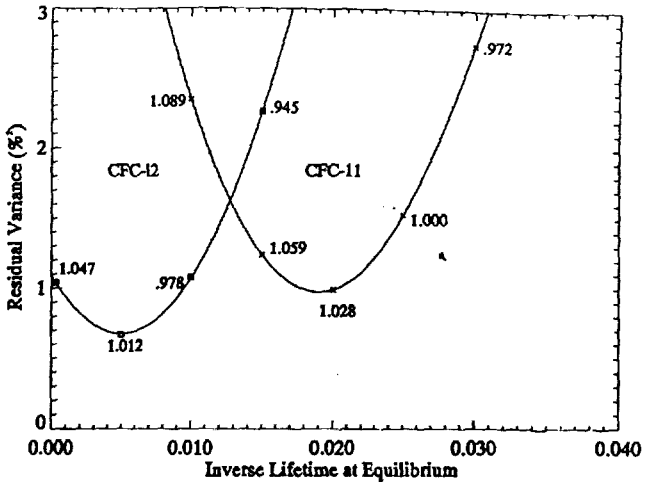

Figure 8. The residual variances (%² expressed relative to the measurements) obtained by combining the differences between the model results, using the *Fisher* [1993] releases, and the measurements at the five sites. For each assumed equilibrium lifetime (years) the figures on the curve indicate the calibration factor (α) by which the measurements would have to be multiplied so as to produce the best fit to the model results for the prescribed lifetime. The minima of the curves indicate the inverse lifetimes at equilibrium (per years) which, combined with the corresponding calibration factor, would produce the best fits between the measurements and the model results.

The release estimates for CCl_3F and CCl_2F_2 are given in Tables 5 and 6 and in Figure 9. Good agreement with the Fisher estimates is indicated. However, the ALE/GAGE emission estimates for 1979 and 1980 for both species are larger than the *Fisher* [1993] values (but the estimated cumulative emissions of CCl_3F and CCl_2F_2 at this time are smaller). This difference widens if the *Golombek and Prinn* [1993] calculated lifetimes are used. It should be noted that the first 6 months of operation (i.e., 1978) was a start-up period during which we are somewhat less confident in the data than during all the remaining years. Because 12-month smoothing is used, the release estimates for 1979 may be in error (in particular for CCl_2F_2). Nevertheless, the pre-1979/1980 cumulative emission differences remain. The agreement with the Fisher estimates would be improved if the closed cell foam uses of CCl_3F possessed the short lifetime discussed by *Gamlen et al.* [1986] and if smaller emissions from nonreporting countries had occurred in 1979 and 1980.

The ALE/GAGE measurements provide strong evidence that worldwide emissions of CCl_3F and CCl_2F_2 decreased in 1989 and 1990. Allowing for inaccuracies in the estimates, we calculate 1990 emissions of $249 \pm 28 \times 10^6$ kg for CCl_3F and $366 \pm 30 \times 10^6$ kg for CCl_2F_2. Our 3-year smoothed estimate of the 1986 combined emissions of the two gases (the base year for the Montreal Protocol) is 777×10^6 kg.

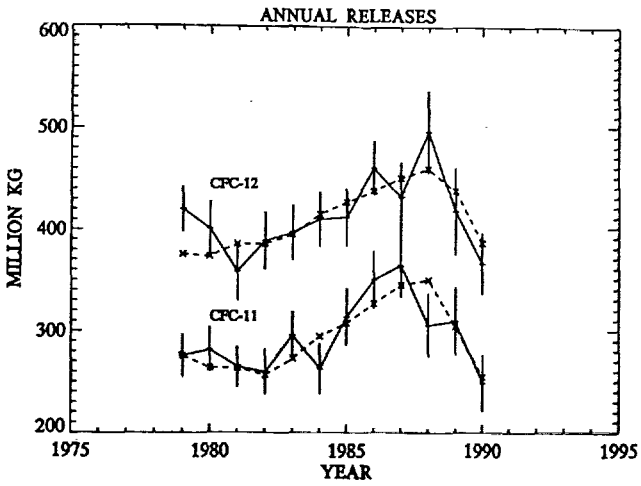

Figure 9. Annual releases of CCl_3F and CCl_2F_2 and 1σ uncertainties estimated from 13 years of ALE/GAGE data (points are joined by a full line); in these calculations the equilibrium lifetimes of CCl_3F and CCl_2F_2 are 44 and 180 years, respectively. These are compared against the most recent estimates of world releases [*Fisher*, 1993] (crosses joined by a dashed line).

The precison of this estimate is $46/3\sqrt{3} = 9 \times 10^6$ kg and the accuracy is approximately 46×10^6 kg. The 1990 emissions expressed as a ratio to the smoothed 1986 emissions exhibit a decrease of 21 ± 5% and the 1989 emissions are 6 ± 7% smaller than the 1986 emissions (the 1990 ratio is 20% if the *Golombek and Prinn* [1993] lifetimes are used and possible inaccuracies do not affect these estimates). The reduction in the 1990 emissions is not significantly different from the Fisher estimate of 16% although it suggests that recent, nonreported emissions might be being overestimated.

In response to the recent decrease in the emissions, the accumulation rates of CCl_3F and CCl_2F_2 have begun to decrease, as was discussed in the empirical model section. This may be more clearly seen in Figure 10 in which the lower tropospheric means and the global means at the ends of each calendar year have been plotted. These values are the results of the two-dimensional model calculations using the estimated annual releases and the prescribed lifetimes. Calculated in this way, these model results are a best fit to the measurements. The smaller annual concentration increases in 1989 and 1990 may be noted.

11. Conclusion

ALE/GAGE measurements of the chlorofluorocarbons, CCl_3F and CCl_2F_2, between July 1978 and June 1991 at five globally distributed locations have been analzyed. Adjustments to the measurements for shifts in the secondary calibration standards which apparently occurred between 1984 and 1991 have been made. The adjusted ALE/GAGE measurements have been shown to be in excellent agreement with shipboard measurements south of 30°S and archived air samples collected at Cape Grim, Tasmania, since 1978. The measurements have been placed on the Scripps Institution of Oceanography, SIO 1993, calibration scale which represents a reduction in CCl_3F concentrations by approximately 5.2% and an increase in CCl_2F_2 concentrations by 3.9% compared to *Cunnold et al.* [1986].

The ALE/GAGE data can usefully be broken into two periods with markedly different characteristics. Applying an empirical model separately to the first 10 years of data (July 1978 to June 1988) and the last 3 years (July 1988 to June 1991), we determined a slow increase in the atmospheric trends of CCl_3F and CCl_2F_2 in the lower troposphere in the first 10 years and a rapid decrease in the trends over the past 3 years. During the first 10 years the trend averaged 9.2 and 17.3 ppt/yr, respectively, for CCl_3F and CCl_2F_2. In contrast, the trends averaged 7.0 and 15.7 ppt/yr, respectively, in the last 3 years and these trends were decreasing at rates of 2.4 and 2.9 ppt/yr^2. The trends were observed to decrease first in the northernmost semihemisphere, as is to be expected based on the source distributions of these gases.

Atmospheric lifetimes of CCl_3F and CCl_2F_2 have been obtained by the analysis procedures initially described by *Cunnold et al.* [1983*a*]. The worldwide release estimates [*Fisher*, 1993] used in these calculations utilize *AFEAS* [1992] figures for production by reporting companies but are different from the worldwide release estimates by the *CMA* [1983]. Equilibrium lifetimes for CCl_3F of 44^{+17}_{-10} years and of 180^{+820}_{-81} years for CCl_2F_2 have been inferred. In contrast to the previous lifetime estimates given by *Cunnold et al.* [1986], there is now good agreement between the estimates obtained by the trend and inventory techniques. This results primarily from the new calibration factors and the revised estimates of worldwide releases. Uncertainties remain in the trend estimates primarily because of release uncertainties. Uncertainties in the inventory lifetime estimates are produced by a combination of uncertainties in absolute calibration, in release and in global simulations with a two-dimensional model.

These lifetimes have been used to infer annual releases of the chlorofluorocarbons. Model releases are adjusted in each year sequentially until agreement is obtained between the observed and calculated annual mean concentrations. The

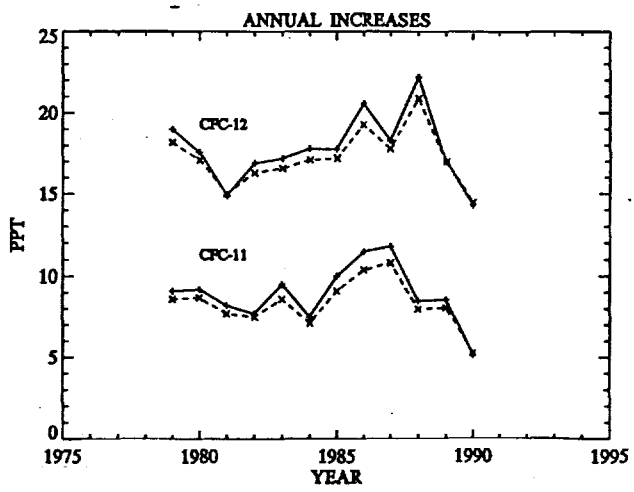

Figure 10. Annual global rates of increase (ppt/yr) of CCl_3F and CCl_2F_2 estimated by combining ALE/GAGE observations and two-dimensional model calculations. (a) In the lower troposphere, 500–1000 mbar (pluses and solid lines) and (b) the entire atmosphere (crosses and dashed lines).

estimated releases of both CCl_3F and CCl_2F_2 in 1979 and 1980 are larger than the *Fisher* [1993] estimates, but in contrast, the accumulated emission prior to 1979 are smaller than the Fisher estimates. These differences could be reduced by assuming shorter lifetimes for the CCl_3F used in closed cell foams, and a more rapid buildup of nonreported emissions of CCl_2F_2 in this time period. It was also inferred that the releases of both chlorofluorocarbons in 1989 and 1990 were less than those in 1988 and the combined 1990 release of CCl_3F and CCl_2F_2 was estimated to be 21 ± 5% less than in 1986. The 1990 releases were estimated to be 249 ± 28 × 10^6 kg for CCl_3F and 366 ± 30 × 10^6 kg for CCl_2F_2. This decrease is a little larger than that calculated from production figures by *Fisher* [1993], suggesting the possibility that recent nonreported emissions are being overestimated. It was suggested that global release estimates from GAGE data for years after 1990 could be more accurate than the estimates obtained from worldwide production figures.

The decrease in the annual releases is associated with smaller increases in the globally integrated (i.e., both horizontally and vertically integrated) atmospheric content of the chlorofluorocarbons in the past few years. Over the period 1979–1988 the global atmospheric inventory is estimated to have been increasing, on average, 8.6 ppt/yr for CCl_3F and 17.6 ppt/yr for CCl_2F_2. In 1990, however, the estimated increase in inventory was 5.3 ppt/yr for CCl_3F and 14.5 ppt/yr for CCl_2F_2.

Acknowledgments. This research was supported by NASA grants NAGW-732 and 474 (R. Prinn), NAGW-729 (F. Alyea, D. Cunnold), NAGW-280 (A. Crawford, R. Rasmussen), and NAGW-2034 (R. Weiss, B. Miller); Chemical Manufacturers Association (contract FC-85-567 (P. Simmonds) and FC-87-640 (P. Fraser)); NOAA (contract NA85-RAC05103 (P. Simmonds)); DOE (UK) (contract PECD 7/10/54, P. Simmonds); CSIRO, Aspendale, Victoria, Australia (P. Fraser); Bureau of Meteorology, Melbourne, Victoria, Australia (P. Fraser). Valuable local support at the ALE/GAGE stations was provided by D. Brown (Mace Head, Ireland), P. Sealey (Ragged Point, Barbados), NOAA staff (Cape Matatula, Samoa), and L. Porter (Cape Grim, Tasmania). We thank R. A. Rasmussen (Oregon Graduate Institute) for his substantial contributions to the maintenance of calibration standards for the ALE/GAGE program and for his contributions to the operation of the Cape Meares and Cape Matatula stations. The shipboard measurements and SIO calibrations were supported by grants from the Chemical Oceanography program of the U.S. NSF, and we thank J. Bullister, P. Salameh, F. Van Woy, and M. Warner for their valuable assistance with these aspects of the work.

References

Alternative Fluorocarbons Environmental Acceptability Study, (AFEAS), Chlorfluorocarbons (CFC's) 11 and 12: Annual production for the years 1931–1975 and annual production and sales for the years 1976–1990, Washington, D. C., 1991.

AFEAS, Chlorofluorocarbons (CFC's) 11 and 12: Annual production for the years 1931–1975 and annual production and sales for the years 1976–1991, Washington, D. C., 1992.

Albritton, D. L., Stratospheric ozone depletion, Global processes, in *Ozone Depletion, Greenhouse Gases, and Climate Change*, pp. 10–18, National Academy Press, Washington, D. C., 1989.

Anderson, J., D. Toohey, and W. Brune, Free radicals within the Antarctic vortex: The roll of CFCs in Antarctic ozone loss, *Science*, *251*, 39–46, 1991.

Borisenkov, Y. P., and Y. Y. Kazekov, Effect of freons and halocarbons on the ozone layer of the atmosphere and climate, technical report, U.N. Environ. Programme, New York, 1977.

Bullister, J. L., Atmospheric chlorofluoromethanes as tracers of ocean circulation and mixing: Measurement and calibration techniques and studies in the Greenland and Norwegian Seas, Ph.D. thesis, 172 pp., Univ. of Calif., San Diego, 1984.

Bullister, J. L., and R. F. Weiss, Determination of CCl_3F and CCl_2F_2 in seawater and air, *Deep Sea Res.*, *35*, 839–853, 1988.

Chemical Manufacturers Association (CMA), World production and release of chlorofluorocarbons 11 and 12 through 1982, report, Fluorocarbon Program Panel, Washington, D. C., 1983.

Cunnold, D. M., Data and results, paper presented at the NASA Workshop on Concentrations, Lifetimes and Trends of CFCs, Halons and Related Speices, Blakeney House, England, January 1992.

Cunnold, D., and R. Prinn, Comment on "Tropospheric OH in a three-dimensional chemical tracer model: An assessment based on observations of CH_3CCl_3" by C. M. Spivakovsky et al., *J. Geophys. Res.*, *96*, 17,391–17,393, 1991.

Cunnold, D., R. Prinn. R. Rasmussen, P. Simmonds, F. Alyea, C. Cardelino, A. Crawford, P. Fraser, and R. Rosen, The Atmospheric Lifetime Experiment, 3, Lifetime methodology and application to three years of $CFCl_3$ data, *J. Geophys. Res.*, *88*, 8379–8400, 1983*a*.

Cunnold, D. M., R. G. Prinn, R. A. Rasmussen, P. G. Simmonds, F. N. Alyea, C. A. Cardelino, and A. J. Crawford, The Atmospheric Lifetime Experiment, 4, Results for CF_2Cl_2 based on 3 years data, *J. Geophys. Res.*, *88*, 8401–8414, 1983*b*.

Cunnold, D., R. Prinn, R. Rasmussen, P. Simmonds, F. Alyea, C. Cardelino, A. Crawford, P. Fraser, and R. Rosen, The atmospheric lifetime and annual release estimates for $CFCl_3$ and CF_2Cl_2 from 5 years of ALE data, *J. Geophys. Res.*, *91*, 10,797–10,817, 1986.

Fisher, D., *NASA Report on Concentrations, Lifetimes and Trends of CFC's, Halons and Related Species*, chap. 2, in press, 1993.

Fraser, P., S. Penkett, M. Gunson, R. Weiss, and F. S. Rowland, *NASA Report on Concentrations, Lifetimes and Trends of CFC's, Halons and Related Species*, chap. 1, in press, 1993.

Gamlen, P. H., B. C. Lane, P. M. Midgley, and J. M. Steed, The production and release to the atmosphere of CCl_3 and CF_2Cl_2 (chlorofluorocarbons CFC-11 and CFC-12), *Atmos. Environ.*, *20*, 1077–1085, 1986.

Golombek, A., and R. Prinn, A global three-dimensional model of the circulation and chemistry of $CFCl_3$, CF_2Cl_2, CH_3CCl_3, CCl_4, and N_2O, *J. Geophys. Res.*, *91*, 3985–4001, 1986.

Golombek, A., and R. G. Prinn, Global three-dimensional model calculations of perhalocarbon and nitrous oxide distributions and lifetime, in *NASA Report on Concentrations, Lifetimes and Trends of CFC's, Halon and Related Species*, chap. 1, in press, 1993.

Hartley, D., and R. Prinn, Feasibility of determining surface emissions of trade gases using an inverse method in a three-dimensional chemical transport model, *J. Geophys. Res.*, *98*, 5183–5197, 1993.

Keeling, C. D., R. B. Bacastow, A. E. Bainbridge, C. A. Ekdahl, Jr., P. R. Guenther, and L. S. Waterman, Atmospheric carbon dioxide variations at Mauna Loa Observatory, Hawaii, *Tellus*, *28*, 538–551, 1976.

Prather, M., European sources of halocarbons and nitrous oxide: Update 1986, *J. Atmos. Chem.*, *6*, 375–406, 1988.

Prather, M., M. McElroy, S. Wofsy, G. Russell, and D. Rind, Chemistry of the global troposphere: Fluorocarbons as tracers of air motion, *J. Geophys. Res.*, *92*, 6579–6613, 1987.

Prinn, R., D. Cunnold, R. Rasmussen, P. Simmonds, F. Alyea, A. Crawford, P. Fraser, and R. Rosen, Atmospheric emissions and trends of nitrous oxide deduced from 10 years of ALE/GAGE data, *J. Geophys. Res.*, *95*, 18,369–18,385, 1990.

Prinn, R., et al., Global average concentration and trend for hydroxyl radicals deduced from ALE/GAGE trichloroethane (methyl chloroform) data for 1978–1990, *J. Geophys. Res.*, *97*(D2), 2445–2461, 1992.

Rasmussen, R. A., and J. E. Lovelock, The Atmospheric Lifetime Experiment, 2, Calibration, *J. Geophys. Res.*, *88*, 8369–8378, 1983.

Simmonds, P. G., and R. G. Derwent, Measurements of ozone and other radiatively active gases at Mace Head in the Republic of Ireland, *Atmos. Environ.*, *25*(A), 1795–1808, 1990.

Simmonds, P. G., D. M. Cunnold, G. J. Dollard, T. J. Davies, A. McCulloch, and R. G. Derwent, Evidence of the phase-out of

CFC use in Europe over the period 1987–1990, *Atmos. Environ.*, *26*(A), 1397–1407, 1993.

Solomon, S., Progress towards a quantitative understanding of Antarctic ozone depletion, *Nature*, *347*, 347–354, 1990.

United Nations Environmental Programme (UNEP), *Montreal Protocol on Substances that Deplete the Ozone Layer*, September 16, 1987, Montreal, 1987.

UNEP, Revised report on data on production, imports, exports and consumption of substances listed in Annex A of the Montreal Protocol, *UNEP/OZL.Pro.2/2/Add.4/Rev./1*, 1990.

Weiss, R. F., C. D. Keeling, and H. Craig, The determination of tropospheric nitrous oxide, *J. Geophys. Res.*, *86*, 7197–7202, 1981.

Weiss, R. F., J. L. Bullister, R. H. Gammon, and M. J. Warner, Atmospheric chlorofluoromethanes in the deep equatorial Atlantic, *Nature*, *314*, 608–610, 1985.

World Meteorological Organization (WMO), The Montreal Protocol on substances that deplete the ozone layer, *WMO Bull.*, *37*, 94–97, 1988.

Yokahata, A., Y. Makide, and T. Tominaga, A new calibration method for the measurement of CCl_4 concentration at 10^{-10} v/v level and the behavior of CCl_4 in the atmosphere, *Bull. Chem. Soc. Jpn.*, *58*, 1308–1314, 1985.

F. N. Alyea and D. M. Cunnold, School of Earth and Atmospheric Sciences, Georgia Institute of Technology, Atlanta, GA 30332.

A. J. Crawford, Center for Atmospheric Studies, Oregon Graduate Institute, Beverton, OR 97006.

P. J. Fraser, Division of Atmospheric Research, CSIRO, Aspendale, Victoria, Australia.

B. R. Miller and R. F. Weiss, Scripps Institution of Oceanography, University of California, La Jolla, CA 92093-0220.

R. G. Prinn, Center for Global Change Science, MIT, Cambridge, MA 02139.

P. G. Simmonds, Department of Biogeochemistry, University of Bristol, Bristol, BS8 1TS England.

(Received August 31, 1992; revised September 15, 1993; accepted September 21, 1993.)

C-2

JOURNAL OF GEOPHYSICAL RESEARCH, VOL. 97, NO. D2, PAGES 2445-2461, FEBRUARY 20, 1992

Global Average Concentration and Trend for Hydroxyl Radicals Deduced From ALE/GAGE Trichloroethane (Methyl Chloroform) Data for 1978–199

R. PRINN,[1] D. CUNNOLD,[2] P. SIMMONDS,[3] F. ALYEA,[2] R. BOLDI,[1] A. CRAWFORD,[4] P. FRASER,[5] D. GUTZLER,[6] D. HARTLEY,[1] R. ROSEN,[6] AND R. RASMUSSEN[4]

Atmospheric measurements at several surface stations made between 1978 and 1990 of the anthropogenic chemical compound 1,1,1-trichloroethane (methyl chloroform, CH_3CCl_3) show it increasing at a global average rate of 4.4 ± 0.2% per year (1σ) over this time period. The measured trends combined with industrial emission estimates are used in an optimal estimation inversion scheme to deduce a globally averaged CH_3CCl_3 tropospheric (and total atmospheric) lifetime of 5.7 (+0.7, −0.6) years (1σ) and a weighted global average tropospheric hydroxyl radical (OH) concentration of (8.7 ± 1.0) × 10^5 radical cm^{-3} (1σ). Inclusion of a small loss rate to the ocean for CH_3CCl_3 of 1/85 $year^{-1}$ does not affect the stated lifetime but lowers the stated OH concentration to (8.1 ± 0.9) × 10^5 radical cm^{-3} (1σ). The rate of change of the weighted global average OH concentration over this time period is determined to be 1.0 ± 0.8% per year (1σ) which has major implications for the oxidation capacity of the atmosphere and more specifically for methane (CH_4), which like CH_3CCl_3 is destroyed primarily by OH radicals. Because the weighting strongly favors the tropical lower troposphere, this deduced positive OH trend is qualitatively consistent with hypothesized changes in tropical tropospheric OH and ozone concentrations driven by tropical urbanization, biomass burning, land use changes, and long-term warming. We caution, however, that our deduced rate of change in OH assumes that current industry estimates of anthropogenic emissions and our absolute calibration of CH_3CCl_3 are accurate. The CH_3CCl_3 measurements at our tropical South Pacific station (Samoa) show remarkable sensitivity to the El Nino-Southern Oscillation (ENSO), which we attribute to modulation of cross-equatorial transport during the northern hemisphere winter by the interannually varying upper tropospheric zonal winds in the equatorial Pacific. Thus measurements of this chemical compound have led to the discovery of a previously unappreciated aspect of tropical atmospheric tracer transport.

1. INTRODUCTION

The hydroxyl radical (OH) is arguably the single most important oxidizing agent in the troposphere. It is produced in daylight hours primarily from the reaction of water vapor with $O(^1D)$ and secondarily by reduction of the hydroperoxy radical (HO_2) by NO, O_3, HO_2, and organoperoxy radicals [e.g., *Donahue and Prinn*, 1990]. It is destroyed on a time scale of about 1 s by oxidizing CO, SO_2, NO_2, and a wide range of hydrocarbons, including methane (CH_4). Direct measurement of tropospheric OH is very difficult with long-baseline spectroscopy possessing a sensitivity level not much lower than ambient OH levels [*Callies et al.*, 1989]. An alternative, indirect approach to OH measurement is to determine the rate of loss of a chemical whose sources are known and whose major sink is reaction with OH. This approach can be used with a globally dispersed chemical like 1,1,1-trichloroethane (CH_3CCl_3) to yield a weighted global average OH concentration [*Singh*, 1977; *Lovelock*, 1977; *Makide and Rowland*, 1981; *Prinn et al.*, 1983*b*, 198 *Khalil and Rasmussen*, 1984; *Fraser et al.*, 1986*a*] or with locally dispersed chemical to yield a local OH concentrati [*Prinn*, 1985].

Measurements of CH_3CCl_3 (common name, methyl chl roform) have been carried out since 1978 as a part of t Atmospheric Lifetime Experiment (ALE) and its success the Global Atmospheric Gases Experiment (GAGE). V previously used the first 7 years of these data to deduce weighted global average tropospheric OH concentration (7.7 ± 1.4) × 10^5 radical cm^{-3} and a global avera CH_3CCl_3 atmospheric lifetime of 6.3 (+1.2, −0.9) yea [*Prinn et al.*, 1987]. In view of the general significance of O in tropospheric chemistry and more specifically the predi tion that tropospheric OH levels may be changing [*Thom son and Cicerone*, 1986; *Isaksen and Hov*, 1987], it is als important to determine (or at least place constraints on) th temporal trend in OH. In this paper we update our earli analysis by reporting the first 12 years of ALE/GAG CH_3CCl_3 data and using these data to determine the tim average and (for the first time) the linear temporal trend i the CH_3CCl_3 lifetime and thus the OH concentration. W also report evidence for an effect of the Southern Oscillatio (SO) on Pacific CH_3CCl_3 measurements.

2. EXPERIMENT

Trichloroethane is analyzed at the ALE/GAGE stations i real time using microprocessor-controlled gas chromatc graphs with silicone-packed columns and electron captur detectors [*Prinn et al.*, 1983*a*]. The ALE/GAGE station are located in Cape Grim, Tasmania (41°S, 145°E); Poir Matatula, American Samoa (14°S, 171°W); Ragged Point Barbados (13°N, 59°W); Cape Meares, Oregon (45°N

[1]Center for Global Change Science, MIT, Cambridge, Massachusetts.
[2]School of Earth and Atmospheric Sciences, Georgia Institute of Technology, Atlanta.
[3]Department of Geochemistry, University of Bristol, Bristol, United Kingdom.
[4]Center for Atmospheric Studies, Oregon Graduate Institute, Beaverton.
[5]Division of Atmospheric Research, CSIRO, Aspendale, Victoria, Australia.
[6]Atmospheric and Environmental Research, Incorporated, Cambridge, Massachusetts.

Paper number 91JD02755.
0148-0227/92/91JD-02755$05.00

124°W); Adrigole, Ireland (52°N, 10°W); and Mace Head, Ireland (53°N, 10°W) (this station replaced the Adrigole station beginning in 1987).

Absolute calibration of the CH_3CCl_3 measurements is carried out by comparing alternate analyses of (Nafion-dried) air and on-site (Nafion-dried) calibration gas [*Prinn et al.*, 1983*a*]. Both before and after use at the site the on-site calibration gas tank is analyzed relative to working secondary standards [*Rasmussen and Lovelock*, 1983] maintained at the Oregon Graduate Institute before 1989 and at the Commonwealth Scientific and Industrial Research Organization after 1989. This calibration procedure assumes a linear relation between instrument response R and mixing ratio χ (i.e., in the general expression $R \propto \chi^{(1-\varepsilon)}$, the nonlinearity parameter $\varepsilon = 1 - d \ln R/d \ln \chi = 0$). For small values of ε, $\Delta \ln R$, and $\Delta \ln \chi$ the error in χ due to nonlinearity is approximately $-\varepsilon\chi\Delta \ln R$ [*Prinn et al.*, 1990]. The linearities of the instruments at each of the five sites and of the instrument used to analyze the on-site calibration tanks relative to the secondary standards have been investigated using a suite of test tanks with mixing ratios ranging from 0.5 to 1.3 times present atmospheric concentrations. From these tests we find $\varepsilon = 0.00 \pm 0.04$ for CH_3CCl_3. The largest difference between unknowns and standards for CH_3CCl_3 in ALE/GAGE is a factor of 2 (i.e., $\Delta \ln R \leq 0.7$). Thus the largest error in χ due to nonlinearity is approximately $\varepsilon \times 0.7 \times 100 = 0.0 \pm 2.8\%$, and this error would apply to 1990 atmospheric analyses in northern mid-latitudes calibrated against our original 1978 secondary standards. This instrumental nonlinearity contributes an uncertainty to our quoted CH_3CCl_3 trends of about $0.0 \pm 0.2\%$ per year which, while not negligible, is small compared to the observed CH_3CCl_3 trends. The above ε values could also reflect in part the finite accuracy with which the individual tanks for testing nonlinearity can be prepared.

The absolute calibration of the working secondary standards is based on *Khalil and Rasmussen* [1984]. This means that the so-called ALE/GAGE calibration factor (ξ) for CH_3CCl_3 is currently 0.80 ± 0.08 compared to the original calibration factor of 1.00 ± 0.15 which was based on *Rasmussen and Lovelock* [1983]. A recent intercomparison between ALE/GAGE and a Japanese standard (Y. Makide, private communication, 1991) yielded $\xi = 0.56$ for the Japanese standard. The consistency of the latter ξ value with ALE/GAGE measurements and industry emissions is discussed later. For determination of long-term trends the long-term stability of the secondary standards is an important consideration. The relative stability of CH_3CCl_3 is checked using a set of specially maintained secondary standard tanks which are periodically analyzed relative to the original secondary tank 033 as described by *Rasmussen and Lovelock* [1983]. For the seven surviving members of this set (tank numbers 022, 028, 030, 032, 036, 004, and 017) measured (relative to tank 033) in 1987 and 1989, the values differed by 0.1 ± 2.0 ppt (parts per trillion by number) and 0.3 ± 2.3 ppt, respectively, from the original 1978 values; these differences are not statistically different from zero (stated uncertainties are standard deviations which are $\sqrt{7}$ times the error in the mean). This result does not of course test whether tank 033 itself is drifting. If the drift in the seven test tanks relative to tank 033 is indicative of the magnitude of the possible drift in 033 itself, then this implies the possibility of a linear drift in the secondary standards of 0.01 ± 0.22 to 0.03 ± 0.21 ppt yr^{-1} (i.e., 0.01 ± 0.20 to 0.0 0.19% per year). These possible drifts are clearly s compared to the measured atmospheric trends in CH_3C but we make the caveat that the long-term trends reporte this paper depend on explicit assumptions concerning stability of CH_3CCl_3 in the above set of test tanks.

Finally, as a measure of the combined effects of ins mental nonlinearity, calibration stability, and accuracy secondary calibration tank preparation, three "archi tanks were filled during the first year of ALE/GAGE were analyzed approximately 12 years later relative secondary calibration tanks 363, 366, and 382. The aver difference between these archive tanks analyzed 12 ye after filling and Cape Grim ALE/GAGE measurements m at the time they were filled was 3.2 ± 1.7 ppt (3.6 ± 1.9 corresponding to an annual change of 0.26 ± 0.14 ppt y ($0.3 \pm 0.2\%$ per yr^{-1}). The latter annual change is com rable to the uncertainty in the long-term CH_3CCl_3 trend to measurement variability (see below).

3. Observations

In the first phase of ALE/GAGE (ALE, 1978–198 HP5840 gas chromatographs taking four calibrated air m surements per day were used, while in the second ph (GAGE, 1981 to present) the HP5840 instruments were fi run together with and then replaced by HP5880 instrume taking 12 air measurements per day. Agreement betwe ALE and GAGE instruments for CH_3CCl_3 was excelle with the small differences largely attributable to the fin accuracy with which the separate calibration tanks used f the two instruments can be prepared (e.g., *Fraser et* [1986*b*] for the Cape Grim station).

3.1. *High-Frequency Variability*

A special feature of the ALE/GAGE approach to lon term trace gas measurements is its ability to resolve impo tant short-term variations in trace gas concentrations. Th ability is illustrated in Figure 1 which shows measuremen to-measurement variations in CH_3CCl_3 (and for comparisoi one of the other ALE/GAGE gases, CF_2Cl_2) over a period 2 years. Pollution events, identified by simultaneous lar positive increases in CH_3CCl_3 and CF_2Cl_2, are quite evide at Ireland, Oregon, and Tasmania. These are associated wit regional circulation changes bringing air to the stations fro nearby industrial regions. Between these pollution event westerlies coming off the ocean bring relatively clean back ground air to these three stations. Except for a few in stances, pollution events are rare or absent at the tropica stations on Barbados and Samoa. Instead, the large north t south gradients in CH_3CCl_3 (and CF_2Cl_2) combined wit significant interannual and intra-annual changes in the trop ical circulation lead to variations at these tropical sites of distinctly different nature.

Specifically, at Barbados during July–December there ar significant simultaneous decreases (and sometimes in creases) in both CH_3CCl_3 and CF_2Cl_2 that can be attributec to enhanced south-to-north (or for the increases, north-to south) transport of air in the north equatorial Atlantic at thi time of year. Similarly, at Samoa during the northern hemisphere (boreal) winter there are in certain years (e.g., 1988 a shown) large simultaneous increases in both CH_3CCl_3 and CF_2Cl_2 which can be attributed to enhanced transport of air

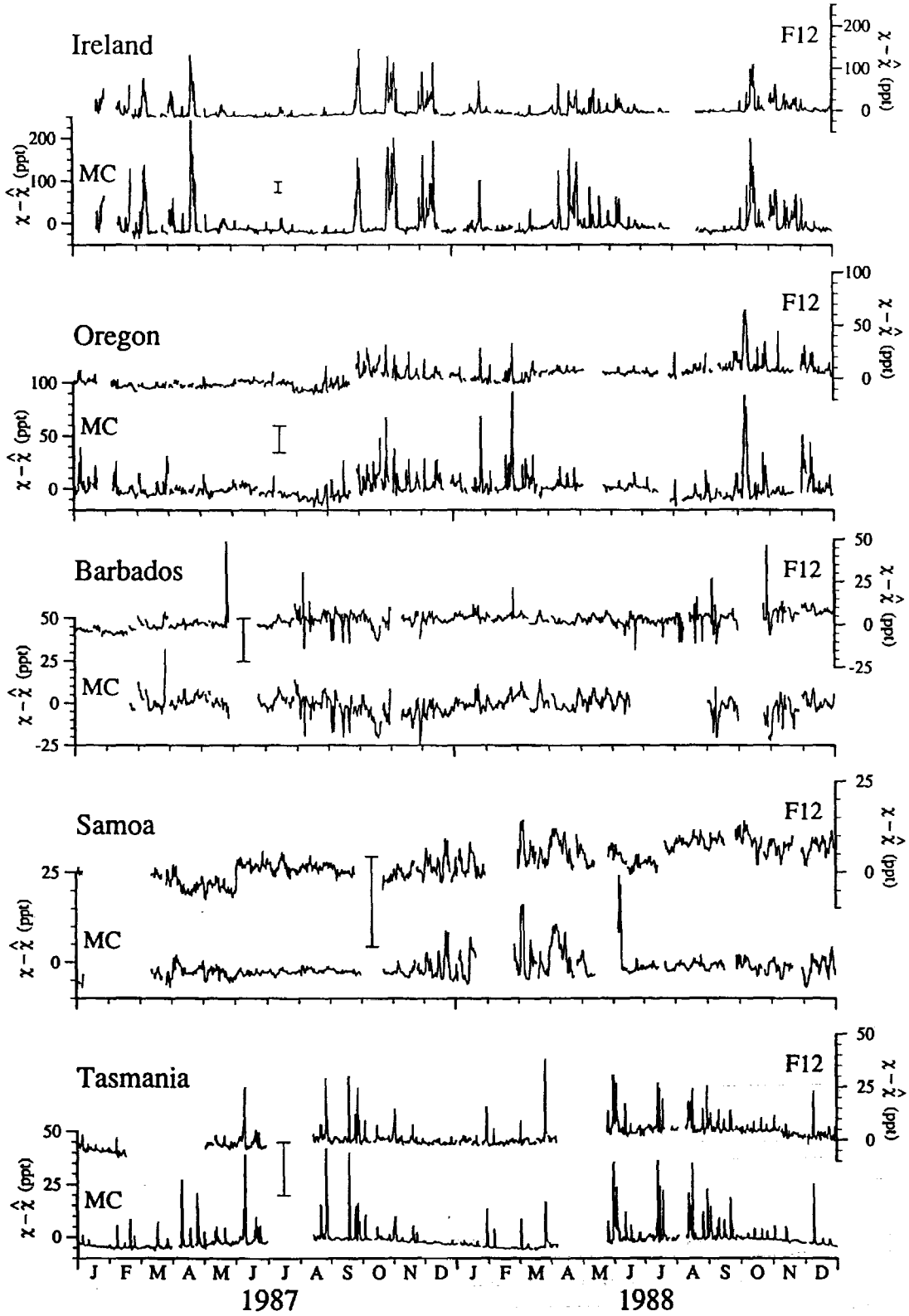

Fig. 1. Twelve-hour averages of the high-frequency (12 per day) measurements of CH_3CCl_3 (MC) and CF_2Cl_2 (F12) during 1987–1988 at the five ALE/GAGE stations with time average and linear trend removed illustrating pollution events at mid-latitude stations and large-scale meridional transport-induced variations at tropical stations. The high-frequency CH_3CCl_3 and CF_2Cl_2 variations are highly correlated as expected. Units are parts per trillion by molecular number in dry air designated ppt. Note the different concentration scales used for mid-latitude and tropical stations. The vertical bar on each station denotes 25 ppt.

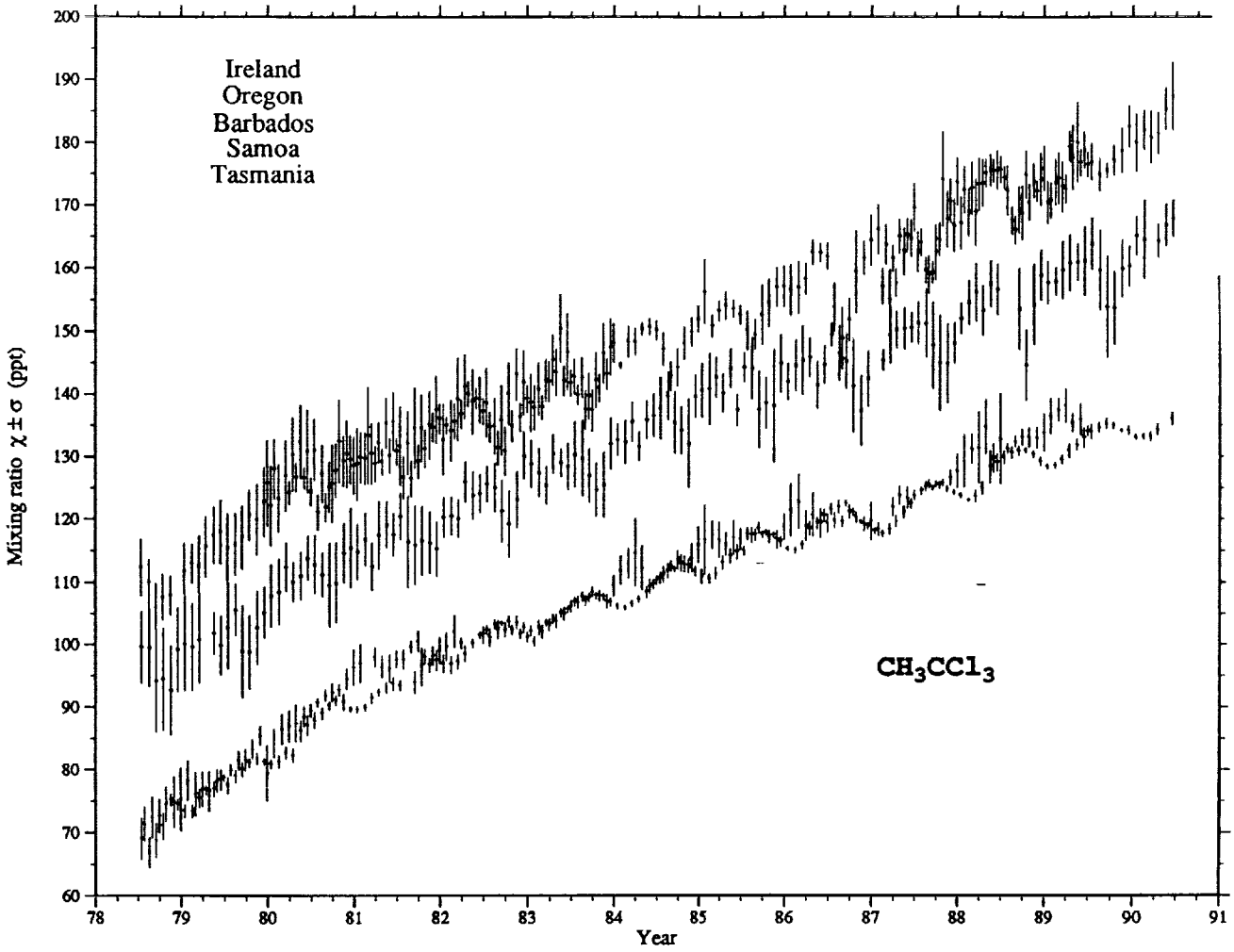

Plate 1. Monthly mean concentrations and standard deviations for CH_3CCl_3 during 1978–1990 at the five ALE/GAGE stations. Pollution events have been removed from the mid-latitude stations. The Ireland station was located at Adrigole for 1978–1983 and Mace Head for 1987–1990. Units are parts per trillion by number (ppt).

from the northern hemisphere during this season. This process and its relation to the Southern Oscillation (SO) will be discussed later. Note that the latitudinal gradient (parts per trillion per degree) of CH_3CCl_3 is about twice that of CF_2Cl_2, accounting for the generally greater amplitude of these circulation-induced variations for CH_3CCl_3 than for CF_2Cl_2 at both of these tropical sites [*Hartley and Prinn*, 1991].

For many of the analyses undertaken in this paper, the ALE/GAGE measurements, when averaged over time scales of a month or longer, are intended to be indicative of the air in a large atmospheric region. Specifically for the CH_3CCl_3 lifetime determinations in this paper this region consists of the air between the surface and 500 mbar in the semihemisphere in which the station lies. Hence periods of obvious local CH_3CCl_3 pollution occurring at Ireland, Oregon, and Tasmania are specifically omitted from the data used to define the monthly means and standard deviations discussed in the following sections.

3.2. *Monotonic and Periodic Variations*

Monthly mean mixing ratios χ and standard deviations σ computed from the 120 to 360 measurements made each month at each ALE/GAGE station are illustrated in Plate 1 and tabulated in Table 1. As discussed elsewhere [*Prinn et al.*, 1983*a*, *b*; *Fraser et al.*, 1986*a*; *Prinn et al.*, 1987], the latitudinal gradients of concentration, the larger standard deviations in the northern hemisphere than in the southern hemisphere, and the distinct annual cycles in concentration can be explained at least qualitatively in terms of distances from sources (largely northern mid-latitude), intensity and seasonality of the global circulation, and the seasonal cycle in the reaction

$$OH + CH_3CCl_3 \rightarrow H_2O + CH_2CCl_3 \qquad (1)$$

caused by the seasonal cycle (with summer maximum) in OH concentrations.

To describe the monotonic and periodic features of the data, the monthly mean mixing ratios χ_i at station i are described conveniently by an empirical model comprised of orthogonal functions either monotonic or periodic in time. Specifically,

$$\chi_i = a_i + b_i P_1\left(\frac{t}{6} - 1\right) + d_i P_2\left(\frac{t}{6} - 1\right) + c_i \cos(2\pi t) + s_i \sin(2\pi t) + p_i \cos(2\pi t/t_0) + q_i \sin(2\pi t/t_0) \qquad (2)$$

where t is time (in years) measured from the beginning of the record, P_1 and P_2 are Legendre polynomials of the order of 1 and 2, respectively, and $t_0 = 2.4$ years is the assumed period of the quasi-biennial oscillation (QBO). The maximum likelihood estimates of a_i, b_i, d_i, p_i, q_i, c_i, and s_i obtained by weighting each χ_i by its inverse variance are given in Table 2. Note from Table 2 (and also Plate 1) that statistically significant annual cycles (described by c_i, s_i) are evident in Ireland, Oregon, Barbados, and Tasmania. An annual cycle is barely evident in Samoa from the coefficients in Table 2, but cycles become quite evident if one divides the data into periods corresponding to extrema in the SO, as discussed later. A statistically significant QBO is evident at Barbados (0.8 ppt amplitude) but is marginal or absent at the other stations. This general conclusion still holds when we assume $t_0 = 2.25$ years for the QBO with only slight changes in the amplitude and phase at Barbados relative to the $t_0 = 2.4$-year case. A similar result for Barbados (but not Tasmania) was found for ALE/GAGE N_2O data [*Prinn et al.*, 1990].

The 12-year averages of the CH_3CCl_3 mixing ratios and trends at each station are given by the a_i and $b_i/6$ values, respectively, in Table 2. Averaging these a_i and $b_i/6$ values at Tasmania, Samoa, Barbados, and Ireland plus Oregon we obtain a "global" 12-year average mixing ratio of 124.5 ppt and trend of 5.5 ± 0.2 ppt yr^{-1} (i.e., $4.4 \pm 0.2\%$ per year) with uncertainties being 1σ. As noted earlier, the CH_3CCl_3 trend is large compared to the inferred errors associated with drifting standards and the maximum inferred errors associated with instrumental nonlinearities. Negative values for the rate of change in the trend ($d_i/12$) at all stations except Cape Meares mean that the annual rate of increase of CH_3CCl_3 is overall decreasing with time, consistent with an approach to a steady state.

Because the annual cycle in CH_3CCl_3 at some of the stations is not a simple 12-month harmonic, equation (2) has limitations for application to these stations. To provide further analysis of the annual cycle we compute monthly mean residuals R by subtracting monotonic variations (as described by an unweighted cubic polynomial fit to the data) from the χ values, thus leaving the periodic variations in the residuals. For each month we then determine the 12-year average residual, its standard deviations, and its standard error. To illustrate persistence and further address fluctuations, we also compute the autocorrelation coefficient $A(t)$ for time lags of t months with a value being considered significant at the 95% level if $A(t) > 2/\sqrt{n}$ where n (≤ 144) is the total number of monthly residuals [e.g., *Hartley and Prinn*, 1991].

The residuals and autocorrelations for Ireland, Oregon, Barbados, and Tasmania are given in Figure 2. It is evident that only Tasmania possesses a nearly simple 12-month harmonic annual cycle. Barbados and Oregon have a significant annual cycle, but the cycles consist of fairly constant positive residuals for 9 months and relatively larger negative residuals for 3 months requiring superposition of a number of harmonics to describe them. Ireland also possesses a significant annual cycle requiring superimposed harmonics to fit it. Negative residuals in Barbados in September–November are associated with transport from the south of air with anomalously low CH_3CCl_3 mixing ratios. As a result the standard deviations σ (Table 1) are about 50% higher during September–November than during the rest of the year. Transitions from positive to negative residuals during the local summer in Ireland, Oregon, and Tasmania are certainly due in part to faster chemical destruction (equation (1)), but circulation and proximity to sources are additional contributors in Ireland and Oregon and to a lesser extent in Tasmania.

3.3. *Interannual Variations and the Southern Oscillation*

Examination of Plate 1 shows that in some years there is a sharp seasonal maximum in CH_3CCl_3 at Samoa during the first few months of the year (e.g., years 1981, 1984, 1985, 1986, 1988, 1989) so that the CH_3CCl_3 measurements at Samoa and Tasmania are anticorrelated. However, in other years (particularly 1983 and 1987) this boreal winter maximum is not present, and the CH_3CCl_3 mixing ratios at Samoa and Tasmania are highly correlated. In conjunction with the absence of the boreal winter maximum in 1983 and 1987 the standard deviations σ at Samoa are depressed relative to other years (see Figure 3). The periods from mid-1982 to mid-1983 and from mid-1986 to mid-1987 were characterized by strong SO "warm event" or El Nino conditions in the tropical Pacific, suggesting that the dramatic circulation changes associated with swings of the SO affect the mixing ratio of CH_3CCl_3 at Samoa.

Southern Oscillation-methyl chloroform relationships are specifically examined by correlating standard indices of the tropical Pacific circulation used by the U.S. National Meteorological Center (NMC) to monitor the SO with monthly mean methyl chloroform fluctuations. These indices (to be described later) are specifically intended to describe interannual variability and so are defined in terms of departures from a climatological seasonal cycle. To make meaningful quantitative comparisons of the time series of these indices with fluctuations of methyl chloroform, it is therefore necessary to remove both the long-term trend and a mean seasonal cycle from the latter.

To match the definitions of the SO indices, monthly concentration anomalies δR at each station are defined by subtracting from the residuals R the climatological (i.e., 12-year average) monthly mean value of the residuals. Similarly, monthly standard deviation anomalies $\delta\sigma$ are defined by removing climatological (i.e., 12-year average) monthly means of the standard deviations σ.

Before discussing correlations with tropical circulation indices, it is instructive to compare the standard deviation (s) and 1-month lag autocorrelation $a(1)$ statistics of the δR and $\delta\sigma$ time series, shown in two columns of Table 3. The pairs of standard deviations are nearly the same at the three Northern Hemisphere sites and are about a factor of 2 larger than the corresponding values at Tasmania. Standard deviations at Samoa are slightly smaller than those at the northern hemisphere sites, and s is least in Tasmania. Tropospheric eddy activity is vigorous in the vicinity of Tasmania [*Trenberth*, 1981], so the small s value here is undoubtedly due to the fact that CH_3CCl_3 is much more homogeneously distributed in the deep southern hemisphere than in the northern hemisphere.

The autocorrelation statistic provides some measure of the coherence of month-to-month variability apart from the seasonal cycle. Four of the δR series exhibit a substantial degree of autocorrelation (between 0.5 and 0.7). The notable exception is Barbados, where there is very little persistence

TABLE 1. Monthly Mean Mixing Ratio χ (ppt), Standard Deviations σ (ppt), and Number of Measurements Each Month N of CH_3CCl_3 at the ALE/GAGE Sites Over the Period July 1978 to June 1990

		Ireland			Oregon			Barbados			Samoa			Tasmania		
Year	Month	χ	σ	N	χ	σ	N	χ	σ	N	χ	σ	N	χ	σ	
1978	7	112.1	4.6	224		...		99.6	5.8	144	71.1	2.9	61	68.8	3.4	
1978	8	109.7	3.7	185		...		99.5	6.2	200	72.1	3.4	125	66.6	2.6	1
1978	9	105.8	3.9	235		...		94.3	8.2	168	72.4	2.9	126	68.5	2.9	
1978	10	107.4	3.8	151		...		94.6	8.2	111	74.2	2.9	108	70.7	2.2	
1978	11	107.7	3.3	92		...		92.8	7.1	125	74.6	4.2	97	74.9	1.1	
1978	12		...			...		99.3	6.7	129	75.0	5.1	57	74.2	1.0	
1979	1	111.5	4.6	74		...		100.2	7.5	114	78.0	3.3	18	73.1	1.2	
1979	2	112.7	3.2	25		...		99.7	7.0	112	75.9	3.6	95	73.1	1.2	
1979	3	112.2	5.0	68		...		100.8	6.9	95	76.6	2.9	117	75.2	1.6	1
1979	4	115.4	4.9	62		...			...		76.3	3.4	120	76.5	0.9	1
1979	5	117.2	4.6	81		...		101.9	3.3	80	77.9	2.0	122	76.7	1.4	1
1979	6	117.7	5.1	68		...		100.0	4.7	40	78.5	0.7	114	78.1	1.8	1
1979	7	115.1	5.6	136		...		102.8	6.7	88	79.7	1.1	118	77.2	1.4	8
1979	8	115.8	5.0	104		...		105.6	4.1	117	81.2	1.7	111	78.7	1.2	11
1979	9	116.8	5.1	94		...		99.0	7.4	134	81.3	1.9	102	79.7	1.3	10
1979	10	120.3	4.1	53		...		98.8	5.9	127	83.0	1.8	115	80.8	0.9	9
1979	11	119.7	5.8	72		...		102.8	5.9	90	85.2	1.7	113	81.5	1.1	11
1979	12	122.5	5.7	69	125.5	7.0	55	105.2	4.1	130	79.2	4.7	102	81.0	0.7	8
1980	1	121.9	6.4	58	127.7	4.9	71	107.9	5.0	133	84.0	2.4	100	80.6	0.9	9
1980	2	123.0	5.5	106		...		108.5	5.2	105	86.3	2.6	122	81.0	1.1	7
1980	3	126.7	5.7	89	123.9	2.0	20	112.5	3.8	104	86.7	2.7	103	82.4	1.2	11
1980	4	130.0	6.0	103	126.4	2.4	78	110.1	3.1	79	87.1	3.1	116	82.0	1.3	4
1980	5	132.0	6.0	60	126.3	1.8	93	111.0	3.8	137	88.2	1.8	115	85.9	1.8	7
1980	6	130.6	6.7	115	124.1	2.4	114	113.9	3.4	147	89.2	1.2	94	86.8	1.8	8
1980	7	130.7	5.0	111	120.8	2.9	85	112.9	4.6	129	90.5	0.8	117	87.6	1.5	9
1980	8	126.9	4.7	111	121.6	2.5	81	111.3	3.5	59	91.6	1.0	117	88.7	1.1	9
1980	9	124.8	4.2	104	125.3	6.3	103	109.6	6.6	126	92.1	1.6	103	90.0	0.8	6
1980	10	127.4	4.4	81	132.1	6.7	111	109.9	6.4	126	92.5	1.1	17	90.8	1.0	7
1980	11	129.0	4.2	77	130.1	5.5	118	114.6	4.7	117	94.2	1.8	63	90.5	1.5	9
1980	12	129.2	4.0	66	128.2	4.6	104	115.5	6.3	118	96.1	3.0	100	89.4	0.6	8
1981	1	128.5	5.9	118	129.5	4.2	121	114.8	4.4	138	96.7	3.2	42	89.4	0.7	5
1981	2	129.4	4.2	60	133.0	7.8	107	116.8	4.2	119		...		89.7	0.7	4
1981	3	130.2	4.9	96	128.5	2.9	120	112.5	3.7	100	97.8	1.7	30	91.2	1.0	8
1981	4	131.9	3.3	46	128.8	2.2	106	117.4	5.3	104	96.2	1.9	136	92.1	0.7	76
1981	5	135.0	4.0	59	129.8	2.9	104	119.1	3.6	123	95.9	2.4	123	92.8	1.0	86
1981	6	135.3	4.7	79	130.5	2.3	108	117.6	3.4	110	97.4	1.5	113	93.4	1.1	60
1981	7	131.4	6.3	120	126.4	3.5	116	120.4	3.7	86	97.4	1.7	73	93.2	1.0	53
1981	8	131.9	5.1	112	126.2	3.0	107	116.4	7.2	95	99.4	1.1	104		...	
1981	9	134.2	6.5	75	128.9	2.8	84	115.9	6.2	95	100.3	1.8	79	93.7	2.0	78
1981	10	134.2	5.4	58	130.9	3.1	73	116.6	5.4	128	97.8	1.4	97	96.2	3.2	52
1981	11	134.7	5.5	85	134.3	2.4	68	116.3	4.8	110	97.9	1.7	64	96.5	1.3	100
1981	12	137.2	5.4	87	135.7	2.5	96	115.3	4.3	108	98.8	2.3	87	97.1	1.8	420
1982	1	132.4	5.8	85	134.6	1.5	87	120.3	3.1	104	99.5	2.4	68	96.6	1.6	393
1982	2	133.8	4.9	100	135.3	2.9	54	120.5	3.0	68	101.9	2.7	64	96.5	1.5	362
1982	3	138.9	6.7	83	136.4	2.3	91	120.1	3.0	110	100.0	1.1	54	97.0	1.3	347
1982	4	140.9	5.2	69	139.6	2.1	98	126.0	3.3	119		...		98.2	1.5	390
1982	5	138.5	5.3	41	138.9	1.8	52	123.8	3.8	123		...		99.9	0.9	371
1982	6	138.8	3.7	85	136.9	2.2	110	124.1	3.0	118	101.3	1.5	18	101.2	0.7	413
1982	7	138.3	5.5	69	134.4	2.5	67	125.6	2.8	49	100.9	1.6	108	102.0	0.9	377
1982	8	134.5	4.6	115	131.0	2.8	112	125.0	3.9	83	102.2	1.7	101	102.9	0.9	344
1982	9	135.5	5.6	110	130.5	4.0	63	121.3	4.9	115	102.1	1.3	104	103.1	0.5	369
1982	10	139.7	5.0	98	134.5	2.6	71	119.2	5.2	71	102.1	0.9	121	103.4	1.0	445
1982	11	142.8	4.2	111	135.9	2.3	66	123.1	4.5	120	101.4	0.9	99	103.2	1.1	359
1982	12	141.5	5.2	125	138.8	2.3	51	130.1	3.6	152	100.9	1.0	93	102.4	0.9	463
1983	1	138.2	4.6	81	137.5	3.6	100	128.8	3.8	130	100.2	0.9	61	101.9	1.0	455
1983	2	140.5	4.3	65	137.5	2.0	71	127.4	3.9	122	101.8	1.2	97	102.4	1.3	314
1983	3	141.9	3.5	122	141.6	3.4	87	125.4	3.0	122	102.9	1.1	88	103.2	0.7	452
1983	4	145.1	4.1	89	143.1	3.8	96	130.4	3.1	133	103.5	1.2	101	103.8	0.9	354
1983	5	150.1	5.5	106	141.7	2.5	91	129.0	2.2	126	104.7	1.2	119	104.8	0.9	310
1983	6	146.4	6.2	96	141.3	2.2	107	128.4	3.7	132	105.9	1.1	106	105.4	0.7	374
1983	7	142.4	3.0	65	139.4	1.7	86	130.3	5.2	123	106.5	1.1	122	106.6	0.9	353
1983	8	142.3	3.3	80	137.1	3.2	93	129.7	6.0	126	106.8	1.0	125	107.4	0.9	387
1983	9	139.3	3.7	97	137.0	3.4	342	126.9	4.3	103	108.2	1.0	116	107.3	0.9	372
1983	10	141.9	4.6	119	140.5	2.3	228	124.7	4.3	90	107.6	1.0	117	107.6	0.7	419
1983	11	146.1	4.9	78	142.8	2.6	267	125.5	5.2	123	106.6	1.3	84	107.4	0.7	384
1983	12	147.1	4.6	107	147.8	3.2	233	132.1	4.1	123	109.1	1.8	122	106.5	0.8	459
1984	1		...		144.3	0.6	24	132.6	2.5	129	111.6	2.4	114	105.9	0.7	397
1984	2		...		148.0	2.6	341	132.3	3.4	124	112.7	2.5	106	105.6	0.5	357
1984	3		...		147.9	2.3	353	135.5	3.1	86	114.4	5.5	109	106.3	0.7	417

TABLE 1. (continued)

		Ireland			Oregon			Barbados			Samoa			Tasmania		
Year	Month	χ	σ	N	χ	σ	N	χ	σ	N	χ	σ	N	χ	σ	N
1984	4		···		150.0	1.1	383	131.6	2.3	93	111.9	3.6	112	107.0	0.7	345
1984	5		···		150.3	1.4	345	135.8	3.1	93	109.1	1.3	122	108.1	1.0	256
1984	6		···		149.8	1.6	404	136.5	3.4	96	110.0	0.9	104	109.4	0.9	210
1984	7		···		146.8	2.8	328	137.6	4.9	110	111.0	1.4	112	110.3	1.1	239
1984	8		···		142.5	2.4	241	139.6	3.9	117	112.3	1.0	109	111.5	1.3	286
1984	9		···		143.8	3.1	231	135.4	4.9	123	113.2	1.7	114	111.8	0.6	272
1984	10		···		147.7	2.8	166	134.2	3.8	129	112.6	1.4	78	112.6	1.5	322
1984	11		···		149.6	2.4	216	132.0	7.1	118	113.5	2.4	104	112.2	1.3	406
1984	12		···		151.6	2.2	269	139.6	3.4	104	115.6	3.0	120	111.4	1.0	460
1985	1		···		155.9	5.2	229	140.5	4.3	133	116.5	5.7	119	110.6	1.3	425
1985	2		···		150.5	1.9	231	140.8	5.7	107	117.2	2.4	109	110.3	0.9	307
1985	3		···		152.9	1.7	243	142.6	3.2	124	116.4	2.9	111	111.1	1.1	413
1985	4		···		153.7	2.3	267	140.1	3.1	128	115.7	2.0	118	112.8	1.2	406
1985	5		···		153.2	1.4	191	144.0	3.1	143	116.8	2.9	112	113.8	1.3	341
1985	6		···		152.2	1.6	254	137.4	2.5	74	116.5	1.8	116	114.4	1.3	369
1985	7		···		149.7	3.2	229	144.2	2.4	60	117.3	1.1	233	114.6	0.9	286
1985	8		···		149.1	2.5	175	144.0	4.8	141	117.2	1.0	397	117.1	1.3	175
1985	9		···		152.2	4.9	181	137.5	6.0	113	117.3	0.7	282	118.2	1.0	266
1985	10		···		154.1	3.9	236	138.5	4.1	167	116.9	1.2	195	117.5	0.6	302
1985	11		···		156.6	3.2	198	138.1	9.0	424	116.5	1.6	515	117.1	0.7	243
1985	12		···		156.8	3.3	99	144.8	4.6	435	118.5	2.3	554	116.0	1.0	344
1986	1		···		156.1	4.1	187	141.9	2.9	372	121.2	4.4	422	114.9	0.5	348
1986	2		···		156.5	4.2	264	144.5	4.1	342	122.5	4.5	393	114.7	0.6	310
1986	3		···		157.9	2.6	210	145.3	5.5	418	118.6	2.6	317	115.5	0.8	342
1986	4		···		162.1	2.1	204	145.8	3.1	460	120.4	3.6	443	118.1	1.2	288
1986	5		···		162.0	1.5	197	141.4	3.8	344	119.1	2.5	346	119.0	1.1	275
1986	6		···		161.5	2.3	297	144.6	3.1	270	119.0	1.6	285	120.2	1.2	312
1986	7		···		153.4	4.0	339	149.4	1.8	288	119.5	1.4	316	121.2	1.0	290
1986	8		···		148.4	5.1	332	146.5	4.4	317	119.3	0.9	273	121.6	1.2	307
1986	9		···		151.4	3.5	307	145.2	4.4	304	120.9	1.2	306	122.2	0.6	282
1986	10		···		159.0	6.6	181	141.2	7.4	323	120.0	1.1	347	120.7	0.8	113
1986	11		···		161.2	2.7	206	137.3	5.5	324	118.9	1.3	298	119.2	0.5	158
1986	12		···		164.0	4.1	168	142.4	4.4	238	119.4	3.1	355	118.6	0.7	293
1987	1		···		165.7	4.0	175		···		118.1	1.2	50	117.8	0.7	324
1987	2	156.8	2.9	57	163.4	3.2	189	145.3	1.6	59		···		117.3	0.7	287
1987	3	154.7	4.8	200	161.1	2.2	274	149.4	4.6	241	121.7	1.5	157	118.0	1.0	305
1987	4	157.4	2.3	189	164.6	2.8	224	150.2	3.0	288	123.5	1.6	321	119.3	1.1	202
1987	5	162.3	3.9	241	164.8	2.8	326	150.4	3.3	262	123.1	1.8	337	120.7	1.1	301
1987	6	164.4	3.0	310	169.3	4.0	273	150.5	2.4	53	123.5	0.9	316	122.1	0.9	274
1987	7	162.3	3.3	289	163.6	2.2	295	151.3	3.4	264	124.2	0.8	364		···	
1987	8	159.3	2.1	295	158.6	3.1	299	151.2	5.4	327	125.3	0.9	369	124.8	1.0	151
1987	9	159.0	1.8	300	162.1	4.4	236	147.7	6.9	319	125.3	0.7	343	124.6	0.5	281
1987	10	164.3	2.7	224	173.8	7.7	233	144.9	7.6	325	125.5	0.6	91	125.0	0.7	259
1987	11	167.5	4.6	240	170.3	3.6	228	144.8	6.4	231	126.3	1.3	340	124.5	0.7	282
1987	12	166.4	4.3	145	173.3	3.9	207	148.1	3.2	343	127.4	2.7	314	123.9	0.6	334
1988	1	166.9	4.2	207	172.0	3.8	251	152.0	2.4	313	128.9	4.3	214	123.4	0.6	251
1988	2	168.6	3.8	247	172.3	4.3	224	154.5	3.5	320	130.9	2.4	37	122.6	0.4	324
1988	3	168.6	5.4	305	172.9	4.2	262	156.1	4.6	321	131.1	5.8	349	123.3	1.1	265
1988	4	173.3	3.8	180	174.7	2.3	282	153.2	3.9	317	134.4	4.4	318	124.5	1.2	60
1988	5	175.3	2.5	213	175.1	1.9	119	157.4	3.6	356	129.4	2.5	159	128.0	2.7	58
1988	6	175.3	3.1	181	175.3	2.2	310	156.6	4.1	203	132.5	7.3	280	128.6	1.4	264
1988	7	174.0	1.8	220	172.0	4.1	168		···		131.0	0.9	298	129.4	1.2	274
1988	8	167.3	2.3	67	165.7	2.3	245		···		132.0	1.0	365	130.2	1.0	196
1988	9	169.0	3.8	337	168.4	4.4	252	153.5	6.4	318	132.7	1.4	229	130.5	0.8	253
1988	10	174.6	3.9	168	170.1	3.0	239	144.5	5.6	73	132.7	1.6	327	130.6	0.5	325
1988	11	173.6	2.7	126	171.9	1.7	243	154.2	6.4	310	132.7	1.7	253	129.9	0.6	286
1988	12	173.9	4.2	284	175.5	3.6	244	158.8	4.0	343	133.5	3.0	346	128.8	0.8	253
1989	1	170.2	3.5	282	170.4	3.0	319	157.7	3.3	343	136.1	2.9	353	128.0	0.6	309
1989	2	173.4	3.7	264	174.0	4.1	182	157.8	2.2	109	137.1	1.9	303	128.2	0.6	247
1989	3	172.7	4.1	88	172.2	2.4	271	159.7	4.5	215	137.8	2.8	72	129.1	0.8	311
1989	4	179.1	2.4	209	177.2	5.2	289	160.8	4.4	301	135.1	1.5	166	130.5	1.2	243
1989	5	179.8	6.5	242	176.5	2.2	351	161.0	2.9	300	135.6	2.6	340	131.5	1.0	258
1989	6	178.6	2.9	256	176.1	2.0	292	161.1	5.5	250	133.7	1.0	337	132.6	1.7	271
1989	7	176.7	2.9	203		···		163.8	4.1	300		···		133.6	1.2	261
1989	8	174.7	2.7	323		···		159.7	6.4	349		···		134.2	0.9	294
1989	9	175.4	1.2	40		···		153.9	8.0	301		···		134.8	1.0	255
1989	10	176.9	2.5	145		···		153.7	5.8	318		···		134.5	0.7	228
1989	11	178.5	3.6	117		···		159.9	4.6	278		···		133.8	0.5	241
1989	12	182.3	3.3	83		···		160.3	3.1	309		···		133.8	0.9	279
1990	1	179.7	4.6	232		···		165.2	3.1	328		···		132.7	0.6	322
1990	2	181.8	3.2	168		···		164.5	6.2	256		···		132.8	0.6	259

TABLE 1. (continued)

Year	Month	Ireland			Oregon			Barbados			Samoa			Tasmania	
		χ	σ	N	χ	σ	N	χ	σ	N	χ	σ	N	χ	σ
1990	3	180.6	4.3	198		...			...			...		132.8	0.9
1990	4	181.3	3.3	240		...		164.3	2.6	272		...		133.9	1.1
1990	5	185.2	3.5	160		...		166.8	3.4	228		...			...
1990	6	187.2	5.5	319		...		167.9	2.9	223		...		135.6	1.2

Units are parts per trillion by number. For Oregon (beginning September 1983), Barbados (beginning August 1985), Samoa (beginning 1985), and Tasmania (beginning July 1981) the ALE (HP5840) and GAGE (HP5880) monthly data are combined by weighting equally A and GAGE monthly means to determine χ and ALE and GAGE individual measurements to determine σ. The calibration fa $\xi = 0.80$ is included here. Data excludes "pollution events."

of monthly anomalies. The largest autocorrelation, 0.68 at Tasmania, is consistent with the above suggestion of a near-homogeneous distribution of methyl chloroform; monthly anomalies would tend to persist in such an environment. Time series of $\delta\sigma$, the monthly anomalies of intramonthly standard deviation, exhibit less autocorrelation (generally between 0.3 and 0.5) than the series of δR. The largest $\delta\sigma$ autocorrelation, 0.65, is again found at Tasmania.

The Southern Oscillation is a vast fluctuation of the coupled ocean-atmosphere system involving the entire tropical Pacific [*Rasmusson and Wallace*, 1983]. Profound interannual circulation changes in the tropical atmosphere occur in conjunction with the SO. To monitor these changes, the NMC formulates and publishes indices of the tropical circulation that have been shown empirically to provide useful descriptions of the state of the SO [*Chelliah*, 1990]. The indices are derived from observed monthly mean near-equatorial pressure, zonal wind, and outgoing longwave radiation (a proxy for large-scale convection). We will show results based on just one of the indices, denoted U8C. This index is derived from the monthly mean analyses of 850 mbar zonal wind averaged over the area bounded by 5°N, 5°S, 175°W, and 140°W which lies just to the north of Samoa. A positive U8C index denotes an easterly anomaly. Because the indices (and circulation anomalies represented by them) are mutually correlated, for our purposes the U8C index can be interpreted as a general index of the SO.

"Cold" (La Nina) and "warm" (El Nino) event years are conveniently defined by calculating annual averages of U8C for 12-month periods starting each July and ending the following June. Years with annually averaged U8C < -0.75 are defined as warm SO events; two such years, 1982/1983 and 1986/1987, meet this criterion. Similarly, 1983/1984, 1984/1985, 1985/1986, and 1988/1989 are defined as cold (La Nina) events with annually averaged U8C > 0.75. T residuals and autocorrelations for all years at Samoa shown in Figure 3, but because averaging all of the ye together masks the SO effect, we also show in Figure 3 residuals and autocorrelations separately for the warm ev (specifically July 1982–June 1983 and July 1986–June 19 and cold event (specifically July 1983–June 1986 and J 1988–June 1989) periods. The difference in phases a structure of the annual cycles associated with the two extrema are very evident. The climatological (12-year av age) seasonal cycles of R and σ in Figure 3 include a bro boreal winter-spring maximum for R and σ and summ autumn maximum for R and minimum for σ. The cold ev composites for R and σ are both slight amplifications of t climatological (12-year average) cycle. During warm eve the winter-spring maximum for R and σ disappears, so th the phase of the annual cycle of R reverses and the int monthly standard deviation σ has practically no seasonali remaining at a low level (just above 1 ppt) throughout t year.

Correlations r(U8C) between the δR and $\delta\sigma$ series and t U8C index are shown in the right-hand column of Table To ascertain the significance of r(U8C), the autocorrelati statistics are used to calculate the degrees of freedo present in each δR and $\delta\sigma$ series [*Leith*, 1973]. Assuming first-order Markov process to model the decay of autocorr lation with lag, we estimate the effective time betwe independent samples in each time series and derive a 5 nonzero significance threshold for r(U8C). This is not rigorous significance test because an a priori t test is beir applied a posteriori to the correlations (i.e., it is expected b chance that 5% of the calculated values of r(U8C) wi exceed the 5% significance threshold), but the test sti serves as a useful standard.

TABLE 2. Optimally Determined Coefficients (With 1σ Uncertainties) in Empirical Model (Equation (2)) Fit to Data in Table 1

Site	a_i	$b_i/6$	$d_i/12$	c_i	s_i	p_i	q_i
Adrigole/MaceHead, Ireland*	148.0 ± 0.4	5.8 ± 0.1	−0.15 ± 0.08	0.8 ± 0.2	−1.6 ± 0.2	0.8 ± 0.5	−0.2 ± 0.5
Cape Meares, Oregon†	147.7 ± 0.2	5.7 ± 0.1	0.11 ± 0.05	−1.4 ± 0.2	−2.6 ± 0.2	0.5 ± 0.3	−0.2 ± 0.3
Ireland plus Oregon*	147.5 ± 0.2	5.8 ± 0.1	−0.08 ± 0.03	−0.4 ± 0.2	−2.2 ± 0.2	0.5 ± 0.3	−0.3 ± 0.3
Ragged Point, Barbados*	133.0 ± 0.2	5.6 ± 0.1	−0.26 ± 0.04	1.2 ± 0.2	−2.1 ± 0.2	0.5 ± 0.2	−0.6 ± 0.2
Point Matatula, Samoa‡	109.8 ± 0.5	5.3 ± 0.2	−0.36 ± 0.11	−0.2 ± 0.2	−0.5 ± 0.2	0.3 ± 0.4	0.5 ± 0.4
Cape Grim, Tasmania*	107.5 ± 0.3	5.3 ± 0.1	−0.43 ± 0.06	0.8 ± 0.2	1.3 ± 0.2	0.2 ± 0.3	−0.2 ± 0.3

The mean concentration for the 12-year time interval 1978–1990 is given by a_i, the mean trend by $b_i/6$, and the mean rate of change o the trend by $d_i/12$. Units are parts per trillion (ppt) for a_i, p_i, q_i, c_i, and s_i, ppt/yr for $b_i/6$, and ppt/yr^2 for $d_i/12$.

*July 1978 to June 1990.

†March 1980 to June 1989.

‡July 1978 to June 1989.

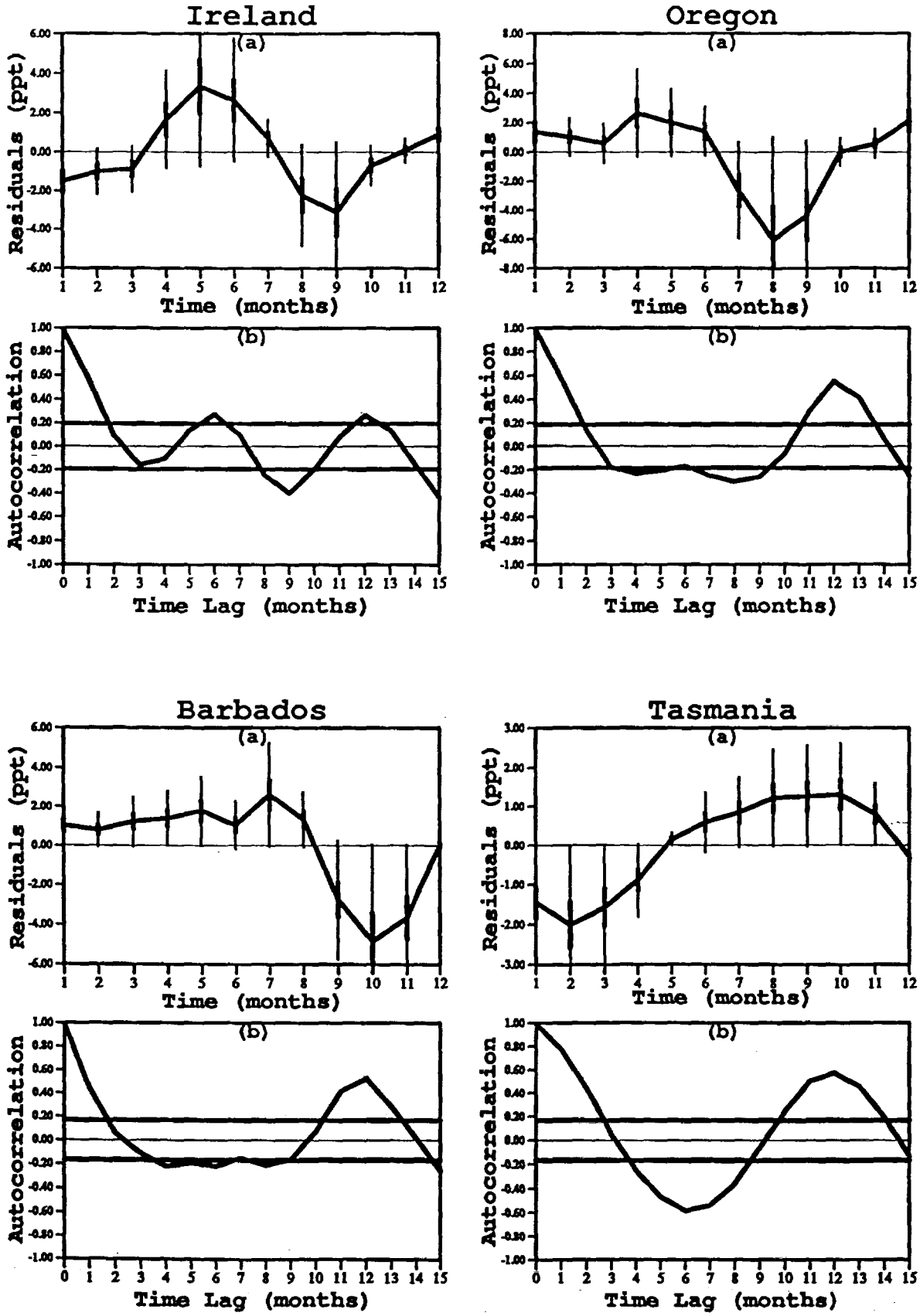

Fig. 2. For the Ireland, Oregon, Barbados, and Tasmania ALE/GAGE stations we show (*a*) 12-year average of monthly mean residuals R, its standard deviation (thin vertical bars) and its standard error (thick vertical bars) with parts per trillion (ppt) units; (*b*) autocorrelation coefficient $A(t)$ for time lags of t months with a repeat cycle being significant if $A(t)$ lies outside the limits shown by horizontal lines.

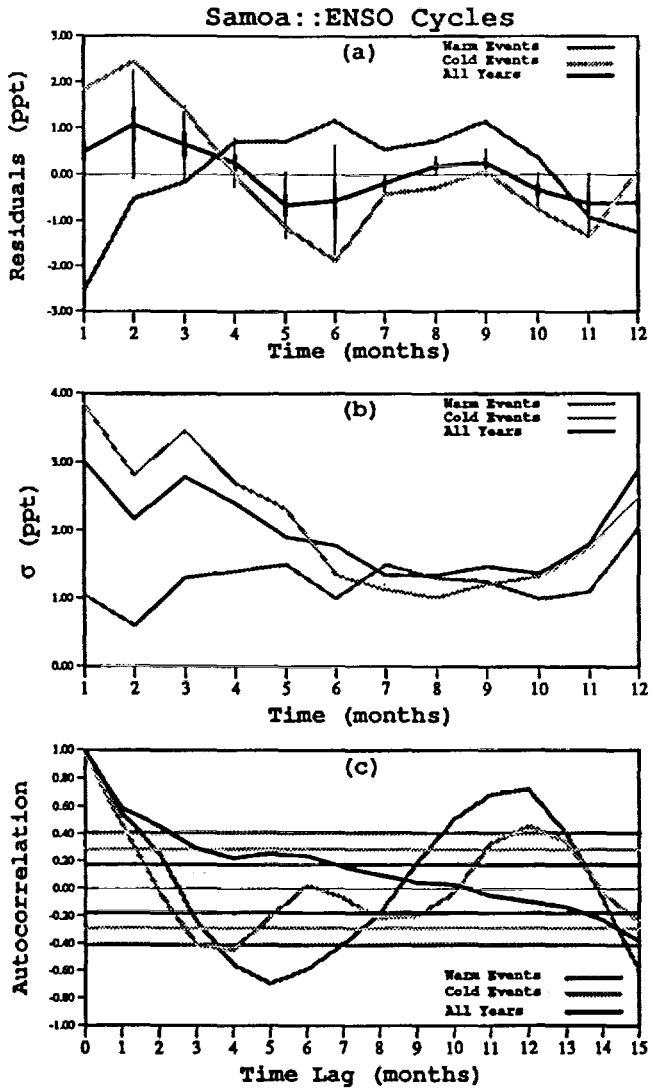

Fig. 3. For the Samoa station we show (*a*) average of monthly mean residuals (parts per trillion (ppt)) over ENSO warm event and cold event years and over all years; error bars as in Figure 3, (*b*) average of standard deviation of monthly means (ppt) over ENSO warm and cold event years and over all years; and (*c*) autocorrelation coefficients as in Figure 3 computed for ENSO event years and all years.

The correlation between δR at Samoa and U8C is 0.54, satisfying the 5% nonzero significance threshold criterion. The strong correlation is also quite evident in the actual time series for δR (Samoa) and U8C shown together in Figure 4. Correlations at Samoa with other SO indices not shown in Table 3 also exceed 0.4. The sign of the correlations indicates that positive anomalies of δR are associated with easterly zonal wind anomalies at 850 mbar in the central equatorial Pacific (i.e., strong trade winds), westerly zonal wind anomalies aloft, and depressed large-scale convection along the equator near the date line. The opposite relationships are also implied: negative δR anomalies are associated with weak trades, easterly anomalies aloft, and enhanced equatorial convection. Thus positive (negative) anomalies of methyl chloroform at Samoa are associated with cold (warm) SO conditions. The $\delta\sigma$ series at Samoa is also positively correlated with U8C, although this correlation is smaller

TABLE 3. Standard Deviations s (Units Parts Per Trilli and 1-Month Lag Autocorrelations $a(1)$ of Monthly Mea δR and $\delta\sigma$ at Each Site

	s	$a(1)$	r(U8C)
Ireland			
δR	2.2	0.63	0.14 (0.
$\delta\sigma$	1.2	0.52	−0.02 (0.
Oregon			
δR	2.1	0.50	0.14 (0.
$\delta\sigma$	1.1	0.31	−0.18 (0.
Barbados			
δR	2.1	0.18	0.08 (0.
$\delta\sigma$	1.2	0.30	0.00 (0.
Samoa			
δR	1.8	0.62	0.54 (0.
$\delta\sigma$	1.0	0.36	0.31 (0.
Tasmania			
δR	1.0	0.68	−0.06 (0.
$\delta\sigma$	0.5	0.65	−0.01 (0.

See text for details of the detrending algorithm used to ger δR and $\delta\sigma$. Right-hand column shows correlation coefficients a δR, $\delta\sigma$, and U8C, an index of the Southern Oscillation. The no 5% nonzero significance threshold for r(U8C) is shown in pare ses; correlations exceeding this threshold are underlined.

than that involving δR. Correlations derived from the c four sites are insignificant.

To explain the SO-CH_3CCl_3 relationship, we propose fluctuations of the large-scale zonal wind field across near-equatorial Pacific strongly modulate the cr equatorial transport of CH_3CCl_3. Throughout the yea zonally averaged westerly zonal winds in both hemisph are separated by a band of zonally averaged easterlies the equator [*Newell et al.*, 1972], forming a critical line inhibits cross-equatorial propagation of large-scale Ro waves, which account for much of the eddy activity (and suggest, the transports of trace gases as well) in the tr sphere [*Holton*, 1979]. Across the central and eastern cific, however, the climatological upper tropospheric z winds are westerly during the boreal winter and sp [*Newell et al.*, 1972], forming a "westerly duct" porous t but the largest scale waves [*Webster and Holton*, 1982]

Fluctuations of the SO are associated with profo circulation changes across the Pacific. Cold events characterized by enhanced easterly trade winds near surface and enhanced westerly winds in the upper tro sphere with anomalies typically reaching extreme val during the boreal winter, thereby facilitating cross-equato propagation of waves through the westerly duct [*Web and Holton*, 1982]. Enhanced high-frequency (intramonth eddy activity is also observed during these periods [*A and Webster*, 1985]. Warm event conditions are associa with anomalies of winds and eddy energy of the oppo signs; during strong SO warm events the westerlies aloft dramatically restricted [*Arkin*, 1982] and the westerly d effectively closes.

Samoa is located just to the south of the equatorial Pac westerly duct. Fluctuations of δR and $\delta\sigma$ at Samoa consistent with this dynamical picture, considering t nearly all of the CH_3CCl_3 reaching Samoa originates in northern hemisphere: increased (decreased) mean transpo and intramonthly variance occur during cold (warm) events, corresponding to positive (negative) values of U8

Thus the climatological boreal winter maximum

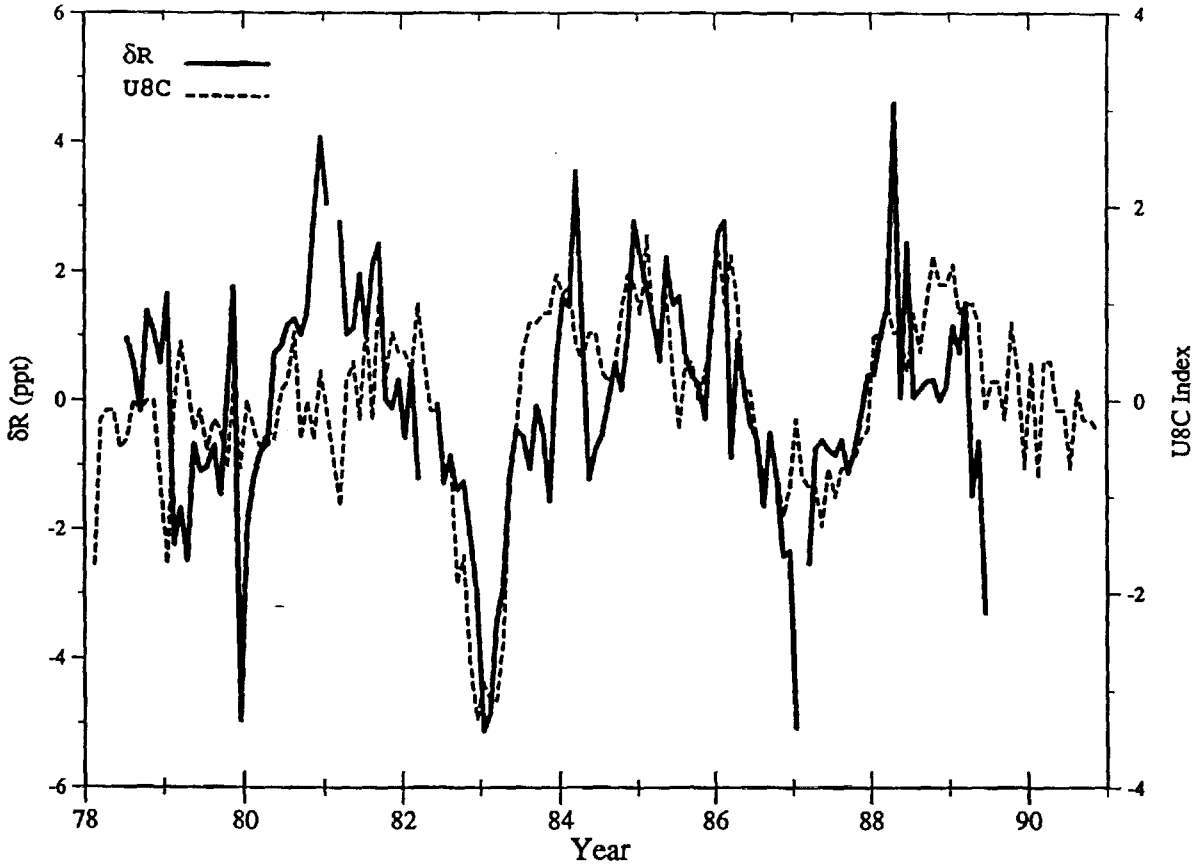

Fig. 4. Monthly methyl chloroform concentration anomalies δR (parts per trillion (ppt)) at Samoa and monthly values of the ENSO index U8C over the period 1978–1990.

CH_3CCl_3 and its intramonthly variability at Samoa appear to result from the seasonal maximum in tropospheric cross-equatorial transport from the northern hemisphere. During cold event years this transport is enhanced. During warm event years the westerly duct is effectively closed and transport from the northern hemisphere is significantly diminished. During these periods, chemical destruction processes can assume a larger role in modulating month-to-month fluctuations of CH_3CCl_3 concentration at Samoa. Specifically, the chemical sink (reaction, equation (1)) would tend to yield a decrease during December–February in CH_3CCl_3 mixing ratios (as observed in Samoa in warm event years and in all years in Tasmania). This is because humidity, ozone concentrations, and ultraviolet fluxes (and thus OH concentrations) as well as temperatures (and thus the rate constant for the reaction in (1)) are both expected to maximize in this time period. The warm event years are characterized by higher than normal (by ~1°C) surface temperatures and thus presumably higher than normal absolute humidities, in the vicinity of Samoa [*Bottomley et al.*, 1990]. These conditions would both tend to increase the influence of the chemical sink at Samoa. Note also that during extreme warm events the mixing ratios of CH_3CCl_3 at Samoa and Tasmania are almost identical, indicating a remarkably homogeneous distribution of CH_3CCl_3 in the South Pacific at these times.

4. Inverse Problems

To interpret the CH_3CCl_3 measurements in terms of surface emissions, atmospheric circulation, and atmospheric destruction, we utilize an optimal estimation inversion technique [*Cunnold et al.*, 1983, 1986]. The technique includes the use of a two-dimensional model of the global atmosphere consisting of eight tropospheric boxes (or grid points) and four upper atmospheric boxes. The four lower tropospheric boxes (or grid points) are intended to provide predictions for comparing with the ALE/GAGE stations in the four semi-hemispheres. Mean inverse advective times (V_{ik}) and eddy diffusive times (t_{ik}) in the model vary seasonally and are specified from meteorological observations and an optimal fit to global ALE/GAGE data for $CFCl_3$ [*Cunnold et al.*, 1986; *Prinn et al.*, 1990].

The 12-month running means for the lower tropospheric mixing ratios χ_1, χ_3, χ_5, and χ_7 predicted in this model are used to compare with monthly mean ALE/GAGE observations rather than the monthly mean model mixing ratios. This is because this box model is not capable of accurately simulating oscillations associated with the measurement technique (e.g., periodic renewal of on-site calibration tanks) or natural meteorological oscillations (e.g., weather patterns, SO, etc.). To account in a statistical way for these unsimulated oscillations, the model output is augmented by two empirical statistical models that are designed to describe the spectrum of the differences (residuals) between the observations and the 12-month running mean model predictions [*Cunnold et al.*, 1986]. Lower frequencies in this spectrum were fitted with a first-order autoregressive model common to all sites with a correlation of 0.5 after 1 month (see Figures 2 and 3 for correlations); higher frequencies

were modeled by assuming that the spectra at each site were the same as those found in the residuals between the observations and the empirical model fit to the observations described earlier (2).

The optimal estimation scheme produces a best guess of the unknown y_i (contained in vector y) and their errors σ_i based on minimizing the squares of the deviations between the logarithms of the observed (vector x) and model-calculated (vector x_c) monthly mean mixing ratios at each ALE/GAGE site. The vector y is updated with each new month of data using

$$\Delta y = CP'[PCP' + N]^{-1}(x - x_c) \qquad (3)$$

where P (transpose P') is a matrix of the partial derivatives of the elements of x_c (the model predictions) with respect to the elements of y (the unknowns), N is a diagonal matrix whose nonzero elements are the squares of the standard errors in the elements of x (i.e., the standard deviations in the monthly observations), and C is a matrix whose diagonal elements are the variance (i.e., σ_i^2) of the elements of y (the unknowns) based on an objective combination of a priori estimates of the uncertainties in the unknowns and the uncertainties in the measurements. The matrices P and C are updated during the inversion process as described by *Cunnold et al.* [1983]. Estimates of unknowns y_i and errors σ_i can be obtained with each ALE/GAGE station data alone or all station data sets simultaneously.

We have interpreted the ALE/GAGE measurements in two different ways. First, using these measurements and industrial CH_3CCl_3 surface emissions estimates, we calculate the CH_3CCl_3 tropospheric lifetime τ (or equivalently a weighted average OH radical concentration) and its temporal trend over the 12 years of the experiment. Second, we specify the tropospheric lifetime τ and then we calculate the total annual global CH_3CCl_3 emission for each ALE/GAGE year using the measurements. In the latter case, the fractions assumed emitted into each semihemisphere are equated to their fractions in the industrial emission estimates.

4.1. *Lifetimes and Hydroxyl Radical Concentrations*

Accurate determination of the CH_3CCl_3 atmospheric lifetime requires accurate estimates of its industrial emissions over the globe. *Prinn et al.* [1987] presented their estimates of emissions and their uncertainties for the period 1951–1985 based on the then best available industry data. *Midgley* [1989] has recently reported the results of a more extensive industry-led effort to gather the sales data needed to determine these emissions.

In this paper we compute 1970–1990 emissions from the sales estimates of *Midgley* [1989] for 1970–1988, P. Midgley (private communication, 1991) for 1989, and assume 1990 sales equal the sum of the 1989 sales and the difference between the 1989 and 1988 sales. All sale numbers are first adjusted for the combined effects of manufacturing losses, incineration, and incarceration by multiplying them by $\phi = 0.99 \pm 0.006$ based on industry information [*Midgley*, 1989]. For 1981–1990, emissions are computed from adjusted sales assuming time delays of 0.25 years for sales for solvent end uses and 0.75 years for sales for other end uses [*Midgley*, 1989]. For 1970–1980 we take into account these time delays by assuming that the fraction α of total annual sales held in user inventories for release in the following year equals 0.006 $\pm$ 0.013 which is the average value of α for 1981–1 Combining the uncertainties in sales of $\pm 2.1\%$ [*Mid* 1989] with those given above for ϕ and α, we deduc uncertainty in each annual emission estimate for 1970– of $\pm 2.2\%$ (1σ). Additional emission scenarios with maxir and minimum trends over the relevant 12 years of A GAGE (1978–1990) are computed by constraining them t within the 2σ limits for each annual emission estim Finally, for the years 1950–1969 the previous emis estimates by *Prinn et al.* [1987] are used. These emiss are input into the four lower tropospheric boxes in our m using estimates of emissions by latitude from Midgley [1 P. Midgley, private communication, 1991] for 1980–1 and *Prinn et al.* [1987] for 1950–1979. All of the emiss related data used in this paper are summarized in Table

In the 1970–1985 time period where the estimates over the Table 4 estimates generally lie between 1 and 2σ of *Prinn et al.* [1987] estimates, and the 16-year total emissi in the two studies differ by only 1.7%. However, the tre in the emissions in the two estimates are quite different v the *Prinn et al.* [1987] estimates being consistently la than the Table 4 estimates for 1970–1976 and consiste smaller for 1980–1985. As noted in *Prinn et al.* [19 estimates of the lifetime of CH_3CCl_3 based on fitting trends in its concentration are quite sensitive to uncertain in the trends in the emissions, so that we expect the Tab emission estimates to yield a significantly different lifeti computed from fitting the CH_3CCl_3 trends than the ear *Prinn et al.* [1987] emission estimates. The other two me ods we use for computing lifetimes which focus on fitting global CH_3CCl_3 content and latitudinal gradient are significantly altered by the differences between these t emission scenarios.

As shown by *Prinn et al.* [1987], the chemical lifetime methyl chloroform in the upper atmospheric box is taken 6 years based on the three-dimensional model of *Golom and Prinn* [1986]. Because only about 11% of the to CH_3CCl_3 destruction occurs in the upper atmospheric b the assumed lifetime in this box is not critical. The lifetime in the ith tropospheric box is assumed to be given by

$$\tau_i^{-1} = k_i A[\mathrm{OH}]_i^* \qquad (4$$

where k_i is the temperature-dependent rate constant [*L More et al.*, 1990] for the reaction in (1) in the box i, [OH is a theoretical estimate of the OH concentration in the b [*Logan et al.*, 1981; *Prinn et al.*, 1983*b*], and A is unknown dimensionless coefficient by which the theoretic estimates are to be multiplied to provide an optimal between the model and CH_3CCl_3 observations. As noted i *Prinn et al.* [1983*b*, 1987] the estimates of the glob tropospheric lifetime τ (or equivalently the global weight average tropospheric OH concentration) are quite insen tive to the choice of $[\mathrm{OH}]_i^*$; the lifetimes and OH conce trations deduced for individual tropospheric boxes are course proportional to $[\mathrm{OH}]_i^*$. This latter insensitivity al enables a simple a posteriori adjustment of the derived value or OH concentrations to take account of a sm oceanic sink, as discussed later.

As fully discussed by *Cunnold et al.* [1983, 1986], *Prinn al.* [1983, 1987], and *Cunnold and Prinn* [1991], we dete mine lifetimes based on three features of the measurement Our first method focuses on optimally fitting the measure

TABLE 4. Global Emissions Derived From *Midgley* [1989] and P. Midgley (Private Communication, 1990) and Percentage Emissions in Each Semihemisphere Based on Above References for 1980–1989 and on *Prinn et al.* [1987] for 1970–1979

Year	Global Emission	Error, 2σ	Maximum Trend	Minimum Trend	Percentage Emissions			
					90°–30°N	30°–0°N	0°–30°S	30°–90°S
1970	153	7	153	153	97.5	1.0	0.4	1.1
1971	173	8	173	173	97.3	1.1	0.4	1.2
1972	224	10	224	224	97.2	1.2	0.4	1.2
1973	276	12	276	276	97.1	1.2	0.4	1.3
1974	311	14	311	311	97.0	1.3	0.4	1.3
1975	304	13	304	304	96.8	1.3	0.5	1.4
1976	402	18	402	402	96.7	1.4	0.5	1.4
1977	475	21	475	475	96.6	1.4	0.5	1.5
1978	518	23	495	541	96.3	1.4	0.6	1.7
1979	501	22	482	520	95.7	1.6	0.9	1.8
1980	546	24	531	561	94.0	1.6	1.5	2.9
1981	544	24	532	556	94.2	2.0	1.3	2.5
1982	518	23	510	526	93.9	2.1	1.4	2.6
1983	530	23	526	534	94.4	2.0	1.3	2.3
1984	579	25	579	579	93.6	2.7	1.5	2.2
1985	587	26	591	583	93.5	2.7	1.5	2.3
1986	596	26	604	588	91.6	3.9	1.8	2.7
1987	617	27	629	605	91.2	4.9	1.5	2.4
1988	659	29	674	644	90.3	5.9	1.5	2.3
1989	701	31	720	682	91.3	5.2	1.4	2.1
1990	743	33	766	720	91.3	5.2	1.4	2.1

Also shown are global emissions with maximum and minimum trends consistent with the 2σ errors for 1978–1990 (see text). All 1990 values are extrapolations from available data. Emission units are 10^9 gm yr^{-1}.

fractional trends in CH_3CCl_3 ("trend" method). In Table 5 we show the estimates of $1/\tau$ using this method that are obtained with each station data set alone (Adrigole, Ireland, and Cape Meares, Oregon, data are combined for this purpose) and all data sets simultaneously. The trend method also provides an estimate of the calibration factor $\xi = 0.77$ consistent with the ALE/GAGE $\xi = 0.8 \pm 0.08$. A calibration factor $\xi = 0.56$ (Y. Makide, private communication, 1991) yields a much poorer fit to the data (also see *Cunnold and Prinn* [1991]). Our two other methods focus on optimally fitting the measured global content of CH_3CCl_3 ("content" method) and the measured concentrations at individual stations relative to the global average ("gradient" method). Estimates of $1/\tau$ based on these two methods are also provided in Table 5.

4.2. *Trends in Hydroxyl Radical*

With 12 years of ALE/GAGE CH_3CCl_3 data in hand it is of considerable interest to address the possibility of a temporal trend in OH. For this purpose we first compute the CH_3CCl_3 lifetime and weighted global average OH concen-

TABLE 5. Tropospheric Lifetime Estimates for Methylchloroform Derived From Trends in ALE/GAGE Data at Each Site and for All Sites Combined

Case	Reciprocal Lifetime, $year^{-1}$	Lifetime, years	Weight Given to Site in Optimal Estimation of Lifetime
Ireland and Oregon	0.222 ± 0.011	4.5	0.27
Ragged Point, Barbados	0.219 ± 0.013	4.6	0.22
Point Matatula, Samoa	0.191 ± 0.014	5.2	0.19
Cape Grim, Tasmania	0.201 ± 0.010	5.0	0.32
All sites from trend	0.210 ± 0.006	4.8	
All sites from trend, with emission trend uncertainty included	$0.210^{+0.037}_{-0.022}$	4.8	
Global atmospheric content, with emission and calibration uncertainty included	0.164 ± 0.031	6.1	
Latitudinal gradient	0.166 ± 0.030	6.0	
Annualized content	0.167 ± 0.011	6.0	
Variable lifetime	0.169 ± 0.025	5.9	
Best estimate	0.175 ± 0.020	5.7	

Uncertainties are 1σ and include allowance for potential biases of the time series inferred from the variance of the individual site lifetime estimates. Also given are lifetimes derived from the global atmospheric content and from the latitudinal gradient. All results assume a stratospheric lifetime of 6 years. The annualized content and variable lifetime cases allow the lifetime to vary over time.

TABLE 6. Estimates of CH_3CCl_3 Tropospheric Lifetime (Years) and Global Average Tropospheric OH Concentrations (10^5 radical cm^{-3}) Deduced From ALE/GAGE Measurements and Emission Estimates (10^9 gm yr^{-1}) of Table 4 in the Indicated Years

Year	Lifetime	OH Concentration	Emissions, Table 4	Emissions, ALE/GAGE	
				τ = 5.6 Years	τ = 5.9 Years
1979	6.7 ± 0.5	7.4 ± 0.5	501 ± 22	552 ± 13	536 ± 13
1980	6.2 ± 0.4	8.0 ± 0.5	546 ± 24	577 ± 16	559 ± 16
1981	5.6 ± 0.2	8.8 ± 0.3	544 ± 24	544 ± 6	525 ± 6
1982	6.2 ± 0.3	8.0 ± 0.4	518 ± 23	556 ± 17	536 ± 17
1983	6.4 ± 0.3	7.7 ± 0.3	530 ± 23	583 ± 13	562 ± 13
1984	6.0 ± 0.3	8.2 ± 0.4	579 ± 25	609 ± 11	587 ± 12
1985	5.9 ± 0.2	8.4 ± 0.3	587 ± 26	608 ± 11	586 ± 11
1986	5.6 ± 0.2	8.8 ± 0.3	596 ± 26	595 ± 9	572 ± 9
1987	6.4 ± 0.3	7.7 ± 0.4	617 ± 27	672 ± 14	648 ± 14
1988	5.8 ± 0.2	8.5 ± 0.3	659 ± 29	671 ± 6	646 ± 6
1989	5.4 ± 0.3	9.1 ± 0.5	701 ± 31	676 ± 23	650 ± 23

Also shown are emissions (10^9 gm yr^{-1}) estimated from ALE/GAGE measurements assuming constant tropospheric lifetimes τ of either 5.6 or 5.9 years. Uncertainties are 1σ.

tration using the content method but now considering each year individually and utilizing the 12-month running mean ALE/GAGE observations (since the network is too sparse to define the global trend in any single year). We use the Table 4 emission estimates for the best guess, maximum trend, and minimum trend scenarios. The results from this method designated the "annualized content" method are summarized in Tables 5 and 6. From these annual numbers we deduce a statistically significant positive linear trend in the global OH concentration of 1.0 ± 0.6% per year (1σ).

As an alternative approach we also repeated the analysis in section 4.1 using the full 12 years of data but now expressing the unknown $1/\tau$ (or equivalently A) as a linear function of time (i.e., $1/\tau = 1/\tau(0) + td(1/\tau)/dt$) and deducing the two unknowns $1/\tau(0)$ and $d(1/\tau)/dt$. In this "variable lifetime" method the calibration factor ξ must be specified instead of estimated. The percentage trend in OH (i.e., 100 d ln $(1/\tau)/dt$) thus determined is also 1.0 ± 0.6% per year (1σ) for ξ = 0.80. Inclusion of an uncertainty in ξ of ±0.08 yields a percentage trend in OH of 1.0 ± 0.8% per year (1σ). The average (i.e., mid-1984) τ value for 1979–1989 using this variable lifetime method is 5.9 (+1.0, −0.8) year (1σ) including the stated uncertainty in ξ. A comparison of the predicted and observed CH_3CCl_3 concentrations for this case is given in Figure 5. Assuming ξ = 0.56 (Y. Makide, private communication, 1991) yields a significantly different average lifetime (3.6 years) and OH trend (−0.7 ± 0.6% per year), but in this case, the root-mean-square residual between model and observation is 4.2% compared to 0.8% for ξ = 0.80.

Combining with equal weight the lifetime estimates based on the annualized content and variable lifetime methods and the three methods discussed in section 4.1 (Table 5), we obtain a best estimate of $1/\tau$ = 0.175 ± 0.020 $year^{-1}$ corresponding to a tropospheric lifetime estimate for CH_3CCl_3 of 5.7 (−0.6, +0.7) years, a value for A in (4) of 0.743 ± 0.083, and a value for the global average OH radical concentration (weighted by the product of the CH_3CCl_3 density and the temperature dependence (exp $(-1800/T)$) of the reaction in (1)) of (8.7 ± 1.0) × 10^5 radical cm^{-3} (all stated uncertainties are 1σ). For a stratospheric lifetime of 6 years [*Golombek and Prinn*, 1986] the tropospheric lifetimes τ quoted above can be converted to total atmospheric lifetimes τ_{tot} using the formula $1/\tau_{tot} = 0.895/\tau + 0.018$. Thus the best estimate tropospheric lifetime τ = 5.7 (−0.6, years corresponds to a best estimate total atmos lifetime $\tau_{tot} \approx \tau$. Multiplying the above A value by the [value in each tropospheric box in our model we obta following regional values for the OH radical concentrat units of 10^5 radical cm^{-3}: 5.5 ± 0.6 (30°–90°N), 11.7 (0°–30°N), 11.0 ± 1.2 (0°–30°S), and 6.0 ± 0.7 (30°–90 the four lower troposphere (500–1000 mbar) boxes; ar ± 0.6 (30°–90°N), 11.2 ± 1.3 (0°–30°N), 11.7 ± 1.3 (0°– and 6.8 ± 0.8 (30°–90°S) in the four upper tropos (200–500 mbar) boxes.

The ocean, by simple dissolution followed by sinki depth and/or by aqueous phase chemical destruction, additional sink for CH_3CCl_3. *Golombek and Prinn* [estimated a loss time τ_0 to the ocean for CH_3CCl_3 of 9 years which is very small relative to the atmosp CH_3CCl_3 sink. Later, *Wine and Chameides* [1989] prop that hydrolysis of CH_3CCl_3 in ocean water may be significant yielding a much shorter loss time to the oce 22–42 years. Recently, *Butler et al.* [1991] report showing subsaturation of CH_3CCl_3 in the mid-Pacific Oc and based on these data they estimate a loss time tc ocean of 62–134 years. To a sufficient approximatior tropospheric OH concentrations deduced above ca corrected for a small oceanic sink by multiplying then the coefficient A) by the factor $\beta = 1 - \tau/\tau_0$. Combinin estimate of τ = 5.7 years from this paper with the estima $\tau_0 = 85^{+49}_{-23}$ years from *Butler et al.* [1991] yields β = 0. 0.02, implying the above OH concentrations are too hig 7 ± 2%. Specifically, the weighted global average concentration is (8.1 ± 0.9) × 10^5 radical cm^{-3} (1σ) inc ing this ocean sink.

4.3. *Emissions*

By specifying the lifetime τ of CH_3CCl_3, an alterna inverse problem can be solved in which the annual gl CH_3CCl_3 emissions are the unknowns. The results assun τ is constant are shown in Table 6. The stated uncertain in these derived emissions do not include the uncertaint ξ. Results are shown for τ = 5.6 years (the average τ for three methods in section 4.1) and τ = 5.9 years (the ave τ for the two methods in section 4.2). In this case, i

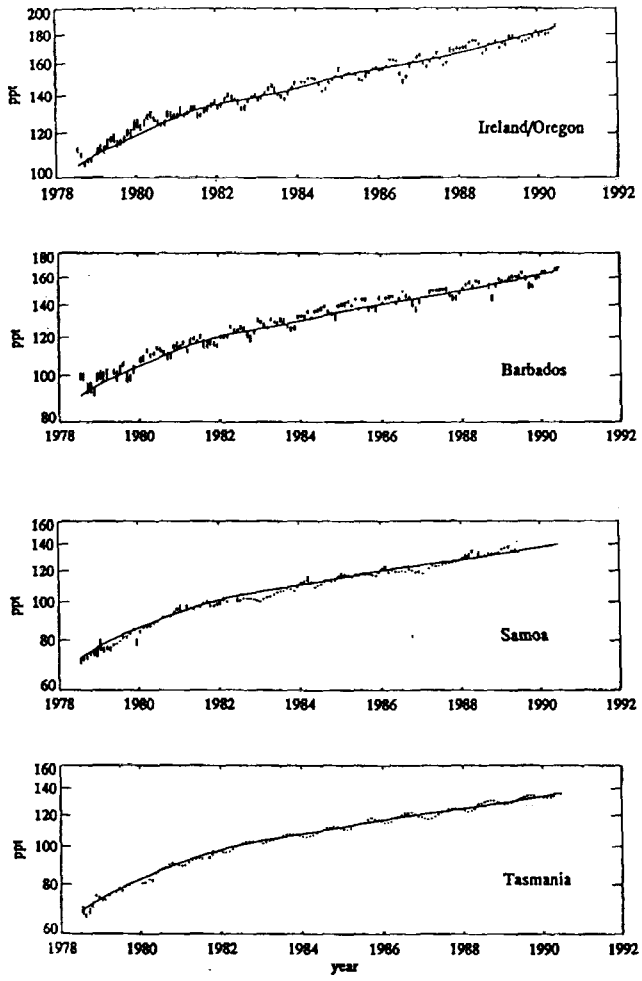

Fig. 5. Model predictions of CH_3CCl_3 concentrations (parts per trillion (ppt)) for $\tau = 5.9$ years and $d \ln (1/\tau)/dt = 0.01$ year^{-1} compared to ALE/GAGE monthly mean measurements. Error bars shown are standard errors taking into account individual measurement autocorrelations.

apparent that the trend in emissions deduced from the ALE/GAGE data is significantly less than that in the emissions given in Table 4 which were deduced from industry data [*Midgley*, 1989]. This is simply another way of demonstrating that the industry-derived emissions imply that τ is not constant but is slowly decreasing with time.

4.4. *Methane Lifetime and Emissions*

Methane is a chemically and radiatively important atmospheric gas with diverse and geographically dispersed natural and anthropogenic sources [*Cicerone and Oremland*, 1988; *Quay et al.*, 1991]. Because the major recognized tropospheric sink for methane is reaction with OH with a rate constant whose temperature dependence is very similar to that for methyl chloroform, the weighted average OH concentrations deduced by combining the five methods in sections 4.1 and 4.2 can legitimately be used together with observed temperatures and methane distributions [*Steele et al.*, 1987; *Blake and Rowland*, 1988] to calculate an average tropospheric lifetime for CH_4 [*Prinn et al.*, 1987]. Using the rate constant for the reaction

$$CH_4 + OH \rightarrow CH_3 + H_2O \qquad (5)$$

recently reported by *Vaghjiani and Ravishankara* [1991], we calculate an average tropospheric lifetime (tropospheric content divided by destruction rate due to OH) for CH_4 of 11.1 (+1.4, −1.1) years (1σ), whereas using the earlier rate constant evaluation reported by *DeMore et al.* [1990], we compute a lifetime of 9.3 (+1.2, −0.8) years (1σ). The stated CH_4 lifetimes do include an oceanic sink of 1/85 year^{-1} for CH_3CCl_3 in deducing OH concentrations, but the stated uncertainties do not include the uncertainty in any of the relevant rate constants.

The above CH_4 lifetime using the *Vaghjiani and Ravishankara* [1991] rate constant can be combined with the observed 1978–1990 average global atmospheric CH_4 content $M = 4.65 \times 10^{15}$ gm and the observed 1978–1990 average CH_4 trend $dM/dt = 4.5 \times 10^{13}$ gm yr^{-1} [*Blake and Rowland*, 1988; D. Blake and S. Rowland, private communication, 1991 (hereinafter referred to as BR91)] to determine the 1978–1990 average global annual CH_4 emission $E = (470 \pm 50) \times 10^{12}$ gm year^{-1} (1σ). The emissions by each individual source type deduced by *Cicerone and Oremland* [1988] and *Quay et al.* [1991] which utilized a CH_4 lifetime of 9.6 years [*Prinn et al.*, 1987] can be simply renormalized to give this new global emission estimate.

The positive trend in OH (section 4.2) has important implications for methane and for all other relatively long-lived trace gases which like CH_3CCl_3 are destroyed predominantly by OH. Specifically, in a one-box atmospheric model the rate of change of the temporal trend of such a trace gas is given by

$$\frac{d^2M}{dt^2} = \frac{dE}{dt} - \frac{1}{\tau}\left(\frac{dM}{dt} + \frac{M d \ln [OH]}{dt}\right) \qquad (6)$$

where E is the global emission rate and the inverse lifetime $1/\tau$ is proportional to the weighted global average OH concentration [OH]. From *Blake and Rowland* [1988; BR91] for the 1978–1990 time period $d^2M/dt^2 = -2.3 \times 10^{12}$ gm yr^{-2}. Using $\tau = 11.1$ year, $d \ln [OH]/dt = 0.01$ year^{-1}, and M and dM/dt from above, we thus determine the 1978–1990 average rate of change of the global methane emission rate $dE/dt = 6 \times 10^{12}$ gm yr^{-2}. Ignoring the OH trend (i.e., $d \ln [OH]/dt = 0$), we obtain $dE/dt = 1.8 \times 10^{12}$ gm yr^{-2} which is about one third of the (presumably correct) value including the trend. Thus we conclude that the OH trend derived from CH_3CCl_3 is a major contributor to the presently observed (BR91) slowing of the rate of increase in atmospheric methane (i.e., negative d^2M/dt^2).

5. CONCLUSION

We have presented a summary of high-frequency real-time atmospheric measurements made between 1978 and 1990 of the anthropogenic chemical compound 1,1,1-trichloroethane (methyl chloroform, CH_3CCl_3). Analysis of these data indicates that CH_3CCl_3 is increasing at a global average rate over this time period of 4.4 ± 0.2% per year (1σ), reaching a global average concentration of about 157 ppt in mid-1990. Interpretation of these data has led to important new conclusions relevant to atmospheric chemistry and atmospheric transport.

The first set of conclusions refer to the hydroxyl radical

which is the major recognized oxidant in the global atmosphere and the major sink for CH_3CCl_3. The measured CH_3CCl_3 concentrations and trends combined with industrial emission estimates have been used in an optimal estimation inversion scheme to deduce a globally averaged CH_3CCl_3 atmospheric lifetime of 5.7 (+0.7, −0.6) years (1σ) which is significantly less than our previous estimate [*Prinn et al.*, 1987]. We derived a weighted global average tropospheric hydroxyl radical (OH) concentration of 8.7 (± 1.0) × 10^5 radical cm^{-3} (1σ) which reduces to an estimate of 8.1 (± 0.9) × 10^5 radical cm^{-3} (1σ) if we include an oceanic loss rate for CH_3CCl_3 of 1/85 $year^{-1}$. The rate of change of the weighted global average OH concentration over this time period is determined to be 1.0 ± 0.8% per year (1σ) which has major implications for all longer-lived species which like CH_3CCl_3 are destroyed predominantly by OH radicals. This positive trend in OH is evident if we use for CH_3CCl_3 the simple one-box atmospheric model applied to CH_4 in section 4.4. Specifically, rearranging (6) and using the 1978–1990 mean dE/dt from Table 4, the 1978–1990 mean M, dM/dt, and d^2M/dt^2 deduced from a_i, $b_i/6$ and $d_i/12$ in Table 2, and the average of the τ values obtained by the variable lifetime and annualized content methods in Table 5, we obtain

$$100\left(\frac{d\ \ln\ [OH]}{dt}\right) = 100\left(\frac{\tau}{M}\frac{dE}{dt} - \frac{\tau}{M}\frac{d^2M}{dt^2} - \frac{d\ \ln\ M}{dt}\right)$$

$$= 3.9 + 1.4 - 4.4 = 0.9\%\ yr^{-1}. \quad (7)$$

Note also that an average upward drift in calibration or an average overestimate in the industrial emission trend would need to be as large as 1% per year for 12 years to negate this deduced positive trend.

While we caution that this deduced rate of change assumes that current industry estimates of anthropogenic emissions and our absolute calibration of CH_3CCl_3 are very accurate, there are theoretical reasons to expect a positive trend for OH in the tropical lower troposphere which is the region strongly weighted in the quoted global average. First, the sensitivity of OH to NO_x levels above 100 ppt [*Liu et al.*, 1988] combined with the 2–3% per year growth in (largely urban) population in tropical countries [*World Resources Institute*, 1990] should be resulting in increasing tropical urban OH levels. Second, *Keller et al.* [1991] compute a significant increase (e.g., a factor of 6 for the dry season) in predicted local OH concentrations when natural tropical forest is replaced by cultivated areas with much higher NO_x levels. Tropical deforestation is currently proceeding at a rate of about 0.6–1.3% per year [*World Resources Institute*, 1990]. Third, these local effects could be exported since *Fishman et al.* [1991] have provided observational evidence that tropical biomass burning (a major land clearing mechanism) yields elevated ozone levels (and thus presumably OH levels) over an area of the tropics and southern subtropics very much larger than the areas being burned. Finally, as discussed in section 3.3, a general warming of the tropics as may be occurring [e.g., *Angell*, 1988] could (in the absence of negating cloud cover changes) lead to a greater CH_3CCl_3 destruction rate and a positive OH trend. These factors combined make a 1% per year increase in OH in the tropical lower troposphere at least a theoretically feasible result.

The second set of conclusions refer to the processes which determine interhemispheric transport and its interar variations. The CH_3CCl_3 measurements at our tro South Pacific station (Samoa) show remarkable sensitivi the El Niño-Southern Oscillation (ENSO) which we attri to modulation of cross-equatorial transport during the n ern hemisphere winter by the interannually variable u tropospheric zonal winds in the equatorial Pacific re Specifically, during the mature phase of ENSO warm e years the December–May tropical Pacific upper tropospl westerlies across the central and eastern equatorial Pa are significantly reduced or reversed thereby inhib cross-equatorial propagation of Rossby waves, and thu propose cross-equatorial transport in general. It is signifi that high-frequency surface measurements of a chem compound have in this way yielded important new insi into mechanisms for interhemispheric transport.

Acknowledgments. This research was supported by N (grants NAGW-732 and 474 (R. Prinn), NAGW-729 (F. Alyea Cunnold), and NAGW-280 (A. Crawford, R. Rasmussen)); Ch cal Manufacturers Association (contract FC-85-567 (P. Simmo and FC-87-640 (P. Fraser)); Department of Environment, Ur Kingdom (P. Simmonds); NOAA (contract NA85-RAC05103 Simmonds)); CSIRO, Aspendale, Victoria, Australia (P. Fra Bureau of Meteorology, Melbourne, Victoria, Australia (P. Fra and NSF (grant ATM-8819825 (D. Gutzler)). D. Hartley ackn edges an NSF Fellowship. Valuable local support at the A GAGE stations was provided by D. Brown (Mace Head, Ireland Sealey (Ragged Point, Barbados), NOAA staff (Point Matat Samoa), and L. Porter (Cape Grim, Tasmania). We thank D. S for manuscript preparation. Two anonymous reviewers provi helpful comments on the manuscript.

REFERENCES

Angell, J., Variation and trends in tropospheric and stratosph global temperatures, 1958–87, *J. Clim.*, *1*, 1296–1313, 1988.

Arkin, P., The relationship between interannual variability in 200 mb tropical wind field and the Southern Oscillation, *M Weather Rev.*, *110*, 1393–1404, 1982.

Arkin, P., and P. Webster, Annual and interannual variability tropical-extratropical interaction: An empirical study, *M Weather Rev.*, *113*, 1510–1523, 1985.

Blake, D., and S. Rowland, Continuing worldwide increase tropospheric methane, 1978 to 1987, *Science*, *239*, 1129–11 1988.

Bottomley, M., C. Folland, J. Hsiung, R. Newell, and D. Park *Global Ocean Surface Temperature Atlas*, 313 pp., U. K. Me orological Office and Massachusetts Institute of Technolo 1990.

Butler, J., J. Elkins, T. Thompson, B. Hall, T. Swanson, and Koropalov, Oceanic consumption of CH_3CCl_3: Implications tropospheric OH, *J. Geophys. Res.*, *96*, 22,347–22,355, 1991.

Callies, J., H.-P. Dorn, U. Platt, and D. Ehhalt, Tropospheric C concentration measurements by laser long-path absorption sp troscopy, in *Ozone in the Atmosphere*, edited by R. Bojkov and Fabian, pp. 772–775, A. Deepak, Hampton, Va., 1989.

Chelliah, M., The global climate for June–August 1989: A season near normal conditions in the tropical Pacific, *J. Clim.*, *3*, 13 161, 1990.

Cicerone, R., and R. Oremland, Biogeochemical aspects of atm spheric methane, *Global Biogeochem. Cycles*, *2*, 299–327, 198

Cunnold, D., and R. Prinn, Comment on "Tropospheric OH in three-dimensional chemical tracer model: An assessment bas on observations of CH_3CCl_3" by C. M. Spivakovsky et al., *Geophys. Res.*, *96*, 17,391–17,393, 1991.

Cunnold, D., R. Prinn, R. Rasmussen, P. Simmonds, F. Alyea, Cardelino, A. Crawford, P. Fraser, and R. Rosen, The atm spheric lifetime experiment, 3, Lifetime methodology and app cation to three years of $CFCl_3$ data, *J. Geophys. Res.*, *8* 8379–8400, 1983.

Cunnold, D., R. Prinn, R. Rasmussen, P. Simmonds, F. Alyea, (

Cardelino, A. Crawford, P. Fraser, and R. Rosen, The atmospheric lifetime and annual release estimates for $CFCl_3$ and CF_2Cl_2 from 5 years of ALE data, *J. Geophys. Res.*, *91*, 10,797–10,817, 1986.

De More, W., S. Sander, D. Golden, M. Molina, R. Hampson, M. Kurylo, C. Howard, and A. Ravishankara, Chemical kinetics and photochemical data for use in stratospheric modelling, *NASA JPL Publ. 90-1*, 217 pp., 1990.

Donahue, N., and R. Prinn, Nonmethane hydrocarbon chemistry in the remote marine boundary layer, *J. Geophys. Res.*, *95*, 18,387–18,411, 1990.

Fishman, J., K. Fakhruzzaman, B. Cros, and D. Nganga, Identification of widespread pollution in the southern hemisphere deduced from satellite analyses, *Science*, *252*, 1693–1695, 1991.

Fraser, P., P. Hyson, R. Rasmussen, A. Crawford, and A. Khalil, Methane, carbon monoxide and methylchloroform in the southern hemisphere, *J. Atmos. Chem.*, *4*, 3–42, 1986*a*.

Fraser, P., N. Derek, R. O'Brien, R. Shepherd, R. Rasmussen, A. Crawford, and L. Steele, Intercomparison of halocarbon and nitrous oxide measurements 1976–1984, in *Baseline 83–84*, edited by R. Francey and B. Forgan, pp. 17–26, Commonwealth Sci. and Ind. Res. Organ., Aspendale, Australia, 1986*b*.

Golombek, A., and R. Prinn, A global three-dimensional model of the circulation and chemistry of $CFCl_3$, CF_2Cl_2, CH_3CCl_3, CCl_4, and N_2O, *J. Geophys. Res.*, *91*, 3985–4001, 1986.

Hartley, D., and R. Prinn, Comment on "Tropospheric OH in a three-dimensional chemical tracer model: An assessment based on observations of CH_3CCl_3" by C. M. Spivakovsky et al., *J. Geophys. Res.*, *96*, 17,383–17,387, 1991.

Holton, J., *An Introduction to Dynamic Meteorology*, 391 pp., Academic, San Diego, Calif., 1979.

Isaksen, I. S. A., and O. Hov, Calculation of trends in the tropospheric concentration of O_3, OH, CH_4, and NO_x, *Tellus*, *39*(B), 271–285, 1987.

Keller, M., D. Jacob, S. Wofsy, and R. Harriss, Effects of tropical deforestation on global and regional atmospheric chemistry, *Clim. Change*, *19*, 139–158, 1991.

Khalil, A., and R. Rasmussen, Methylchloroform: Global distribution, seasonal cycles, and anthropogenic chlorine, *Chemosphere*, *13*, 789–800, 1984.

Leith, C., The standard error of time-average estimates of climatic means, *J. Appl. Meteorol.*, *12*, 1066–1069, 1973.

Liu, S., et al., Oxidizing capacity of the atmosphere, in *The Changing Atmosphere*, edited by S. Rowland and I. Isaksen, pp. 219–232, John Wiley, New York, 1988.

Logan, J., M. Prather, S. Wofsy, and M. McElroy, Tropospheric chemistry: A global perspective, *J. Geophys. Res.*, *86*, 7210–7254, 1981.

Lovelock, J., Methyl chloroform in the troposphere as an indicator of OH radical abundance, *Nature*, *267*, 32, 1977.

Makide, Y., and S. Rowland, Tropospheric concentrations of methyl chloroform, CH_3CCl_3, in January 1978 and estimates of the atmospheric residence times for hydrohalocarbons, *Proc. Natl. Acad. Sci. U.S.A.*, *78*, 5933–5973, 1981.

Midgley, P., The production and release to the atmosphere of 1,1,1-trichloroethane (methyl chloroform), *Atmos. Environ.*, *23*, 2663–2665, 1989.

Newell, R., J. Kidson, D. Vincent, and G. Boer, *The General Circulation of the Tropical Atmosphere*, vol. 1, 258 pp., MIT Press, Cambridge, Mass., 1972.

Prinn, R., On the feasibility of quantitative analysis of atmospheric OH by titration, *Geophys. Res. Lett.*, *12*, 597–600, 1985.

Prinn, R., P. Simmonds, R. Rasmussen, R. Rosen, F. Alyea, C. Cardelino, A. Crawford, D. Cunnold, P. Fraser, and J. Lovelock, The Atmospheric Lifetime Experiment, 1, Introduction, instrumentation, and overview, *J. Geophys. Res.*, *88*, 8352–8367, 1983*a*.

Prinn, R., R. Rasmussen, P. Simmonds, F. Alyea, D. Cunnold, B. Lane, A. Crawford, and C. Cardelino, The Atmospheric Lifetime Experiment, 5, Results for CH_3CCl_3 based on 3 years of data, *J. Geophys. Res.*, *88*, 8415–8426, 1983*b*.

Prinn, R., D. Cunnold, R. Rasmussen, P. Simmonds, F. Alyea, A. Crawford, P. Fraser, and R. Rosen, Atmospheric trends in methylchloroform and the global average for the hydroxyl radical, *Science*, *238*, 945–950, 1987.

Prinn, R., D. Cunnold, R. Rasmussen, P. Simmonds, F. Alyea, A. Crawford, P. Fraser, and R. Rosen, Atmospheric emissions and trends of nitrous oxide deduced from 10 years of ALE/GAGE data, *J. Geophys. Res.*, *95*, 18,369–18,385, 1990.

Quay, P., et al., Carbon isotopic composition of atmospheric CH_4: Fossil and biomass burning source strengths, *Global Biogeochem. Cycles*, *5*, 25–47, 1991.

Rasmussen, R., and J. Lovelock, The Atmospheric Lifetime Experiment, 2, Calibration, *J. Geophys. Res.*, *88*, 8369–8378, 1983.

Rasmusson, E., and J. Wallace, Meteorological aspects of the 1982–83 El Nino-Southern Oscillation, *Science*, *222*, 1195–1202, 1983.

Singh, H., Atmospheric halocarbons: Evidence in favor of reduced average hydroxyl concentration in the troposphere, *Geophys. Res. Lett.*, *4*, 101–104, 1977.

Steele, L., P. Fraser, R. Rasmussen, M. Khalil, T. Conway, A. Crawford, R. Gammon, K. Masarie, and K. Thoning, The global distribution of methane in the troposphere, *J. Atmos. Chem.*, *5*, 125–171, 1987.

Thompson, A. M., and R. J. Cicerone, Possible perturbations to atmospheric CO, CH_4, and OH, *J. Geophys. Res.*, *91*, 10,853–10,864, 1986.

Trenberth, K., Observed Southern Hemisphere eddy statistics at 500 mb: Frequency and spatial dependence, *J. Atmos. Sci.*, *38*, 2585–2605, 1981.

Vaghjiani, G., and A. Ravishankara, New measurement of the rate coefficient for the reaction of OH with methane, *Nature*, *350*, 406–409, 1991.

Webster, P., and J. Holton, Cross-equatorial response to middle-latitude forcing in a zonally varying basic state, *J. Atmos. Sci.*, *39*, 722–733, 1982.

Wine, P., and W. Chameides, Possible atmospheric lifetimes and chemical reaction mechanisms for selected HCFCs, HFCs, CH_3CCl_3, and their degradation products against dissolution and/or degradation in seawater and cloud water, in *Scientific Assessment of Stratospheric Ozone: 1989*, *WMO Rep. 20*, vol. 2, pp. 271–295, World Meteorological Organization, Geneva, 1989.

World Resources Institute, *World Resources 1990–91*, 383 pp., Oxford University Press, New York, 1990.

F. Alyea and D. Cunnold, School of Earth and Atmospheric Sciences, Georgia Institute of Technology, Atlanta, GA 30332.

R. Boldi, D. Hartley, and R. Prinn, Center for Global Change Science, Massachusetts Institute of Technology, 54-1312, Cambridge, MA 02139.

A. Crawford and R. Rasmussen, Center for Atmospheric Studies, Oregon Graduate Institute, Beaverton, OR 97006.

P. Fraser, Division of Atmospheric Research, CSIRO, Aspendale, 3195 Victoria, Australia.

D. Gutzler and R. Rosen, Atmospheric and Environmental Research, Incorporated, Cambridge MA 02139.

P. Simmonds, Department of Geochemistry, University of Bristol, Bristol BS8-ITS, United Kingdom.

(Received July 2, 1991;
revised October 30, 1991;
accepted October 30, 1991.)

JOURNAL OF GEOPHYSICAL RESEARCH, VOL. 88, NO. C13, PAGES 8353–8367, OCTOBER 20, 1983

The Atmospheric Lifetime Experiment
1. Introduction, Instrumentation, and Overview

R. G. PRINN,[1,2] P. G. SIMMONDS,[3] R. A. RASMUSSEN,[4] R. D. ROSEN,[5,6] F. N. ALYEA,[2,7]
C. A. CARDELINO,[2,7] A. J. CRAWFORD,[4] D. M. CUNNOLD,[2,7]
P. J. FRASER,[8] AND J. E. LOVELOCK[9]

The Atmospheric Lifetime Experiment is designed to determine accurately the atmospheric concentrations of the four halocarbons $CFCl_3$, CF_2Cl_2, CCl_4, and CH_3CCl_3, and also of N_2O with emphasis on measurement of their long-term trends in the atmosphere. Comparison of these concentrations and trends for the four halocarbons with estimates of their industrial emission rates then enables calculations of their global circulation rates and globally averaged atmospheric lifetimes. The experiment utilizes automated dual-column electron-capture gas chromatographs which sample the background air about 4 times daily at the following globally distributed sites: Adrigole, Ireland (52°N, 10°W); Cape Meares, Oregon (45°N, 124°W); Ragged Point, Barbados (13°N, 59°W); Point Matatula, American Samoa (14°S, 171°W); and Cape Grim, Tasmania (41°S, 145°E). We review the climatology of these "clean air" sites and their ability to describe the global air mass. The instrumentation and methods for data acquisition and processing are then described. An overview of the data obtained and the trends derived during the 3-year period from July 1978 through June 1981 for each of the five species being measured is presented. The comparative behavior of the species with latitude and time is emphasized. The global average surface concentrations of $CFCl_3$, CF_2Cl_2, CH_3CCl_3, CCl_4, and N_2O are increasing at annually averaged rates of 5.7, 6.0, 8.7, 1.8, and 0.2% per year, respectively, at the midpoint of the 3-year period of the measurements.

1. Introduction

Current concerns about the accumulation of the compounds $CFCl_3$, CF_2Cl_2, CH_3CCl_3, CCl_4, and N_2O in the atmosphere are based on their possible deleterious effects on the stratospheric ozone layer [*Molina and Rowland*, 1974*a*, *b*; *McConnell and Schiff*, 1978; *Crutzen*, 1974] and on surface climate [*Ramanathan*, 1975; *Wang et al.*, 1976]. These possible effects stem from the fact that these compounds are sources of either chlorine or nitrogen oxides which can catalytically destroy ozone [*Stolarski and Cicerone*, 1974; *Crutzen*, 1970], and they are also strong infrared absorbers in window regions of the atmosphere. The only major sink for $CFCl_3$, CF_2Cl_2, CCl_4, and N_2O that has so far been identified is photodissociation in the stratosphere. If photodissociation is the only sink, then $CFCl_3$, for example, presently has an atmospheric lifetime of approximately 78 years whereas CF_2Cl_2 has a lifetime of approximately 220 years [*Golombek*, 1982]. These very long lifetimes, combined with current release rates of chlorofluorocarbons, lead to the prediction that these chlorofluorocarbons will reach sufficiently high atmospheric concentrations in 20 or 30 years time to produce discernable effects on ozone and climate. The determination of the actual atmospheric lifetimes of $CFCl_3$ and CF_2Cl_2 is thus of considerable importance. Similar comments apply to CCl_4 and N_2O which also appear to have lifetimes of decades. The principal sink for CH_3CCl_3 appears to be its reaction with the OH radical [*Cox et al.*, 1976], and a measurement of its atmospheric lifetime provides a potentially accurate indicator of tropospheric OH concentrations [*Lovelock*, 1977].

Before 1977, existing chlorofluorocarbon observations had been used to suggest that the lifetimes of $CFCl_3$ and CF_2Cl_2 were several decades or more [*Rowland and Molina*, 1976; *Pack et al.*, 1977]. However, it was also pointed out that a lifetime as short as 10–15 years was not inconsistent with the observations when one takes into account the variability and accuracy of the data [*Sze and Wu*, 1976; *Jesson et al.*, 1977; *Cunnold et al.*, 1978]. This is an important point. With chlorofluorocarbon lifetimes of only 15 years, for example, the predicted depletion of the ozone layer would be reduced by a factor of about 5 for $CFCl_3$ and about 11 for CF_2Cl_2.

In the absence of sufficiently accurate observations, talk of short (i.e., 10–15 years) or long (i.e., 78–200 years) chlorofluorocarbon lifetimes is largely conjectural. A detailed theoretical study has shown that a network of four ground stations appropriately spaced around the globe and making at least daily measurements with existing experimental methods could, with 3–4 years of operation, prove or disprove the existence of a 10–15 year lifetime [*Cunnold et al.*, 1978]. This study also concluded that the effect of systematic errors in instrument precision and calibration and in estimates of chlorofluorocarbon release rates to the atmosphere could be minimized by determining the trend over several years, rather than attempting to assess the instantaneous global atmospheric chlorofluorocarbon content.

Based on this study we began an experiment entitled the "Atmospheric Lifetime Experiment" (ALE), which utilizes the following five globally distributed coastal measurement stations: (1) Adrigole, Ireland, 52°N, 10°W; (2) Cape Meares, Oregon, 45°N, 124°W; (3) Ragged Point, Barbados, 13°N, 59°W; (4) Point Matatula, American Samoa, 14°S, 171°W; (5) Cape Grim, Tasmania, 41°S, 145°E. Operations began in February 1978 at Adrigole; in April 1978 at Cape Grim; in May

[1]Department of Earth, Atmospheric, and Planetary Sciences, Massachusetts Institute of Technology.
[2] CAP, Inc.
[3]Department of Geochemistry, University of Bristol.
[4]Department of Environmental Science, Oregon Graduate Center.
[5]Environmental Research and Technology, Inc. Now at Atmospheric and Environmental Research, Inc.
[7]School of Geophysical Sciences, Georgia Institute of Technology.
[8]Division of Atmospheric Physics, CSIRO.
[9]Department of Engineering and Cybernetics, University of Reading.

Paper number 3C0674.
0148-0227/83/003C-0674$05.00

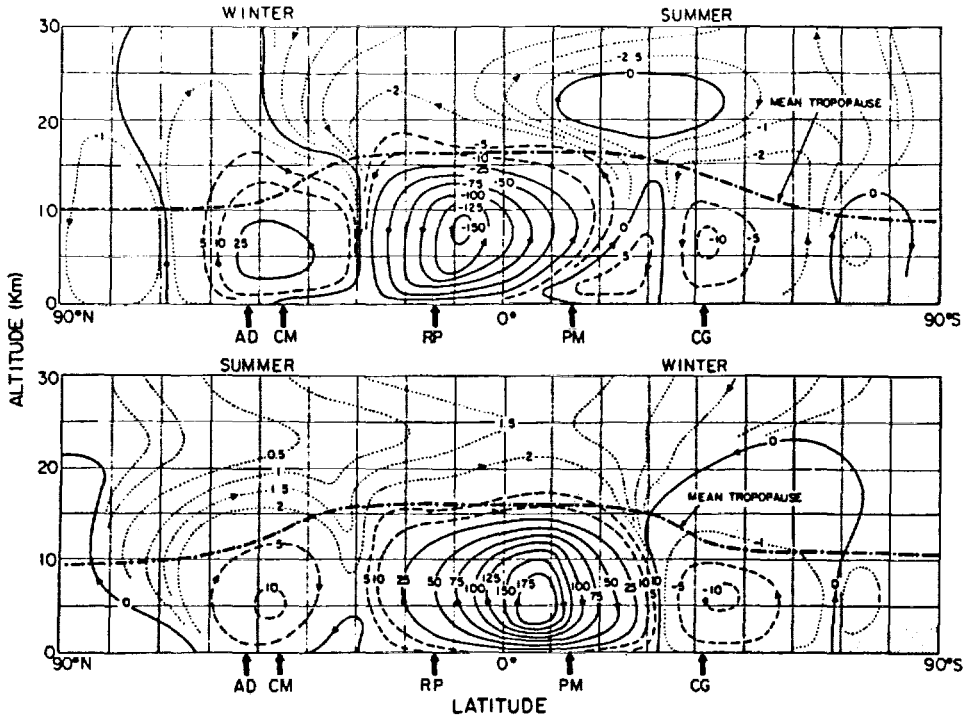

Fig. 1. The location of the ALE stations in relation to the summer and winter zonally averaged circulations from *Louis* [1975]. Units for the streamlines are 10^{12} gm/s. The symbols AD, CM, RP, PM, and CG represent Adrigole, Cape Meares, Ragged Point, Point Matatula, and Cape Grim, respectively.

1978 at Samoa; in July 1978 at Ragged Point; and, finally, in December 1979 at Cape Meares.

Each of the ALE stations is intended to be representative of one of the four equal mass subdivisions of the global atmosphere. The placement of the stations in relation to the global mean meridional circulation [after *Louis*, 1975] is shown in Figure 1. It is apparent that our choice of stations provides a good degree of symmetry in the sampling of each hemisphere and that the two tropical stations are firmly placed in the tropical Hadley cell, while the three mid-latitude stations are centered below the weak indirect cells. The placement of the stations in relation to seasonally averaged global 850 mbar horizontal streamlines [after *Newell et al.*, 1972] is shown in Figure 2. It is evident that the tropical stations should experience steady, largely easterly winds, whereas the mid-latitude stations should experience generally westerly winds, though these are sometimes disrupted strongly by the passage of cyclones and anticyclones.

In general, the sites were chosen to ensure as much as possible that clean oceanic air would be sampled. The station in Ireland is located on the west coast some 50 m above sea level and 400 m from the coast of Bantry Bay; the Oregon station is 30 m above sea level and immediately overlooking the ocean; and the Barbados site is on the east coast about 18 m above sea level and 15 m from the ocean. The Samoa station is located at the National Oceanic and Atmospheric Administration (NOAA) site some 30 m above sea level and samples air through a 15 m high intake tube above the station building. Finally, the Tasmania station was located on the northwest coast about 93 m above the sea level and 80 m from the shoreline prior to February 1980 and 80 m above sea level and 35 m from the shoreline (and 165 m north of the old site) after that date. The latter site change was necessitated by the then ongoing construction of the new Cape Grim Baseline Air Pollution Station (BAPS). The ALE instrument was finally moved into the BAPS station in 1982.

Because most of the industrial emissions of $CFCl_3$, CF_2Cl_2, CCl_4, and CH_3CCl_3 occur in the northern hemisphere at mid-latitudes, it was considered highly desirable that two stations operate at these latitudes. Adrigole often receives polluted air from industrial England and Europe, while Cape Meares appears to receive largely unpolluted Pacific air. Both polluted and unpolluted air comprise the total air inventory in the northern hemisphere mid-latitudes, and operation of both stations avoids the biases that could result from reliance on any one station alone.

At each station, a temperature-controlled, windowless building houses the instrumentation, and each site has a local caretaker who makes usually daily maintenance checks on the equipment. The instrumentation is described in detail in section 2. The primary instrument is a microprocessor-controlled Hewlett-Packard 5480A dual-channel electron capture gas chromatograph, and measurements are taken usually four times daily of atmospheric $CFCl_3$, CF_2Cl_2, CH_3CCl_3, CCl_4, and N_2O. At all the ALE sites, except Barbados, measurements are also available for some of these latter species that have been made independently of the ALE program [*Pack et al.*, 1977; *Fraser and Pearman*, 1978*a*; *Rasmussen et al.*, 1981; *De Luisi*, 1981; *Rasmussen and Khalil*, 1981].

To interpret the chromatograms in terms of actual concentrations, accurate daily onsite calibration of the instruments to keep both systematic "drifts" and random errors to a minimum is imperative. A method using reference cylinders of air calibrated directly or indirectly by using dilution, exponential dilution, and coulometric techniques has been devised and appears sufficient to meet our particular calibration demands. These reference cylinders are prepared by using primary standards and then shipped to the ALE sites. There, they

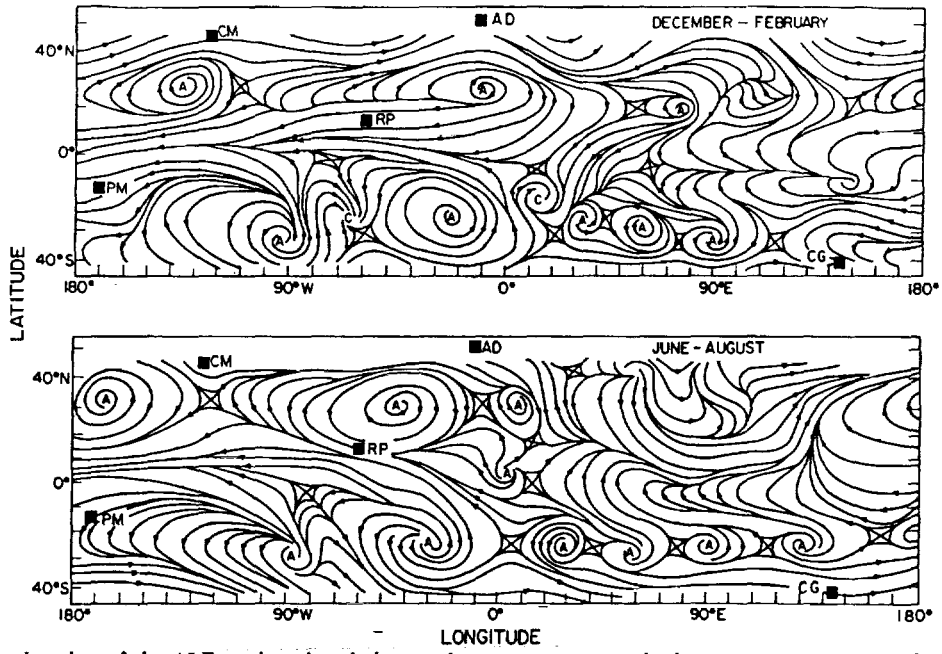

Fig. 2. The location of the ALE stations in relation to the mean summer and winter streamlines at the 850 mbar pressure level from *Newell et al.* [1972]. As in Figure 1, the stations are represented by the symbols AD, CM, RP, PM, and CG.

are usually used for approximately 3 months and then returned for remeasurement against the primary standards. A complete description of the calibration techniques used in the ALE program appears in a following paper [*Rasmussen and Lovelock*, this issue].

In this paper we provide an overview of 3 years of finalized, calibrated data from the Adrigole, Ragged Point, Point Matatula, and Cape Grim stations and 18 months of data from Cape Meares. Taking into account the four-times daily measurement runs with their accompanying calibration runs and the fact that $CFCl_3$ is analyzed on two independent chromatographic columns, the raw data base comprises $\sim 2 \times 10^5$ chromatographic peaks. The manner in which these data are processed, with due consideration for possible instrumental malfunction and local pollution, is outlined in section 3. In section 4 we present an overview of the measurement of all five species being analyzed at the five sites emphasizing the overall performance of the experiment and the comparative behavior of the species with latitude and time. Further details and interpretations of the observations of $CFCl_3$, CF_2Cl_2, CH_3CCl_3, CCl_4, and N_2O in terms of their individual sources, sinks, and, where possible, their atmospheric lifetimes are provided by *Cunnold et al.* [this issue (*a*), (*b*)], *Prinn et al.* [this issue], *Simmonds et al.* [this issue], and R. A. Rasmussen et al. (unpublished manuscript, 1983), respectively.

Finally, we emphasize that the chlorofluorocarbons are excellent tracers for global scale atmospheric mixing and may be used in particular to test global circulation models (e.g., *Golombek*, 1982]. They also provide a convenient tracer for determining oceanic mixing rates [*Lovelock et al.*, 1973]. For these and other potential applications a complete digital record of all of the data from the first 3 years of ALE is available [*Alyea*, 1983].

2. Instrumentation

All five ALE stations are equipped with the same microprocessor-controlled Hewlett Packard 5840A dual channel electron-capture gas chromatograph. Each channel is operated independently with separate chromatographic columns and detectors. Channel "P" contains a 1.8 m by 6.4 mm column packed with 80–100 mesh Porasil D which separates, in order of elution, N_2O, CF_2Cl_2, and $CFCl_3$ using a 2 or 3 ml air sample. Channel "S" analyses a 5 or 7 ml air sample for $CFCl_3$, CH_3CCl_3, and CCl_4 on a 1.8 m by 6.4 mm column packed with 10% SP2100 silicone coated on 100–120 mesh Suplecoport. Both columns are maintained isothermally at an oven temperature of 50°C. The carrier gas is a specially purified grade of 95% argon + 5% methane, containing less than 5 ppm of oxygen. Diffusion-resistant high purity regulators with stainless steel diaphragms are used on all carrier gas cylinders, and the respective flow rates for the "P" and "S" channels are 30 and 50 ml min^{-1}.

Several precautions are necessary to ensure that the carrier gases are both halocarbon-free and of a consistent quality at each station and from tank to tank. First, the carrier gas is passed through a 0.46 m × 2.5 mm stainless steel pipe filled with a mixture of 5 Å and 13X molecular sieves. Further 5 Å sieve traps (0.15 m by 6.4 mm) are in line on each channel after the flow controllers. In addition, as a final precaution, the injection ports (0.10 m by 6.4 mm) are maintained at 270°C and filled with palladized asbestos to destroy catalytically any trace halocarbons that might escape the molecular sieve filters. Each electron capture detector is heated separately, 320°C for channel "P" and 250°C for channel "S" for the Atlantic stations and 350°C for both channels at the three Pacific stations.

A block diagram of the experimental arrangement is illustrated in Figure 3. Outside air is drawn into each of the instruments by means of a noncontaminating metal bellows pump (MB-41, Metal Bellows Corp.) along a stainless steel line that is securely attached to a large pole so that the air intake is at least 2.0 m above the roof of the instrument building. A stainless steel funnel with small mesh screen is inverted at the beginning of the sampling line to prevent insects or water

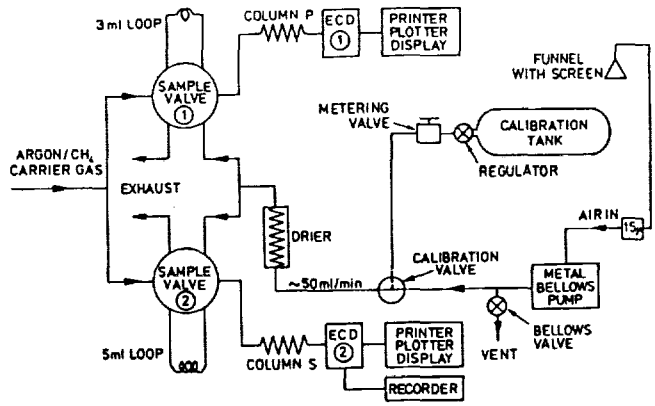

Fig. 3. Air sampling and calibration flow system at the ALE stations. ECD refers to the electron capture detector. See text for further details.

from entering the line. There is also a small 15 μm filter en route to the pump to prevent the intrusion of dust. The incoming air is first reduced to a nominal flow rate of 50 ml min^{-1} by means of a simple flow divider and vent valve. It then passes through a three-way switching valve (Valco Instruments, Inc.) followed by a special dryer [*Foulger and Simmonds*, 1979], fabricated from type 815 Nafion® tubing, which reduces the water content of the sample to an approximately constant 700 ppmv. Dry ambient air then enters each of the gas sampling valve loops which are thermostatted at 50°C within the chromatographic oven.

The air sampling calibration schematic is also shown in Figure 3. The high pressure in the calibration tank (nominally 400–500 psig) is reduced to 10 psi, without contamination, via an ultraclean stainless steel regulator (Veriflo UHP 660-580-2-SS-M1). After each analysis of an ambient air sample, the position of the three-way switching valve is changed by a pre-programed instruction from the microprocessor, thereby initiating a flow of calibration gas into the two gas sample loops. The gas flows are stopped just before injection, providing a precise and reproducible sample. Flow meters are incorporated on the exit lines from each gas sampling valve, thus enabling the local caretaker to readily confirm that the flow rates are within certain specified limits.

It is important to note that the electron capture detector (ECD) signal outputs from channel "P" are processed with constant current mode electronics. This form of signal processing has also been used for channel "S" at Oregon, Tasmania, and Samoa (with the exception of a 6-month period at Samoa from November 10, 1978, to May 8, 1979, when a constant frequency detector was used). The constant current or pulse frequency feedback mode of detection has been adopted by the majority of commercial gas chromatograph manufacturers because of its wide dynamic range. However, some caution is necessary with this method, since compounds to which electrons strongly attach can produce a response that varies nonlinearly with concentration, except at very high carrier gas flow rates [*Lovelock*, 1974]. This problem can be largely overcome by the separate analysis of a calibration

TABLE 1. ALE Program Sequence at Adrigole and Barbados

Time	Run	Column/Measurement	
1600–1700	17	SA	caretaker reset run
1700–1800	1	SA	
1800–1900	2	SC	
1900–2000	3	PC	
2000–2100	4	PA	
2100–2300			wait 2 hours
2300–2400	5	SA	
2400–0100	6	SC	
0100–0200	7	PC	
0200–0300	8	PA	
0300–0500			wait 2 hours
0500–0600	9	SA	
0600–0700	10	SC	
0700–0800	11	PC	
0800–0900	12	PA	
0900–1100			wait 2 hours
1100–1200	13	SA	
1200–1300	14	SC	
1300–1400	15	PC	
1400–1500	16	PA	
1500–1600			wait 1 hour

P = Porasil column; S = silicone column; A = ambient air measurement; C = calibration gas measurement.

TABLE 2. ALE Program Sequence at Cape Meares, Samoa, and Tasmania

Time	Run	Column/Measurement	
900–1000	12	SA	auto reset
1000–1100	1	SA	
1100–1200	2	SC*	
1200–1300	3	SA*	
1300–1400	4	SA*	
1400–1500	5	SC*	
1500–1600	6	SA	
1600–1700	7	PA	
1700–1800	8	PC*	
1800–1900	9	PA*	
1900–2000	10	PA*	
2000–2100	11	PC*	
2100–2200	12	SA	auto reset
2200–2300	1	SA	
2300–2400	2	SC*	
2400–0100	3	SA*	
0100–0200	4	SA*	
0200–0300	5	SC*	
0300–0400	6	SA	
0400–0500	7	PA	
0500–0600	8	PC*	
0600–0700	9	PA*	
0700–0800	10	PA*	
0800–0900	11	PC*	

*Data used for data base.

P = Porasil column; S = silicone column; A = ambient air measurement; C = calibration gas measurement.

standard as close in concentration to ambient as possible and under the same conditions of analysis. This procedure is routinely followed in the ALE program so that calibration and air analyses are usually only 1 hour apart.

At the Adrigole and Barbados stations, constant frequency (4 kHz) electronics have been used to process the signal outputs from the "S" channel detector. Although the signal is slightly noisier by this method, it is potentially an absolute method of analysis where the coulometric reaction of halocarbons and electrons can be used to calculate halocarbon concentrations within the detector [*Lovelock and Watson*, 1978; *Grimsrud and Kim*, 1979; *Gobby et al.*, 1980]. Also, since halocarbon measurements had been made at the Adrigole station commencing in 1970 by using the constant frequency electronics [*Pack et al.*, 1977], it was desirable to continue with this method to maintain continuity in this long time series of measurements.

Although the signal outputs from both "P" and "S" channels are recorded automatically onto a thermal printer-plotter, the analog output from the "S" channel is also processed through additional electronics and displayed on a backup potentiometric recorder. In the design and construction of these electronics we have included some additional relay circuits that operate under control of the HP5840A microprocessor and permit the programed operation of ancillary equipment, such as the on-off cycles for the metal bellows pump and the potentiometric recorder. An extra signal cable from a small frequency meter has also been incorporated into the HP5840A detector housing to monitor the frequency of the constant current "P" channel. This frequency measurement is a valuable and sensitive indicator of the overall cleanliness and stability of the "P" channel detector. Recently, at Adrigole, Samoa, Tasmania, and Oregon, provision has been made for duplicate recording of the digital output onto cassette tape, using a Techtran 815-17 data logger. This option not only provides a backup in the event of a printer-plotter failure, but also allows rapid inspection of the data record for system malfunctions.

Besides the chromatographic apparatus, each station except Tasmania is air conditioned (the refrigerant of choice is $CHClF_2$). The air within the instrument buildings is analyzed regularly to guard against any leaks that might develop in the air conditioner. Positioning of the air intake sample line upwind, and well above and away from the building, also minimizes the risk of any contamination. All stations also contain either a barohydrothermograph or a hydrothermograph which provide a continuous record of station pressure, humidity, and temperature.

The main stresses to all of the instrumentation are periods of low voltage (most common at Samoa) and power outages (frequent at Barbados and Samoa). Because these power problems have been particularly severe at the Samoan station an Uninterruptible Power Supply (Elgar Corp.) was installed in the spring of 1981.

Each of the stations follows the same basic analysis and calibration procedures. However, there are minor technical differences, including time differences in the sequences of ambient air and calibration analyses to optimize individual instruments to the local conditions. When the ALE stations were first established, 10 ambient air measurements were recorded throughout a 24-hour cycle with two calibration measurements at 12-hourly intervals. However, in September 1978 it was decided to introduce a different sequence, to increase the frequency of calibration measurements, and to allow for differences in the availability of caretaker support at individual stations. Tables 1 and 2 show sequences adopted for the Atlantic and Pacific stations since September 1978, respectively.

At most sites a local caretaker or trained technician makes a daily visit to the station to verify routine performance of the

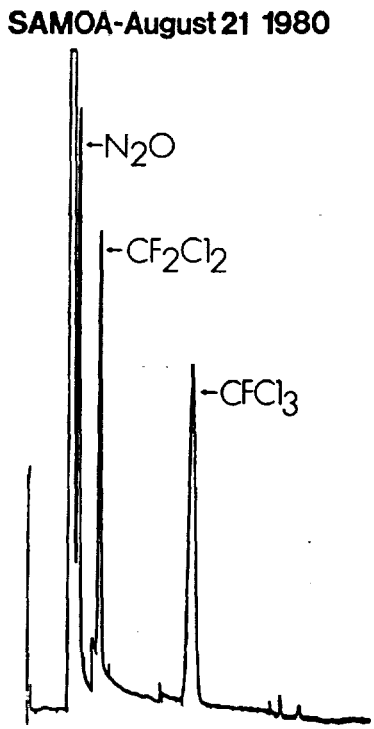

Fig. 4. Analysis of 3 ml of ambient air at the Samoan station on the "P" channel. The 1.8 m by 6.4 mm column utilized is isothermal (50°C) and packed with Porasil D (80–100 mesh).

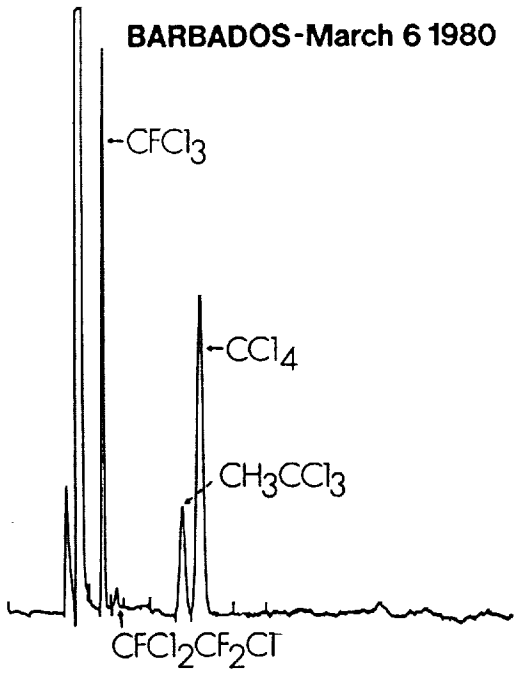

Fig. 5. Analysis of 5 ml of ambient air at the Barbados station on the "S" channel. The 1.8 m by 6.4 mm column is isothermal (50°C) and packed with 10% SP2100 silicone on 100–120 mesh Supelcoport.

instrumentation and when necessary to replace consumables (e.g., printer-plotter paper, carrier gas, etc.). Any unusual events, including power failures or abnormal weather conditions, are recorded, and any instrumental malfunctions are immediately reported to the station scientist. Because power failures and low voltages can often scramble the microprocessor program, the caretakers also have the ability to reinstate the correct instructions by editing the program directly from the microprocessor keyboard.

Each station is visited at least quarterly by the station scientist for detailed servicing of the instrument and for replacement of the calibration gas tank. Cross-calibration of both old and new calibration tanks is performed on-site, and the used tank that typically still contains between 200 and 300 psi of gas is returned for remeasurement against the primary standard [see *Rasmussen and Lovelock*, this issue]. If a new calibration tank is found to have an anomalously low pressure or if there are obvious discrepancies during the cross calibration, the suspect tank is not used but exchanged for a second calibration tank which is always held in reserve.

Each visit specifically includes replacement of all molecular sieve filters and Nafion® dryers, as well as diagnostic checks on electronic components, chromatographic performance, and electron capture detector standing currents and frequencies. Considerable care is taken to be certain that cleaning and/or replacement of components has not disturbed the internal consistency or accuracy of the measurements in which we aim to maintain 1% precision of analysis at ambient levels.

3. Data Acquisition and Processing

Data are printed out automatically by the HP5840A and consist specifically of the retention times and integrated peak areas for each species. Usually, these integrated peak areas are sufficiently accurate to be used directly to compute species concentrations. However, the integration for species with smaller peaks, particularly CH_3CCl_3 and CCl_4, often lacks the

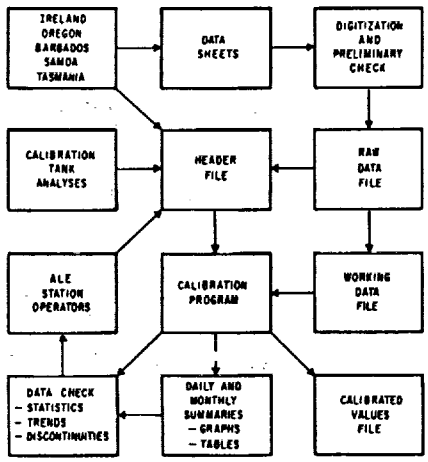

Fig. 6. Flow diagram outlining the data processing scheme used in the ALE program.

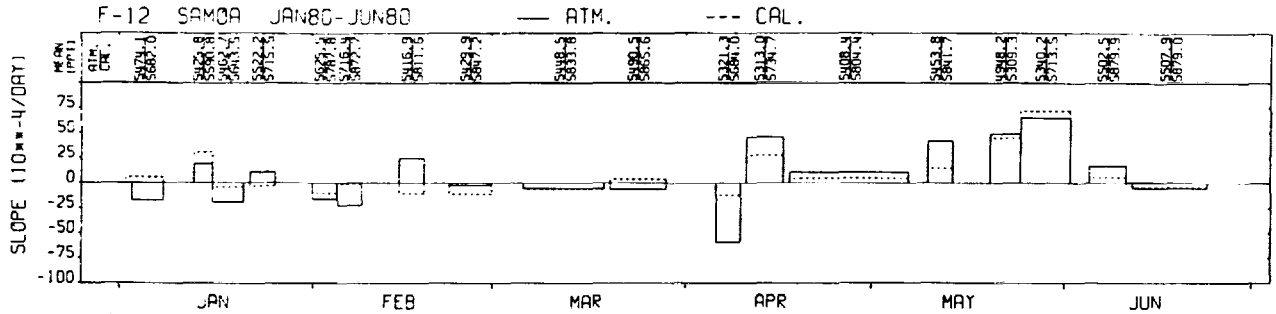

Fig. 7. Histograms showing fractional linear trends in the raw data values for CF_2Cl_2 in ambient air (solid histograms) and calibration tanks (dashed histograms) over major time segments during the 6-month period January–June 1980 at Point Matatula, Samoa. The mean raw data values (ATM or CAL) in arbitrary units that are used to normalize the histograms for each segment are shown along the top border.

instrumental precision required, and for this reason we make manual measurements of the relevant peak heights. Examples of the automatic print out for each channel are shown in Figures 4 and 5. The analysis of a 3-ml air sample at Samoa (Figure 4) shows the resolution of N_2O, CF_2Cl_2, and $CFCl_3$ on the Porasil D column (channel "P"). Similarly, the Barbados chromatogram (Figure 5) illustrates the separation of $CFCl_3$, CH_3CCl_3, and CCl_4 in a 5-ml air sample on the SP2100 silicone column, (channel "S").

It should be mentioned that the columns used in the ALE program were selected from practical experience as the most suitable for the direct analysis of trace halocarbons in ambient air. Nevertheless, they are relatively low resolution packed columns, and the possibility exists for coelution of other minor atmospheric components with the halocarbon species measured by ALE. Fortunately, there is close agreement between atmospheric concentrations of $CFCl_3$, CF_2Cl_2, CH_3CCl_3, and CCl_4 determined by electron-capture gas chromatography and gas chromatography-mass spectrometry methods [*Grimsrud and Rasmussen*, 1975; *Cronn and Harsch*, 1979; *Penkett*, 1981]. Furthermore, the additional specificity obtained from the mass spectrometry methods confirms the absence of any major coeluting species. Independent measurements by *Simmonds* [1980] of clean maritime air on chromatographic columns with completely different retention characteristics from those used in the ALE program further establishes that the major atmospheric halocarbons determined in ALE do in fact elute as single chromatographic peaks.

Standard procedures have been developed for the processing of all ALE data. The important steps are outlined in Figure 6 in the form of a flow diagram. Raw chromatographic data from the five sites are first transferred to daily data sheets which summarize the atmospheric and calibration tank analyses on each column in the form of chromatographic peak areas (or occasionally peak heights) together with comments on any unusual aspects of the day's operations. Information on these data sheets is later transferred to computer cards, and daily means and standard deviations are computed. These latter statistics, together with a simple visual inspection of the data, form part of a routine check. Any obviously unusual data is investigated to check if transcription errors, automatic peak area integrator malfunctions, and related problems have occurred; if so, the appropriate corrections are made. After this check, an immutable "raw data file" is created that forms the basis for all subsequent processing.

A "working data file" is formed from the raw data file, and a separate "header file" is created, which among other items contains information on the calibration tank used at the site for each measurement and the concentrations of halocarbons and nitrous oxide in this tank. Also included is information on whether independent evidence for pollution exists; whether the data comprises peak areas or heights; and whether power failures, changes of calibration or carrier gas tanks, and related interruptions of the normal station routine have occurred. The "header file" also labels any statistically unusual data for later checking.

A calibration program then uses the information in the working data and header files to calibrate the data by using the basic relationship

$$x = x_0 \frac{A}{C}$$

where x is the calibrated mixing ratio for the appropriate species, x_0 is the mixing ratio of the species in the on-site calibration tank, and A and C are the areas (or heights) of the chromatographic peaks for the atmospheric and calibration tank analyses respectively. In most cases, x_0 is an average value determined from analysis of the calibration tanks before and after their use at the station; for two (out of a total of 51) tanks used, analyses were available only prior to their use. In general, C refers to the nearest calibration tank analysis in time to the atmospheric analysis for the two Atlantic stations and to the arithmetic mean of the calibration tank analyses immediately before and after the atmospheric analysis for the three Pacific stations. The choice of separate procedures for the Atlantic and Pacific stations arises from the different sequences of calibration tank and atmospheric analyses at the two sets of stations. We have discerned no statistical differences between the Atlantic and Pacific stations attributable to this slight difference in their calibration procedures. At all stations if the normal calibration tank analyses are missing or if there has been a break in instrument operation, then C is defined as the nearest value or arithmetic mean value depending on the proximity of the atmospheric analysis to the surrounding calibration tank analyses. Also, in the first few months of operation of the Irish, Barbadan, Samoan, and Tasmanian stations, the frequency of calibration tank analyses was less than that adopted later, and again an appropriate choice of the nearest or arithmetic mean value was therefore used.

After the calibration procedure, a "calibrated values file" is created which contains all the raw and calibrated data together with any subsidiary information on the data contained in the header file. Also, any data suspected on statistical grounds is at this point carefully investigated. Only if an independently verifiable malfunction in the measurement system (e.g., sam-

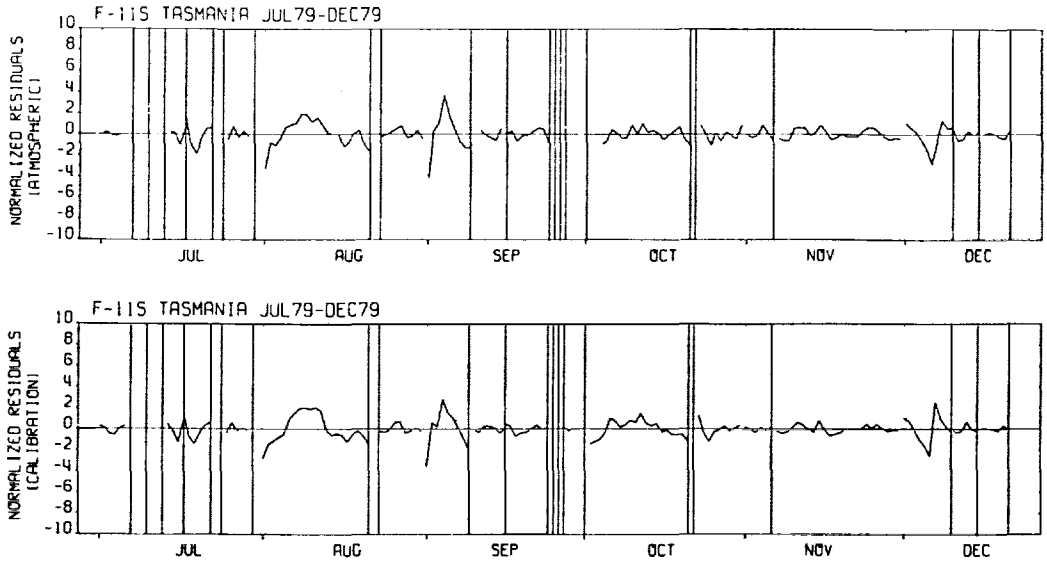

Fig. 8. Residuals obtained at Cape Grim, Tasmania, after subtracting the mean linear trends over major time segments from the daily mean raw chromatographic values for $CFCl_3$ on the "S" channel. Overall period shown is July–December 1979. Residuals are presented as percentages of the mean raw data value during each time segment. Residuals for atmospheric raw data are shown in the top graph and those for the calibration tank in the bottom.

pling valve problems, detector deterioration, automatic integrator malfunction) or a pollution episode (as defined in section 4) is identified, are such data corrected or deleted in the calibrated values file. A permanent record of all of these corrections or deletions is maintained in the header file. We emphasize that the original raw and working data files are never altered as a result of such investigations. In addition, the original chromatograms generated at all the stations are permanently stored for future reference.

A "monthly summaries file" is also created which contains tabulations of the calibrated daily and monthly means and standard deviations for atmospheric $CFCl_3$ (silicone column), $CFCl_3$ (Porasil column), CF_2Cl_2, CH_3CCl_3, CCl_4, and N_2O at each station. From this file, monthly summary sheets and plots of the daily mean data in 6–12 month segments are generated. These are used as aids in the extensive review of the data set by the experimenters which are made at 6 monthly intervals. In addition, to aid in the review of instrumental performance, linear trends and residuals are computed separately for the calibration tank and atmospheric measurements, and the correlation between these two sets of residuals is also determined.

We are particularly concerned with the evaluation of two temporal scales of instrument performance: potential long-term instrumental drift over many days or weeks and fairly rapid oscillations which may occur from day to day. Figure 7 contains an example of an analysis of instrumental drift for a 6-month period at Point Matatula. Specifically illustrated are the fractional linear trends of the raw chromatographic values recorded over time segments of days to weeks when the instrument was operating continuously. The solid histograms represent ambient air measurements, and the dashed histograms the calibration tank measurements. The mean raw data values for each time segment used to normalize the histograms (ATM/CAL) are recorded along the top border of the figure. Note particularly that the magnitudes of the linear trends are small (considerably less than 1% per day), their signs fairly random, and that their values tend to be similar for both the ambient air and the calibration samples. These illustrated results are generally typical of all of the data collected at the ALE sites and help substantiate the calibration technique used in the ALE program.

The typical day to day behavior of the instruments is depicted in Figure 8. Here we show for a 6-month period at Cape Grim the residuals obtained after subtracting the mean linear trends (over time segments of continuous instrument operation) from the daily mean raw chromatographic values. These residuals have been normalized by the raw mean values in each time segment and are thus displayed as percentages for the ambient air measurements (top) and the calibration tank measurements (bottom). We see that the residuals are reasonably small (less than ~4%) and show similar patterns for both ambient air and calibration measurements. Again, these results suggest that the high level of performance of the instruments, coupled with the ALE on-site calibration technique, provides a system capable of generating reliable atmospheric concentrations with very good precision. All of the ALE stations and species demonstrate similar long- and short-term performances with few anomalies except when definite instrument problems have been identified, in which case the data is in any case not valid and therefore rejected.

Finally, the calibrated mixing ratios for each species stored in the ALE files have absolute values dependent on values assigned to the primary standards adopted for the experiment. However, recent independent determinations of the absolute concentrations of ALE species in these primary standards indicate that small corrections to these assigned values are in general required [see *Rasmussen and Lovelock*, this issue]. For consistency in the ALE program, the formal values assigned to the primary standards are not altered as estimates of absolute concentrations improve. Rather, the appropriate factor ξ, by which all the ALE mixing ratios for a given species should be multiplied to provide their true atmospheric values, is determined based on the best information currently available on absolute calibration. The ξ values for $CFCl_3$, CF_2Cl_2, CH_3CCl_3 and CCl_4 are at present estimated to be 0.96 ± 0.02, 0.95 ± 0.02, 1 ± 0.3, and 0.81 ± 0.04, respectively (95% confidence; see *Rasmussen and Lovelock* [this issue]). The ξ

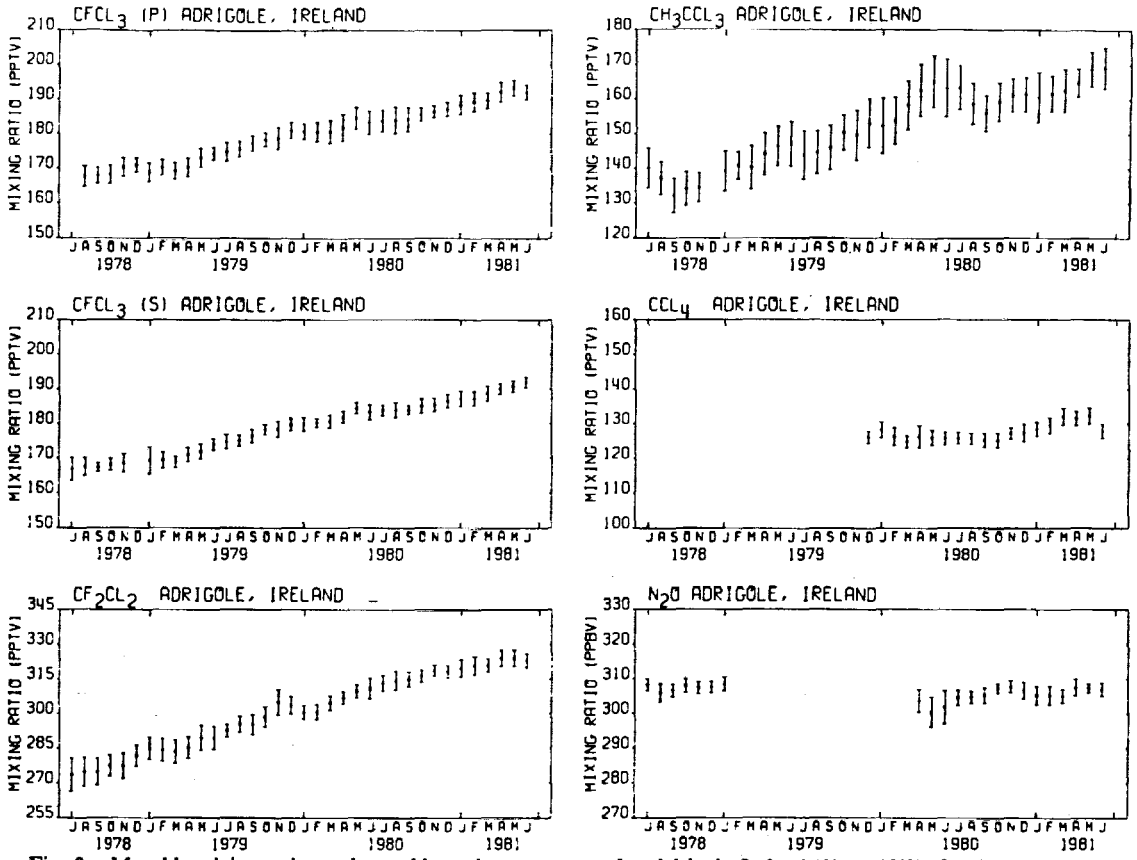

Fig. 9. Monthly mixing ratios and monthly variances measured at Adrigole, Ireland (52°N, 10°W) for $CFCl_3$ using the silicone (F11S) and Porasil (F11P) columns, CF_2Cl_2 (F12) and N_2O using the Porasil column, and CH_3CCl_3 and CCl_4 using the silicone column. The mixing ratios plotted here and in Figures 10–13 have been multiplied by the absolute calibration factors ξ discussed in the text and therefore represent our present best estimates for the absolute concentrations of these compounds.

value for N_2O has not yet been precisely determined. For purposes of a preliminary presentation of the ALE N_2O data in this paper we adopt an interim value for $\xi = 0.92$; a more precise evaluation will be given by R. Rasmussen et al. (unpublished manuscript, 1983). We emphasize that the absolute concentrations (but not the fractional trends in space and time) presented here for N_2O are dependent on the above interim ξ value.

4. Summary of Results

The quality of the data obtained in the first 3 years of the ALE program is well above our initial expectations. In particular, the overall accuracy for $CFCl_3$ and CF_2Cl_2 has equalled or exceeded our original goals which were based on the required accuracies for measurements to be used in atmospheric lifetime determinations. Although the ALE instruments have been optimized for the latter two chlorofluorocarbons, it is clear from the record that good quality data are also being obtained for CH_3CCl_3, CCl_4, and N_2O.

The monthly mean mixing ratios χ and monthly variances determined in the ALE program for $CFCl_3$ (using the silicone column), $CFCl_3$ (using the Porasil column), CF_2Cl_2, CH_3CCl_3, CCl_4, and N_2O are illustrated for each ALE station in Figures 9–13. As was discussed in the papers devoted to each of the ALE species, the values of $\ln \chi$ obtained at each site can be conveniently fit with an empirically determined function containing terms that are linear, quadratic, and simple harmonic (period = 12 months) in time. At the midpoint of the second year of the ALE program, the annually averaged mixing ratio X and trend $\partial X/\partial t$ for each species at each site can be determined from the $\ln \chi$ functions by using

$$X = \int_{-1/2}^{+1/2} \exp\{\ln \chi(t)\}\, dt$$

$$\frac{\partial X}{\partial t} = \int_{-1/2}^{+1/2} \frac{\partial \ln \chi(t)}{\partial t} \exp\{\ln \chi(t)\}\, dt$$

where t is time in years measured from January 1, 1980. Global-average values for the mixing ratio $\bar{X}$ and the trend $\overline{\partial \ln X/\partial t}$ of each ALE compound can then be deduced by

TABLE 3. Global-Average Mixing Ratios $\bar{X}$ and Trends $\overline{\partial \ln X/\partial t}$ for the Second Year of the ALE Program Determined by Averaging the Annual-Average Values X and $\partial X/\partial t$ From Each of the ALE Sites, Respectively

Compound	$\bar{X}$	$\overline{\partial \ln X/\partial t}$, percent yr^{-1}
$CFCl_3$ (silicone)	168 pptv	5.6
$CFCl_3$ (Porasil)	168 pptv	5.7
CF_2Cl_2	285 pptv	6.0
CH_3CCl_3	123 pptv	8.7
CCl_4	118 pptv	1.8
N_2O	306 ppbv	0.2

The Adrigole and Cape Meares stations are averaged as one station when their measurements overlap in time. The values of $\bar{X}$ tabulated here have been multiplied by the appropriate absolute calibration factor ξ (see text).

TABLE 4. Annual-Average Mixing Ratios X in the Northern Hemisphere (NH) and Southern Hemisphere (SH) for the Second Year of the ALE Program Obtained by Averaging the X Values From the NH and SH ALE Stations

Compound	X(NH)	X(SH)	X(NH)/X(SH)
$CFCl_3$ (silicone)	175 pptv	160 pptv	1.09
$CFCl_3$ (Porasil)	175 pptv	161 pptv	1.09
CF_2Cl_2	296 pptv	274 pptv	1.08
CH_3CCl_3	143 pptv	104 pptv	1.37
CCl_4	121 pptv	115 pptv	1.05
N_2O	307 ppbv	306 ppbv	1.003

The Adrigole and Cape Meares stations are averaged as one station where their measurements overlap in time. The values of X tabulated here have been multiplied by the appropriate absolute calibration factor ξ (see text).

averaging the X and $\partial X/\partial t$ values obtained at each station and are given in Table 3.

The latitudinal distributions of the ALE species are summarized in Table 4 where we give the annual-average mixing ratios X (at $t = 0$) for each ALE compound in the northern and southern hemispheres, respectively. These are obtained by averaging appropriately the X values at each station in the relevant hemisphere. Also tabulated are the ratios of the northern and southern hemisphere X values.

An examination of Table 3 shows that of the five ALE species CH_3CCl_3 is accumulating the most rapidly and N_2O the least rapidly. In particular, the e folding times for mixing ratios for current rates of accumulation are approximately 11, 17, 18, 53, and 500 years for CH_3CCl_3, CF_2Cl_2, $CFCl_3$, CCl_4, and N_2O, respectively. If the emission fluxes of these compounds remain constant and their rates of destruction remain proportional to their concentrations, then these latter e folding times will steadily increase as each species approaches a steady state (zero trend).

From Table 4 it is evident that CH_3CCl_3 has the largest interhemispheric gradient and N_2O the smallest. These interhemispheric gradients are in general a function of the spatial and temporal variations of the sources and sinks for each species and of the strength of the global atmospheric circulation. For the four ALE halocarbons, CH_3CCl_3, $CFCl_3$, CF_2Cl_2, and CCl_4, which all have largely northern hemisphere sources, the global cumulative industrial emission at the end of 1980 is 26, 14, 13, and 6%, respectively, more than the cumulative emission at the end of 1978. These differences in the recent rates of growth of the emissions of these compounds are an important factor in determining the differences in their interhemispheric ratios. Indeed, their observed interhemispheric ratios are in the same order as their recent rates of growth in emission. There are, of course, other factors involved, and these are discussed in the detailed papers devoted to each of the ALE compounds referenced earlier.

We have found that the geography and meteorology of the ALE sites are very important for understanding the history of the air parcels being sampled and, in particular, for identifying those times when the stations are sampling highly polluted air from populated areas. At Adrigole, particularly in winter, the passage of secondary lows over Europe may enable polluted air from eastern Ireland, Wales, England, and continental Europe to reach Adrigole [*Pack et al.*, 1977]. Indeed, Adrigole

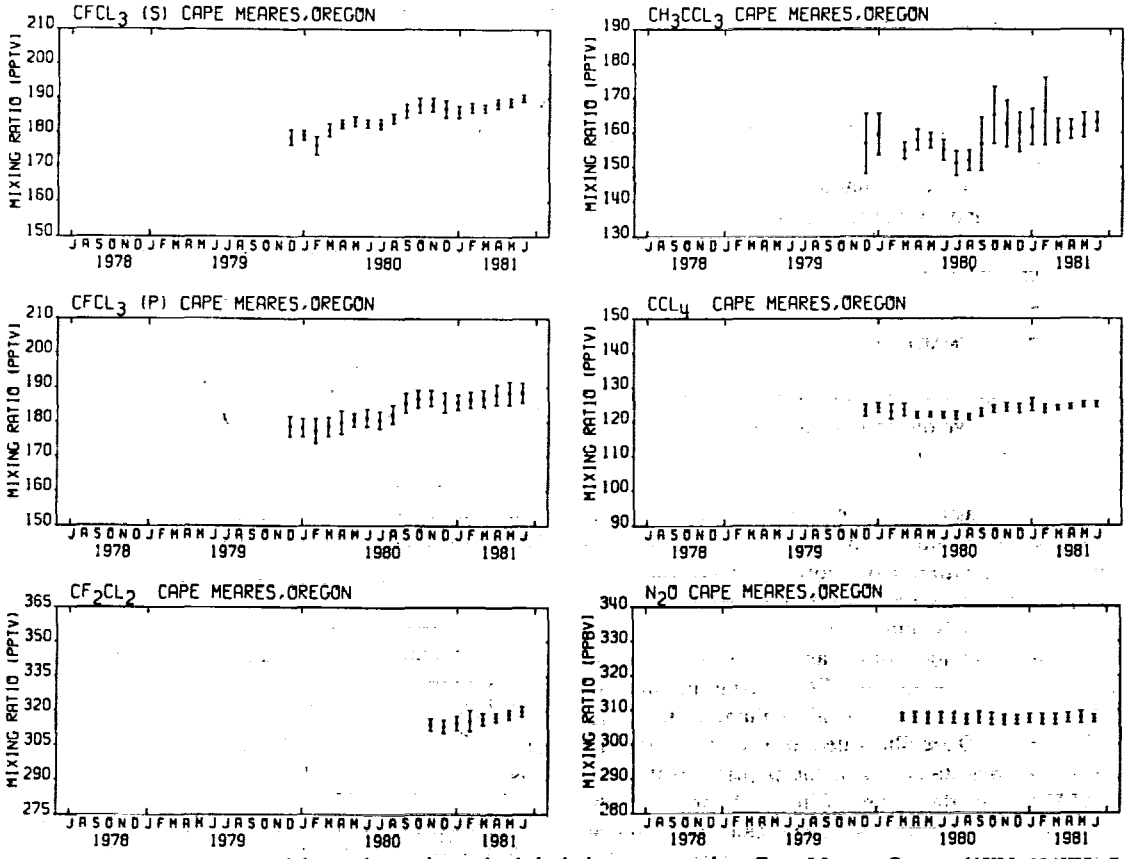

Fig. 10. Monthly mean mixing ratios and standard deviations measured at Cape Meares, Oregon (45°N, 124°W). See Figure 9 for notation and discussion of calibration factors ξ.

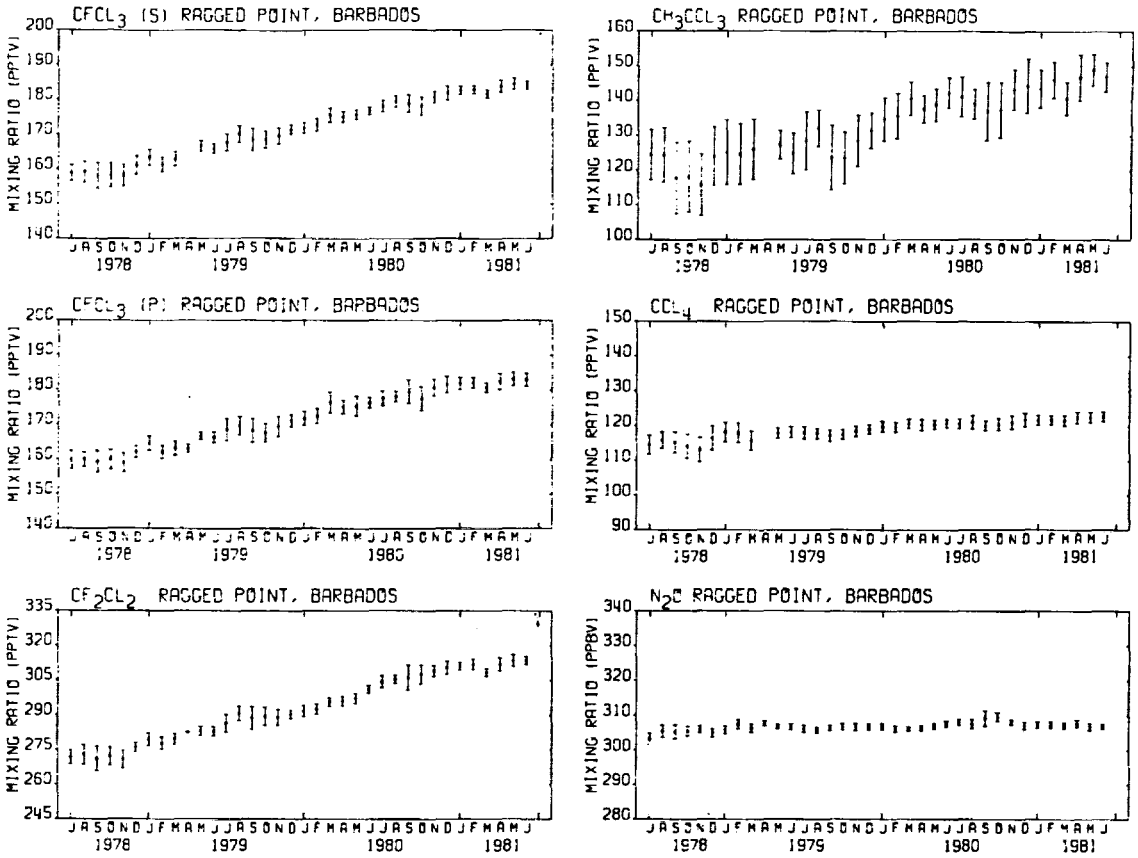

Fig. 11. Monthly mean mixing ratios and standard deviations measured at Ragged Point, Barbados (13°N, 59°W). See Figure 9 for notation and discussion of calibration factors ξ.

is the most polluted of the ALE sites, as evidenced by episodic rapid increases in the ALE halocarbon concentrations. For this reason, three independent approaches were taken to recognize these pollution episodes at Adrigole.

First, we found that pollution could be reliably forecast with the aid of weather maps. In particular, the presence of prolonged ENE to ESE winds at all levels associated with an occluding low to the south of Adrigole correlated very well with extended periods (>1–2 days) of pollution, although the timing of pollution events forecasted in this way was occasionally a day or so off. Second, perchloroethylene is observed as a minor chromatographic peak at Adrigole, and this short-lived species can be associated with air masses that have passed over industrial perchloroethylene sources at most a few days earlier. Third, high levels of perchloroethylene are generally well correlated with rapid rises in the ALE halocarbons $CFCl_3$, CF_2Cl_2, and CH_3CCl_3 and with the meteorological forecasts of pollution at this site. In practice, high perchloroethylene levels and/or marked simultaneous increases in $CFCl_3$, CF_2Cl_2, and CH_3CCl_3 are used as indicators of polluted air at Adrigole. Using these criteria, approximately one third of the measurements at Adrigole contain evidence of some pollution.

There is very little evidence from the ALE data for any significant pollution at Cape Meares. This is conversant with the meteorology of this site. Specifically, for pollution to reach Cape Meares from the large urban areas of California, the prolonged presence of a Pacific high located to the southeast of this station appears necessary. A study of the daily synoptic situation during 1978 indicates that 35% of the time a high existed in such a conducive location, but on only a few occasions did it persist longer than 3 days. Because it would take at least 3 days for polluted air to travel clockwise around the high pressure area and arrive at Cape Meares, we conclude that only about 5% of the time during the year can pollutants from California potentially reach Cape Meares. Moreover, even when the Pacific high persists in the required postion SE of Cape Meares, a trough is often present over southern California and northern Mexico giving rise to a NE wind over the urban areas of California. This latter wind would move pollutants on a more southward track toward Mexico rather than westward ultimately to reach Oregon.

Barbados is under the influence of easterly winds essentially all of the year so that almost without exception the air that arrives over Barbados is of oceanic origin with the nearest potential source of pollution being west Africa. An analysis of 850 mbar streamlines (see Figure 2) indicates that the arrival at Barbados of air parcels of southern hemispheric origin (characterized by lower than normal halocarbon concentrations) is most likely during summer (June–August) and least likely during winter (December–February). This is also the conclusion expected from the annual movements of the Intertropical Convergence Zone (see Figure 1). Barbados also occasionally shows rapid increases in $CFCl_3$, CF_2Cl_2, and CH_3CCl_3 during evening hours when the island is dominated by calm conditions. In such situations, pollutants apparently build up near the ground in the populated inland areas of the island during the day and drain outward toward the coastal ALE site in the early evening. The island is usually flushed of this polluted air by about midnight, and halocarbon levels

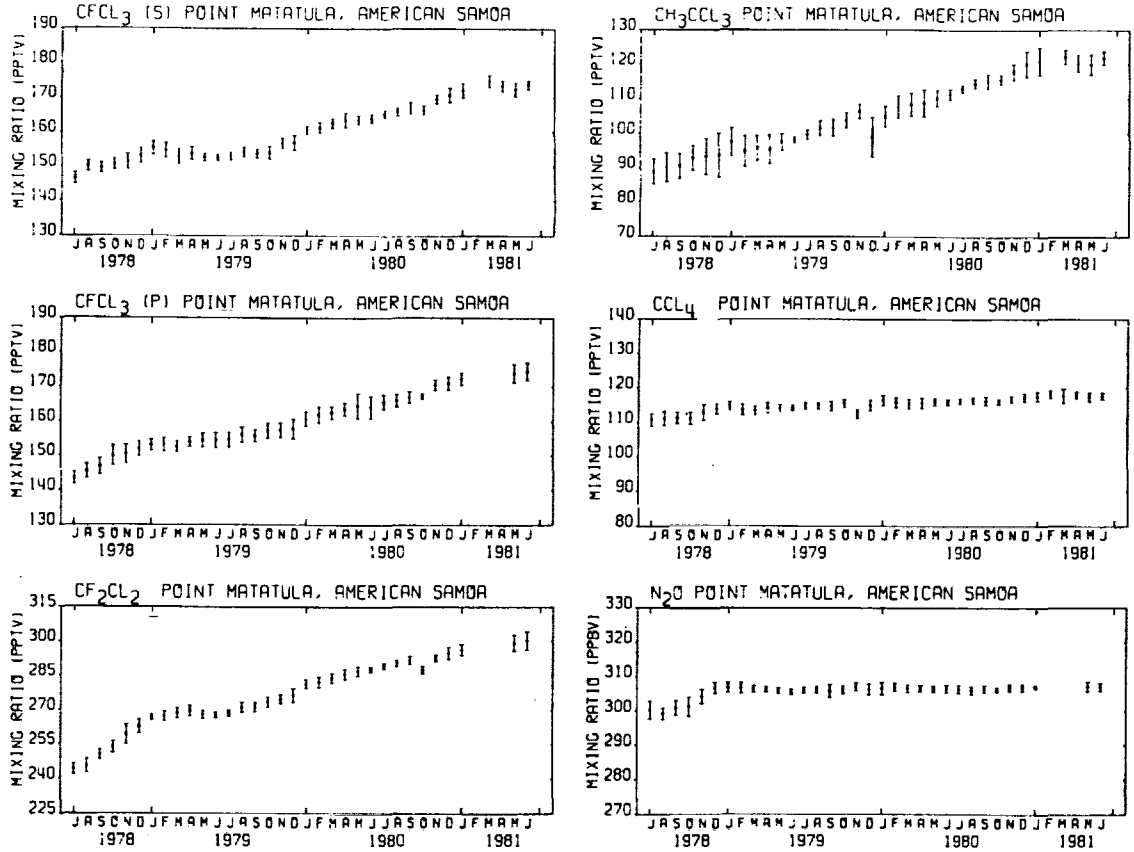

Fig. 12. Monthly mean mixing ratios and standard deviations measured at Point Matatula, American Samoa (14°S, 171°W). See Figure 9 for notation and discussion of calibration factors ξ.

appear to return to normal by early morning. To identify these short pollution episodes, a record of calm and hazy days at Ragged Point is maintained by the station caretaker.

During the southern summer the Intertropical Convergence Zone influences the Samoan latitudes. In particular, the circulation is affected by a monsoon low that forms to the west of Samoa and which enables northern hemisphere air (characterized by higher than normal halocarbon concentrations) occasionally to reach this station. Since air parcels arriving at Samoa are almost exclusively of oceanic origin, significant pollution is extremely rare at this site.

At Cape Grim, Tasmania, the majority (~56%) of winds blow from the southwest sector, and winds from other directions may be contaminated by the Australian mainland or Tasmania. In summer, high pressure dominates over Tasmania, and local sea breezes generally minimize instances of polluted air. However, in the winter and during the transition seasons, highs to the northeast of Tasmania may cause air from the Australian mainland to reach Cape Grim. For example, *Fraser and Pearman* [1978*b*] have identified Melbourne as an occasional source of high levels of $CFCl_3$ at Cape Grim. Such identifiable pollution occurs about 10 days per year at this site as evidenced by the ALE data record. Otherwise, Tasmania is an excellent clean air site.

The existence of annual cycles in the general circulation of the atmosphere and the possible existence of annual cycles in the emission rates of some of the ALE species suggests a search for such cycles in the ALE data. At Adrigole (Figure 9), a significant annual cycle is evident for CH_3CCl_3 with peak values occurring in late spring, but cycles are difficult to discern for the other four species. At Cape Meares (Figure 10), there is insufficient data to reach any definite conclusions about annual variations. The data at Barbados (Figure 11) indicate small amplitude cycles in CH_3CCl_3, CCl_4, and CF_2Cl_2 with peaks in late spring, late spring, and late summer, respectively. The cycles in CCl_4 and CH_3CCl_3 are consistent with southern hemisphere air parcels having the greatest likelihood of reaching this station in summer and fall and least in winter and spring, but the cycle in CF_2Cl_2 is apparently not. However, a detailed examination of the daily rather than monthly mean data does indicate short episodes of anomalously low CF_2Cl_2 mixing ratios at Barbados in the summer and fall which is consistent with the occasional sampling of southern hemisphere air in these latter two seasons [*Cunnold et al.*, this issue (*b*)].

At Samoa (Figure 12) we see the most pronounced evidence of annual cycles. Maximum mixing ratios are clearly observed in late summer and minima in late winter for CF_2Cl_2 and CCl_4 and for $CFCl_3$ on both columns. A similar but less clearly discernable cycle is evident for CH_3CCl_3 but with a maximum mixing ratio in the late spring. The observation of peak mixing ratios in late summer for the two chlorofluorocarbons is consistent with northern hemisphere air having the greatest probability of reaching Samoa in this season. Finally, the Tasmanian results (Figure 13) indicate an annual cycle for CH_3CCl_3 with a peak in late winter, but cycles in the other species are not evident.

The observed variations in trace species measurements are a function of both the precision of the actual measurements and the true atmospheric variability of the species. It is sometimes possible to separate these two influences. For example, the monthly variances in the observed mixing ratios plotted in

Figures 9–13 often show a marked decrease in magnitude after the first 6 months of operation of a particular measurement station. This decrease is very obvious in the data at Tasmania (Figure 13) and is due to the improvements in instrumental precision in this early period. Conversely, for those species and stations discussed above with recognized annual cycles, there is generally a correlation between peak mixing ratios and maximum monthly variances (see Figures 11 and 12 in particular). This correlation is expected since peak mixing ratios indicate air masses originating closer to the sources of the respective species and therefore exhibiting maximum variability. Similarly, inspection of Figures 9–13 shows a general decrease in monthly variances as we move from the northern to southern hemisphere stations. The Cape Grim station shows the least variability for all the ALE species, and this behavior is certainly expected for the four halocarbons since this station is the furthest from the major northern hemisphere anthropogenic sources of these compounds.

The lack of a substantial latitudinal gradient in the N_2O mixing ratio indicates that the N_2O sources are much more evenly distributed over the globe than the halocarbon sources. Thus, a comparison of N_2O monthly variances with those of the halocarbons can sometimes be used to differentiate between instrumental and atmospheric effects. In particular, when the N_2O monthly variances are positively correlated with the halocarbon monthly variances, then important instrumental rather than atmospheric effects on the variances are implicated. For example, the large variances in both N_2O and the halocarbons in the first several months of data at Barbados (Figure 11) lead us to suspect an instrumental rather than an atmospheric cause for the increased variability in the data in this early period. In this respect, the simultaneous measurement of several different species in the ALE program enables a number of cross checks on instrumental performance and true atmospheric variability which would not otherwise be possible for a single species.

At each station it is evident that CH_3CCl_3 has the largest monthly variances; typically, this variance is ~5% for CH_3CCl_3, ~2% for $CFCl_3$, CF_2CCl_2, and CCl_4, and ~0.5% for N_2O. The ALE data indicate that the lifetime of CH_3CCl_3 [*Prinn et al.*, this issue] is significantly shorter than that of $CFCl_3$, CF_2Cl_2, and CCl_4 [*Cunnold et al.*, this issue (*a*), (*b*); *Simmonds et al.*, this issue]. *Junge* [1974] has argued that such an inverse relationship between lifetime and variance σ is expected for species with similar distributions of sources and sinks. In particular, he suggested $\log \sigma \propto \log 1/\tau$ which appears to be roughly consistent with ALE σ and τ values for the halocarbons.

Although it is not evident in Figures 9–13, we have found that after significant adjustments have been made to the instrument, a short period sometimes elapses before the instrument stabilizes. Occasionally, small stepwise changes in the individual mean species concentrations are produced by such instrumental adjustments or by changing a calibration tank. The data record is currently insufficient to determine whether these small step-wise changes will average to zero over a long term. The general quality of ALE data particularly for the chlorofluorocarbons is usually sufficiently high for these few

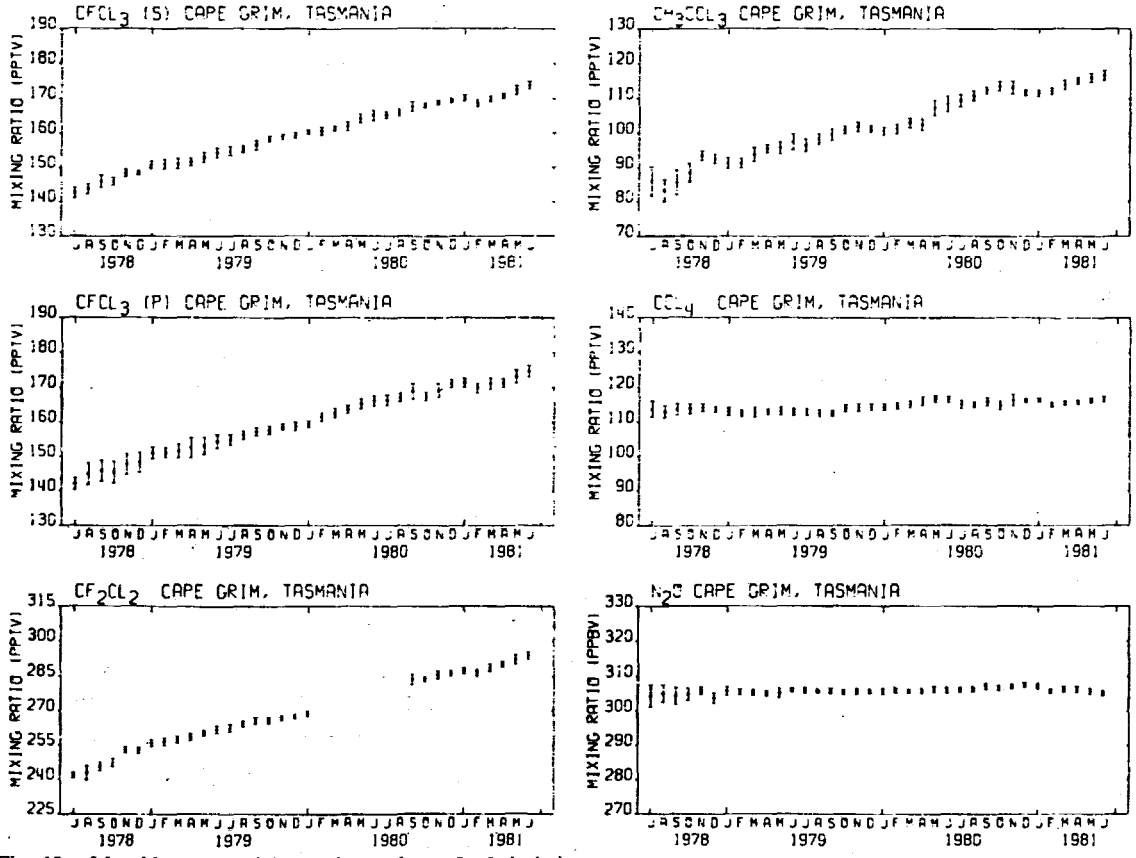

Fig. 13. Monthly mean mixing ratios and standard deviations measured at Cape Grim, Tasmania (41°S, 145°E). See Figure 9 for notation and discussion of calibration factors ξ.

small step-wise changes to make a nonnegligible contribution to the total error in the trend. Thus, although the trend errors are lower than anticipated, there is room for further improvement by minimizing the frequency of interruptions to instrumental operation. Indeed, a general improvement in instrument precision in the ALE program is already evident from the temporal decrease in the monthly variances for each species over the first 3 years. Thus, while monthly variances in the first year indicated effects due to differing performance of the instruments as well as to station location, the monthly variances in the third year are a function largely of the latitude of the ALE site.

5. Concluding Remarks

The major goal of the ALE experiment was to measure the trends of long-lived atmospheric species with sufficient precision to define accurately their atmospheric lifetimes, global circulation rates, and source-sink balances. Prior to the experiment we expected on theoretical grounds a systematic change in the observed chlorofluorocarbon trends with latitude based on source locations and interhemispheric transport rates. We also expected important seasonal and other temporal periodicities in the data. All these expected effects are clearly evident in the data which we have presented in this paper.

The measurements of $CFCl_3$, CF_2Cl_2, CH_3CCl_3, and CCl_4 in the ALE program indicate that reliance on only occasional measurements at varied locations for the determination of their lifetimes and circulation rates is in general hazardous. The atmospheric variability of these species on daily, weekly, seasonal, and annual time scales is significant and must be determined adequately before accurate conclusions can be drawn from the data. To define adequately the seasonal variations in species, it is apparent that a minimum of 2 years of data is required. To recognize even interannual variations (e.g., biennial oscillations) it is also clear that a minimum of 3 years of data is necessary. Thus, quite apart from the arguments by *Cunnold et al.* [1978] quoted earlier, conclusions concerning long-lived atmospheric species which are based on only 1 or 2 years of data are subject to criticism. This is certainly evident by inspection of the $CFCl_3$ lifetimes which would have been reported from the ALE experiment had we relied on only 1 or 2 years of data (namely, 45 and 105 years, respectively, using the observed trends). These values differ significantly from the value of 83 years deduced after 3 years of data became available [*Cunnold et al.*, this issue (*a*)].

In this and the following papers the data from the first 3 years of the ALE program are presented and analyzed. The ALE program is now in its fifth year of operation, and we are optimistic that at least 6 years of data will eventually be obtained.

Acknowledgments. The existence and success of the Atmospheric Lifetime Experiment owes much to the efforts of Bruce Lane, Ian Jones, and John Diggle of Imperial Chemical Industries. In their official roles as representatives of the Fluorocarbon Program Panel, Chemical Manufacturers Association, they have played an important role not only in the managerial but in the scientific aspects of the experiment. At the ALE stations we would like to acknowledge the local help from Graham Wise and Kim Briggs (Australian Department of Science and Technology) in Tasmania; Don Nelson (National Atmospheric and Oceanic Administration) in Samoa; Cornelius Shea in Barbados; Jeff Weiderholt in Oregon; and Andrew Lovelock and Michael O'Sullivan in Ireland. We also thank C. Curthoys for her help in the data handling for the Adrigole and Ragged Point stations. This research was supported by the Fluorocarbon Program of the Chemical Manufacturers Association. Nominal support has also been provided by the Atmospheric Chemistry Program of NSF (to R.G.P.) and the Upper Atmosphere Research Program of NASA (to R.A.R.).

References

Alyea, F., The Atmospheric Lifetime Experiment: A guide to the ALE data tape, *NASA Tech. Memo.*, 1983.

Cox, R., R. Derwent, A. Eggleton, and J. Lovelock, Photochemical oxidation of halocarbons in the troposphere, *Atmos. Environ.*, *10*, 305–308, 1976.

Cronn, D. R., and D. E. Harsch, Determination of atmospheric halocarbon concentrations by GC-MS, *Anal. Lett.*, *12*, 1489–1496, 1979.

Crutzen, P., The influence of nitrogen oxides on the atmospheric ozone content, *Q. J. R. Meteorol. Soc.*, *96*, 320–325, 1970.

Crutzen, P., Estimates of possible variations of total ozone due to natural causes and human activities, *Ambio*, *3*, 201–210, 1974.

Cunnold, D., F. Alyea, and R. Prinn, A methodology for determining the atmospheric lifetime of fluorocarbons, *J. Geophys. Res.*, *83*, 5493–5500, 1978.

Cunnold, D., R. Prinn, R. Rasmussen, P. Simmonds, F. Alyea, C. Cardelino, A. Crawford, P. Fraser, and R. Rosen, The Atmospheric Lifetime Experiment, 3, Lifetime metholology and application to 3 years of $CFCl_3$ data, *J. Geophys. Res.*, this issue (*a*).

Cunnold, D., R. Prinn, R. Rasmussen, P. Simmonds, F. Alyea, C. Cardelino, and A. Crawford, The Atmospheric Lifetime Experiment, 4, Results for CF_2Cl_2 based on 3 years of data, *J. Geophys. Res.*, this issue (*b*).

De Luisi, J., Geophysical monitoring for climatic change, 9, *Summary Rep. for 1980*, NOAA Environ. Res. Lab., Boulder, Colo., 1981.

Foulger, B. E., and P. G. Simmonds, Drier for field use in the determination of trace atmospheric gases, *Anal. Chem.*, *51*, 1089–1090, 1979.

Fraser, P., and G. Pearman, Atmospheric halocarbons in the southern hemisphere, *Atmos. Environ.*, *12*, 839–844, 1978*a*.

Fraser, P., and G. Pearman, The Australian atmospheric halocarbon monitoring programme, in *Proceedings of the International Clean Air Conference, Brisbane*, edited by E. White, pp. 703–716, Ann Arbor Science, Ann Arbor, Mich., 1978*b*.

Gobby, P. L., E. P. Grimsrud, and S. W. Warden, Improved model of the pulsed electron capture detector, *Anal. Chem.*, *52*, 473–482, 1980.

Golombek, A., A global three-dimensional model of the circulation and chemistry of long-lived atmospheric species, Ph.D. thesis, Mass. Inst. of Technol., Cambridge, 1982.

Grimsrud, E. P., and S. H. Kim, Stoichiometry of the reaction of electrons with bromotrichloromethane in an electron capture detector, *Anal. Chem.*, *51*, 537–541, 1979.

Grimsrud, E. P., and R. A. Rasmussen, Survey and analysis of halocarbons in the atmosphere by gas chromatography-mass spectrometry, *Atmos. Environ.*, *9*, 1014–1017, 1975.

Jesson, J., P. Meakin, and L. Glasgow, The fluorocarbon-ozone theory, II, Tropospheric lifetimes—An estimate of the tropospheric lifetime of $CFCl_3$, *Atmos. Environ.*, *11*, 449–508, 1977.

Junge, C., Residence time and variability of tropospheric trace gases, *Tellus*, *26*, 477–488, 1974.

Louis, J. F., Mean meridional circulation, The Natural Stratosphere of 1974: CIAP Monograph 1, *Rep. DOT-TST-75-51*, pp. 6:23–6:31, *U.S. Dep. of Transp.*, Washington, D. C., 1975.

Lovelock, J. E., The electron capture detector: Theory and practice, *J. Chromatogr.*, *99*, 3–12, 1974.

Lovelock, J. E., Methyl chloroform in the troposphere as an indicator of OH radical abundance, *Nature*, *267*, 32, 1977.

Lovelock, J. E., and A. J. Watson, Electron-capture detector: Theory and practice, II, *J. Chromatogr.*, *158*, 123–138, 1978.

Lovelock, J., R. Maggs, and R. Wade, Halogenated hydrocarbons in and over the Atlantic, *Nature*, *241*, 194–196, 1973.

McConnell, J., and H. Schiff, Methyl chloroform: Impact on stratospheric ozone, *Science*, *199*, 174–177, 1978.

Molina, M., and F. Rowland, Stratospheric sink for chlorofluoromethanes: Chlorine catalysed destruction of ozone, *Nature*, *249*, 810–812, 1974*a*.

Molina, M., and F. Rowland, Predicted present stratospheric abundances of chlorine species from photodissociation of carbon tetrachloride, *Geophys. Res. Lett.*, *1*, 309–312, 1974*b*.

Newell, R., J. Kidson, D. Vincent, and G. Boer, *The General Circulation of the Tropical Atmosphere and Interactions With Extra-Tropical Latitudes*, vol. 1, pp. 122–123, MIT Press, Cambridge, Mass., 1972.

Pack, D., J. Lovelock, G. Cotton, and C. Curthoys, Halocarbon behaviour from a long time series, *Atmos. Environ.*, *11*, 329–344, 1977.

Penkett, S. A., The application of analytical techniques to the understanding of chemical processes occurring in the atmosphere, *Toxicol. Environ. Chem. Rev.*, *3*, 291–321, 1981.

Prinn, R., R. Rasmussen, P. Simmonds, F. Alyea, D. Cunnold, B. Lane, C. Cardelino, and A. Crawford, The Atmospheric Lifetime Experiment, 5, Results for CH_3CCl_3 based on 3 years of data, *J. Geophys. Res.*, this issue.

Ramanathan, V., Greenhouse effect due to chlorofluorocarbons: Climatic implications, *Science*, *190*, 50–52, 1975.

Rasmussen, R., and M. Khalil, Global Atmospheric distribution and trend of methylchloroform (CH_3CCl_3), *Geophys. Res. Lett.*, *8*, 1005–1007, 1981.

Rasmussen, R., and J. Lovelock, The Atmospheric Lifetime Experiment, 2, Calibration, *J. Geophys. Res.*, this issue.

Rasmussen, R., M. Khalil and R. Dalluge, Atmospheric trace gases in Antarctica, *Science*, *211*, 285–287, 1981.

Rowland, F., and M. Molina, Estimated future atmospheric concentrations of $CFCl_3$ (fluorocarbon 11) for various hypothetical tropospheric removal rates, *J. Phys. Chem.*, *80*, 2049–2051, 1976.

Simmonds, P., The atmospheric lifetime experiment, first quarterly report, contract FC-79-280, Chem. Mfr. Assoc., Washington, D. C., 1980.

Simmonds, P., F. Alyea, D. Cunnold, J. Lovelock, R. Prinn, R. Rasmussen, B. Lane, C. Cardelino, and A. Crawford, The Atmospheric Lifetime Experiment, 6, Results for CCl_4 based on 3 years of data, *J. Geophys. Res.*, this issue.

Stolarski, R., and R. Cicerone, Stratospheric chlorine: A possible sink for ozone, *Can. J. Chem.*, *52*, 1610–1615, 1974.

Sze, N., and M. Wu, Measurements of fluorocarbons 11 and 12 and model validation: An assessment, *Atmos. Environ.*, *10*, 1117–1125, 1976.

Wang, W., Y. Yung, A Lacis, T. Mo, and J. Hansen, Greenhouse effects due to man-made perturbations of trace gases, *Science*, *194*, 685–690, 1976.

F. N. Alyea, C. A. Cardelino, and D. M. Cunnold, School of Geophysical Sciences, Georgia Institute of Technology, Atlanta, GA 30332.

A. J. Crawford and R. A. Rasmussen, Department of Environmental Science, Oregon Graduate Center, Beaverton, OR 97006.

P. J. Fraser, Division of Atmospheric Physics, CSIRO, Aspendale, Victoria, Australia.

J. E. Lovelock, Department of Engineering and Cybernetics, University of Reading, Reading, England.

R. G. Prinn, Earth, Atmospheric, and Planetary Sciences, Massachusetts Institute of Technology, Cambridge, MA 02139.

R. D. Rosen, Atmospheric and Environmental Research, Inc., Cambridge, MA 02139.

P. G. Simmonds, Department of Geochemistry, University of Bristol, Bristol, England.

(Received July 9, 1982;
revised March 28, 1983;
accepted April 25, 1983.)

JOURNAL OF GEOPHYSICAL RESEARCH, VOL. 88, NO. C13, PAGES 8369–8378, OCTOBER 20, 1983

The Atmospheric Lifetime Experiment 2. Calibration

R. A. RASMUSSEN

Department of Environmental Science, Oregon Graduate Center

J. E. LOVELOCK

Department of Engineering and Cybernetics, University of Reading

The calibration standards used in the Atmospheric Lifetime Experiment (ALE) for $CFCl_3$, CF_2Cl_2, CH_3CCl_3, and CCl_4 are described. This includes the preparation of the primary standards by static dilution and their propagation and stability for the period 1977–1982. Two independent assessments of the absolute concentrations of the primary standards used to initiate the ALE measurements in 1977–1978 are reported. For consistency in the ALE program the values assigned to the primary standards and subsequent working standards used in the field were not altered during the experiment when results of better estimates of the original concentration values were obtained. Rather, the appropriate factors ζ, by which the ALE mixing ratios for a given species should be multiplied to obtain our best estimate of the current concentration of a given species, are provided.

INTRODUCTION

A special and necessary feature of the ALE program is the accurate daily on-site calibration of the instruments. This is accomplished by using specially prepared reference tanks of air which are shipped to the ALE sites where they are usually used for approximately 3 months. At any one time there are usually two reference tanks maintained at each site, one being used and the other serving as a backup.

These calibration tanks are prepared by using clean air from the Cape Meares station and the concentrations of CCl_3F, CCl_2F_2, CH_3CCl_3, CCl_4, and N_2O in the tanks are determined relative to primary standards. The determination of these concentrations is carried out both before and after the use of the tank at a particular site. Each determination consists of at least six separate analyses to ensure that errors in the concentrations in these tanks relative to the primary standards are not important in subsequent analyses of the ALE data for trends and lifetimes.

The absolute concentrations of the primary and secondary standards used in the ALE measurements program were determined by static dilution techniques. This work was done prior to the initiation of ALE. The work in early 1975 [*Grimsrud and Rasmussen, 1975a*] using gas chromatographic/mass spectrometric (GC/MS) analysis established the following ambient concentrations at 45°N for $CFCl_3$, 125 ± 8; CF_2Cl_2, 230 ± 10; CH_3CCl_3, 100 ± 15; and CCl_4, 120 ± 15 (pptv). These background concentrations were significantly higher than values obtained by others using only electron capture gas chromatography (EC/GC). This was especially significant for CF_2Cl_2 which was consistently about twice the values of *Hester et al.* [1974] and *Lovelock* [1974*a*]. In view of the relatively straightforward principles of mass spectrometric analyses as compared to the less well understood electron capture detector at this time, we regarded the higher values for CF_2Cl_2 as being correct. Direct EC/GC analyses of the primary and the secondary standards prepared were consistent with the GC/MS results.

Further preparations of primary standards for various trace gases by using static dilution methods were continued through 1976 and 1977. The results for the halocarbons were consistent with the primary standards developed in 1975. The experimental details for preparing the primary standards for $CFCl_3$, CF_2Cl_2, CH_3CCl_3, and CCl_4 from pure materials have been previously described [*ALE Principle Investigators*, 1981]. The efforts between 1975 and 1977 established the expertise to prepare absolute concentrations for $CFCl_3$ and CF_2Cl_2 to ± 5 to 10% and CH_3CCl_3 and CCl_4 to ± 15 to 20%. The work also developed containers free from contamination and determined the storage stability of $CFCl_3$, CF_2Cl_2, CH_3CCl_3, CCl_4, and N_2O in standards used in the laboratory. These developments were tested in several interlaboratory calibration studies [*Rasmussen et al.*, 1976; *Rasmussen*, 1978; *Rasmussen and Pierotti*, 1978; *Rasmussen and Khalil*, 1981]. Accordingly, when the ALE program started in the fall of 1977, the accuracy of the primary standards in use in Rasmussen's laboratory was accepted as the provisional reference standards for the ALE study. Subsequently, two additional studies were designed by Lovelock to determine independently the absolute calibration values assigned to the ALE primary standards. These additional studies involved the use of a large exponential dilution chamber and the calculation of the absolute concentrations by coulometry.

The propagation of the primary standards in the ALE program is discussed in the following sections. Considerable care is taken to confirm continuously the accuracy of the propagation of the ALE standards over time and between the various ALE stations. This is because, in order to determine the trends of trace gases for the ALE program, the errors in relative concentrations are much more important than the errors in absolute concentrations.

PROPAGATION OF ALE SECONDARY STANDARDS

The concentrations of $CFCl_3$, CF_2Cl_2, CH_3CCl_3, and CCl_4 assigned in 1977 to the ALE standards were determined by direct comparison with the standards used in the 1976 interla-

Paper number 3C1028.
0148-0227/83/003C-1028$05.00

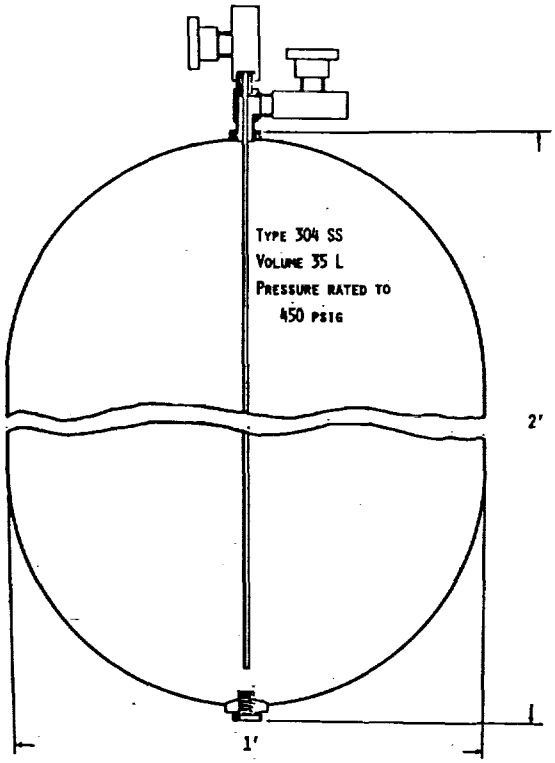

Fig. 1. Modified and internally SUMMA® treated type G-1 stainless steel tank of 35 l used for ALE calibration standards.

boratory calibration exchange [*Rasmussen and Pierotti*, 1978]. Through the fall and winter of 1977 a dozen high pressure (>400 psig) tanks of clean ambient air were collected and calibrated against these standards. The values assigned to the ALE standards were the best estimates available at the time the project started. These are referred to as our "working values." The new calibration tanks were designated secondary working standards. The approach served to provide a sufficient number of reference standards for laboratory and field use while conserving the primary standards. The design was also intended to check the stability of the stored mixture by periodic comparison of the secondary standards with each other and with the parent primary standard. Such cross tests would reveal drift, degradation, or variable stability of the halocarbons measured. Periodic re-examination of the standards was expected to reveal changes as small as ±2% for CFC's and N_2O and ±4% for the other species (i.e., twice that of the precision of analysis). Except in the event that all of the secondary standards as well as the primary standards, each with its own concentration in the different tanks, deteriorated at a similar rate (a possibility considered below), the validity of the long-term stability of the standards could be accurately determined.

The secondary standards are prepared in aircraft surplus breathing oxygen tanks (type G-1, 35 L static volume). The tanks are made of stainless steel (type 304) of a nonshatterable design limited to 450 psig. Their light weight (9.1 kg) provides ease of handling and shipment. The stainless steel fabrication was selected because it could be passivated by the SUMMA® electropolish, thereby greatly improving the quality of the surface in contact with the stored gas compared to previously used steel cylinders. The ¼-inch NPT openings on each end of the G-1 tanks also greatly facilitated the immersion of the tanks in the SUMMA® solution and subsequent washing. The tanks are sealed at the bottom end with a stainless steel plug and fitted on the top with two stainless steel bellow valves (Nupro®, SS 4-H-4) welded to a purge tee assembly (Figure 1). After being assembled and leak tested, the tanks are internally steam cleaned and baked out (150°C) for 24 hours while being flushed with zero air. Measurements for the desorption of residual halocarbon contaminants are made on the tanks (filled to 5 psig with a halocarbon-free air) after a week or two of storage.

Since 1978 the secondary standards have been prepared at the Cape Meares station by cryogenically liquefying clean ambient air into the tanks. This is accomplished by floating the tanks in liquid nitrogen (LN_2). When the bottom of the tank has reached equilibrium with the LN_2 (−196°C), the side valve is opened and clean air is drawn into the tank by the vacuum created as liquid air forms on the bottom surface. The filling is accelerated by pumping air into the tank, using an ultra-clean metal bellow pump (Metal-Bellow Corp., model 158). Data from the in situ real-time analyses at the Cape Meares station compared with the analyses of the air collected in the tanks during the same period show no significant differences. The amount of air compressed is typically ~1000 l, resulting in pressures of ~450 psig. The water condensed in the tanks by compression is removed by draining, and the concentrations of $CFCl_3$, CF_2Cl_2, CH_3CCl_3, and CCl_4 are determined against the primary standards of OGC. The dew point of the air withdrawn from the tanks is typically −26 to −24°C over the pressure range of 450–100 psig. Experience with the standards prepared in this manner has shown them to have excellent stability for the ambient levels of the halocarbons of interest. The stability for CCl_4 is especially important since storage of this species in the steel medical oxygen cylinders used in 1975–1976 was of varying reliability. Also, the stainless steel tanks have provided excellent stability for CHF_2Cl, CH_3Cl, and CH_4. It should be noted that before the air sample withdrawn from the tanks is injected into the gas chromatographs, it is dried to an H_2O mixing ratio of 700 ppm or less by an 815 Nafion® drier [*Foulger and Simmonds*, 1979]. This procedure has further standardized the analysis to dry air.

To date some 190 tanks have been prepared; 51 of them have been used at the five ALE stations. The stability of the halocarbons and N_2O in these high pressure tanks is shown (Table 1) for three typical tanks used in the ALE project. The tanks were analyzed before being sent to the field stations and upon their return. Further periodic analyses were done to better validate long-term stability of a given tank and to reassure the internal consistency in the primary calibration values. All of the concentrations in the tanks have been determined by direct comparison with primary standard 033. This standard is one of three (033, 034, 035) established in the spring of 1978 that is traceable to the 1975–1976 primary standards via the 1976 interlaboratory calibration study. As shown by the data in Table 1, the precision of analysis has improved since 1978, essentially because of the changeover from manual peak height measurements to electronic integration of peak heights (HP3388A reporting integrator) in 1979 and further optimization of the instrument (PE3920-B) dedicated to calibration analyses. The continuity in these calibration standards has been used to measure the halocarbons at the South Pole in Antarctica and in the U.S. Pacific Northwest (~45°N)

TABLE 1. Stability of Species in Three of the ALE Secondary Calibration Tanks

Run	Date (Month/Day/Year)	F-11, ppt		F-12, ppt		CH_3CCl_3, ppt		CCl_4, ppt		N_2O, ppb	
		$\bar{x}$	σ	$\bar{x}$	σ	$\bar{x}$	σ	$\bar{x}$	σ	$\bar{x}$	σ
					Tank 023						
Original	04/09/78	167.4	1.4	280.8	2.9	162.8	2.5	143.2	1.5	335.2	1.8
Rechecked	12/06/78	164.8	1.7	280.0	1.6	166.0	4.5	142.5	0.8	333.5	2.1
Rechecked	04/10/79	167.5	0.8	281.3	2.0	164.7	2.2	145.7	1.2	335.5	0.5
Rechecked	02/01/80	166.8	0.4	279.0	0.6	164.5	0.8	145.8	0.4	334.8	0.4
Rechecked	09/03/81	166.4	0.8	281.8	2.6	162.9	0.7	144.4	0.9	334.6	1.1
Rechecked	02/22/82	166.8	0.4	280.0	2.8	163.5	0.8	144.3	1.0	336.8	1.0
					Tank 017						
Original	04/09/78	168.5	0.6	285.3	2.9	134.5	2.8	146.8	1.5	332.8	1.6
Rechecked	12/04/78	169.2	0.8	282.8	1.1	128.3	1.2	146.2	0.8	332.3	1.2
Rechecked	04/11/79	168.0	0.0	283.2	1.0	129.2	0.8	144.2	1.0	333.3	0.5
Rechecked	01/30/80	168.7	0.5	284.2	0.8	129.7	0.5	143.2	1.5	333.8	0.8
Rechecked	08/29/80	168.8	0.4	284.3	0.8	129.7	0.5	142.7	0.5	335.2	1.2
Rechecked	09/04/81	169.2	0.8	282.2	1.2	130.5	1.0	141.3	1.0	333.3	1.0
Rechecked	02/15/82	169.3	0.5	279.6	1.9	130.7	0.5	139.2	0.4	334.8	0.8
					Tank 028						
Original	04/09/78	168.5	1.0	281.5	1.2	148.9	2.8	146.8	1.9	335.4	1.4
Rechecked	01/24/79	167.5	0.6	282.0	0.6	149.0	1.3	146.0	1.1	335.0	0.0
Rechecked	04/24/79	167.8	0.4	283.0	1.3	150.7	0.8	146.3	0.5	333.3	1.2
Rechecked	08/29/79	167.2	1.2	282.0	1.1	148.7	0.8	145.7	1.4	334.3	0.5
Rechecked	02/05/80	168.0	0.6	284.5	0.5	148.3	1.4	145.5	0.5	334.5	0.5
Rechecked	05/18/81	168.7	0.5	283.5	1.8	146.7	1.4	145.3	0.8	334.5	0.6
Rechecked	03/12/82	168.3	0.4	281.8	0.4	147.7	1.0	145.1	0.7	335.8	1.1

during January of each year from 1975 to 1980 [*Rasmussen and Khalil*, 1981].

Propagating standards (especially for $CFCl_3$) within the same margin of precision ($\pm 1\%$) as required of the precision of analysis ($< \pm 1\%$) has been a major part of the experiment. Verifying the stability of halocarbons and N_2O in these secondary standards required that the tanks be rechecked every few months to once a year. The standards are usually calibrated twice before being sent to a field station, upon return and periodically thereafter. This system of periodic cross calibrations began in 1977.

Figures 2*a*, 2*b*, 2*c*, and 2*d* shows the stability of $CFCl_3$, CF_2Cl_2, CH_3CCl_3, and CCl_4 in the first tanks used in 1978 for several months at Adrigole, Barbados, Samoa, and Tasmania. Some of the tanks were redeployed in the field after being rechecked at the Oregon Graduate Center (OGC). This is possible since the initial tank pressures are >400 psig, and <100 psig are used during the field calibration period. Tests have shown that the halocarbons and N_2O are unchanged in the tanks down to pressures of <100 psig. The data plotted are the percent changes from their originally assigned values determined by analyses against one or more of the primary standards. For example, the $CFCl_3$ concentration in the tanks is $\sim 170 \pm 1$ pptv/v. The $\pm 0.5\%$ deviation shown in Figure 2*a* for $CFCl_3$ after nearly 4 years is equivalent to 0.8 pptv/v, which is within the overall accuracy required of the measurement. Similar results are shown in Figures 2*b*, 2*c*, and 2*d* for CF_2Cl_2, CH_3CCl_3, and CCl_4.

The data in the graphs have been analyzed mathematically and the conclusion drawn that there is little change in the assigned values of any of the species in the tanks. The calculated average drift for all of the tanks showed no statistical change at the $\alpha = 0.05$ level. Similarly, when each tank was considered individually, none was found to be drifting at statistically significant rates, $\alpha = 0.05$. Inspection of Figures 2*a*, 2*b*, 2*c*, and 2*d* indicates that the greatest changes between successive analyses occurred in the first 12–14 months after the calibration began. Changes in the experimental procedures and greater accuracy in the electronic measurement of the chromatographic peaks during this period are believed to be responsible for the improvement.

Further analyses were performed to determine if the concentrations of a given species ($CFCl_3$, etc.) stored in similar tanks under equivalent conditions could drift at the same rate. The principle source of any such steady state drift is presumed to be a heretogeneous surface reaction. The basis for this concern was that all of the ALE secondary standards are stored under identical conditions of tank type (G-1, type 304 SS), volume (35 l), pressure (>400 psig), and represent a limited concentration range of 100–200 pptv/v. In this respect, heterogeneous reaction on the walls of the flasks could be important. Therefore, 26 air samples collected cryogenically in May–June 1978 in smaller 1.6 l stainless steel bottles were studied over an equivalent period similar to the analysis schedule for the larger ALE tanks. These samples were equivalent in concentration range (90–180 pptv/v), pressure (>400 psig) and type (304 SS). The only major difference was the smaller volume-to-surface ratio of 0.99 for the 1.6 l bottles versus 2.46 for the 35 l ALE tanks. Table 2 shows the statistical analysis comparing the concentrations of $CFCl_3$, CF_2Cl_2, CH_3CCl_3, and CCl_4 determined after 26 months (Δ_1) and 42 months (Δ_2) against the original values referenced to the same primary standards at the 95% confidence limit. The quoted errors do not include the uncertainty in the assigned values of the 35 l ALE tanks.

For the species $CFCl_3$, CF_2Cl_2, and CH_3CCl_3 the 1.6 l tanks do not show any decrease relative to the ALE tanks and hence refute any hypothesis that the levels in the tanks are

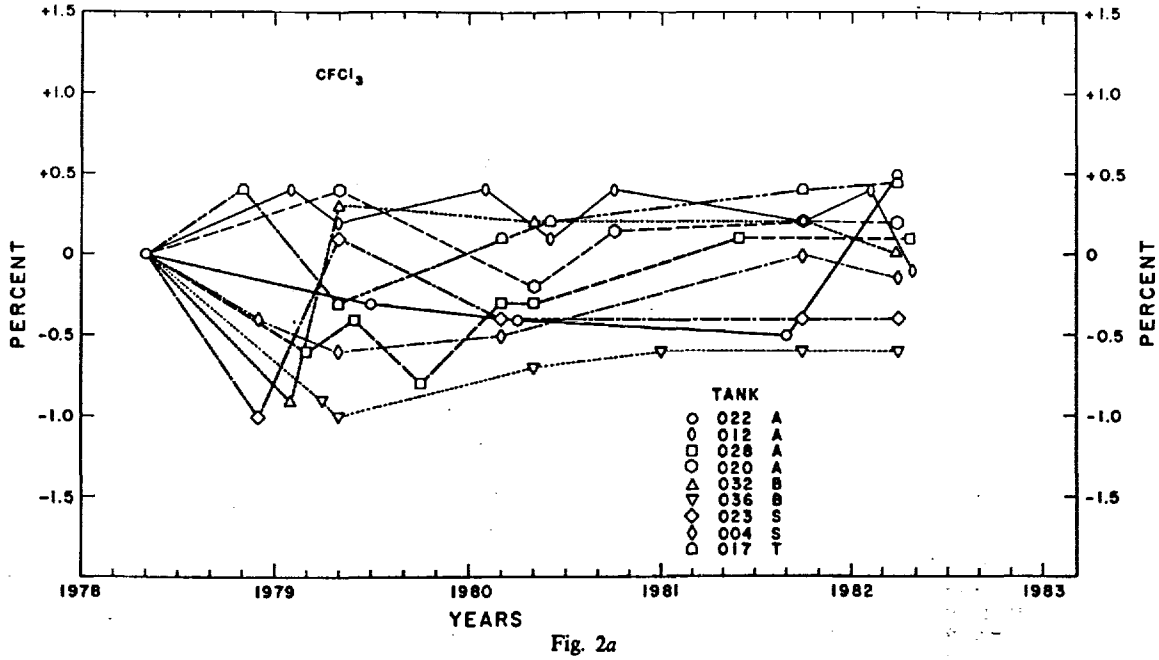

Fig. 2a

Fig. 2. Percent changes of $CFCl_3$, CF_2CL_2, CH_3CCl_3, and CCl_4 from original values as determined against primary standard in subsequent analyses over 4 years. Assigned concentrations in pptv at time 0: (*a*) $CFCl_3$: 022, 169; 012, 170; 028, 168; 020, 169, 032, 174; 036, 174; 023, 167; 004, 169; 017, 168. (*b*) CF_2Cl_2: 022, 283; 012, 285; 028, 282; 020, 284; 032, 292; 036, 293; 023, 281; 004, 282; 017, 285. (*c*) CH_3CCl_3: 022, 143; 012, 150; 028, 149; 020, 143; 036, 137; 023, 163; 004, 144; 017, 134. (*d*) CCl_4: 022, 144, 012, 148; 028, 147; 020, 146; 032, 151; 036, 151; 023, 143; 004, 145.

declining due to heterogeneous surface reactions, which would result in a relatively greater concentration decline in the 1.6 l tanks than in the 35 l tanks.

The slight increase in the 1.6 l tanks (e.g., CF_2Cl_2) compared with the 35 l tanks is of unknown origin. In these small tanks any volume dependent effect, such as outgassing from the PTFE tape used to seal in the valve, would be magnified by a factor of 22 over the effect in the 35 l tanks. If such a phenomenon is the origin of the slight increase in the 1.6 l tanks, the magnitude of the increase for the 35 l tanks is negligible.

For the species CCl_4 the concentration in the 1.6 l tanks relative to the 35 l tanks is shown in Figure 3. The behavior is clearly variable. Four of the tanks lose 45–80% of their CCl_4 in 26 months, four other 1.6 l tanks lose 10–20% in 42 months, and the remaining 18 tanks form a group spread around 7% change. The least square fit line for this subset is -0.2% year^{-1} $\pm 0.3\%$ year^{-1}; clearly the eight rapidly decreasing tanks are not typical of the ALE tanks, as the relative calibration of the ALE tanks does not show any such rapidly declining tanks. The ALE tanks (see insert in Figure 3) are more typical of the subset of the 18 1.6 l tanks. From this

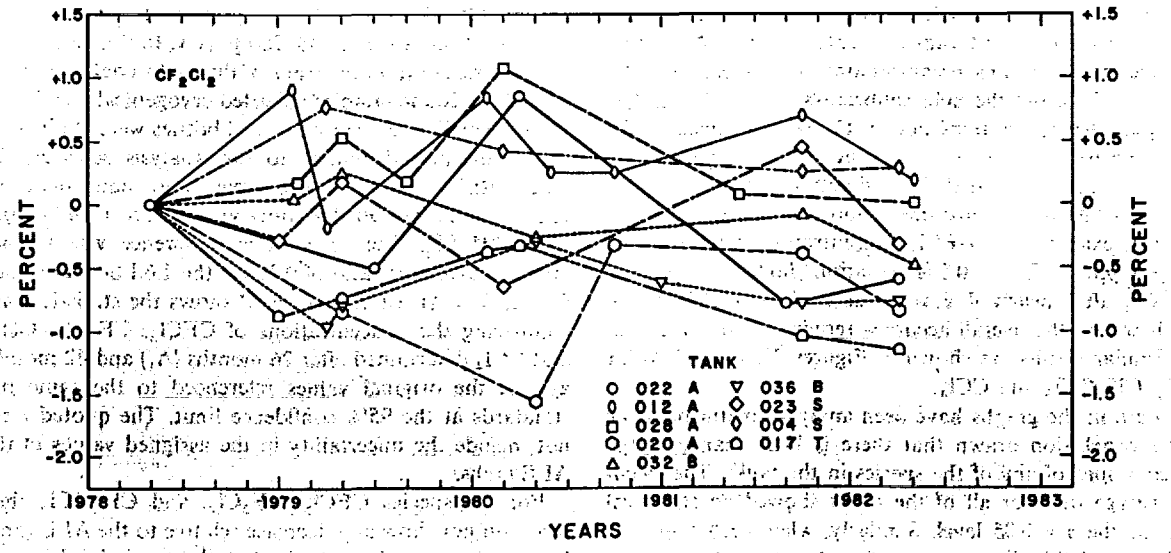

Fig. 2b

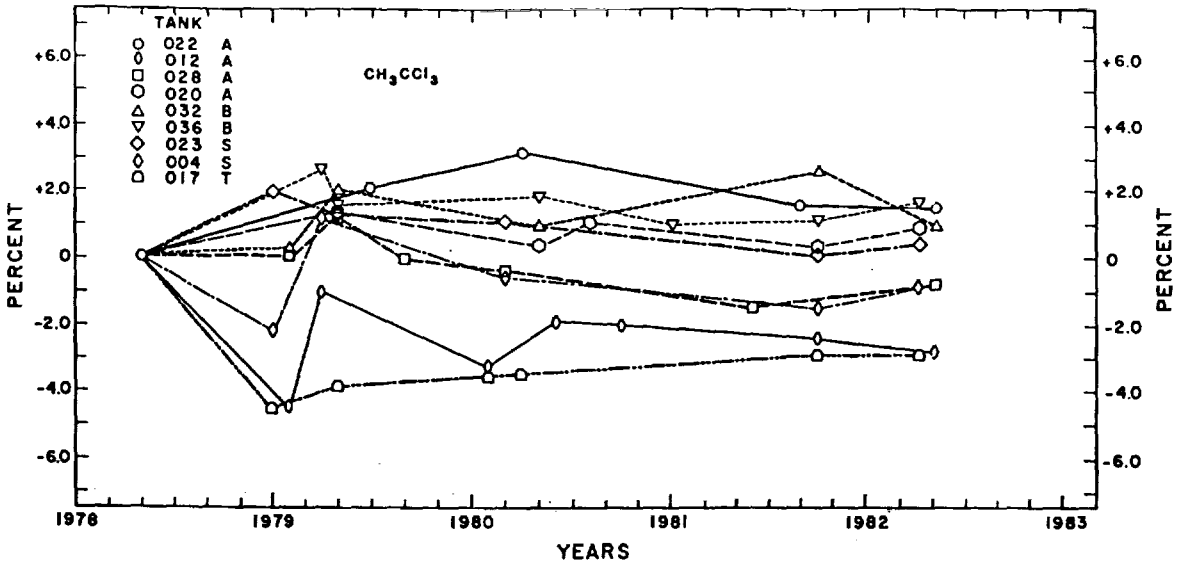

Fig. 2c

subset we estimate the decline of the ALE tanks from heterogeneous surface reaction could be $-0.2 + 0.3\%$ year^{-1}/1.4 or $-0.15 \pm 0.2\%$ year^{-1} or -0.2 ± 0.3 pptv year^{-1}.

This result is not statistically different from zero, but is indicative of a slight decline.

Absolute Calibration

Exponential dilution

This method involves dispersing uniformly an accurately measured amount of a pure compound (~1 mg level) into a known volume of sufficient size to give in a single almost error-free step an aerial concentration at a part per billion or less. The known volume can conveniently be a sealed empty room or capacity 50–100 cubic metres. If the room were hermetically sealed and the walls were made of material which was wholly inert to the test vapor, the vapor concentration would persist indefinitely and the air of the room would constitute a primary standard. In practice, although possible, the construction of a room to these specifications is expensive. A more realistic alternative is to take a room of more conventional construction and arrange to provide it with positive pressure clean air ventilation at a known rate and also to keep the air of the room vigorously stirred by using a powerful fan. In these circumstances, the vapor concentration in the room is uniform but is undergoing dilution at a constant rate. By observing the rate of decay of the test vapor and also that of some reference gas, such as hydrogen, the concentration at the time zero can be found which corresponds to that which would persist in an ideal leak-free room. Furthermore, since the vapor concentration nearly always decays exponentially, the logarithm of its concentration is a linear function of the elapsed time from the start of the dilution. Accurate standard concentrations down to one tenth the initial concentration can be established from the rate of dilution and the elapsed time. The decay of concentration C with time t is that of a first-order reaction

$$\frac{dC}{dt} = -\frac{U}{V}C \qquad (1)$$

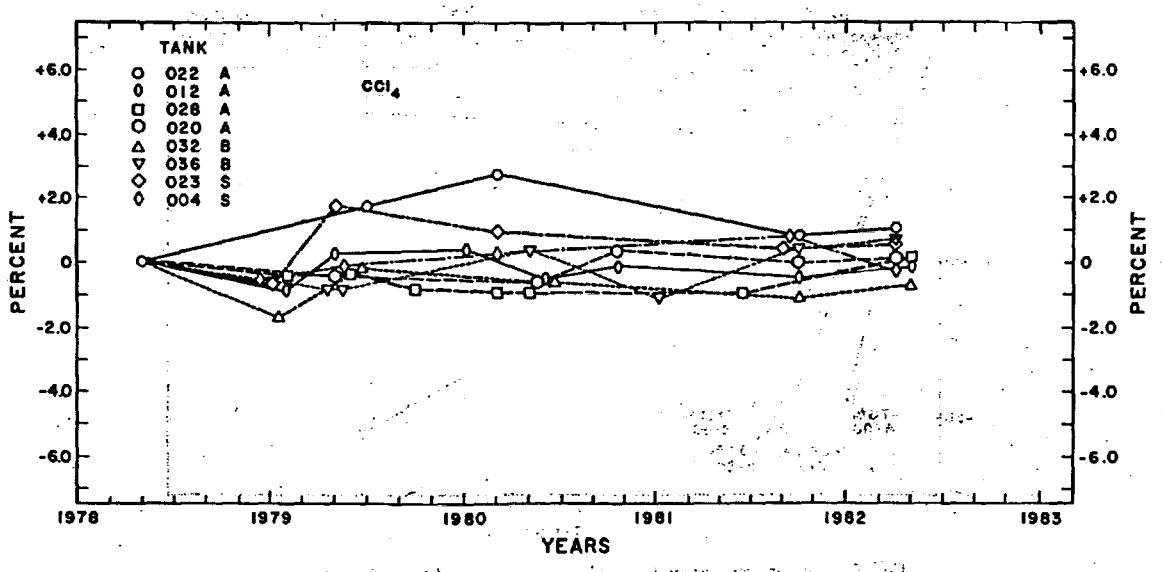

Fig. 2d

TABLE 2. Time Course Changes in Halocarbon Concentrations in 1.6 l Bottles

	Δ'_1, pptv/yr	Δ'_2, pptv/yr
$CFCl_3$	0.13 (±0.4)	1.2 (±0.4)
CF_2Cl_2	1.4 (±0.6)	0.3 (±1.0)
CH_3CCl_3	−0.4 (±0.4)	1.5 (±0.6)
CCl_4	−1.4 (±1.0)	−1.4 (±1.0)

where V is the chamber volume and U the flow rate of ventilating air, or equivalently

$$\ln C(t) = \ln C(0) - \frac{U}{V} t \tag{2}$$

From (2) it follows that the logarithm of the concentration is a linear function of time from the start of the dilution and that the intercept at time zero is the logarithm of the concentration expected for an ideal leak-tight chamber.

In practice, there may be a constant concentration of the test substance in the ambient air C_a. Equation (2) then becomes

$$\ln [C(t) - C_a] = \ln [C(0) - C_a] - \frac{U}{V} t \tag{3}$$

It is usual to take measurements of the incoming air for 2 hours before and after a dilution experiment so that the quantity C_a can be found and seen to be constant.

The dilution chamber was constructed from plaster board fastened to a rigid wooden framework. The lines of contact between the plasterboards were sealed with masking tape and the entire room was then covered with three coats of a water-based acrylic resin paint. The chamber was supported inside the upper part of an ancient barn, the lower part of which housed the ventilation blower, and analytical and other equipment.

The chamber was stirred by a meter diameter axial flow fan mounted 30 cm above the center of the flood of the chamber. The mixing time was measured by releasing hydrogen and observing the time to reach a steady constant level with a continuous hydrogen analyzer. It was 20 s for 95% mixing. The chamber was ventilated by blowing in air drawn from a point outside and upwind. For this, an industrial vacuum cleaner was used which gave a flow of 100 m^3 h^{-1} and hence a ventilation rate of 2 h^{-1}. The ventilation rate was kept constant by controlling the motor speed electronically. No attempt was made to measure the air flow of the ventilating blower. The rate of chamber ventilation was instead taken from the observed decay rate of the reference gas hydrogen and sometimes from the decay rate of other gases such as N_2O, CF_2Cl_2, and CF_2ClBr.

The air inside the chamber was passed out for analysis or storage by two stainless steel bellow pumps (MB-158, Metal Bellows Corp.). One of these passed air from the chamber to the analytical laboratory along 100 m of 3 mm diameter aluminum tubing; the other was used to fill stainless steel sample vessels of 1 l capacity to a pressure of 2 atm. When filling these vessels they were flushed for 5 min with air from the chamber before the valves on the vessel were closed at the time chosen to store the air sample. The air received in the laboratory from the chamber flowed at 1 l min^{-1} and all but 0.03 l min^{-1} were passed to waste. The small remainder flowed continuously through a sample loop usually 0.5 ml in volume and mounted in the oven of the gas chromatograph. The pressurized vessels were analyzed by using the same sample loop and analytical system.

The temperature and atmospheric pressure were recorded during each experiment. The chamber is sited about 1 km from the nearest other inhabitation (a small farm house) and is about 20 km from the Atlantic Ocean on the northwest coast of the southwest peninsula of England. Dilution experiments are made only on days when the air mass over the region is oceanic and when the wind is blowing from a westerly quarter. As a further check for clean air the presence of trichloroethylene and tetrachloroethylene in the air are taken as indicators of pollution.

The gas chromatograph was a Hewlett Packard 5830A, and, wherever possible, the same columns and conditions of analy-

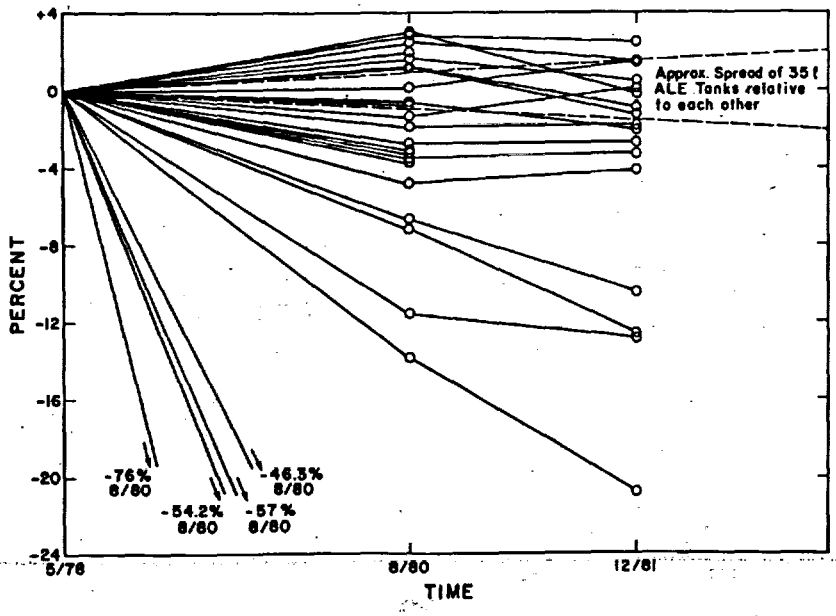

Fig. 3. Percent change in 1.6 l CCl_4 values versus ALE (35 l) CCl_4 values.

sis as those used in the ALE stations were used. For nitrous oxide and the lighter fluorocarbons, a column of glass 150 cm long and 5 mm internal diameter filled with Porasil B was used, usually at 50°C and with a flow rate of the carrier gas of 30 ml min^{-1}. For the other halocarbons, a 300-cm column also of 5 mm diameter glass filled with 12% OV101 on Chromosorb W (100–120 mesh) was used. The temperature of this column was also 50°C, but the flow rate was usually 40 ml min^{-1}. The detector was a Hewlett Packard electron capture detector with a radioactive source. This detector differed from the commercial version in that the ceramic insulator had been replaced with a PTFE version. This was found necessary since the original insulator had a resistance of approximately 1000 megohms above 300°C (a potential source of inaccuracy).

The detector was operated in both the constant current variable frequency mode (CC), where the frequency is the signal, and in the constant pulse fixed frequency mode (FF), where the detector ion current provides the signal. In either mode the operating conditions of the detector (i.e., temperature, flow rate, etc.) were identical. The carrier gases used were either 90% argon 10% methane mixtures or nitrogen. With both gases, traces of oxygen and other electron-attaching contaminants were removed by doping the gas with about 0.1% of hydrogen and then passing it through a reactor filled with palladium catalyst at 300°. When operated in the constant pulse frequency mode, the detector for $CFCl_3$ and CCl_4 can also function as an internal standard and provide an independent absolute analysis. The theory and practice of this independent "coulometric" method are described later in this paper.

In most of the experiments the text mixture was prepared by a vacuum volumetric procedure. Pure samples of halocarbons were degassed by freezing and thawing on a vacuum line and then used to fill an accurately known volume (5.023 ml) with vapor at a known pressure in the range 10–40 torr. The pressure was measured by a calibrated glass bourdon gauge and by a silicone fluid manometer. The volumetric sample was then frozen into an evacuated ampoule held at −180°C in liquid nitrogen. The ampoule was sealed by a gas flame while the sample was still frozen in the liquid nitrogen.

In a few experiments the less volatile halocarbons were prepared gravimetrically by adding them from a 10 microliter syringe to a weighed volume of heptane in a small flask. The quantity added was found by reweighing. The reference gas hydrogen was introduced from a 0.02 m^3 pressure vessel in which it was held at 3 atm pressure. Both the hydrogen and the test vapors were released into the chamber at the point of input of the ventilation blower so as to ensure a rapid mixing with the chamber air. The glass ampoule was broken either manually or by an electrically driven vice. In a typical experiment, air samples from the chamber, with the fan and pumps running, were taken and analyzed at 15 min intervals for 2 hours. The samples were then introduced and analysis continued for 5 more hours. At chosen times after the start of the experiment, pressure vessels were filled with air from the chamber and set aside for later analysis. The analysis of the air passed to the gas chromatograph proceeded automatically under the control of its own microprocessor.

Figure 4 shows typical exponential dilution experiments for $CFCl_3$ and CCl_4. In general, the chlorofluorocarbons and hydrogen show a remarkable agreement, excellent linearity, and a very high precision of measurement. Hydrogen was measured using a thermal conductivity detector with air as the carrier gas. The concentration covered was from between 0.1 and 1.1 down to 100 ppm. No independent check of linearity of the response of the detector over this range was made. Less satisfactory results were obtained for methyl chloroform and CCl_4, where strong evidence of adsorption, probably on the glass ampoule, is shown by the anomalously low values of the first observations evident in Figure 4 (bottom). The following sources of errors have been uncovered: (1) a sample loop which adsorbed some of the test compounds; (2) fluctuations in the rate of flow of ventilating air; (3) adsorption of sample on the surfaces of the glass ampoule in which the sample was introduced to the chamber; (4) inaccuracies in the automatic integration of peak areas by the chromatograph; and (5) slow changes in detector sensitivity usually attributable to the emergence of contaminants from the column.

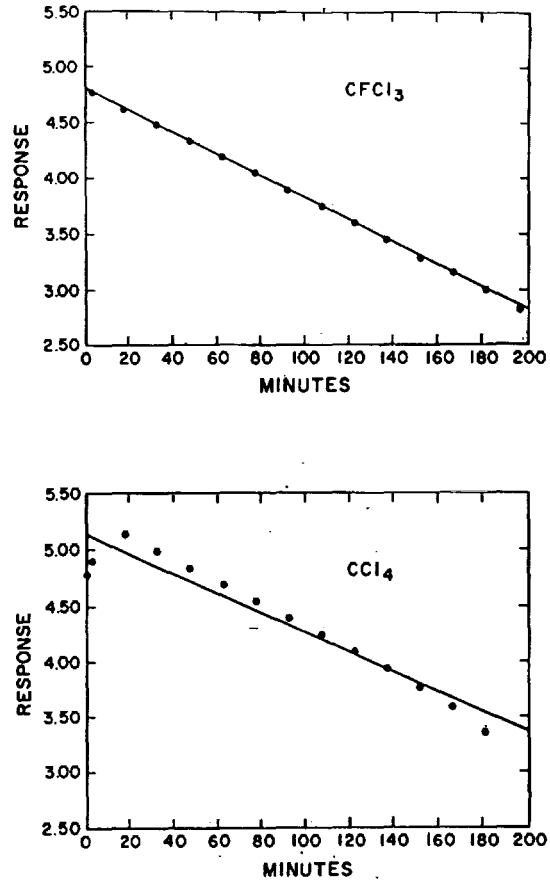

Fig. 4. Least square line of exponential dilution results for $CFCl_3$ and CCl_4.

Each of these has been treated individually, and there has been a marked improvement in the quality of the measurements. The most intractable problems are those due to the adsorption of the test substances on surfaces, particularly that of the ampoule used to dispense the sample mixture. For the less volatile compounds, methyl chloroform and carbon tetrachloride, this problem has not yet been overcome.

The standard samples produced in the exponential dilution chamber have been used to calibrate ALE standards 043 and 044 at levels that cover the ambient range. By using a 5 ml sample loop (as at the ALE stations) it was found that dilution in the chamber could not be followed accurately much below 1.5 times the ambient concentration of the test substance. To allow for calibration in the range of concentrations around

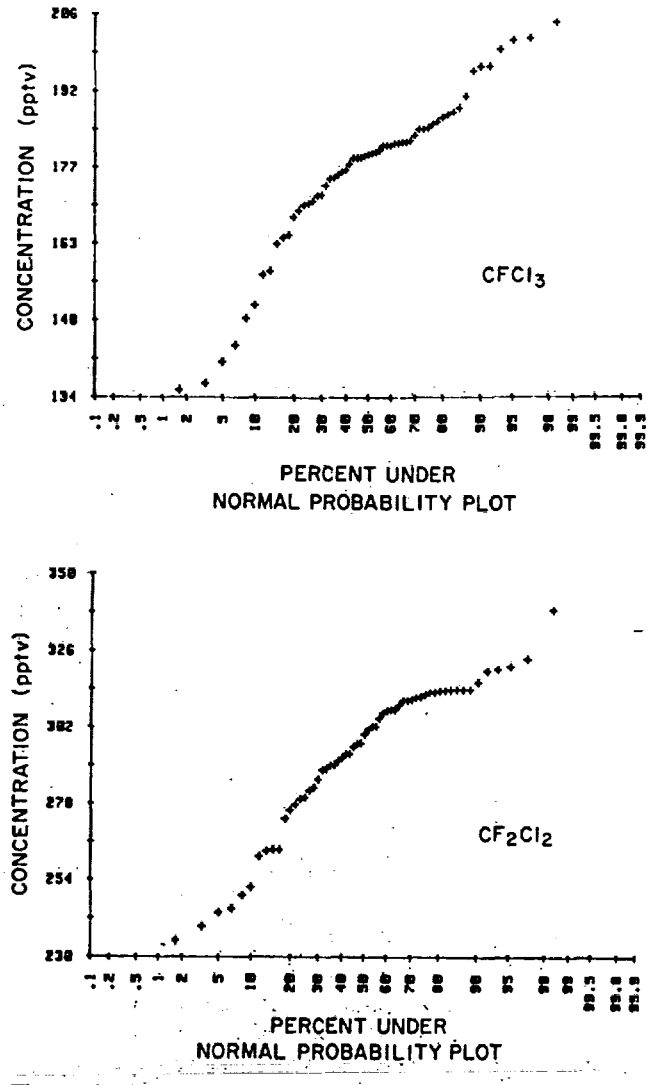

Fig. 5. Statistical distribution of exponential dilution results for $CFCl_3$ and CF_2Cl_2.

and below ambient levels, the expedient of using a smaller sample loop was used. A loop size of 0.7 ml was chosen so that at a total concentration of about 7 times ambient the same chromatographic peak area was obtained as with ambient air in a 5 ml loop. The accuracy of the 0.7 ml/5 ml sample loop volume ratio was verified experimentally as follows. The sample loops used in calibration by exponential dilution were always calibrated by filling with water and weighing. A trace of surfactant was added to the water to avoid the trapping of small bubbles. The uncertainty about their volumes and the ratio of them is likely to be one of the lesser sources of error. Figure 5 shows the statistical distribution of the results from the 59 independent exponential dilution-calibration experiments conducted to date for $CFCl_3$ and CF_2Cl_2. In this figure a normal or gaussian distribution of data would be represented by a straight line with its intercept on the 50% line being the mean value. In the real data, a slightly skewed gaussian distribution is evident for both $CFCl_3$ and CF_2Cl_2; the distributions are narrower on the high mixing ratio side than on the low mixing ratio side. The reasons for this slight skewness are not yet evident.

Table 3 summarizes the means and standard deviations in the various series of experiments carried out over the past 2 years which collectively comprise the total of 59 experiments conducted to date. We note that the mean values for $CFCl_3$ (177 pptv) and CF_2Cl_2 (294 pptv) are only 1 and 3% lower than the working values for ALE standards 043 and 044, respectively.

The problems with the performance of methyl chloroform and CCl_4 in the dilution chamber noted earlier are at present sufficiently severe to prevent a precise determination of their concentrations in the ALE standards.

Coulometry

A few molecular species, particularly halocarbons, are ionized irreversibly by their reaction with free electrons in the electron capture detector. Moreover, experiments indicate that for each molecule ionized one electron is lost. This intensely ionizing reaction can therefore serve as the basis of a gas-phase coulometer in which absolute measurements of trace quantities of halocarbons is possible.

The general principles and details of suitable coulometric detectors have been described by *Lovelock et al.* [1971], *Lovelock* [1974*b*], and *Lovelock* [1978]. Briefly, it is possible to calculate for known analytical conditions the fraction f of a compound which is ionized. Hence, with the detector in the constant pulse frequency mode, the chromatographic peak area in coulombs is obtained, and after dividing by f an estimate of the number of molecules present can be found by applying Faraday's Law. The quantities which need to be known for this calculation are the total rate of injection of electrons by ionization, the recombination rate of electrons and positive ions, the gas flow rate, the rate constant for the reaction between the compound and free electrons, and the loss rate of electrons by diffusion to the walls and electrodes. All of these are either known or can be determined experimentally.

Coulometry was used to determine the absolute concentrations of $CFCl_3$ and CCl_4 in the first reported measurements of their atmospheric abundance [*Lovelock et al.*, 1973]. The choice of this novel calibration procedure was dictated by the then extreme difficulty of accurately preparing standards at the parts per trillion level, particularly in view of the high background of halocarbons in a laboratory environment. Since that time the method has not been extensively utilized, and its accuracy has been occasionally questioned [e.g., *National Academy of Sciences*, 1975]. However, the experiments of *Lovelock et al.* [1971] and *Lovelock* [1978] have recently been independently confirmed under more rigorous experimental conditions by *Grimsrud and Kim* [1979] and *Gobby et al.* [1980]. Based on this, we must regard coulometry as a legitimate alternative method for determining absolute concentrations, at least for the strongly electron-absorbing species $CFCl_3$ and CCl_4.

The results of 33 analyses of $CFCl_3$ and 16 of CCl_4 in ALE standards 043 or 044 by coulometry are shown in Table 4. The absolute concentration (166 pptv) estimated for $CFCl_3$ in the ALE tanks is 6% less than obtained from the exponential dilution experiment using the ECD in the constant current mode. These results lie well within the standard deviations of the estimates made by the totally independent exponential dilution technique (Table 3). In Table 4 a value is also given for CF_2Cl_2 even though this compound cannot be accurately estimated by coulometry. The value determined (282 pptv) is based on the assumption that the same ratio of $CFCl_3/CF_2Cl_2$ is measured by the ECD in the coulometry mode as in

TABLE 3. Calibration of ALE Standards 043 and 044 by Exponential Dilution

	$CFCl_3$, pptv		CF_2Cl_2, pptv		Number of Experiments
	Mean	Standard Deviation*	Mean	Standard Deviation*	
Experiment					
March–July 1979	173.8	±22.5	275.2	±28.0	21
July–Sept. 1979	182	± 5.4	314	± 4.2	15
Nov. 1979 to Feb. 1980	172.2	± 7.7	294	±12.3	12
April–Oct. 1980	179.9	± 3.6	307.6	± 7.9	11
Total†	177	±15(±2)‡	294	±24(±3)‡	59
Working values†					
043	178	±5%§	302	±10%§	
044	179	±5%	305	±10%	

*The probable error of a single dilution experiment involving 15–20 analyses is usually 0.5%. The standard deviations given are for the quoted number of independent dilution experiments carried out over the time periods indicated.
†Values quoted to nearest pptv.
‡Error in the mean (divide standard deviation by $\sqrt{59}$)
§Absolute accuracy of working values estimated in 1978.

the constant current mode. Both modes provide the very accurate ratioed measurement of $CFCl_3/CF_2Cl_2$ as long as the operating conditions of the detector are the same. Accordingly, $CFCl_3$ is in effect an internal standard between the two modes, and the concentration of CF_2Cl_2 is locked in by its ratio to $CFCl_3$. Therefore, the estimate of CF_2Cl_2 by coulometry, albeit indirect, is a valid independent method for calculating the absolute concentration of CF_2Cl_2 in the ALE standards. As far as CCl_4 measured in the ALE standards 043 and 044 is concerned, coulometry has indicated values in the range of 107–137 pptv with a mean value of 122 ± 7 pptv in the two ALE standards.

Calibration Factor

The absolute calibration of the ALE working data set is based on comparisons with the ALE primary standards whose absolute concentrations were determined by static dilution techniques as discussed. For consistency in the ALE program, the values assigned to these working standards are not altered as a result of the independent checks of absolute calibration and calibration propagation using the exponential dilution and coulometry experiments. Rather, at any particular time the appropriate factor ξ, by which all the ALE mixing ratios for a given species should be multiplied, will be based on the best information available at that time on absolute calibration. At the moment our best estimate for this factor for $CFCl_3$ and CF_2Cl_2 is obtained by averaging with equal weight the results of the two independent calibration studies described. The factors (with estimated 2σ error) are

$CFCl_3$

$$\xi \simeq \frac{177(\pm 4) + 166(\pm 2)}{2 \times 178.65}$$

$$= 0.96 \pm 0.02$$

CF_2Cl_2

$$\xi \simeq \frac{294(\pm 6) + 282(\pm 4)}{2 \times 303.5}$$

$$= 0.95 \pm 0.02$$

The absolute calibration factor ξ for CH_3CCl_3 is poorly known. Based on independent exponential dilution and coulometry analyses we deduce $\xi \simeq 1 \pm 0.15$ (1σ). Further work is clearly needed before a more precise statement can be made.

Absolute calibration for CCl_4 is, at present, relatively

TABLE 4. Calibration of ALE Standards 043 and 044 by Coulometry

	$CFCl_3$, pptv		CF_2Cl_2, pptv*		CCl_4, pptv		Number of Experiments
	Mean	Standard Deviation	Mean	Standard Deviation	Mean	Standard Deviation	
Experiment							
Feb. 1979	166.3	±4.1	282.7	±7.0	117.8	±8.1	6
June 1979	169.0	±2.3	287.3	±3.9			6
Aug. 1979	167.3	±2.2	284.4	±3.7	125.4	±5.5	10
Oct. 1980	164.4	±4.9	279.5	±8.3			11
Total†	166	±5(±1)‡	282	±8(±2)‡	122	±7(±2)‡	33
Working values†							
043	178	±5%§	302	±10%§	150	±20%§	
044	179	±5%	305	±10%§	149	±20%	

*Derived assuming that the ratio of CF_2Cl_2 to $CFCl_3$ is as determined by the exponential dilution technique.
†Values quoted to nearest pptv.
‡Error in the mean (divide standard deviation by $\sqrt{33}$ and/or $\sqrt{16}$).
§Absolute accuracy of working values estimated in 1978.

poorly defined. The calibration factor ξ based solely on the coulometry studies if $\xi \simeq 0.81 \pm 0.03$ (2σ). The absolute calibration factor ξ for N_2O is still being determined and will be reported separately.

CONCLUSIONS

Maintaining high precision in the relative calibrations of $CFCl_3$, CF_2Cl_2, CH_3CCl_3, and CCl_4 during the source of the ALE program has been very successful. Overall, the concentrations of the trace gases in the ALE cal tanks have been exceptionally stable. Periodic audits made over 4 years of the assigned concentrations against primary standards have shown no drift for any of the five species. This is quite remarkable for CCl_4 since this species has a reputation for disappearing in stainless steel vessels over time. However, an experiment using similar type samples, containers, and conditions but of very different volume to surface ratios demonstrated that even the trace levels of CCl_4 at the ~140 pptv level did not change in 4 years. The exquisite stability of all of the species in the ALE calibration standards used during the course of the experiment is very important for calculating their lifetimes. Actually, a series of internally consistent and very accurately determined relative calibrations standards was a higher requisite of the study than absolute accuracy.

Two studies, exponential dilution and coulometry, successfully determined independently the absolute calibration values of $CFCl_3$, CF_2Cl_2, and CCl_4 assigned to the ALE primary standards. The results of the exponential dilution experiment gave mean values for $CFCl_3$ and CF_2Cl_2 only 1 and 3% lower, respectively, than the values assigned to the ALE standards. Correspondingly, the coulometric method suggested that $CFCl_3$ values in the ALE standards were 6% lower than those obtained with the exponential dilution method. However, the coulometric value for CCl_4 was ~20% lower than that assigned to the ALE tanks. Accordingly, appropriate factors, ξ, by which all of the ALE mixing ratios for a given species should be multiplied to obtain the best estimate of absolute value were determined during the course of the study. These adjustments are submitted only for the purpose of providing a reliable estimate at this time and should not be construed to be the permanent values. As regards absolute calibration, more work is needed before all of the uncertainties in the $CFCl_3$, CF_2Cl_2, CH_3CCl_3, and CCl_4 absolute concentrations are minimized.

Acknowledgments. We thank the many colleagues who encouraged us and contributed to this work. We thank J. Wiederholt, R. Dalluge, and R. Gunawardena of the Oregon Graduate Center for their care in performing the measurements and maintaining the ancillary instrumentation necessary for the internal consistency in the high precision analyses. We also thank all of our ALE team members: Fred Alyea, Steve Crawford, Derek Cunnold, Paul Fraser, Donald Prinn, Rick Rosen, and Peter Simmonds for their contributions, as well as Bruce Lane and Aslam Khalil for their advice and guidance. The research was supported by the Chemical Manufacturers Association. Nominal support has also been provided by the Atmospheric Chemistry Program of NSF and the Upper Atmospheric Research Program of NASA to R. A. Rasmussen.

REFERENCES

ALE Principle Investigators, The Atmospheric Lifetime Experiment, vol. I, The First Two Years, Special Report, Chem. Manufacturers Assoc., February 1981.

Foulger, B., and P. Simmonds, Drier for field use in the determination of trace atmospheric gases, *Anal. Chem., 51*, 1089–1090, 1979.

Gobby, P., E. Grimsrud, and S. Warden, Improved model of the pulsed electron capture detector, *Anal. Chem., 52*, 473–482, 1980.

Grimsrud, E. P., and S. H. Kim, Stoichiometry of the reaction of electrons with bromotrichloromethane in an electron capture detector, *Anal. Chem., 51*, 537–541, 1979.

Grimsrud, E. P., and R. A. Rasmussen, Analysis of chlorofluorocarbons in the troposphere by gas chromatography-mass spectrometry, *Atmos. Environ., 9*, 1010–1013, 1975*a*.

Grimsrud, E. P., and R. Rasmussen, Survey and analysis of halocarbons in the atmosphere by GC-MS, *Atmos. Environ., 9*, 1014–1017, 1975*b*.

Hester, N., E. Stephens, and O. Taylor, Fluorocarbons in the Los Angeles basin, *J. Air Pollut. Control Assoc., 24*, 591–595, 1974.

Lovelock, J., Atmospheric halocarbons and stratospheric ozone, *Nature, 252*, 292–294, 1974*a*.

Lovelock, J., Electron capture detector, Theory and practice, *J. Chromatogr., 99*, 3–12, 1974*b*.

Lovelock, J., Electron capture detector, Theory and practice, II, *J. Chromatogr., 158*, 123–138, 1978.

Lovelock, J., R. Maggs, and E. Adlard, Gas phase coulometry by thermal electron attachment, *Anal. Chem., 43*, 1962–1965, 1971.

Lovelock, J., R. Maggs, and R. Wade, Halogenated hydrocarbons in and over the Atlantic, *Nature, 241*, 194–196, 1973.

National Academy of Sciences, *Halocarbons: Effects on Stratospheric Ozone*, Washington, D. C., 1976.

Rasmussen, R., Interlaboratory comparison of fluorocarbon measurement, *Atmos. Environ., 12*, 2505–2508, 1978.

Rasmussen, R., M. A. K. Khalil, Interlaboratory comparison of flurocarbons 11, 12, methylchloroform and nitrous oxide measurements, *Atoms. Environ., 15*, 1559–1568, 1981.

Rasmussen, R., and D. Pierotti, Interlaboratory calibration of atmospheric nitrous oxide measurements, *Geophys. Res. Lett., 5*, 353–355, 1978.

Rasmussen, R., J. Krasnec, and D. Pierotti, N_2O analysis in the atmosphere via electron capture-gas chromatography, *Geophys. Res. Lett., 3*, 615–618, 1976.

Rasmussen, R., D. Harsch, P. Sweany, J. Krasnec, and D. Cronn, Determination of atmospheric halocarbons by a temperature-programmed gas chromatographic freezeout concentration method, *J. Air Pollut. Control Assoc., 27*, 579–581, 1977.

Rasmussen, R., M. A. K. Khalil, and R. W. Dalluge, Atmospheric trace gases in Antarctica, *Science, 211*, 285–287, 1981.

J. E. Lovelock, Department of Engineering and Cybernetics, University of Reading, Reading, United Kingdom.

R. A. Rasmussen, Department of Environmental Science, Oregon Graduate Center, 19600 N.W. Walker Road, Beaverton, OR 97006.

(Received July 16, 1982;
revised June 9, 1983;
accepted June 13, 1983.)

JOURNAL OF GEOPHYSICAL RESEARCH, VOL. 88, NO. C13, PAGES 8379–8400, OCTOBER 20, 1983

The Atmospheric Lifetime Experiment 3. Lifetime Methodology and Application to Three Years of $CFCl_3$ Data

D. M. CUNNOLD,[1,2] R. G. PRINN,[2,3] R. A. RASMUSSEN,[4] P. G. SIMMONDS,[5] F. N. ALYEA,[1,2] C. A. CARDELINO,[1,2] A. J. CRAWFORD,[4] P. J. FRASER,[6] AND R. D. ROSEN[7,8]

Observations of the chlorofluorocarbon $CFCl_3$ obtained several times daily over the period July 1978 to June 1981 at Adrigole, Ireland (52°N, 10°W); Ragged Point, Barbados (13°N, 59°W); Point Matatula, American Samoa (14°S, 171°W); and Cape Grim, Tasmania (41°S, 145°E) are reported. In addition, observations at Cape Meares, Oregon (45°N, 124°W) are given for the period January 1980 to June 1981. On January 1, 1980, the average mixing ratio of $CFCl_3$ in the lower troposphere is estimated to have been 168 pptv, and this is calculated to have been increasing 5.7% annually. An optimal estimation procedure for deriving the atmospheric lifetime of $CFCl_3$ by using a nine-box two-dimensional model of the atmosphere is described. In this procedure, model parameters are estimated based upon minimizing the differences between the temporal trends observed and those calculated in the two-dimensional model. Assuming that the only destruction of $CFCl_3$ occurs in the stratosphere, the lifetime, on January 1, 1980, estimated by the trend technique is 83^{+73}_{-27} years; the lifetime estimated from the global inventory of $CFCl_3$ is 70^{+89}_{-25} years. The maximum likelihood current lifetime estimate obtained by combining the estimates from both analysis techniques is 78 years.

1. INTRODUCTION

The compound trichlorofluoromethane ($CFCl_3$) is a remarkably inert atmospheric constituent that appears to have an exclusively anthropogenic origin. It is important both as a source of chlorine atoms in the stratosphere which can catalytically destroy ozone [*Molina and Rowland*, 1974*a*, *b*; *Stolarski and Cicerone*, 1974] and as an absorber of infrared radiation which contributes to the energy balance of the earth [*Ramanathan*, 1975].

The possible impact of $CFCl_3$ (and other related halocarbons) on the ozone layer has resulted in an extensive research program involving atmospheric and laboratory measurements together with a variety of models designed to study the complex chemical, dynamical, and radiative interactions which are involved in the maintenance of the ozone layer [see *NASA*, 1979; *World Meteorological Organization*, 1981 for extensive reviews].

Current models predict that if $CFCl_3$ (and CF_2Cl_2) were to continue to be released into the atmosphere at the rates prevalent in 1977, the steady state reduction of stratospheric ozone that will be reached about 200 years in the future would be 5–9% [*National Academy of Sciences*, 1982]. These predictions assume that the sole important sink for both $CFCl_3$ and CF_2Cl_2 is stratospheric photodissociation and that current models are correctly calculating the photodissociation rate. Owing to the correlations that exist between ultraviolet fluxes and $CFCl_3$ or CF_2Cl_2 concentrations in the stratosphere a two- or three-dimensional model is required to predict accurately the global photodissociation rates and thus the atmospheric lifetimes of these species. Using a two-dimensional model, *Ko and Sze* [1982] and *Owens et al.* [1982] predict a lifetime for $CFCl_3$ at steady state of 65 years and 60 years, respectively, while *Golombeck* [1982], using a three-dimensional model, predicts a present-day lifetime for $CFCl_3$ of 78 years. These lifetimes differ because the present ratio of tropospheric to stratospheric $CFCl_3$ concentrations is greater than that at steady state due to the 3–4 year transport time between the surface and the middle stratosphere. Both models assume O_2 and O_3 ultraviolet cross sections that are apparently too large to explain recent in situ measurements of stratospheric ultraviolet fluxes [*Frederick and Mentall*, 1982]. Thus, these predicted lifetimes may be significantly larger than the true lifetimes for $CFCl_3$ photodissociation.

Measurements of $CFCl_3$ available prior to 1978 were not sufficiently accurate to enable an experimental determination of the present day $CFCl_3$ lifetimes other than to rule out lifetimes less than ~15 years [*Sze and Wu*, 1976; *Jesson et al.*, 1977; *Cunnold et al.*, 1978]. The determination of the true lifetime of $CFCl_3$ is of paramount importance in assessing the potential impact of $CFCl_3$ on the ozone layer. For example, if the present lifetime of $CFCl_3$ were 39 years instead of 78 years as quoted above, the predicted steady state reduction of ozone by $CFCl_3$ would be only about 50% of that predicted in current models.

Based on a theoretical study by *Cunnold et al.* [1978], the Atmospheric Lifetime Experiment (ALE) was initiated in 1978 and was designed to measure accurately the rates of increase of $CFCl_3$, CF_2Cl_2, CH_3CCl_3, CCl_4, and N_2O and to use this data to estimate lifetimes for the four halocarbons. An overview of the experiment is provided in *Prinn et al.* [this issue (*a*)]. The ALE utilizes automated dual-column electron-capture gas chromatographs that sample the background air about four times daily at the following five globally distributed sites: Adrigole, Ireland (52°N, 10°W); Cape Meares, Oregon (45°N, 124°W); Ragged Point, Barbados (13°N, 59°W); Point Matatula, American Samoa (14°S, 171°W); and Cape Grim, Tasmania (41°S, 145°E). Details of the instrumentation are also provided in *Prinn et al.* [this issue (*a*)], and the

[1] School of Geophysical Sciences, Georgia Institute of Technology.
[2] CAP, Inc.
[3] Department of Meteorology and Physical Oceanography, Massachusetts Institute of Technology.
[4] Department of Environmental Science, Oregon Graduate Center.
[5] Department of Geochemistry, University of Bristol.
[6] Division of Atmospheric Physics, CSIRO.
[7] Environmental Research and Technology, Inc., Concord, Massachusetts.
[8] Now at Atmospheric and Environmental Research, Inc.

Paper number 3C0669.
0148-0227/83/003C-0669$05.00

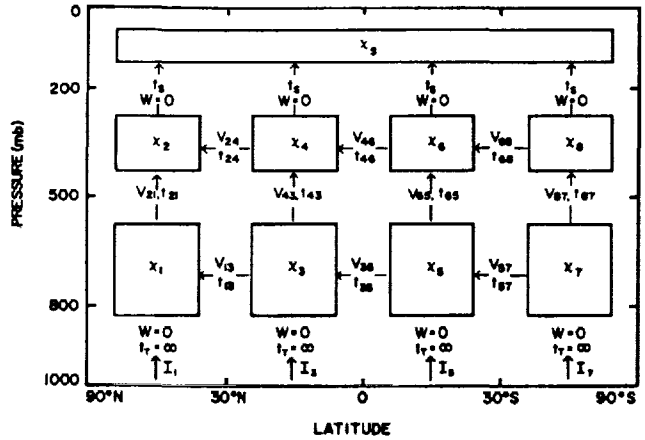

Fig. 1. Schematic of the nine-box two-dimensional model of the atmosphere. Values of the diffusion coefficients t_{ij} and inverse advection times V_{ij} are given in Table 1. Atmospheric release of halocarbons is assumed to occur directly into boxes 1, 3, 5, and 7.

methods for on-site calibration of the data are given in *Rasmussen and Lovelock* [this issue].

In this paper we first present the details of an optimal estimation technique which is used in this and in subsequent papers [*Cunnold et al.*, this issue; *Prinn et al.*, this issue (*b*); Simmonds *et al.*, this issue; R. A. Rasmussen et al., unpublished manuscript, 1983] to analyze the ALE data for the five species measured in the program. We then present the global data set obtained specifically for $CFCl_3$ during ALE and discuss the estimates of $CFCl_3$ from industrial sources during and prior to the ALE measurements. On the basis of these measurements and emission estimates we then analyze the $CFCl_3$ trends and total atmospheric content to determine its atmospheric lifetime. The analysis includes a careful assessment of all possible sources of error so that the accuracy of our final lifetime estimates can be quantified.

2. Data Analysis Technique

The lifetime of each ALE species determined from the ALE data is based on the equation [*Cunnold et al.*, 1978]:

$$\frac{1}{\chi_G}\frac{d\chi_G}{dt} = \frac{I}{\int_0^t I(t')e^{(t'-t)/\tau}\,dt'} - \frac{1}{\tau} \tag{1}$$

where χ_G is the globally averaged mixing ratio of the ALE species, $I(t)$ is the historical information on the worldwide release of the species (for $CFCl_3$ see *Chemical Manufacturers Association* (CMA) [1982] and τ is its atmospheric lifetime. The lifetime determination is thus based on temporal trends observed in the ALE data. This approach minimizes the effects of uncertainties in absolute calibration and release [*Cunnold et al.*, 1978]. However, the trend for ln χ_G (where ln denotes the natural log) is not constant in time, and it is thus inappropriate to determine merely the trend in ALE data by using a linear regression analysis. A more sophisticated approach is needed to provide the best estimate of atmospheric lifetime from the ALE observations.

The lifetime analysis uses optimal estimation theory [e.g., *Gelb*, 1974]. A simplified picture of how this mathematical procedure is applied to the ALE data is obtained by assuming that the ALE measures χ_G (which of course it does not). Equation (1) then represents our numerical model in which the unknown parameter τ is to be estimated from the data. By using (1) and an a priori estimate of the lifetime (τ_0), the trend $D(= d[\ln \chi_G]/dt)$ is first calculated for each month of the ALE observations based upon the global release data for the appropriate ALE species. By changing the lifetime slightly (i.e., $\Delta\tau/\tau \ll 1$), the derivative $\Delta\tau/\Delta D$ is also calculated. Then the estimate of the lifetime provided by the ALE data would be

$$\hat{\tau} = \tau_0 + \frac{1}{N}\sum_{i=1}^{N}\left(\frac{\Delta\tau}{\Delta D}\right)(\hat{D} - D) \tag{2}$$

where $\hat{D}$ is the monthly trend derived from the ALE data and N is the number of months of observation.

The optimal estimation approach possesses several convenient mathematical features that makes it particularly useful for supplying the best estimate of the lifetime. It can be applied recursively so that each month of data can be analyzed sequentially as it is received; the lifetime estimate at the end of any month of data reflects all the data analyzed prior to that time. Because the contribution to the estimate from an individual month of data is weighted by σ_m^{-2}, where σ_m is the

TABLE 1. Transport Parameters Used in the Two-Dimensional Model

Pressure, mbar	Latitudes	Parameters	Winter, Dec.–Feb.	Spring, March–May	Summer, June–Aug.	Fall, Sept.–Nov.
750	30°N	t_{13} (days)	116	116	261	139
	0	t_{35}	495	712	363	712
	30°S	t_{57}	167	167	116	116
350	30°N	t_{24}	29	35	85	52
	0	t_{46}	124	178	124	178
	30°S	t_{68}	52	42	29	42
500	all latitudes	$t_{21} = t_{43} = t_{65} = t_{87}$	38	38	38	38
200	all latitudes	t_s	1440	1440	1440	1440
750	30°N	V_{13}^{-1} (days)	−1506	581	1882	−442
	0	V_{35}^{-1}	−69	−376	50	126
	30°S	V_{57}^{-1}	1506	1075	753	1506
350	30°N	V_{24}^{-1}	1506	−581	−1882	442
	0	V_{46}^{-1}	69	376	−50	−126
	30°S	V_{68}^{-1}	−1506	−1075	−753	−1506
500	48.6°N	V_{21}^{-1}	−1506	581	1882	−442
	14.5°N	V_{43}^{-1}	−72	−228	52	98
	14.5°S	V_{65}^{-1}	65	279	−54	−137
	48.6°S	V_{87}^{-1}	−1506	−1075	−753	−1506

TABLE 2. Sensitivity of $CFCl_3$ Partial Derivatives, $\partial \ln \chi_c/\partial(1/\tau)$ and $d/dt\,[\partial \ln \chi_c/\partial(1/\tau)]$, to Two-Dimensional Model Parameter Variations for January 1, 1980

τ_1, years	τ_2, years	τ_3, years	τ_4, years	F	$\frac{\partial \ln \chi_c}{\partial(1/\tau)}$, years Box 1	Box 3	Box 5	Box 7	$\frac{d}{dt}\left[\frac{\partial \ln \chi_c}{\partial(1/\tau)}\right]$ Box 1	Box 3	Box 5	Box 7	Parameter Varied in Calculating Derivatives	Release Data Used
60	8	10^4	3	2	−4.56	−4.70	−5.01	−5.04	−0.42	−0.40	−0.40	−0.39	τ_3	*CMA* [1981*a*] injected into box 1
81	12	10^4	3	1.8	−4.26	−4.44	−4.76	−4.79	−0.41	−0.41	−0.41	−0.41	τ_3	*CMA* [1982] injected into box 1
67	8	10^4	4	1.4	−4.04	−4.28	−4.54	−4.58	−0.36	−0.41	−0.36	−0.36	τ_3	*CMA* [1982] latitudinally distributed
61	10	240	4	1.4	−7.26	−7.47	−8.00	−8.06	−0.44	−0.46	−0.39	−0.39	τ_1	*CMA* [1982] latitudinally distributed

standard error of the measurement of the monthly mean, missing data are straighforwardly accounted for. Optimal estimation theory also provides an estimate of the uncertainty in the lifetime based on the addition of these standard errors.

The calculation of lifetimes from the ALE data is complicated by the fact that the ALE does not measure χ_G but, instead, provides a time series of species measurements at each of five surface sites. Equation (1) is therefore replaced by a limited resolution two-dimensional model of the atmosphere. Optimal estimation theory may then be applied to the time series at each site to provide five estimates of the lifetime or may be applied to all sites simultaneously to provide a single best estimate. It may be noted that using a two-dimensional model introduces "unknowns" (e.g., transport rates) in addition to the lifetime into the analysis. Fortunately, not only is the lifetime estimate fairly insensitive to uncertainties in transport rates but the analysis may be modified to include an estimate of these transport rates. However, it is important to reduce the resolution of the model as much as possible so that the number of unknowns is minimized without compromising the ability of the model to provide a good simulation of the ALE data.

2.1 *The Two-Dimensional Model*

All the ALE species possess measurable latitudinal gradients. Since the locations of the ALE sites had been chosen to be representative of the four equal mass subdivisions in the atmosphere [see *Prinn et al.*, this issue (*a*)], the minimum number of latitudinal subdivisions in the two-dimensional model is four. To resolve adequately the gross characteristics of the zonally averaged circulation in the troposphere (in particular the tropical Hadley cell), we divide the troposphere into two layers in the vertical. The stratospheric circulation is unimportant relative to the tropospheric circulation in the global dispersion of ALE species (and thus for simulating the ALE data) since the species all have surface sources. Therefore, the stratosphere (which is important as a known photochemical sink for all the ALE species) is represented by a single box. The "ad hoc" two-dimensional model thus contains eight tropospheric boxes and one stratospheric box.

Transport in the model is parameterized by using zonally averaged velocities and eddy diffusion coefficients. To minimize the number of uncertain parameters in this model, parameterized eddy transfer by diffusion coefficients of the K_{yz} form (y = latitude, z = altitude) is neglected in the computations. Such a transfer must be accounted for in this model by the K_{zz} and K_{yy} terms; therefore, caution is necessary before applying the model to species other than those that are injected into the boundary layer at mid-latitudes at a very slow rate (i.e., which produce an increase in the global content $\simeq$5–10%/year). Using estimates of velocities and diffusion coefficients derived from *Newell et al.* [1969], we find that the latitudinal gradients observed in the ALE may be approximately simulated merely by scaling each of the horizontal diffusion coefficients by a single factor F of order unity. Thus, we assume that F is the only unknown aspect of the transport rates that needs to be determined in the optimal estimation procedure.

Model boundaries are chosen specifically at the equator, 30° latitude, and the poles, and at the ground, 500, 200, and at 0 mbar (for a schematic representation including the numbering

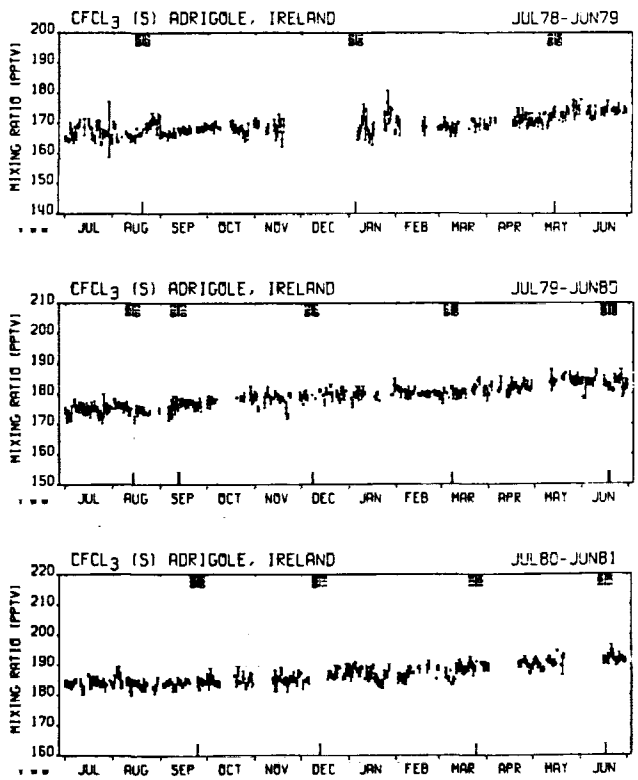

Fig. 2. $CFCl_3$ daily means (pptv) and standard deviations at Adrigole, Ireland (52°N, 10°W) on the silicone channel for the period July 1978 to June 1981. Changes of the calibration gas tank are noted on the upper abscissae.

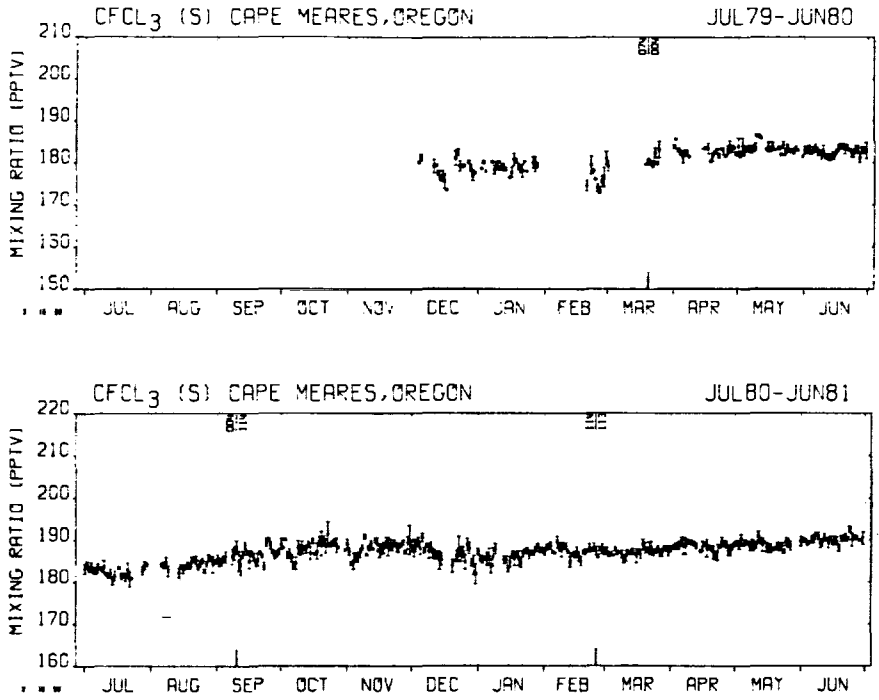

Fig. 3. $CFCl_3$ daily means (pptv) and standard deviations at Cape Meares, Oregon (45°N, 124°W) on the silicone channel for the period December 1979 to June 1981. Changes of the calibration gas tank are noted on the upper abscissae.

system for the boxes, see Figure 1). Mean meridional transport between boxes i and j is represented by an inverse time constant V_{ij}, while eddy diffusion between these boxes is assumed to occur at a rate $(t_{ij})^{-1}$. Assuming input to box 1 occurs at a rate I_1, (kgm/yr), mass continuity in box 1 requires that

$$\frac{d\chi_1}{dt} = V_{13}\bar{\chi}_{13} - V_{21}\bar{\chi}_{21} - \frac{(\Delta\chi)_{13}}{t_{13}} + \frac{(\Delta\chi)_{21}}{t_{21}} + \frac{I_1}{M_1} \qquad (3)$$

where χ_1 is the mass mixing ratio of the species in box 1,

$$\bar{\chi}_{ij} = \frac{1}{2}(\chi_i + \chi_j)$$

$$(\Delta\chi)_{ij} = \chi_i - \chi_j$$

and M_1 is the total mass of air in box 1. To this equation we may add a destruction process for halocarbons equal to χ_1/τ_t, where τ_t is the lifetime for the species in the troposphere. For box 3, for example, the equation is

$$\frac{d\chi_3}{dt} = -V_{13}\bar{\chi}_{13} + V_{35}\bar{\chi}_{35} - V_{43}\bar{\chi}_{43} + \frac{(\Delta\chi)_{13}}{t_{13}} - \frac{(\Delta\chi)_{35}}{t_{35}} + \frac{(\Delta\chi)_{43}}{t_{43}} - \frac{\chi_3}{\tau_t} + \frac{I_3}{M_3} \qquad (4)$$

The equations for boxes 2, 4, 6, and 8, which are in the upper troposphere, reflect the differing masses of air in upper and lower tropospheric and stratospheric boxes. For box 2, we have, for example,

$$\frac{d\chi_2}{dt} = \frac{5}{3}V_{24}\bar{\chi}_{24} + \frac{5}{3}V_{21}\bar{\chi}_{21} - \frac{(\Delta\chi)_{24}}{t_{24}} - \frac{5}{3}\frac{(\Delta\chi)_{21}}{t_{21}} - \frac{2}{3}\frac{\chi_u - \chi_s}{\tau_s} - \frac{\chi_2}{\tau_t} \qquad (5)$$

where $\chi_u = (\chi_2 + \chi_4 + \chi_6 + \chi_8)/4$, χ_s is the average (stratospheric) mixing ratio above 200 mbar and t_s is the transfer time between the troposphere and stratosphere. The equation

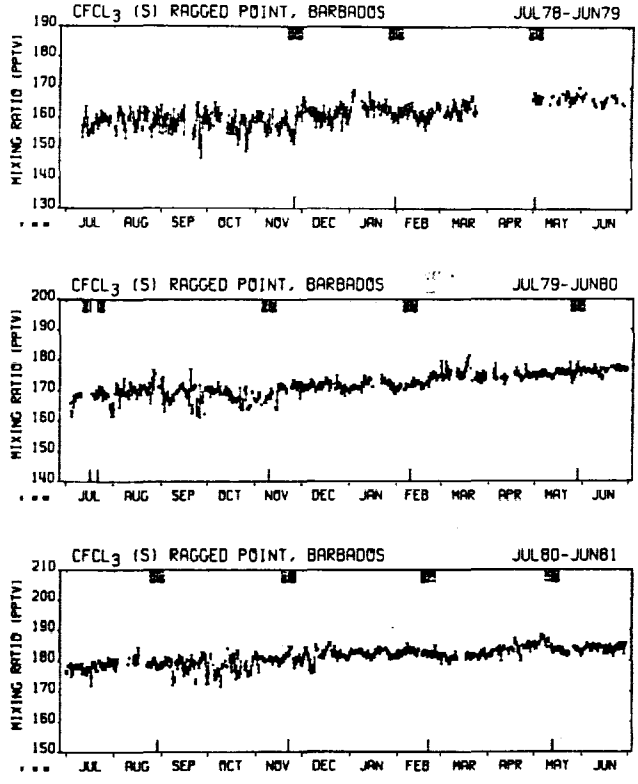

Fig. 4. $CFCl_3$ daily means (pptv) and standard deviations at Ragged Point, Barbados (13°N, 59°W) on the silicone channel for the period July 1978 to June 1981. Changes of the calibration gas tank are noted on the upper abscissae.

for χ_s is

$$\frac{d\chi_s}{dt} = \frac{\chi_u - \chi_s}{t_s} - \frac{\chi_s}{\tau_s} \tag{6}$$

where τ_s is the stratospheric lifetime of the species (resulting from photodissociation). We shall define $r = \chi_s/\chi_u$.

By using equations (4)–(6), the overall lifetime of the species in the atmosphere is

$$\tau = \frac{\tau_s(1 + \chi_s/4\bar{\chi}_t)}{\tau_s/\tau_t + (\chi_s/4\bar{\chi}_t)} \tag{7}$$

where $\bar{\chi}_t$ = the average tropospheric mixing ratio

$$= \frac{5}{32}(\chi_1 + \chi_3 + \chi_5 + \chi_7) + \frac{3}{32}(\chi_2 + \chi_4 + \chi_6 + \chi_8)$$

Note that the lifetime τ of the species is dependent on $\chi_s/\bar{\chi}_t$ and is thus time dependent. In particular, for the ALE species $\chi_s/\bar{\chi}_t$ is increasing with time so that τ decreases with time if $\tau_s < \tau_t$.

To prescribe the t_{ij} values for horizontal diffusion we utilize the results of *Newell et al.* [1969]. The horizontal diffusion rates are then multiplied by the factor F (which is determined from the optimal estimation analysis as providing the best fit to the species gradients observed in ALE).

To provide a smooth temporal variation of horizontal diffusion throughout the year, we represent t_{ij} by a four-term series

$$t_{ij} = \frac{a_0}{2} + a_1 \cos\left(\frac{2\pi t}{T}\right) + b_1 \sin\left(\frac{2\pi t}{T}\right) + b_2 \sin\left(\frac{4\pi t}{T}\right) \tag{8}$$

where $T = 360$ days and $t = 0$ corresponds to January 1. The constants, a_0, a_1, b_1, and b_2 are chosen so that t_{ij} averaged over a season equals the t_{ij} determined by using the seasonal-average data from *Newell et al.* [1969].

The tropospheric vertical diffusion times t_{ij} are assumed to be latitudinally and seasonally invariant and correspond to a vertical diffusion coefficient of 0.375×10^5 cm^2/s at 500 mbar. The exchange time t_s between troposphere and stratosphere is taken as 4 years. The time constants V_{ij}^{-1} due to horizontal and vertical zonally averaged motion are determined from the stream functions given by *Newell et al.* [1969]. In a manner similar to that for horizontal diffusion, we represent the seasonally averaged horizontal velocities by a four-term Fourier series in time. In this model, vertical transfer is dominated by vertical diffusion and therefore we have not found it necessary to represent the seasonal variation of vertical velocity by a time series. A summary of the box model parameters is given in Table 1.

For each ALE species, integration of the box model proceeds from 1970, using the current best estimates for annual releases in boxes 1, 3, 5, and 7 for the species (see section 4 for $CFCl_3$ releases). The release prior to 1970 has been included assuming an exponential release prior to that time (which sums to the tabulated total release). This assumption results in an analytic integration of equation (1) so that the destruction prior to 1970 can be estimated. The effect of this assumption has been tested by repeating a few calculations starting from 1960. Differences are insignificant after approximately 1974 (since for any compound with lifetime $\tau \gg 4$ years the 1970 release would have become uniformly distributed in the atmosphere by 1974). The integration uses a four-cycle time-stepping scheme [*Lorenz*, 1971] with six hour cycles.

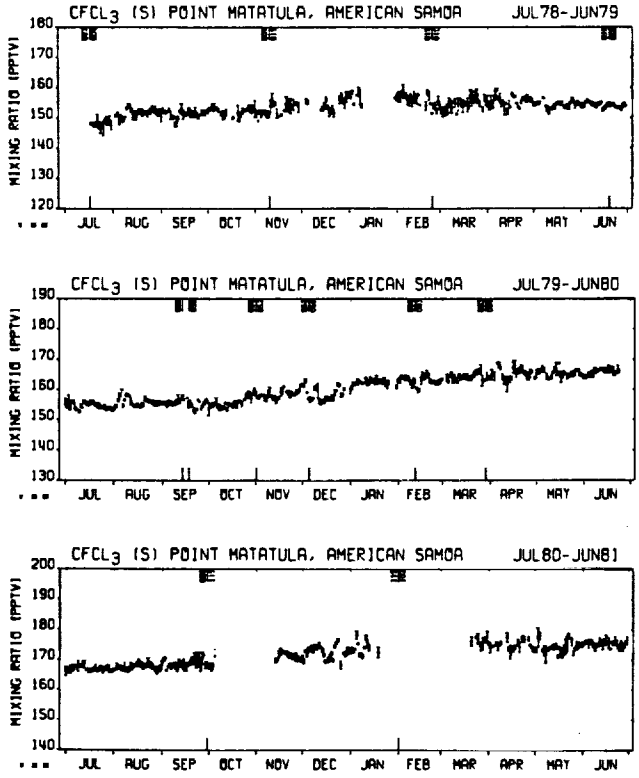

Fig. 5. $CFCl_3$ daily means (pptv) and standard deviations at Point Matatula, American Samoa (14°S, 171°W) on the silicone channel for the period July 1978 to June 1981. Changes of the calibration gas tank are noted on the upper abscissae.

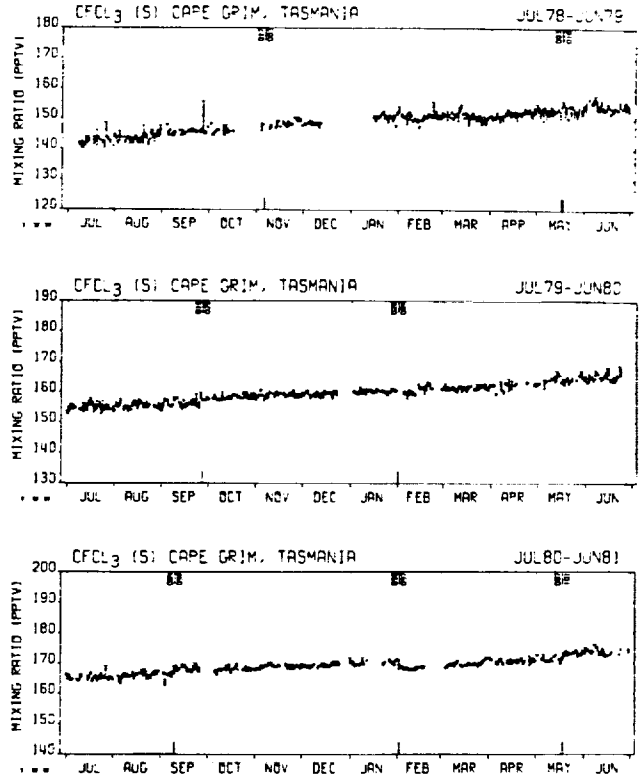

Fig. 6. $CFCl_3$ daily means (pptv) and standard deviations at Cape Grim, Tasmania (41°S, 145°E) on the silicone channel for the period July 1978 to June 1981. Changes of the calibration gas tank are noted on the upper abscissae.

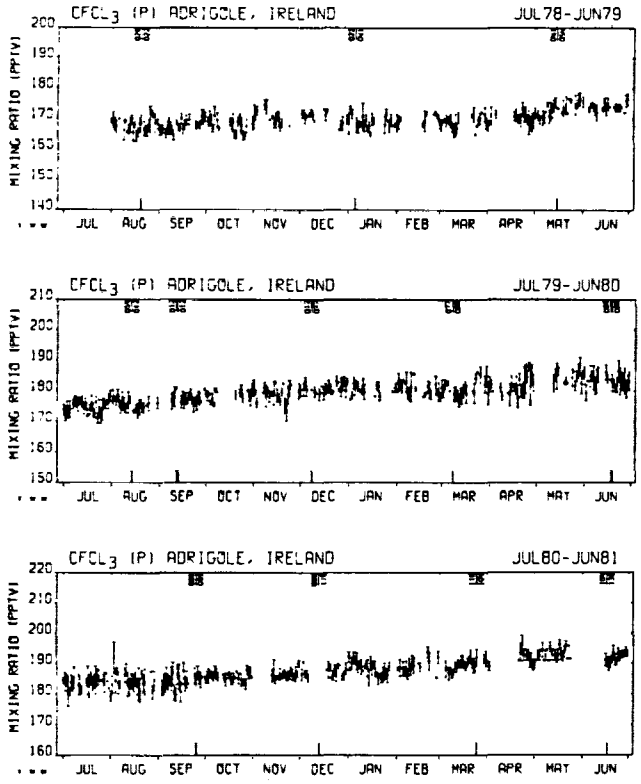

Fig. 7. $CFCl_3$ daily means (pptv) and standard deviations at Adrigole, Ireland (52°N, 10°W) on the Porasil channel for the period July 1978 to June 1981. Changes of the calibration gas tank are noted on the upper abscissae.

2.2 *The Optimal Estimation Procedure*

This procedure is used to provide estimates of the atmospheric lifetimes of the four ALE halocarbons and of the rate of horizontal mixing in the atmosphere. Since $CFCl_3$, CF_2Cl_2, and CH_3CCl_3 possess sufficiently accurately known release distributions, ALE measurements of these species all contribute to providing an estimate of the rate of horizontal mixing. Therefore, the procedure is set up so as to provide simultaneous estimates of the lifetimes of $CFCl_3$, CF_2Cl_2, CH_3CCl_3, and the horizontal diffusion factor (F). Measurements of $CFCl_3$ on the silicone and Porasil columns are treated independently, separate lifetimes being estimated from each data set. For mathematical convenience, we work with the logarithm of measured and calculated mixing ratios rather than instanteous mixing ratio trends. Then, to ensure that the lifetime estimate will be based on trend information, we multiply the absolute concentrations measured at each ALE site by an unknown factor A of order unity to be estimated from the measurements. This allows any disagreement between the time-averaged atmospheric inventory estimated from the ALE data and that derived from the two-dimensional model to appear in A. Adrigole, Ireland, and Cape Meares, Oregon, measurements both provide information on the concentrations of ALE species at mid-latitudes of the northern hemisphere. To avoid overweighting this atmospheric region in the estimate of lifetime, Adrigole and Cape Meares data have therefore been optimally combined into a single time series with a weight factor inversely proportional to the variance of each individual month's estimate of the mixing ratio.

The state vector, which describes the unknown parameters, would thus take the form

$$\mathbf{y}_1 = (A_1, \tau_1, A_2, \tau_2, A_3, \tau_3, A_4, t_4, F)$$

However, in order that the system possess maximum linearity during the optimal estimation procedure, we replace A by ln A, F by ln F, and τ by $1/\tau$. The state vector thus becomes:

$$\mathbf{y} = (\ln A, \tau_1^{-1}, \ln A_2, \tau_2^{-1}, \ln A_3, \tau_3^{-1}, \ln A_4, \tau_4^{-1}, \ln F) \quad (9)$$

The update equation for the state according to optimal esti-

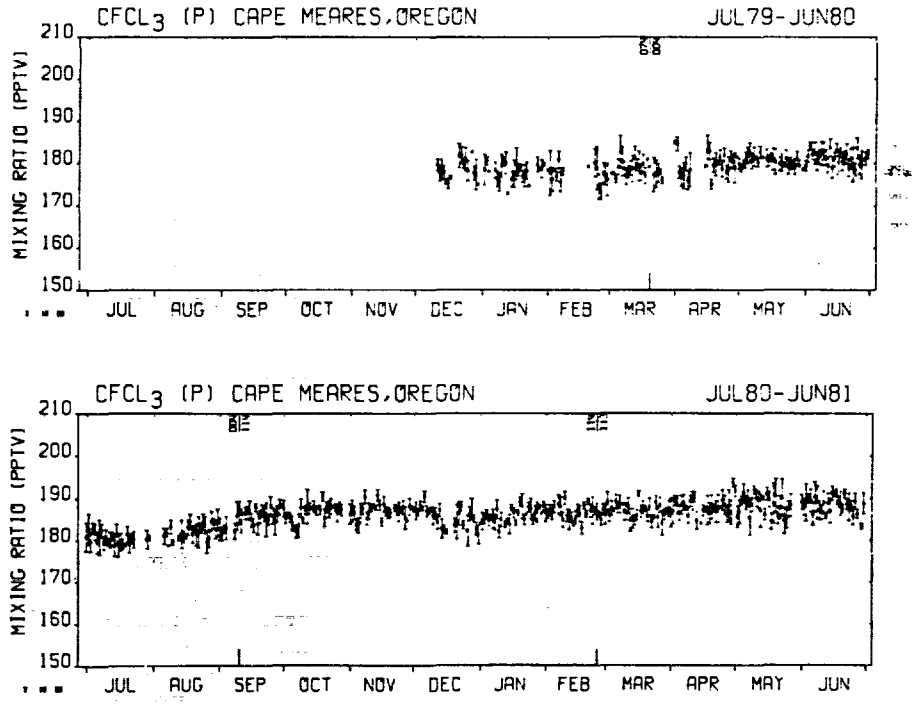

Fig. 8. $CFCl_3$ daily means (pptv) and standard deviations at Cape Meares, Oregon (45°N, 124°W) on the Porasil channel for the period December 1979 to June 1981. Changes of the calibration gas tank are noted on the upper abscissae.

mation theory is

$$\mathbf{y} = \mathbf{y}_0 + \mathbf{G}(\mathbf{x} - \hat{\mathbf{x}}) \tag{10}$$

where $\mathbf{y}_0$ is the a priori estimate of the state vector; $\mathbf{x}$ is a 16 component vector consisting of the natural logarithms of the measured monthly mean mixing ratios, χ_m, of $CFCl_3(S)$, $CFCl_3(P)$, CF_2Cl_2, and CH_3CCl_3 at Adrigole, Cape Meares, Ragged Point, Point Matatula, and Cape Grim (monthly mean rather than instantaneous values were used to reduce computation time and because the time scales relevent to determining the lifetime were seasonal or longer); $\hat{\mathbf{x}}$ is a similar vector of the species mixing ratios, χ_c, calculated by the two-dimensional model; and G is a 9×16 matrix usually referred to as the gain matrix. Equation (10) provides a prescription for updating the state vector after each month of ALE observations (using y from the previous month as the current a priori estimate). Smaller updates will automatically be performed on those state vector elements for which the a priori knowledge is greater.

The gain matrix is given by

$$\mathbf{G} = \mathbf{C}_0\mathbf{P}'[\mathbf{P}\mathbf{C}_0\mathbf{P}' + \mathbf{N}]^{-1} \tag{11}$$

where $\mathbf{C}_0$ is the (a priori) covariance matrix whose diagonal elements are the variances of the elements of the state vector and whose off-diagonal elements represent covariation between those elements. The matrix P (with transpose P') is a matrix of the partial derivatives of the elements of $\hat{\mathbf{x}}$ with respect to the elements of y (for example, $\partial(\ln \chi_c)/\partial(1/\tau)$); these derivatives are computed by using the two-dimensional model. The matrix N is the noise matrix of the measurements which is a diagonal matrix whose nonzero elements are the variances associated with the standard errors (σ) of the estimates of the monthly mean measured values at each site. It may be noted that if P is a square matrix and the measurements are noisy ($\mathbf{N} \to \mathbf{O}$), the gain matrix is equal to $\mathbf{P}^{-1}$. Noisy measurements, on the other hand ($\mathbf{N} \gg \mathbf{P}\mathbf{C}_0\mathbf{P}'$), would provide a gain much less than $\mathbf{P}^{-1}$.

The covariance matrix is also updated based on the measurements by using the equation

$$\mathbf{C} = \mathbf{C}_0 - \mathbf{G}\mathbf{P}\mathbf{C}_0 \tag{12}$$

On the basis of the preceding paragraph, we see that noisy measurements will leave C virtually unaltered while for almost noiseless measurements C tends to zero. The diagonal elements of C are interpreted as the variance (i.e., uncertainty) of the elements of the state vector based on a combination of the a priori uncertainties and the uncertainties in the measurements. The off-diagonal elements of C are the covariances between the elements of the state vector based on the a priori and measurement information and reflect the degree of interdependence of the element estimates.

Each additional period (e.g. 1 month) of ALE data is used to update the previous estimate of the state vector. The two-dimensional model results indicate that the response of the calculated concentrations to small variations of the state vector elements is approximately linear. This permits us to avoid substantial computation by performing a linear adjustment as an approximation for the model's two-dimensional prediction at time-step $m + 1$

$$\hat{\mathbf{x}}_{m+1} = \hat{\mathbf{x}}_{m+1}{}^0 + \mathbf{P}_{m+1}(\mathbf{y}_m - \mathbf{y}_0) \tag{13}$$

where $\hat{\mathbf{x}}_{m+1}{}^0$ is calculated with the two-dimensional model by using the estimated state vector at time-step zero. Calculations

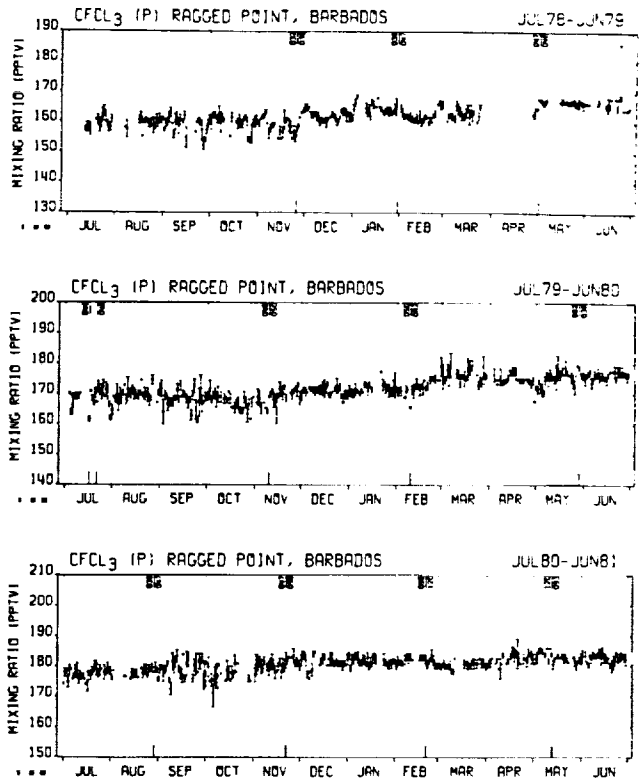

Fig. 9. $CFCl_3$ daily means (pptv) and standard deviations at Ragged Point, Barbados (13°N, 59°W) on the Porasil channel for the period July 1978 to June 1981. Changes of the calibration gas tank are noted on the upper abscissae.

with the two-dimensional model, moreover, indicate that the partial-derivative matrix P is relatively insensitive to changes in the state vector elements; a constant "average" value of P is therefore utilized throughout. It should be noted, however, that $\partial/\partial t$ (P) is not assumed to be zero but must be precisely specified because this will control the lifetime estimate. This may be seen by noting that one element of $\partial/\partial t$ (P) is

$$\frac{\partial}{\partial t}\left\{\frac{\partial \ln \chi_c}{\partial(1/\tau)}\right\} = \frac{\partial}{\partial(1/\tau)}\left(\frac{\partial \ln \chi_c}{\partial t}\right) \tag{14}$$

which expresses the sensitivity of the trend to the inverse lifetime. In practice, a constant "average" value is assumed for $\partial/\partial t$ (P).

Equations (10)–(13) constitute the optimal estimation procedure. During its application to the 36 month data set, month by month, no additional two-dimensional model calculations are made. The assumptions of constancy in $\partial(\ln \chi_c)/\partial(1/\tau)$ and its time derivative for $CFCl_3$ are justified in Table 2 where it is shown, in particular, that these two derivatives are relatively insensitive to changes of τ (as well as to several other parameters). It may be noted, however, that the derivative $\partial(\ln \chi_c)/\partial(1/\tau)$ is sensitive to whether the $CFCl_3$ sink is in the stratosphere or the troposphere. We shall return to this point when the results are discussed. Since the assumption of constant partial derivatives is an approximation, after the lifetime has been estimated from the 3 year data set, the two-dimensional model is rerun by using this lifetime and the entire 3 year data set is reprocessed. As expected, the convergence of this procedure to produce a final estimate of the lifetime is rapid. The principal sensitivity of the results to the partial derivatives is therefore in estimating uncertainty limits.

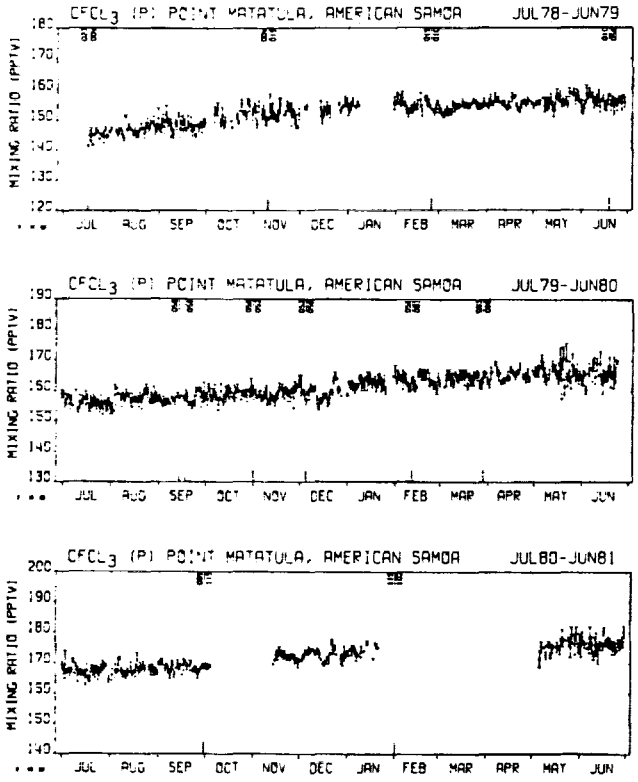

Fig. 10. $CFCl_3$ daily means (pptv) and standard deviations at Point Matatula, American Samoa (14°S, 171°W) on the Porasil channel for the period July 1978 to June 1981. Changes of the calibration gas tank are noted on the upper abscissae.

Additional information about the optimal estimation approach is provided in the appendix, in which some useful limiting cases are discussed. In particular, the second limiting case in the appendix (results (A5) and (A6)) provides important insight into what happens when optimal estimation is used to analyze the four stations' time series to estimate a state vector consisting of a calibration error, a lifetime, and a horizontal transport factor. The lifetime estimate would be determined by a combination of the temporal trend and of the site to site differences (since $\partial(\ln \chi_c)/\partial(1/\tau)$ is not the same at all sites). If the horizontal transport factor is unconstrained, then most of the latitudinal gradient information would be used to update the transport factor and the lifetime would be primarily based on trend information. If, on the other hand, three species were to be used simultaneously to deduce a "best" estimate of the transport factor, an anomalous latitudinal gradient of one species could make a significant contribution to the estimated lifetime of that species (because the transport factor would be constrained by the other two species). For this reason, in the analysis that follows, lifetime estimates will be presented for each station's time series analyzed separately by using the two-dimensional model results that provide the best fit to all the ALE data. The individual station lifetime estimates thus obtained will be based upon the prescribed partial derivatives and the two-dimensional model calculation that provides the best fit to the optimal combination of the data from all the sites. In addition, the optimal lifetime estimates based upon combining the data at all the sites are artificially forced to be based purely on the trends at each site by setting the partial derivatives, $\partial(\ln \chi_c)/\partial(1/\tau)$, equal to the four box mean values. In effect, we are saying that small differences between the mean observed concentrations at each site and the two-dimensional model results are most likely due to uncertainties in the latitudinal distributions of releases as well as to minor inadequacies in the model's ability to simulate global transport. We assume, however, that these minor limitations of the model simulation have negligible impact on the trends at each site and reason that adjusting the transport factor to provide the best fit to the mean latitudinal gradient for the species should provide the best prediction of the temporal trends at each site. (Dr. Oehlert of the Department of Statistics, Princeton University, has pointed out that with these approximations our procedure for estimating the $CFCl_3$ trend lifetime is equivalent to generalized least squares estimation of the parameters y^1 and y^2 in the equation

$$x^i(t) - \hat{x}^i(t) = (y^1 - y_0{}^1) + (y^2 - y_0{}^2)[-4.40 - 0.031(t - 18)]$$

where the superscripts denote elements of the state vector, $\mathbf{y}$, and the ln (chlorofluorocarbon mixing ratio) vector, $\mathbf{x}$, and t is expressed in months with month 1 being July 1978.)

3. Global Trichlorofluoromethane Data

Figures 2–11 show the daily $CFCl_3$ data for the period July 1978 to June 1981 at the five ALE sites on the silicone (denoted $CFCl_3$ (*S*)) and Porasil (denoted $CFCl_3$ (*P*)) columns of the gas chromatograph. These data have all been adjusted by the ALE absolute calibration factor, $\xi = 0.96$, for $CFCl_3$ determined by *Rasmussen and Lovelock* [this issue]. The ALE instrument at Cape Meares, Oregon, has only operated since December 1979. At each site the ambient air is usually sampled four times daily, and the calibration tank is sampled between each ambient air measurement. The error bars at-

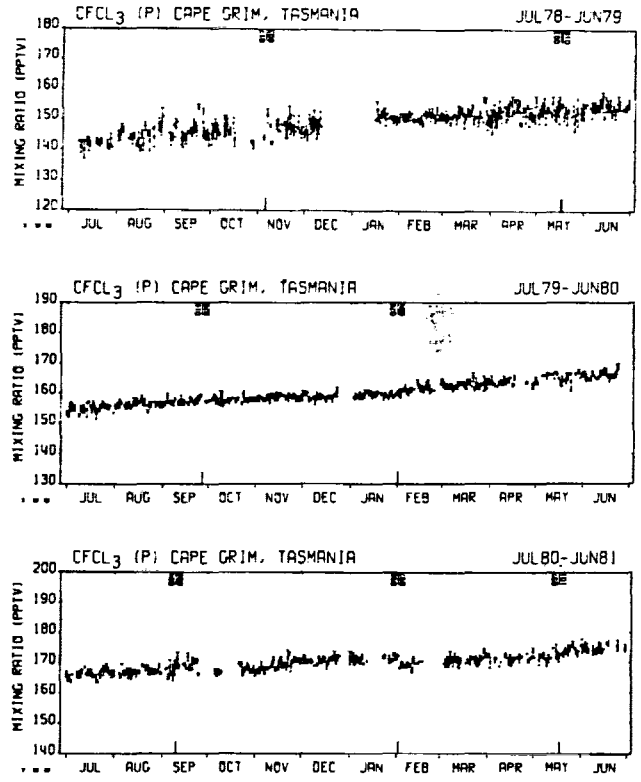

Fig. 11. $CFCl_3$ daily means (pptv) and standard deviations at Cape Grim, Tasmania (41°S, 145°E) on the Porasil channel for the period July 1978 to June 1981. Changes of the calibration gas tank are noted on the upper abscissae.

tached to each daily mean value reflect ± 1 standard deviation derived from the four calibrated air measurements.

The ALE calibration tanks have been measured against a standard tank, as described in *Rasmussen and Lovelock* [this issue], to a precision better than 0.5% for $CFCl_3$ prior to shipment to the ALE sites and again following the return of the tanks to Oregon. Additional measurements have been made on some of the tanks from time to time over the 3-year period; for this 3-year period, the standard deviation of the mean $CFCl_3$ values is typically 0.5%. Based on these results, discontinuities in the ALE data record for $CFCl_3$ resulting from calibration tank changes (the calibration cylinders used and the changing dates are indicated on the upper abscissae of Figures 2–11) should generally not exceed 1%.

Considering the data records in order from the northern to the southern hemisphere, the Adrigole, Ireland, record contains the most data gaps. This is primarily related to elevated values of $CFCl_3$ that occur there simultaneously with increased concentrations of CF_2Cl_2, CH_3CCl_3, and perchloroethylene. These events, which generally last a few days, are attributed to regional polution and have been removed from the data set. Additional gaps in the data record occur because of problems with the electrical supply in the spring and summer of 1981 and because of a deteriorating detector on the silicone column in December 1978 and January 1979 which was finally replaced on February 20, 1979. The $CFCl_3$ (P) data has also been removed from the first month because of inadequate Porasil channel operation during this initial time period.

At Cape Meares, Oregon, pollution occurs only rarely, and the F-11S and F-11P records are relatively continuous from December 1979 onward. Moving farther south to Ragged Point, Barbados, it is clear that the first 6 months of measurements of $CFCl_3$ on the silicone column were less precise than those after May 1979. During April 1979, the Ragged Point, Barbados, instrument was out of operation, and, prior to its return to operation on May 1, 1979, a new detector was installed on the silicone column and the electronics was improved. There appears to be an increase in $CFCl_3$ variability during every September and October. This is believed to result from the combined effects of intense storms, including hurricanes, on the island's power supply resulting in disequilibration of the instrument and of real decreases in $CFCl_3$ produced by the occurrence of air over Ragged Point, Barbados, with a southern hemisphere origin.

At Point Matatula, American Samoa, power supply problems have been even more severe than elsewhere and have resulted in the instrument being burned out in October 1980 and again in January 1981. Following this, the instrument did not return to full operation until May 1981. On November 10, 1978, the sample loop was changed on the Porasil column from 3 to 2 ml and from 5 to 7 ml on the silicone column. Prior to that time, the accuracy and precision of the Porasil column measurements are questionable because the three Porasil channel species $CFCl_3$, CF_2Cl_2, and N_2O all exhibit an upward drift and CF_2Cl_2 and N_2O show a discontinuity coinciding with the change in the sample loop size (and the calibration tank change from 004 to 019).

The variability of $CFCl_3$ at Cape Grim, Tasmania, is least. Here, also, the sample loop was changed in November 1978 from 4 ml to 3 ml on the Porasil channel and from 5 ml to 7 ml on the silicone channel. Pollution, identified by substantial simultaneous increases of $CFCl_3$ and CF_2Cl_2, occasionally occur associated with a northwesterly wind; these events have been removed from the data set. In December 1978, the air intake valve became contaminated; it was replaced in January 1979.

The data shown in Figures 2–11 have been processed to yield monthly means and standard deviations. The results are given in Table 3. All the analysis of ALE $CFCl_3$ data to yield lifetimes is based upon the data given in Table 3.

The optimal estimation code described in the previous section has first been used to fit an empirical model to these monthly mean values. The form of the empirical model assumed is

$$\ln \chi_i = a_i + b_i\left(\frac{t-18}{12}\right) + d_i\left(\frac{t-18}{12}\right)^2 + c_i \cos\left(\frac{2\pi t}{12}\right) + s_i \sin\left(\frac{2\pi t}{12}\right) \quad (15)$$

where χ_i is expressed in pptv and t is given in months with month 1 being July 1978. The data is thus being fitted with a linear trend, a curvature term and an annual cycle. For the Cape Meares, Oregon, data, the curvature term has been omitted ($d_i = 0$) since the data extends over only approximately 18 months. The optimal estimation code provides maximum likelihood estimates of the parameters a_i, b_i, d_i, c_i, and s_i with each month's observations being weighted by

$$\sigma^{-2} = \left(\frac{\sigma_m^2}{n_m} + \sigma_0^2\right)^{-1} \quad (16)$$

where σ_m is the standard deviation of the measurements during month m, n_m is the number of measurements made in month m divided by 12 (to allow for the typical observed correlation between individual measurements over periods ~ 3 days), and σ_0^2 is the variance of the residuals of the monthly mean observations relative to the fitted empirical model (calculated a posteriori). It may be noted that if σ_0^2 dominates this expression, each month's data receives equal weight in estimating the trend. For $CFCl_3$, σ_0^2 is typically roughly twice σ_m^2/n_m; moreover, the short term precision of the instrument ($\sim\sigma_m$) has tended to improve slightly with time at some sites so that more recent data will receive a little more weight than the 1978–1979 data.

After the optimal fit has been obtained, the autocovariance of the monthly residuals (and its Fourier transform) are calculated. Because the monthly residuals are found to be correlated, σ_0^2 underestimates the uncertainty. In calculating the variance of the estimate of a_i, for example, σ_0^2 should be replaced by

$$\sigma_0^2(1 + 2\gamma(1) + 2\gamma(2) + \cdots)$$

where $\gamma(m)$ is the expected value of the autocorrelation of the residuals at lag m months. To estimate this multiplicative factor from a time series of limited duration, it is customary to give less weight to the sample autocovariances at the longer lags. For example, in determining the Fourier transform of the autocovariance series a Parzen window [*Parzen*, 1964] is often used as a weighting function. We have used a Parzen window with 8 degrees of freedom ($M = 8$) to obtain the power spectrum of the residuals and to supply weighting factors on the sample autocorrelations used in estimating the multiplicative factors for the uncertainties in the coefficients in (15). The multiplicative factor to be estimated for b_i for 36 months of

TABLE 3a. Monthly-Averaged $CFCl_3$ (Silicone Column) Mixing Ratios χ (pptv), Their Standard Deviations σ_m (pptv), and the Number of Measurements During Each Month (N) Determined From Measurements at the Five ALE Sites Over the Period July 1978 through June 1981

Month	Adrigole, Ireland			Cape Meares Oregon			Ragged Point Barbados			Pt. Matatula, Amer. Samoa			Cape Grim, Tasmania		
	χ	σ_m	N	χ	σ_m	N	χ	σ_m	N	χ	σ_m	N	χ	σ_m	N
7-78	166.9	3.3	223				158.9	2.3	144	148.1	1.6	61	142.6	1.5	62
8-78	167.7	2.6	188				159.3	3.0	202	151.7	1.5	124	143.7	1.4	128
9-78	167.4	1.2	233				158.2	3.6	169	151.2	1.5	121	146.0	1.8	74
10-78	168.3	1.7	151				158.3	3.4	110	152.3	1.5	98	146.0	1.2	42
11-78	168.7	2.6	92				158.3	3.1	125	153.0	2.2	95	148.4	1.1	54
12-78	-	-	-				161.2	2.6	129	154.8	2.2	59	148.5	.6	40
1-79	169.4	3.8	80				163.5	2.3	114	157.1	1.9	18	150.9	1.1	52
2-79	169.4	2.3	25				161.5	2.1	113	156.4	2.1	93	151.1	1.3	91
3-79	169.0	1.6	68				162.9	2.0	96	154.6	2.2	114	151.2	1.4	107
4-79	171.1	2.0	63				-	-	-	155.5	1.8	119	151.8	1.2	104
5-79	172.0	2.2	83				166.7	1.4	67	154.4	1.2	122	153.0	1.4	107
6-79	174.0	1.6	71				165.9	1.3	40	154.3	.9	116	154.4	1.3	104
7-79	174.7	2.0	137				167.7	2.4	88	154.8	1.2	116	154.9	1.2	89
8-79	175.1	1.6	106				170.0	2.4	113	155.9	1.3	112	155.4	1.0	112
9-79	176.4	1.9	96				168.6	3.2	130	155.4	1.2	100	156.6	1.3	101
10-79	178.3	1.4	53				168.6	2.4	126	155.7	1.8	115	158.4	.8	94
11-79	178.5	2.3	76				169.6	2.3	90	158.5	1.4	112	159.2	.7	102
12-79	179.7	1.7	69	178.7	2.2	59	171.5	1.3	128	158.6	2.2	102	159.5	.8	79
1-80	179.8	1.9	58	179.2	1.3	70	171.8	1.5	108	162.4	1.2	99	160.4	.6	96
2-80	180.3	1.2	108	176.2	2.7	25	172.7	1.7	92	163.1	1.5	124	160.7	1.2	70
3-80	180.7	1.8	90	180.8	1.8	24	175.5	2.0	99	164.4	1.3	107	161.6	.7	109
4-80	182.0	1.6	103	182.6	1.2	84	175.0	1.5	77	165.3	2.1	112	162.0	1.2	60
5-80	184.5	1.6	61	183.4	1.3	97	175.7	1.3	136	165.4	1.2	111	164.4	1.2	76
6-80	183.4	2.2	114	182.7	1.2	114	176.6	1.1	129	165.8	1.2	94	165.3	1.4	84
7-80	183.9	1.5	111	182.6	1.4	91	178.1	1.6	129	167.1	1.1	116	165.4	1.0	92
8-80	184.0	2.1	110	184.2	1.3	82	179.4	1.6	56	167.7	1.2	113	166.1	1.0	91
9-80	184.1	1.2	105	186.4	1.9	110	178.8	2.5	124	168.9	1.6	94	167.8	1.3	75
10-80	185.2	2.0	83	188.1	2.1	111	178.2	2.6	122	168.2	1.2	15	168.1	.7	79
11-80	185.5	1.9	76	188.2	1.9	122	180.8	1.5	118	171.4	1.2	64	169.0	.6	93
12-80	186.6	1.9	66	187.0	2.5	107	181.8	2.0	125	172.6	2.0	97	169.4	.6	83
1-81	187.3	2.2	118	186.1	1.7	127	182.6	1.2	138	173.9	2.1	42	170.2	.8	54
2-81	187.3	2.0	66	187.4	1.3	106	182.8	1.2	115	-	-	-	168.8	1.0	44
3-81	188.7	2.2	98	187.2	1.2	126	181.6	1.2	100	176.5	1.7	27	169.9	.8	82
4-81	190.1	1.5	50	188.5	1.3	113	183.7	1.7	97	175.2	1.5	122	170.9	.7	75
5-81	190.8	1.6	62	188.9	1.2	104	184.5	1.6	123	174.1	2.0	119	172.4	1.2	83
6-81	192.0	1.5	77	190.1	1.1	112	184.1	1.2	109	175.5	1.2	113	173.9	1.0	61

The ALE measured values have all been converted to mixing ratios by multiplication by the absolute calibration factor $\xi = 0.96$.

observation may be shown to be

$$M = (1 + 1.7\gamma(1) + 1.4\gamma(2) + 1.3\gamma(3) + \cdots)$$

Having estimated this multiplicative factor, the empirical model calculation is repeated with σ_0^2 in the noise matrix replaced by $\sigma'^2_0 = M\sigma_0^2$ where M is not permitted to be less than unity. This step produced increases in the error bars ranging from zero at Barbados to approximately 50% at American Samoa. The multiplicative factors for a_i, d_i, c_i, and s_i were also estimated from the power in the smoothed spectrum at zero frequency (a_i), at a frequency of 1/6 years^{-1} (d_i), and 1 year^{-1} (c_i and s_i). These factors were not markedly different from M, and because the uncertainty in the estimates of these multiplicative factors is substantial (perhaps a factor of 2), no further adjustments of the error bars for a_i, d_i, c_i, and s_i were made.

The resulting estimates of the coefficients in equation (15), together with the 1σ uncertainty limits for the $CFCl_3$ data, are

TABLE 3*b*. Monthly-Averaged $CFCl_3$ (Porasil Column) Mixing Ratios χ (pptv), Their Standard Deviations σ_m (pptv), and the Number of Measurements During Each Month (N) Determined From Measurements at the Five ALE Sites Over the Period July 1978 through June 1981

Month	Adrigole, Ireland			Cape Meares, Oregon			Ragged Point, Barbados			Pt. Matatula, Amer. Samoa			Cape Grim, Tasmania		
	χ	σ_m	N	χ	σ_m	N	χ	σ_m	N	χ	σ_m	N	χ	σ_m	N
7-78	-	-	-				159.8	2.6	123	145.0	1.7	52	142.1	1.7	56
8-78	167.8	2.9	200				159.9	2.1	102	147.1	2.0	86	145.0	3.2	70
9-78	168.0	2.3	213				159.4	3.1	136	148.4	2.4	102	145.9	3.1	66
10-78	168.3	2.7	159				159.9	2.8	85	151.6	2.9	58	145.5	3.2	47
11-78	170.4	2.7	107				159.1	2.7	79	152.1	2.7	87	147.8	3.0	59
12-78	171.0	2.0	40				162.2	1.7	104	153.6	2.1	40	148.4	2.9	39
1-79	169.0	2.7	76				164.6	2.0	88	154.8	1.6	23	151.1	1.7	52
2-79	170.2	2.2	32				162.2	1.9	86	154.8	2.0	95	151.3	1.4	96
3-79	169.2	2.4	69				163.2	2.0	73	154.3	1.5	119	151.7	2.0	106
4-79	170.3	2.7	58				163.2	1.2	4	155.6	1.4	114	152.6	2.9	102
5-79	173.1	2.7	86				166.8	1.0	76	156.1	2.0	116	153.2	2.5	102
6-79	174.2	1.8	65				166.4	1.5	42	156.1	2.2	113	154.5	2.0	93
7-79	174.8	2.7	108				168.6	3.2	77	156.3	2.1	113	155.0	1.4	90
8-79	175.7	2.3	82				169.5	2.6	91	157.7	2.2	109	156.4	1.2	108
9-79	177.3	2.2	65				168.3	3.4	101	157.4	1.8	113	157.3	1.2	91
10-79	178.5	2.0	55				167.6	2.6	81	159.0	2.2	115	157.8	1.2	93
11-79	176.8	3.2	68				169.4	2.9	68	159.2	2.1	123	158.8	.9	103
12-79	181.1	2.3	73	178.8	2.9	59	171.1	1.7	101	159.6	2.9	102	158.9	1.2	81
1-80	180.8	2.2	46	178.4	2.6	75	171.7	2.0	88	162.5	2.1	90	159.5	.9	94
2-80	180.7	2.8	67	177.4	3.6	57	172.4	2.1	74	163.7	2.3	111	161.6	1.2	72
3-80	180.7	3.3	75	178.7	2.8	81	176.4	3.0	87	164.4	1.8	111	162.8	1.3	116
4-80	181.9	3.7	81	179.9	3.4	81	175.1	1.9	80	165.3	1.8	90	163.8	1.1	63
5-80	184.6	3.1	46	180.6	1.9	96	175.4	2.8	105	166.3	3.6	102	165.5	1.4	70
6-80	183.4	3.4	88	181.2	2.6	114	176.3	1.5	96	165.9	3.3	84	166.3	1.4	80
7-80	183.8	3.1	91	180.6	2.5	89	177.6	2.1	97	167.4	2.1	111	166.5	1.4	94
8-80	184.0	3.8	87	182.3	2.6	84	178.1	1.5	54	167.8	1.8	99	167.3	1.2	93
9-80	184.3	3.5	83	185.6	2.9	100	179.4	3.4	90	168.8	1.6	85	169.1	2.2	75
10-80	185.7	1.9	85	186.8	2.5	95	177.5	3.5	52	169.0	.8	14	167.6	1.2	51
11-80	186.5	1.7	61	187.0	2.2	109	180.7	2.4	84	172.3	1.5	54	169.3	1.9	106
12-80	187.2	2.0	54	185.8	2.9	98	181.4	2.3	80	172.8	1.9	94	171.2	1.2	80
1-81	188.4	2.8	95	185.9	2.2	130	181.8	1.6	92	174.0	1.7	34	171.5	1.2	52
2-81	189.3	2.8	50	186.6	2.3	96	182.0	1.4	79	-	-	-	169.9	1.3	44
3-81	189.7	2.3	81	187.0	2.4	117	180.7	1.3	76	-	-	-	171.3	1.5	92
4-81	192.2	2.9	45	188.1	2.9	107	182.5	2.3	73	-	-	-	171.5	1.2	62
5-81	193.3	2.2	74	188.5	3.4	104	183.1	1.8	71	175.8	2.7	84	173.2	1.8	86
6-81	192.1	2.1	61	188.6	2.9	111	182.9	1.8	86	176.4	2.6	109	174.8	1.6	65

The ALE measured values have all been converted to mixing ratios by multiplication by the absolute calibration factor $\xi = 0.96$.

given in Table 4. It should be noted that the mean concentration of $CFCl_3$ (and, hence, its latitudinal gradient) and its temporal trend are extremely well defined while the curvature and the seasonal variation are relatively poorly defined. In particular, the annual cycle is fairly weak at all sites except Point Matatula, American Samoa. The consistency between the silicone and Porasil channels is generally good (i.e., the agreement between the data obtained from the two channels is consistent within the cited uncertainty limits). Exceptions to this statement occur at Point Matatula, American Samoa and at Cape Meares, Oregon. At Point Matatula, the difference primarily results from the first 9 months of operation. As noted earlier, the sample loop sizes were changed at this site after approximately 4 months of operation and an anomalous increase of $CFCl_3$, N_2O, and CF_2Cl_2 occurred on the Porasil column during these first 4 months. Also, a constant frequency detector was temporarily used on the silicone column for 6 months after the changes of the sample loop sizes. The Point Matatula, American Samoa, $CFCl_3$ data will, therefore, receive a lower weight in the estimation of lifetime because of

TABLE 4. Empircal Model Fit (Equation (15)) to the 3 Years of $CFCl_3$ Data Given in Tables 3*a* and 3*b*

Site	a_i	b_i	d_i	c_i	s_i	Variance of Residuals, $\sigma_0^2 \times 10^6$
			$CFCl_3$ (S)			
Adrigole, Ireland	5.184 ± 0.002	0.050 ± 0.002	−0.002 ± 0.002	0.001 ± 0.002	0.002 ± 0.002	27
Cape Meares, Oregon	5.190 ± 0.002	0.040 ± 0.004*		−0.001 ± 0.002	0.005 ± 0.002	30
Ragged Point, Barbados	5.145 ± 0.002	0.057 ± 0.002	−0.005 ± 0.002	0.002 ± 0.002	0.001 ± 0.002	36
Point Matatula, American Samoa	5.077 ± 0.004	0.056 ± 0.003	0.009 ± 0.004	−0.006 ± 0.003	−0.007 ± 0.003	73
Cape Grim, Tasmania	5.073 ± 0.001	0.065 ± 0.001	−0.008 ± 0.001	−0.001 ± 0.001	0.002 ± 0.001	14
			$CFCl_3$ (P)			
Adrigole, Ireland	5.186 ± 0.003	0.051 ± 0.002	−0.001 ± 0.003	0.001 ± 0.003	0.002 ± 0.003	38
Cape Meares, Oregon	5.179 ± 0.002	0.045 ± 0.004*		−0.004 ± 0.002	0.005 ± 0.002	18
Ragged Point, Barbados	5.145 ± 0.002	0.053 ± 0.002	−0.004 ± 0.002	0.001 ± 0.002	0.001 ± 0.003	48
Point Matatula, American Samoa	5.084 ± 0.003	0.062 ± 0.002	0.000 ± 0.003	−0.004 ± 0.003	−0.005 ± 0.003	35
Cape Grim, Tasmania	5.075 ± 0.002	0.067 ± 0.002	−0.008 ± 0.002	−0.001 ± 0.002	0.001 ± 0.002	21

*Calculated from 18-month data set (this implies the trend is characteristic of month 27 as opposed to month 18 at other sites).

the large variance of the residuals produced by the first 9 months of operation. At Cape Meares, Oregon, it is also the first few months of operation which lead to the different mean $CFCl_3$ concentrations on the two columns.

In processing the data to produce lifetimes, the Adrigole, Ireland, and Cape Meares, Oregon, data have been combined into a single time series for each column. These time series have also been processed through the empirical model algorithm. They give, for $CFCl_3$ (*S*): $a_i = 5.185$, $b_i = 0.049$, with a residual variance of 2×10^{-5}; and for $CFCl_3$ (*P*): $a_i = 5.183$, $b_i = 0.048$ with a residual variance of 2.2×10^{-5}. The annually averaged mixing ratios and trends for January 1, 1980, obtained by using (15) and averaging in each semi-hemisphere are, respectively, 179 pptv and 8.6 pptv/year (Adrigole/Cape Meares); 172 pptv and 9.4 pptv/year (Ragged Point); 161 pptv and 9.6 pptv/year (Point Matatula); and 160 pptv and 10.5 pptv/year (Cape Grim). Averaging these semi-hemispheric results indicates that the average mixing ratio in the lower troposphere is 168 pptv, and it is increasing at a rate of 9.5 pptv/year (5.7%/year). All these quoted mixing ratios and trends refer to the middle of the 3-year data set (i.e., January 1, 1980).

4. Trichlorofluoromethane Emissions

Estimates of global annual emission rates for $CFCl_3$ through 1975 have been published by *McCarthy et al.* [1977]. These emission rates have been updated for each year since 1975 by using the same model and assumptions as *McCarthy et al.* [1977], and these updates are available in a series of reports from the Chemical Manufacturers Association (CMA). The most recent of these reports [*CMA*, 1982] contains emission estimates for the period 1921–1981.

Since the original analysis of *McCarthy et al.* [1977], more information has become available on the production of $CFCl_3$ in Eastern Europe and the U.S.S.R., on the losses of $CFCl_3$ during production, and on the end uses of $CFCl_3$ and their emission characteristics. This information implies that certain of the assumptions used by *McCarthy et al.* [1977] and *CMA* [1981*a*] are invalid. In particular, production in Eastern Europe and the U.S.S.R. after 1975 is underestimated, emission in $CFCl_3$ during manufacture amounting to 1.5% of production is ignored, the delay in release of $CFCl_3$ from open-cell foams after manufacture is overestimated, and the use of $CFCl_3$ in hermetically sealed refrigeration is overestimated. An update of the report *CMA* [1981*a*] has recently been completed which incorporates the above corrections [*CMA*, 1982]. We will use these updated emission rates in the analysis of ALE data (Table 5) but calculations, using the old emission rates, are also presented.

The calculation of global circulation rates from ALE data (and to a lesser extent the deduction of atmospheric lifetimes) requires at least an approximate knowledge of the latitude distribution of the above $CFCl_3$ emissions. While exact information about this latter distribution is lacking, there is enough information available to provide estimates with an accuracy sufficient for our purposes. In particular, we compute

TABLE 5. World Production and Release of $CFCl_3$ in Million Kilograms/Year

Year	Annual Production	Annual Release	Accumulated Production	Accumulated Release
1970	241.0	209.0	1707.5	1470.2
1971	266.6	229.7	1974.2	1699.9
1972	311.1	259.1	2285.3	1959.0
1973	354.3	296.5	2639.5	2255.5
1974	377.5	327.0	3017.1	2582.5
1975	323.4	318.3	3340.5	2900.7
1976	350.7	325.3	3691.2	3226.0
1977	332.8	313.7	4024.0	3539.8
1978	323.3	294.6	4347.3	3834.4
1979	306.5	276.1	4653.9	4110.5
1980	309.3	264.8	4963.2	4375.2
1981	310.1	264.3	5273.3	4639.5

From *Chemical Manufacturers Association* [1982].

TABLE 6. $CFCl_3$ Lifetime Estimates Derived From the Trend at Each ALE Site

Site	Reciprocal Lifetime, $(\text{years})^{-1} \pm 1\sigma$	Lifetime, (years) $\pm 1\sigma$	Approximate Weight Given to Station in Optimal Code
	Silicone Column		
Adrigole, Ireland/ Cape Meares, Oregon	0.0208 ± 0.0040	48^{+12}_{-8}	0.2
Ragged Point, Barbados	0.0067 ± 0.0038	149^{+196}_{-54}	0.2
Point Matatula, American Samoa	0.0221 ± 0.0075	45^{+23}_{-11}	0.1
Cape Grim, Tasmania	0.0077 ± 0.0026	130^{+66}_{-33}	0.5
	Porasil Column		
Adrigole, Ireland/ Cape Meares, Oregon	0.0230 ± 0.0042	43^{+10}_{-6}	0.3
Ragged Point, Barbados	0.0176 ± 0.0045	57^{+19}_{-12}	0.2
Point Matatula, American Samoa	0.0087 ± 0.0056	115^{+208}_{-45}	0.2
Cape Grim, Tasmania	0.0018 ± 0.0038	$556^{+\infty}_{-377}$	0.3

the fractions of the annual emission of $CFCl_3$ released in each semi-hemisphere by using the formulae

$$f(90°\text{N}-30°\text{N}) = \left(\frac{8}{9}B - \frac{1}{2}\varepsilon + D - \alpha\right)\Big/(B + C + D)$$

$$f(30°\text{N}-0°) = \left(\frac{1}{2}\alpha + \frac{1}{9}B + \frac{1}{2}\varepsilon\right)\Big/(B + C + D)$$

$$f(0°-30°\text{S}) = \frac{7}{12}C/(B + C + D) \tag{17}$$

$$f(30°\text{S}-90°\text{S}) = \left(\frac{5}{12}C + \frac{1}{2}\alpha\right)\Big/(B + C + D)$$

where α is the annual production of India plus Argentina [*CMA*, 1981*b*]; B and C are the annual total sales by CMA reporting companies in the northern and southern hemispheres, respectively [*CMA*, 1976, 1977, 1978, 1979, 1980, 1981*b*]; D is the annual total production by Eastern Europe, U.S.S.R., India, and Argentina [*CMA*, 1982]; and ε is the total of annual exports from the European Economic Community (EEC) to countries outside the EEC [*Department of Environment*, 1979; *Committee of European Communities*, 1980, 1981; *Bevington and Wallace*, 1981]. We assume EEC exports are released equally in the 90°N–30°N and 30°N–0° regions, and the India plus Argentina production is released equally in the 30°N–0° and 30°S–90°S regions. The distributions of emissions within each hemisphere resulting from sales by CMA reporting companies are determined from the locations of the reporting companies and their subsidiaries. Sales by the reporting companies were increased by 1.5% to account for $CFCl_3$ emission during manufacture.

Using equation (17), we calculate average f values for the 5-year period 1976–1980 of 0.785, 0.160, 0.031, and 0.024 in the 90°N–30°N, 30°N–0°, 0°–30°S, and 30°S–90°S semi-hemispheres, respectively. For the $CFCl_3$ lifetime calculations in the following section, we have used these average f values for the 10-year period July 1, 1971, to June 30, 1981. These f values are consistent with independent estimates of the global distribution of $CFCl_3$ and CF_2Cl_2 consumption in 1974 [*Department of Environment*, 1979].

Prior to July 1, 1971, we assume that $CFCl_3$ emissions are confined to the 90°N–30°N region. We note that interhemispheric mixing of $CFCl_3$ is sufficiently fast so that the behavior of $CFCl_3$ during the ALE program is insensitive to assumptions about f values for periods several years or more prior to the program.

5. Trend Estimate of Lifetime

The algorithm used to derive lifetimes of the chlorofluorocarbons must be appropriately constrained by a priori and measurement uncertainties. In the results to be presented here for $CFCl_3$ (as well as in the results for the other ALE species presented in the following papers) a priori error bars have been specified at artificially large values so that the estimates obtained are based solely on the ALE data. As was explained in section 2, the algorithm is constrained to produce a trend estimate of the lifetime by allowing it to estimate simultaneously an absolute calibration factor A for each species. We argue that the best estimate of the horizontal transport factor, F, is derived from the latitudinal distributions of the mean concentrations of the ALE species. As will be discussed in section 6, seasonal variations assumed in the model transport rates tend to produce an overprediction of the observed seasonal variations of the ALE species. Therefore, in the calculation of lifetimes, based upon trends over a 3 year period, the two-dimensional model results have been prefiltered by replacing each month's calculated value by a 12 month average. As shown in Table 2, the partial derivatives, $\partial(\ln \chi_c)/\partial(1/\tau)$, differ from site to site; there is therefore a tendency for the algorithm to adjust the lifetime (as well as F) so as to minimize differences between the calculated and the observed latitudinal gradients. Therefore, as indicated in section 3, to force the algorithm to base its lifetime estimates only on the temporal trends at the ALE sites, the latitudinal mean value of $\partial(\ln \chi_c)/\partial(1/\tau)$ is used to process the $CFCl_3$ data from each site.

In presenting the lifetime estimates it is useful to first give the results obtained by processing each ALE station's time series individually with the optimal code. This is achieved by fixing all the state vector elements except for the absolute calibration factor A and the lifetime τ for the species being examined. The transport factor F is fixed at the value (1.6) which gives the best fit to all the ALE data. In these calculations, the partial derivatives used are those calculated on the basis of a tropospheric lifetime $\tau_t = 10^4$ years and a varying stratospheric lifetime τ_s (see line 3 in Table 2). The lifetime estimates obtained for each site and their error bars are given in Table 6. Approximate weights which are used (internally) in the algorithm to produce a maximum likelihood optimally

TABLE 7. Reciprocal $CFCl_3$ Lifetime Estimates ($Years^{-1}$) and Their Standard Errors as Function of Time Obtained by Averaging and by Optimally Combining the Lifetime Estimates at the ALE Sites

Time Period, month/year	$CFCl_3$ (S)		$CFCl_3$ (P)	
	Optimal Combination	Average (Equal Weight)	Optimal Combination	Average (Equal Weight)
7/78–6/79	0.0238 ± 0.0103	0.0415 ± 0.0221	0.0205 ± 0.0120	0.0205 ± 0.0199
7/80–6/81	0.0379 ± 0.0089	0.0303 ± 0.0103	0.0317 ± 0.0104	0.0264 ± 0.0138
7/78–6/80	0.0069 ± 0.0035	0.0177 ± 0.0127	0.0121 ± 0.0041	0.0138 ± 0.0072
7/79–6/81	0.0155 ± 0.0032	0.0075 ± 0.0115	0.0121 ± 0.0037	0.0098 ± 0.0086
7/78–6/81	0.0114 ± 0.0018	0.0144 ± 0.0041	0.0127 ± 0.0021	0.0128 ± 0.0046

combined estimate are also given in Table 6. These weights and the uncertainties in reciprocal lifetimes are based upon the estimated variances in the measurements which are derived by the same procedure as was used in the empirical model fit. In fact, we have used the ${\sigma'_0}^2$ (see equation (16)) determined from the residuals with respect to the best fit empirical models (instead of with respect to the best fit two-dimensional model calculation). These ${\sigma'_0}^2$ reflect short ($\lesssim$1–2 years) time scale variations in the data and by using these values in the noise matrix we avoid biasing the all-site lifetime estimate by variations on a time scale of 3 years or more which might be produced at an individual site by year to year climatological variations which are not described by the two-dimensional model.

Table 6 shows that there exist significant (i.e., $> 1\sigma$) differences both between the lifetimes estimate of the ALE sites and between the lifetime estimates on the two columns at the same site. These differences indicate that the uncertainties (i.e., σ^2 in equation (16)) inserted into the optimal estimation procedure may be low by a factor of approximately 2 (this factor was estimated by using a variation of the student t test). That is to say, it appears that $CFCl_3$ trends at individual sites are being biased by variations of instrumental or atmospheric origin on time scales longer than approximately 1 year. The fact that the $CFCl_3$ (S) and $CFCl_3$ (P) lifetime estimates are significantly different at most sites suggests that these biases probably are of instrumental origin. If the site to site differences, as reflected in the standard errors in the average estimate of lifetimes given in Table 7, are examined as a function of time, a tendency for the standard errors to vary as $N^{-3/2}$, where N is the number of years of observations, is noted. This suggests that variations of time scale 1 or 2 years may exist in the ALE record (which may be unaccounted for in the procedure used to determine σ^2) but that longer term variations are small.

In Table 7 we present the results for lifetime estimates obtained by using the optimal code which processes data from all four ALE stations simultaneously. We note that the individual station lifetimes given in Table 6 may be optimally combined by using the weights given in that table to yield a result which is almost the same as that obtained with the optimal code (in which the weights are slightly time-dependent). From Table 7 the optimally estimated reciprocal lifetime of $CFCl_3$ is .0121 $years^{-1}$ giving a lifetime of 83 years. It may be noted from Table 6 that for the silicone column data, Point Matatula, American Samoa, is receiving very little weight while Cape Grim, Tasmania, is contributing substantially to this lifetime estimate. Some justification for this distribution of weighting is given in Figures 12 and 13 in which the residuals formed by differencing the monthly observations and the two-dimensional model calculation (for a lifetime of 83 years) are given. In Figure 12 it may be noted that the residuals on the silicone column are exceptionally large during the first 18 months of operation at Point Matatula, American Samoa, while those at Cape Grim, Tasmania, are exceptionally small. Clearly, the trend at Point Matatula is much less precisely determined than that at Cape Grim. It is encouraging to note that while the individual site data on the Porasil column is more evenly weighted in obtaining the optimal estimate of lifetime, the combined estimate for this column is similar to that for the silicone column. Additional confidence in the optimally estimated result is obtained by noting that it seems to be converging faster than the average result (cf. the 2 and 3 year results in Table 7). It does seem appropriate, however, to use the average site to site differences in lifetime to provide an estimate of the reciprocal lifetime uncertainty since we have already recognized that the effect of temporal autocorrelations on the error bars is quite uncertain and that the optimally estimated uncertainty appears to be unrealistically small. An upper limit to the uncertainty is then obtained by assuming that the Porasil and silicone columns do not provide independent estimates of the lifetime. The uncertainty limit on the reciprocal lifetime, therefore, is

$$\frac{(0.0041^2 + 0.0046^2)^{1/2}}{2} = 0.0044 \text{ years}^{-1}$$

It was noted in the description of the $CFCl_3$ data that a question existed about the validity of the data on the Porasil channel at Point Matatula, American Samoa, during July–October 1978. Figure 13 indicates that the residuals during this period appear to be no worse than at other times during the first 18 months, and it is interesting to note that the optimal estimate of lifetime for that site does not change during the period July 1978 to January 1979 when the data is processed backward in time.

The estimated lifetime of 83 years applies to the middle of the ALE data record (January 1, 1980) and corresponds in our calculations to $\tau_s = 11$ years (and $\tau_t = 10{,}000$ years). These instantaneous or present-day lifetimes in the two portions of the atmosphere lead to a steady state lifetime (when the stratospheric content is no longer delayed relative to the tropospheric content) of 70 years.

6. Lifetime Determination by the Atmospheric Inventory Technique

To estimate the atmospheric inventory of $CFCl_3$ from the surface observations obtained in ALE, concentrations must be estimated at other locations in the atmosphere and, in particular, in the stratosphere. We argue that the two-dimensional model provides a good fit to the available data and that the model results, therefore, may be directly used to estimate the

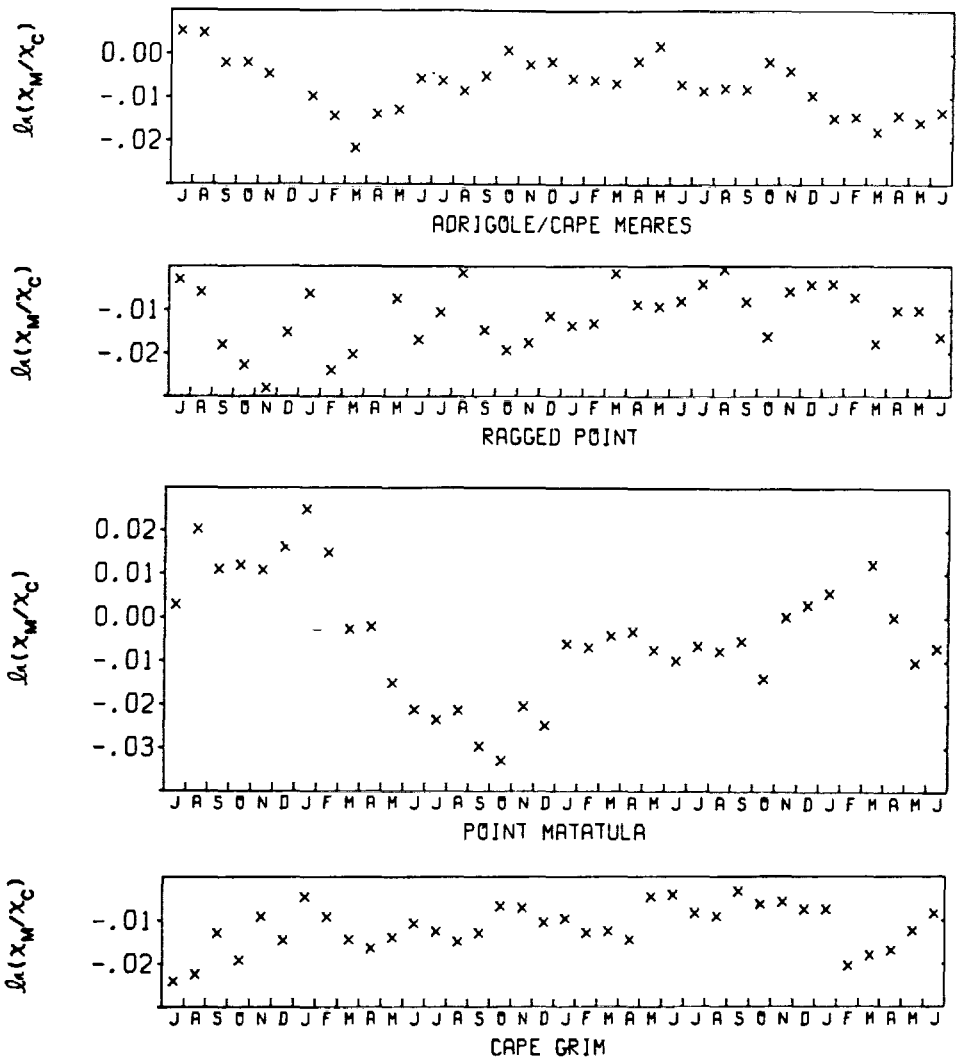

Fig. 12. $CFCl_3$ (S) residuals with respect to a two-dimensional model calculation with lifetime 83 years on January 1, 1980 (the trend best fit model). Residuals are given as the natural log of the ratio of the observed to the calculated mixing ratio.

atmospheric inventory. The following paragraphs provide not only observational support for the model results but also an assessment of the uncertainty limits on the atmospheric contents in each region of the atmosphere. The inventory lifetime and its uncertainty is then derived.

In the lower troposphere (the region below 500 mbar in the model), the atmospheric inventory is estimated to be the average of the mixing ratios in the four boxes in which the ALE supplies measurements multiplied by the mass of this region of the atmosphere. In support of this estimate and for ease of comparison with the ALE and other $CFCl_3$ measurements in the lower troposphere, the model results in each of the four lower tropospheric boxes have been fitted with an empirical model similar to that used to fit the ALE data, namely,

$$\ln \chi_c = a + b\left(\frac{t-18}{12}\right) + d\left(\frac{t-18}{12}\right)^2 + c_1 \cos\left(\frac{2\pi t}{12}\right) + c_2 \cos\left(\frac{4\pi t}{12}\right) + s_1 \sin\left(\frac{2\pi t}{12}\right) + s_2 \sin\left(\frac{4\pi t}{12}\right) \quad (18)$$

This empirical model is used to represent output from the two-dimensional model for the period July 1978 to June 1981. Since the model output is relatively smooth, containing variations on approximately the seasonal scale or longer, it is meaningful to derive both annual and semiannual terms in (18). The resulting empirical model coefficients are given in Table 8.

A comparison of the coefficients in Table 8 against those given in Table 4 reveals that the two-dimensional model slightly underpredicts the observed latitudinal variation of a_t. For comparison, this same model provides an excellent fit to the latitudinal variation observed for CF_2Cl_2 [*Cunnold et al.*, this issue], but it substantially underpredicts the observed latitudinal variation of methyl chloroform [*Prinn et al.*, this issue (*b*)]. The optimal code gives a horizontal transport factor F of approximately 1.6 which is based primarily on fitting the $CFCl_3$ and CF_2Cl_2 distributions which are more precisely determined than is the methyl chloroform distribution. Table 8, when compared with Table 4, indicates that the two-dimensional model does not simulate the observed $CFCl_3$ seasonal cycle very well (except at American Samoa), in general overpredicting its magnitude. We are currently attempting to use this result to derive additional information about large-scale transport in the atmosphere.

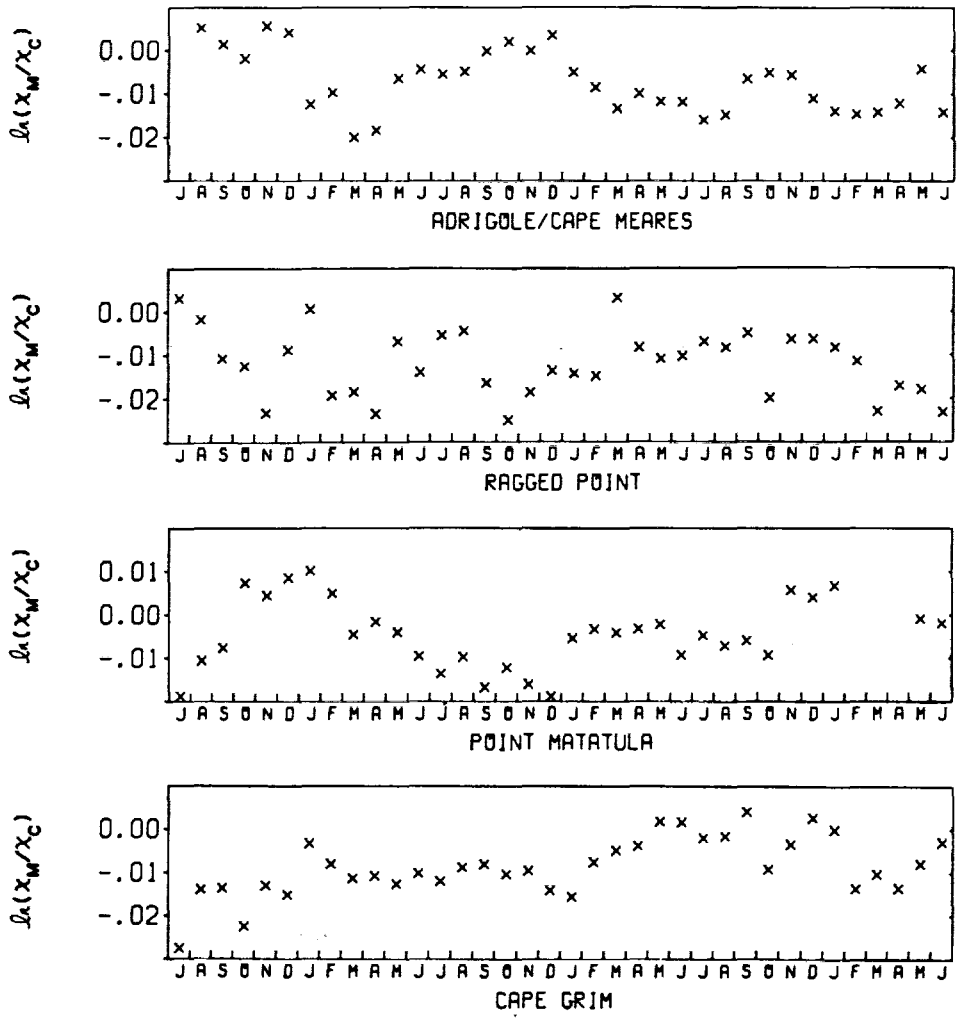

Fig. 13. $CFCl_3$ (P) residuals with respect to a two-dimensional model calculation with lifetime 83 years on January 1, 1980 (the trend best fit model). Residuals are given as the natural log of the ratio of the observed to the calculated mixing ratio.

Additional information about the use of our model together with ALE results for describing the atmospheric inventory of the lower troposphere may be obtained by comparing the model predictions against other measurements at different times and places. This comparison is given in Table 9 and is based on filtering seasonal variations out of the two-dimensional model results and adding the small seasonal cycle observed in the ALE to correct the model's seasonal predictions. Table 8 clearly exhibits some disagreement with respect to absolute calibration. It should be noted not only that the ALE absolute calibration experiments [*Rasmussen and Lovelock*, this issue] give $\xi = 0.96$ based on exponential dilution and coulometric techniques but also that absolute calibration by coulometry alone provides an even smaller ξ factor. Since some of the earliest measurements utilized coulometry, we suspect this to be a significant contributor to the absolute calibration differences. Of more importance, however, to this paper is the degree of agreement in the latitudinal distribution. The agreement appears to be within the precision of the various measurements except for *Lovelock*'s [1973] observations. It is to be noted (Table 4) that after identifiable pollution events have been removed that Adrigole, Ireland, and Cape Meares, Oregon, data give essentially the same concentration of $CFCl_3$. It is, therefore, concluded that *Lovelock*'s [1973] observations in the North Atlantic may have been influenced by regional, temporary pollution. It is also noteworthy that Point Barrow, Alaska (70°N latitude) exhibits a mixing ratio 2–3% higher than that at Niwot Ridge, Col-

TABLE 8. Empirical Model Fit (equation (18)) to the Two-Dimensional Model Calculations Which Provide the Best Fit to ALE-Determined Trends for $CFCl_3$ (Current Lifetime = 83 Years)

Box Number	a	b	d	c_1	c_2	s_1	s_2	$\ln^{-1} a$, pptv
1	5.190	0.051	−0.002	0.001	0.000	0.006	0.002	179.5
3	5.156	0.055	−0.004	−0.007	0.004	−0.012	−0.003	173.5
5	5.091	0.061	−0.005	−0.004	−0.003	−0.008	0.001	162.6
7	5.082	0.062	−0.004	0.001	−0.001	0.002	0.000	161.1

TABLE 9. Comparison Between Best (Trend) Fit Two-Dimensional Model and Non-ALE Observations of $CFCl_3$

Date of Measurement	Box 1 Mean Reported Measurement, pptv	Box 1 Calculated Mixing Ratio	Box 3 Mean Reported Measurement, pptv	Box 3 Calculated Mixing Ratio	Box 5 Mean Reported Measurement, pptv	Box 5 Calculated Mixing Ratio	Box 7 Mean Reported Measurement, pptv	Box 7 Calculated Mixing Ratio	Reporter
Nov. 1971	70	81	50	78	43	67	39	66	*Lovelock et al.* [1974]
Nov.–Dec. 1972			67	90	64	77	60	76	*Wilkniss et al.* [1975]
March–April 1974	95	112	86	105	76	96			*Wilkniss et al.* [1975]
March 1976			128	131	118	121			*Rasmussen et al.* [1977]
Sept. 1978	169	170	164	162	155	149			*Deluisi* [1981]
Jan. 1, 1980	179	180	172	174	162	165	160	162	ALE

Date of Measurement	Box 2 Mean Reported Measurement, pptv	Box 2 Calculated Mixing Ratio	Box 4 Mean Reported Measurement, pptv	Box 4 Calculated Mixing Ratio	Box 6 Mean Reported Measurement, pptv	Box 6 Calculated Mixing Ratio	Box 8 Mean Reported Measurement, pptv	Box 8 Calculated Mixing Ratio	Reporter
Fall 1976			135	138	131	127	128	126	*Rasmussen and Krasnec* [1977]

orado (40°N latitude) [*DeLuisi*, 1981]. The implicit assumption of a linear gradient within a two-dimensional model box is therefore reasonable for box 1 which, because most of the atmospheric injection occurs in this box, might be considered to be where the assumption is particularly questionable. We conclude, therefore, that the two-dimensional model is providing an accurate simulation of $CFCl_3$ in the lower troposphere. Moreover, since the observed difference between the mid-latitude northern hemisphere and mid-latitude southern hemisphere mixing ratios is only 11%, the precision of the estimate of the atmospheric inventory in the lower troposphere by the two-dimensional model is probably $\pm 1\%(1\sigma)$.

The only available latitude survey of $CFCl_3$ in the upper troposphere of which we are aware is by *Rasmussen and Krasnec* [1977]. From Table 8 it is noted that the model overpredicts the observed gradient. The predicted gradient can be reduced by increasing transport rates in the model and, in particular, the vertical transport rate. However, the two-dimensional model predicts that the average mixing ratio in the upper troposphere is, in any case, approximately 99% of that in the lower troposphere. Any increase in vertical transport rates can only increase this ratio to 100%; it therefore seems reasonable to use the calculated mixing ratio to estimate the atmospheric inventory and to assume that there exists an uncertainty of $\pm 1\%$ (1σ) in this estimate.

Stratospheric observations of $CFCl_3$ have been reported by several authors with the most extensive set of measurements being given by *Goldan et al.* [1980] (see also the recent WMO report [*World Meteorological Organization*, 1981]). If the measurements are referenced to height above the tropopause [see *Goldan et al.*, 1980, Figure 15] the altitude profile in the stratosphere is relatively independent of latitude. If a mean profile and the envelope of the measurements are constructed from the available measurements, the average mixing ratio above the tropopause (adjusted to January 1, 1980) is calculated to be 0.58 ± 0.10 (1σ) of that below the tropopause. In this calculation the uncertainty limits have been extended beyond the envelope derived from Figure 15 of *Goldan et al.* [1980] to include profiles measured by other investigators [e.g., *Heidt et al.*, 1975; *Fabian et al.*, 1979]. The principal cause of uncertainty in this calculation is the profile in the region from a few kilometers below the tropopause to a few kilometers above the tropopause. Using a troposphere to stratosphere transport time (t_s) of 4 years, a similar upper troposphere-to-stratosphere mixing ratio ratio (r) is obtained in the two-dimensional model. A somewhat different stratosphere to troposphere mixing ratio ratio has recently been obtained in a three-dimensional model by *Golombeck* [1982]. Using the temperatures, stream functions, and velocity potentials from *Cunnold et al.* [1975] and the presently accepted photodissociation cross section of $CFCl_3$, Golombeck obtained a globally averaged ratio of approximately 0.70 on January 1, 1981 (i.e., 1σ greater than our calculated value of 0.6). A similar ratio can be obtained in our two-dimensional model by using t_s approximately equal to 3 instead of 4 years. For the present, however, we shall be guided by our interpretation of the northern hemisphere measurements of $CFCl_3$ in the stratosphere (corresponding to $t_s = 4$ years) but recognize that this may result in an underestimate of the stratospheric content by approximately 14%. (Note that a change of t_s to 3 years from 4 years shortens the atmospheric lifetime determined by the trend technique by just 1 year.)

According to the optimal estimation algorithm discussed in section 5, the (trend) estimated lifetime of 83 years results in an overprediction of the atmospheric inventory of $CFCl_3$ on January 1, 1980, by 1.0%. This result corresponds to pressure weighting and summing the mixing ratio scaling factors discussed above to give an atmospheric inventory derived from the ALE network equal to

$$(0.5 \times 1 + 0.3 \times 0.99 + 0.2 \times 0.99 \times 0.58)\bar{\chi}_{ALE} = (0.91 \pm 0.03)\bar{\chi}_{ALE}$$

where $\bar{\chi}_{ALE}$ is the global mean mixing ratio in the lower troposphere determined by averaging the four ALE determined mixing ratios and multiplying by ξ. This gives a global chlorofluorocarbon content of approximately 3730×10^6 kg on January 1, 1980 (using 5.137×10^{18} kg for the mass of the atmosphere) which may be compared against the accumulated release prior to that time equal to 4110×10^6 kg and to a content of 3780×10^6 kg for a lifetime of 83 years. The lifetime estimated by the atmospheric inventory technique may be obtained by applying the partial derivatives given in Table 2 to the 1.0% underprediction cited above. Using the average

value of the partial derivative $\partial(\ln \chi_c)/\partial(1/\tau)$ equal to -4.4 in the lower troposphere, we obtain an atmospheric inventory lifetime of 70 years for January 1, 1980. Since this lifetime is shorter than that calculated for stratospheric photodissociation alone (78 years, *Golombeck* [1982]), this result may also be interpreted as being produced by stratospheric photodissociation combined with a small tropospheric sink. In that case, the partial derivative from line 4 of Table 2 ($= -7.7$) would be used to yield an atmospheric lifetime equal to

$$\left(0.0128 + \frac{4.4}{7.7} \times 0.0014\right)^{-1} = 74 \text{ years}$$

7. Discussion

To specify completely the uncertainty limits on the trend and inventory lifetimes, uncertainties in release must be assessed and combined with the measurement uncertainties. In this section, upper and lower limits on the release uncertainties will first be discussed based on calculations with a release code similar to that used by *McCarthy et al.* [1977]. To convert such uncertainties to uncertainties in lifetime, additional calculations were performed with the two-dimensional model. In such calculations, all the transport parameters were usually fixed and τ_s was varied so as to obtain a match between the observed and the calculated mixing ratios in the lower troposphere. It should be noted that this procedure resulted in some change in r, a parameter that was poorly defined by observation. Generally, it was found that the partial derivative $\partial \ln\chi/\partial(1/\tau) = -4.4$ (see line 3 of Table 2) provided a good estimate of the change in the inventory lifetime. Changes in release may be interpreted in this way by noting that a change in the accumulated release (R), Δ ln R, will produce a similar change in ln χ which must then be compensated for by a change in τ_s. The trend lifetime uncertainty may be derived from the change in I/R, where I is the average annual release for 1979 and 1980, and using $\partial(I/R)/\partial(1/\tau) = 0.36$.

The principal $CFCl_3$ production uncertainties involve how much $CFCl_3$ is produced in the Peoples Republic of China, which might be 1% of world production, which is neglected in the CMA production estimates, and how much is produced in the U.S.S.R. During the period 1970–1975, U.S.S.R. production data [*Borisenkov and Kazakov*, 1977] exhibited an average increase of 24% annually. The new *CMA* [1982] release estimates have assumed an increase of 18% since that time. If the difference between these two trends is assumed to be the (2σ) uncertainty in the U.S.S.R. production in the period 1975–1980, this translates into an uncertainty of approximately 0.5% (1σ) in world production in the ALE period of observation. Finally, while the CMA reporting company production numbers are believed to be accurate, there exists some loss (and release) during production. The revised CMA release estimates assume the loss is 1.5%; however, an uncertainty of 0.5% seems reasonable for this estimate. Combining the three sources of uncertainty discussed above as random errors, we obtain an uncertainty of $\pm 1.2\%$ (1σ). To translate this into an uncertainty in lifetime it will be assumed that this error in production translates into an error in release by aerosol cans, open-cell foams, and other prompt release uses for $CFCl_3$.

Two major uses of $CFCl_3$ have historically been its use as a propellant in aerosol cans and its use in the inflation of open-cell foams. In both cases, the delay in release relative to production is somewhat uncertain. For aerosol cans, a release delay of 6 months is assumed and the uncertainty in this is probably ± 1 month (1σ). For open-cell foams, there are indications that the $CFCl_3$ is lost almost immediately after injection, and the delay is therefore likely to be considerably shorter than 6 months. However, since aerosol cans dominate this release category, it seems reasonable to use ± 1 month release delay uncertainty for the entire category.

The third major use of $CFCl_3$ is in closed-cell foams. CMA's release scenarios for this category assumes 10% immediate release followed by steady loss over a 20 year period. Based on the work of *Brandreth and Ingersoll* [1980], *CMA* [1980*b*] estimate that the $CFCl_3$ in a typical closed-cell foam possesses a half-life of approximately 80 years. We believe, however, that even if this emission estimate is correct that the products containing these foams (e.g., houses and refrigerators) have a shorter half-life than this and that, therefore, 80 years is likely to be a (2σ) upper limit on the lifetime. In our calculations we use 10 years and 80 years to provide $\pm 2\sigma$ limits on the uncertainty in release delay for this use category.

The effect of these three release uncertainties is summarized in Table 10. Production, prompt release, and closed-cell foam lifetime uncertainties contribute almost equally to the uncertainty in the (reciprocal) inventory lifetime combining to give a 1σ error of 0.0051 years^{-1}. For the trend technique, the prompt release and closed-cell foam uncertainties contribute approximately equally to the reciprocal lifetime uncertainty and combine to give a 1σ of 0.0036 years^{-1}. The uncertainty due to release (0.0036 years^{-1}) can be combined with measurement uncertainties (0.0044 years^{-1}) to give an uncertainty in the trend reciprocal lifetime of 0.0057 years^{-1}. Based on the trend lifetime estimate of 83 years, this translates into upper and lower (1σ) limits on the lifetime of 156 and 56 years. The lower limit on the lifetime in the presence of stratospheric photodissociation (giving a lifetime of 78 years), combined with a tropospheric sink, may be found by using a partial derivative of 0.42 instead of 0.37 (from Table 2) and is

$$\left[0.0128 + (0.0057 - 0.0007) \times \frac{0.37}{0.42}\right]^{-1} = 58 \text{ years}$$

To estimate the inventory lifetime uncertainty, the effect of the release uncertainty (0.0051 years^{-1}) needs to be combined with the effect of the 2% uncertainty in absolute calibration (0.0045 years^{-1}) and with the effect of the 3.3% uncertainty in translating ALE measurements to an atmospheric overburden. This last uncertainty consisted of a 1% uniform uncertainty in the mixing ratio throughout the atmosphere (giving 0.0023 years^{-1}) together with an uncertainty primarily in r (resulting from uncertainties in t_s). The effect of the uncertainty in r has been derived by determining the changes in t_s and τ_s which would produce the prescribed change in $r(=0.1)$ together with no change in the mixing ratio in the lower troposphere (giving an inverse lifetime uncertainty of 0.0036 years^{-1}). Combining these errors gives an uncertainty in the reciprocal lifetime estimated by the atmospheric inventory technique of 0.0080 years^{-1} and gives upper and lower (1σ) limits on the 70-year inventory lifetime of 159 and 45 years. This lifetime estimate and uncertainty range is based on the assumption that the stratosphere is the only sink for $CFCl_3$; allowing for a tropospheric sink (using a partial derivative of -7.7 in place of -4.4) would give a lifetime of 74^{+38}_{-19} years where the upper

TABLE 10. Effect of Release Uncertainties on the $CFCl_3$ Reciprocal Lifetime Estimated Using $\partial(\ln R)/\partial(1/\tau) = 4.4$ years and $\partial(I/R)/\partial(1/\tau) = 0.36$ Where I and R are Expressed in Million kg

Release Scenario	Increase in Accumulated Release (R) to the End of 1979, 10^6 kg	$\Delta(1/\tau)$ Inventory Technique, years^{-1}	Average Change in Annual Release for the Period/Accumulated Release 1979–1980	$\Delta(1/\tau)$ Trend Technique, years^{-1}
1.2% additional production released as in the prompt release category	58	0.003	0.0001	—
5 month delay in prompt release category (versus 6 months used in *McCarthy et al.* [1977])	19	0.001	−0.0006	−0.002
Loss of $CFCl_3$ from closed-cell foams occurs over 10 years (this provides 2σ error so results have been divided by 2 to get 1σ error)	67	0.004	0.0011	0.003
Loss of $CFCl_3$ from closed-cell foams occurs over 80 years (results have been divided by 2 to get 1σ error)	−67	−0.004	−0.0011	−0.003

limit has no physical meaning since it exceeds the 78 year lifetime assumed to be due to stratospheric photodissociation.

Finally, to facilitate comparison of our results with previous estimates of the lifetime of $CFCl_3$, the optimal estimation procedure has been used to provide estimates of the lifetime based upon the pre-1982 CMA release figures [*CMA*, 1981*a*]. The trend estimate of the lifetime is 79 years in this case and the atmospheric inventory estimate is 115 years assuming the presence of stratospheric destruction only.

8. Conclusions

Observations of chlorofluorocarbon $CFCl_3$ obtained several times daily over the period July 1978 to June 1981 at Adrigole, Ireland (52°N, 10°W); Ragged Point, Barbados (13°N, 59°W); Point Matatula, American Samoa (14°S, 171°W); and Cape Grim, Tasmania (41°S, 145°E) have been described as well as observations for the period January 1980 to June 1981 at Cape Meares, Oregon (45°, 124°W). A procedure for estimating two-dimensional model parameters that provide the best fit to these observations in a weighted least squares sense has also been described. By using weighting factors based on the uncertainties in the monthly mean measurements, the data was first fit with an empirical model consisting of a linear trend, a curvature term, and an annual cycle. This model indicated that latitudinal differences were well defined by the observations with an average difference between northern and southern hemisphere mid-latitudes of 11%. A latitudinal progression in the temporal trend consistent with the northern hemisphere injection of chlorofluorocarbons was also noted. Only at American Samoa was there clear evidence of an annual cycle in the observations. Averaging the observations from the four semi-hemispheres of the globe, the average mixing ratio of $CFCl_3$ in the lower troposphere on January 1, 1980, was 168 pptv, and it was increasing at 5.7% per annum at that time.

Substitution of the empirical model by a nine-box, two-dimensional model of the atmosphere allowed atmospheric lifetimes to be estimated from the data. Based on the temporal trends in the ALE data in each of the four latitudinal regions, a lifetime of 83 years on January 1, 1980, was obtained. These calculations were based on assuming that stratospheric photodissociation was the only sink for $CFCl_3$. The estimated lifetime may be compared against recently reported estimates from model calculations of 78 years [*Golombeck*, 1982] and 74 years [*Owens et al.*, 1982]. The steady state lifetime was projected to be 70 years.

The lifetime of $CFCl_3$ was independently estimated based upon the average atmospheric inventory of $CFCl_3$ over the period July 1978 to June 1981. The average inventory is estimated to be 3730×10^6 kg; this corresponds to a lifetime of 70 years if there were no tropospheric destruction of $CFCl_3$ and to a lifetime of 74 years if stratospheric destruction were fixed to correspond to an atmospheric lifetime of 78 years.

Uncertainties in these estimates of lifetime were assessed. For the trend technique, the uncertainty resulted from differences between the measured and the predicted trends at each site and from uncertainty in the rate of release of $CFCl_3$ into the atmosphere. It was argued that the trend differences principally resulted from measurement errors rather than from inadequacies in the two-dimensional model and that the release uncertainty was dominated by the uncertain lifetime of $CFCl_3$ used in closed-cell foams and by the uncertain delay in release relative to production for the prompt release uses of $CFCl_3$ [*CMA*, 1982]. These uncertainties produced a (1σ) uncertainty range of 56–156 years for the trend lifetime estimate under the conditions of stratospheric destruction only (and a

lower limit of 58 years if stratospheric destruction were fixed at a value corresponding to a lifetime of 78 years).

Uncertainties in the lifetime estimated by the atmospheric inventory technique were also assessed. These consisted of a 2% uncertainty in the absolute calibration, a 3.3% uncertainty in translating measurements of $CFCl_3$ at the surface into a global inventory—primarily due to uncertainty in the stratospheric content—and uncertainties in the release of $CFCl_3$ into the atmosphere of approximately 2%. The last of these uncertainties consisted of production uncertainties, principally related to whether or not the Peoples Republic of China is producing chlorofluorocarbons and uncertainties in the releases from closed-cell foams. These uncertainties were combined to give a range for the lifetime estimate by the atmospheric inventory technique 70^{+89}_{-25} years for stratospheric destruction only and a range of 74^{+38}_{-19} years for the case of fixed stratospheric destruction. A note of caution on these uncertainty limits is that the absolute calibration uncertainty was derived from studies by just two investigators [*Rasmussen and Lovelock*, this issue].

Finally, the two independent techniques for obtaining a lifetime may be combined to yield a maximum likelihood estimate of the lifetime of 78 years. In deriving this estimate, the trend technique is favored because of the slightly smaller uncertainty limits associated with its estimate (this was one of the anticipated results of the ALE experiment suggested in *Cunnold et al.* [1978]).

APPENDIX

Analysis using the optimal estimation procedure may most easily be understood by considering the following example of its application to the estimation of two elements of a state vector from two measurements of a single specie. Let the a priori covariance matrix be

$$\mathbf{C}_0 = \begin{pmatrix} C_1 & 0 \\ 0 & C_2 \end{pmatrix}$$

the partial derivative matrix be

$$\mathbf{P} = \begin{pmatrix} p_1 & p_2 \\ p_1' & p_2' \end{pmatrix} = \begin{pmatrix} \dfrac{\partial \ln \chi_{c_1}}{\partial S_1} & \dfrac{\partial \ln \chi_{c_2}}{\partial S_2} \\ \dfrac{\partial \ln \chi_{c_2}}{\partial S_1} & \dfrac{\partial \ln \chi_{c_2}}{\partial S_2} \end{pmatrix}$$

where χ_c is a calculated mixing ratio of $CFCl_3$ and it is assumed that $p_1 = p_1'$ corresponding to the first state vector element being a calibration "error" (in which case $p_1 = p_1' = 1$), and the noise matrix of the measurements be

$$\mathbf{N} = \begin{pmatrix} \sigma_1^2 & 0 \\ 0 & \sigma_2^2 \end{pmatrix}$$

If δ_i and δ_2 are the deviations of the measurements from the model predictions made by using the state factor, $(S_1^0, S_2^0) \equiv (\ln A, 1/\tau)$, then it can be shown that the new estimates of the state vector are

$$S_1 = S_1^0 + \frac{c_1 p_1 \{\delta_1[\sigma_2^2 + c_2 p_2'(p_2' - p_2)] + \delta_2[\sigma_1^2 - c_2 p_2(p_2' - p_2)]\}}{(c_1 p_1^2 + c_2 p_2^2)\sigma_2^2 + (c_1 p_1^2 + c_2 p_2'^2)\sigma_1^2 + c_1 c_2 p_1^2 (p_2' - p_2)^2} \quad \text{(A1)}$$

and

$$S_2 = S_2^0 + \frac{c_2\{\delta_1[\sigma_2^2 p_2 - c_1 p_1^2(p_2' - p_2)] + \delta_2[\sigma_1^2 p_2' + c_1 p_1^2(p_2' - p_2)]\}}{(c_1 p_1^2 + c_2 p_2^2)\sigma_2^2 + (c_1 p_1^2 + c_2 p_2'^2)\sigma_1^2 + c_1 c_2 p_1^2 (p_2' - p_2)^2} \quad \text{(A2)}$$

These solutions provide two interesting limiting cases. First, if $p_2 = p_2'$,

$$S_1 = S_1^0 + \left(\frac{c_1 p_1}{c_1 p_1^2 + c_2 p_2^2}\right) \cdot \left(\frac{\sigma_2^2 \delta_1 + \sigma_1^2 \delta_2}{\sigma_1^2 + \sigma_2^2}\right) \quad \text{(A3)}$$

and

$$S_2 = S_2^0 + \left(\frac{c_2 p_2}{c_1 p_1^2 + c_2 p_2^2}\right) \cdot \left(\frac{\sigma_2^2 \delta_1 + \sigma_1^2 \delta_2}{\sigma_1^2 + \sigma_2^2}\right) \quad \text{(A4)}$$

Thus, the measured deviations (δ) are weighted inversely as their uncertainty and contribute to updates of both S_1 and S_2 in the proportion $c_1 p_1 : c_2 p_2$. This situation may arise when we attempt to deduce the calibration error and the lifetime from just a few months of data at a single site since dp_2/dt is small.

The more interesting limiting case is when $\sigma_1^2 = \sigma_2^2 \simeq 0$. Then

$$S_1 = S_1^0 + \frac{p_2'\delta_1 - p_2\delta_2}{p_1(p_2' - p_2)} = S_1^0 + \frac{\delta_1 + \delta_2}{2p_1} + \frac{p_2' + p_2}{2p_1}\frac{(\delta_1 - \delta_2)}{(p_2' - p_2)} \quad \text{(A5)}$$

$$S_2 = S_2^0 + \frac{\delta_2 - \delta_1}{p_2' - p_2} \quad \text{(A6)}$$

Thus, for two measurements at a single site at different times, the lifetime, S_2, will be determined by the trend method. For measurements at the same time at different locations the lifetime (or the diffusion coefficient factor if it is the unknown) will be determined by the horizontal gradient. In either case, the absolute calibration error, S_1, receives an update from the mean underprediction, $(\delta_1 + \delta_2)/2$, together with a contribution from the update of S_2, $(\delta_2 - \delta_1)/(p_2^1 - p_2)$. This effect produces nonzero off-diagonal elements in the covariance matrix.

A second useful example of the application of the optimal estimation analysis to ALE data is obtained for a series of measurements (all having equal uncertainty) of a single specie at a single station. Then it can be shown analytically that, for $\sigma^2 \to 0$ the update of the lifetime is given by

$$\Delta\left(\frac{1}{\tau}\right) = \frac{N\sum_{i=1}^{N} p_i\delta_i - \left(\sum_{i=1}^{N} p_i\right)\left(\sum_{i=1}^{N} \delta_i\right)}{\sum_{i=1}^{N}\sum_{j=1}^{i}(p_i - p_j)^2} \equiv \frac{R\sigma_\delta}{\sigma_p} \quad \text{(A7)}$$

where

$$R = \frac{\sum_{i=1}^{N}(p_i - \bar{p})(\delta_i - \bar{\delta})}{N\sigma_p\sigma_\delta}$$

and overbar denotes the mean of the N observations. The variance of this estimate can be shown to equal

$$\frac{\sigma_\delta^2}{N\sigma_p^2}$$

which is identical to the result given in equation (4) of *Cunnold et al.* [1978].

Acknowledgments. This research was supported by the Flurocarbon Program Panel of the Chemical Manufacturers Association. Nominal support has also been provided by the Upper Atmosphere Research Program of NASA (to R.A.R.). We are particularly grateful to Bruce Lane of the Fluorocarbon Panel for his unceasing efforts to determine the accuracy and precision of the $CFCl_3$ release estimates.

REFERENCES

Bevington, C., and A. Wallace, Aspects of effecting further reductions in chlorofluorocarbon usage in the EEC, Final Rep. (and Addendum) to the Commission of European Communities, Metra Consulting Group Limited, London, 1981.

Borisenkov, Ye. P., and Yy. Ye. Kazekov, Effect of freons and halocarbons on the ozone layer of the atmosphere and climate, report, United Nations Environ. Programme, New York, 1977.

Brandreth, D., and H. Ingersoll, Accelerated aging of rigid polyurethane foam, paper presented at Proceedings of the International Conference on Cellular and Non-Cellular Urethanes, Plastics Industry, Strasbourg, France, June 1980.

Chemical Manufacturers Association, Environmental analysis of fluorocarbons FC-11, FC-12, and FC-22, Rep. of the Fluorocarbon Program Panel, Washington, D.C. 1976.

Chemical Manufacturers Association, Environmental analysis of fluorocarbons FC-11, FC-12, and FC-22, of the Fluorocarbon Program Panel, Washington, D. C., 1977.

Chemical Manufacturers Association, World production and sales of fluorocarbons FC-11 and FC-12: 1977, Rep. of the Fluorocarbon Program Panel, Washington, D. C., 1978.

Chemical Manufacturers Association, World production and salesof fluorocarbons FC-11 and FC-12: 1978, Rep. of the Fluorocarbon Program Panel, Washington, D. C., 1979.

Chemical Manufacturers Association, World production and sales of fluorocarbons FC-11 and FC-12: 1979, Rep. of the Fluorocarbon Program Panel, Washington, D. C., 1980*a*.

Chemical Manufacturers Association, U.S. emissions of CFC-11 from rigid plastic foams, final report, contract FC-79-275, Arthur D. Little, Washington, D. C., 1980*b*.

Chemical Manufacturers Association, World production and release of chlorofluorocarbons 11 and 12 through 1980, Rep. of the Fluorocarbon Program Panel, Washington, D. C., 1981*a*.

Chemical Manufacturers Association, World production and sales of fluorocarbons FC-11 and FC-12: 1980, Rep. of the Fluorocarbon Program Panel, Washington, D. C., 1981*b*.

Chemical Manufacturers Association, World production and release of chlorofluorocarbons 11 and 12 through 1981, Rep. of the Fluorocarbon Program Panel, Washington, D. C., 1982.

Commission of European Communities, Chlorofluorocarbons in the environment, Communication to the Council, *COM(80)339*, 1980.

Commission of European Communities, Information and basis for evaluation for the pursuit of chlorofluorocarbons in the environment, Communication to the Council, *COM(81)261*, 1981.

Cunnold, D., F. Alyea, N. Phillips, and R. Prinn, A three-dimensional dynamical-chemical model of atmospheric ozone, *J. Atmos. Sci., 32*, 170–194, 1975.

Cunnold, D., F. Alyea, and R. Prinn, A methodology for determining the atmospheric lifetime of fluorocarbons, *J. Geophys. Res., 83*, 5493–5500, 1978.

Cunnold, D., M., R. G. Prinn, R. A. Rasmussen, P. G. Simmonds, F. N. Alyea, C. A. Cardelino, and A. J. Crawford, The Atmospheric Lifetime Experiment, 4,: Results for CF_2Cl_2 based on 3 years data, *J. Geophys. Res.*, this issue.

DeLuisi, J. J., Geophysical monitoring for climatic change, Summary report 1980, Air Resources Lab., Boulder, Colo., December 1981.

Department of Environment, Chlorofluorocarbons and their effect on stratospheric ozone, Second report, *Pollut. Pap. 15*, Central Directorate on Environ. Pollut., Her Majesty's Stationery Office, London, 1979.

Fabian, P., R. Borchers, K. W. Weiler, U. Schmidt, A. Volz, D. H. Ehhalt, W. Seiler, and F. Muller, Simultaneously measured vertical profiles of H_2, CH_4, CO, N_2O, $CFCl_3$, and CF_2Cl_2 in the midlatitude stratosphere and troposphere, *J. Geophys. Res., 84*, 3149–3154, 1979.

Frederick, J., and J. Mentall, Solar irradiance in the stratosphere: Implications for the Herzberg continuum absorption of O_2, *Geophys. Res. Lett., 9*, 461–464, 1982.

Gelb, A., *Applied Optimal Estimation*, M.I.T. Press, Cambridge, Mass., 1974.

Goldan, P. D., W. C. Kuster, D. L. Albritton, and A. L. Schmeltekopf, Stratospheric $CFCl_3$, CF_2Cl_2, and N_2O height profile measurements at several latitudes, *J. Geophys. Res., 85*, 412–423, 1980.

Golombeck, A., A global three-dimensional model of the circulation and chemistry of long-lived atmospheric species, Ph.D. Thesis, Mass. Inst. of Tech., Cambridge, 1982.

Heidt, L. E., R. Lueb, W. Pollack, and D. H. Ehhalt, Stratospheric profiles of CCl_3F and CCl_2F_2, *Geophys. Res. Lett., 2*, 445–447, 1975.

Jesson, J., P. Meakin, and L. Glasgow, The fluorocarbon-ozone theory, 2, Tropospheric lifetimes: An estimate of the tropospheric lifetime of $CFCl_3$, *Atmos. Environ., 11*, 449–508, 1977.

Ko, M. K. W., and N. D. Sze, A 2-D model calculation of atmospheric lifetimes for N_2O, CFC-11, and CFC-12, *Nature, 297*, 317–319, 1982.

Lovelock, J. E., R. J. Maggs, and R. J. Wade, Halogenated hydrocarbons in and over the Atlantic, *Nature, 241*, 194–196, 1973.

Lorenz, E., An N-cycle time-differencing scheme for stepwise numerical integration, *Mon. Weather Rev., 99*, 644–648, 1971.

McCarthy, R. L., F. A. Bower, and J. P. Jesson, The fluorocarbon-ozone theory, 1, Production and release: World production and release of CCl_3F and CCl_2F_2 (fluorocarbons 11 and 12) through 1975, *Atmos. Environ., 2*, 491–497, 1977.

Molina, M. J., and F. S. Rowland, Stratospheric sink for chlorofluoromethanes: Chlorine catalysed destruction of ozone, *Nature, 249*, 810–812, 1974*a*.

Molina, M. J., and F. S. Rowland, Predicted present stratospheric abundances of chlorine species from photodissociation of carbon tetrachloride, *Geophys. Res. Lett., 1*, 309–312, 1974*b*.

National Academy of Sciences, Causes and effects of stratospheric ozone reduction: An update, Washington, D. C., 1982.

NASA, The stratosphere: Present and Future, *NASA Ref. Publ. 1049*, 1979.

Newell, R. E., D. G. Vincent, and J. W. Kidson, Interhemispheric mass exchange from meteorological and trace substance observations, *Tellus* 21, 641–647, 1969.

Owens, A. J., J. M. Steed, C. Miller, D. L. Filkin, and J. P. Jesson, The atmospheric lifetimes of CFC 11 and CFC 12, *Geophys. Res. Lett., 9*, 700–703, 1982.

Parzen, E., An approach to empirical time series analysis, *Radio Sci. J. Res., 68D*, 551–565, 1964.

Prinn, R. G., P. G. Simmonds, R. A. Rasmussen, R. D. Rosen, F. N. Alyea, C. A. Cardelino, A. J. Crawford, D. M. Cunnold, P. J. Fraser, and J. E. Lovelock, The Atmospheric Lifetime Experiment, 1, Introduction, instrumentation and overview, *J. Geophys. Res.*, this issue (*a*).

Prinn, R. G., R. A. Rasmussen, P. G. Simmonds, F. N. Alyea, D. M. Cunnold, B. Lane, A. J. Crawford, and C. Cardelino, The Atmospheric Lifetime Experiment, 5, Results for CH_3CCl_3 based on 3 years of data, *J. Geophys. Res.*, this issue (*b*).

Ramanathan, V., Greenhouse effect due to chlorofluorocarbons: Climatic implications, *Science, 190*, 50–52, 1975.

Rasmussen, R. A., and J. Krasnec, Interhemispheric survey of minor upper atmospheric constituents during October–November 1976, *NASA TMX-73630*, 1977.

Rasmussen, R. A., and J. E. Lovelock, The Atmospheric Lifetime Experiment, 2, Calibration, *J. Geophys. Res.*, this issue.

Rasmussen, R. A., D. Pierotti, and J. Krasnec, Cruise report of the Alpha Helix, Washington State Univ., Pullman, 1977.

Simmonds, P. G., F. N. Alyea, D. M. Cunnold, J. E. Lovelock, R. G. Prinn, R. A. Rasmussen, B. C. Lane, C. A. Cardelino, and A. J. Crawford, The Atmospheric Lifetime Experiment, 6, Results for CCl_4 based on 3 years of data, *J. Geophys. Res.*, this issue.

Stolarski, R. S., and R. J. Cicerone, Stratospheric chlorine: A possible sink for ozone, *Can. J. Chem., 52*, 1610–1615, 1974.

Sze, N. D., and M. F. Wu, Measurements of fluorocarbons 11 and 12 and model validation: An assessment, *Atmos. Environ., 10*, 1117–1125, 1976.

Wilkniss, P. E., J. W. Swinnerton, R. A. Lamontagne, and D. J. Bresson, Trichlorofluoromethane in the troposphere, distribution and increase, 1971 to 1974, *Science, 187*, 832–834, 1975.

World Meteorological Organization, The stratosphere 1981, Theory

and measurements, *WMO Global Ozone Res. and Monit. Proj. Rep.* 11, Geneva, Switzerland, 1982.

F. N. Alyea, C. A. Cardelino, and D. M. Cunnold, School of Geophysical Sciences, Georgia Institute of Technology, Atlanta, GA 30332.

A. J. Crawford and R. A. Rasmussen, Department of Environmental Science, Oregon Graduate Center, Beaverton, OR 97005.

P. J. Fraser, Division of Atmospheric Physics, CSIRO, Aspendale, Victoria, Australia.

R. G. Prinn, Department of Meteorology and Physical Oceanography, Massachusetts Institute of Technology, Cambridge, MA 02139.

R. D. Rosen, Atmospheric and Environmental Research, Inc., Cambridge, MA 02139.

P. G. Simmonds, Department of Geochemistry, University of Bristol, Bristol, England.

(Received July 12, 1982;
revised March 29, 1983;
accepted April 25, 1983.)

JOURNAL OF GEOPHYSICAL RESEARCH, VOL. 88, NO. C13, PAGES 8401-8414, OCTOBER 20, 1983

The Atmospheric Lifetime Experiment 4. Results for CF_2Cl_2 Based on Three Years Data

D. M. CUNNOLD,[1,2] R. G. PRINN,[2,3] R. A. RASMUSSEN,[4] P. G. SIMMONDS,[5] F. N. ALYEA,[1,2] C. A. CARDELINO,[1,2] AND A. J. CRAWFORD[4]

Observations of dichlorodifluoromethane obtained several times daily over the period July 1978 to June 1981 at Adrigole, Ireland (52°N, 10°W), Ragged Point, Barbados (13°N, 59°W), Point Matatula, American Samoa (14°S, 171°W), and Cape Grim, Tasmania (41°S, 145°E), are reported. Observations at Cape Meares, Oregon (45°N, 124°W), are also given for the period November 1980 to June 1981. On January 1, 1980, the average mixing ratio of dichlorodifluoromethane in the lower troposphere is estimated to have been 285 pptv and to have been increasing at 6.0%/year. The atmospheric lifetime of this compound is estimated from this data by adjusting its destruction rate in a two-dimensional model of the atmosphere so as to provide the best fit to the observations. Assuming destruction of CF_2Cl_2 in the stratosphere only, the lifetime estimate for January 1, 1980, by the inventory technique is 69^{+36}_{-18} years. The trend technique principally provides a lower limit to the lifetime of 81 years. The results suggest a need for further assessment of dichlorodifluoromethane release estimates, particularly those from the USSR and eastern Europe.

1. INTRODUCTION

Measurements during the 1970s indicate that dichlorodifluoromethane (CF_2Cl_2) is steadily accumulating in the atmosphere. This accumulation is not surprising since the atmospheric lifetime of dichlorodifluoromethane, owing to its only recognized sink (stratospheric photodissociation), is calculated by *Golombeck* [1982] to be about 222 years (currently) and by *Owens et al.* [1982] to be 120 years (at steady state). For reference in this paper we shall assume an intermediate value of 180 years to represent the lifetime on January 1, 1980, resulting from stratospheric photodissociation only. The major uncertainty in this figure is the result of uncertainties in the relevant absorption cross sections and in the transport of CF_2Cl_2 into and through the lower stratosphere. Despite the observed accumulation, model calculations indicate that current CF_2Cl_2 (and $CFCl_3$) levels are not high enough to produce detectable effects on ozone [*Penner*, 1982]. However, the very long lifetime, combined with current industrial release rates of CF_2Cl_2, leads to the prediction that it could have marked effects on ozone by the end of this century [*World Meteorological Organization*, 1982]. The magnitude of the ultimate effect depends upon many factors, including the future release rates of chlorofluorocarbons into the atmosphere, the rate of chemical interactions involving certain radical species in the stratosphere and with other source gases whose concentrations are increasing (A. J. Owens et al., unpublished manuscripts, 1983), and the true (rather than theoretical) atmospheric lifetime of CF_2Cl_2.

Atmospheric observations of dichlorodifluoromethane during the 1970s have been fewer than for trichlorofluoromethane, and while it has been obvious that dichlorodifluoromethane has been accumulating in the atmosphere, precise experimental estimates of its lifetime have not been made. If dichlorodifluoromethane were to possess an additional sink comparable with its stratospheric photodissociation, its ultimate effect on atmospheric ozone would be reduced approximately 50%.

Cunnold et al. [1978] calculated that a network of four surface measurement sites around the world could, with three to four years of measurements, substantially reduce the uncertainties in then existing estimates of the $CFCl_3$ and, by implication, the CF_2Cl_2 lifetime. This study, moreover, emphasized that because the rate of increase of these two chlorofluorocarbons with time was changing during the late seventies, their temporal trends in the atmosphere could be used to deduce a lifetime. Furthermore, such a lifetime estimate substantially eliminated instrumental absolute calibration uncertainties and absolute errors in production and release that would alias results obtained by a direct analysis of the instantaneous atmospheric inventory of these chlorofluorocarbons.

On the basis of the above theoretical work, experimental measurements of $CFCl_3$, CF_2Cl_2, CH_3CCl_3, CCl_4, and N_2O were instigated and have been made almost continuously, at approximately 6-hour intervals, by using HP5840A gas chromatographs at Adrigole, Ireland, Ragged Point, Barbados, Point Matatula, American Samoa, and Cape Grim, Tasmania, since July 1978 and at Cape Meares, Oregon, since January 1980. An overview of the experiment, which is known as the atmospheric lifetime experiment (ALE) is provided in *Prinn et al.* [this issue (*a*)]. The calibration techniques are discussed by *Rasmussen and Lovelock* [this issue]. The technique for the simultaneous analysis of all the ALE data to determine species lifetimes and global circulation rates is described by *Cunnold et al.* [this issue] and applied specifically to $CFCl_3$. It is therefore recommended that this latter paper be consulted before the present paper. In this paper we first present the ALE results for the three year period July 1978 through June 1981 for the chlorofluorocarbon CF_2Cl_2. The analysis of these results in terms of the industrial emission rates, global circulation, and atmospheric lifetime of CF_2Cl_2 are then discussed in detail.

[1]School of Geophysical Sciences, Georgia Institute of Technology.
[2]CAP, Inc.
[3]Department of Meteorology and Physical Oceanography, Massachusetts Institute of Technology.
[4]Department of Environmental Science, Oregon Graduate Center.
[5]Department of Geochemistry, University of Bristol.

Paper number 3C0670.
0148-0227/83/003C-0670$05.00

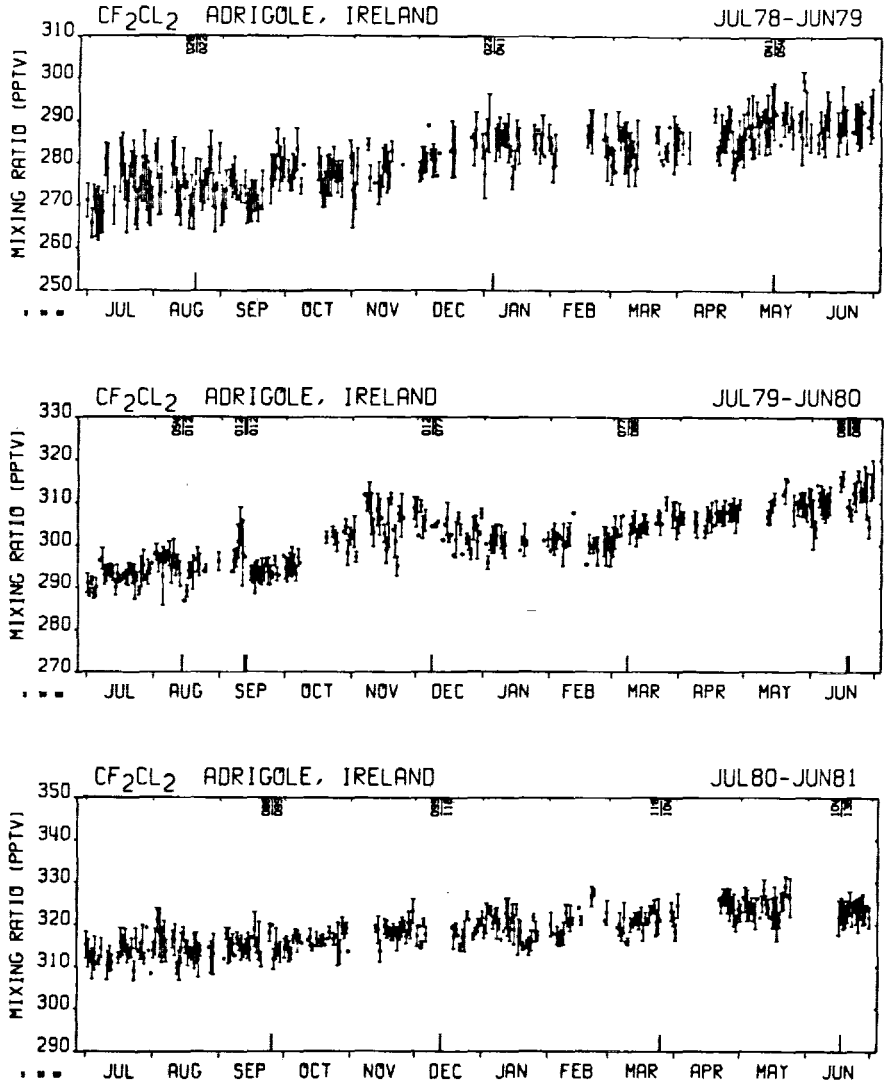

Fig. 1. CF_2Cl_2 daily means (pptv) and standard deviations at Adrigole, Ireland (52°N, 10°W) for the period July, 1978 to June, 1981. Changes of the calibration gas tank are noted on the upper abscissae.

2. GLOBAL CF_2Cl_2 DATA

Figures 1–5 show the daily CF_2Cl_2 data for the period July 1978 to June 1981. The range of the (~4) measurements on each day is indicated by the error bars that correspond to one standard deviation. Each measurement has been calibrated by direct comparison with the known concentration of CF_2Cl_2 in the on site calibration tank and an absolute calibration factor of 0.95 [*Rasmussen and Lovelock*, this issue] has been applied to all the data. The chromatographic analysis of CF_2Cl_2 uses a Porasil column and an electron capture detector.

The Adrigole, Ireland, CF_2Cl_2 data (Figure 1) contains the most gaps, primarily because of the elimination of pollution events that have been identified by correlated increases of $CFCl_3$, CF_2Cl_2, and CH_3CCl_3 and with elevated levels of

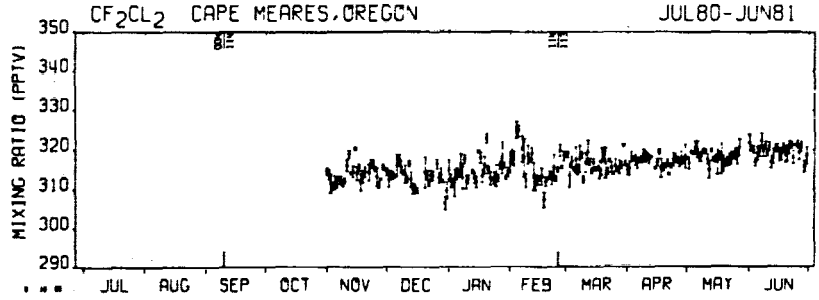

Fig. 2. CF_2Cl_2 daily means (pptv) and standard deviations at Cape Meares, Oregon (45°N, 124°W) for the period December, 1979 to June, 1981. Changes of the calibration gas tank are noted on the upper abscissae.

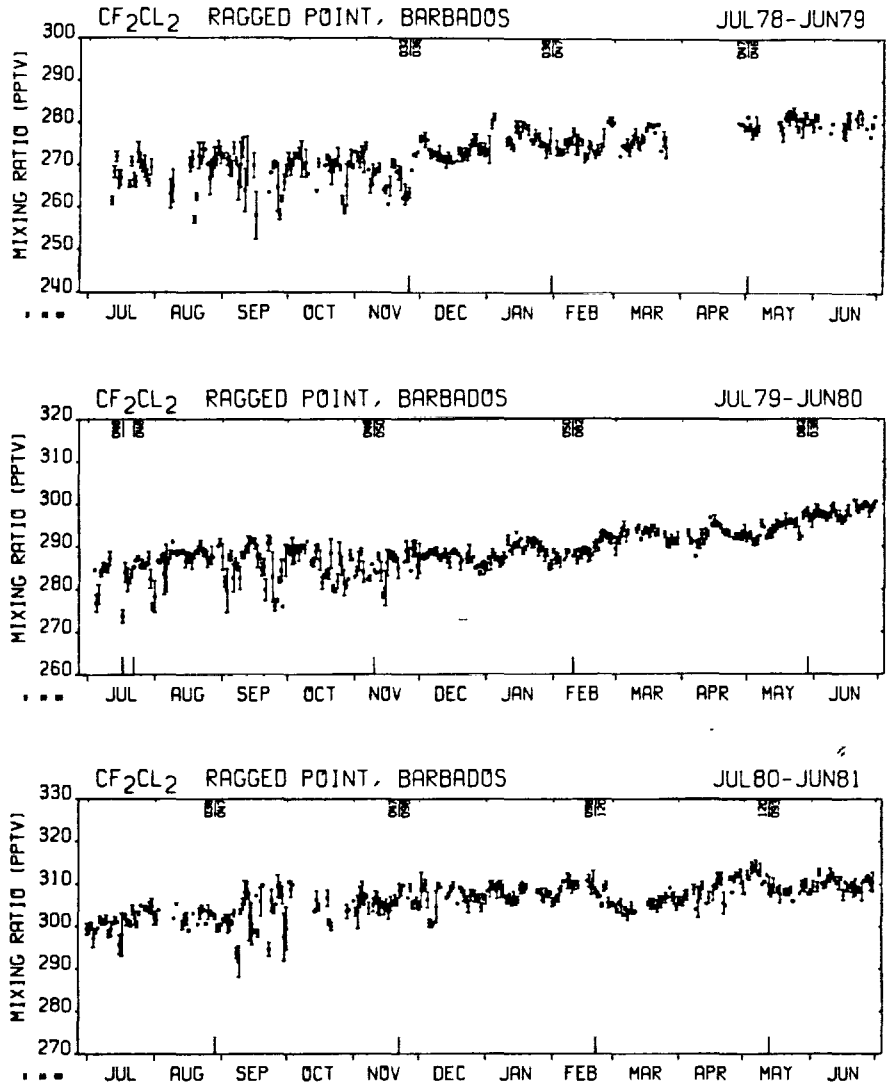

Fig. 3. CF_2Cl_2 daily means (pptv) and standard deviations at Ragged Point, Barbados (13°N, 59°W) for the period July, 1978 to June, 1981. Changes of the calibration gas tank are noted on the upper abscissae.

perchloroethylene. These events generally last for a few days. In the spring and summer of 1981, electrical supply problems occurred at Adrigole, which produced some gaps in the CF_2Cl_2 record at that time.

At all sites the precision of the measurements appears to vary from time to time. A deterioration of instrumental precision is usually associated with the aging of components; sudden increases in precision, on the other hand, may be produced by a major overhaul of the instrument. Changes in precision are also associated with occasional decisions by the field investigators to report chromatogram peak heights instead of the usual machine-derived areas. The latter decisions are usually associated with a substantial degradation in the instrument's normal sensitivity and have usually been made to apply to extended periods of time rather than to isolated events. The manual measurement of peak heights often results in a more precise, but not necessarily more accurate, estimate of the CF_2Cl_2 concentration.

The CF_2Cl_2 record at Cape Meares covers only nine months because of contamination during the first nine months of operation at this site by a leaky air conditioner in the ALE building. As may be seen from the continuity of the data after October 1980 pollution events at Cape Meares, Oregon, are rare (only at Adrigole, Ireland, is the perchloroethylene level sufficiently high to provide an independent assessment of regional pollution).

The CF_2Cl_2 record at Ragged Point, Barbados, is noteworthy for the substantial day to day variability occurring in July through November of each year. This may, in part, be due to effects on the island's power supply resulting from the intense storms, including hurricanes, that occur at this time of year. There is, however, strong evidence, based on simultaneous decreases of $CFCl_3$, CF_2Cl_2, and CH_3CCl_3, that southern hemisphere air is occasionally intruding into the northern hemisphere at this time of year. The instrument was out of operation in April 1979 because of difficulties in obtaining necessary supplies.

The most severe problems associated with the electrical supply and with the remoteness, and therefore inaccessibility, of the ALE sites have been experienced at Point Matatula, American Samoa. The instrument was burned out by surges in the electrical supply in October 1980 and

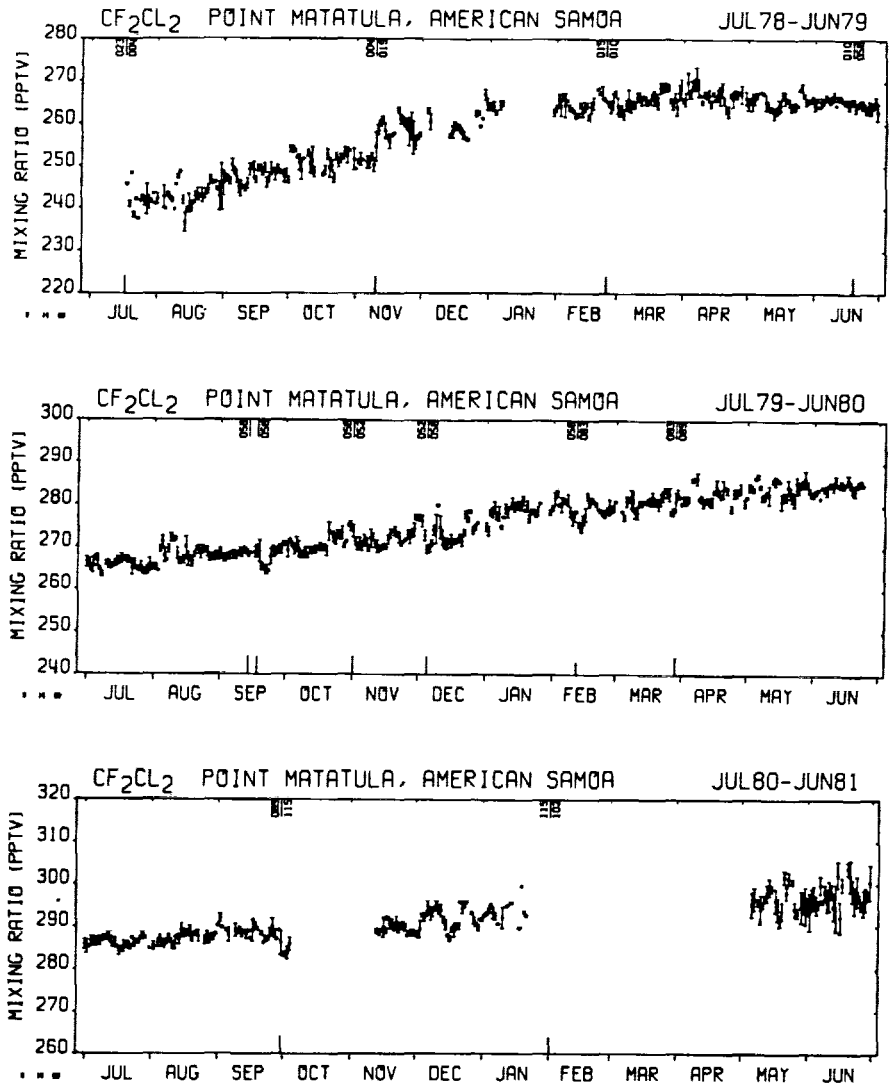

Fig. 4. CF_2Cl_2 daily means (pptv) and standard deviations at Point Matatula, American Samoa (14°S, 171°W) for the period July, 1978 to June, 1981. Changes of the calibration gas tank are noted on the upper abscissae.

January 1981; it did not return to full operation until May 1981. A visual inspection of the CF_2Cl_2 record at Point Matatula suggests that there is a discontinuity in the record occurring on November 10, 1978. At that time the sample loop size was changed from 3 to 2 ml; we are, however, unaware of any reason why this should have produced such a discontinuity. However, the N_2O record, which has been very stable since November 1978 and which is also obtained on the Porasil column, exhibited an anomalous trend during the first four months of operation. This suggests that the trend of CF_2Cl_2 from July to November 1978 may be anomalous. It is interesting to note that there often exists at Point Matatula as well as at all the other sites a characteristic "down then up" signature that is produced over the course of the week following a change of calibration tanks.

Before discussing the data at Cape Grim, Tasmania, a note on the calibration tanks is necessary. The CF_2Cl_2 in the ALE calibration tanks was measured to a precision of 0.5% prior to shipment to the sites and (except for a few tanks that were inadvertently emptied during return shipment) again on return to Oregon. Some of these tanks have been rechecked for calibration and returned to the ALE sites, while others have been monitored occasionally in Oregon over the three-year period. In most cases, the calibrated value of the tanks has been found to be maintained to a precision of better than 0.5% [*Rasmussen and Lovelock*, this issue]. Any discontinuities in the ALE data record due to replacement of the calibration tank (indicated on the upper abscissae of the figures) should not generally, therefore, exceed approximately 1%. Tank 084, which was used at Cape Grim, Tasmania between February and September 1980, however, showed a drift in CF_2Cl_2 of approximately 0.8 pptv/month over the period January 1980 to November 1981, a change far larger than that for any other ALE tank. Because no reasonable assumption about the calibrated value of CF_2Cl_2 in this tank removed discontinuities in the ALE record, this period has been removed from the Cape Grim, Tasmania CF_2Cl_2 data. At Cape Grim, the sample loop size on the Porasil column was changed from 4 to 3 ml on November 4, 1978, and as at Point Matatula, a visual inspection of the record suggests the possible presence of a discontinuity associated with this change. During the period December 1978 to January 1979, the air sample inlet valve became obviously contaminated, and this period has been removed

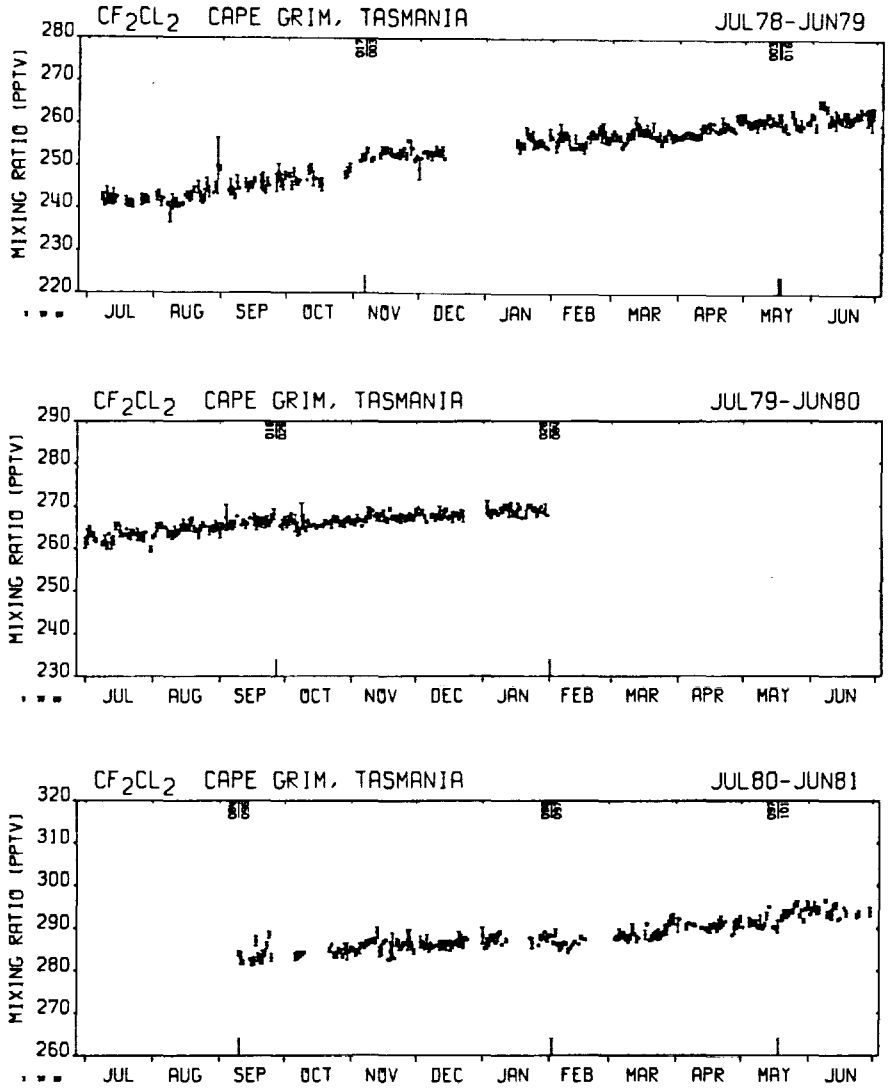

Fig. 5. CF_2Cl_2 daily means (pptv) and standard deviations at Cape Grim, Tasmania (41°S, 145°E) for the period July, 1978 to June, 1981. Changes of the calibration gas tank are noted on the upper abscissae.

from the record. Overall, however, we note that there appears to be, not unexpectedly, less variability of CF_2Cl_2 at Cape Grim, Tasmania, than at the other sites, which should result in a more precise estimate of the trend there.

The data shown in Figures 1–5 has been processed to yield monthly means and standard deviations. The results are given in Table 1. The analysis of the data to yield lifetimes is based on the data in Table 1.

The optimal estimation code described in *Cunnold et al.* [this issue] has been used to determine the best fit empirical model to the monthly mean values derived from the data shown in Figures 1–5. The form of the empirical model used is

$$\ln \chi_i = a_i + b_i\left(\frac{t-18}{12}\right) + d_i\left(\frac{t-18}{12}\right)^2 + c_1 \cos\left(\frac{2\pi t}{12}\right) + s_1 \sin\left(\frac{2\pi t}{12}\right) \quad (1)$$

where χ_i is expressed in pptv and t is given in months with month 1 being July 1978. The data is thus being fitted with a linear trend, a curvature, and an annual cycle. Since the Cape Meares, Oregon, record contained only nine months of data, no attempt was made to model it. The analysis procedure provides maximum likelihood estimates of the above parameters, weighting each months' data by

$$\sigma^{-2} = \left(\frac{\sigma_m^2}{n_m} + \sigma'^2_0\right)^{-1} \quad (2)$$

where σ_m is the standard deviation of the measurements during the month m, n_m is the number of observations made during the month divided by 12 (to allow for a typical observed three-day correlation between the measurements), and $\sigma_0'^2$ is the variance of the residuals of the monthly mean observations relative to the empirical model (σ_0^2) (determined a posteriori and given in Table 2) multiplied by a factor M. For CF_2Cl_2, σ_0^2 is typically about twice σ_m^2/n_m. The factor M was obtained, as described in *Cunnold et al.* [this issue], from an examination of the temporal autocovariance of the residuals and is intended to account for the effect of month to month autocorrelations on the uncertainty of estimating a trend b_i in the data. This factor produced

TABLE 1. Monthly Averaged CF_2Cl_2 Mixing Ratios χ (pptv), Their Standard Deviations σ_m (pptv), and the Number of Measurements During Each Month (N) Determined From Measurements at the Five ALE Sites Over the Period July 1978 Through June 1981

	Adrigole, Ireland			Cape Meares, Oregon			Ragged Point, Barbados			Point Matatula, American Samoa			Cape Grim, Tasmania		
Month	χ	σ_m	N	χ	σ_m	N	χ	σ_m	N	χ	σ_m	N	χ	σ_m	N
July 1978	273.7	7.1	235				269.0	2.9	124	241.7	2.3	42	241.9	1.2	54
Aug. 1978	275.0	6.2	200				270.2	4.2	102	243.1	2.9	80	243.0	3.0	86
Sept. 1978	274.9	5.7	214				268.5	5.3	132	247.9	2.0	98	245.8	1.8	65
Oct. 1978	277.7	4.5	159				269.4	3.9	84	251.3	2.5	68	247.6	1.7	50
Nov. 1978	277.5	5.4	107				268.2	3.8	79	256.8	4.2	84	253.1	1.2	66
Dec. 1978	281.9	4.6	45				273.4	2.0	104	260.1	2.9	48	252.9	1.3	43
Jan. 1979	285.1	4.7	76				276.7	2.7	88	264.2	1.1	20	256.0	1.4	50
Feb. 1979	284.4	4.8	32				275.1	2.6	86	264.7	2.0	98	256.7	1.6	98
March 1979	283.7	4.9	69				276.8	2.4	74	265.9	2.2	119	257.6	1.4	112
April 1979	285.4	4.6	58				280.0	.2	4	266.9	2.2	108	258.9	1.5	110
May 1979	289.7	5.3	86				280.3	1.9	76	265.3	1.7	105	260.7	1.1	104
June 1979	289.6	4.9	65				280.2	1.9	42	265.1	1.2	114	262.2	1.6	97
July 1979	292.7	2.8	107				283.7	3.8	77	265.9	1.3	116	263.0	1.5	92
Aug. 1979	295.5	3.4	79				287.7	2.9	99	268.5	2.1	113	264.7	1.2	108
Sept. 1979	295.4	4.3	74				285.9	4.7	107	268.5	1.9	116	266.0	1.3	89
Oct. 1979	298.7	4.4	54				286.6	3.8	101	270.7	2.2	116	266.1	1.3	100
Nov. 1979	305.1	5.5	68				286.2	3.3	76	272.1	1.9	122	267.3	1.0	103
Dec. 1979	303.7	3.7	73	...	...	...	287.5	1.7	105	273.6	2.8	102	267.8	.9	79
Jan. 1980	300.7	2.9	46	...	...	...	288.8	2.3	109	278.6	1.9	91	268.9	1.0	94
Feb. 1980	300.8	3.2	64	...	...	...	289.7	2.2	90	279.3	2.2	111	...	...	...
March 1980	304.8	3.1	75	...	...	...	292.6	1.7	89	281.0	2.0	112	...	...	...
April 1980	307.0	2.6	81	...	...	...	293.1	1.9	83	282.7	2.1	93	...	...	...
May 1980	309.8	2.9	45	...	...	...	294.2	2.1	105	284.0	2.0	101	...	...	...
June 1980	311.0	4.6	88	...	...	...	298.2	1.5	97	284.7	1.1	82	...	...	...
July 1980	313.3	3.3	91	...	...	...	301.2	2.6	97	286.3	1.2	110	...	...	...
Aug. 1980	314.4	4.1	88	...	...	...	302.3	1.8	51	287.5	1.3	93	...	...	...
Sept. 1980	315.1	3.2	83	...	...	...	303.0	5.2	89	288.8	1.7	78	284.0	2.2	52
Oct. 1980	316.4	2.6	84	...	...	...	304.4	4.0	31	284.5	1.6	13	284.1	1.0	46
Nov. 1980	318.7	2.4	61	314.0	2.6	106	305.9	2.3	87	289.7	1.4	54	285.9	1.7	102
Dec. 1980	318.3	2.7	54	313.2	2.8	97	307.1	2.8	78	291.8	2.6	96	286.4	1.1	76
Jan. 1981	319.8	3.7	95	314.6	3.1	127	307.9	1.6	92	293.3	2.3	36	287.6	1.2	51
Feb. 1981	320.9	3.9	50	315.8	4.6	95	308.7	2.2	79	...	...	...	286.7	1.3	41
March 1981	321.0	2.8	80	316.4	2.6	112	305.2	1.6	76	...	...	...	289.0	1.6	91
April 1981	324.0	3.4	45	317.1	1.8	106	308.8	2.8	71	...	...	...	290.6	1.1	61
May 1981	324.1	3.5	75	318.4	2.0	96	310.3	2.5	72	296.2	3.4	83	292.4	1.9	84
June 1981	323.0	3.0	61	319.9	2.1	107	310.3	1.7	86	297.2	3.9	100	294.1	1.3	68

The ALE measured values have all been converted to mixing ratios by multiplication by the absolute calibration factor $\xi = 0.95$.

increases of approximately 50% in the uncertainty limits for Point Matatula, American Samoa, and Cape Grim, Tasmania, an increase of approximately 20% at Ragged Point, Barbados, and no increase at Adrigole, Ireland.

The resulting empirical model coefficients and their estimated (1σ) uncertainty limits are given in Table 2. The mean concentrations of CF_2Cl_2 at each site (and hence the latitudinal gradients) and the linear trends are apparently precisely determined by the ALE data set. The annual cycle is apparently weak (as it is for the other ALE species) except at Point Matatula, American Samoa; its amplitude and phase there is reasonably consistent with that observed for $CFCl_3$. The curvatures of the trends are fairly well defined and, as we shall see, are in the direction of, but are of larger magnitude than is to be expected from the atmospheric release data. The empirical model fit indicates that we should expect to give significantly less weight to the data from Point Matatula than to other sites in determining the atmospheric lifetime of CF_2Cl_2 since the trend is less precisely determined there.

In the processing of the data to obtain lifetimes, the data from Adrigole, Ireland, and Cape Meares, Oregon, was combined (optimally, each site receiving weight $(\sigma_m^2/n_m)^{-1}$) into a single time series in order to avoid overweighting mid-latitudes of the northern hemisphere. If this time series is processed with the empirical model estimation procedure, we obtain $a_i = 5.709$, $b_i = 0.060$, and a residual variance of 25×10^{-6}. Thus, despite the limited nature of the Cape Meares, Oregon, data, it has a discernable effect on the trend deduced at northern hemisphere mid-latitudes. From Table 1, this effect is evidently produced because Cape Meares possesses a mixing ratio of CF_2Cl_2 that is typically about 5

TABLE 2. Empirical Model Fit (Equation (1)) to Three Years of CF_2Cl_2 Mixing Ratio Data

Site	a_i	b_i	d_i	c_i	s_i	Variance of Residuals ($\sigma_0^2 \times 10^6$)
Adrigole, Ireland	5.708 ± 0.002	0.063 ± 0.002	−0.008 ± .002	−0.001 ± 0.002	0.003 ± 0.002	27
Ragged Point, Barbados	5.669 ± 0.002	0.055 ± 0.002	−0.002 ± .002	0.001 ± 0.002	0.004 ± 0.002	35
Point Matatula, American Samoa	5.622 ± 0.003	0.064 ± 0.003	−0.011 ± .004	−0.003 ± 0.003	−0.010 ± 0.003	60
Cape Grim, Tasmania	5.600 ± 0.003	0.063 ± 0.002	−0.007 ± .003	0.000 ± 0.002	−0.001 ± 0.002	29

TABLE 3. World Production and Release of CF_2Cl_2 in Million Kilograms/Year (From *Chemical Manufacturers Association* [1982])

Year	Annual Production	Annual Release	Accumulated Production	Accumulated Release
1970	336.8	313.4	3015.5	2691.1
1971	360.5	337.5	3376.0	3028.6
1972	401.7	368.3	3777.7	3396.9
1973	447.4	408.1	4225.0	3805.1
1974	473.5	443.5	4698.5	4248.6
1975	418.5	434.6	5117.0	4683.1
1976	455.6	425.9	5572.6	5109.1
1977	434.9	410.3	6007.6	5519.4
1978	433.2	384.9	6440.7	5904.2
1979	428.8	388.4	6869.6	6292.6
1980	433.4	392.5	7303.0	6685.1
1981	449.2	412.2	7752.2	7097.4

pptv lower than that at Adrigole, Ireland (during November, 1980 to June, 1981). It seems premature to interpret this difference as corresponding to real differences in atmospheric CF_2Cl_2 concentrations because such a difference has existed between almost simultaneous, but relatively independent, measurements of $CFCl_3$ at one site [*Cunnold et al.*, this issue]. While it is unclear which site is providing the more realistic estimate of the northern hemisphere mid-latitude mixing ratio, it is interesting to note that the trend obtained at Adrigole alone is anomalously high relative to the other ALE sites and that there is no significant difference between the $CFCl_3$ mixing ratios at Adrigole and Cape Meares [*Cunnold et al.*, this issue].

Processing the data at northern hemisphere mid-latitudes as a single time series allows an estimate of the mixing ratio of CF_2Cl_2 and its temporal trend in the lower troposphere to be made. On January 1, 1980, the annually averaged ratios and trends derived from the empirical model were 302 pptv and 17.8 pptv/year at Adrigole and Cape Meares, respectively, 290 pptv and 16.0 pptv/year at Ragged Point, 277 pptv and 17.5 pptv/year at Point Matatula, and 271 pptv and 16.9 pptv/year at Cape Grim. Using an (unweighted) average of the data in the four latitudinal subdivisions of the globe, we find that in the lower troposphere the mixing ratio of CF_2Cl_2 was 285 pptv, and it is calculated to have been increasing at 17.1 pptv (6.0%) per annum at that time.

3. DICHLORODIFLUOROMETHANE EMISSIONS

For the annual global emission rates of CF_2Cl_2 we use the latest estimates by the Chemical Manufacturers Association for the period 1931–1981 [*Chemical Manufacturers Association*, 1982] (see Table 3). As discussed by *Cunnold et al.* [this issue], these latter estimates constitute an update of some earlier estimates that had incorporated certain invalid assumptions [*Chemical Manufacturers Association*, 1981]. In particular, production in eastern Europe and the USSR after 1975 had been underestimated, emission of CF_2Cl_2 during manufacture amounting to 2.5% of production had been ignored, and the use of CF_2Cl_2 in hermetically versus non-hermetically sealed refrigeration had been seriously overestimated. We shall use the Chemical Manufacturers Association (CMA) 1982 data in our analysis but computations using the CMA 1981 data will also be presented.

The fractions f of the annual global emission of CF_2Cl_2 that occur in each semi-hemisphere are computed in the manner discussed by *Cunnold et al.* [this issue] for $CFCl_3$. Average f values calculated from available data for the five year period 1976–1980 are 0.789, 0.141, 0.038, and 0.032 in the 90°N–30°N, 30°N–0°, 0°–30°S, and 30°S–90°S regions, respectively. We assume these average f values are valid for the ten year period July 1, 1971, to June 30, 1981. Prior to July 1, 1971, we assume that CF_2Cl_2 emissions are confined to the 90°N–30°N sector.

4. TREND ESTIMATE OF LIFETIME

The algorithm used to derive the atmospheric lifetime of CF_2Cl_2 is described in *Cunnold et al.* [this issue]. It consists of a two-dimensional model of the atmosphere in which the atmospheric lifetime of CF_2Cl_2, together with an absolute calibration factor and a global transport factor, are varied so as to provide calculated mixing ratios and temporal trends at the ALE sites that best simulate the observations. The use of an absolute calibration factor as an unknown forces the algorithm to base its estimate of lifetime on the temporal trends in CF_2Cl_2. A global transport factor F is estimated so as to provide the best possible simulation of the latitudinal distribution of CF_2Cl_2 (and simultaneously $CFCl_3$ and to a lesser extent of CH_3CCl_3 [see *Cunnold et al.*, this issue; *Prinn et al.*, this issue (*b*)]). In essence, we are assuming that the best simulation of the latitudinal distribution of these halocarbons will provide the most accurate prediction of the temporal trends at each ALE site. However, as will be indicated in section 5, the model does not simulate the observed seasonal variations in CF_2Cl_2 very well. Although it is, in principle, possible to determine transport coefficients that provide a better simulation of the (weak) annual cycles at each site (and this is under investigation), for the purpose of this paper we have filtered the calculated, unrealistically strong annual cycles out of the two-dimensional model results by using a twelve-month running mean filter. This should result in a more stable estimate of the lifetime at each site as a function of time.

In the calculation of lifetimes, the partial derivatives given in Table 4 were used, and since the lifetime is very long, the partial derivatives corresponding to a variation in the stratospheric lifetime τ_s were selected. Since $\partial(ln\chi)/\partial(1/\tau)$ is different at each site, there would be a tendency for the algorithm to adjust the lifetime in response to an imprecise simulation of the mean latitudinal distribution of CF_2Cl_2. We believe, however, that such an imprecision would most likely be related to inadequacies in either the model's description of transport or the latitudinal distribution of release. Therefore,

TABLE 4. Sensitivity of CF_2Cl_2 Partial Derivatives $[\partial ln\chi/\partial(1/\tau)]$ and $(d/dt)[\partial ln\chi/\partial(1/\tau)]$, to Two-Dimensional Model Parameter Variations for January 1, 1980

τ, Years	τ_s, Years	τ_t, Years	t_s, Years	F	$\partial ln\chi/\partial(1/\tau)$, Years				$d/dt\ [\partial ln\chi/\partial(1/\tau)]$				Parameter Varied in Calculating Derivatives	Release Scenario
					Box 1	Box 3	Box 5	Box 7	Box 1	Box 3	Box 5	Box 7		
169	50	296	4	2	−8.92	−9.20	−9.74	−9.80	−0.39	−0.39	−0.41	−0.40	τ_t	CMA 1982 latitudinally distributed
192	29	10^4	4	2	−5.46	−5.62	−6.00	−6.40	−0.37	−0.37	−0.38	−0.38	τ_s	CMA 1982 latitudinally distributed

Here τ, τ_s, and τ_t represent the atmospheric, the stratospheric, and the tropospheric lifetimes, respectively, of CF_2Cl_2. Boxes 1, 3, 5, and 7 designate the lower troposphere (500–1000 mb) in the 90°N–30°N, 30°N–0°, 0°–30°S, and 30°S–90°S regions, respectively.

the mean $\partial(ln\chi)/\partial(1/\tau)$ and $(d/dt)(\partial ln\chi/\partial(1/\tau))$ were used at all the ALE sites (= −5.8 and −0.37 on January 1, 1980).

The three-year data set was first processed separately for each site (except the two northern hemisphere mid-latitude sites that were combined) by fixing $F = 1.6$ and estimating the absolute calibration factor and the lifetime from that site's data alone. It should be noted that the results obtained are only approximately correct because they were obtained by using those two-dimensional model results that provided the best simulation of all the ALE data and then by using the partial derivatives to provide an estimate of the lifetime, which would produce a calculated trend equal to that observed at an individual site. Fortunately, the relevant derivative, $(d/dt)(\partial ln\chi\partial(1/\tau))$ is insensitive to variations in the CF_2Cl_2 lifetime (this is demonstrated for $CFCl_3$ in Table 2 of *Cunnold et al.* [this issue]).

Site by site estimates of the lifetime are given in Table 5. The trend at Ragged Point, Barbados, suggests a comparatively short lifetime, while that at Point Matatula, American Samoa, indicates an excessively long lifetime. The scatter of the lifetime results may be understood through an examination of the residuals given by the measured divided by the calculated mixing ratios. Figure 6, which is based upon the model calculation that gave the best fit to the trend in all the CF_2Cl_2 data, indicates that data from Point Matatula during the first year and data from Cape Grim, Tasmania, during the first four months of operation (when a different sample loop was used) may be inconsistent with the data obtained during the remainder of the three-year period. If the data for these periods are ignored, reciprocal lifetimes of 0.0021 and 0.0054 $years^{-1}$ are obtained at Point Matatula and Cape Grim, respectively. It, therefore, seems reasonable to give significantly less weight to these two sites in the global estimation of lifetime and, as indicated in Table 5, the optimal estimation algorithm provides a plausible distribution of weights. (A preliminary examination of an additional six months of ALE data confirms that the lifetime derived from the 3-year data set at Point Matatula and Cape Grim is too long and that even the reduced weighting given to these stations in the optimal code may be producing too long a global lifetime.)

The weights used in the optimal estimation algorithm are similar to those used in fitting an empirical model to the data (see equation (2)). They account for the short (≤ 1–2 years) temporal autocorrelations in the data but result in an unbiased combined (5 site) lifetime estimate if, for example, a particular site is providing a trend produced by real climatological changes not being simulated by the two-dimensional model (because the anomalous long-term trend at this site would not be included in its weighting factor).

Simultaneous processing of the CF_2Cl_2 data at the five ALE sites yields the (trend) estimates of lifetime given in Table 6. The optimal estimate of inverse lifetime for the three-year period equal to 0.0013 $years^{-1}$ is preferred over the value 0.0005 $years^{-1}$ (although these estimates are not significantly different) because of the uncertainties in the Point Matatula and Cape Grim data for the first year of operation. The results indicate, however, that there are sources of "noise" in addition to those accounted for by the values of σ^2 (equation (2)). For example, Table 5 indicates that there are site to site differences in the lifetime estimates that are not accounted for by the uncertainty limits assigned to the individual lifetime estimates. For $CFCl_3$ these differences appear to be instrumentally induced because they also existed between independent measurements at the same site [*Cunnold et al.*, this issue]. The estimates for the first and third years of operation in Table 6 should also be noted, however. They suggest (because of the site to site consistency) that the atmospheric release during the first year is being underestimated, while that for the third year is being overestimated. In order for our uncertainty limits to reflect these additional sources of potential error, we shall assume, for mathematical convenience, that the overall uncertainties at each site are in direct proportion to the uncertainties given in Table 5. All the optimally obtained uncertainty limits should then be multiplied by a constant factor that may be estimated by applying the student's t test to the results given in Table 6. To account for the site to site differences in the lifetime estimate, the uncertainty limits would have to be increased

TABLE 5. CF_2Cl_2 Reciprocal Lifetime Estimates Derived From the Trend at Each ALE Site

Site	Reciprocal Lifetime (Years), $\pm 1\sigma$	Lifetime (Years), $\pm 1\sigma$	Approximate Weight Given to Station in Optimal Code
Adrigole, Ireland/Cape Meares, Oregon	0.0041 ± 0.0036	244^{+1756}_{114}	0.4
Ragged Point, Barbados	0.0117 ± 0.0043	85^{+50}_{23}	0.25
Point Matatula, American Samoa	−0.0105 ± 0.0071	∞	0.1
Cape Grim, Tasmania	−0.0034 ± 0.0044	1000 → ∞	0.25

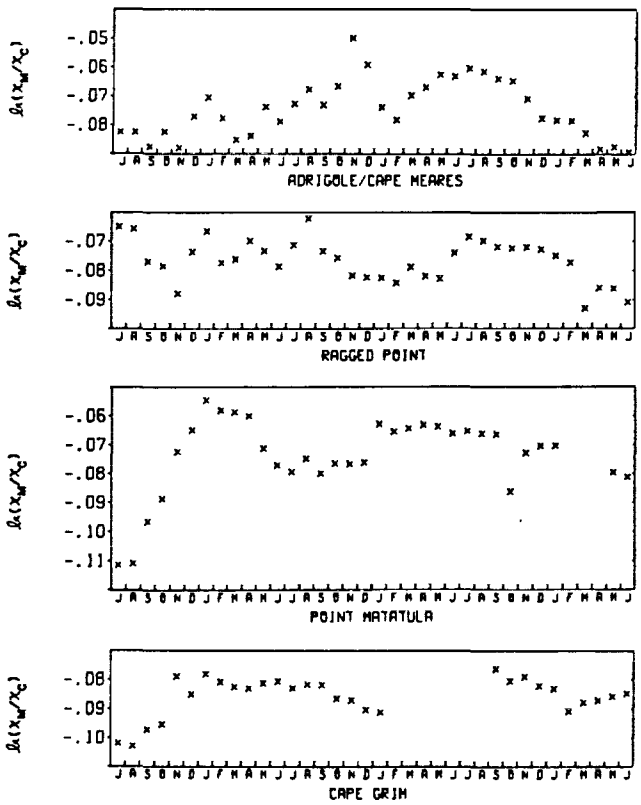

Fig. 6. CF_2Cl_2 residuals with respect to a two-dimensional model calculation with lifetime 769 years on January 1, 1980 (the trend best fit model). Residuals are given as the natural log. of the ratio of the observed to the calculated mixing ratio.

by a factor of approximately 2. However, to account for the year to year differences in the lifetime estimate given in Table 6, a factor of approximately 4 is indicated. This implies a reciprocal lifetime with uncertainty limits of 0.0013 ± 0.0090. The trend estimate of the CF_2Cl_2 lifetime appropriate to January 1, 1980, is then 769 years with lower and upper limits of 97 years and ∞.

5. The Lifetime Determined by the Atmospheric Inventory Technique

As for $CFCl_3$ [*Cunnold et al.*, this issue], it is argued that the two-dimensional model provides a realistic simulation of the global distribution of CF_2Cl_2 in the atmosphere to the extent that it is known and that the two-dimensional model provides a way to extrapolate the surface observations in ALE into an atmospheric inventory of CF_2Cl_2.

In the lower troposphere (the region below 500 mb in the model), the globally averaged mixing ratio is estimated to be equal to the average of the ALE measurements from each

TABLE 6. CF_2Cl_2 Reciprocal Lifetime Estimates ($years^{-1}$) for January 1, 1980, as Function of Time Obtained by Giving Equal Weight to and by Optimally Combining the Lifetime Estimates at the ALE Sites

Time Period (Month/Year)	Optimal Combination	Average
July 1978–June 1979	−0.0376 ± 0.0122	−0.0456 ± 0.0290
July 1980–June 1981	0.0770 ± 0.0111	0.0584 ± 0.0141
July 1978–June 1980	−0.0170 ± 0.0044	−0.0147 ± 0.0109
July 1979–June 1981	0.0170 ± 0.0039	0.0125 ± 0.0069
July 1978–June 1981	0.0013 ± 0.0022	0.0005 ± 0.0048

semi-hemisphere. In support of this estimate and to facilitate comparison with non-ALE measurements of CF_2Cl_2, it is useful to represent the two-dimensional model predictions in the empirical model form:

$$ln\chi = a + b\left(\frac{t-18}{12}\right) + d\left(\frac{t-18}{12}\right)^2 + c_1\cos\left(\frac{2\pi t}{12}\right) + c_2\cos\left(\frac{4\pi t}{12}\right) + s_1\sin\left(\frac{2\pi t}{12}\right) + s_2\cos\left(\frac{4\pi t}{12}\right) \quad (3)$$

Here it is meaningful to seek both annual and semi-annual variations in the relatively smooth two-dimensional model results. The coefficients of this series for the period July 1978 to June 1981 are given in Table 7 with t = 1 (month) corresponding to July 1978.

A comparison of Table 7 against Table 2 indicates that the mean latitudinal distribution of CF_2Cl_2 (coefficient a) is very well simulated by the two-dimensional model (with a transport factor F equal to 1.6), and although the seasonal variation at Point Matatula is acceptably simulated, the seasonal variation at Ragged Point is not. Because of the overprediction of the seasonal cycle at Ragged Point, Barbados, the seasonal cycle was filtered out of the two-dimensional model before processing the ALE results to obtain the lifetime, and an investigation of how to improve the simulation of the Ragged Point results has begun. It may also be noted that the simulation of the curvature terms (d) is poor, and this is reflected in the time dependence of the lifetime estimates given in Table 6.

Table 8 contains a comparison of the two-dimensional model predictions, which provide the best simulation of the temporal trends observed in the ALE, to latitudinal distributions observed by Rasmussen et al. and by the NOAA GMCC network of stations [*DeLuisi*, 1981]. In this comparison, the seasonal variations in the lower troposphere have been removed from the two-dimensional model results and the seasonal variations observed at the ALE sites have been added. It may first be noted that the calculated mixing ratios

TABLE 7. Empirical Model Fit (Equation (3)) to the Two-Dimensional Model Calculations That Provide the Best Fit to the Measured Trends

Box Number	a	b	d	c_1	c_2	s_1	s_2	$\ln^{-1}a$, pptv
1	5.775	0.056	−0.000	0.002	0.000	0.005	0.002	322.1
3	5.744	0.058	−0.001	−0.006	0.003	−0.010	−0.003	312.3
5	5.688	0.060	−0.002	−0.003	−0.003	0.006	0.000	295.3
7	5.681	0.061	−0.002	0.001	−0.001	0.002	0.000	293.2

Boxes 1, 3, 5, and 7 refer to the lower troposphere at northern hemisphere mid-latitudes and tropical latitudes and at southern hemisphere tropical and mid-latitudes, respectively.

TABLE 8. Comparison Between Best (Trend) Fit Two-Dimensional Model Calculations and Non-ALE Observations

	Box 1		Box 3	
Date of Measurement	Mean Reported Measurement, pptv	Calculated Mixing Ratio	Mean Reported Measurement, pptv	Calculated Mixing Ratio
March 1976			214	241
Jan. 1978	280	289		
Sept. 1978	296	301	295	291
Jan. 1, 1980	302	324	290	313
	Box 2		**Box 4**	
Date of Measurement	Mean Reported Measurement, pptv	Calculated Mixing Ratio	Mean Reported Measurement, pptv	Calculated Mixing Ratio
June 1976	228	253	221	247
Fall 1976			226	253

Lateral boundaries of the boxes lie at 90°N, 30°N, 0°, 30°S and 90°S. Vertical boundaries lie at 1000 mb, 500 mb, and 200 mb. The predicted concentrations for an atmospheric lifetime of CF_2Cl_2 of 180 years may be estimated by decreasing the values given by 2%.

exceed those measured in the ALE and all the other programs (indicating that the inventory lifetime is shorter than the trend lifetime). Second, it should be noted that Dr. Rasmussen's calibration standards have been widely used in the past but only in the ALE program has a factor of 0.95 been applied to the measurements to obtain absolute concentrations. Of more relevance for this paper, however, is the model's ability to simulate observed latitudinal variations, and here the agreement is regarded as acceptable. The NOAA-GMCC data [*DeLuisi*, 1981], moreover, indicates that during the ALE period of observation the mixing ratio at Niwot Ridge, Colorado (40°N latitude) was no more than 1% different (lower) than that at Point Barrow, Alaska (70° latitude). ALE data also suggest that the 30°N to 90°N region is relatively uniformly mixed for CF_2Cl_2 since Adrigole, Ireland, typically exhibits not more than 2% more CF_2Cl_2 than Cape Meares, Oregon. It is, therefore, concluded that the two-dimensional model is providing a realistic simulation of the latitudinal distribution of CF_2Cl_2. Moreover, since the observed northern hemisphere to southern hemisphere mid-latitude difference is only 11%, the two-dimensional model estimate of the mean CF_2Cl_2 content in the lower troposphere probably possesses a precision of approximately 1% (1σ).

In the upper troposphere, Table 8 suggests that the two-dimensional model overpredicts the observed gradient. Tests indicate that the calculated gradient may be reduced by adjusting the transport rate and, in particular, by decreasing the vertical transport rate. The model, however, indicates that the average mixing ratio in the upper troposphere is approximately 99% of that in the lower troposphere. Since it is unlikely that the average mixing ratio in the upper troposphere exceeds the average mixing ratio in the lower troposphere, and the observations suggest 99% may be an underestimate of the ratio, the model calculations are assumed to be realistic for inventory purposes and we shall attach an uncertainty of 1% (1σ) to the resulting inventory ratio for the two regions.

An extensive series of stratospheric observations of CF_2Cl_2 have been reported by *Goldan et al.* [1980] (see also *World Meteorological Organization* [1982]). In their Figure 16, *Goldan et al.* [1980] showed that if the altitude profiles were referenced to altitude above the tropopause, the profiles were relatively independent of latitude. On the basis of these observations, which were made in 1976 through 1979, it is estimated that the average mixing ratio in the stratosphere (using pressure weighting) was 0.67 of that in the upper troposphere. Uncertainty limits on this ratio, obtained by regarding the envelope of the observations as providing $\pm 2\sigma$ limits, are ± 0.07 (1σ) with the principal uncertainty being the profile shape in the region from a few kilometers below, to a few kilometers above, the tropopause. Using an upper troposphere box to stratosphere box (350 mb to 100 mb) transfer time (t_s) of four years, a ratio of 0.70 was obtained for 1977 in the two-dimensional model in good agreement with the ratio derived from observations.

On January 1, 1980, the two-dimensional model indicates that the globally averaged mixing ratio is 0.944 times that in the lower troposphere. On the basis of the uncertainty limits given in the preceding paragraphs, we conclude that the globally averaged mixing ratio of CF_2Cl_2 may be obtained from the ALE data by multiplying the latitudinally-averaged value by the factor (1σ error limits)

$$(0.944 \pm 0.02)$$

In a three-dimensional chemical model that utilizes CMA 1982 release rates, and stream functions, velocity potentials, and ozone concentrations from a recent run of the three-dimensional model of *Cunnold et al.* [1975], it has been calculated that on January 1, 1981, this factor was approximately 0.951 [*Golombeck*, 1982]. While this factor lies within our assumed error limits, it suggests that our calculations may underestimate the atmospheric content of CF_2Cl_2 by approximately 1% and that a value of $t_s = 3$ years may produce a more realistic simulation of atmospheric transport between the troposphere and stratosphere.

The algorithm used to derive the trend lifetime indicated that the deduced CF_2Cl_2 lifetime of 769 years results in an overprediction of the mixing ratio in the lower troposphere (relative to observations) by 0.077 in $ln\chi$. The global CF_2Cl_2 content on January 1, 1980, was estimated from ALE data (applying the factor of 0.944 determined from the two-dimensional model) to have been 5780×10^6 kg which may be compared against the model inventory (for $\tau = 769$ years) of 6220×10^6 kg and the accumulated release prior to that time of 6293×10^6 kg. The lifetime estimated by the atmospheric inventory technique may be obtained by applying the average value of the partial derivative, $\partial(ln\chi)/\partial(1/\tau)$, given in Table 4, to the $ln\chi$ discrepancy of 0.077. The inventory estimate of the lifetime is shorter than that ob-

of CF_2Cl_2 in the Lower Troposphere (Boxes 1, 3, 5, and 7) and in the Upper Troposphere (Boxes 2, 4, 6, and 8)

Box 5		Box 7		
Mean Reported Measurement, pptv	Calculated, Mixing Ratio	Mean Reported Measurement, pptv	Calculated, Mixing Ratio	Reporter
196	227			*Rasmussen et al.* [1977]
		244	258	*Rasmussen et al.* [1981]
273	270			*DeLuisi* [1981]
278	298	271	294	ALE

Box 6		Box 8		
Mean Reported Measurement, pptv	Calculated, Mixing Ratio	Mean Reported Measurement, pptv	Calculated, Mixing Ratio	Reporter
217	231	212	228	*Robinson and Harsch* [1978]
220	237	217	235	*Rasmussen and Krasnec* [1977]

tained by the trend technique and implies either a shorter stratospheric lifetime or a small tropospheric sink (or a combination thereof). Assuming destruction in the stratosphere only, using a partial derivative of −5.8 years, a lifetime of 69 years on January 1, 1980, is obtained. If, on the other hand, a stratospheric sink τ_s = 27 years is assumed (based on the calculations by *Golombeck* [1982] and *Owens et al.* [1982]), τ^{-1} = 0.0056 years^{-1}, the $ln\chi$ discrepancy to be interpreted as a tropospheric sink would be 0.052. Applying a partial derivative of −9.4 years to this discrepancy, a lifetime of $[0.0056 + (0.052/9.4)]^{-1}$ = 90 years is obtained (and a tropospheric lifetime $\tau_t \simeq$ 150 years).

6. Discussion

To specify completely the uncertainty limits on the trend and inventory lifetimes, uncertainties in release must be assessed and combined with the measurement uncertainties. In this section, upper and lower limits on the release uncertainties will first be discussed based on calculations with a release code similar to that used by *McCarthy et al.* [1977]. To convert these uncertainties to uncertainties in lifetime, additional calculations were performed with the two-dimensional model. In these calculations, all the transport parameters were usually fixed, and τ_s was varied so as to obtain a match between the observed and calculated mixing ratios in the lower troposphere. It should be noted that this procedure resulted in some change in r, the stratospheric to tropospheric mixing ratio ratio, which is poorly defined by observation. Generally, it was found that the partial derivative $\partial ln\chi/\partial(1/\tau) = -5.8$ (see line 2 of Table 4) provided a good estimate of the change in the inventory lifetime. Changes in release may be interpreted in this way by noting that a change in the accumulated release (R), ΔlnR, will produce a similar change in $ln\chi$, which must then be compensated for by a change in τ_s. The trend lifetime uncertainty may be derived from the change in I/R, where I is the average annual release for 1979 and 1980, and by using $\partial(I/R)/\partial(1/\tau) = 0.3$ years.

The production of CF_2Cl_2 in the United States and Europe should be known very precisely since it is in the industries' interest to keep an accurate record of production. No allowance has, however, been made in the industry figures for production in the Peoples Republic of China, which might amount to 0.5% of world production (1σ); moreover, the production in the USSR and eastern Europe after 1975 is relatively poorly defined. The CMA release estimate (1981) arbitrarily assumed a 3% growth in production in the USSR and eastern Europe since 1975, while the revised release scenario [*Chemical Manufacturers Association*, 1982] assumed an 18% growth rate. This substantial increase in the estimated release of CF_2Cl_2 in eastern Europe is primarily based upon the startup of a plant with a capacity of 30×10^6 kg/year in Volgograd (European Chemical News, Nov. 17, 1980, p. 40). It is evident from the construction of this plant and of another that is not yet operational that the demand for fluorocarbons in eastern Europe and the USSR has been rising rapidly. We shall therefore assume that the 3% growth rate represents a lower limit (2σ) on the growth. This translates into a change in the accumulated production of 0.4% (1σ) and a significant change in the trend of release. Some CF_2Cl_2 is released during production and the CMA estimate of this loss (2.5%) is probably accurate to 0.5% (1σ). In order to translate these uncertainties to uncertainties in lifetime, we shall make the assumption that the additional production during manufacture and in the Peoples Republic of China is added to the prompt release category. The uncertainty in production in the USSR and eastern Europe will be treated separately.

In the prompt release category, which for CF_2Cl_2 primarily consists of aerosol propellant usage, a five to six month delay in release relative to production was assumed in the CMA estimates. We estimate that an uncertainty (1σ) of one month is appropriate for this use category. In the second most important CF_2Cl_2 release category—the use in non-hermetically sealed refrigeration and air conditioning—a release delay of four years relative to production was assumed in the CMA calculations. This delay is believed to be accurate to ± 0.5 years (CMA Fluorocarbon Panel, private communication, 1983). The CMA 1982 estimates are also based on a 3.5% to 96.5% split between usage in hermetically sealed and non-hermetically sealed containers versus an approximately 40/60 split used in CMA 1981. A one-sided error bar of 5% (1σ) allows for the fact that this split estimate is tentative and that the proportion of usage in domestic refrigerators and freezers in the United States, on which it is based, may have been larger in the rest of the world than in the United States in recent years. *McCarthy et al.* [1977] estimates that CF_2Cl_2 in rigid foams has an escape time of six months; even if 25% of these foams were of the foamed in place variety (as for $CFCl_3$), which results in an escape time

TABLE 9. Effect of Release Uncertainities on the CF_2Cl_2 Reciprocal Lifetime Estimated by Using $\partial(lnR)/\partial(1/\tau) = 5.8$ years and $\partial(I/R)/\partial(1/\tau) = 0.3$ years

Release Scenario	Increase in Accumulated Release (R) to the end of 1979 ($\times 10^6$kg)	$\Delta(1/\tau)$ Inventory Technique, years^{-1}	Average Change in Annual release for the Period/Accumulated Release 1979–1980, $\Delta(I/R)$	$\Delta(1/\tau)$ Trend Technique, years^{-1}
0.7% additional production/release released as in the prompt release category.	+44	+0.001	...	...
One-month decrease (increase) in prompt release category (versus 5.5 months used in CMA 1982).	±16	±0.000	±0.0004	±0.001
Uncertainty in production in eastern Europe corresponding to a 2σ error equal to 3% growth since 1975 versus 18%.	±27	±0.001	±0.0016	±0.005
0.5 year decrease (increase) in delay in release relative to production for non-hermetically sealed use.	±60	±0.002	±0.0004	±0.001
8.5/91.5 hermetic/non-hermetic split versus 3.5/96.5 used in CMA 1982.	−38	−0.001	−0.0002	−0.001
Totals	±80	±0.002	±0.0017	±0.006

of order 20 years, there would be negligible impact on the atmospheric lifetime estimates. This uncertainty is not, therefore, included in Table 9.

The effect of the release uncertainties discussed above on the atmospheric lifetime is summarized in Table 9. For the trend estimate of lifetime, the unknown growth of production in the USSR and eastern Europe clearly represent a significant uncertainty. If the release uncertainty (0.006 years^{-1}) is combined with the uncertainty due to measurement errors of 0.009 years^{-1}, the uncertainty in the reciprocal lifetime is 0.011 years^{-1}. For the deduced trend lifetime of 769 years, this gives a (1σ) uncertainty range of 81 years to ∞. If the stratospheric lifetime is fixed at 27 years (τ^{-1} = 0.0056 years^{-1}), the lower limit (1σ) on the lifetime resulting from stratospheric photodissociation and tropospheric destruction is

$$\left(0.0056 + 0.0067 \times \frac{0.375}{0.398}\right)^{-1} = 84 \text{ years}$$

This would correspond to $\tau_t \simeq 140$ years.

The uncertainty in the inventory estimate of the inverse lifetime is produced by the combination of an uncertainty of 0.002 years^{-1} in the reciprocal lifetime from release uncertainties (see Table 9), an uncertainty of 2% (→ 0.02/5.8 = 0.0034 years^{-1}) in absolute calibration [*Rasmussen and Lovelock*, this issue] and the uncertainty in translating ALE measurements to an atmospheric overburden. This last uncertainty consisted of a 1% uniform uncertainty in the mixing ratio throughout the atmosphere (giving 0.002 years^{-1}) together with an uncertainty in the stratospheric content produced in our model by uncertainties in t_s. The effect of this uncertainty has been derived by determining the changes in t_s and τ_s, which would produce a prescribed change in r (= 0.07) together with no change in the mixing ratio in the lower troposphere (where the mixing ratio should equal that observed in the ALE). Combining the result of this last calculation (0.002 years^{-1}) with the other uncertainties gives 0.005 years^{-1}. This gives uncertainty limits ($\pm 1\sigma$) on the lifetime of CF_2Cl_2 resulting from destruction in the stratosphere only of 51 to 105 years. If the contribution to the atmospheric lifetime resulting from stratospheric destruction is fixed at τ_s = 27 years, the atmospheric lifetime was calculated to be 90 years and the uncertainty limits may be obtained by using the partial derivative $\partial(ln\chi)/\partial(1/\tau) = -9.4$ years in place of −5.8 years (see Table 4). This gives a reciprocal lifetime uncertainty of 0.005 × 5.8/9.4 = 0.003 years^{-1} and a (1σ) uncertainty range on the lifetime of 71 and 123 years. Using the two-dimensional model, this lifetime range corresponds to an uncertainty range for τ_t of approximately 100 to 360 years.

Assuming destruction of CF_2Cl_2 in the stratosphere only, the inverse lifetime derived by the trend technique (0.0013 ± 0.0110 years^{-1}) may be optimally combined with that from the inventory technique (0.0145 ± 0.0050 years^{-1}) to give a maximum likelihood lifetime estimate for January 1, 1980, of 82 years. In contrast to the results for $CFCl_3$ [*Cunnold et al.*, this issue], the inventory technique is giving the more precise estimate of lifetime for the three year data set. This is the result of a greater than expected accuracy of the inventory technique rather than of unexpectedly poor accuracy in the trend technique. Moreover, the fact that the 1σ uncertainty limits barely overlap suggests a need for further investigation of the uncertainties. For the trend technique, the principal uncertainties are produced by the (im)precision of the trend estimate from three years of data and by a tendency of the data to imply a larger (and smaller) than estimated release in the first (and last) years of operation of the ALE network. For the inventory technique, the principal uncertainty arises from absolute calibration, and here we

note that independently calibrated measurements in the North Atlantic by *Bullister and Weiss* [1983] exhibit 1.5% higher concentrations than our measurements at Adrigole. Such a change in absolute calibration would lead to an inventory lifetime of 84 years.

To facilitate comparison of the ALE lifetime estimates for CF_2Cl_2 with those obtained in previous studies, our calculations have been repeated by using the CMA 1981 release estimates in place of those given by CMA 1982. The revised estimate of release [*Chemical Manufacturers Association*, 1982] gives 474×10^6 kg more in the accumulated release through 1979 primarily because of a reclassification of most of the hermetically sealed usage as non-hermetically sealed. It should thus be noted, therefore, that previous model calculations [e.g., *Owens et al.*, 1982] predict lower tropospheric concentrations of CF_2Cl_2 that are several percent lower than those measured in ALE. The reciprocal lifetime estimate obtained by the trend technique for this release scenario is -0.0140 years^{-1}, which corresponds to the observed trend exceeding that predicted in the case of absolutely no atmospheric destruction of CF_2Cl_2 by 0.5%/year. The inventory lifetime estimate is 1250 years.

Our results may now be compared with the analysis of a longer period but significantly less comprehensive data set by *Rowland et al.* [1982], which showed inconsistency with the CMA 1981 release estimates. Rowland et al. estimated an atmospheric inventory of 6180×10^6 kg on January 1, 1980, which may be compared against our estimate of 5780×10^6 kg. The difference between the estimates is primarily produced by the absolute calibration factor $\xi = 0.95$. The accumulated release at that time is estimated to be 6293×10^6 kgm [*Chemical Manufacturers Association*, 1982] or 5819×10^6 kg [*Chemical Manufacturers Association*, 1981]. Destruction of CF_2Cl_2 by stratospheric photodissociation provides agreement within $\pm 1\sigma$ uncertainty limits for the ALE estimated inventory not only with the CMA 1982 release estimates (which, in fact, imply some additional destruction) but also with the CMA 1981 release estimates. The trend technique, on the other hand, applied to the ALE data set gives results that are reasonably consistent with the 1982 release estimates but that are inconsistent with the 1981 releases (as Rowland et al. emphasized in their analysis). Furthermore, in contrast to the five years of data analyzed by Rowland et al., the latitudinal distribution of CF_2Cl_2 obtained by the ALE over the three year period is consistent with the latitudinal distribution of $CFCl_3$ and with reasonable values of transport rates ($F \simeq 1.6$). We conclude that the ALE data together with the CMA 1982 release estimates are more consistent than the data analyzed by *Rowland et al.* [1982] together with the CMA 1981 releases. However, both analyses suggest that there has been a significant reduction in the atmospheric release of CF_2Cl_2 between 1979 and 1981, which is not contained in the release estimates.

These results indicate a need to determine better the trend of CF_2Cl_2 in the atmosphere (which should be possible from the fourth and fifth years of ALE data) and a need to assess further the atmospheric release of CF_2Cl_2. Here, the principal needs are to obtain data on the production and uses of CF_2Cl_2 in the USSR and eastern Europe (which it is estimated now accounts for approximately 25% of world production) since 1975 and to reassess the proportion and lifetime of CF_2Cl_2 used in non-hermetically sealed (as opposed to hermetically sealed) equipment throughout the world.

7. CONCLUSIONS

Observations of dichlorodifluoromethane several times daily over the period July 1978 to June 1981 at Adrigole, Ireland (52°N, 10°W), Ragged Point, Barbados (13°N, 59°W), Point Matatula, American Samoa (14°S, 171°W), and Cape Grim, Tasmania (41°S, 145°E) have been described, as well as observations for the period November 1980 to June 1981 at Cape Meares, Oregon (45°N, 124°W). Using the optimal estimation procedure described in *Cunnold et al.* [1982], the data at each site was first fitted by an empirical model consisting of a linear trend, a curvature, and an annual cycle. Averaging the mean concentrations and the trends from each latitude region, the average mixing ratio of dichlorodifluoromethane in the lower troposphere on January 1, 1980, was estimated to have been 285 pptv and it was calculated to have been increasing at 6.0% per year at that time.

The ALE data was processed to obtain the CF_2Cl_2 lifetime by determining the lifetime that when inserted into the two-dimensional model of the atmosphere gave the best simulation of the data in a weighted least mean square sense. Independent estimates of the lifetime were obtained by simulating the temporal trends in each latitude region (the trend lifetime) and by simulating the observed mixing ratios (the inventory lifetime). The lifetime estimates depended on whether it was assumed that destruction of CF_2Cl_2 occurred in the troposphere or stratosphere. Two destruction scenarios were used: all destruction occurring in the stratosphere and destruction in the stratosphere at a rate given by $\tau = 180$ years ($\tau_s = 27$ years) combined with some tropospheric destruction.

The trend lifetime derived from the ALE data is 769 years for stratospheric destruction only (the second destruction scenario is physically meaningless in this case). The inventory lifetime is 69 years for stratospheric destruction only and 90 years for the combined stratospheric/tropospheric destruction scenario (with the lifetime of CF_2Cl_2 in the troposphere being estimated to be approximately 150 years). The atmospheric inventory for January 1, 1980, was estimated to have been 5780×10^6 kg.

Uncertainties in these estimates of lifetime were assessed. For the trend lifetime these consisted of contributions from measurement uncertainties and from release uncertainties—principally related to the trend of production and release of CF_2Cl_2 in the USSR and eastern Europe. These were combined to indicate that within $\pm 1\sigma$ limits the lifetime is longer than 81 years for destruction in the stratosphere and longer than 84 years if the stratospheric lifetime is fixed at 36 years.

Uncertainty in the inventory estimate of lifetime resulted principally from the absolute calibration of CF_2Cl_2 in the reference cylinders (which was derived from the experiments of *Rasmussen and Lovelock* [this issue]) and from the ability of the two-dimensional model to extrapolate surface measurements to an atmospheric inventory. The combined effect of the uncertainties was to give a lifetime range of 51–105 years, assuming only stratospheric destruction, and of 71–123 years, assuming a stratospheric lifetime of 27 years.

Finally, it was noted that the ALE observed trends were inconsistent with the original CMA release estimate [*Chemical Manufacturers Association*, 1981] but that the revised release estimates [*Chemical Manufacturers Association*, 1982] resulted in a trend lifetime that was consistent with a photodissociation only sink for CF_2Cl_2 and in inventory estimates that suggested either the existence of an additional

atmospheric sink of CF_2Cl_2 or that stratospheric photodissociation rates are being underestimated in current models. In addition, however, the trend data indicated that the atmospheric release of CF_2Cl_2 in 1978/1979 and 1980/1981 may have been underestimated and overestimated, respectively. Since the USSR and eastern Europe are now believed to account for approximately 25% of the world production of CF_2Cl_2, there is a need to assess further the year release of CF_2Cl_2 there since 1975.

Acknowledgments. This research was supported by the Fluorocarbon Program Panel of the Chemical Manufacturers Association. Nominal support has also been provided by the Upper Atmosphere Research Program of NASA (to R.A.R.). We are particularly grateful to B. Lane of the Fluorocarbon Program Panel for his unceasing efforts to determine the accuracy and precision of the CF_2Cl_2 release estimates and to R. Rosen of Environmental Research and Technology (now at Atmospheric and Environmental Research (AER)) for his professional and timely processing of the ALE data and for his suggestions regarding the analysis of the ALE results. We also thank our colleagues P. Fraser and J. Lovelock for their contributions to the ALE measurements and the data analysis.

REFERENCES

Bullister, J. L., and R. F. Weiss, Anthropogenic chlorofluorocarbons in the Greenland and Norwegian Seas, *Science, 221*, 265–267, 1983.

Chemical Manufacturers Association, World production and release of chlorofluorocarbons 11 and 12 through 1980, Rep. of the Fluorocarbon Program Panel, Washington, D. C., 1981.

Chemical Manufacturers Association, World production and release of chlorofluorocarbons 11 and 12 through 1981, Rep. of the Fluorocarbon Program Panel, Washington, D. C., 1982.

Cunnold, D., F. Alyea, N. Phillips, and R. Prinn, A three-dimensional dynamical-chemical model of atmospheric ozone, *J. Atmos. Sci., 32*, 170–194, 1975.

Cunnold, D., F. Alyea, and R. Prinn, A methodology for determining the atmospheric lifetime of fluorocarbons, *J. Geophys. Res., 83*, 5493–5500, 1978.

Cunnold, D. M., R. G. Prinn, R. A. Rasmussen, P. G. Simmonds, F. N. Alyea, C. A. Cardelino, A. J. Crawford, P. J. Fraser, and R. D. Rosen, The Atmospheric Lifetime Experiment, 3, Lifetime methodology and application to 3 years of $CFCl_3$ data, *J. Geophys. Res.*, this issue.

DeLuisi, J. J., Geophysical monitoring for climatic change no. 9, *Summary Rep. 1980*, edited by J. J. DeLuisi, p. 163, Air Resour. Lab., Boulder, Colo., Dec. 1981.

Goldan, P. D., W. C. Kuster, D. L. Albritton, and A. L. Schmeltekopf, Stratospheric $CFCl_3$, CF_2Cl_2, and N_2O height profile measurements at several latitudes, *J. Geophys. Res., 85*, 413–423, 1980.

Golombeck, A., A global three-dimensional model of the circulation and chemistry of long-lived atmospheric species, Ph.D. thesis, Mass. Inst. of Technol., Cambridge, 1982.

McCarthy, R. L., F. A. Bower, and J. P. Jesson, The fluorocarbon-ozone theory, I, Production and release—World production and release of CCl_3F and CCl_2F_2 (fluorocarbons 11 and 12) through 1975, *Atmos. Environ., 2*, 491–497, 1977.

Owens, A. J., J. M. Steed, C. Miller, D. L. Filkin, and J. P. Jesson, The atmospheric lifetimes of CFC 11 and CFC 12, *Geophys. Res. Lett., 9*, 700–703, 1982.

Penner, J. E., Trend prediction for O_3: An analysis of model uncertainty with comparison to detection thresholds, *Atmos. Environ., 16*, 1109–1115, 1982.

Prinn, R. G., P. G. Simmonds, R. A. Rasmussen, R. D. Rosen, F. N. Alyea, C. A. Cardelino, A. J. Crawford, D. M. Cunnold, P. J. Fraser, and J. E. Lovelock, The Atmospheric Lifetime Experiment, 1, Introduction, instrumentation, and overview, *J. Geophys. Res.*, this issue.

Prinn, R. G., R. A. Rasmussen, P. G. Simmonds, F. N. Alyea, D. M. Cunnold, B. Lane, A. J. Crawford, and C. Cardelino, The Atmospheric Lifetime Experiment, 5, Results for CH_3CCl_3 based on 3 years of data, *J. Geophys. Res.*, this issue.

Rasmussen, R. A., and J. Krasnec, Interhemispheric survey of minor upper atmospheric constituents during October–November, 1976, *NASA TMX-73630*, March 1977.

Rasmussen, R. A., and J. E. Lovelock, The Atmospheric Lifetime Experiment, 2, Calibration, *J. Geophys. Res.*, this issue.

Rasmussen, R., D. Pierotti, and J. Krasnec, Cruise report of the alpha helix, *Report to NSF*, Wash. State Univ., Pullman, 1977.

Rasmussen, R. A., M. A. K. Khalil, and R. W. Daluge, Atmospheric trace gases in Antarctica, *Science, 211*, 285–287, 1981.

Robinson, E., and D. E. Harsch, A halocarbon survey in the Pacific area from 80°N to 49°S, June, 1976, *Final Rep. 78/13-24*, Chem. Mfr. Assoc., Washington, D.C., June 1978.

Rowland, F. S., S. C. Tyler, D. C. Montague, and Y. Makide, Dichlorodifluoromethane, CCl_2F_2, in the earth's atmosphere, *Geophys. Res. Lett., 9*, 481–484, 1982.

World Meteorological Organization, The stratosphere 1981: Theory and measurements, *Rep. 11*, 359 pp., WMO Global Ozone Res. and Monit. Proj., Geneva, Switzerland, 1982.

F. N. Alyea, C. A. Cardelino, and D. M. Cunnold, School of Geophysical Sciences, Georgia Institute of Technology, Atlanta, GA 30332.

A. J. Crawford and R. A. Rasmussen, Department of Environmental Science, Oregon Graduate Center, Beaverton, OR 97005.

R. G. Prinn, Department of Meteorology and Physical Oceanography, Massachusetts Institute of Technology, Cambridge, MA 02139.

P. G. Simmons, Department of Geochemistry, University of Bristol, Bristol, England.

(Received July 12, 1982;
revised March 29, 1983;
accepted April 25, 1983.)

JOURNAL OF GEOPHYSICAL RESEARCH, VOL. 88, NO. C13, PAGES 8415–8426, OCTOBER 20, 1983

The Atmospheric Lifetime Experiment 5. Results for CH_3CCl_3 Based on Three Years of Data

R. G. PRINN,[1,2] R. A. RASMUSSEN,[3] P. G. SIMMONDS,[4] F. N. ALYEA,[2,5] D. M. CUNNOLD,[2,5] B. C. LANE,[6] C. A. CARDELINO,[2,5] AND A. J. CRAWFORD[3]

We present gas chromatographic determinations of the concentrations of CH_3CCl_3 at Adrigole (Ireland), Cape Meares (Oregon), Ragged Point (Barbados), Point Matatula (American Samoa), and Cape Grim (Tasmania) for the 3-year period July 1978 through June 1981. The determinations involve approximately four measurements each day with on-site calibration. The absolute values and trends for these observed concentrations are interpreted in terms of the industrial production, global circulation rate, and atmospheric lifetime of CH_3CCl_3 by using an optimal estimation technique that incorporates a nine-box model of the atmosphere. The globally and annually averaged trend in the lower troposphere at the midpoint of the second year of the experiment is 8.7% per year, and the inferred global atmospheric content of CH_3CCl_3 at this midpoint is 2.58×10^9kg. The global atmospheric lifetime deduced by using the observed trends and global content together with current estimates of industrial CH_3CCl_3 emissions is $10.2^{+5.2}_{-2.6}$ years. This deduced lifetime is sufficiently long to imply that the observed variability in the data on seasonal and shorter time scales must be dominated by meteorological (and perhaps industrial emission) variabilities rather than by spatial and temporal variations in the rate of chemical destruction of CH_3CCl_3 by OH. However, the observed variations on annual and longer time scales are sensitive to the spatially and temporally averaged OH concentrations. In particular, the globally averaged tropospheric OH concentration compatible with the above-deduced CH_3CCl_3 lifetime is $(5 \pm 2) \times 10^5$ molecule cm^{-3}; in reasonable agreement, for example, with the value of $(6.5^{+3}_{-2}) \times 10^5$ molecule cm^{-3} deduced by Volz et al. (1981) from measurements of CO. Our results are sensitive to constraints imposed on uncertainties in the CH_3CCl_3 emissions and absolute mixing ratios. If we decrease emissions by ≤8% in the years 1976–1978 and increase emissions in 1979–1981 to compensate, and if absolute mixing ratios are decreased by about 18%, then the best estimate of the lifetime from our data decreases to 6.5 years.

1. INTRODUCTION

The compound 1,1,1-trichloroethane (methyl chloroform) is a relatively long-lived atmospheric constituent with a predominantly or exclusively anthropogenic origin. The reaction of CH_3CCl_3 with the OH radical is its principal recognized atmospheric sink [*Yung et al.*, 1975; *Cox et al.*, 1976]. It has therefore been proposed as a potentially accurate indicator of tropospheric OH concentrations [*Singh*, 1977*a*; *Lovelock*, 1977]. It has also been identified as a potentially significant source of reactive chlorine compounds in the stratosphere [*McConnell and Schiff*, 1978; *Crutzen et al.*, 1978]. It is therefore important to understand the global mass balance for this species and, in particular, to reconcile its observed atmospheric concentrations with its anthropogenic sources and globally averaged atmospheric lifetime.

There have been two basic approaches used to estimate the globally averaged lifetime τ of CH_3CCl_3. The first involves utilization of independent information to define the concentrations of the principal known scavenger of CH_3CCl_3 (namely OH) and thus to define τ. Utilizing CH_3CCl_3 industrial emission data, the OH (or τ) values can then be checked by comparing calculated spatial and temporal CH_3CCl_3 distributions with observations. The second approach involves utilizing directly the observed CH_3CCl_3 distributions and emission estimates to infer the lifetime through global mass balance calculations.

Using the first approach with a horizontally averaged model, *Yung et al.* [1975], *Cox et al.* [1976], *Crutzen and Fishman* [1977], and *McConnell and Schiff* [1978] estimated τ values of 3, 1.1, 6–10.7, and 8 years, respectively. With the same approach, but utilizing two-dimensional box or grid models of varying complexity, *Chameides and Tan* [1981], *Logan et al.* [1981], and *Derwent and Eggleton* [1978, 1981] computed τ values of 4.6–15, 5, 5.4, and 3.6–6 years, respectively. The second approach has been used in a horizontally averaged model by *Singh* [1977*a*], *Rasmussen and Khalil* [1981], and *Makide and Rowland* [1981] to deduce τ values of 7.2 ± 1.2, 6–10, and 6.9 ± 1.2 years, respectively. Finally, using two-dimensional models with the second approach, *Lovelock* [1977], *Neely and Plonka* [1978], *Singh* [1977*b*], *Chang and Penner* [1978], and *Singh et al.* [1979] compute lifetimes of 5–10, 3.3 ± 0.7, 8.3, 11.3, and 8–10 years, respectively. Clearly, these estimates vary considerably, and this is due not only to the two basic approaches taken but also to the differences in the estimates of the tropospheric concentrations of OH and its rate of reaction with CH_3CCl_3; to the uncertainties in the industrial emissions, concentrations, and spatial and temporal trends of CH_3CCl_3; and, finally, to the varying complexity of the atmospheric models involved.

The approach involving a consideration of the global mass balance is clearly the more direct for deducing CH_3CCl_3 lifetimes and provides atmospheric OH concentrations as an important corollary. Some of the problems associated with

[1] Department of Earth, Atmospheric and Planetary Sciences, Massachusetts Institute of Technology.
[2] CAP, Inc.
[3] Department of Environmental Science, Oregon Graduate Center.
[4] Department of Geochemistry, University of Bristol.
[5] School of Geophysical Sciences, Georgia Institute of Technology.
[6] ICI Americas, Inc.

Paper number 3C0675.
0148-0227/83/003C-0675$05.00

this approach, in particular systematic errors in industrial emissions and absolute atmospheric concentrations, can be alleviated through sufficiently accurate determinations of the global trend in CH_3CCl_3 concentrations. The use of trend measurements for determining atmospheric lifetimes has been discussed in detail by *Cunnold et al.* [1978] with specific application to the compounds $CFCl_3$ and CF_2Cl_2. By analogy with these latter compounds we expect that measurements of CH_3CCl_3 trends at several globally distributed sites should provide an accurate determination of the CH_3CCl_3 lifetime, unaffected by systematic errors of the aforementioned type.

The 'Atmospheric Lifetime Experiment' (ALE) was initiated to measure accurately the rates of increase of the atmospheric concentrations of the five long-lived atmospheric constituents: $CFCl_3$, CF_2Cl_2, CH_3CCl_3, CCl_4, and N_2O [*Prinn et al.*, this issue]. One of the goals of the experiment was to use the observed trends in concentration to deduce, where possible, the atmospheric lifetimes of these constituents. In this paper we present absolute concentrations and trends in CH_3CCl_3 concentrations obtained during ALE in the period July 1978 through June 1981. These observations are then interpreted in terms of the industrial emission, global circulation, and atmospheric lifetime of CH_3CCl_3.

The ALE utilizes automated dual-column electron capture gas chromatographs which sample the background air about four times daily at the following five globally distributed sites: Adrigole, Ireland (52°N, 10°W); Cape Meares, Oregon (45°N, 124°W); Ragged Point, Barbados (13°N, 59°W); Point Matatula, American Samoa (14°S, 171°W)'; and Cape Grim Tasmania (41°S, 145°E). Details concerning the instrumentation and station operation are provided by *Prinn et al.* [this issue]. Methyl chloroform is analyzed by using a silicone column with either a constant frequency (Ireland; Barbados: November 10, 1978, to May 8, 1979, at Samoa) or constant current (Oregon; Samoa, except November 10, 1978, to May 8, 1979; Tasmania) detector. Details concerning the technique for absolute and relative calibration of the data are given by *Rasmussen and Lovelock* [this issue]. Reference cylinders of air, which are analyzed relative to a primary standard, are shipped to the ALE sites, where they are used for approximately 3 months and then returned for reanalysis. The primary standard for CH_3CCl_3 is described by *Rasmussen and Lovelock* [this issue]. Details concerning data processing, including formulae used for data calibration and methods used for discerning locally polluted air from clean background air, are provided in *Prinn* et al. [this issue]. Periods in which local pollution is unambiguously identified are omitted from the data presented in this paper. Such pollution periods are largely restricted to the Adrigole ALE station, and their inclusion in the data would make this station nontypical of the 30°N–90°N atmospheric mass [*Prinn et al.*, this issue]. However, a complete digital record of all measurements taken in the ALE program, including those taken during pollution periods, is available to the interested reader [*Alyea*, 1983].

The CH_3CCl_3 data are analyzed in this paper by using a nine-box model (eight tropospheric boxes and one stratospheric box) of the global atmosphere and an optimal estimation technique for calculating lifetimes, as described in detail by *Cunnold et al.* [this issue (*a*)]. Industrial emission rates for CH_3CCl_3, which are required for estimation of lifetimes, are obtained from various chemical industry sources. Methyl chloroform is widely used as an industrial vapor degreasin solvent, particularly in the sheet metal industry, whic supplies automobile manufacturers.

2. Global Methyl Chloroform Data

Daily averaged CH_3CCl_3 mixing ratios and their dail standard deviations determined from the measurements a the five ALE sites in the period from July 1978 through Jun 1981 are shown in Figures 1–5. The monthly averaged mixin ratios $\bar{\chi}$(in pptv) and their standard deviations σ at each sit in this period are reported in Table 1. In the figures the time of calibration tank changes (and the calibration tank num bers) are indicated along the top of each plot. To obtain ou current best estimates of the absolute concentration o CH_3CCl_3 in the atmosphere, all values reported in Figures 1- 5 and Table 1 assume that the calibration factor $\xi = 1.0 \pm 0.15$ [*Rasmussen and Lovelock*, this issue].

The variation in the CH_3CCl_3 mixing ratios χ(pptv) over seasonal and longer time scales is conveniently described at station i by the function

$$\ln \chi_i = a_i + b_i\left[\frac{t-18}{12}\right] + d_i\left[\frac{t-18}{12}\right]^2 + c_i \cos\left[\frac{2\pi t}{12}\right] + s_i \sin\left[\frac{2\pi t}{12}\right] \quad (1)$$

where t is time measured in months with month 1 being July 1978. The coefficients a_i, b_i, d_i, c_i, and s_i have been determined from the monthly mean $\bar{\chi}$ and σ values given in Table 1 by using the method described by *Cunnold et al.* [this issue (*a*)]. Values of the latter coefficients for each of the five ALE stations are given in Table 2. An estimate of the globally averaged mixing ratio and trend of CH_3CCl_3 in the lower troposphere may be derived by suitably averaging the time series obtained in each latitude region. For this purpose, as well as for all the other data processing reported in this paper, the Adrigole, Ireland, and Cape Meares, Oregon, data have been optimally combined into a single time series. Thus, at northern hemisphere mid-latitudes we derive $a_i = 5.021$, $b_i = 0.069$, $d_i = -0.013$, $c_i = 0.001$, and $s_i = -0.009$. Using the various time series, we deduce at the midpoint of the second year of the experiment (January 1, 1980) that the annually averaged surface mixing ratios and trends are, respectively, 152 pptv and 10.3 pptv/yr at Adrigole/Cape Meares; 133 pptv and 9.3 pptv/yr at Ragged Point; 106 pptv and 12.3 pptv/yr at Point Matatula; and 103 pptv and 11.1 pptv/yr at Cape Grim. Averaging these four values yields a globally averaged surface mixing ratio and trend of 123 pptv and 10.7 pptv (8.7%) per year, respectively.

The locations of the five ALE stations were deliberately chosen to represent, as much as possible, the four major equal mass subdivisions of the global atmosphere. To the extent that this goal is accomplished, the globally averaged trends quoted above are valid. In this respect our principal concern must be with any major deviations from a monotonic gradient in CH_3CCl_3 concentrations with latitude. Available data [*Rasmussen and Khalil*, 1981] suggest that a small deviation does exist (mixing ratios at 70°N are 3–6% less than those at Cape Meares, while those at 90°S are about equal to those at Cape Grim). This suggests that our use of only Cape Meares and Adrigole (which show similar mixing ratios) may lead us to overestimate slightly the average

TABLE 1. Monthly Averaged CH_3CCl_3 Mixing Ratios $\bar{\chi}$ (pptv) and Their Standard Deviations σ (pptv) Determined from Measurements at the Five ALE Sites Over the Period July 1978 through June 1981

	Adrigole, 52°N, 10°W			Cape Meares, 45°N, 124°W			Ragged Point, 13°N, 59°W			Point Matatula, 14°S, 171°W			Cape Grim, 41°S, 145°E		
Month	$\bar{\chi}$	σ	N	$\bar{\chi}$	σ	N	$\bar{\chi}$	σ	N	$\bar{\chi}$	σ	N	$\bar{\chi}$	σ	N
7-78	140.1	5.7	224				124.5	7.2	144	88.9	3.6	61	86.0	4.3	52
8-78	137.2	4.7	185				124.4	7.8	200	90.1	4.2	125	83.3	3.2	124
9-78	132.3	4.9	235				117.8	10.3	168	90.5	3.6	126	85.6	3.6	74
10-78	134.2	4.8	151				118.2	10.2	111	92.8	3.6	108	88.5	2.8	44
11-78	134.6	4.1	92				115.9	8.9	125	93.2	5.2	97	93.6	1.4	57
12-78	—	—	—				124.1	8.4	129	93.7	6.4	57	92.7	1.3	38
1-79	139.3	5.7	74				125.2	9.3	114	97.5	4.1	18	91.4	1.5	52
2-79	140.9	3.9	25				124.7	8.7	112	94.8	4.5	95	91.4	1.4	92
3-79	140.3	6.2	68				126.1	8.6	95	95.7	3.7	117	93.9	2.0	109
4-79	144.2	6.1	62				—	—	—	95.3	4.2	120	95.6	1.2	106
5-79	146.5	5.7	81				127.4	4.1	80	97.4	2.5	122	95.8	1.7	107
6-79	147.1	6.4	68				124.9	5.8	40	98.1	0.9	114	97.6	2.3	104
7-79	143.9	7.0	136				128.5	8.3	88	99.6	1.4	118	96.6	1.8	89
8-79	144.7	6.2	104				132.1	5.2	117	101.5	2.1	111	98.4	1.5	112
9-79	146.1	6.4	94				123.7	9.3	134	101.6	2.4	102	99.7	1.6	101
10-79	150.4	5.1	53				123.6	7.4	127	103.8	2.2	115	101.0	1.1	94
11-79	149.6	7.2	72				128.5	7.3	90	106.4	2.1	113	101.9	1.4	110
12-79	153.1	7.0	69	156.8	8.7	55	131.5	5.1	130	98.9	5.8	102	101.3	0.9	81
1-80	152.3	8.0	58	159.6	6.0	71	134.8	6.2	133	105.0	3.0	100	100.7	1.1	94
2-80	153.8	6.8	106	—	—	—	135.6	6.5	105	107.8	3.2	122	101.2	1.4	72
3-80	158.3	7.1	89	154.9	2.4	20	140.6	4.8	104	108.4	3.3	103	103.0	1.4	114
4-80	162.6	7.5	103	158.0	3.0	78	137.6	3.9	79	108.9	3.9	116	102.5	1.6	44
5-80	165.1	7.4	60	157.9	2.3	93	138.8	4.7	137	110.3	2.3	115	107.4	2.2	76
6-80	163.2	8.3	115	155.1	3.0	114	142.3	4.3	147	111.5	1.5	94	108.5	2.2	83
7-80	163.4	6.3	111	151.0	3.6	85	141.1	5.7	129	113.1	1.0	117	109.5	1.8	93
8-80	158.7	5.9	111	151.9	3.0	81	139.1	4.3	59	114.5	1.3	117	110.9	1.4	92
9-80	156.0	5.2	104	156.7	7.8	103	137.0	8.3	126	115.1	2.0	103	112.4	1.0	69
10-80	159.3	5.5	81	165.1	8.3	111	137.4	7.9	126	115.6	1.3	17	113.5	1.3	78
11-80	161.2	4.8	75	162.6	6.8	118	143.3	5.8	117	117.8	2.3	63	113.2	1.8	96
12-80	161.5	5.0	66	160.2	5.8	104	144.3	7.8	118	120.1	3.7	100	111.8	0.8	85
1-81	160.6	7.3	118	161.8	5.2	121	143.5	5.5	138	120.9	4.0	42	111.7	0.9	54
2-81	161.7	5.2	60	166.3	9.8	107	146.0	5.2	119	—	—	—	112.1	0.9	44
3-81	162.7	6.1	96	160.7	3.6	120	140.7	4.7	100	122.2	2.0	30	114.0	1.3	86
4-81	164.9	4.1	46	161.1	2.8	106	146.8	6.6	104	120.3	2.4	136	115.1	0.9	76
5-81	168.8	5.0	59	162.3	3.6	104	148.9	4.5	123	119.9	2.9	123	116.0	1.3	86
6-81	169.1	5.9	79	163.2	2.8	108	146.9	4.2	110	121.8	1.9	113	116.8	1.4	60

Values tabulated assume an absolute calibration factor $\xi = 1$. The number N of measurements made each month is also tabulated.

mixing ratio in the 30°N–90°N semihemisphere. In contrast, our neglect of polluted air at Adrigole will cause us to underestimate slightly the mixing ratios in this semihemisphere. Present indications are that these two offsetting errors are of similar magnitude and are therefore not expected to have an important effect on our estimate of the global CH_3CCl_3 trend. These combined errors are also expected to lead to an uncertainty of, at most, 1% in the global CH_3CCl_3 content.

The coefficients c_i and s_i define the magnitude and phase of the annual cycle at each site. Maxima occur in late spring at Adrigole, Ragged Point, and Point Matatula and in late winter at Cape Meares and Cape Grim. It is apparent from Table 2 that these seasonal cycles are not very well defined by our 3-year data set, but they are nevertheless much larger than, and possess phases different from, those for $CFCl_3$ and CF_2Cl_2 [*Cunnold et al.*, this issue (*a*), (*b*)]. Annual cycles are expected for CH_3CCl_3 because of the seasonal oscillations in atmospheric circulation, particularly if, as observed, a significant meridional concentration gradient exists. Cycles are also expected because of the seasonal variation in CH_3CCl_3 destruction by OH, but only if the CH_3CCl_3 destruction time is less than or equal to the interhemispheric mixing time.

In examining the data at Adrigole, Ireland (Figure 1), it is evident that this site shows higher σ values for CH_3CCl_3 relative to the two southern hemisphere sites and that identifiable pollution periods (producing the small gaps in the data) are frequent. The large gap in the presented data from November 24, 1978, until January 4, 1979, was caused by obvious detector contamination in this period, resulting in the data being discarded.

Greater atmospheric variability (and therefore larger σ's) at Adrigole than at the southern hemisphere sites is expected because of the relative proximity of Adrigole to the predominantly northern mid-latitude sources of CH_3CCl_3. However, the larger σ values may also be due to the fact that Adrigole uses a constant frequency detector, while the two southern hemisphere stations use constant current detectors [*Prinn et al.*, this issue]. This latter explanation is supported by a comparison of the σ values at Samoa during the 6-month period when a constant frequency detector was temporarily used (November 10, 1978, to May 8, 1979) with the σ values following this period when the constant current detector was reinstated. It is also supported by the similarity of σ values at Adrigole and Ragged Point, where a constant frequency detector is also in use. It is not supported however by the often similar σ's at Adrigole and Cape Meares, where a constant current detector is used. Apparently both instrumental differences and true atmospheric variability are involved in explaining the station-to-station differences in standard deviations.

The standard deviations at Cape Meares, Oregon (Figure 2), are clearly anomalously high in the period from September 1980 through February 1981. There are no instrumental or calibration reasons to suspect the data in this period, although it corresponds largely to the period of use of

TABLE 2. Coefficients in the Empirical function (Equation (1) in Text) Describing the Long-Term Variation of the Natural Logarithm of the CH_3CCl_3 Mixing Ratios (With Calibration Factor $\xi = 1$) at the Five ALE Sites

i	Station	a_i	b_i	d_i	c_i	s_i	σ_{ti}^2
1	Adrigole	5.026 ± 0.007	0.077 ± 0.006	−0.013 ± 0.007	0.017 ± 0.007	−0.007 ± 0.007	2.89 × 10⁻
2	Cape Meares	5.038 ± 0.005	0.037 ± 0.010	—	−0.015 ± 0.006	−0.011 ± 0.007	2.62 × 10⁻
3	Ragged Point	4.889 ± 0.007	0.070 ± 0.006	−0.001 ± 0.008	0.011 ± 0.007	−0.012 ± 0.008	4.94 × 10⁻
4	Point Matatula	4.656 ± 0.005	0.116 ± 0.004	−0.005 ± 0.005	−0.006 ± 0.005	0.005 ± 0.005	2.31 × 10⁻
5	Cape Grim	4.626 ± 0.005	0.109 ± 0.005	−0.012 ± 0.006	0.000 ± 0.006	0.010 ± 0.006	2.43 × 10⁻

The coefficients for Cape Meares are computed from 18 months of data (January 1980 to June 1981). The coefficients for all other station refer to the 36-month period from July 1978 to June 1981. The quoted error bars for the coefficients include the effects of any nonwhit distribution of residuals. There is insufficient data at Cape Meares to adequately define values for d_2. Values of the variance σ_{ti}^2 of th residuals of the monthly mean observations relative to the empirical function for each station are also tabulated.

calibration tank number 114. (The phenomenon may indicate presently unrecognized local sources for CH_3CCl_3 at this station.) Other than this latter phenomenon, we have no reason to suspect any important effects of local pollution in the CH_3CCl_3 data at this site. The data gap from late January to mid-March 1980 is due to problems encountered during the start-up of this station.

As already noted, the CH_3CCl_3 measurements at Ragged Point, Barbados (Figure 3), show similar standard deviations to those at Adrigole. A visual inspection also indicates an apparent oscillation in the observed mixing ratios with a 1–2 month period. Identifiable local pollution does occur at this site, but it is isolated and infrequent and is evident largely in the last year of the CH_3CCl_3 data. The gap in data from late March through April 1979 was due to a temporary inability to deliver chromatographic carrier gas tanks to the site. On May 1, 1979, a new constant frequency detector was installed with an obvious improvement in instrumental precision.

The daily standard deviations of the measurements at Point Matatula, Samoa (Figure 4) are about half of those at Barbados, and the 1–2 month oscillations in the Barbadian data are not discernible in the Samoan data. As noted earlier, a temporary constant frequency detector was used in the period from November 10, 1978, to May 8, 1979. There is no evidence for local CH_3CCl_3 pollution at this site. The absence of data for 3 weeks in January 1979 was caused by a bee restricting the outside air intake. Gaps in the data from early October through early November 1980 and from late January through late February 1981 were due to instrumental damage caused by extremely poor voltage regulation in the power supply of American Samoa.

The Tasmanian CH_3CCl_3 data (Figure 5) generally shows the lowest σ's of any of the sites, which, as noted earlier, we believe is due to a combination of the remoteness of this site from the major CH_3CCl_3 sources and the use of the constant current detector. On November 4, 1978, the silicone column sample volume was changed from 5 to 7 ml, resulting in an obvious increase in the precision of the measurements. Occasional periods of identifiable pollution do occur at Cape Grim (about 10 days per year), and these periods have been omitted from the data presented, using the criteria given in *Prinn et al.* [this issue]. The instrument was inoperative in the latter half of October 1978. The data gap from December 11, 1978, through January 16, 1979, is due to identified contamination of an input valve.

3. Global Budget of Methyl Chloroform

As outlined by *Cunnold et al.* [1978] there are two principal methods for analyzing globally distributed observations of a long-lived atmospheric trace species, such a CH_3CCl_3, in terms of its sources and sinks. In one approacl the measured total global atmospheric content $c(t)$ o CH_3CCl_3 at time t is expressed in terms of its known releas rate $R(t)$ and unknown lifetime τ through the equation

$$c(t) = \int_0^t R(t')e^{(t'-t)/\tau}\,dt' \qquad (2$$

In the other approach the measured globally averaged trenc in CH_3CCl_3 mixing ratio $\chi(t)$ is expressed in terms of the known $R(t)$ and the unknown τ through the equation

$$\frac{1}{\chi}\frac{d\chi}{dt} = \frac{1}{c}\frac{dc}{dt} = \frac{R(t)}{\int_0^t R(t')e^{(t'-t)/\tau}\,dt'} - \frac{1}{\tau} \qquad (3)$$

The relative sensitivity of these two approaches to errors in

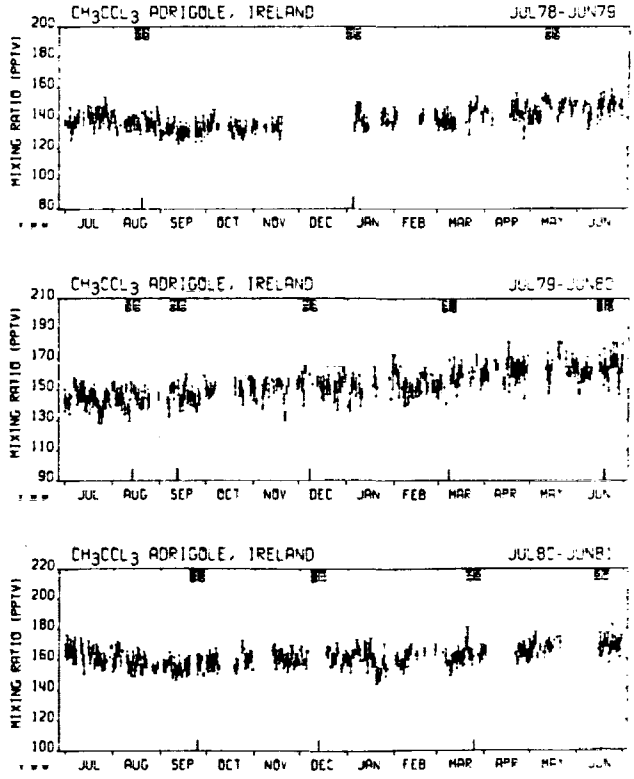

Fig. 1. Daily averaged CH_3CCl_3 mixing ratios (pptv) and their standard deviations (pptv) determined at Adrigole, Ireland (52°N, 10°W), during the period July 1978 through June 1981. Measured values presented here and in Figures 2–6 assume an absolute calibration factor $\xi = 1$.

the concentrations χ or c and the release rates R leads one to generally favor the trend technique over the global content technique for accurately defining τ. In this section we first review our knowledge of the global release rates of CH_3CCl_3 and their probable accuracy. We then analyze the ALE CH_3CCl_3 data by using both of the above methods.

3.1 *Methyl Chloroform Emissions*

Neely and Plonka [1978] have presented global production and atmospheric release estimates for 1,1,1-trichloroethane computed by the Dow Chemical Company for the period 1951–1976. We also have an update of these estimates which provides release data for 1977–1979 (W. B. Neely and H. Farber, private communication, 1982). Independent of these Dow Chemical Company data, we also have obtained through one of our authors (B. C. L.) the global CH_3CCl_3 sales estimates for the period 1977–1981 computed by Imperial Chemical Industries, PLC. These latter estimates include the fraction of the total sales applicable to each of the four equal mass subdivisions of the global atmosphere. The available data are summarized in Tables 3 and 4.

The year-to-year fluctuations in the ratio of the annual production to the annual release discernible in the Dow Chemical Company estimates are evidently due to year-to-year changes in the inventory held by the manufacturers. For example, inventories were obviously building up in the middle 1970's, evidently as a result of 1,1,1-trichloroethane replacing the solvent trichloroethylene as the use of the latter compound become increasingly regulated.

In order to relate the available data on annual production $P(t)$, sales $S(t)$, inventory $I(t)$, and releases $R(t)$, we make the reasonable assumption that a constant fraction f of the CH_3CCl_3 sales in each year is emitted to the atmosphere and that there is no important time lag between the sale and use of this compound. Thus for the year t

$$R(t) = \begin{cases} fS(t) \\ f(P(t) - I(t) + I(t-1)) \end{cases} \quad (4)$$

The fraction f is less than unity as a result of decomposition of CH_3CCl_3 during storage and use, of its use as an intermediate in production of other chemicals, and most important,

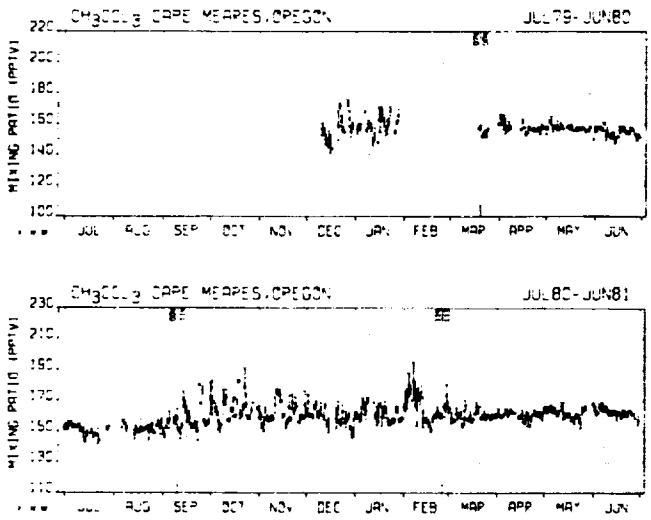

Fig. 2. As in Figure 1, but for Cape Meares, Oregon (45°N, 124°W), for the period January 1980 through June 1981.

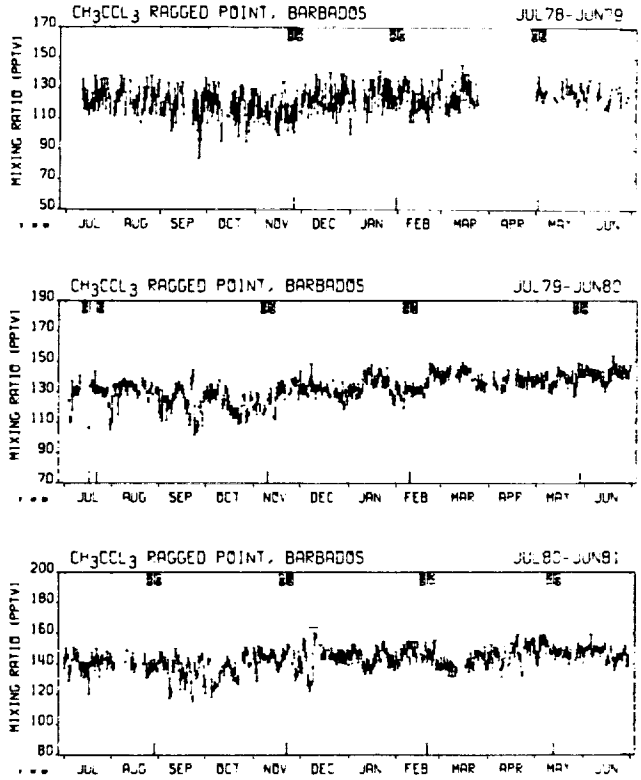

Fig. 3. As in Figure 1, but for Ragged Point, Barbados (13°N, 59°W).

of incineration or incarceration of concentrated organic solutions in which CH_3CCl_3 was used as the solvent. Using (4), the value of f appropriate to the Dow Chemical Company estimates is simply

$$f = \frac{\sum_{t=1951}^{t=1976} R(t)}{\left[\sum_{t=1951}^{t=1976} P(t)\right] - I(1976)} = 0.94 \quad (5)$$

where we have assumed $I(1976) = P(1976)/8$, which is typical of inventories in the industry. This f value is consistent with an independent estimate by Imperial Chemical Industries, PLC, implying only about 5% of CH_3CCl_3 sold is incarcerated or incinerated. Using (4) and (5), we have converted the $S(t)$ values for 1977–1981 from Imperial Chemical Industries, PLC, to $R(t)$ values, which can be compared to the $R(t)$ values estimated by the Dow Chemical Company for 1977–1979 (see Table 4). The global $R(t)$ estimates for 1977, 1978, and 1979 from Imperial Chemical Industries, PLC, are 1.0% higher, 6.1% lower, and 3.4% lower, respectively, than the corresponding estimates for these 3 years by the Dow Chemical Company. The agreement between these two essentially independent estimates is encouraging.

Based on these considerations, we have adopted the *Neely and Plonka* [1978] release data for 1951–1976. We assume that the percentages applicable to each semihemisphere in this period vary linearly between 1951 and 1977. Values assumed for 1951 are 100% for 90°N–30°N and 0% for the other three semihemispheres. Values assumed for 1977 are those given in Table 4.

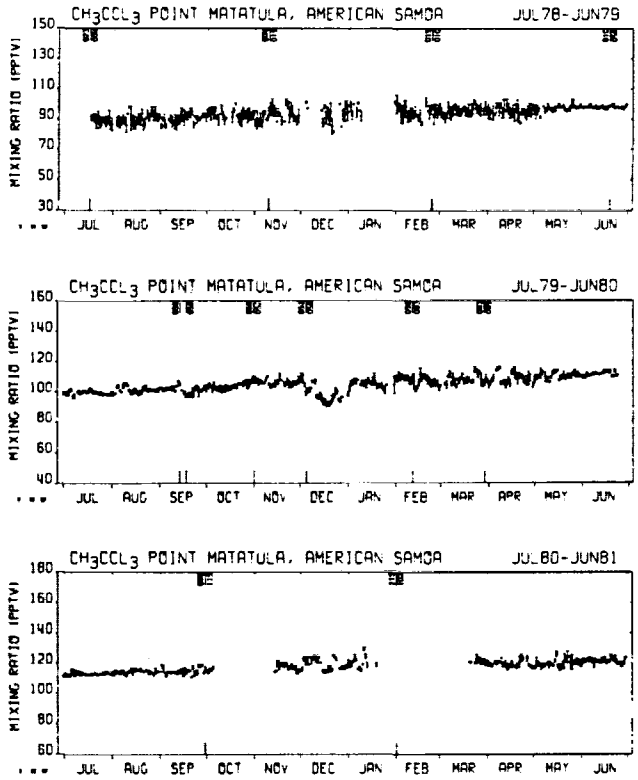

Fig. 4. As in Figure 1, but for Point Matatula, American Samoa (14°S, 171°W).

For the 1977–1979 period we adopt an average of the two global release estimates given in Table 4, since we have no reason to prefer one estimate from the other. The percentages applicable to each semihemisphere are assumed to be those estimated from Imperial Chemical Industries, PLC, data during this period.

As far as can be gauged from the data in Tables 3 and 4 and from industry sources polled by one of our authors (B. C. L.), the large inventory fluctuations evident in the middle and late 1970's are not expected in the 1979–1981 period because of the now-relative stability in supply versus demand for CH_3CCl_3. Thus any fractional changes in global production from 1979 to 1981 should have produced similar fractional changes in sales and releases. Data on production of CH_3CCl_3 in the United States are readily available [*U.S. International Trade Commission*, 1979, 1980, 1981]. In particular, a comparison of the annual data for 1979 and 1980 indicates production of CH_3CCl_3 decreased by 3.36% from 1979 to 1980, and a comparison of the annual data for 1980 and the preliminary annual data for 1981 indicates production increased by 0.76% from 1980 to 1981. Because of the international character of the sheet metals industry, and thus of the use of CH_3CCl_3 in its primary role as a degreaser, changes in production in the United States should be at least qualitatively indicative of worldwide trends. Therefore, we have assumed a 3.36% decrease from 1979 to 1980 and a 0.76% increase from 1980 to 1981 in the Dow Chemical Company estimates of global releases. With these 1980 and 1981 estimates and/or extrapolations in hand, we then adopt an average of the Imperial Chemical Industries, PLC, and Dow Chemical Company global release values for the 1980–1981 period, with the percentages of release in each semihemisphere being those calculated from the Imperial Chemical Industries, PLC, data alone.

A completely objective estimate of the probable errors in these adopted release values is not possible at present. However, we note that the number of different companies involved in CH_3CCl_3 production and the number of different release scenarios associated with CH_3CCl_3 end uses are both significantly less than the corresponding numbers for the chlorofluorocarbons $CFCl_3$ and CF_2Cl_2, for example. This is undoubtedly one of the major reasons behind the strong agreement between the independent release estimates by Dow Chemical Company and Imperial Chemical Industries PLC, for 1977–1979. The fractional differences ε between these latter two estimates and their mean in the 5 years 1977-1981 have a standard deviation σ, given by

$$\sigma = 100 \sqrt{\frac{\sum_{n=1}^{n=10} \varepsilon_n^2}{9}} \quad (6)$$

$$= 1.8\%$$

and we make the reasonable assumption that this latter σ value is a measure of the standard error in the release estimates adopted in this paper. That is, the 95% confidence limits on our release estimates are $\pm 2 \times 1.8\% = \pm 3.7\%$.

One important caveat about the above release estimates should be emphasized. They neglect any possible production of CH_3CCl_3 in Eastern Europe, U.S.S.R., and the Peoples Republic of China. Such unknown production is expected to be small in relation to the known production included in Tables 3 and 4 because of the unimportance of the automobile industry in these countries relative to the rest of the

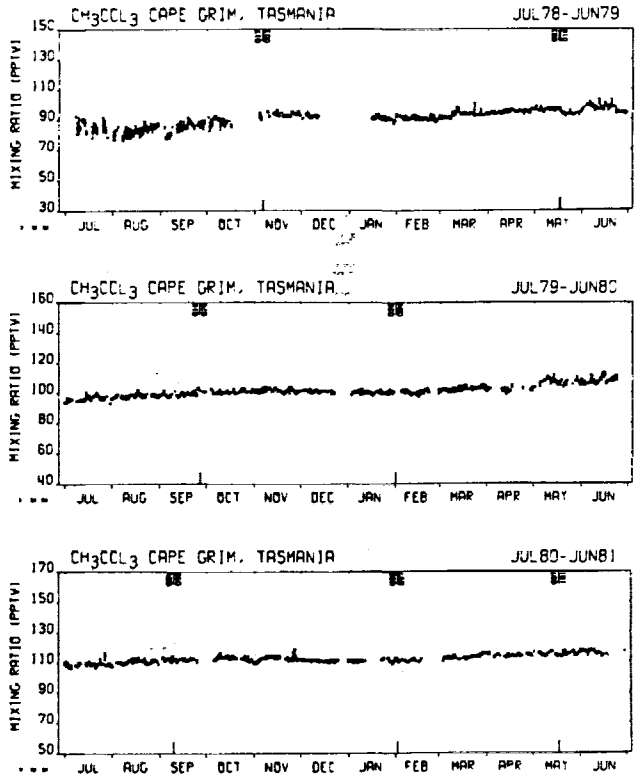

Fig. 5. As in Figure 1, but for Cape Grim, Tasmania (41°S, 145°E).

TABLE 3. Estimates of Global Production and Atmospheric Releases for CH_3CCl_3 for the Period 1951–1976

Year	Production	Releases	Year	Production	Releases
1951	0.1	0.1	1964	64.3	56.6
1952	0.2	0.2	1965	82.4	72.9
1953	1.0	1.0	1966	116.0	108.7
1954	2.9	2.7	1967	145.4	130.5
1955	8.4	8.0	1968	158.1	145.0
1956	13.8	12.4	1969	167.6	148.1
1957	20.6	19.6	1970	181.2	154.5
1958	21.8	20.7	1971	191.2	166.7
1959	31.8	30.3	1972	266.8	230.1
1960	38.0	36.1	1973	349.7	339.8
1961	39.9	38.0	1974	389.1	362.4
1962	59.3	56.2	1975	373.7	364.2
1963	58.0	50.7	1976	437.1	415.4

Units are 10^9 g yr^{-1} (after *Neely and Plonka* [1978]).

world. However, the possibility that we are systematically underpredicting CH_3CCl_3 releases by a small fraction should be kept in mind in interpreting our results. For example, recent measurements by *Rasmussen et al.* [1982] suggest the release of this chemical in the Peoples Republic of China. Also, as we will discuss later, the ALE data are compatible with a larger upward trend in the annual releases in recent years than that given in Tables 3 and 4.

TABLE 4. Estimates of Global and Semihemispheric Sales and Atmospheric Releases of CH_3CCl_3 for the Period 1977–1981

	Global	90°N–30°N	30°N–0°	0°–30°S	30°S–90°S
		1977			
Sales*	483.6	96.67%	1.36%	0.47%	1.50%
ICI†	454.6	96.67%	1.36%	0.47%	1.50%
Releases					
Dow‡	443.9	—	—	—	—
		1978			
Sales*	497.5	96.38%	1.41%	0.55%	1.66%
ICI†	467.7	96.38%	1.41%	0.55%	1.66%
Releases					
Dow‡	498.3	—	—	—	—
		1979			
Sales*	535.5	96.36%	1.40%	0.56%	1.68%
ICI†	503.4	96.36%	1.40%	0.56%	1.68%
Releases					
Dow‡	521.0	—	—	—	—
		1980			
Sales*	544.2	95.96%	1.65%	0.60%	1.79%
ICI†	511.5	95.96%	1.65%	0.60%	1.79%
Releases					
Dow¶	503.5	—	—	—	—
		1981			
Sales*	544.2	95.96%	1.65%	0.60%	1.79%
ICI†	511.5	95.96%	1.65%	0.60%	1.79%
Releases					
Dow¶	507.3	—	—	—	—

Units are 10^9 g yr^{-1} for the global estimates and percentages of the appropriate global estimates for the semihemispheric data.

*Imperial Chemical Industries, PLC estimates. Data for South African sales have been divided equally between the two southern semihemispheres.

† Computed in this paper by using equations (4) and (5).

‡W. B. Neely and H. Farber, Dow Chemical Co., private communication, 1982.

¶Estimated in this paper by extrapolation (see text).

3.2 *Methyl Chloroform Lifetimes*

The optimal estimation technique used in this paper to derive the atmospheric lifetime of CH_3CCl_3 from the $\bar{\chi}$, σ, and R values given in Tables 1–4 is fully described in *Cunnold et al.* [this issue (*a*)]. The technique includes the use of a nine-box model of the global atmosphere. Mean advective and eddy diffusive transports between the boxes are completely specified, except that the amplitude of all the horizontal eddy diffusive transports are expressed in terms of an unknown dimensionless amplitude factor F of order unity. The lifetime τ_s of CH_3CCl_3 in the stratospheric box (90°S–90°N, 0–200 mbar) is assumed to be 6 years, based on stratospheric destruction of CH_3CCl_3 by OH and ultraviolet radiation computed in a three-dimensional global circulation model [*Golombek*, 1982].

The principal recognized sink for CH_3CCl_3 in the troposphere is the reaction

$$OH + CH_3CCl_3 \rightarrow H_2O + CH_2CCl_3 \qquad (7)$$

By comparison, the loss of CH_3CCl_3 by transfer to ocean water is negligible [*Neely and Plonka*, 1978]. In our analysis of the data we wish to recognize the fact that the distribution of the principal tropospheric scavenger of CH_3CCl_3, namely OH, varies significantly with latitude and the fact that the chemical lifetimes and global transport times of CH_3CCl_3 may conceivably be comparable. Under these circumstances, the use of a globally averaged lifetime would be inappropriate [*Logan et al.*, 1981; *Derwent and Eggleton*, 1981]. We have therefore allowed for the existence of different lifetimes τ_i in each of our eight tropospheric boxes. The inverse lifetimes τ_i^{-1} are defined by

$$\tau_i^{-1} = \begin{cases} k_i[\mathrm{OH}]_i \\ [5.4 \times 10^{-12} \exp(-1820/T_i)]A[\mathrm{OH}]_i^* \ (s^{-1}) \end{cases} \qquad (8)$$

where k_i is the rate constant for the reaction of OH with CH_3CCl_3 in the ith box [*Jeong and Kaufman*, 1979; *Kurylo et al.* 1979]; $[OH]_i$ and $[OH]_i^*$ are the actual and assumed average concentrations, respectively, of OH (molecule cm^{-3}) in the ith box; T_i is the average temperature (°K) of the ith box; and A is an unknown dimensionless and box-independent amplitude factor of order unity. The prediction of the globally averaged tropospheric lifetime τ_t is therefore equivalent to the prediction of the factor A, which relates our assumed OH concentrations to the actual ones. That is, the

TABLE 5. Methyl Chloroform Atmospheric Lifetime Estimates and Their Standard Deviations $^{\sigma}$ Derived From the Trend at Each ALE Site

Site	Reciprocal Lifetime, $yr^{-1} \pm 1^{\sigma}$	Lifetime, years, $\pm 1^{\sigma}$	Approximate Weight Given to Station in Optimal Code
Adrigole, Ireland/Cape Meares, Oregon	0.143 ± 0.024	$7.0^{+1.3}_{-1.0}$	0.2
Ragged Point, Barbados	0.162 ± 0.029	$6.2^{+1.3}_{-1.0}$	0.1
Pt. Matatula, American Samoa	0.009 ± 0.019	111.0^{∞}_{-75}	0.4
Cape Grim, Tasmania	0.065 ± 0.021	$15.4^{+7.3}_{-3.8}$	0.3

relative OH concentrations in the eight boxes are specified, but the absolute OH concentrations are predicted.

For our assumed values for OH in each box we have chosen the computed annual average OH concentrations at 15° and 45° latitudes for land and sea surfaces given in Figure 27*b* of *Logan et al.* [1981]. Annual rather than seasonal average values are chosen since the box-to-box mixing times are much shorter than the CH_3CCl_3 destruction times in each box and also because most of the CH_3CCl_3 destruction occurs in the tropics, where the seasonal variations in OH are relatively small. There are, of course, several other model OH distributions we could choose from the literature. However, the Logan et al. distributions appear typical and are extensively compared to other calculations in their paper. Using (8), these assumed OH concentrations yield the following values for $A\tau_i$: 18.6 years in the 90°N–30°N, 200–500 mbar box; 6.4 years in the 90°N–30°N, 500–1000 mbar box; 6.2 years in the 30°N–0°, 200–500 mbar box; 2.1 years in the 30°N–0°, 500–1000 mbar box; 5.9 years in the 0°–30°S, 200–500 mbar box; 2.2 years in the 0°–30°S, 500–1000 mbar box; 14.9 years in the 30°S–90°S, 200–500 mbar box; and 5.8 years in the 30°S–90°S, 500–1000 mbar box.

The analysis of the CH_3CCl_3 data to determine the value of A (or equivalently the tropospheric lifetime) utilizes a box-model transport factor F, equal to 1.6, which is principally determined by the more precisely defined latitudinal distributions of $CFCl_3$ and CF_2Cl_2 [*Cunnold et al.*, this issue (*a*, *b*)]; in fact, this value of F results in an 11% underprediction of the latitudinal gradient of CH_3CCl_3 that will be discussed later. Using this latter transport factor, the $R(t)$ values given in Tables 3 and 4, and applying the estimation technique to each time series individually, we obtain the atmospheric lifetime estimates given in Table 5. Averaging the reciprocal lifetime estimates from the four time series with equal weight gives an atmospheric lifetime of methyl chloroform of $10.5^{+0.7}_{-0.8}$ years where the uncertainty limits correspond to the standard error of the four series mean. This may be translated into a tropospheric lifetime (and thus a value for A) by using the expression which is valid for our box model

$$\frac{4+r}{\tau} = \frac{4}{\tau_t} + \frac{r}{\tau_s} \tag{9}$$

where τ, τ_s, and τ_t are the atmospheric, stratospheric (6 years), and tropospheric lifetimes, respectively, and r is the ratio of the stratospheric mixing ratio to the average mixing ratio in the upper troposphere. Using a troposphere to stratosphere transfer time (t_s) of 4 years (as used for $CFCl_3$ and CF_2Cl_2 by *Cunnold et al.* [this issue (*a*, *b*)], we obtain $r = 0.47$ on January 1, 1980. This may be compared with a value of about 0.58 obtained in the three-dimensional model simulation of the methyl chloroform distribution by *Golombeck* [1982] (which would correspond to a t_s value of approximately 3 years). Using (9) with $r = 0.47$ gives a tropospheric lifetime of methyl chloroform of $11.5^{+9.6}_{-3.5}$ years and a value of $A = 0.37 \pm 0.17$ (using $r = 0.58$ yields τ_t and A values differing by only about 2% from these).

It is apparent that the ALE measurements yield an A value less than unity. An A value equal to unity corresponds to a tropospheric lifetime in the box model of approximately 4.3 years (and using (9) an atmospheric lifetime of 4.5 years). Values of A less than unity thus correspond to lifetimes greater than 4.3 years, which is significantly longer than the global atmospheric transport time. When $A < 1$, the lifetime estimates should not, therefore, be strongly dependent on the assumed latitudinal distribution of OH. In fact our computations show that assuming a uniform distribution of OH in the troposphere produces a change in the lifetime estimate by only approximately 0.1%. In other words, while CH_3CCl_3 measurements provide a useful measure of the globally averaged tropospheric OH concentration, they are not useful for determining the latitudinal distribution of this radical.

We also note that the long lifetimes deduced here imply that the behavior of CH_3CCl_3 on seasonal and shorter time scales at the ALE sites must be dominated by meteorological (and perhaps industrial release) variations and not by seasonal or higher frequency variations in OH. For example, by multiplying the seasonal average OH concentrations predicted by *Logan et al.* [1981] by $A = 0.37$ we deduce chemical lifetimes in the 90°N–30°N, 500–1000 mbar box of ~65 years in winter and ~9 years in summer. For comparison, the diffusive exchange times in our model (using $F = 1.6$) between this latter box and the adjacent 30°N–0° box are very much shorter: namely, ~0.2 years in winter and ~0.45 years in summer.

The optimal lifetime estimate (as opposed to the four-station average estimate given above) is obtained by weighting each monthly observation by

$$\sigma^{-2} = \left(\frac{\sigma_m^2}{n_m} + M\sigma_0^2 \right)^{-1} \tag{10}$$

where σ_m is the standard deviation of the measurements during month m, n_m is the number of measurements made in month m divided by 12 (to allow for the typical observed three-day correlation between individual measurements), σ_0^2 is the variance of the residuals of the monthly mean

observations relative to the fitted empirical model (equation (1)) as given in Table 2, and M is a factor (~1.4 for Adrigole/Cape Meares and Cape Grim and ~1 for the other two sites) that increases the variances to reflect the month-to-month autocorrelation of the residuals [see *Cunnold et al.*, this issue (*a*, *b*)]. The optimal estimate of the atmospheric lifetime is $15.4^{+7.3}_{-3.8}$ years and may be approximately obtained by weighting the individual station estimates by the weights given in Table 5. This optimal estimate is obviously strongly influenced by the two southern hemisphere estimates of lifetime that (particularly at Point Matatula) are substantially longer than those for the northern hemisphere.

To provide further insight into these results, we have plotted in Figure 6 the month-by-month residuals $\ln(\chi_m/\chi_c)$ for each station where the mixing ratios χ_m and χ_c are those measured by ALE and those calculated in the nine-box model (with τ = 10.5 years and F = 1.6), respectively. It is apparent that the observed mixing ratios at the two southern hemisphere stations (and thus the latitudinal gradient) are not well predicted in the model. There is a slight downward temporal trend in the residuals at Adrigole/Cape Meares and Ragged Point, a slight upward trend at Cape Grim, and a pronounced upward trend at Point Matatula. This means that the underprediction of the latitudinal gradient is generally decreasing with time and that, as already noted, the derived τ values at Adrigole/Cape Meares and Ragged Point are slightly less than 10.5 years, while those at Cape Grim and Point Matatula are slightly greater and much greater, respectively, than 10.5 years. Neglect of the first few months of data at each station could be justified on the basis of general startup problems. This would tend to decrease the temporal trends in the residuals at all stations except Point Matatula and thus bring the τ values derived from these stations into closer agreement with the average τ value (10.5 years).

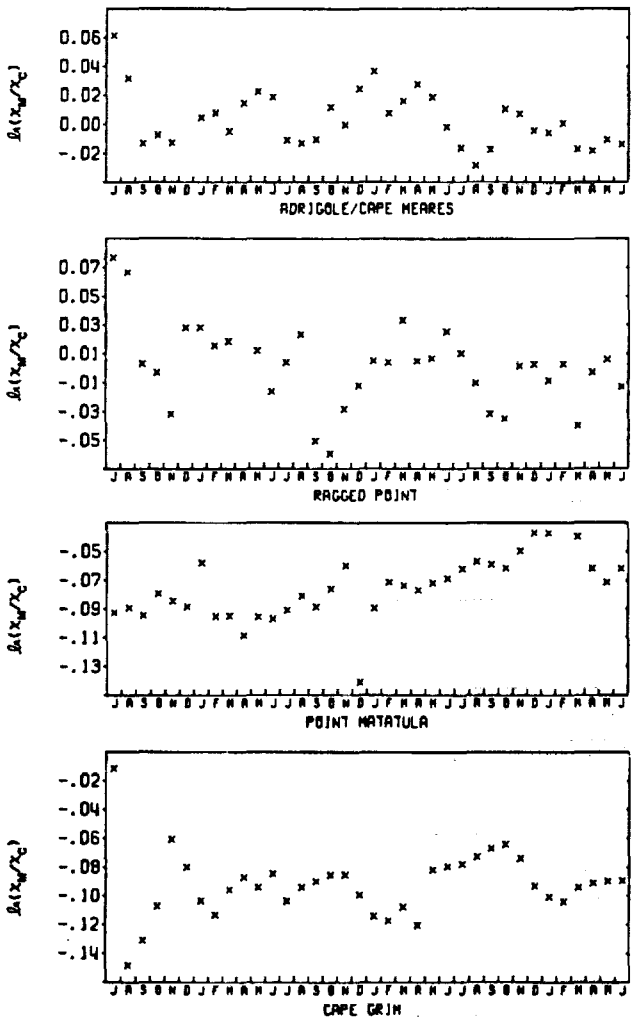

Fig. 6. Values for methyl chloroform of the natural logarithm of the ratio of the monthly mean measured (χ_m) and calculated (χ_c) mixing ratios. Calculated mixing ratios are 12-month running mean values obtained from the nine-box model with F = 1.6 and τ = 10.5 years.

TABLE 6. Reciprocal Atmospheric Lifetime Estimates (years^{-1}) and Their Standard Deviations σ for Methyl Chloroform as a Function of Time Obtained by Averaging and by Optimally Combining the Lifetime Estimates at the ALE Sites

Time Period, month/year	Optimal Combination $\pm 1\sigma$, year^{-1}	Average $\pm 1\sigma$, year^{-1}
7/78–6/79	0.246 ± 0.059	0.131 ± 0.067
7/80–6/81	0.124 ± 0.051	0.132 ± 0.030
7/78–6/80	0.086 ± 0.021	0.094 ± 0.027
7/79–6/81	0.044 ± 0.019	0.083 ± 0.033
7/78–6/81	0.070 ± 0.011	0.095 ± 0.035

The optimal estimate of τ (15.4 years) is suspicious because this estimate gives greatest weight to Point Matatula, which from its anomalously long lifetime (Table 5) and from the residuals illustrated in Figure 6 is behaving quite differently from the other three stations. Moreover, recently obtained CH_3CCl_3 data for the period July–December 1981 suggest that the Point Matatula lifetime estimate based on the July 1978–June 1981 period is an artifact. The optimal lifetime is further suspect when we compare the lifetime estimates obtained by optimally combining and by averaging the individual station estimates for several time periods, as shown in Table 6. Here it is to be noted that in contrast to the results for $CFCl_3$ and CF_2Cl_2 [*Cunnold et al.*, this issue (*a*, *b*)] the standard error of the estimate of the mean does not decay as $N^{-3/2}$, where N is the number of years of observation, which would be the case for random errors. Apparently, the optimal estimate is not adequately accounting for the differences between individual station estimates, and also, one or more sites is giving a steadily biased estimate of the lifetime over the 3-year period. Also, in contrast to the results for $CFCl_3$ and CF_2Cl_2, the optimal estimate appears to be converging more slowly than the estimate obtained by averaging. For these reasons we reject the optimally combined estimate of lifetime for CH_3CCl_3 and recommend the four-station average lifetime estimate of $10.5^{+6.2}_{-2.8}$ years as the current best estimate by the trend method.

This latter estimate of the lifetime is independent of the absolute calibration factor ξ for the CH_3CCl_3 mixing ratios. The quoted error bars do not, however, include uncertainties in CH_3CCl_3 releases. If the difference between the two estimates of release given in Table 4 in the period 1977–1981 (suggesting 1 σ errors of only 1.8%) were to be regarded as an estimate of the total release uncertainty, the effect on the lifetime estimate would be small, and the uncertainty in the lifetime would be dominated by the measurement uncertainties already discussed. However, if the release errors are much larger than 1.8%, particularly if the trend in the releases is in error, then our lifetime estimates and their

uncertainties can be substantially affected. We will demonstrate this point shortly.

It is apparent that the trend technique applied to the ALE data is yielding τ estimates similar to the largest estimates by previous workers as quoted in the introduction. We should address, therefore, the question of whether the CH_3CCl_3 lifetimes derived by using the trend technique are consistent with the release history $R(t)$ and present global content of this species $c(t)$ as expressed by (2). The ALE CH_3CCl_3 data at each station, when combined with runs of our nine-box model, enable us to estimate a $c(t)$ value for January 1, 1980, of 2580×10^6 kg. Using the emission data in Tables 3 and 4, we then estimate $\tau = 9.8$ years.

To assess errors in this latter τ estimate we first note that our deduced random error of $\pm 1.8\%$ in $R(t)$ is much less than the errors in $c(t)$ so we will specifically consider τ uncertainties caused by $c(t)$ uncertainties only. Our assessment of $c(t)$ is deduced, in essence, from the globally averaged lower tropospheric CH_3CCl_3 mixing ratio $\bar{\chi}$ (obtained from ALE measurements) and from the ratio r of the globally averaged stratospheric to upper tropospheric mixing ratio (obtained from models). Uncertainties in $\bar{\chi}$ include a standard error of 15% in the absolute calibration factor ξ [*Rasmussen and Lovelock*, this issue] and an error ~1% resulting from equating Cape Meares and Adrigole measurements with their semihemispheric average. Uncertainty in r is ~23%, based on the difference between the r values computed in our nine-box model and in the *Golombek* [1982] three-dimensional model.

The uncertainty in $\bar{\chi}$ is converted into an uncertainty in τ by using $\partial(\ln \bar{\chi})/\partial(1/\tau) = -4.4$ years (derived from the nine-box model), giving $\Delta(1/\tau) = 0.032$ year^{-1}. The uncertainty in r uses $\partial r/(\partial(1/\tau) = -25.9$ years (also derived from the nine-box model) to give $\Delta(1/\tau) = 0.004$ year^{-1}. Combining these two uncertainties in $1/\tau$ gives an atmospheric lifetime estimate by the global content technique of $\tau = 9.8^{+4.5}_{-2.3}$ years.

It is apparent that lifetimes τ computed with (2) are consistent with those computed by the trend method. For example, the trend lifetime of 10.5 years that we derived, when combined with the emission history of CH_3CCl_3, yields a value of $c(t)$ only 2.7% greater than the $c(t)$ value inferred from ALE observations. This discrepancy obviously lies well within the error bars on the observationally derived $c(t)$ value. Using (9) with $r = 0.47$, the τ value determined by the global content technique corresponds to $A = 0.40 \pm 0.15$ and $\tau_t = 10.6^{+6.5}_{-2.9}$ years.

As noted earlier, our nine-box model (with transport factor $F = 1.6$ and lifetime $\tau = 10.5$ years) does not predict as large a latitudinal gradient for CH_3CCl_3 as that observed by ALE. There are three possibilities we have investigated that could remove this discrepancy. The first is that, at present, we are significantly underestimating southern hemispheric releases of $CFCl_3$ and CF_2Cl_2, and therefore the value of $F = 1.6$ derived from these compounds (and used here for CH_3CCl_3) is causing erroneously high rates of meridional mixing in our model. If instead we use $F = 1.0$ (with $\tau = 10.5$ years) for CH_3CCl_3, we find that the difference between observed and calculated CH_3CCl_3 latitudinal gradients is largely removed. However, if we wish to use $F = 1.0$ to explain the $CFCl_3$ and CF_2Cl_2 data also [*Cunnold et al.*, this issue (*a*, *b*)], the required spatial redistributions of the releases of these latter two compounds are much larger than we can justify.

A second possibility is that the 3 years of ALE measurements presently available for CH_3CCl_3 are inadequate for definition of long-term trends and, in particular, are providing significant overestimates of these trends. Lower trends would lead to lower estimates of τ. Thus τ becomes more comparable to the interhemispheric mixing time, which therefore leads to larger predicted latitudinal CH_3CCl_3 gradients. Indeed, if we take $\tau = 5$ years rather than 10.5 years there is strong agreement (using $F = 1.6$) between the gradients in the model and observations (except that the model now overpredicts the Adrigole to Ragged Point gradient by ~4% and underpredicts the Ragged Point to Cape Grim gradient by ~4%). However, this 5-year lifetime assumption in the model leads to underestimations of the global lower-tropospheric temporal trend and absolute mixing ratio by about 17% and 28%, respectively. Also, the trends calculated at each station with $\tau = 5$ years differ much more from the observed trends than those computed by using $\tau = 10.5$ years.

A third possibility is that the rate of increase in the release of CH_3CCl_3 in the last few years is being underestimated. This would cause us to underestimate the latitudinal gradient since releases are almost exclusively confined to the northern hemisphere. To investigate this possibility, we have redistributed the official releases $R(t)$ given in Tables 3 and 4 for the years $t = 1976$–1981 to produce modified releases $R'(t)$ (in units of 10^9 g yr^{-1}), defined in terms of $R(t)$ by the formula

$$R'(t) = R(t) + 12.95\,(t - 1978.5) \qquad (11)$$

Specifically, the $R'(t)$ values are, respectively, 7.8%, 4.3%, and 1.3% less than the official values in 1976, 1977, and 1978 and 1.3%, 3.8%, and 6.4% greater in 1979, 1980, and 1981 (however, the total releases are the same for the modified and official releases). Using these modified releases with $F = 1.6$, the calculated Adrigole to Cape Grim gradient differs by only 2.7% from the observed gradient (as noted earlier the official releases lead to an 11% underprediction of this gradient). The modified releases lead to $1/\tau = 0.154 \pm 0.078$ year^{-1} ($\tau = 6.5^{+6.3}_{-2.2}$ years) when we average with equal weight the $1/\tau$ values derived from the trends in the four semihemispheres. This may be compared to $1/\tau = 0.095 \pm 0.035$ year^{-1} ($\tau = 10.5^{+6.2}_{-2.8}$ years) for the official releases.

Of the three possible explanations discussed above we consider the third to be the least unlikely. We emphasize, however, that even this third explanation possesses objectionable features. In particular, the $1/\tau$ estimates for the modified releases vary even more widely from station to station than the estimates given in Table 5, which use the official releases. In other words the modified releases provide a poorer simulation of the temporal trends than the official releases. Also using the τ value of 6.5 years derived from the modified releases, we obtain a global CH_3CCl_3 content that is 18% less than that inferred from the ALE data. The calibration factor ξ would need to be 0.82 to remove the latter disagreement; this value lies outside our 1σ but inside our 2σ limits on ξ. Finally, the suggested modifications to the releases clearly exceed our suggested probable error in $R(t)$ of $\pm 3.7\%$ (95% confidence). However, as already noted, the estimates of $R(t)$ and their probable errors involved certain assumptions whose validity is difficult to assess. Perhaps a combination of an increasing f value (e.g., resulting from a lowering of user inventories), increasing

Communist production (presently ignored), and an underestimate of 1980 and 1981 production outside the United States could lead to an increased trend in the releases of the type expressed by (11). However, this is certainly speculative, and the lifetime estimate of $6.5^{+6.2}_{-2.2}$ years derived with the modified releases must be rejected at the present time.

4. CONCLUSIONS

Averaging the inverse trend lifetime of 0.095 ± 0.035 year^{-1} and the inverse global-content lifetime of 0.102 ± 0.032 year^{-1} calculated for CH_3CCl_3 from the ALE data and the official CH_3CCl_3 releases, we obtain $\tau = 10.2^{+5.2}_{-2.6}$ years. Using (9), this latter τ value provides an estimate of $\tau_t = 11.0^{+7.8}_{-3.2}$ years, which corresponds to $A = 0.39 \pm 0.16$. Since $A = 1$ in our nine-box model corresponds to a global tropospheric average OH concentration [OH] $\sim 1.2 \times 10^6$ molecule cm^{-3}, then the CH_3CCl_3 ALE data implies [OH] $\sim 1.2 \times 10^6 A = (5 \pm 2) \times 10^5$ molecule cm^{-3}.

In the *Logan et al.* [1981] two-dimensional model (whose OH concentrations are used to define our standard model), $A \sim 1^{+1.0}_{-0.5}$ and [OH] $\sim (1.2^{+1.2}_{-0.6}) \times 10^6$ molecule cm^{-3}. The two-dimensional diagnostic model of *Chameides and Tan* [1981] has [OH] $\sim (4.2^{-3.8}_{-2.0}) \times 10^5$ molecule cm^{-3}, while the two-dimensional model of *Volz et al.* [1981] implies [OH] $\sim (6.5^{+3}_{-3}) \times 10^5$ molecule cm^{-3} on the basis of an analysis of ^{14}CO measurements. The small differences between the ALE-derived result and the results from the latter two models are not statistically significant, but it is apparent that the ALE results imply tropospheric OH concentrations ~2.5 times less than those computed by Logan et al. Since the latter model is carefully constrained by using observed concentrations of H_2O, O_3, CO, CH_4, NO, NO_2, and HNO_3 and also attempts to include all the important known OH production and loss processes, the disagreement with the ALE results may conceivably be due to presently unrecognized sources or sinks for tropospheric OH.

For the reasons discussed in detail in section 3 we have rejected the CH_3CCl_3 lifetime of 15.4 years that was deduced from ALE by using the optimal trend method and the lifetime of 6.5 years required to simultaneously fit the ALE latitudinal gradients of CH_3CCl_3, CF_2Cl_2, and $CFCl_3$. If we included these rejected estimates with the two we consider valid (four-station average trend lifetime = 10.5 years, global content lifetime = 9.8 years), we would obtain an average lifetime of 9.6 years compared to our preferred value of 10.2 years.

Our model results are in qualitative agreement with the model results of *Derwent and Eggleton* [1981]. They found a reasonable fit to northern hemispheric CH_3CCl_3 trend observations by using $\tau = 5$ years, but this lifetime was far too short to explain the then available southern hemispheric observations. For comparison, if we ignored in our model the two southern hemisphere ALE stations, we would deduce a two-station average trend lifetime of 6.6 years. The southern hemispheric CH_3CCl_3 trends are significantly greater than those in the northern hemisphere and imply globally averaged lifetimes significantly greater than those derived from northern hemisphere trends alone.

The ALE program has provided the most extensive measurements of the global concentrations and trends for CH_3CCl_3 and the most accurate determination of its atmospheric lifetime yet obtained. Continued measurements of this species at the ALE sites should result in a significant improvement in our knowledge of its lifetime and thus of global average OH concentrations. In particular, it is important to establish whether the significant differences between trends in the two hemispheres persist as further years of ALE data are obtained. Also, the need for improvement in the absolute calibration of CH_3CCl_3 concentrations in the atmosphere in order to improve the accuracy of the τ values derived by using the global content method is readily apparent.

Finally, we note that we have been unable to explain simultaneously the ALE observations of the latitudinal gradients of CH_3CCl_3, $CFCl_3$, and CF_2Cl_2 by using the same global meridional mixing rates. We have suggested that this problem may be at least partly alleviated if we have underestimated the rate of increase in CH_3CCl_3 emissions over the last few years. With the greater data base made available through the fourth and fifth years of the ALE program we intend to estimate emissions, lifetimes, and global mixing rates, optimally. However, it is clear that additional research on CH_3CCl_3 emissions is urgently needed, and until such research has been accomplished the lifetime of 6.5 years for CH_3CCl_3, estimated with our modified release scenario, must be held in abeyance.

Acknowledgments. We thank our colleagues in the ALE program, Richard Rosen, James Lovelock, and Paul Fraser, for their extensive contributions to the ALE measurements and data analysis. This research was supported by the Fluorocarbon Project of the Chemical Manufacturers Association. Nominal support was also provided by the Atmospheric Chemistry Program of NSF (to R.G.P.) and the Upper Atmosphere Research Program of NASA (to R.A.R.).

REFERENCES

Alyea, F., The Atmospheric Lifetime Experiment: A guide to the ALE data tape, *NASA Tech. Memo.*, in press, Washington, D.C., 1983.

Chameides, W., and A. Tan, A two-dimensional diagnostic model for tropospheric OH: An uncertainty analysis, *J. Geophys. Res.*, *86*, 5209–5223, 1981.

Chang, J., and J. Penner, Analysis of global budgets of halocarbons, *Atmos. Environ.*, *12*, 1867–1873, 1978.

Cox, R., R. Derwent, A. Eggleton, and J. Lovelock, Photochemical oxidation of halocarbons in the troposphere, *Atmos. Environ.*, *10*, 305–308, 1976.

Crutzen, P., and J. Fishman, Average concentrations of OH in the troposphere and the budgets of CH_4, CO, H_2, and CH_3CCl_3, *Geophys. Res. Lett.*, *4*, 321–324, 1977.

Crutzen, P., I. Isaksen, and J. McAfee, The impact of the chlorocarbon industry on the ozone layer, *J. Geophys. Res.*, *83*, 345–363, 1978.

Cunnold, D., F. Alyea, and R. Prinn, A methodology for determining the atmospheric lifetime of fluorocarbons, *J. Geophys. Res.*, *83*, 5493–5500, 1978.

Cunnold, D., R. Prinn, R. Rasmussen, P. Simmonds, F. Alyea, C. Cardelino, A. Crawford, P. Fraser, and R. Rosen, The Atmospheric Lifetime Experiment, 3, Lifetime methodology and application to 3 years of $CFCl_3$ data, *J. Geophys. Res.*, this issue (*a*).

Cunnold, D., R. Prinn, R. Rasmussen, P. Simmonds, F. Alyea, C. Cardelino, and A. Crawford, The Atmospheric Lifetime Experiment, 4, Results for CF_2Cl_2 based on 3 years of data, *J. Geophys. Res.*, this issue (*b*).

Derwent, R., and A. Eggleton, Halocarbon lifetimes and concentration distributions calculated using a two-dimensional tropospheric model, *Atmos. Environ.*, *12*, 1261–1269, 1978.

Derwent, R., and A. Eggleton, Two-dimensional model studies of methyl chloroform in the troposphere, *Q. J. R. Meteorol. Soc.*, *107*, 231–242, 1981.

Golombek, A., A global three-dimensional model of the circulation and chemistry of long-lived atmospheric species, Ph.D. thesis, Mass. Inst. of Technol., Cambridge, 1982.

Jeong, K., and F. Kaufman, Rates of the reactions of 1,1,1-trichloroethane and 1,1,2-trichloroethane with OH, *Geophys. Res. Lett.*, *6*, 757–759, 1979.

Kurylo, M., P. Anderson, and O. Klais, A flash-photolysis resonance-fluorescence investigation of the reaction OH + CH_3CCl_3 → H_2O + CH_2CCl_3, *Geophys. Res. Lett.*, *6*, 760–762, 1979.

Logan, J., M. Prather, S. Wofsy, and M. McElroy, Tropospheric chemistry: A global perspective, *J. Geophys. Res.*, *86*, 7210–7254, 1981.

Lovelock, J., Methyl chloroform in the troposphere as an indicator of OH radical abundance, *Nature*, *267*, 32, 1977.

Makide, Y., and S. Rowland, Tropospheric concentrations of methyl chloroform, CH_3CCl_3, in January 1978 and estimates of the atmospheric residence times for hydrohalocarbons, *Proc. Natl. Acad. Sci. U.S.*, *78*, 5933–5973, 1981.

McConnell, J., and H. Schiff, Methyl chloroform: Impact on stratospheric ozone, *Science*, *199*, 174–177, 1978.

Neely, W., and J. Plonka, Estimation of time-averaged hydroxyl radical concentration in the troposphere, *Environ. Sci. Technol.*, *12*, 317–321.

Prinn, R., P. Simmonds, R. Rasmussen, R. Rosen, F. Alyea, C. Cardelino, S. Crawford, D. Cunnold, P. Fraser, and J. Lovelock, The atmospheric Lifetime Experiment, 1, Introduction, instrumentation, and overview, *J. Geophys. Res.*, this issue.

Rasmussen, R., and M. Khalil, Global atmospheric distribution and trend of methyl chloroform, *Geophys. Res. Lett.*, *8*, 1005–1007, 1981.

Rasmussen, R., and J. Lovelock, The Atmospheric Lifetime Experiment, 2: Calibration, *J. Geophys. Res.*, this issue.

Rasmussen, R., M. Khalil and J. Chang, Atmospheric trace gases over China, *Environ. Sci. Technol.*, *16*, 124–126, 1982.

Singh, H., Atmospheric halocarbons: Evidence in favor of reduced average hydroxyl concentration in the troposphere, *Geophys. Res. Lett.*, *4*, 101–104, 1977*a*.

Singh, H., Preliminary estimation of average tropospheric OH concentrations in the northern and southern hemispheres *Geophys. Res. Lett.*, *4*, 453–456, 1977*b*.

Singh, H., L. Salas, H. Shigeishi, and E. Schribner, Atmospheric halocarbons, hydrocarbons, and sulfur hexafluoride: Global distributions, sources, and sinks, *Science*, *203*, 899–903, 1979.

U.S. International Trade Commission, Synthetic Organic Chemicals: U.S. Production and Sales, 1979, *Publ. 1099*, p. 269, Washington, D.C., 1979.

U.S. International Trade Commission, Synthetic Organic Chemicals: U.S. Production and Sales, 1980, *Publ. 1183*, p. 265, Washington, D.C., 1980.

U.S. International Trade Commission, Preliminary Report on U.S. Production of Selected Synthetic Organic Chemicals, Preliminary Totals, in press, Washington, D.C., 1981.

Yung, Y., M. McElroy, and S. Wofsy, Atmospheric halocarbons: A discussion with emphasis on chloroform, *Geophys. Res. Lett.*, *2*, 397–399, 1975.

Volz, A., D. Ehhalt, and R. Derwent, Seasonal and latitudinal variation of ^{14}CO and the tropospheric concentration of OH radicals, *J. Geophys. Res.*, *86*, 5163–5171, 1981.

F. N. Alyea, C. A. Cardelino, and D. M. Cunnold, School of Geophysical Sciences, Georgia Institute of Technology, Atlanta, GA 30332.

A. J. Crawford and R. A. Rasmussen, Department of Environmental Science, Oregon Graduate Center, Beaverton, OR 97006.

B. C. Lane, ICI Americas, Inc., Wilmington, DE 19897.

R. G. Prinn, Department of Earth, Atmospheric and Planetary Sciences, Massachusetts Institute of Technology, Cambridge, MA 02139.

P. G. Simmonds, Department of Geochemistry, University of Bristol, Bristol, England.

(Received July 8, 1982;
revised March 28, 1983;
accepted April 25, 1983.)

JOURNAL OF GEOPHYSICAL RESEARCH, VOL. 88, NO. C13, PAGES 8427–8441, OCTOBER 20, 1983

The Atmospheric Lifetime Experiment 6. Results for Carbon Tetrachloride Based on 3 Years Data

P. G. SIMMONDS,[1] F. N. ALYEA,[2] C. A. CARDELINO,[2] A. J. CRAWFORD,[3] D. M. CUNNOLD,[2] B. C. LANE,[4] J. E. LOVELOCK,[5] R. G. PRINN,[6] AND R. A. RASMUSSEN[3]

The automated electron capture gas chromatographic determination of the atmospheric concentrations of CCl_4 are reported for the period July 1978 to June 1981 at five coastal monitoring stations, Adrigole (Ireland), Cape Meares (Oregon), Ragged Point (Barbados, West Indies), Point Matatula (American Samoa), and Cape Grim (Tasmania). Daily measurements at approximately 6-hourly intervals are always complimented by an equivalent number of on-site calibration measurements. Estimates of CCl_4 emissions to the atmosphere from known industrial sources are compared with the measured trends and the absolute values of the observed concentrations. A globally averaged atmospheric lifetime for CCl_4 is calculated by using an optimal estimation technique incorporating a nine-box model of the atmosphere. The average global concentration of CCl_4 from July 1978 to June 1981 in the lower troposphere was 118 pptv, and it was increasing 2.1 pptv/year over this period. Both the absolute concentration observed and its trend are consistent with the calculated releases of CCl_4 and its expected destruction by stratospheric photolysis.

1. INTRODUCTION

The measurement of carbon tetrachloride (CCl_4) in the Atmospheric Lifetime Experiment (ALE) has special interest for several reasons. CCl_4 is a major halocarbon in terms of its measured tropospheric concentration and represents one of the major sources of industrial halogen in the stratosphere. With a suspected long atmospheric lifetime, it is implicated therefore in those model calculations which predict the long-term depletion of stratospheric ozone. Furthermore, it is intricately linked with the other major atmospheric halocarbons, $CFCl_3$ and CF_2Cl_2, through its main use as a starting material for their industrial production. In fact, the majority viewpoint contends that the observed atmospheric burden of CCl_4 is simply a man-made global pollutant [*Altshuller*, 1976; *Singh et al.*, 1976; *Galbally*, 1976; *Neely*, 1977] with an atmospheric lifetime that lies between 40 and 100 years. However, *Lovelock et al.* [1973] have suggested that CCl_4 might also have an atmospheric origin. Indeed, there is some evidence for the photochemical conversion of chlorinated alkenes to CCl_4 [*Singh et al.*, 1975].

A considerable number of tropospheric measurements of CCl_4 have been made over the last decade, and these are summarized in a number of reports and publications (*Fraser and Pearman*, 1978; *Galbally*, 1976; *Grimsrud and Rasmussen*, 1975; *Hanst et al.*, 1975; *Lillian et al.*, 1975; *Lovelock et al.*, 1973; *National Academy of Science* (NAS), 1976; *National Research Center* (NRC) 1978; *Ohta et al.*, 1976; *Pack et al.*, 1977; *Pearson and McConnell*, 1975; *Penkett et al.*, 1979; *Pierotti et al.*, 1976*a*, *b*, 1980; *Rasmussen et al.*, 1981; *Simmonds et al.*, 1974; *Singh et al.*, 1977*a*, *b*, 1979; *Su and Goldberg*, 1976; *Tyson et al.*, 1978; *Wilkness et al.*, 1973].

Random measurements from place to place and at different times show predictably high variability, and it is difficult to discern tropospheric sinks or predict accurate atmospheric residence times from such data. Furthermore, differences in the methods and frequency of calibration used by individual investigators reveal substantial disagreement in terms both of absolute concentrations and of the reported growth rates of CCl_4.

The ALE program was instigated to provide a long time series of accurate halocarbon measurements where high precision in the analysis and calibration could be maintained primarily through the use of daily on-site calibration. The basic principles, scientific objectives, and analytical methods of the ALE program have already been reported [*Prinn et al.*, this issue]. Details of the calibration procedures are discussed by *Rasmussen and Lovelock* [this issue].

The three years of CCl_4 measurements (July 1978 to June 1981) obtained by the ALE monitoring network have been analyzed with the assistance of a nine-box model (eight tropospheric boxes and one stratospheric box) and an optimal estimation technique for calculating lifetimes as described by *Cunnold et al.* [this issue (*a*)]. Coupled with a more rigorous estimate of the industrial releases, these results allow us to reexamine the question of CCl_4 in the global environment.

2. GLOBAL CARBON TETRACHLORIDE DATA

The daily average CCl_4 mixing ratios (pptv) and their standard deviations σ determined from the measurements at each of the five ALE stations are shown in Figures 1–5. The times of calibration tank changes and tank numbers are indicated along the top of each figure. The monthly average mixing ratios $\bar{\chi}$ (pptv), the standard deviations (σ), and the number of measurements (N) are reported in Table 1. These are our current best estimates of the absolute concentration of CCl_4 in the atmosphere and assume a calibration factor $\xi = 0.81$ [*Rasmussen and Lovelock*, this issue].

Greater variability is expected and observed at the Adrigole station (Figure 1) compared with the other ALE sites due to its relative proximity to northern European sources, and this is reflected in the data when the arrival of "polluted air" is usually evident by a rapid increase in the concentrations of $CFCl_3$, CF_2Cl_2, and CH_3CCl_3, as well as the appearance of a

[1]Department of Geochemistry, University of Bristol.
[2]School of Geophysical Sciences, Georgia Institute of Technology.
[3]Department of Environmental Science, Oregon Graduate Center.
[4]ICI Americas, Inc.
[5]Department of Engineering and Cybernetics, University of Reading.
[6]Department of Meteorology and Physical Oceanography, Massachusetts Institute of Technology.

Paper number 3C1149.
0148-0227/83/003C-1149$05.00

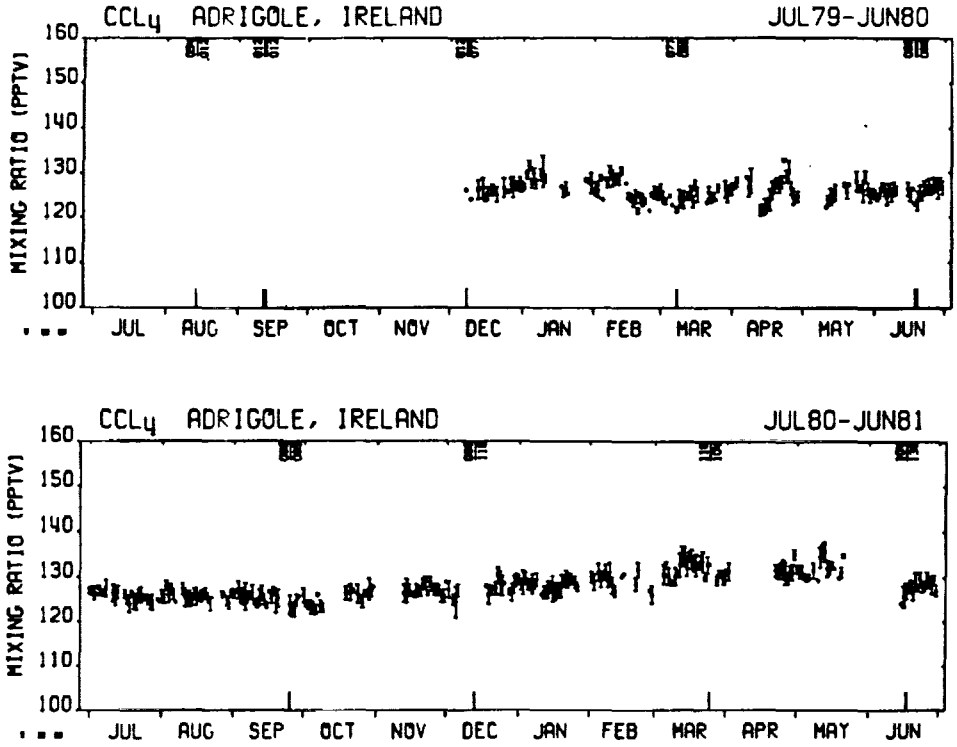

Fig. 1. The daily average mixing ratios in pptv of CCl_4 at Adrigole, Ireland, covering the period December 1979 through June 1981. Times of calibration tank changes and tank numbers are indicated along the top of each figure.

substantial peak for perchloroethylene (PCE). It is important to note that these days of identifiable pollution have been removed from the data record in Figure 1 and also from the calculation of monthly means, etc. However, the entire ALE data set including all "pollution events" are to be published as a NASA technical memorandum [*Alyea*, 1983]. The CCl_4 data at Adrigole was also unusually variable from July 1978 through November 1979 even after removal of the obvious pollution episodes. Analysis has shown that this is due to variability in the measurements of the calibration gas rather than the ambient air. Although some of this data can be recovered, we have less confidence in its quality, and it has therefore not been included in the present study.

Halocarbon measurements did not commence at the Cape

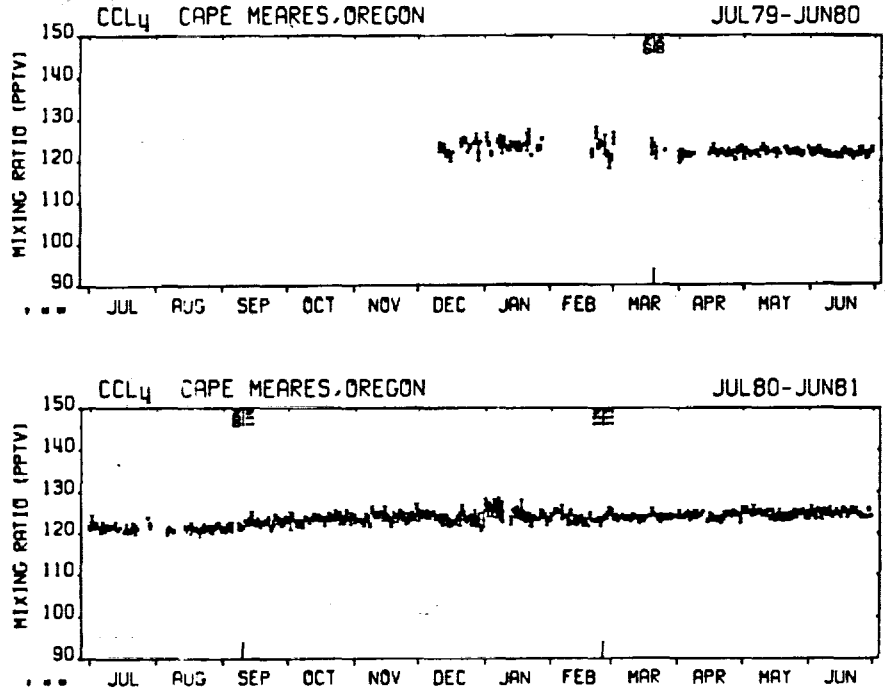

Fig. 2. The daily average mixing ratios in pptv of CCl_4 at Cape Meares, Oregon, covering the period January 1980 through June 1981.

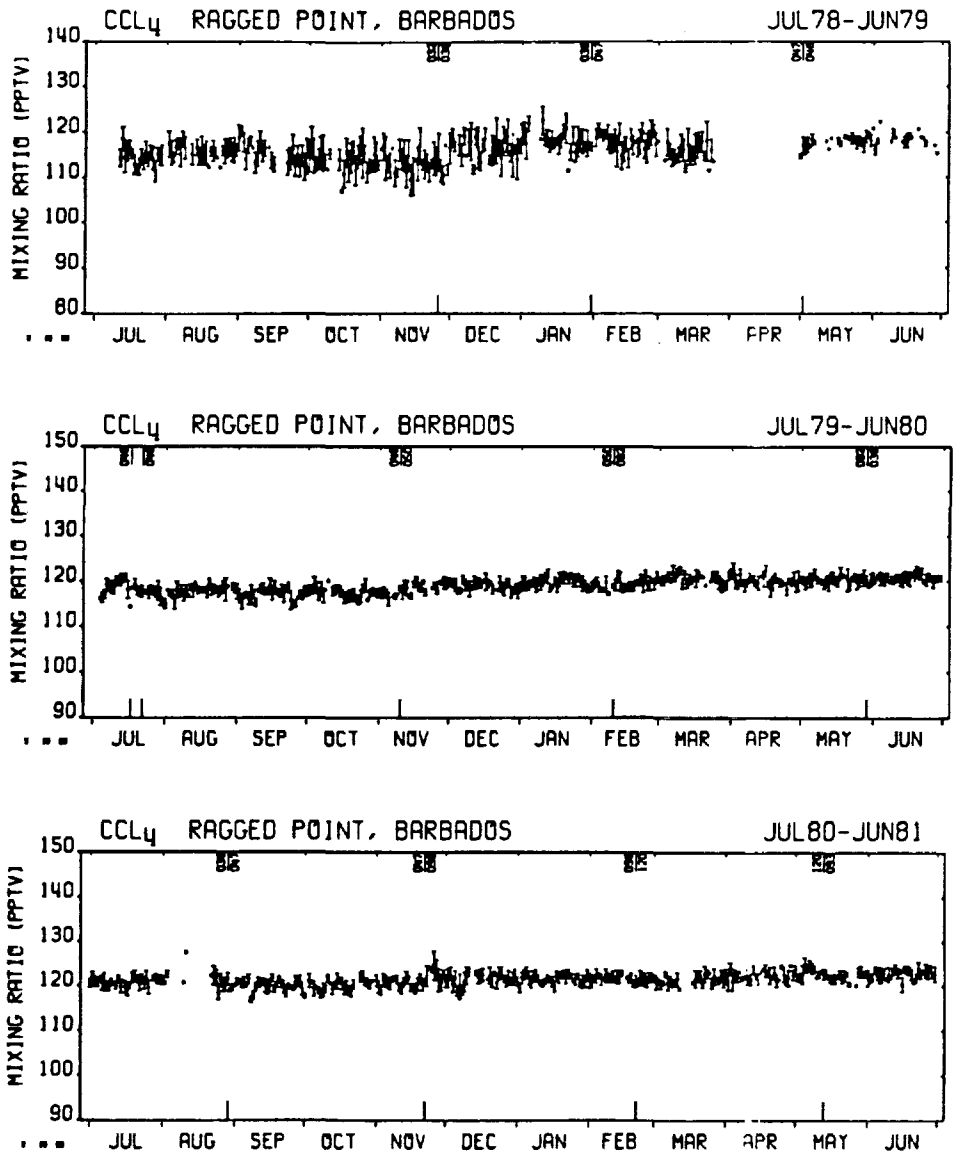

Fig. 3. The daily average mixing ratios in pptv of CCl_4 at Ragged Point, Barbados, covering the period July 1978 through June 1981.

Meares, Oregon, station (Figure 2) until December 1979 and the data gaps from the end of January to mid-March 1980 are due to problems encountered during the start-up of this station.

The Barbados station (Figure 3) 3-year data set is essentially complete with only two significant gaps. No data was collected during April 1979 due to carrier gas supply problems, while a major hurricane shut down the station for most of August 1980. The greater variability in the data record observed at Adrigole and Barbados is also partly attributed to the use of the constant frequency electronics in processing the signal output from the electron capture detector (ECD), which generally produces a noisier signal [*Prinn et al.*, this issue]. On May 1, 1979, a new ECD was installed at Barbados with an obvious improvement in instrumental precision.

Several data gaps are evident in the Samoan record (Figure 4) with 3 weeks lost in January 1979 caused by an insect restricting the outside air intake. Generally poor regulation in the American Samoa power supply and several major power failures caused instrumental damage with the loss of data from early October through the beginning of November 1980 and again from late January through February 1981. It should be noted that a constant frequency detector was used temporarily in the period from November 10, 1978, to May 8, 1979. Also on November 10, 1978, the sample loop size was changed from 5 ml to 7 ml on the silicone column channel.

The Tasmanian data (Figure 5) is the least variable of all the ALE sites and is essentially free of any significant pollution. Only about 10 days per year are observed in which anomously high levels of $CFCl_3$ and CF_2Cl_2 are recorded, and these days have been omitted from the data presented. Data are missing from the last half of October 1978 due to instrumental problems, and a larger data gap is evident from December 11, 1978, to January 16, 1979, caused by contamination of the input gas sampling valve. Power failure problems in January and February 1981 also resulted in the loss of small segments of data. Precision was clearly improved after November 4, 1978, when the sample valve loop size was increased from 5 ml to 7 ml.

The CCl_4 monthly averaged mixing ratios $\bar{\chi}$ and their

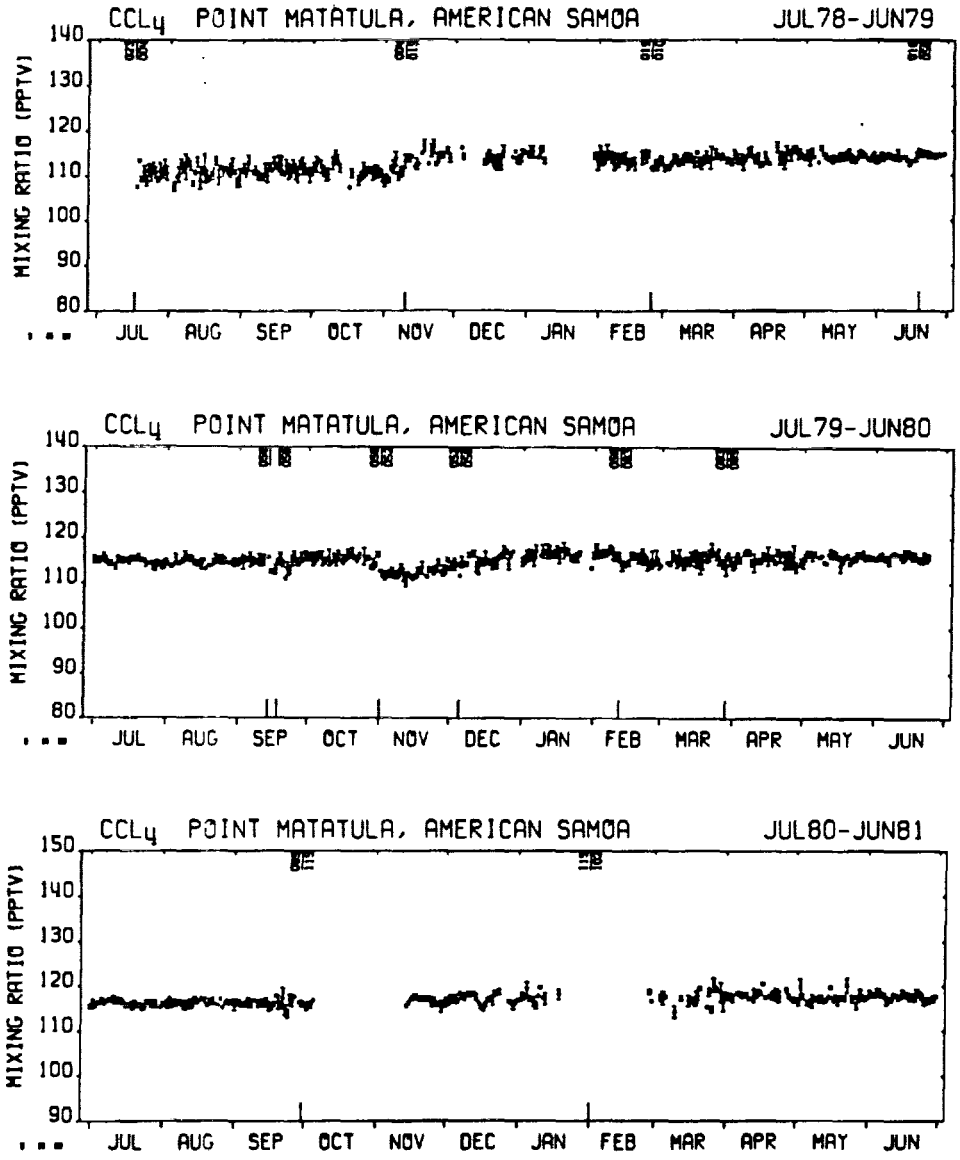

Fig. 4. The daily average mixing ratios in pptv of CCl_4 at Point Matatula, American Samoa, covering the period July 1978 through June 1981.

monthly standard deviations σ listed in Table 1 have been processed with the optimal estimation code described in *Cunnold et al.* [this issue (*a*)] to determine the coefficients of the empirical model,

$$\ln \chi_t = a_t + b_t \left\{\frac{t-18}{12}\right\} + c_t \cos\left\{\frac{2\pi t}{12}\right\} + s_t \sin\left\{\frac{2\pi t}{12}\right\} \quad (1)$$

which provided the best fit to the observations at each site. Here, χ_t is the CCl_4 mixing ratio expressed in pptv, and t is measured in months with the first month being July 1978. In this estimation procedure, each month of observations is weighted by

$$\sigma^{-2} = \left(\frac{\sigma_m^2}{n_m} + \sigma_0'^2\right)^{-2} \quad (2)$$

where σ_m is the standard deviation of the measurements during month m and n_m is the number of measurements during the month divided by 12 (to allow for the typically observed correlation between individual measurements over periods ~3 days). $\sigma_0'^2$ is the variance of the residuals at an individual site with respect to the empirical model (σ_0^2) increased by a factor, M, which allows for the effect of the observed month-to-month autocorrelation of the residuals on the precision of estimating a trend from the data [see *Cunnold et al.*, this issue (*a*)]. In the CCl_4 observations, M is $\lesssim 1.4$ at all sites except Cape Grim (where $M \simeq 2.5$) and $\sigma_0'^2$ is approximately 2 (Barbados; Samoa; and Cape Meares, Oregon) to 5 (Adrigole, Ireland, and Tasmania) times σ_m^2/n_m. Table 2 gives the calculated coefficients; it should be noted in the interpretation of the results that the trend b_t is determined from just 19 months of data at Cape Meares, Oregon, and Adrigole, Ireland.

Table 2 indicates that the mean concentration at each site, and hence the latitudinal distribution of CCl_4, and its temporal trend is precisely determined by the ALE data. Moreover, the annual cycle of CCl_4 is generally weak and ill defined except at mid-latitudes of the northern hemisphere. In that case, however, the annual cycle has been determined from just 19 months of data and may therefore be atypical and in fact differs in amplitude and phase from that obtained from $CFCl_3$

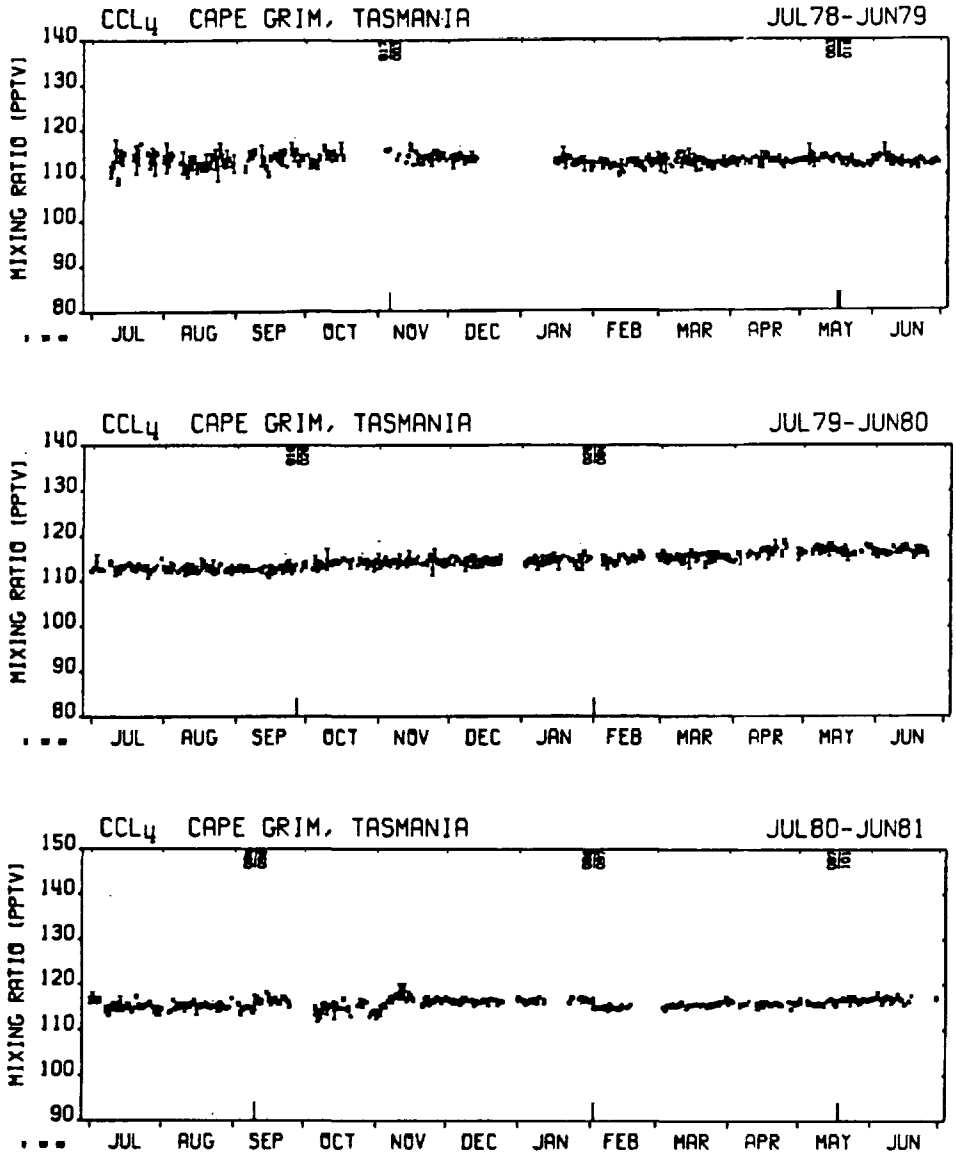

Fig. 5. The daily average mixing ratios in pptv of CCl_4 at Cape Grim, Tasmania, covering the period July 1978 through June 1981.

and CF_2Cl_2 [*Cunnold et al.*, this issue (*a*), (*b*)]. It may be noted that Adrigole, Ireland, possesses a CCl_4 mixing ratio approximately 2% larger than that at Cape Meares, Oregon. Although this difference is most likely related to the proximity of Adrigole to where CCl_4 is injected into the atmosphere, it is curious that only CF_2Cl_2 of the other ALE species gives any indication (based upon just 8 months of data) of such a difference between these two mid-latitude northern hemisphere sites.

Further processing of the ALE data requires a combination of the Adrigole and Cape Meares records in order to provide a time series typical of mid-latitudes of the northern hemisphere. Since there exists a significant difference between the mean concentrations of CCl_4 at the two sites, it is inappropriate to combine optimally the two time series. Instead, to provide an unbiased estimate of the CCl_4 concentration in this semi-hemisphere, each month's data at the two sites has been averaged (both sites have provided monthly data continuously since December 1979); each month's average has been assigned an uncertainty $\sigma_m/\sqrt{n_m} = (\sigma_a^2/n_a + \sigma_c^2/n_c)^{1/2}/2$ where σ_a, n_a, σ_c, and n_c are the standard deviations and the estimated number of independent measurements at Adrigole and Cape Meares in month m. The combined times series has been processed to yield empirical model coefficients and gives $a_l = 4.815$ and $b_l = 0.020$.

The annually averaged mixing ratios and trends for January 1, 1980, obtained using the empirical model are 123 pptv, 2.5 pptv/year at Adrigole/Cape Meares; 119 pptv, 2.5 pptv/year at Ragged Point; 115 pptv, 2.1 pptv/year at Point Matatula; and 115 pptv, 1.4 pptv/year at Cape Grim. Averaging these results, the average mixing ratio in the lower troposphere in the period July 1978 to June 1981 was 118 pptv, and it was increasing 2.1 pptv/year (1.8%/year).

3. Global Budget of Carbon Tetrachloride

Two principal methods are used in analyzing the globally distributed measurements obtained from the ALE monitoring network in terms of the sources and sinks of carbon tetrachloride. In the first approach, the measured total atmospheric content $C(t)$ of CCl_4 at time t is expressed in terms of its

TABLE 1. Monthly Averaged CCl_4 Mixing Ratios χ (pptv), Their Standard Deviations σ (pptv), and the Number of Measurements During Each Month (N) Determined From Measurements at the Five ALE Stations Over the Period July 1978 Through June 1981

	Adrigole, Ireland			Cape Meares, Oregon			Ragged Point, Barbados			Point Matatula, American Samoa			Cape Grim Tasmania		
Month	χ	σ	N	χ	σ	N	χ	σ	N	χ	σ	N	χ	σ	N
July 1978	–	–	–				114.6	2.7	144	110.7	1.8	61	113.8	2.3	54
Aug. 1978	–	–	–				116.0	2.3	200	111.1	2.0	125	113.1	1.8	124
Sept. 1978	–	–	–				115.3	3.0	165	111.4	1.6	126	113.7	1.6	72
Oct. 1978	–	–	–				114.3	3.5	111	111.2	1.7	106	113.9	1.4	44
Nov. 1978	–	–	–				113.2	3.6	134	113.0	2.3	97	114.3	1.1	70
Dec. 1978	–	–	–				116.6	3.5	131	114.0	1.5	60	113.8	0.8	47
Jan. 1979	–	–	–				118.3	2.8	121	114.9	1.1	18	113.1	1.1	58
Feb. 1979	–	–	–				118.1	2.8	118	113.8	1.5	95	112.6	1.0	92
March 1979	–	–	–				115.9	2.8	94	113.6	1.2	117	112.9	1.3	111
April 1979	–	–	–				–	–	–	114.3	1.5	110	113.2	0.8	115
May 1979	–	–	–				117.9	1.5	80	114.2	1.0	121	113.2	1.1	110
June 1979	–	–	–				118.3	1.5	40	114.2	0.8	115	113.0	1.0	112
July 1979	–	–	–				118.1	1.7	104	114.9	0.9	118	113.0	1.0	94
Aug. 1979	–	–	–				117.9	1.5	123	114.9	0.9	111	112.8	0.9	118
Sept. 1979	–	–	–				117.2	1.6	136	114.8	1.3	99	112.8	0.8	106
Oct. 1979	–	–	–				117.6	1.4	134	115.6	1.1	115	114.1	1.0	94
Nov. 1979	–	–	–				118.5	1.5	96	112.6	1.2	115	114.4	1.1	110
Dec. 1979	126.1	1.7	53	123.4	1.7	55	119.2	1.3	129	115.0	1.5	102	114.5	0.9	85
Jan. 1980	128.2	2.3	61	124.1	1.5	74	119.9	1.5	132	116.5	1.5	99	114.5	1.0	94
Feb. 1980	126.4	2.5	108	123.0	2.2	31	119.6	1.4	105	115.9	1.5	122	114.8	0.9	72
March 1980	124.8	1.7	89	123.5	1.8	10	120.8	1.4	128	115.5	1.4	105	115.3	0.9	117
April 1980	126.3	3.2	104	122.1	0.9	87	120.4	1.5	124	115.7	1.5	115	116.2	1.2	79
May 1980	126.0	2.1	61	122.1	0.8	98	120.5	1.3	137	116.0	1.0	116	116.8	0.9	88
June 1980	125.8	1.8	114	122.0	0.8	114	120.9	1.1	147	116.0	0.8	94	116.6	0.8	85
July 1980	125.9	1.6	110	121.7	1.1	91	120.9	1.4	129	116.2	0.7	117	115.3	1.1	105
Aug. 1980	125.7	1.5	119	121.3	0.9	82	121.2	1.9	47	116.4	0.8	117	115.2	0.7	102
Sept. 1980	125.2	1.9	109	122.6	1.1	112	120.2	1.4	125	116.3	1.2	100	116.1	1.1	74
Oct. 1980	125.2	2.0	79	123.7	1.1	126	120.6	1.7	126	116.1	0.7	17	114.9	1.2	81
Nov. 1980	127.2	1.6	79	124.2	1.2	123	121.2	1.9	118	116.8	0.9	63	116.5	1.5	101
Dec. 1980	127.3	2.5	66	123.9	1.3	119	121.7	1.9	117	117.3	1.1	98	116.4	0.5	96
Jan. 1981	128.3	1.9	120	125.0	1.9	132	121.7	1.4	138	117.6	1.3	42	116.6	0.6	54
Feb. 1981	129.4	2.3	66	123.8	1.2	111	121.8	1.3	119	118.3	1.1	4	115.1	0.6	46
March 1981	132.1	2.4	101	124.1	0.7	128	121.7	1.5	99	117.8	1.9	54	115.7	0.6	88
April 1981	131.5	2.0	53	124.4	0.8	113	122.6	1.6	110	118.0	1.0	136	115.8	0.6	80
May 1981	132.3	2.3	62	125.0	0.9	123	122.7	1.5	123	117.4	1.2	123	116.3	0.6	99
June 1981	127.8	2.0	78	125.0	0.9	115	122.9	1.4	110	117.7	0.9	111	116.9	0.7	62

known release rate $I(t)$ and unknown lifetime τ through the equation

$$C(t) = \int_0^t I(t')e^{(t'-t)/\tau}\,dt' \tag{3}$$

The second approach is based upon the temporal derivative of this equation in the form

$$\frac{1}{C}\frac{dC}{dt} = \frac{I(t)}{\int_0^t I(t')e^{(t'-t)/\tau}\,dt'} - \frac{1}{\tau} \tag{4}$$

For each approach a two-dimensional model is used to relate measured mixing ratios (χ) to the atmospheric content and to relate the global trend in CCl_4 to the trends, $1/\chi(d\chi/dt)$, measured at each ALE site. The two techniques provide relatively independent estimates of the lifetime because uncertainties in absolute calibration are an important part of the overall uncertainty in the first approach but are relatively unimportant in the second approach.

3.1. *Emissions of Carbon Tetrachloride*

There have been many important changes in the industrial usage of CCl_4 since significant production commenced in the early 1900's. As was noted by *Galbally* [1976] and *Singh et al* [1976], prior to 1950 world production of CCl_4 was dominated by the United States. Principal uses were as an indus-

TABLE 2. Empirical Model Fit (Equation (1)) Together With 1σ Uncertainty for the Three Years of CCl_4 Data Given in Table 1

Site	a_i	b_i	c_i	s_i	Variance of Residuals ($\sigma^2 \times 10^6$)
Adrigole, Ireland	4.825 ± 0.003	0.027 ± 0.006	−0.002 ± 0.004	−0.013 ± 0.004	78
Cape Meares, Oregon	4.802 ± 0.002	0.016 ± 0.004	−0.006 ± 0.002	−0.004 ± 0.003	25
Ragged Point, Barbados	4.779 ± 0.001	0.021 ± 0.002	0.002 ± 0.002	−0.004 ± 0.002	43
Point Matatula, American Samoa	4.745 ± 0.001	0.018 ± 0.002	−0.001 ± 0.002	−0.003 ± 0.002	38
Cape Grim, Tasmania	4.740 ± 0.002	0.012 ± 0.003	0.001 ± 0.002	0.000 ± 0.002	47

It should be noted that the date at Adrigole and Cape Meares covers the period Dec. 1979 to June 1981.

TABLE 3. Annual United States and World Production of the Two Chlorofluorocarbons, $CFCl_3$ (CFC-11) and CF_2Cl_2 (CFC-12) From 1958 to 1980

Year	Annual U.S. Production[a] CFC-11 + CFC-12, KT	Annual World Production[b] CFC-11 + CFC-12, KT	United States, World, %
1958	82.5	102.9	80.2
1959	98.7	123.3	80.0
1960	108.3	149.1	72.6
1961	119.9	169.0	70.9
1962	150.9	206.2	73.2
1963	162.2	239.7	67.7
1964	170.7	281.2	60.7
1965	200.4	312.9	64.0
1966	207.1	357.2	58.0
1967	223.1	402.6	55.4
1968[c]	249.0	463.6	53.7
1969	274.9	531.2	51.7
1970	281.1	578.0	48.6
1971	293.6	627.1	46.8
1972	335.1	712.2	47.0
1973[c]	355.4	801.8	44.3
1974	375.7	851.2	44.1
1975	300.5	742.1	40.5
1976	283.1	799.7	35.4
1977	256.6	756.6	33.9
1978	236.2	735.3	32.1
1979	209.7	702.3	29.9
1980	200.7	695.6	28.8

KT = 1000 metric tons.
[a]Data taken from International Trade Commission (Synthetic Organic Chemicals).
[b]Data taken from *Alexander Grant Report-DuPont Calculations* [1981].
[c]Data are extrapolated in these years and are therefore less certain.

trial solvent, dry cleaning agent, fire extinguisher, grain fumigant, and rodenticide. However, recognition and concern about the toxicological effects of CCl_4 has led to substitution of its uses as a dry cleaning agent and fire extinguisher by other less toxic chemicals. Any growth in the continuing applications of CCl_4 is expected, therefore, to be minor owing to the shift away from its dispersive uses to other solvents.

In 1931, CCl_4 began to be used as an intermediate in the production of chlorofluorocarbons, a use that has grown steadily until very recently with the advent of the chlorofluorocarbon/ozone controversy. It is also significant that from 1958 to 1980, when accurate production figures are available [*Alexander Grant Report-DuPont Calculations*, 1981], that the percentage of U.S. chlorofluorocarbon production relative to world production has declined from 80 to about 30% (see Table 3). Since CCl_4 production parallels the production of chlorofluorocarbons, it is apparent that there has been a similar shift in the global pattern of CCl_4 usage.

Assuming for the moment that there are no natural sources of CCl_4, then releases to the atmosphere can be estimated from a detailed knowledge of the various industrial uses of CCl_4, but most importantly from an inventory of its consumption as a chemical feedstock. One approach to obtaining such an estimate is to sum the percentages lost for each of the uses of CCl_4 using data compiled mainly from U.S. sources and then estimating the percentage U.S. production/world production to obtain a figure for global release [*NAS*, 1976; *NRC*, 1978]. An alternative approach, and the one used here, is to determine the apparent U.S. domestic consumption of CCl_4 from available government figures for production plus imports less exports. The majority of this CCl_4 will be converted into the chlorofluorocarbons, CF_2Cl_2, and $CFCl_3$, and this amount can be calculated from the stochiometry and by assuming that the efficiency of this chemical process is 97%. In fact, recent figures released by the Chemical Manufacturers Association calculate that the average loss of CCl_4 during its conversion into the two chlorofluorocarbons is 2.9% ($\sigma = \pm 0.6\%$) over the period 1965–1979 [*Chemical Manufacturers Association*, 1983]. Therefore, CCl_4 not used in the production of chlorofluorocarbons must be accounted for by all other industrial uses and is a reasonable estimate of the fraction eventually released to the atmosphere [*Edwards et al.*, 1982]. CCl_4 release estimates for the United States are summarized in Table 4 by using this approach, in which it has been further assumed that 95% of all nonchemically reacted CCl_4 is released. This loss is also expressed as a percentage of U.S. consumption in Table 4, and it should be noted that the annual variability includes any changes in inventories as well as actual consumption.

To derive a world estimate of CCl_4 release is more difficult since only limited records of CCl_4 production are available from other countries. However, concern over the potential depletion of ozone by chlorofluorocarbons has resulted in the accumulation of detailed and accurate records for their production and release on a global basis [*Alexander Grant Report-DuPont Calculations*, 1981]. As there is likely to be close parity between CCl_4 and chlorofluorocarbon production, we can use the percentage U.S./world chlorofluorocarbon figures to estimate world CCl_4 production based on available U.S. CCl_4 production data. Furthermore, we assume that production losses, etc., in other countries will be proportionally similar to those of the United States because of comparable technologies.

Global release estimates for CCl_4 are summarized in Tables 5–7. Table 5 covers the years 1908–1930 and is based on data taken from the National Research Council report [*NRC*,

C-3

TABLE 4. United States Releases of Carbon Tetrachloride

Year	Apparent Domestic Consumption of CCl_4,[a] KT	Consumed in CFC-11 Production,[b] KT	Consumed in CFC-12 Production,[b] KT	Apparent Release CCl_4, KT	Percent U.S. Consumption, %
year					
1958	141.9	26.43	78.14	37.30	26.30
1959	166.8	31.63	93.46	41.70	25.00
1960	168.8	37.90	98.95	31.90	18.90
1961	174.1	47.61	103.19	23.30	13.40
1962	219.4	65.31	123.69	30.40	13.90
1963	235.5	73.36	129.33	32.80	13.90
1964	243.1	77.74	135.54	29.80	12.30
1965	269.3	89.24	161.43	18.60	6.90
1966	293.9	89.18	170.31	34.40	11.70
1967	323.7	95.40	184.19	44.10	13.60
1968	346.3	110.10[d]	201.40[d]	34.70[d]	10.30[d]
1969	400.4	124.87	218.68	56.80	14.20
1970	458.6	127.99	223.29	107.40	23.40
1971	457.7	135.02	231.72	90.90	19.90
1972	457.4	156.84	261.25	39.30	8.60
1973	475.0	167.70[d]	275.60[d]	31.70	6.70[d]
1974	534.7	178.50	289.90	66.30	12.40
1975[c]	406.2	141.15	233.81	31.20	7.70
1976[c]	381.1	128.89	224.87	27.30	7.20
1977[c]	355.5	110.62	210.86	34.00	9.60
1978[c]	321.8	101.33	194.67	25.80	8.00
1979[c]	283.0	90.50	172.16	20.30	7.20
1980[c]	285.7	81.19	171.05	33.50	11.70
Average					13.2[e]

KT = 1000 metric tons.
[a]Source: International Trade Commission (Synthetic Organic Chemicals).
[b]Assumes 97% efficiency of conversion of CCl_4 into CFC-11 and CFC-12.
[c]1975–1980 Uses ITC production + imports − exports (import and export figures from U.S. Department of Commerce).
[d]Extrapolated data.
[e]Average 1958–1971, 16%; average 1972–1980, 8.8%.

1978], with only minor modifications. Table 6 commences in 1931 and takes into account the conversion of CCl_4 into chlorofluorocarbons in estimating global CCl_4 emissions by subtracting the fraction of CCl_4 used as a chemical feedstock and by assuming 95% release of the residual CCl_4. The estimates for production losses and percentage U.S./world CCl_4 production are again taken from the National Research Council report [*NRC*, 1978]. For Table 7, world CCl_4 production is derived from the comparable percentage chlorofluorocarbon figures in Table 3 and reflects the progressive decline in U.S. production relative to the rest of the world, especially during the last decade.

World CCl_4 emissions are estimated from the data in Table 4, which expresses CCl_4 release as a percentage of U.S. consumption. Because production figures for CCl_4 include both sales and inventory changes, we prefer to use average percentages to avoid any distortion due to inventory changes in a given year. Average consumption figures were calculated, therefore, for the years 1972–1980 (8.8%) when most accurate data were available and for the years 1958–1971 (16%) when the data is less accurate. Annual world CCl_4 emissions were then calculated for each of these time periods (see column 8, Table 7) and again assuming that 95% of the nonfeedstock CCl_4 is eventually released. It is also significant that, using 1976 as an example, the cummulative emissions calculated by this method are at least 20% higher than those derived by the *NRC* [1978].

These CCl_4 release estimates probably still underestimate slightly the actual emissions since production figures for chlorofluorocarbons and CCl_4 are very limited from the U.S.S.R., Peoples Republic of China, and eastern European countries. Furthermore, end usage patterns in these countries could be different with a larger fraction of CCl_4 total production being used dispersively.

The cumulative emission of 3427 ktons of CCl_4 at the end of 1980 can therefore be regarded as a lower limit, and we must next attempt to estimate an upper limit for the global release of CCl_4. From Table 3, we can see that about 10 years elapsed (from 1958 to 1968) before production of chlorofluorocarbons in the rest of the world equalled production in the United States. If this 10 year lag-time is also a reasonable reflection of CCl_4 production and uses, we can further assume that releases of CCl_4 in the rest of the world as a percentage of the rest of the world production would be roughly proportional to release in the United States 10 years earlier as a percentage of U.S. production. Using this assumption, we have then calculated annual CCl_4 emissions in the rest of the world beginning in 1958, but the calculation is based on U.S. release rates calculated for 1948. Each year's release, calculated in this way, is then summed with the derived production losses, with 95% of the total CCl_4 finally released to the atmosphere. The cummulative CCl_4 global release at the end of 1980 determined by this method is 3972 ktons, which we have adopted as our upper limit.

In our calculations the atmospheric release after 1970, given in Table 7, is assumed to be injected into the atmosphere in

the proportion 0.787, 0.149, 0.035, and 0.029 in the 90°N–30°N, 30°N–0°, 0°–30°S, and 30°S–90°S semi-hemispheres, respectively. These proportions were determined from the proportions (f values) derived for $CFCl_3$ [*Cunnold et al.*, this issue (*a*)] and CF_2Cl_2 [*Cunnold et al.*, this issue (*b*)] with the relative weights given to $CFCl_3$ and CF_2Cl_2 being determined by the quantities of CCl_4 used in their production. This procedure for determination of f values parallels the procedure used to determine the lower limit on release and is used in the absence of information on the dispersive releases of CCl_4. Prior to 1971, all the release was assumed to be in the 90°N–30°N semi-hemisphere. The atmospheric lifetime of CCl_4 deduced from the ALE data is not significantly dependent on the assumed distribution of release.

3.2. *Removal Processes for Carbon Tetrachloride*

It is generally agreed that the primary mechanism for the removal of CCl_4 from the atmosphere is by stratospheric transport and photolysis. However, estimates of the CCl_4 residence time in the stratosphere vary considerably. *Krey et al.* [1976] estimate an atmospheric lifetime of 18 years; lifetimes calculated by other investigators range from 50 to 100 years [*Atkinson et al.*, 1976; *Galbally*, 1976; *NAS*, 1976; *Singh et al.*, 1976]. Actual measurements [*Pierotti et al.*, 1980; *Seiler et al.*, 1978] of the stratospheric profile of CCl_4 show that its concentration rapidly decreases with altitude ($\sim$14 pptv km^{-1}) and support the view that the stratospheric lifetime may be much shorter than most calculated estimates. Recent calculations by *Golombeck* [1982] based on the photodissociation cross section of CCl_4, in fact, give a stratospheric lifetime of 7.5 years and an atmospheric lifetime of approximately 50 years.

Transfer into the oceans with subsequent hydrolysis is the second most important sink for CCl_4. Based on laboratory measurements, hydrolysis in the oceans is predicted to be extremely slow [*Hine*, 1950; *Radding et al.*, 1977]. However, the e^{-1} depth of CCl_4 is reported to be 50 m [*Lovelock et al.*, 1973], and the rate of transfer across the air/sea interface calculated by different investigators ranges from 1.7×10^{-2} to 7×10^{-3} yr^{-1} [*Galbally*, 1976; *Neely*, 1977; *Pierotti et al.*, 1976b]. This would suggest that the CCl_4 flux to the oceans could be an important sink if the faster rates apply and would be competitive with the stratospheric sink. Unfortunately, the exact removal mechanism by the oceans is uncertain, although speculation suggests that bioaccumulation in marine organisms and subsequent incorporation in sediments could be the dominant loss process [*NAS*, 1976].

Removal of CCl_4 from the troposphere through ion-molecule chemistry, or by gas phase reactions with neutral species, are generally not of sufficient magnitude to be important sinks [*NAS*, 1976]. UV photolysis is not significant in the troposphere [*Rebbert and Ausloos*, 1976], and reaction with OH radicals is also sufficiently slow as to be unimportant as a sink [*Cox et al.*, 1976]. *Galbally* [1976] concludes that reactions of CCl_4 with $O(^3P)$, H, and CH_3 are the only significant atmospheric reactions. Although a fast reaction rate (1.4×10^{-9} cm^3 s^{-1}) has been reported for the reaction of CCl_4 with O^- ions [*Dotan et al.*, 1978], most atmospheric ions are rapidly hydrated to form cluster ions so that charge transfer reactions of this type have little practical effect on overall CCl_4 loss rates. *Campbell* [1976] contends that natural ionization could lead to a CCl_4 removal rate of 2.4×10^{-2} yr^{-1}, even greater than the stratospheric loss rate; however, competition with the more abundant molecular oxygen would negate the importance of this potential sink.

Photodissociation of CCl_4 adsorbed onto silicates has been demonstrated in the laboratory [*Ausloos et al.*, 1977; *Gab et al.*, 1977], and it has been proposed that this phenomenum could provide a sink for CCl_4 in the desert regions of the world, such as the Sahara. If the chemical efficiency of this

TABLE 5. Estimates of Annual World Emissions of CCl_4 From 1908 to 1930

Year	Annual World Production, KT	Annual Production United States, World, %	Production Loss, %	Production Loss, KT	Annual World Emission,* KT	Cumulative World Emission, KT
1908	0.1	100	5.0	0.0	0.1	0.1
1909	0.3	100	5.0	0.0	0.3	0.4
1910	0.2	100	5.0	0.0	0.2	0.6
1911	0.7	100	5.0	0.0	0.7	1.3
1912	0.8	100	5.0	0.0	0.8	2.1
1913	1.0	100	5.0	0.1	1.1	3.2
1914	1.5	100	5.0	0.1	1.5	4.7
1915	2.8	100	5.0	0.1	2.8	7.5
1916	5.1	100	5.0	0.3	5.1	12.6
1917	5.9	100	4.5	0.3	5.9	18.5
1918	6.4	100	4.5	0.3	6.4	24.9
1919	3.3	100	4.5	0.1	3.2	28.1
1920	3.2	100	4.5	0.1	3.1	31.2
1921	1.9	100	4.5	0.1	1.9	33.1
1922	5.1	100	4.5	0.2	5.0	38.1
1923	6.1	100	4.5	0.3	6.1	44.2
1924	6.5	100	4.5	0.3	6.5	50.7
1925	7.7	95	4.0	0.3	7.6	58.3
1926	9.0	95	4.0	0.4	8.9	67.2
1927	7.9	95	4.0	0.3	7.8	75.0
1928	9.4	95	4.0	0.4	9.3	84.3
1929	15.7	95	4.0	0.6	15.5	99.8
1930	15.6	95	4.0	0.6	15.4	115.2

*Annual World Emission assumes 95% release of world production + production loss during manufacture.

TABLE 6. Estimates of Global Atmospheric Releases of CCl_4 From 1931 to 1957

Year	Annual Global Production, KT	Annual Production United States, Global, %	Production Loss, %	Production Loss, KT	Conversion to CFC's 11 and 12, KT[a]	Residual Released (95%), KT[b]	Annal Global Emission, KT	Cumulative Global Emission, KT
								(115.2)
1931	17.5	90	4.0	0.70	0.65	16.0	16.7	131.9
1932	17.8	90	4.0	0.71	0.13	16.8	17.5	149.4
1933	18.0	90	4.0	0.72	0.39	16.7	17.4	166.8
1934	23.6	90	3.5	0.83	0.92	21.8	22.6	189.4
1935	28.1	90	3.5	0.98	1.30	25.5	26.4	215.8
1936	34.5	90	3.5	1.21	2.21	30.7	31.9	247.7
1937	42.3	90	3.5	1.48	4.17	36.2	37.7	285.4
1938	39.3	90	3.5	1.38	3.81	33.7	35.1	320.5
1939	45.6	90	3.5	1.60	5.21	38.4	40.0	360.5
1940	50.7	90	3.5	1.77	6.13	42.3	44.1	404.6
1941	61.3	90	3.5	2.15	8.65	50.0	52.2	456.8
1942	72.8	90	3.0	2.18	8.05	61.5	63.7	520.5
1943	88.3	90	3.0	2.65	11.16	73.3	75.9	596.4
1944	105.7	90	3.0	3.17	22.36	79.2	82.3	678.7
1945	97.2	90	3.0	2.92	26.86	66.8	69.7	748.4
1946	74.8	90	3.0	2.24	22.61	49.6	51.8	800.2
1947	100.4	90	3.0	3.01	27.90	68.9	71.9	872.1
1948	108.2	90	3.0	3.25	35.96	68.6	71.9	944.0
1949	99.3	90	3.0	2.98	39.39	56.9	59.9	1003.9
1950	109.1	90	2.5	2.73	53.02	53.3	56.0	1059.9
1951	123.2	90	2.5	3.08	58.00	61.9	65.0	1124.9
1952	110.5	90	2.5	2.76	64.50	43.7	46.5	1171.4
1953	130.9	90	2.5	3.27	80.97	47.4	50.7	1222.1
1954	118.3	90	2.5	2.96	88.53	28.3	31.2	1253.3
1955	144.9	90	2.5	3.62	105.86	37.1	40.7	1294.0
1956	155.9	88	2.5	3.90	127.62	26.9	30.8	1324.8
1957	169.6	85	2.5	4.24	136.43	31.5	35.7	1360.5

[a]Assumes 97% efficiency of conversion.
[b]Assumes 95% of annual global production CCl_4-CCl_4 converted to CFC's is eventually released.

removal process was 10%, it would account for a CCl_4 destruction time constant of about 20 years [*Alyea et al.*, 1978]. Support for this hypothesis is provided by limited measurements of halocarbons in dusty Saharan atmosphere, which show a small but statistically significant depletion of CCl_4 [*Pierotti et al.*, 1978]. Nevertheless, the exact magnitude of this potentially important sink has yet to be quantitatively determined. Table 8 summarizes the various sinks which have been proposed for CCl_4 in terms of first-order removal rates and estimated lifetimes.

4. CCl_4 Lifetime Estimates

4.1. *Trend Technique*

The two-dimensional atmospheric model described in *Cunnold et al.* [this issue (*a*)] has been used to predict the distribution of CCl_4 in the lower troposphere for both the lower and the upper limit release scenarios given in Table 7. In these calculations, the model transport parameters were the same as those used in simulating the observed latitudinal distributions of $CFCl_3$ and CF_2Cl_2 [*Cunnold et al.*, this issue (*a*)] and the stratospheric lifetime, τ_s, was varied until the best overall fit to the temporal trends at the ALE sites was obtained. As for the other ALE calculations, because the assumed transport parameters lead to an overprediction of the observed seasonal variations at most of the sites, the seasonal variations were filtered out of the two-dimensional model results, using a 12-month averaging procedure. This was done in order to avoid introducing into the residuals seasonal cycles in which we had little confidence because of uncertainties in the modeled seasonal variations of both atmospheric transport and the release of CCl_4 into the atmosphere. To provide a summary of the site-to-site and month-to-month consistency of the data, the monthly differences (residuals) between the model results and the observations expressed in the form $\ln(\chi_m/\chi_c)$ are given in Figure 6, where the mixing ratios χ_m and χ_c are those measured by the ALE and those calculated by using the nine-box model, respectively. For this calculation, the "most probable" release scenario, defined as the average of the upper and lower limit scenarios, was used, and a lifetime of 50 years was assumed.

Examining the trends in the residuals, Figure 6 suggests an underprediction of the linear trend by the two-dimensional model for Ragged Point, Barbados, and an overprediction of the trend for Cape Grim, Tasmania. These differences in trend may be interpreted as variations in the atmospheric lifetime estimates from site to site. Lifetime estimates derived from the data series in each of the four semi-hemispheres of the globe are given in Table 9. These estimates have been obtained by using the optimal estimation procedure of *Cunnold et al.* [this issue (*a*)] with the variances given by equation (2) being used to weight the differences between the monthly observations and the two-dimensional model predictions. The calculations used a partial derivative

$$\frac{\partial}{\partial(1/\tau)}\left[\frac{d(\ln \chi)}{dt}\right] = -0.6$$

This was determined from other two-dimensional model calculations based upon the sensitivity of the average mixing ratio trend at the locations of the ALE sites over the 3-year

TABLE 7. Estimates of Global Atmospheric Releases of CCl_4 From 1958 to 1980

Year	Annual World Production, KT	Annual Production United States, World, %	Production Loss, %	Production Loss, KT	Annual World Emission Calculated as Percent of World Consumption CCl_4,[a] %	Assume 95% Released, KT	Total Annual World Emission[b] Lower Limit, KT	Total Annual World Emission[b] Upper Limit, KT	Cummulative World Lower Limit, KT	Cummulative World Upper Limit, KT
										(1360.5)
1958	177.4	80	2.5	4.4	28.4	27.0	31.4	62.1	1391.9	1422.6
1959	208.5	80	2.0	4.2	33.4	31.7	35.9	67.4	1427.8	1490.0
1960	231.2	73	2.0	4.6	37.0	35.1	39.7	65.2	1467.5	1555.2
1961	245.2	71	2.0	4.9	39.2	37.3	42.2	62.5	1509.7	1617.7
1962	300.5	73	2.0	6.0	48.1	45.7	51.7	66.6	1561.4	1684.3
1963	346.3	68	2.0	6.9	55.4	52.6	59.5	77.8	1620.9	1762.1
1964	398.5	61	2.0	8.0	63.8	60.6	68.6	73.1	1689.5	1835.2
1965	420.8	64	2.0	8.4	67.3	64.0	72.4	64.3	1761.9	1899.5
1966	506.7	58	2.0	10.1	81.1	77.0	87.1	79.0	1849.0	1978.5
1967	588.5	55	2.0	11.8	94.2	89.5	101.3	102.1	1950.3	2080.6
1968[c]	641.2	54	1.5	9.6	102.6	97.5	107.1	86.9	2057.4	2167.5
1969	770.0	52	1.5	11.5	123.2	117.0	128.5	121.0	2185.9	2288.5
1970	935.9	49	1.5	14.0	149.7	142.3	156.3	187.9	2342.2	2476.4
1971	973.8	47	1.5	14.6	155.8	148.0	162.6	178.7	2504.8	2655.1
1972	973.2	47	1.5	14.6	85.6	81.4	96.0	129.6	2600.8	2784.7
1973[c]	1079.5	44	1.5	16.2	95.0	90.3	106.5	137.4	2707.3	2922.1
1974	1215.2	44	1.5	18.2	106.9	101.6	119.8	183.7	2827.1	3105.8
1975	1015.5	40	1.5	15.2	89.4	84.9	100.1	136.7	2927.2	3242.5
1976	1088.9	35	1.5	16.3	95.8	91.0	107.3	148.9	3034.5	3391.4
1977	1045.6	34	1.5	15.7	92.0	87.4	103.4	152.1	3137.9	3543.5
1978	1005.6	32	1.5	15.1	88.5	84.1	99.2	142.8	3237.1	3686.3
1979	943.3	30	1.5	14.1	83.0	78.9	93.0	133.0	3330.1	3819.3
1980	985.2	29	1.5	14.8	86.7	82.4	97.2	152.2	3427.3	3971.5

[a]From 1975 to 1980, annual world production of CCl_4 is derived from U.S. CCl_4 production + imports − exports. For all other years, consumption is equivalent to production because no export/import figures were avaliable. Also from 1958 to 1971, 16% is used to calculate emission, whereas from 1972 to 1980, 8.8% is used (see text).

[b]Total emission is the sum of annual emission (95% release) + production loss.

[c]These years use extrapolated values and are therefore less certain.

data period to small variations in τ_s. The site-to-site differences in the estimates of lifetime correspond to differences between the observed and calculated linear trends at each site divided by this partial derivative. The uncertainty limits on the lifetimes are affected primarily by month-to-month (as opposed to within months) variations in CCl_4 and are significantly larger for Adrigole/Cape Meares than for the other sites because the data record is only approximately half as long at those sites. Applying a student-t test to the site-to-site lifetime differences and to the uncertainty limits assigned to each, it would appear that the uncertainty limits are underestimated by a factor of approximately 2. That is to say, there probably exist long-term drifts (having a period of several years or more), which are probably of instrumental origin [*Cunnold et al.*, this issue (*a*)], which are not predicted by the two-dimensional model and which would not be accounted for by the procedure used to derive the uncertainty limits.

From Figure 6 it appears that the most significant inconsistencies occur in the first few months of ALE operation. It is, therefore, useful to examine the site-to-site consistency as a function of time. Table 10 shows both the optimal and the average lifetime estimates obtained for 1, 2, and 3 year periods

TABLE 8. Sinks and Removal Times for Carbon Tetrachloride

Sink	Removal Time, τ (years)	Removal Rate, $1/\tau$ ($year^{-1}$)	Reference
Stratospheric photolysis	60	1.6×10^{-2}	*NAS* [1976]
	40–59	$1.7–2.5 \times 10^{-2}$	*Galbally* [1976]
	60–100	$1.3–1.6 \times 10^{-2}$	*Singh et al.* [1976]
	18	5.5×10^{-2}	*Krey et al.* [1976]
	50	2.0×10^{-2}	*Golombeck* [1982]
Transfer and hydrolysis in the oceans	59	1.7×10^{-2}	*Pierotti et al.* [1976]
	95–286	$3.5–10.5 \times 10^{-3}$	*Galbally* [1976]
Gas phase reactions			
Reactions with O, H, CH_3	555–1667	$0.6–1.8 \times 10^{-3}$	*Galbally* [1976]
Reaction with OH	>330	$> 3 \times 10^{-3}$	*Cox et al.* [1976]
Biological removal	$333–10^3$	$1.0–3.0 \times 10^{-3}$	*Galbally* [1976]

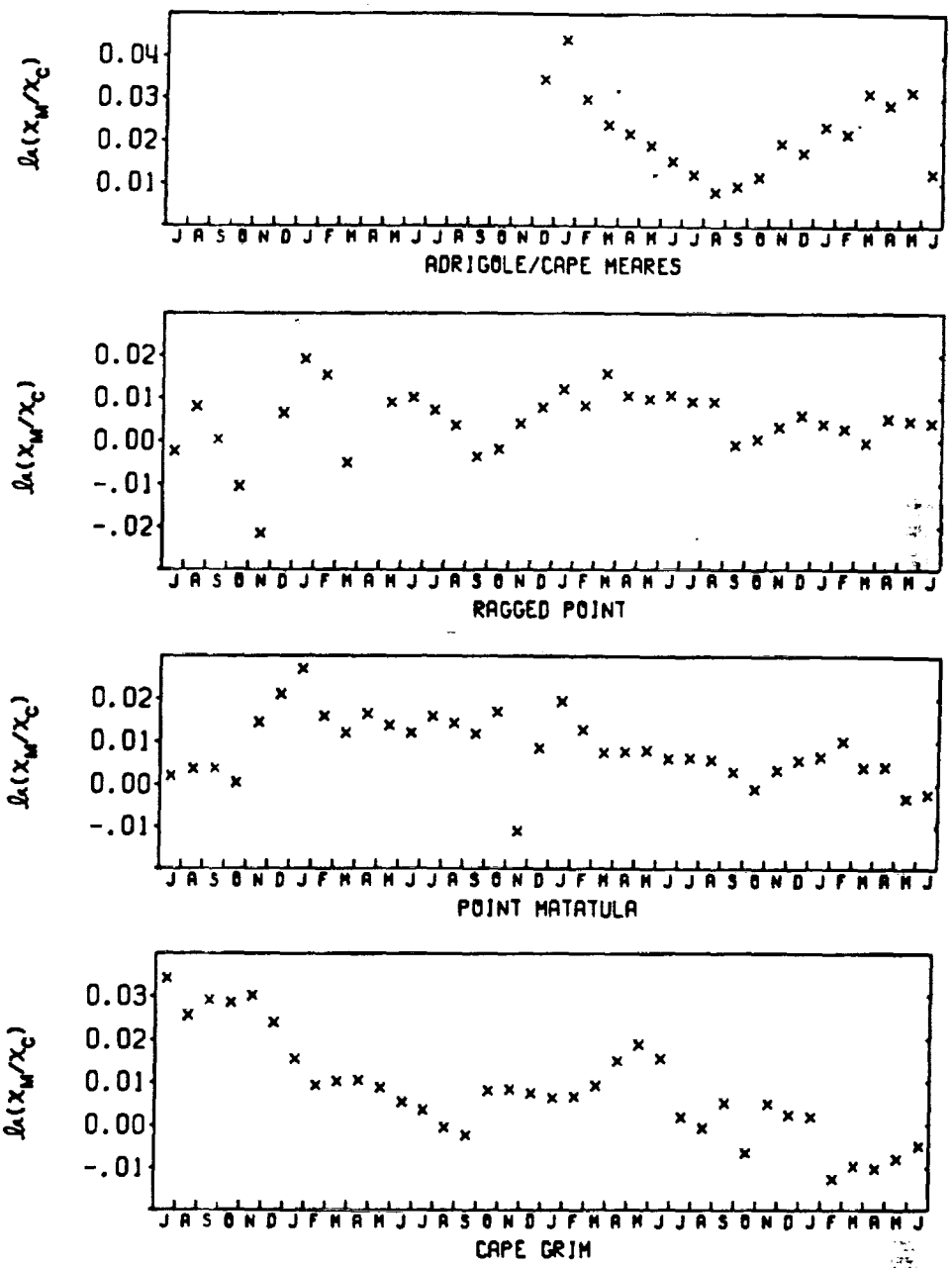

Fig. 6. CCl_4 residuals with respect to a two-dimensional model calculation with only a stratospheric sink corresponding to an atmospheric lifetime of 50 years. Residuals are given as the natural logarithm of the measured mixing ratio divided by the calculated mixing ratio.

(based upon varying the stratospheric lifetime, τ_s). In preparing this table, the data from Adrigole/Cape Meares was omitted in deriving the average lifetime estimate for the period July 1978 to June 1980 since only 7 months of data were available in that time period. The table shows extreme variability of the lifetime estimates during the first year of network operation and, in contrast, very little variation in the second and third years of operation. Both the optimal combination

TABLE 9. CCl_4 Lifetime Estimates (Due to Stratospheric Photodissociation) Derived From the Trend at Each Site Based Upon the Average of the Two Release Scenarios Given in Table 7

Site	Reciprocal Lifetime, (years) $\pm 1\sigma$	Lifetime, (years) $\pm 1\sigma$	Approximate Weight Given to Station in Optimal Code
Adrigole, Ireland/ Cape Meares, Oregon	0.023 ± 0.007	43^{+19}_{-10}	0.1
Ragged Point, Barbados	0.017 ± 0.003	59^{+13}_{-9}	0.3
Point Matatula, American Samoa	0.024 ± 0.003	42^{+6}_{-5}	0.4
Cape Grim, Tasmania	0.035 ± 0.004	29^{+3}_{-3}	0.2

TABLE 10. CCl_4 Reciprocal Lifetime Estimates (years^{-1}) as a Function of Time Obtained by Averaging and by Optimally Combining the Lifetime Estimates at the ALE Sites

Time Period	Optimal Combination	Average
July 1978 to June 1979	0.011 ± 0.009	0.020 ± 0.024
July 1980 to June 1981	0.015 ± 0.007	0.018 ± 0.011
July 1978 to June 1980	0.014 ± 0.003	0.020 ± 0.007
July 1979 to June 1981	0.021 ± 0.003	0.026 ± 0.003
July 1978 to June 1981	0.020 ± 0.002	0.025 ± 0.004

and the average of the lifetime estimates at the "four" sites appear to be converging satisfactorily with time. It is not, however, clear from Table 10 which combination provides the better lifetime estimate. The difference between the two estimates is that the optimal combination gives reduced weight to the Cape Grim (and Adrigole/Cape Meares) record because of the substantial autocorrelation of the residuals shown in Figure 6. It seems intuitively reasonable to give reduced weight to all the data during the first year of operation as well as to the shorter length record at Adrigole/Cape Meares. We shall therefore utilize the weighting reflected in the optimal combination and the lifetime thus derived. However, because the student-t test suggests that the optimal algorithm is underestimating the uncertainty limits (by approximately a factor of 2), we shall use the error bars obtained by averaging. The reciprocal lifetime estimate is thus 0.020 ± 0.004 years^{-1} and atmospheric lifetime of CCl_4 (obtained by the trend technique) is 50^{+12}_{-8} years. Note that these uncertainty limits do not yet include the effect of the uncertainties in release corresponding to our two release scenarios.

4.2. *Inventory Technique*

In previous papers it was argued that the two-dimensional model successfully similates the latitudinal and altitudinal distributions of $CFCl_3$ [*Cunnold et al.*, this issue (*a*)] and CF_2Cl_2 [*Cunnold et al.*, this issue (*b*)]. Figure 6 suggests that the two-dimensional model also successfully simulates the latitudinal distribution of CCl_4; for example, the average increase from Cape Grim, Tasmania, to Ragged Point, Barbados, is 4.0% observationally and 4.2% in the two-dimensional model. The agreement is poorer for the gradient from Cape Grim to Adrigole/Cape Meares (7.6% versus 6.2 ± 0.7% depending on which release scenario is used), and this may indicate that CCl_4 at Adrigole is anomalously high.

It is evident from the ALE experiment, as well as from previous observations, that the atmospheric lifetime of CCl_4 is sufficiently long that CCl_4 is well mixed in the troposphere. In fact, the observed latitudinal gradient is so small (~7%) that we believe that the average mixing ratio derived from the ALE network is likely to be within 0.5% of the average tropospheric mixing ratio of CCl_4. Stratospheric observations [*Pierotti et al.*, 1980; *Seiler et al.*, 1978] indicate that there is CCl_4 in the stratosphere but that its relative decrease with increasing altitude is at least as large as for $CFCl_3$. The three-dimensional model calculations by *Golombeck* [1982] give an atmospheric lifetime for CCl_4 due to stratospheric photodissociation alone of 50 years. Assuming that this is the only destruction process for CCl_4, and using the "most probable" release scenario, our two-dimensional model produces an average mixing ratio in the stratosphere at the end of 1979 equal to 0.6 times the average mixing ratio in the (upper) troposphere. We shall assume a value of 0.6 ± 0.12 (1σ limits) for this ratio. This range is consistent with existing stratospheric observations of CCl_4 and with a ratio of 0.58 ± 0.1 [*Cunnold et al.*, this issue (*a*)] observed for $CFCl_3$. Assuming the stratosphere is 20% of the atmosphere, the average mixing ratio of CCl_4 throughout the atmosphere is estimated to be

$$(0.92 \pm 0.03)\bar{\chi}_{ALE} \tag{5}$$

where $\bar{\chi}_{ALE}$ is the average mixing ratio observed in the ALE experiment. Based upon $\bar{\chi}_{ALE} = 118$ pptv and an atmospheric mass of 5.137×10^{18} kgm, the atmospheric inventory of CCl_4 on January 1, 1980, is therefore estimated to be approximately 3000 kton. This may be compared against the accumulated release up to that time, using the average of the two release scenarios given in Table 7, of 3575 kton.

Using the "most probable" release scenario, an atmospheric lifetime which best simulates the atmospheric inventory is determined by minimizing the differences between the observed and the model-calculated mixing ratios. In this calculation also the differences are weighted according to the precision of the estimates of the monthly mean values (equation (2)). This lifetime, which is based on solving equation (3), is calculated to be 57 years.

4.3. *Uncertainties in the Lifetime Estimates*

Trend estimates of lifetime have been derived from the ALE data by using both the upper and lower limit release scenarios. For the lower limit scenario, the reciprocal lifetime is estimated to be 0.009 years^{-1} (~110 years) while for the upper limit scenario we obtain an estimate of 0.032 years^{-1} (31 years). If we assume that these release scenarios provide $\pm 1\sigma$ upper and lower limits on the release, we conclude that the uncertainty in reciprocal lifetime due to uncertainties in the release data is ± 0.011 years^{-1}. Similar model calculations may also be used to estimate how release uncertainties affect the lifetime estimate calculated by the inventory technique. For the lower and upper limit release scenarios, we obtain reciprocal lifetimes of 0.008 years^{-1} (~120 years) and 0.027 years^{-1} (37 years), respectively. Thus, for the inventory and the trend techniques, release uncertainties produce uncertainties in the reciprocal lifetime of 0.010 and 0.011 years^{-1}, respectively.

If the reciprocal lifetime uncertainty associated with measuring the trend of CCl_4 in the atmosphere (0.004 years^{-1}) is combined with the uncertainty associated with the release of CCl_4 into the atmosphere, the trend reciprocal lifetime uncertainty is $(0.011^2 + 0.004^2)^{1/2}$ years^{-1}. This gives upper and lower (1σ) limits to the trend lifetime of approximately 120 and 31 years, respectively.

The uncertainty in the inventory estimate of reciprocal lifetime arises not only from the release uncertainties described above (0.010 years^{-1}) but also from absolute calibration uncertainties and from the uncertain content of CCl_4 in the stratosphere. From coulometry alone, *Rasmussen and Lovelock* [this issue] estimate that the accuracy of the calibration of the ALE standards is 4%. In the absence of independent corroboration by other measurement techniques, we believe that this uncertainty should be increased. Based on the fact that dilution provides an absolute calibration factor which is approximately 22% more than that derived from coulometry techniques [*Rasmussen and Lovelock*, this issue], we shall assume that the accuracy of calibration of CCl_4 in the ALE standards is 22/2 = 11%. We note that such an absolute calibration uncertainty is consistent with the large differ-

ences in absolute calibration noted by *Rasmussen* [1978]. This uncertainty may be translated into an uncertainty in reciprocal lifetime on the basis of the sensitivity shown in our two-dimensional model of the atmosphere to small changes in the atmospheric lifetime of CCl_4. The model sensitivity is simulated by $\partial(\ln \chi)/\partial(1/\tau) = -8$ years where χ is the simulated globally averaged mixing ratio at the locations of the ALE sites for the 3 years of measurements. Thus, the uncertainty of 11% in absolute calibration is translated into a reciprocal lifetime uncertainty of 0.14 years^{-1}. Neglecting the much smaller uncertainty associated with our estimate of the stratospheric content, the combined uncertainty in the reciprocal lifetime derived from the inventory technique is $(0.014^2 + 0.010^2)^{1/2}$ years^{-1}. This gives an uncertainty range for the inventory lifetime of $57^{+\infty}_{-28}$ years.

The CCl_4 production from photochemically induced oxidation of perchloroethylene [*Singh et al.*, 1975, 1976] would lead to approximately 20 kton/year of additional CCl_4 release during the 1970's (based on PCE production figures obtained from the International Trade Commission) and to an increase in the predicted surface mixing ratio of CCl_4 of approximately 20%. It would, however, lead to a change of only 0.1%/year in the calculated trend over the 3-year period of ALE observations. Hence, this CCl_4 production mechanism does not produce a determinable response in trend or, in fact, in atmospheric inventory based on the uncertainties of the ALE CCl_4 measurements and release estimates.

5. Conclusion

The atmospheric concentrations of CCl_4 have been determined at five coastal sites chosen to represent approximately the four major equal mass subdivisions of the global atmosphere. The data have been fitted with an empirical model including a linear trend and an annual cycle. Averaging the observations from the four semi-hemispheres of the globe, the average mixing ratio of CCl_4 in the lower troposphere on January 1, 1980, is estimated to have been 118 pptv, and it was increasing at 2.1 pptv (1.8%) per year.

Using an optimal estimation technique incorporating a two-dimensional nine-box model of the atmosphere and a prescribed atmospheric release scenario leads to estimates of the atmospheric lifetime of CCl_4 of 50 years (by the trend analysis technique) and 57 years (by the inventory analysis technique). The maximum likelihood combination of these two lifetime estimates is 52 years. Uncertainties in these estimates have been discussed and result from both release and measurement uncertainties for the trend technique and principally from release and absolute calibration uncertainties for the inventory analysis. Based on the current estimate of the atmospheric lifetime of CCl_4 due to stratospheric photodissociation of approximately 50 years and on the admittedly ad-hoc assessment of uncertainties in release and absolute calibration, we note not only remarkable agreement between the lifetime estimates obtained by using the two relatively independent analysis procedures but also consistency between the proposed release scenario and destruction of CCl_4 by photodissociation in the stratosphere only.

Acknowledgments. The successful operation of the ALE monitoring network owes much to the efforts of local individuals at each of the ALE stations. In particular, we would like to acknowledge the help of Paul Fraser (CSIRO, Australia), Graham Wise and Kim Briggs (Australian Department of Science and Technology), Don Nelson (NOAA), Cornelius Shea (Barbados), Michael O'Sullivan (Adrigole, Ireland), and Jeff Widerholt (Oregon Graduate Center). In addition, we are especially grateful to Christine Curthoys for preliminary processing of the raw data and to Andrew Lovelock for his assistance in maintaining and servicing the instrumentation at the Adrigole and Barbados stations. In the preparation of this manuscript we thank Rick Rosen, Graeme Milne, and Brian Foulger for many helpful suggestions and comments. Finally, we thank the Chemical Manufacturers Association who have so generously supported the Atmospheric Lifetime Experiment.

References

Alexander Grant Report-DuPont Calculations, World production and release of chlorofluorocarbons FC-11 and FC-12 through 1980, report, Chemical Mfr. Assoc., Washington, D. C., 1981.

Altshuller, A. P., Average tropospheric concentration of carbon tetrachloride based on industrial production, usage, and emissions, *Environ. Sci. Technol.*, *10*, 596–598, 1976.

Alyea, F. N., The Atmospheric Lifetime Experiment: A guide to the ALE data tape, technical memorandum, Washington, D. C., 1983.

Alyea, F. N., D. M. Cunnold, and R. G. Prinn, Meteorological constraints on tropospheric halocarbon and nitrous oxide destructions by siliceous land surfaces, *Atmos. Environ.*, *12*, 1009–1011, 1978.

Atkinson, R., G. M. Breuer, J. N. Pitts, Jr., and H. L. Sandoval, Tropospheric and stratospheric sinks for halocarbons: Photooxidation, $O(^1D)$ atom, and OH radical reactions, *J. Geophys. Res.*, *81*, 5765–5770, 1976.

Ausloos, P. J., R. E. Rebbert, and L. Glasgow, Photodecomposition of chloromethanes adsorbed on silica surfaces, *J. Res. Nat. Bur. Stand.*, *82*, 1–7, 1977.

Campbell, M., Halocarbon decomposition by natural ionization, *Geophys. Res. Lett.*, *3*, 661–664, 1976.

Chemical Manufacturers Association, Carbon tetrachloride consumption in production of chlorofluorocarbons FC-11 and FC-12, report, Washington, D. C., 1983.

Cox, R. A., R. G. Derwent, A. E. J. Eggleton, and J. E. Lovelock, Photochemical oxidation of halocarbons in the troposphere, *Atmos. Environ.*, *10*, 305–308, 1976.

Cunnold, D. M., R. G. Prinn, R. A. Rasmussen, P. G. Simmonds, F. N. Alyea, C. A. Cardelino, A. J. Crawford, P. J. Fraser, and R. D. Rosen, The Atmospheric Lifetime Experiment, 3, Lifetime methodology and application to 3 years of $CFCl_3$ data, *J. Geophys. Res.*, this issue (*a*).

Cunnold, D. M., R. G. Prinn, R. A. Rasmussen, P. G. Simmonds, F. N. Alyea, C. A. Cardelino, and A. J. Crawford, The Atmospheric Lifetime Experiment, 4, Results for CF_2Cl_2 based on 3 years data, *J. Geophys. Res.*, this issue (*b*).

Dotan, L., D. L. Albritton, F. C. Fesenfeld, G. E. Streit, and E. E. Ferguson, Rate constants for the reactions of O^-, O_2^-, NO_2^-, CO_3^-, and CO_4^- with HCl and ClO^- with NO, NO_2, SO_2, and CO_2 at 300 K, *J. Chem. Phys.*, *68*, 5414–5416, 1978.

Edwards, P. R., I. Campbell, and G. S. Milne, The impact of chloromethanes on the environment, I, The atmospheric chlorine cycle, *Chem. Ind.*, 54–58, 1982.

Fraser, P. J., and G. I. Pearman, Atmospheric halocarbons in the southern hemisphere, *Atmos. Environ.*, *12*, 839–844, 1978.

Gäb, S., J. Schmitzer, H. W. Thamm, H. Parlar, and F. Korte, Photomineralisation rate of organic compounds adsorbed on particulate matter, *Nature*, *270*, 331–333, 1977.

Galbally, I. E., Man-made carbon tetrachloride in the atmosphere, *Science*, *193*, 573–576, 1976.

Golombeck, A., A global three-dimensional model of the circulation and chemistry of long-lived atmospheric species, Ph.D. Thesis, Mass. Inst. of Tech., Cambridge, Mass., 1982.

Grimsrud, E. P., and R. A. Rasmussen, Survey and analysis of halocarbons in the atmosphere by gas chromatography-mass spectrometry, *Atmos. Environ.*, *9*, 1014–1017, 1975.

Hanst, P. C., L. L. Spiller, D. N. Watts, J. W. Spence, and M. F. Miller, Infrared measurements of fluorocarbons, carbon tetrachloride, carbonyl sulfide, and other atmospheric trace gases, *J. Air Pollut. Control Assoc.*, *25*, 1220–1226, 1975.

Hine, J., Carbon dichloride as an intermediate in the basic hydrolysis of chloroform, *J. Am. Chem. Soc.*, *72*, 2438–2445, 1950.

Krey, P. W., R. Lagomarsino, M. Schonberg, and I. E. Toonkel, CCl_4 in ground level air and stratosphere, *Health Safety Lab. Environ. Quart.*, I-21–I-49, 1976.

Lillian, D., H. B. Singh, A. Appleby, L. Lobban, R. Arnts, R. Gumbert, R. Hague, J. Tooney, J. Kazazis, M. Antell, D. Hansen, and B.

Scott, Atmospheric fates of halogenated compounds, *Environ. Sci. Technol.*, *9*, 1042–1048, 1975.

Lovelock, J. E., R. J. Maggs, and R. J. Wade, Halogenated hydrocarbons in and over the Atlantic, *Nature*, *241*, 194–196, 1973.

National Academy of Sciences, *Halocarbons: Effects on Stratospheric Ozone*, Washington, D. C., 1976.

National Research Council, *Chloroform, Carbon Tetrachloride, and Other Halomethanes:* An Environmental Assessment, Washington, D. C., 1978.

Neely, W. B., Material balance analysis of trichlorofluoromethane and carbon tetrachloride in the atmosphere, *Science Total Environ.*, *8*, 267–274, 1977.

Ohta, T., M. Morita, and I. Mizoguichi, Local distribution of chlorinated hydrocarbons in the ambient air in Tokyo, *Atmos. Environ.*, *10*, 557–560, 1976.

Pack, D. H., J. E. Lovelock, G. Cotton, and C. Curthoys, Halocarbon behavior from a long time series, *Atmos. Environ.*, *11*, 329–344, 1977.

Pearson, C. R., and G. McConnell, Chlorinated C_1 and C_2 hydrocarbons in the marine environment, *Proc. R. Soc., London Ser. B*, *189*, 305–332, 1975.

Penkett, S. A., K. A. Brice, R. G. Derwent, and A. E. J. Eggleton, Measurement of CCl_3F and CCl_4 at Harwell over the period January 1975 to November 1977, *Atmos. Environ.*, *13*, 1011–1109, 1979.

Pierotti, D., and R. A. Rasmussen, Interim report on the atmospheric measurement of nitrous oxide and the halocarbons, report, NASA, Washington, D. C., 1976*a*.

Pierotti, D., R. A. Rasmussen, J. Krasnec, and E. Halter, Trip report on cruise of R/V *Alpha Helix* from San Diego, Calif., to San Martin, Peru, report, National Science Foundation, Washington, D. C., 1976*b*.

Pierotti, D., L. E. Rasmussen, and R. A. Rasmussen, The Sahara as a possible sink for trace gases, *Geophys. Res. Lett.*, *5*, 1001–1004, 1978.

Pierotti, D., R. A. Rasmussen, and R. Dalluge, Measurements of N_2O, CF_2Cl_2, $CFCl_3$, CH_3CCl_3, CCl_4, and CH_3Cl in the troposphere and lower stratosphere over North America, *J. Geomag. Geoelectr.*, *32*, 181–205, 1980.

Prinn, R. G., P. G. Simmonds, R. A. Rasmussen, R. D. Rosen, F. N. Alyea, C. A. Cardelino, A. J. Crawford, D. M. Cunnold, P. J. Fraser, and J. E. Lovelock, The Atmospheric Lifetime Experiment, 1, Introduction, instrumentation and overview, *J. Geophys. Res.*, this issue.

Radding, S. B., D. H. Liu, H. L. Johnson, and T. Mill, Review of the environmental fate of selected chemicals, *EPA 560/5-77-003*, U.S. Environ. Prot. Agency, Washington, D. C., 1977.

Rasmussen, R. A., Interlaboratory comparison of fluorocarbon measurements, *Atmos. Environ.*, *12*, 2505–2508, 1978.

Rasmussen, R. A., and J. E. Lovelock, The Atmospheric Lifetime Experiment, 2, Calibration, *J. Geophys. Res.*, this issue.

Rasmussen, R. A., M. A. K. Khalil, and R. Dalluge, Atmospheric trace gases in Antartica, *Science*, *211*, 285–287, 1981.

Rebbert, R. E., and P. J. Ausloos, Gas-phase photodecomposition of carbon tetrachloride, *J. Photochem.*, *6*, 265–276, 1976.

Seiler, W., F. Muller, and H. Oeser, Vertical distribution of chlorofluoromethanes in the upper troposphere and lower stratosphere, *Pure Appl. Geophys.*, *116*, 554–566, 1978.

Simmonds, P. G., S. L. Kerrin, J. E. Lovelock, and F. H. Shair, Distribution of atmospheric halocarbons in the air over the Los Angeles basin, *Atmos. Environ.*, *8*, 209–216, 1974.

Singh, H. B., D. Lillian, A. Appleby, and L. Lobban, Atmospheric formation of carbon tetrachloride from tetrachloroethylene, *Environ. Lett.*, *10*, 253–256, 1975.

Singh, H. B., D. P. Fowler, and T. O. Peyton, Atmospheric carbon tetrachloride, another man-made pollutant, *Science*, *192*, 1231–1234, 1976.

Singh, H. B., L. Salas, H. Shigeishi, and A. Crawford, Urban nonurban relationships of halocarbons, SF_6, N_2O, and other atmospheric constituents, *Atmos. Environ.*, *11*, 819–828, 1977*a*.

Singh, H. B., L. J. Salas, and L. A. Cavanagh, Distribution, sources, and sinks of atmospheric halogenated compounds, *J. Air. Pollut. Control Assoc.*, *27*, 332–336, 1977*b*.

Singh, H. B., L. J. Salas, H. Shigeishi, and E. Scribner, Atmospheric halocarbons, hydrocarbons, and sulfur hexafluoride: Global distributions, sources, and sinks, *Science*, *203*, 899–903, 1979.

Su, C., and E. D. Goldberg, Environmental concentrations and fluxes of some halocarbons, *Marine Pollution Transfer*, edited by H. L. Windom and R. A. Duce, pp. 353–374, Lexington Books, New York, 1976.

Tyson, B. J., J. C. Arvesen, and D. O'Hara, Interhemispheric gradients of CF_2Cl_2, $CFCl_3$, CCl_4, and N_2O, *Geophys. Res. Lett.*, *5*, 535–538, 1978.

U.S. International Trade Commission, Preliminary reports on U.S. production of selected organic chemicals, *Chem. Mark. Reporter*, 1979, 1980, 1981.

Wilkness, P. E., R. A. Lamontagne, R. E. Larson, J. W. Swinnerton, C. R. Dickson, and T. Thompson, Atmospheric trace gases in the southern hemisphere, *Nature*, *245*, 45–47, 1973.

F. N. Alyea, C. A. Cardelino, and D. M. Cunnold, School of Geophysical Sciences, Georgia Institute of Technology, Altlanta, GA 30332.

A. J. Crawford and R. A. Rasmussen, Department of Environmental Science, Oregon Graduate Center, Beaverton, OR 97005.

B. C. Lane, ICI Americas. Inc., Wilmington, DE 19897.

J. E. Lovelock, Department of Engineering and Cybernetics, University of Reading, Reading, Berks, RG6 2AL, United Kingdom.

R. G. Prinn, Department of Meteorology and Physical Oceanography, Massachusetts Institute of Technology, Cambridge, MA 02139.

P. G. Simmonds, Department of Geochemistry, University of Bristol, Bristol, BS8 1TS, United Kingdom.

(Received September 2, 1982;
revised June 20, 1983;
accepted July 5, 1983.)

JOURNAL OF GEOPHYSICAL RESEARCH, VOL. 91, NO. D10, PAGES 10,797–10,817, SEPTEMBER 20, 1986

Atmospheric Lifetime and Annual Release Estimates for $CFCl_3$ and CF_2Cl_2 From 5 Years of ALE Data

D. M. CUNNOLD,[1,2] R. G. PRINN,[2,3] R. A. RASMUSSEN,[4] P. G. SIMMONDS,[5]
F. N. ALYEA,[1,2] C. A. CARDELINO,[1,2] A. J. CRAWFORD,[4]
P. J. FRASER,[6] AND R. D. ROSEN[7]

Atmospheric Lifetime Experiment measurements of $CFCl_3$ and CF_2Cl_2 several times per day at five remote surface sites from July 1978 to June 1983 are reported. For January 1, 1981, the mean latitudinally averaged mixing ratios were 177.5 parts per trillion by volume (pptv) and 300.4 pptv for $CFCl_3$ and CF_2Cl_2, respectively. The atmospheric content at that time is estimated to have been 3,960 million kg of $CFCl_3$ and 6,000 million kg of CF_2Cl_2. The mixing ratios exhibited an annual rate of increase of 9.0 and 15.3 pptv/yr for $CFCl_3$ and CF_2Cl_2, respectively. Trend lifetime estimates for January 1, 1981, from this 5-year data set are 74^{+31}_{-17} years for $CFCl_3$ and 111^{+222}_{-44} years for CF_2Cl_2. On the basis of a comparison of $CFCl_3$ data on two different chromatographic columns, it is shown that the spectrum of measurement errors maximizes at low frequencies but may be relatively flat at periods longer than approximately 3 years. The uncertainties in the trend lifetime estimates are, however, dominated by release uncertainties. Inverting the analysis, assuming stratospheric photodissociation to be the only atmospheric sink of fluorocarbons, yields annual release estimates with an accuracy, based on the precision of the measurement system, of approximtely 8%. Excellent agreement with the Chemical Manufacturers Association release estimates is found for $CFCl_3$; for CF_2Cl_2 the estimates, although exhibiting variability from year to year, suggest that the emissions in the USSR and Eastern Europe have remained roughly constant over the years 1979–1982.

1. INTRODUCTION

Long-term measurements of the atmospheric concentrations of $CFCl_3$, CF_2Cl_2, CH_3CCl_3, CCl_4, and N_2O have been made at Adrigole, Ireland (52°N, 10°W), Cape Meares, Oregon (45°N, 124°W), Ragged Point, Barbados (13°N, 59°W), Point Matatula, American Samoa (14°S, 171°W), and Cape Grim, Tasmania (41°S, 145°E). The Atmospheric Lifetime Experiment (ALE) utilizes automated dual-column electron-capture gas chromatographs which sample the air four times daily. Measurements have been made since approximately mid-1978 at four of the sites and since December 1979 at Cape Meares.

Data for the period from July 1978 to June 1981 and the analysis for the atmospheric lifetimes of the constituents have been reported in a series of six papers [*Prinn et al.*, 1983*a*, *b*; *Rasmussen and Lovelock*, 1983; *Cunnold et al.*, 1983*a*, *b*; and *Simmonds et al.*, 1983]. The years 1984–1985 have been a transition period for ALE during which funding of Adrigole ceased and preparations were made for replacing the HP5840A instruments by HP5880s with the capability of measuring CH_4.

This paper summarizes the data on $CFCl_3$ and CF_2Cl_2 for the 5-year period from July 1978 to June 1983. Separate reports are being written for N_2O and for CH_3CCl_3 and CCl_4. In this report the "3-year" lifetime estimates are updated, and in addition, the analysis is inverted to derive annual global release rates of the gases. Attempts have been made to separate variations of the measured concentrations produced by atmospheric transport from variations of instrumental origin; a separate paper will describe these results. However, at the long periods which affect the determination of lifetimes, evidence will be presented that the dominant measurement residuals are not transport related. The 5-year data set provides a better sample for estimating these long-term variations than the 3-year data set. Accordingly, the analysis reported here results in more precise estimates of lifetimes than were possible from the 3-year data set.

2. THE 5-YEAR DATA SET

Daily mean concentrations and standard deviations for $CFCl_3$ (measured on both the silicone and Porasil columns) and CF_2Cl_2 (which was measured on the Porasil column) for the fourth and fifth years of ALE (July 1981 to June 1983) are shown in Figures 1–3. Corresponding data for the first 3 years may be found in the individual 3-year analysis papers. Figures 4–6 show the complete 5-year data record of monthly means (and standard deviations) at each measurement site, and Tables 1–3 list the monthly mean values for the fourth and fifth years. Absolute calibration factors (ξ) which have been applied to the data are 0.96 for $CFCl_3$ and 0.95 for CF_2Cl_2. These are the same factors which were used for the 3-year data set. Note that pollution events, determined by simultaneous increases in several of the measured gases or from measurements of perchloroethylene at Adrigole, have been omitted from the data set analyzed in this paper. Thus the Adrigole record, in particular, contains many short-term data gaps.

The daily data obtained in 1982 and 1983 are of a similar quality (that is, precision) to that obtained in the second and third year of the ALE experiment. The continuity of the data during the fifth year is remarkable. Following calibration tank changes, approximately 1-week equilibration periods, and discontinuities of approximately 1%, remain a characteristic fea-

[1] School of Geophysical Sciences, Georgia Institute of Technology, Atlanta.
[2] CAP, Incorporated, Atlanta, Georgia.
[3] Department of Earth, Atmospheric, and Planetary Sciences, Massachusetts Institute of Technology, Cambridge.
[4] Department of Environmental Science, Oregon Graduate Center, Beaverton.
[5] Department of Geochemistry, University of Bristol, Bristol, England.
[6] Division of Atmospheric Physics, Commonwealth Scientific and Industrial Research Organization, Aspendale, Victoria, Australia.
[7] Atmospheric and Environmental Research, Inc., Cambridge, Massachusetts.

Paper number 6D0306.
0148-0227/86/006D-0306$05.00

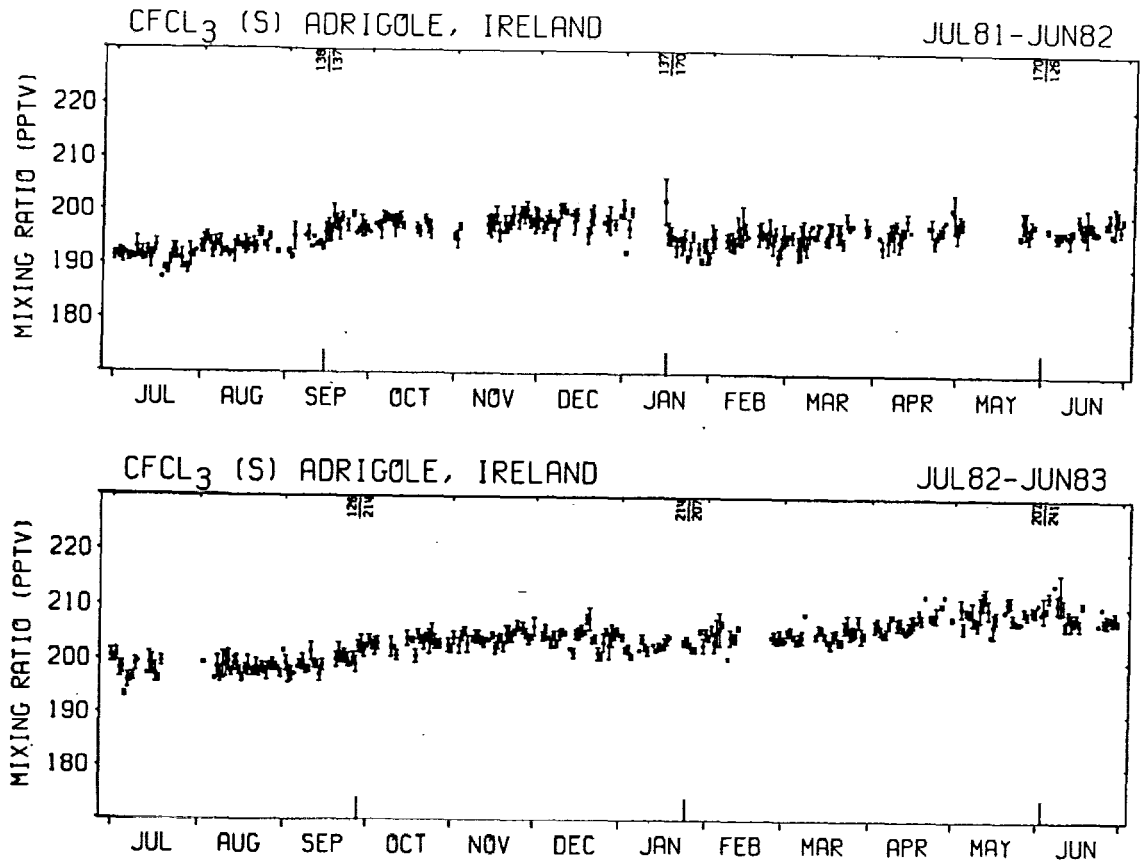

Fig. 1*a*. $CFCl_3$ daily means (pptv) and standard deviations measured on the silicone column at Adrigole, Ireland (52°N, 10°W), for the period July 1981 to June 1983. Changes of the calibration gas tank are noted on the upper abscissae.

ture of the data set (for example, tank 082 at Ragged Point, Barbados). In March and April 1982 the instrument at Point Matatula was almost destroyed by lightning and required complete renovation. In July, August, and September 1981 the Cape Grim instrument was operated incorrectly and a contaminated argon/methane-carrier gas mixture was used. Some of the data was, however, retrievable. In May 1982 the instrument at Cape Grim was moved from the ALE building to the new Commonwealth Scientific and Industrial Research Organization (CSIRO)/Bureau of Meteorology laboratory a short distance away. No discontinuity is evident in the data at that time. This conclusion is, moreover, supported by the simultaneous operation of an HP5880 by one of the authors (P. J. F.) in the laboratory over a period of several months spanning May 1982.

To summarize efficiently the principal long-term components of the ALE data, the time series have been fitted by an empirical model of the form

$$x_{ij} = a_{ij} + b_{ij}\left[\frac{t-t_m}{12}\right] + d_{ij}\left[\frac{t-t_m}{12}\right]^2 + e_{ij}\left[\frac{t-t_m}{12}\right]^3 + c_{ij}\cos\left[\frac{2\pi t}{12}\right] + s_{ij}\sin\left[\frac{2\pi t}{12}\right] \quad (1)$$

where $t = 0$ corresponds to June 15, 1978; t is measured in months; t_m is the midpoint of the data records and is equal to 30.5 months (January 1, 1981), except where subsequently noted; and x_{ij} is the volume mixing ratio of species i at station j. Note that the time series of mixing ratio is modeled in (1) and not its logarithm, which was modeled for the 3-year data set. This change was made because the year-by-year release rate estimates for each species are approximately constant over the 5-year period. The time series should thus be primarily represented by the first two terms of (1).

Weighted least squares fitting of the monthly mean measurements by (1) yields maximum likelihood estimates of the parameters. In this procedure each month's mean receives a weight (σ^{-2}) obtained from the estimated variance of the monthly mean value. This variance is derived from the sum of the variance of the measurements (σ_m^2) during the month about the monthly mean, divided by the number of independent observations n_m (which is approximately 10, based on a correlation time of 3 days) and the variance of the monthly means about the fitted empirical model (σ_0^2, calculated a posteriori). The residuals defining the latter variance are also correlated, by an amount which may be calculated from an analysis of the residuals. This correlation is accounted for by increasing σ_0^2 by a factor $M(\geq 1)$ to give $\sigma_0'^2$. Thus each monthly mean is weighted by

$$\sigma^{-2} = \left[\frac{\sigma_m^2}{n_m} + \sigma_0'^2\right]^{-1} \quad (2)$$

The effect of this weighting is to give a little less weight to the first few months of operation in 1978 (when σ_m^2 was large) and to those months in which only a few acceptable measurements were possible. Note that the procedure gives zero weight to those months in which no observations were possible.

The factor M is determined from the smoothed power spectrum of the residual variability of each individual time series.

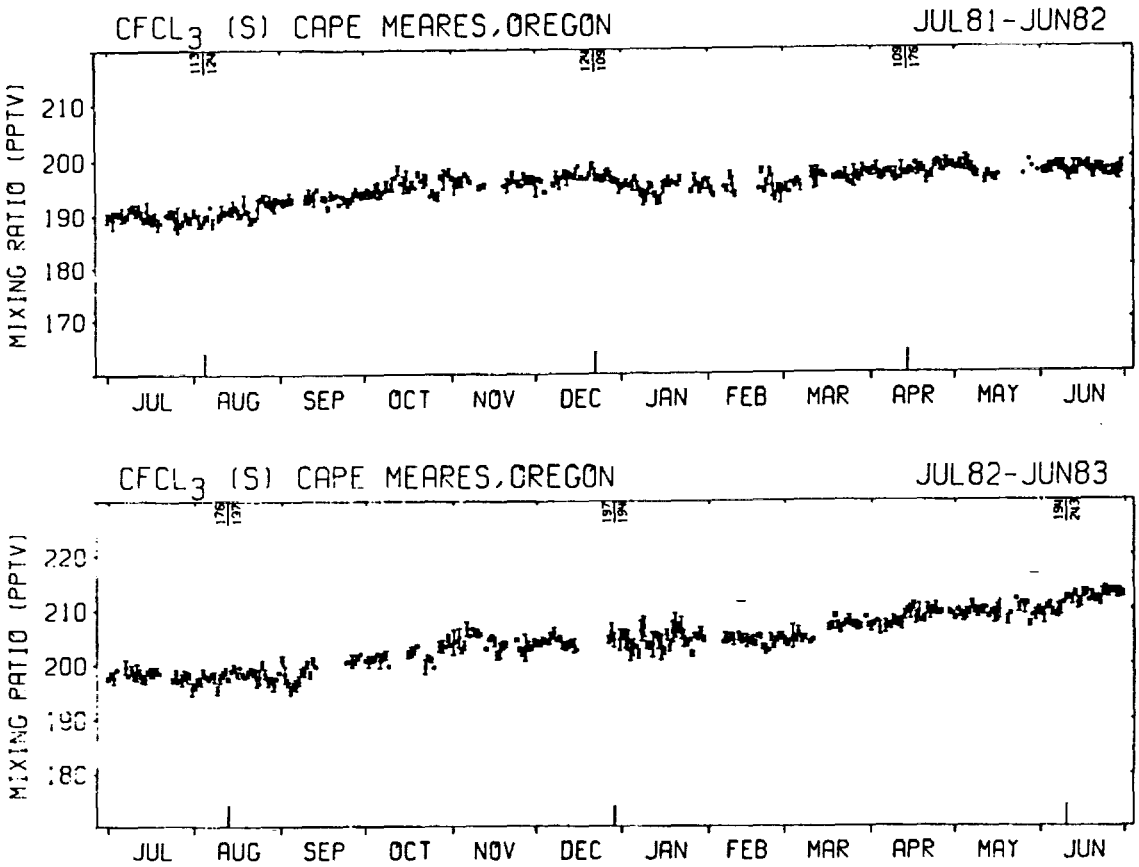

Fig. 1*b*. As for Figure 1*a* at Cape Meares, Oregon, (45°N, 124°W).

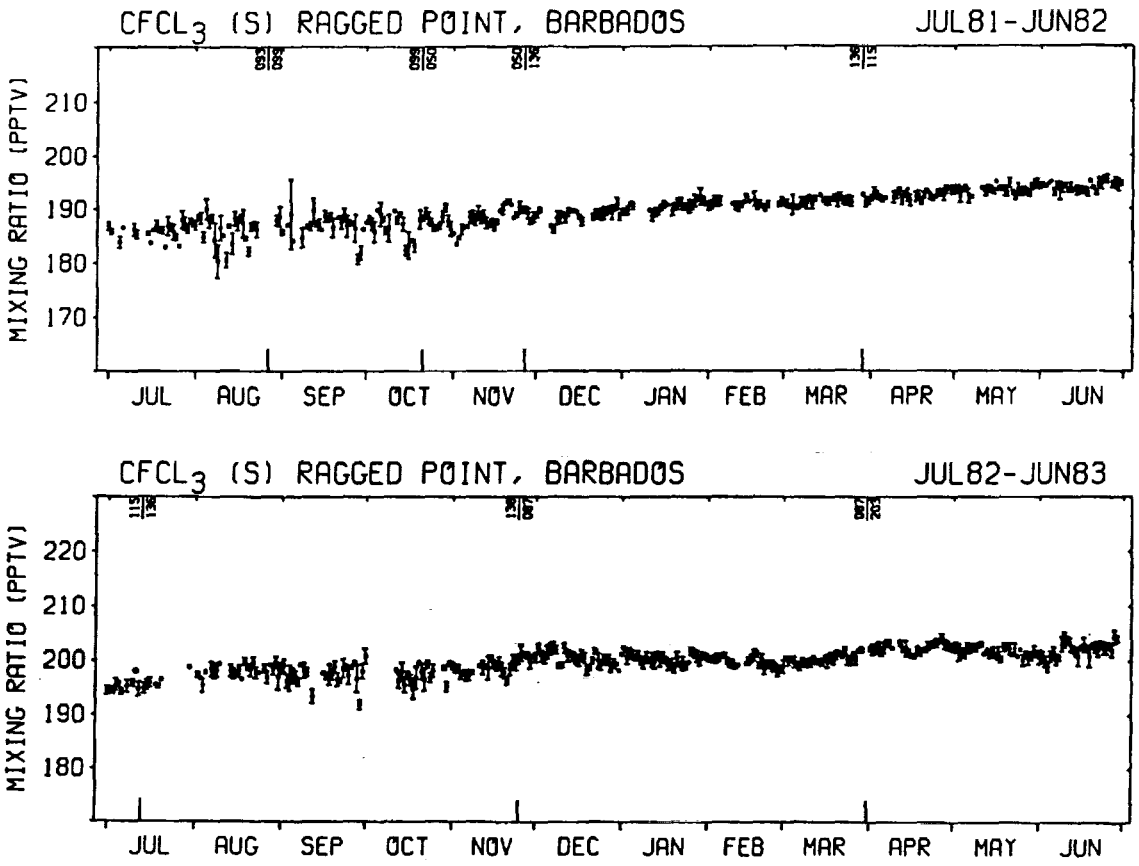

Fig. 1*c*. As for Figure 1*a* at Ragged Point, Barbados (13°N, 59°W).

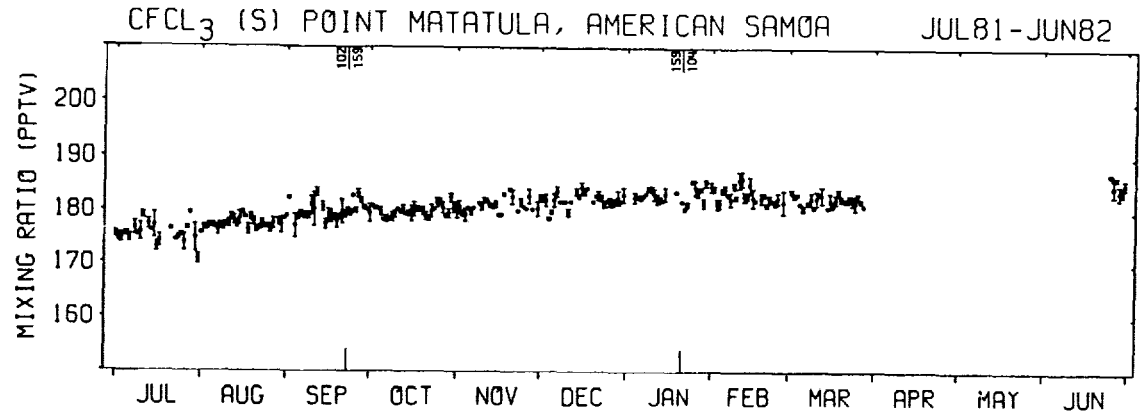

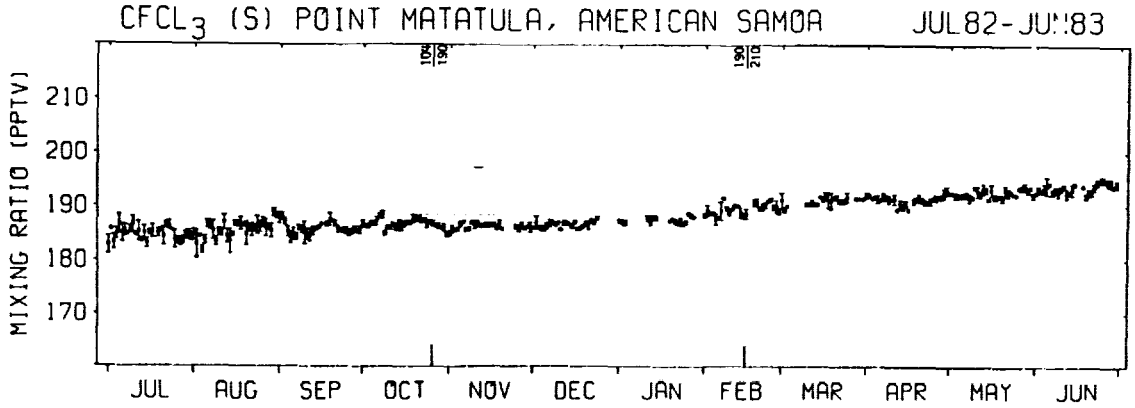

Fig. 1*d*. As for Figure 1*a* at Point Matatula, American Samoa (14°S, 171°W).

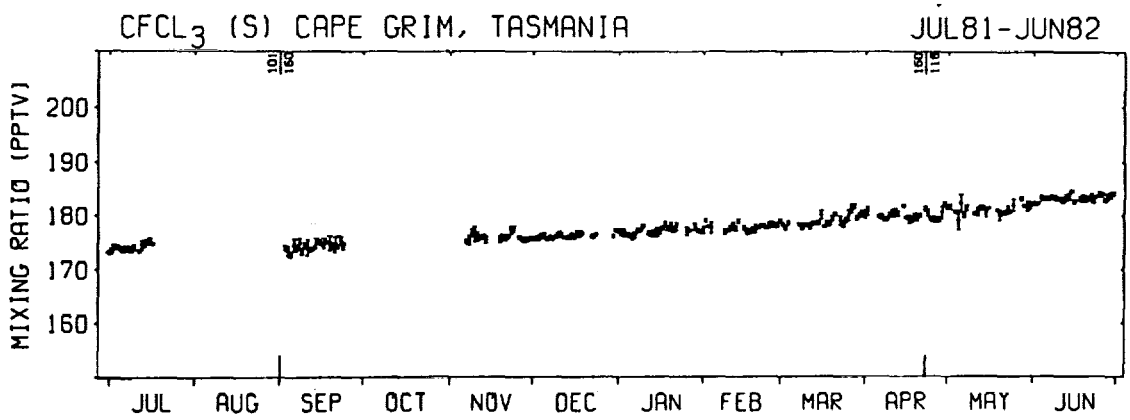

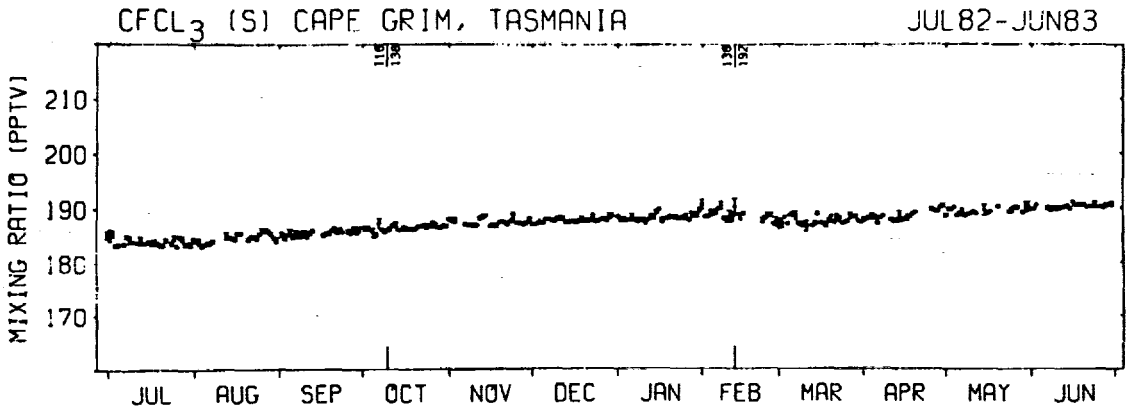

Fig. 1*e*. As for Figure 1*a* at Cape Grim, Tasmania (41°S, 145°E).

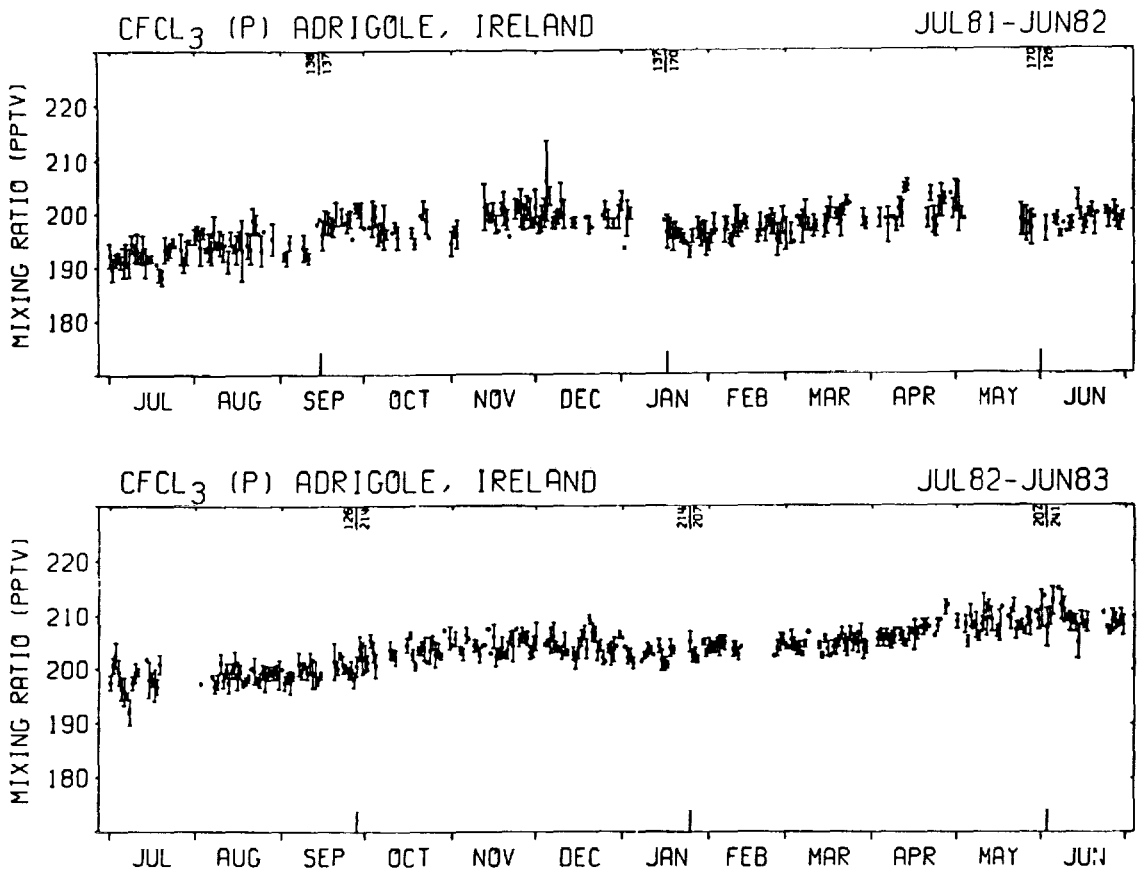

Fig. 2*a*. $CFCl_3$ daily means (pptv) and standard deviations measured on the Porasil column at Adrigole, Ireland (52°N, 10°W), for the period July 1981 to June 1983. Changes of the calibration gas tank are noted on the upper abscissae.

The smoothing was performed using a Parzen window (see, for example, *Chatfield* [1975]) with a bandwidth of approximately 2 cycles per year. Since this paper is particularly concerned with long-term trends in the time series, M is based on the power at the lowest frequencies [see *Cunnold et al.*, 1983*a*]. Table 4 shows the calculated coefficients for the empirical model, together with estimated error bars. The error bars were determined directly from the weighted least squares estimation. Small adjustments were made to the error bars for the annual components, corresponding to variation of the power spectrum between frequencies of 1 cycle per 5 years and 1 cycle per year.

The coefficients a_i, b_i, etc., correspond to the smoothed mixing ratio and trend, etc., at the midpoint of the data record. Because the Cape Meares data record is 18 months shorter than the others, the coefficients for Cape Meares are not directly comparable with those for the other sites. Perhaps the best way to view the Cape Meares data is to compare it against the portion of the Adrigole record which overlaps in time. Table 5 shows that comparison (note that the annual cycle terms are referenced to June 15 in all the time series).

Table 4 indicates a monotonic decrease of fluorocarbon mixing ratio with latitude, starting at the northern hemisphere mid-latitude sites, and trends which are consistent from site to site and, in fact, almost equal when expressed in units of pptv per year (except perhaps for $CFCl_3$ (S) at Samoa). (In this paper the letter S indicates the silicone column and the letter P the Porasil column.) Consistent seasonal cycles of the fluorocarbons exceeding 1σ in the background noise are found at Adrigole, Cape Meares, and Samoa (with amplitudes less than 1 ppt for $CFCl_3$ and less than 2 ppt for CF_2Cl_2) and Barbados continues to exhibit an insignificant annual cycle. Maximum concentrations associated with the seasonal cycle occur in October at Adrigole, November at Cape Meares, and in February in Samoa.

Table 5 indicates that $CFCl_3$ and CF_2Cl_2 concentrations are approximately 1% higher at Adrigole than at Cape Meares. We ascribe this difference to a slight increase in the base level at Adrigole due to a combination of its proximity to local sources of emission, the effect of which has not been entirely removed by filtering, and to a longitudinally nonuniform distribution produced by fluorocarbon releases in North America.

Table 4 also indicates that at the end of 1980, $CFCl_3$ in the lower atmosphere was increasing at an annually averaged rate of 9.0 ppt per year and 1 year later was increasing at 8.8 ppt per year. The globally averaged mixing ratio in the lower atmosphere on January 1, 1981, is estimated to have been 177.5 ppt, thus implying that the rate of increase was 5.1% per year at that time. Also at that time, CF_2Cl_2 was increasing at 15.3 ppt per year (and at the same rate 1 year later). For a CF_2Cl_2 mixing ratio of 300.4 ppt this implies a rate of increase for CF_2Cl_2 of 5.1% per year, equivalent to that of $CFCl_3$.

3. Updated Lifetime Estimates by the Trend Technique

The observed time series of fluorocarbons at each ALE site have been modeled by a nine-box two-dimensional model of the atmosphere [*Cunnold et al.*, 1983*a*]. This model contains

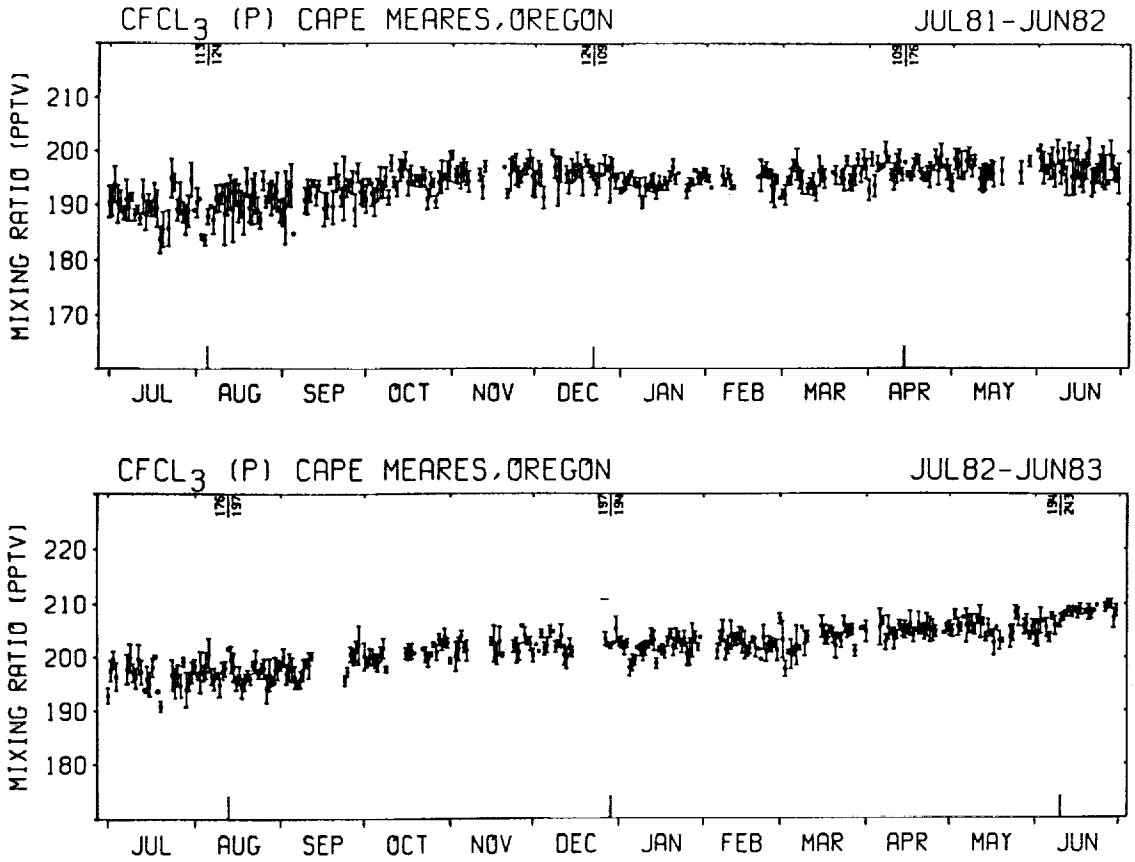

Fig. 2*b*. As for Figure 2*a* at Cape Meares, Oregon (45°N, 124°W).

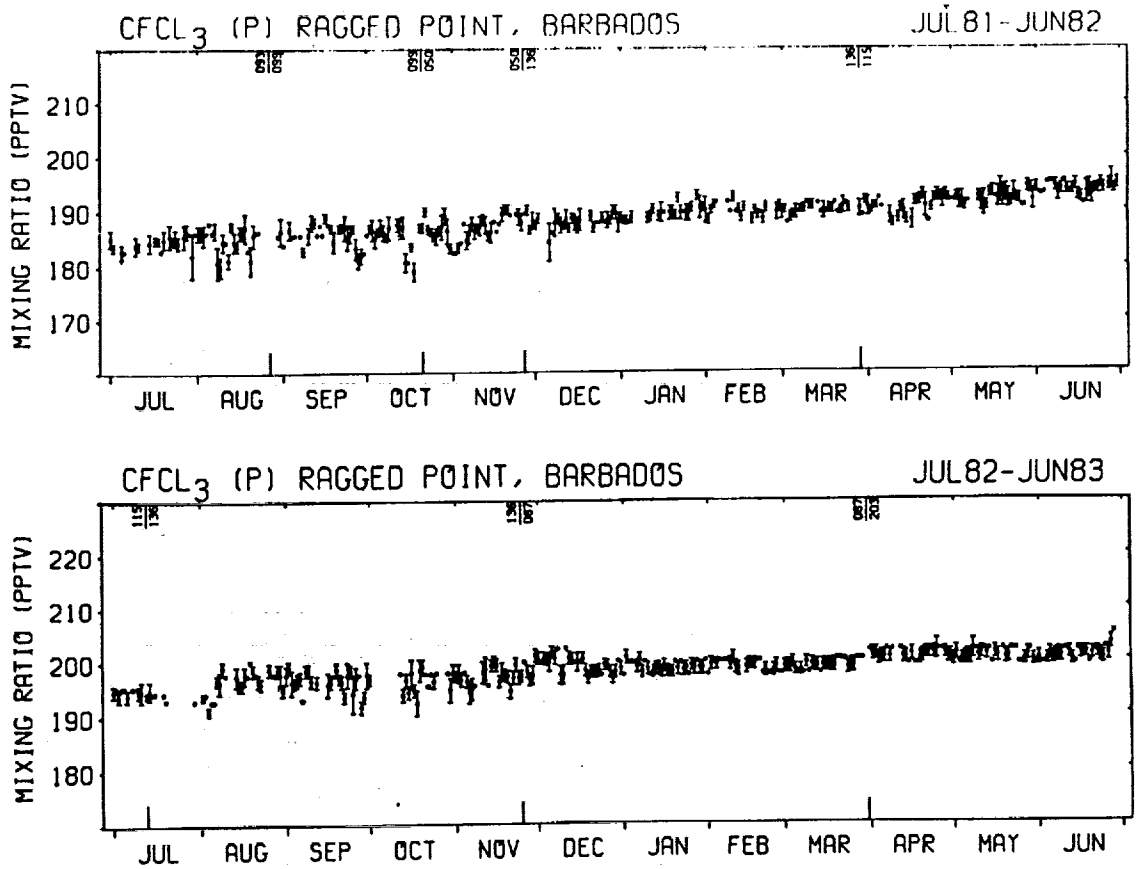

Fig. 2*c*. As for Figure 2*a* at Ragged Point, Barbados (13°N, 59°W).

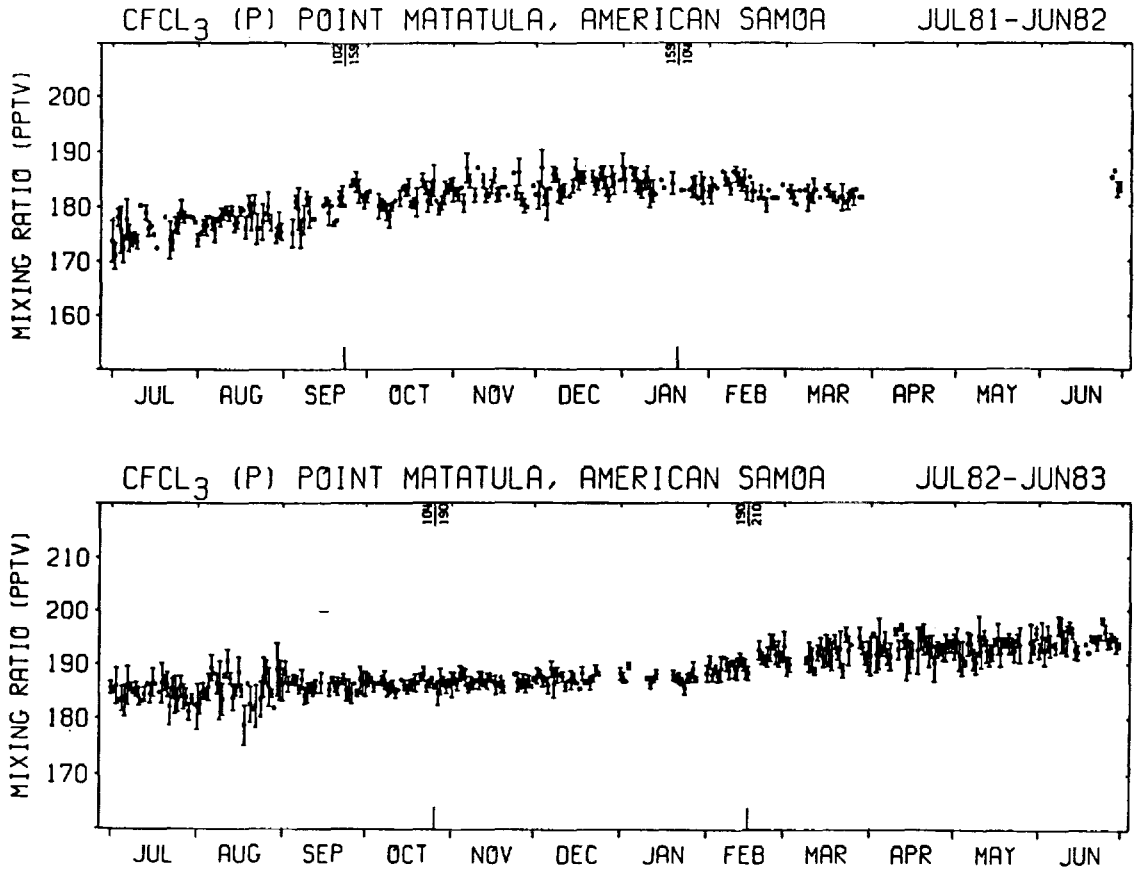

Fig. 2*d*. As for Figure 2*a* at Point Matatula, American Samoa (14°S, 171°W).

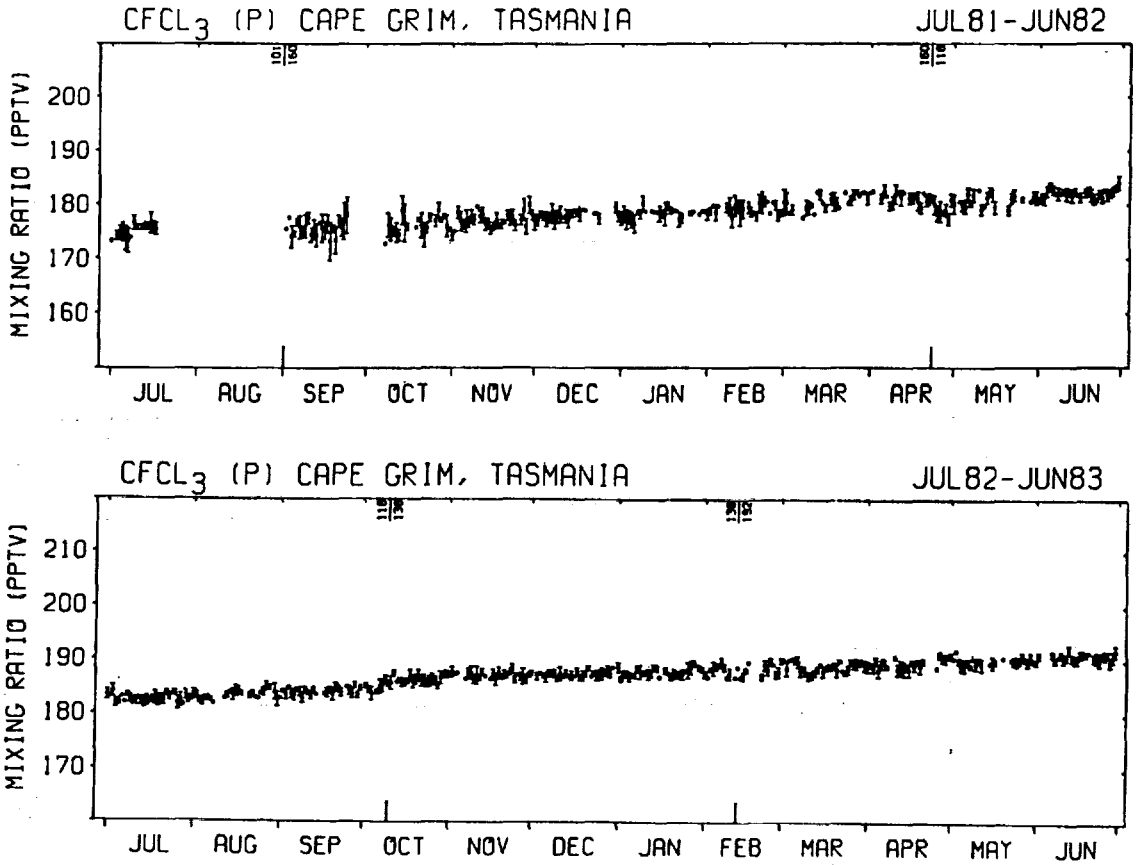

Fig. 2*e*. As for Figure 2*a* at Cape Grim, Tasmania (41°S, 145°E).

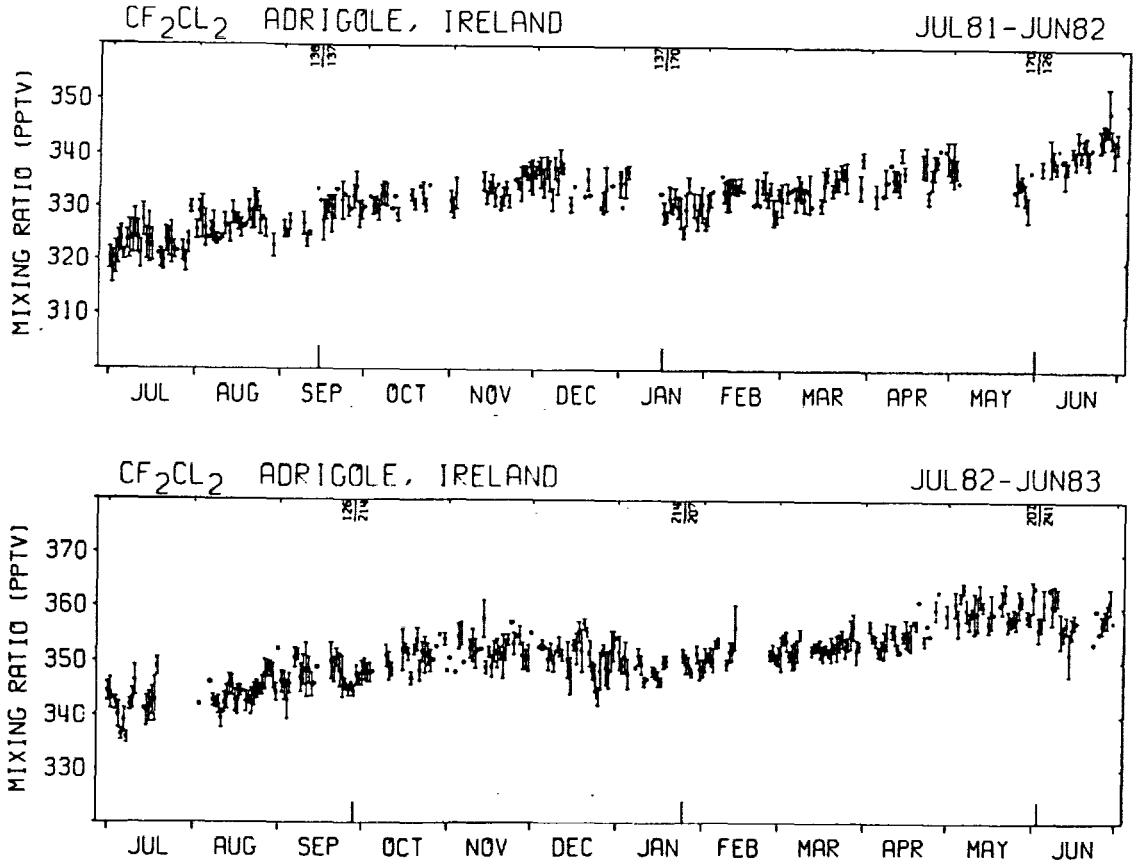

Fig. 3*a*. CF_2Cl_2 daily means (pptv) and standard deviations measured on the Porasil column at Adrigole, Ireland (52°N, 10°W), for the period July 1981 to June 1983. Changes of the calibration gas tank are noted on the upper abscissae.

fixed vertical mixing times and horizontal mixing times which have been fitted to the mean observed latitudinal gradients of $CFCl_3$ and CF_2Cl_2. In the following results the horizontal transport factor F was calculated to be 1.6 (the same value used in analyzing the 3-year data set). This adjustment of the horizontal transport should ensure that the effect of transport on the trends at the ALE sites will be simulated by our model (unless the atmosphere exhibits a systematic change in transport rates over the 5-year period). The specification of the model is completed by prescribing atmospheric release rates, including their latitudinal distribution, and a destruction rate for fluorocarbons in the atmosphere. Assuming the atmospheric release rates are known, the destruction rate can be adjusted (that is, estimated) so as to provide an optimal fit to the ALE data.

The Chemical Manufacturers Association has compiled estimates of the annual emissions of fluorocarbons in a series of reports, including *Chemical Manufacturers Association* (*CMA*) [1983], which contains estimates of the emissions through 1982. In estimating the worldwide emissions for 1983, *CMA* [1984] broke with previous tradition and declined to estimate the emissions in the USSR and Eastern Europe because of the considerable uncertainty about the emissions there in recent years. In 1982 the emissions in the USSR and Eastern Europe were estimated at approximately 6% of the worldwide total for $CFCl_3$ and 20% for CF_2Cl_2. The uncertainty in this portion of the global emissions is expected to have a significant impact on the CF_2Cl_2 lifetime estimate but only a small effect on the $CFCl_3$ lifetime. Because of the smaller contribution to the worldwide emissions, we shall first report lifetime estimates obtained by assuming that the percentage increase of fluorocarbon releases in 1983 in the USSR and Eastern Europe are similar to the percentage increases in emissions estimated for the rest of the world. This assumption about the 1983 emission has a negligible effect on the lifetime estimates, since it impacts only 6 months of our data; this result is referred to as that corresponding to the *CMA* [1983] releases, which included estimates of the USSR and Eastern European releases for the years prior to 1983. The release estimates for the rest of the world given by *CMA* [1984] will be used to assess the effect of the uncertainties in the releases in the USSR and Eastern Europe.

The latitudinal distribution of releases, which primarily affects our estimates of global circulation rates (for example, the factor F) is similar to that assumed by *Cunnold et al.* [1983*a*, *b*]. Thus for $CFCl_3$ we assume that throughout the 5-year period the global release is distributed in the proportions 0.785, 0.160, 0.031, and 0.024 in the 90°–30°N, 30°N–0°, 0°–30°S and 30°–90°S semihemispheres, respectively. For CF_2Cl_2 the proportions assumed are 0.789, 0.141, 0.038, and 0.032, respectively.

The two-dimensional model of atmospheric transport is described by *Cunnold et al.* [1983*a*]. This model can, at best, only be expected to simulate the annual cycle at each site and the variations in fluorocarbon concentrations from year to year produced by the annually averaged emissions. In fact, we find that although the seasonal cycle is well simulated at some sites (for example, Samoa), it is significantly overpredicted at others (for example, Barbados). Thus the variance of the time series residuals are not reduced by including the seasonal cycle

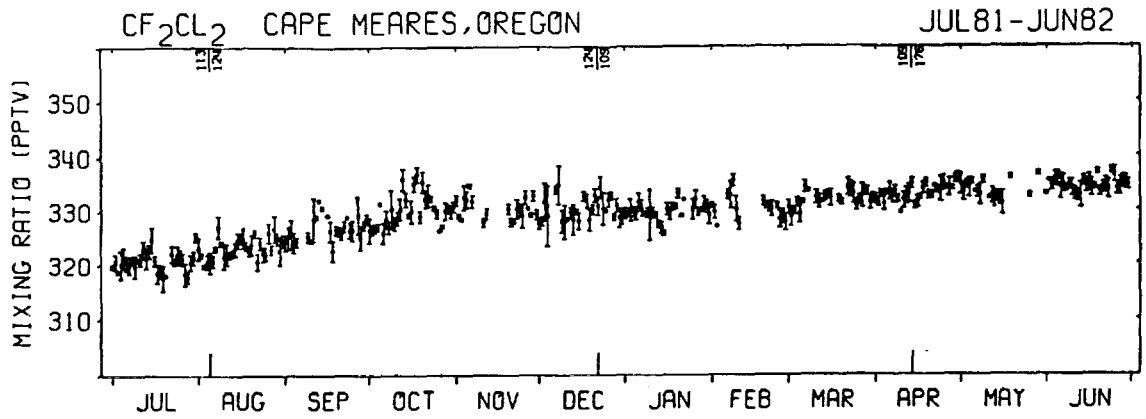

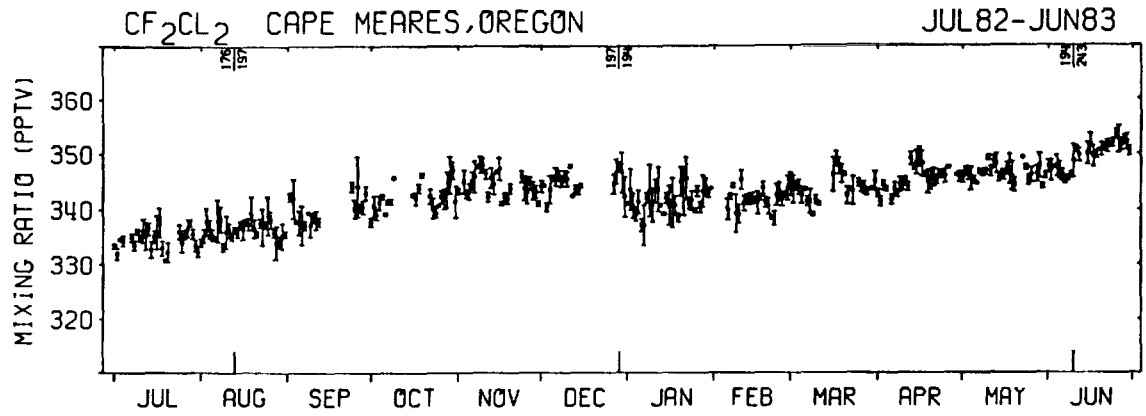

Fig. 3b. As for Figure 3a at Cape Meares, Oregon (45°N, 124°W).

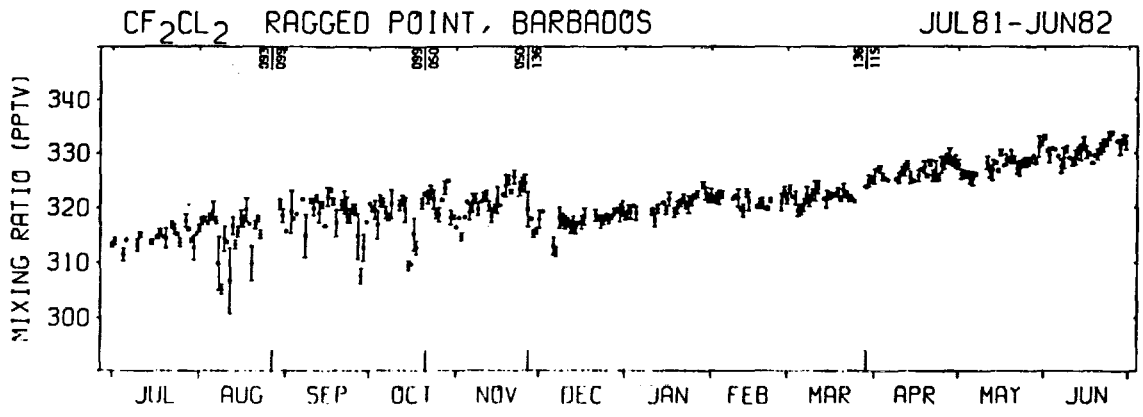

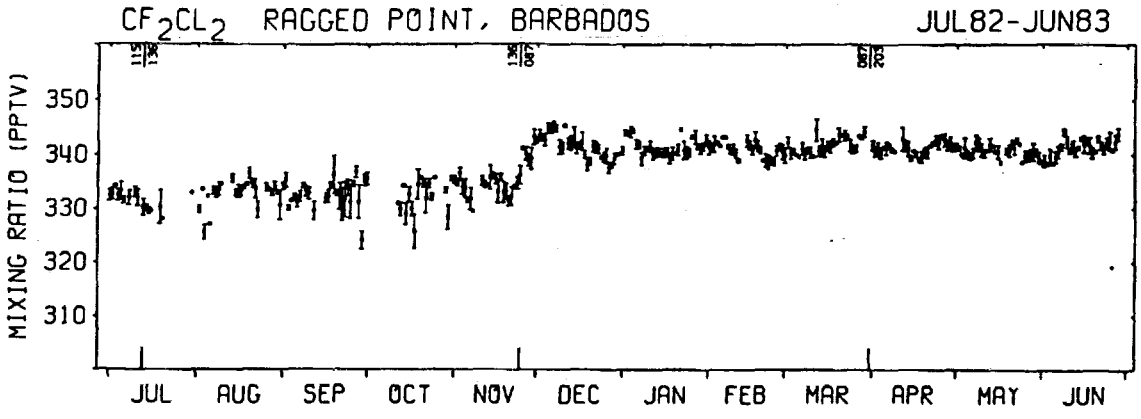

Fig. 3c. As for Figure 3a at Ragged Point, Barbados (13°N, 59°W).

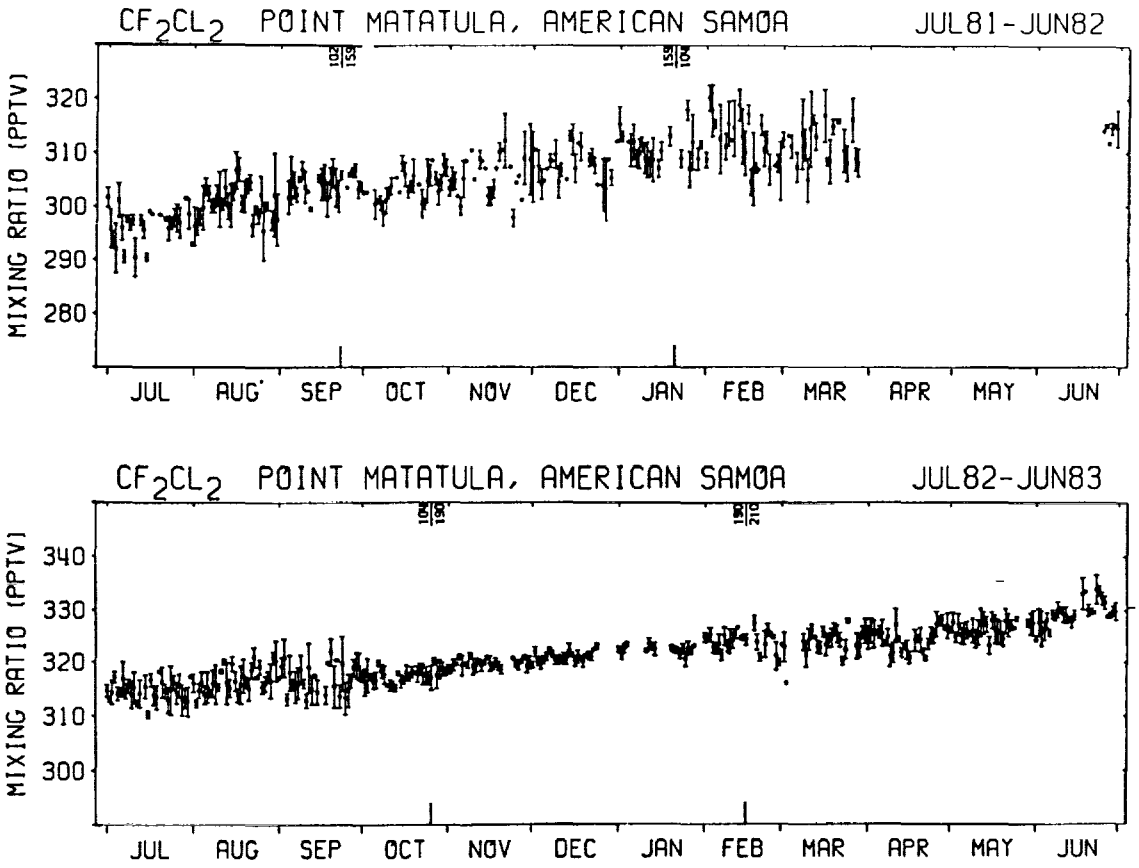

Fig. 3*d*. As for Figure 3*a* at Point Matatula, American Samoa (14°S, 171°W).

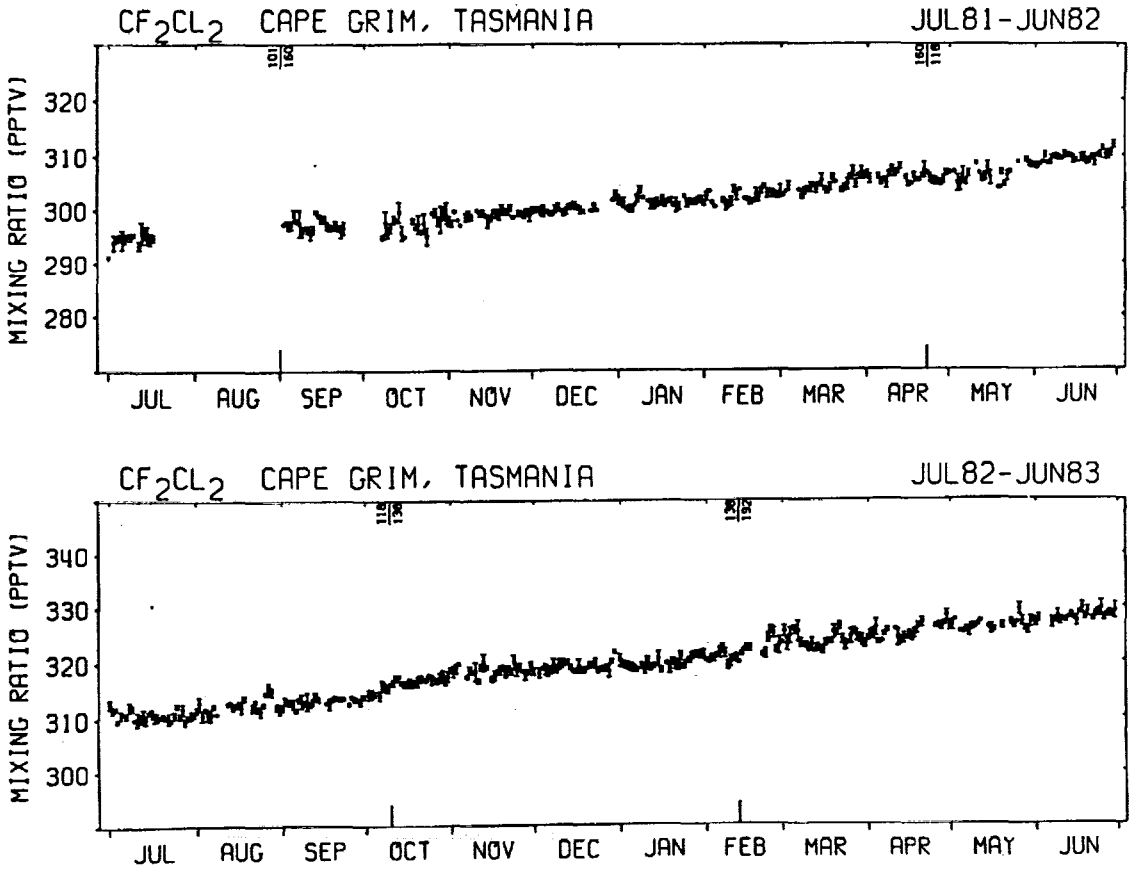

Fig. 3*e*. As for Figure 3*a* at Cape Grim, Tasmania (41°S, 145°E).

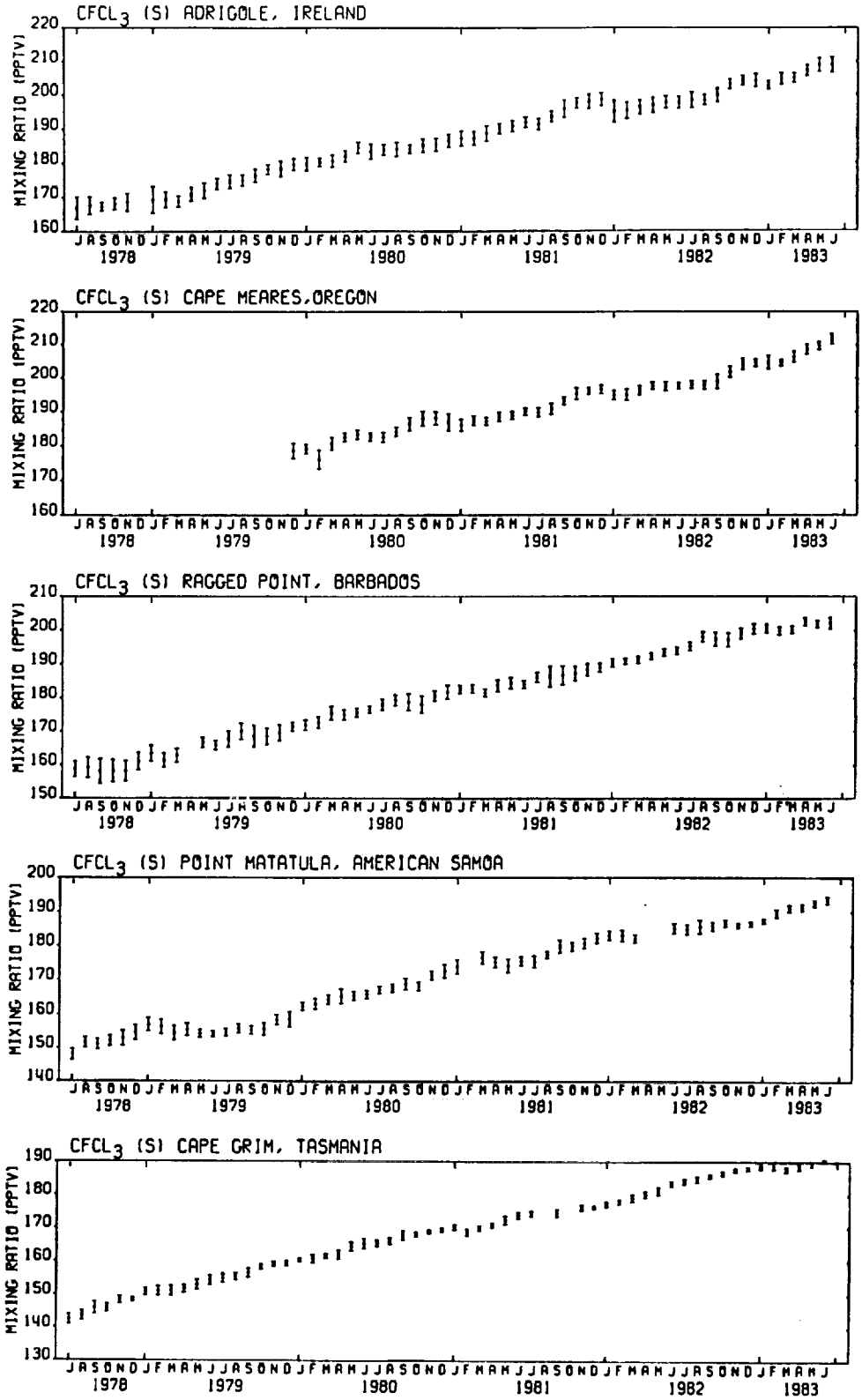

Fig. 4. Monthly means and standard deviations for 5 years of $CFCl_3$ (S) at the five ALE sites.

in the two-dimensional model. Therefore even this cycle in the model is removed, using a 12-month running mean filter, before the model is applied to the determination of lifetimes.

The lifetime estimates produced in this section of the paper are based on long-term trends in the time series. Yet the two-dimensional model does not, for example, simulate the effect of variations in atmospheric transport rates between one year and another. In order to produce unbiased estimates of the lifetimes of the fluorocarbons and expected uncertainty limits, the residual variability of each time series should be examined and modeled.

Figure 7 shows the average of eight smoothed, normalized

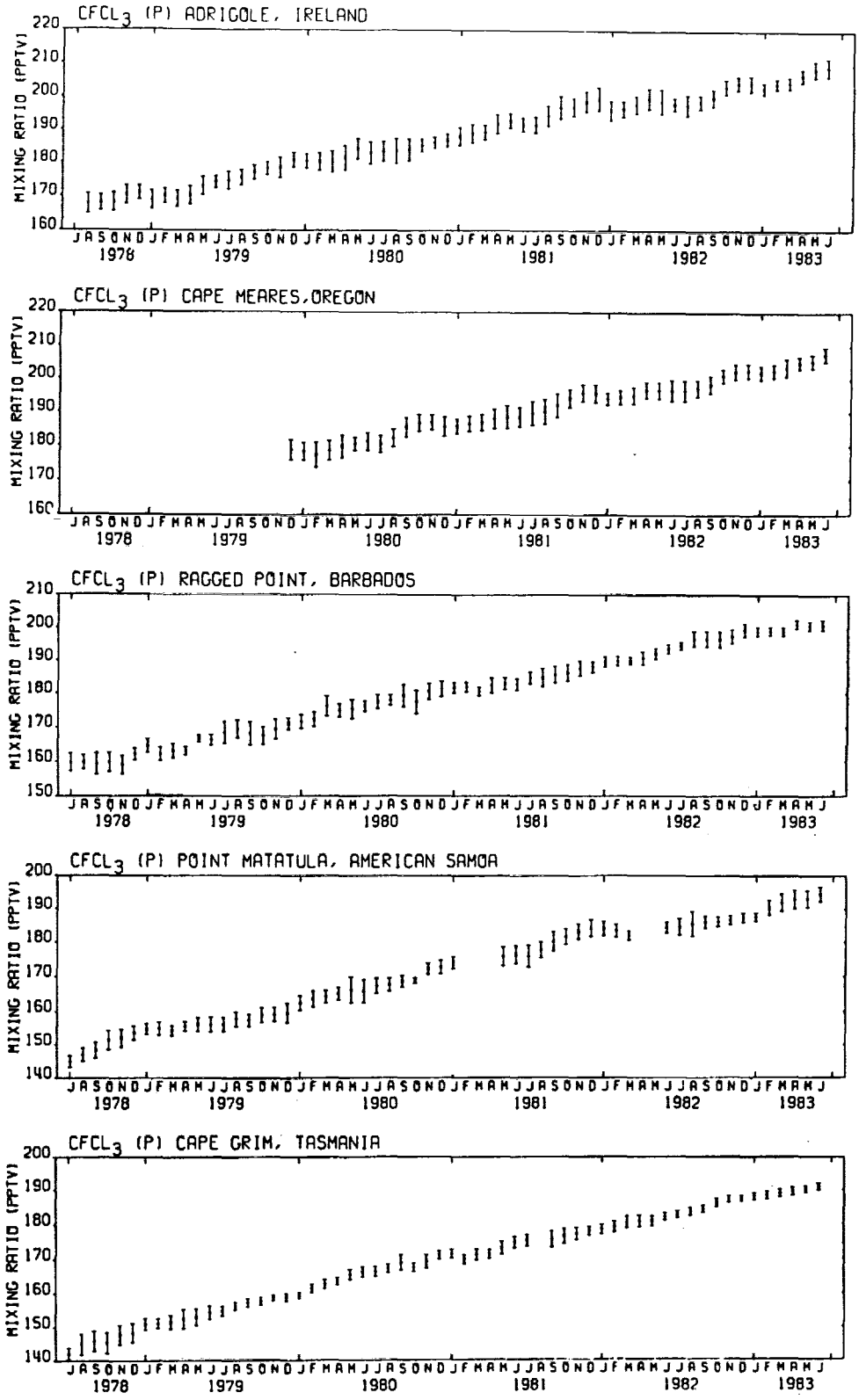

Fig. 5. Monthly means and standard deviations for 5 years of $CFCl_3$ (P) at the five ALE sites.

power spectra corresponding to the time series residuals for $CFCl_3$ after removal of the variation at each site, described by a single, best fit two-dimensional model calculation. The residual trends were not removed prior to calculation of the power spectra. This ensures that the power spectra contain all the unresolved variability, even though the contributions at individual low frequencies may be inadequately characterized by 5 years of data. Prior to calculation of the average, each individual spectrum was normalized such that

$$\int_{-\omega_0}^{\omega_0} P(\omega)\, d\omega = 1$$

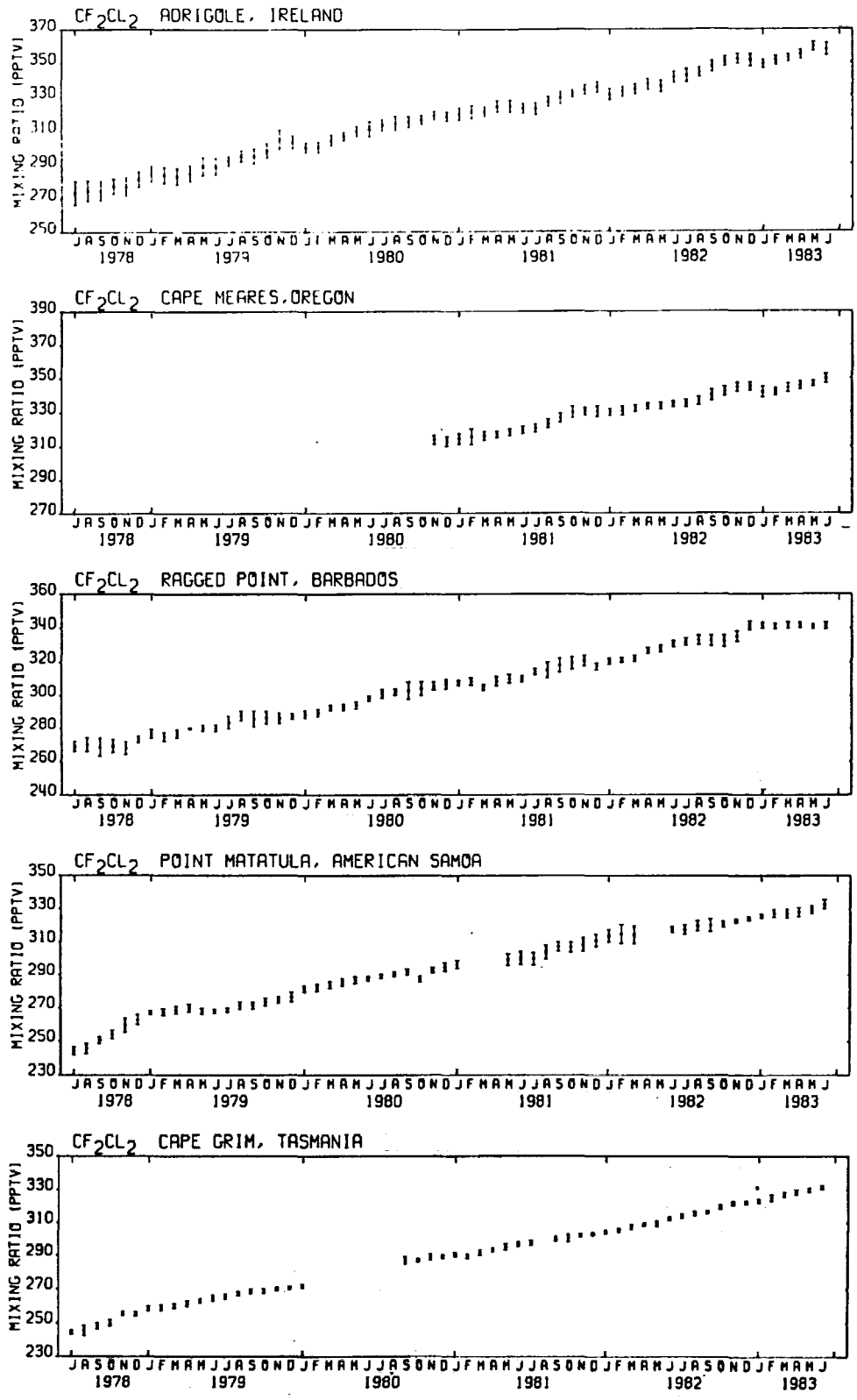

Fig. 6. Monthly means and standard deviations for 5 years of CF_2Cl_2 at the five ALE sites.

where $\omega_0 = 2\pi/2$ months. The average standard deviation of the residuals is 1.4 ppt for $CFCl_3$ (S), 1.2 ppt for $CFCl_3$ (P), and 2.7 ppt for CF_2Cl_2. The error bars at selected periods in Figure 7 indicate the range of variation covered by the eight individual spectra ($\pm 1\sigma$). The smoothing used gives predicted uncertainty limits on an individual spectrum of approximately $\pm 20\%$, corresponding to a smoothing bandwidth of 0.9 cycles per year [e.g., *Chatfield*, 1975]. Since the error bars are considerably wider than $\pm 20\%$ at periods shorter than 1 year, the individual spectra appear to be significantly different from

TABLE 1. Monthly Averaged $CFCl_3$ (Silicone Column) Mixing ratios χ, Their Standard Deviations σ_m, and the Number of Measurements During Each Month (N), Determined From Measurements at the Five ALE Sites Over the Period July 1981 Through June 1983

	Adrigole, Ireland			Cape Meares, Oregon			Ragged Point, Barbados			Point Matatula, American Samoa			Cape Grim, Tasmania		
Month	χ, pptv	σ_m, pptv	N	χ, pptv	σ_m, pptv	N	χ, pptv	σ_m, pptv	N	χ, pptv	σ_m, pptv	N	χ, pptv	σ_m, pptv	N
July 1981	191.4	1.6	125	189.9	1.3	116	186.2	1.4	76	175.4	1.7	71	174.3	0.8	54
Aug. 1981	193.6	1.5	118	190.9	1.6	111	186.4	3.0	95	177.5	1.1	103	...	...	...
Sept. 1981	195.9	2.6	97	193.2	1.1	89	186.8	2.8	95	179.9	1.8	75	174.5	1.1	80
Oct. 1981	197.6	1.5	59	195.5	1.7	112	187.4	2.1	123	179.9	1.2	92	...	...	...
Nov. 1981	198.0	2.1	85	196.2	1.0	81	188.4	1.7	110	180.9	1.4	64	176.2	0.9	77
Dec. 1981	198.6	1.9	87	196.7	1.2	104	189.0	1.2	108	182.3	1.4	87	176.3	0.5	76
Jan. 1982	195.1	3.2	85	195.0	1.3	103	190.5	1.2	104	183.2	1.3	65	177.2	0.8	89
Feb. 1982	195.4	2.4	100	195.1	1.6	62	190.9	0.9	68	183.1	1.6	64	178.0	0.7	86
March 1982	196.3	2.1	83	196.3	1.3	99	191.3	1.0	110	182.2	1.2	62	179.1	1.1	96
April 1982	196.9	2.3	69	197.7	1.1	112	192.5	1.0	119	...	...	...	180.2	1.0	89
May 1982	197.8	1.8	40	197.5	1.2	61	193.5	1.1	123	...	...	...	181.2	1.2	76
June 1982	197.7	1.8	87	197.7	1.0	110	194.0	1.1	118	185.2	1.4	19	183.4	0.7	107
July 1982	198.3	2.3	69	198.0	1.2	91	195.4	1.2	49	184.9	1.4	108	184.1	0.8	106
Aug. 1982	198.4	1.5	114	198.0	1.2	120	198.1	1.4	83	185.7	1.9	113	184.8	0.9	86
Sept. 1982	199.9	2.0	110	199.0	2.1	68	197.5	2.0	115	185.9	1.2	105	185.7	0.6	93
Oct. 1982	203.3	1.5	97	201.9	1.6	75	197.3	2.0	71	186.7	1.0	118	186.5	0.6	117
Nov. 1982	204.4	1.4	111	204.2	1.6	89	199.1	1.5	120	186.1	0.7	95	187.6	0.6	102
Dec. 1982	204.4	2.0	125	204.6	1.2	61	200.4	1.4	151	186.5	0.7	86	188.0	0.5	114
Jan. 1983	202.9	1.2	82	204.8	2.0	114	200.5	1.2	130	187.4	0.7	60	188.4	0.6	111
Feb. 1983	204.9	1.7	65	204.6	1.0	81	199.9	1.2	122	189.6	1.2	90	188.9	1.2	86
March 1983	205.2	1.4	122	206.4	1.6	87	200.3	1.1	122	191.0	1.0	88	187.8	0.8	110
April 1983	207.4	1.6	92	208.6	1.4	102	202.6	1.1	133	191.3	1.0	100	188.5	0.9	87
May 1983	209.0	2.0	103	209.7	1.2	92	201.9	1.1	126	192.5	0.9	117	189.4	0.7	80
June 1983	209.0	2.2	91	211.7	1.5	119	202.2	1.6	132	193.4	1.1	104	190.3	0.4	93

one another on these time scales, corresponding, for example, to meteorological variability associated with the different sites (see, for example, *Prather*, [1985]). On the other hand, at periods longer than 1 year, where the range of variation is approximately $\pm 20\%$, the spectra may be similar (and of the same physical origin).

A comparison of the $CFCl_3$ residuals on the two different chromatographic columns at each site strongly suggests that a substantial portion of this long-term (> 1 year) variability is produced by the measurement system (that is, the combination of the HP5840As and the calibration procedures). It was therefore decided to model this measurement noise with a

TABLE 2. Monthly Averaged $CFCl_3$ (Porasil Column) Mixing ratios χ, Their Standard Deviations σ_m, and the Number of Measurements During Each Month (N), Determined From Measurements at the Five ALE Sites Over the Period July 1981 Through June 1983

	Adrigole, Ireland			Cape Meares, Oregon			Ragged Point, Barbados			Point Matatula, American Samoa			Cape Grim, Tasmania		
Month	χ, pptv	σ_m, pptv	N	χ, pptv	σ_m, pptv	N	χ, pptv	σ_m, pptv	N	χ, pptv	σ_m, pptv	N	χ, pptv	σ_m, pptv	N
July 1981	192.0	2.5	101	189.8	3.6	114	184.9	1.8	58	176.0	3.2	74	175.3	1.6	52
Aug. 1981	194.8	3.0	80	190.3	3.6	112	185.0	2.8	72	177.8	2.3	101	...	...	...
Sept. 1981	197.3	3.4	65	192.1	3.6	94	185.9	2.5	75	180.3	2.9	68	175.7	2.3	79
Oct. 1981	197.5	2.7	43	194.3	2.8	112	186.3	2.5	94	181.6	2.3	92	176.4	2.2	72
Nov. 1981	199.1	3.0	70	195.8	2.6	76	187.8	2.2	81	183.2	2.3	60	177.2	1.7	105
Dec. 1981	199.9	3.5	68	195.6	2.7	105	188.2	1.6	84	184.2	2.5	94	178.0	1.2	84
Jan. 1982	196.4	2.9	66	194.1	1.8	108	189.8	1.5	76	184.1	2.1	66	178.5	1.3	97
Feb. 1982	196.9	2.4	78	194.6	2.1	60	190.1	1.4	56	183.5	1.9	61	179.2	1.5	92
March 1982	198.3	2.6	71	195.2	2.5	98	190.2	1.2	81	182.0	1.3	65	180.6	1.6	79
April 1982	200.1	3.1	59	196.7	2.4	113	190.8	1.9	82	...	...	...	180.8	1.6	94
May 1982	199.2	3.6	34	196.6	2.5	61	192.2	1.6	95	...	...	...	180.9	1.4	68
June 1982	198.3	1.9	76	196.6	3.2	114	193.7	1.3	86	184.4	1.6	12	182.1	1.1	110
July 1982	198.1	3.1	60	196.6	3.1	92	194.6	1.2	46	184.6	2.5	104	182.7	1.0	110
Aug. 1982	199.0	2.0	92	197.3	2.5	117	196.8	2.3	69	185.6	3.7	100	183.6	1.1	89
Sept. 1982	200.3	2.5	87	198.4	2.6	65	196.7	2.3	85	186.0	1.8	104	184.2	1.0	97
Oct. 1982	203.5	2.2	79	201.0	2.0	71	196.6	2.3	53	186.2	1.4	117	186.0	1.2	107
Nov. 1982	204.6	2.0	88	202.3	2.3	64	197.6	2.1	94	186.7	1.3	101	187.2	1.0	97
Dec. 1982	204.6	2.3	100	202.7	2.1	67	199.5	1.9	104	187.4	1.3	94	187.4	0.9	112
Jan. 1983	203.1	1.7	71	202.1	2.1	117	199.1	1.3	101	187.6	1.2	62	188.0	1.1	111
Feb. 1983	204.5	1.5	53	202.7	2.0	87	199.2	1.2	90	190.5	2.2	92	188.4	1.2	79
March 1983	204.8	1.7	98	203.7	2.7	83	199.1	1.2	96	192.0	2.6	83	189.0	1.2	111
April 1983	207.0	1.9	72	205.2	1.8	91	201.2	1.2	90	193.0	2.8	99	189.5	1.2	87
May 1983	208.9	2.4	84	205.6	2.0	97	200.8	1.3	91	193.1	2.6	109	190.1	1.0	83
June 1983	209.4	2.7	78	207.6	2.1	98	201.0	1.5	90	194.5	2.2	99	190.8	1.0	86

TABLE 3. Monthly Averaged CF_2Cl_2 Mixing ratios χ, Their Standard Deviations σ_m, and the Number of Measurements During Each Month (N), Determined From Measurements at the Five ALE Sites Over the Period July 1981 Through June 1983

	Adrigole, Ireland			Cape Meares, Oregon			Ragged Point, Barbados			Point Matatula, American Samoa			Cape Grim, Tasmania		
Month	χ, pptv	σ_m, pptv	N	χ, pptv	σ_m, pptv	N	χ, pptv	σ_m, pptv	N	χ, pptv	σ_m, pptv	N	χ, pptv	σ_m, pptv	N
July 1981	322.7	3.6	101	320.7	2.4	107	314.6	1.7	58	296.8	3.7	66	294.8	1.4	55
Aug. 1981	326.8	2.8	86	323.4	2.5	105	315.4	4.7	72	300.8	4.1	102	...	...	...
Sept. 1981	329.2	3.5	68	326.7	2.7	84	318.3	4.2	75	304.2	3.0	64	297.3	1.4	78
Oct. 1981	331.4	2.1	43	330.0	3.2	101	319.6	3.6	94	303.7	3.1	87	297.6	2.1	76
Nov. 1981	334.0	2.8	70	330.0	2.2	67	320.8	3.1	81	305.3	4.3	52	299.2	1.0	91
Dec. 1981	335.3	3.2	68	330.4	3.0	100	317.6	2.0	84	308.0	3.8	84	300.2	1.0	82
Jan. 1982	331.0	3.4	66	330.0	2.0	100	320.5	1.7	76	310.6	3.7	64	301.4	1.0	97
Feb. 1982	332.5	2.8	78	330.7	2.6	54	321.4	1.3	56	311.8	5.6	57	302.4	1.1	89
March 1982	334.1	3.0	71	332.2	1.9	91	322.2	1.7	82	311.2	5.1	52	304.7	1.4	84
April 1982	337.0	3.3	59	333.4	1.7	99	326.9	1.6	84	...	...	...	306.0	1.0	92
May 1982	335.6	3.5	34	333.5	1.9	58	328.0	1.9	95	...	...	...	306.4	1.6	63
June 1982	341.3	3.4	77	334.6	1.7	113	330.8	1.8	86	314.5	1.8	11	309.5	1.0	109
July 1982	342.2	3.9	58	335.0	2.2	97	331.8	2.0	46	314.5	2.7	91	311.0	1.1	109
Aug. 1982	344.4	2.8	92	336.6	2.4	116	332.9	2.7	69	316.7	3.0	99	312.6	1.4	88
Sept. 1982	347.7	3.2	87	340.0	3.2	53	332.6	3.0	87	317.0	3.8	92	313.4	0.9	94
Oct. 1982	350.7	2.8	79	342.2	2.8	68	332.4	3.3	53	317.7	1.8	113	316.5	1.2	107
Nov. 1982	352.3	2.8	88	344.6	2.5	87	335.2	3.0	94	319.7	1.1	101	318.8	1.1	97
Dec. 1982	351.3	3.6	101	345.0	2.4	62	341.5	2.4	104	321.0	1.2	94	319.2	1.0	112
Jan. 1983	349.2	2.4	71	341.8	3.2	105	341.5	1.7	101	322.4	1.1	62	320.1	1.1	107
Feb. 1983	351.4	2.7	53	342.1	2.2	84	341.1	1.6	89	324.0	2.2	87	322.0	1.8	81
March 1983	352.7	2.2	98	344.4	2.6	83	341.6	1.7	96	324.0	2.6	74	324.0	1.4	111
April 1983	354.9	2.7	74	345.7	2.4	98	341.6	1.4	90	324.8	2.7	98	325.2	1.4	87
May 1983	359.7	2.7	87	346.7	1.7	90	341.0	1.3	91	326.3	2.3	104	326.4	1.1	80
June 1983	358.0	3.6	78	349.8	2.7	102	341.3	1.8	90	329.5	2.7	89	328.0	1.0	87

first-order autoregressive (AR) model. Figure 7 indicates that such a model provides an excellent fit to the average power spectrum if the autocorrelation of the AR model is 0.5 at a time lag of 1 month.

The complete model describing the fluorocarbon time series then consists of three parts: the two-dimensional model, the autoregressive model, which essentially accounts for the variation of the measured trends about the two-dimensional model predictions, and a site-(and species-) dependent model describing meteorological variations and measurement errors, particularly on time scales shorter than approximately 1 year. These last models are needed to account for the uncertainties associated with determining the long-term trend in the individual time series.

Because of a nonlinear dependence of the two-dimensional model on the lifetime τ, the estimation procedure seeks to minimize the squares of the deviations,

$$\ln [x(t)] - \ln [\hat{x}(t)] = a + \left[\frac{1}{\tau} - \frac{1}{\tau_0}\right]\left\{ - \frac{\partial(\ln \hat{x})}{\partial(1/\tau)} - \frac{d}{dt}\left[\frac{\partial(\ln \hat{x})}{\partial(1/\tau)}\right](t - t_0)\right\} \quad (3)$$

in a weighted least squares sense. Here $x(t)$ and $\hat{x}(t)$ are the observed and calculated mixing ratios of an individual fluorocarbon at a particular site, $1/\tau_0$ is the inverse of the lifetime ("inverse lifetime") assumed in the two-dimensional model computation, and a and $1/\tau$ are the absolute calibration factor

TABLE 4. Empirical Model Fit (Equation (1) With t_m = 30.5 Months) to the 5 Years of $CFCl_3$ and CF_2Cl_2 Data

Site	a_i	b_i	d_i	e_i	c_i	s_i	Variance of Residuals $\sigma_0'^2$
			$CFCl_3(S)$				
Adrigole, Ireland	187.5 ± 0.4	8.3 ± 0.5	−0.1 ± 0.2	0.1 ± 0.1	−0.2 ± 0.4	0.5 ± 0.4	4.3
Ragged Point, Barbados	181.2 ± 0.3	9.1 ± 0.3	−0.2 ± 0.1	0.1 ± 0.1	0.1 ± 0.2	0.2 ± 0.2	1.4
Point Matatula, American Samoa	171.4 ± 0.5	10.7 ± 0.6	0.0 ± 0.2	−0.4 ± 0.1	−0.3 ± 0.5	−1.0 ± 0.5	5.7
Cape Grim, Tasmania	169.3 ± 0.3	8.9 ± 0.3	−0.3 ± 0.1	0.2 ± 0.1	−0.2 ± 0.2	0.6 ± 0.2	1.4
			$CFCl_3(P)$				
Adrigole, Ireland	188.4 ± 0.6	8.6 ± 0.5	−0.3 ± 0.2	0.0 ± 0.2	−0.3 ± 0.5	0.3 ± 0.5	4.4
Ragged Point, Barbados	180.5 ± 0.3	8.7 ± 0.4	0.0 ± 0.3	0.0 ± 0.1	0.0 ± 0.3	0.3 ± 0.3	2.0
Point Matatula, American Samoa	172.2 ± 0.4	9.9 ± 0.5	−0.4 ± 0.2	−0.1 ± 0.1	−0.3 ± 0.4	−0.7 ± 0.4	3.9
Cape Grim, Tasmania	170.0 ± 0.2	8.8 ± 0.2	−0.5 ± 0.1	0.2 ± 0.1	−0.1 ± 0.2	0.1 ± 0.2	0.8
			CF_2Cl_2				
Adrigole, Ireland	318.3 ± 0.4	15.0 ± 0.5	−0.5 ± 0.2	0.6 ± 0.1	−0.7 ± 0.4	1.5 ± 0.4	3.2
Ragged Point, Barbados	305.7 ± 0.5	15.9 ± 0.6	0.0 ± 0.2	0.0 ± 0.2	0.0 ± 0.5	0.9 ± 0.5	6.0
Point Matatula, American Samoa	292.8 ± 0.6	14.9 ± 0.7	−0.9 ± 0.2	0.3 ± 0.2	−0.8 ± 0.5	−1.7 ± 0.6	6.9
Cape Grim, Tasmania	286.2 ± 0.4	14.8 ± 0.4	0.0 ± 0.1	0.4 ± 0.1	−0.1 ± 0.3	0.1 ± 0.3	2.7

Values are in units of parts per trillion per volume.

TABLE 5. Comparison of the Empirical Model Coefficients at Adrigole and Cape Meares for the Period December 1979 to June 1983 for $CFCl_3$ and for the Period November 1980 to June 1983 for CF_2Cl_2

Site	a_i	b_i	d_i	c_i	s_i	Variance of Residuals, $\sigma_0'^2$
			$CFCl_3(S)$			
Adrigole, Ireland	193.2 ± 0.7	8.1 ± 0.7	0.2 ± 0.4	−0.3 ± 0.7	0.4 ± 0.7	4.3
Cape Meares, Oregon	192.2 ± 0.6	8.4 ± 0.5	0.9 ± 0.5	−0.5 ± 0.6	0.5 ± 0.6	3.6
			$CFCl_3(P)$			
Adrigole, Ireland	194.2 ± 0.8	8.1 ± 0.9	−0.2 ± 0.4	−0.3 ± 0.8	−0.1 ± 0.8	4.4
Cape Meares, Oregon	191.6 ± 0.4	8.2 ± 0.3	0.2 ± 0.3	−0.7 ± 0.4	0.5 ± 0.4	1.5
			CF_2Cl_2			
Adrigole, Ireland	335.5 ± 0.8	16.6 ± 0.8	2.1 ± 0.7	−1.0 ± 0.6	1.4 ± 0.6	3.2
Cape Meares, Oregon	331.7 ± 0.3	14.3 ± 0.5	−0.8 ± 0.5	−1.2 ± 0.4	1.1 ± 0.4	1.3

Values are in units of parts per trillion per volume; t_m = 39.5 months for $CFCl_3$; t_m = 44.5 months for CF_2Cl_2.

and the inverse lifetime which are being estimated. The partial derivatives are calculated in the two-dimensional model. Each month's squared deviation from (3) is inversely weighted by σ^2 (from equation (2)) plus σ_a^2, which describes the low-frequency energy in the power spectrum of the autoregressive model. After an estimate of $1/\tau$ has been obtained from the entire 60-month data set, the estimation is repeated with revised values of $x(t)$, obtained from a new two-dimensional model calculation which used the latest estimate of $1/\tau$.

In addition to an all-station lifetime estimate, estimates for individual time series were also calculated. In these calculations the two-dimensional model results were fixed, based on that lifetime which provides the best fit to all the time series. The individual site lifetime estimates are thus determined using the partial derivatives. The resulting lifetime estimates are given in Table 6. They may be approximately linearly combined to produce the all-site lifetime estimate.

The 5-year data shows clear evidence of slightly higher fluorocarbon concentrations at Adrigole than at Cape Meares. This difference can produce spurious trends in the combined data for mid-latitudes of the northern hemisphere because of the incomplete record at Cape Meares. This difference was ignored by *Cunnold et al.* [1983*a*, *b*] because it was not judged to be statistically significant based on 19 (or fewer) months of data. The averages of the differences (which are persistent) over the months during which observations were made at both sites are 0.3 ppt (0.2%) for $CFCl_3(S)$, 2.1 ppt (1.2%) for $CFCl_3(P)$ and 5.5 ppt (1.6%) for CF_2Cl_2 (these numbers may be derived from Table 5 if allowance is made for the effect of d_i on the mean). The combined Adrigole/Cape Meares record is obtained by averaging the monthly data after reducing the Adrigole data and increasing the Cape Meares data by one-half of these differences. This procedural change is the principal reason for the differences between the "3-year" lifetime estimates shown in Tables 6 and 7 and those given by *Cunnold et al.* [1983*a*, *b*].

The lifetime estimates vary from site to site but do not exhibit a systematic latitudinal tendency. In order to place a lower bound on how much of this variation is of instrumental origin, the differences between the CFC's inverse lifetime estimates on the silicone and Porasil channels were examined. A standard deviation of 0.003 $year^{-1}$ is calculated, which may be compared against a standard deviation in the eight inverse lifetime estimates for the four sites and two columns, also of 0.003 $year^{-1}$. Thus most of the long-term differences between the $CFCl_3$ measurements and the two-dimensional model results is probably of instrumental origin.

It is useful to examine the convergence of the individual site lifetime estimates using 3 and 5 years of data. The average power spectrum of the residuals (Figure 7) suggests that the spectrum is flattening out at periods longer than approximately 2 years and that it may therefore be possible to extrapolate the effect of measurement errors on uncertainties in the

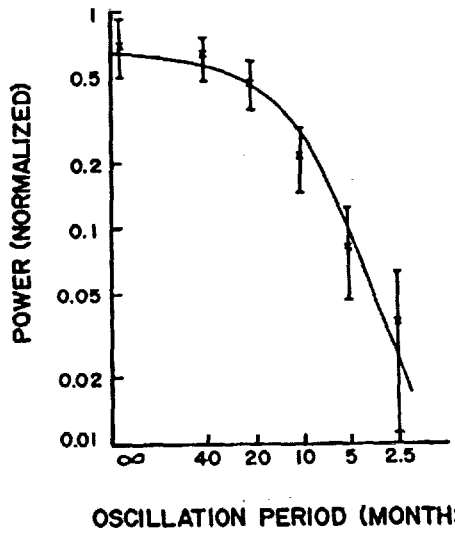

Fig. 7. The smoothed power spectrum of $CFCl_3$ residuals with respect to the two-dimensional model. The vertical lines indicate ±1 standard deviation produced by the eight spectra. The power spectra have been normalized to give an integral with respect to frequency (radians/month) of 0.5. The full line is a first-order autoregressive model fit to the spectrum with a correlation of 0.5 after 1 month.

TABLE 6. Lifetime Estimates for $CFCl_3$ and CF_2Cl_2 Derived From Trends in 5 Years of ALE Data at Each Site

	Reciprocal Lifetime, years^{-1} $\pm 1\sigma$	Lifetime, years $\pm 1\sigma$	Approximate Weight Given to Site in Optimal Estimate of Lifetime
	$CFCl_3$, Silicone Column		
Adrigole, Ireland/ Cape Meares, Oregon	0.017 ± 0.004	59^{+11}_{-10}	0.24
Ragged Point, Barbados	0.009 ± 0.003	111^{+28}_{-36}	0.29
Point Matatula, American Samoa	0.016 ± 0.004	62^{+12}_{-11}	0.17
Cape Grim, Tasmania	0.011 ± 0.003	90^{+19}_{-15}	0.30
	$CFCl_3$, Porasil Column		
Adrigole, Ireland/ Cape Meares, Oregon	0.017 ± 0.003	59^{+9}_{-12}	0.22
Ragged Point, Barbados	0.014 ± 0.003	72^{+13}_{-10}	0.27
Point Matatula, American Samoa	0.012 ± 0.003	83^{+16}_{-28}	0.17
Cape Grim, Tasmania	0.012 ± 0.002	83^{+12}_{-17}	0.34
	CF_2Cl_2		
Adrigole, Ireland/ Cape Meares, Oregon	0.008 ± 0.005	125^{+48}_{-208}	0.24
Ragged Point, Barbados	0.015 ± 0.005	67^{+17}_{-33}	0.25
Point Matatula, American Samoa	0.009 ± 0.005	111^{+40}_{-139}	0.23
Cape Grim, Tasmania	0.004 ± 0.005	$250^{+139}_{-\infty}$	0.28

Error bars for the first 3 years given by *Cunnold et al.* [1983*a*, *b*] do not include allowance for the average bias of individual time series, inferred from the variance of the lifetime estimates.

lifetime estimates for periods longer than 5 years, using a white-noise assumption. Since, however, this spectrum has been smoothed over a bandwith of approximately 0.9 cycles per year, this conclusion has been tested using the individual site results. The variance of the $CFCl_3$ inverse lifetime estimates after 3 years of data is 36×10^{-6} year^{-2} and after 5 years of data it is 7×10^{-6} year^{-2} (cf. Table 6). If the noise is white, the ratio of these variances should be $5^3/3^3 = 4.6$. Thus these results also suggest that the measurement errors may be described by a white-noise spectrum at periods beyond approximately 3 years.

In Table 6 the values indicated as the approximate weights given to individual stations do not vary much, although less than average weight is given to Point Matatula and more than average weight to Cape Grim. The combined lifetime estimates, which are given in Table 7, should therefore be compared principally against the average lifetime estimates given by *Cunnold et al.* [1983*a*]. Table 7 shows that the 5-year data set indicates a lifetime for $CFCl_3$ in 1980, based on its temporal trend, of 75 years. On the basis of our two-dimensional model calculations this corresponds to a steady state lifetime of 63 years; this result (as well as the 3-year result) is in excellent agreement with the $CFCl_3$ lifetime resulting from stratospheric photodissociation calculated by *Owens et al.* [1982], *Ko and Sze* [1982], and *Fraser et al.* [1983].

There is a substantial change in the lifetime estimate for CF_2Cl_2, from an indeterminately long lifetime estimated from the first 3 years of data to a lifetime shorter than that expected to be produced by stratospheric photodissociation. Note, however, that the error bars are substantial. Moreover, in the work by *Cunnold et al.* [1983*b*] we commented on inconsistencies between the estimated emissions for CF_2Cl_2 and the year-to-year variations found in the CF_2Cl_2 measurements. Since CF_2Cl_2 should be even more stable than $CFCl_3$, it is most likely, based on the long lifetimes exhibited by the ALE results, that the only sink of CF_2Cl_2 in the atmosphere is photodissociation in the stratosphere and that the variability in the CF_2Cl_2 lifetime estimates over the ALE measurement period is caused by differences between the estimated and the actual emissions of CF_2Cl_2 into the atmosphere. These differences are probably related to the almost unknown emissions of CF_2Cl_2 in the USSR and Eastern Europe; it should be noted, moreover, that the relative proportion of world production in that region is believed to be substantially higher for CF_2Cl_2 than for $CFCl_3$ [*CMA*, 1983]. The lifetime uncertainties given in Table 7 reflect the differences between the ALE observations and the two-dimensional model results. They thus allow for year-to-year differences between estimated and actual emissions. They do not, however, account for biases in the trends of atmospheric release of fluorocarbons which might be produced by gross uncertainty in the emissions in the USSR and Eastern Europe.

At the current time there is significant uncertainty about the absorption cross section of molecular oxygen. This affects the penetration of solar ultraviolet radiation into the middle and lower stratosphere and hence the calculated photodissociation rates and lifetimes of the fluorocarbons. *Ko and Sze* [1982] have calculated that the *Herman and Mentall* [1982] cross sections produce a change in the steady state lifetime of $CFCl_3$

TABLE 7. Combined Lifetime Estimates by the Trend Technique

	1976–1981		1978–1983	
Species	$1/\tau$	τ, years	$1/\tau$	τ, years
$CFCl_3$ (S)	0.012 ± 0.004	83^{+42}_{-21}	0.013 ± 0.002	77^{+14}_{-10}
$CFCl_3$ (P)	0.010 ± 0.003	100^{+43}_{-23}	0.014 ± 0.001	71^{+6}_{-4}
CF_2Cl_2	-0.003 ± 0.004	$\frac{1000}{\infty}$	0.009 ± 0.002	111^{+32}_{-20}

Error bars include measurement errors but not uncertainties in release.

TABLE 8. Emission Estimates for $CFCl_3$

12-Month Period (July 1 to June 30)	*CMA* [1983] Estimate (World Total)	ALE Estimate	
		$CFCl_3$ (S)	$CFCl_3$ (P)
1978–1979	285	255 ± 31	291 ± 28
1979–1980	270	266 ± 22	264 ± 22
1980–1981	265	271 ± 17	271 ± 26
1981–1982	262	258 ± 18	248 ± 16
1982–1983	266	265 ± 35	259 ± 23

Estimates are given in million kilograms per year.

in a one-dimensional model from 73 to 56 years and of CF_2Cl_2 from 133 to 115 years. Another study, by *Jackman and Guthrie* [1985], indicates that the 1980 lifetime of $CFCl_3$ would change from 67 to 47 years and, for CF_2Cl_2, from 154 to 118 years. These changes correspond to approximately 1σ in our CF_2Cl_2 results and to approximately 2σ in the $CFCl_3$ results. The $CFCl_3$ results favor the original oxygen cross sections, while the $CFCl_2$ results (less strongly) favor the *Herman and Mentall* [1982] results. Considering this ambivalence in our results and the variation in lifetime calculations by different investigators and between models of different dimensions, we conclude that the trend lifetime estimates are currently consistent with both sets of molecular oxygen cross sections.

4. Atmospheric Inventory of Fluorocarbons

The total atmospheric content of $CFCl_3$ and CF_2Cl_2 may be estimated by combining the measured concentrations in the lower troposphere with model results to fill in the concentrations in the rest of the atmosphere. Using the measured mixing ratio of $CFCl_3$ on January 1, 1981, of 177.5 ppt and a model-determined factor of 0.915 [*Cunnold et al.*, 1983*a*] gives a globally averaged mixing ratio of 162.4 parts per trillion by volume (pptv). Assuming an atmospheric mass of 5.137×10^{18} kg [*Trenberth*, 1981], the global inventory of $CFCl_3$ on January 1, 1981, is estimated to have been 3,960 million kg. The uncertainty in this estimate due to modeling uncertainties is 110 million kg (for additional details on the procedure for obtaining these estimates, see *Cunnold et al.*, 1983*a*).

A two-dimensional model computation based on a lifetime of 75 years on January 1, 1981 (that is, the trend estimate of the lifetime) gives a mixing ratio of 178.5 ppt in the lower troposphere at that time. The observed mixing ratio, which is 0.6% smaller, using a model-calculated partial derivative of $\partial(\ln x)/\partial(1/\tau) = -4.4$, implies an inventory estimate of the lifetime of 68 years. This is similar to the inventory estimate of lifetime of 70 years for January 1, 1980, obtained from the first 3 years of ALE data [*Cunnold et al.*, 1983*a*].

The measured mixing ratio of CF_2Cl_2 on January 1, 1981, was 300.4 ppt. For a lifetime of 111 years the model gives a factor of 0.93 for determining the globally averaged mixing ratio (this is a smaller factor than is given by *Cunnold et al.* [1983*b*], which was based on a much larger estimate of the trend lifetime, giving more CF_2Cl_2 in the stratosphere). This gives a global inventory of CF_2Cl_2 on January 1, 1981, of 6,000 million kg. The uncertainty in this estimate due to modeling uncertainties is approximately 130 million kg (1σ). The inventory estimate of the lifetime, based on the worldwide emissions given by *CMA* [1983], is 68 years on January 1, 1981. This is similar to the estimate of 69 years for January 1, 1980, obtained from the 3-year data set [*Cunnold et al.*, 1983*b*].

5. $CFCl_3$ and CF_2Cl_2 Annual Emission Estimates

The ALE data, together with the two-dimensional model, may be used to produce a yearly atmospheric budget of fluorocarbons. If the sink is known, the yearly input into the atmosphere (and annually averaged transport rates to be discussed in a separate paper) may be estimated. Since the lifetime estimates for $CFCl_3$ indicate photodissociation is the only loss process and since CF_2Cl_2 should be even more stable than $CFCl_3$, we shall base our emission estimates on the assumption that photodissociation is the only loss process for both species. The steady state lifetimes assumed in the following calculations are 63 years for $CFCl_3$, corresponding to a current lifetime of 74 years, and 140 years (170 years currently) for CF_2Cl_2, based on *Owens et al.* [1982], *Ko and Sze* [1982], *Golombeck and Prinn* [1986], and *Jackman and Guthrie* [1985]. Small errors in the calculated lifetimes will affect the average emission level (I) over the five-year period, according to the approximate formulae

$$\Delta I(CFCl_3) = 3700\ \Delta(1/\tau) \text{ million kg/yr}$$
$$\Delta I(CF_2Cl_2) = 5900\ \Delta 1/\tau \text{ million kg/yr} \quad (4)$$

The impact of such errors on the year-to-year variations in emission rates is negligible (roughly, 5% of the sensitivity described by equation (4)).

On a time scale of 1 year or less, atmospheric variability produces significant variations in the measured fluorocarbon concentrations. In order to reduce the impact of this variability on the emission estimates, we have utilized the empirical model results, which constitute a smoothed representation of the 5-year data record but which have a sufficient number of degrees of freedom to resolve trends on a time scale of approximately 1 year. The emission estimation procedure is then to use the empirical model results to estimate the fluorocarbon concentrations in each of the four semi-hemispheres between 1000 and 500 mbar and to use the two-dimensional model calculations to estimate the proportion of the atmospheric fluorocarbon content which is between 500 and 200 mbar and that which is in the stratosphere. To utilize the full 5-year ALE data record, 12-month periods are used, starting on July 1 each year.

Table 8 shows the emission estimates. For comparison, Table 8 also shows the emissions obtained by taking 2-year averages of the annual CMA estimates [*CMA*, 1983] (this is an approximate adjustment for the 6-month time difference between the two emission estimates). Error bars on the emission estimates are based upon the residuals with respect to the single "best fit" two-dimensional model computation. Trends in the time series residuals have been estimated for each site for each 12-month period. The variance of the trends from the "four" sites in any 12-month period is used to provide error bars on the emission estimate for that period, on the basis that the emission estimate is approximately determined by the average of the four trends for the year. The assumption here is that the two-dimensional model is able to simulate, and hence account for, the expected dependence of the annual trends on latitude.

The results in Table 8 show excellent agreement between the $CFCl_3$ emissions estimated by *CMA* [1983] and the emissions inferred from the ALE measurements. This agreement extends to the average emission level for $CFCl_3$ over the 5-year period; this is consistent with the overburden lifetime estimate for $CFCl_3$ being similar to the trend estimate of life-

TABLE 9. Emission Estimates for CF_2Cl_2

12-Month Period (July 1 to June 30)	CMA Estimate (Reporting Company Only)	ALE Estimate (World Total)	ALE − CMA = (Estimated Release From Nonreporting Companies)	Previous Column Adjusted for Inventory Discrepancy
1978–1979	339	457 ± 67	118 ± 67	138
1979–1980	335	366 ± 51	31 ± 51	48
1980–1981	337	377 ± 29	40 ± 29	58
1981–1982	339	351 ± 33	12 ± 33	29
1982–1983	341	406 ± 31	65 ± 31	84

Estimates are given in million kilograms per year.

time. The agreement does not, however, hold for CF_2Cl_2. Since the largest uncertainty in the CF_2Cl_2 emissions probably arises from the emissions in the USSR and Eastern Europe, Table 9 shows the differences between the ALE emission estimates and the emission estimates for the rest of the world [*CMA*, 1984]. Column 4 in Table 9 might therefore be interpreted as an estimate of the emissions of CF_2Cl_2 in the USSR and Eastern Europe.

Assuming that the only sink for CF_2Cl_2 is photodissociation in the stratosphere, with a steady state lifetime of 140 years, the differences between the releases for reporting companies estimated by *CMA* [1984] and the estimates made from the ALE data exhibit several significant features. First, it should be noted that our estimate of the atmospheric inventory of fluorocarbons on January 1, 1981, from the ALE data is 6,000 million kg. This may be compared to the inventory from the model calculation based on *CMA* [1983] estimates of release of 6,340 million kg. Excluding the unreported emissions [*CMA*, 1984], primarily in Eastern Europe and the USSR, gives a model-calculated inventory of 5,930 million kg. Thus the ALE-estimated inventory is only 70 million kg greater than the inventory estimated from the release figures for reporting companies only. If the releases in Eastern Europe and the USSR had continued at the 1975 level reported by *Borisenkov and Kasekov* [1977], the model-estimated inventory would be 6,270 million kg. The difference between the estimate based on *CMA* [1983] and the ALE inventory estimate of 6,000 million kg corresponds to the additional destruction which would result from a lifetime of 68 years (the inventory lifetime estimate) relative to an assumed lifetime of 170 years currently.

The releases indicated in column 4 of Table 9 suggest that the CF_2Cl_2 releases by nonreporting companies between 1979 and 1982 were roughly similar to those projected by *CMA* [1983]. Assuming that this release scenario also provides a reasonable way to project the releases backward in time, there then exists an inventory discrepancy of approximately 300 million kg (5%) between the ALE measurements and the predicted releases.

An absolute calibration error in the ALE experiment could account for part of this discrepancy. For example, the mixing ratios reported by *Bullister and Weiss* [1983] were approximately 1.5% higher in the vicinity of Adrigole than those reported here. This could account for approximately 100 million kg. The extrapolation of lower atmosphere measurements to a globally averaged mixing ratio might also contribute approximately 100 million kg to this discrepancy, primarily because of uncertainty about the stratospheric content. However, the inventory agreement found for $CFCl_3$ suggests that the modeling uncertainty is not this large. The release uncertainty having the largest impact on the overburden (cf. Table 9 of *Cunnold et al.* [1983*b*]) is the effective release time for nonhermetically sealed uses of CF_2Cl_2. A prolongation of the release time from 4 to 5 years would reduce the atmospheric release of CF_2Cl_2 by approximately 120 million kg. (A change in the release time for this use would have little impact on the $CFCl_3$ budget, since this does not represent a substantial use of $CFCl_3$.) A combination of such a change in the release rate for CF_2Cl_2 and an absolute calibration error would seem to be required to explain the CF_2Cl_2 observations.

An absolute calibration error would increase the ALE emission estimates in Table 9 and a nonhermetically sealed release delay error would decrease the release estimates determined from production by reporting companies. Internal consistency between the release estimates for nonreporting companies and the measured atmospheric inventory may be obtained by using the estimates in column 5 of Table 9. These estimates were obtained by increasing the ALE emission estimates by 2.5% and decreasing the CMA estimates by 2.5%. Although we consider the release estimates in column 5 to be our best guesses, based on an atmospheric lifetime of CF_2Cl_2 (currently) of 170 years, it should be recognized that not only do these release estimates contain year-by-year random uncertainties associated with the imprecision in the measurement system (as indicated by the error bars given in Tables 8 and 9), but the estimates may be biased because of uncertainty about how to adjust for the inventory discrepancy. These biases consist of absolute calibration uncertainties (2%) and model-associated uncertainties. As described by *Cunnold et al.* [1983*a*, *b*], the latter uncertainties are estimated to be 1% (1σ) for the troposphere and 2% (1σ) for the stratosphere, corresponding to a 10% uncertainty in the content there. Thus possible biases in all our release estimates are expected to be in the range ±5%.

If the current lifetime of CF_2Cl_2 is 118 years [*Jackman and Guthrie*, 1985], using equation (4), our emission estimates for the nonreporting companies would increase by 15 million kg. However, such a lifetime would result in a reduction of the inventory discrepancy by approximately 100 million kg and give a corresponding reduction in the adjusted emissions by approximately 6 million kg. Thus using the *Hermand and Mentall* [1982] cross sections for molecular oxygen leads to an increase in the emission estimates of column 5 (Table 9) of approximately 9 million kg. This would also lead to an increase in the $CFCl_3$ emission estimates, using a lifetime of 47 years [*Jackman and Guthrie*, 1985] of approximately 29 − 9 = 20 million kg.

Interpreting the release from nonreporting companies given in column 5 of Table 9 as being due to production in Eastern Europe and the USSR, the release over the period 1979–1983 averages 55 million kg/yr and possesses no significant trend. On the basis of emissions estimated by *CMA* [1983], these

results could be considered as indicating a growth rate of 18% in the USSR and Eastern Europe from 1975 to 1979, followed by no growth since that time.

The release estimates in Table 8 are based upon the measured year-to-year differences in fluorocarbon concentrations. Thus just as for the lifetime estimates, release estimates obtained from several years of data possess substantially more accuracy than single-year estimates. Our analysis indicates a factor of approximately 2 increase in accuracy for 2-year average release estimates and a factor of 4 increase in accuracy for 3-year average release estimates.

Individual year differences shown in Table 9 are worthy of mention. The large discrepancy in 1978–1979 possesses a substantial error bar because it is primarily the result of the upward trend in the measurements at Samoa and Tasmania during the first 6 months of operation of the ALE instruments. During November 1978, sample loop sizes were changed at both of these sites; the sample loop sizes have remained fixed since that time and the overall consistency of the trends has also been much better (see Figure 6 of *Cunnold et al.*, [1983*b*]). Thus we suspect that the exceptionally large CF_2Cl_2 release estimate in 1978–1979 is caused by startup problems for the ALE network and is not real. The change in the ALE/CMA differences between 1981-1982 and 1982-1983 might be associated with the change in business conditions in the USA and Western Europe during that period. A similar but smaller shift in $CFCL_2$ usage may be noted in Table 8.

Since the ALE sampled only the surface values of fluorocarbons, some year-to-year variation might be caused by interannual variations in the rate of transport of material between the lower and the upper atmosphere on a global scale. The time for transport between 350 and 100 mbar assumed in our two-dimensional model is 4 years. If this time constant is changed to 3 years for a period of 1 year, the change in the tropospheric mixing ratio may easily be estimated by neglecting the effect of any change in the gradient between the troposphere and the stratosphere on atmospheric transport. It is calculated that the tropospheric mixing ratio would be reduced by approximately 0.6% for CF_2Cl_2 and 0.8% for $CFCl_3$ (which possesses a relatively larger vertical gradient between the troposphere and stratosphere). Therefore if such a change in the vertical transport were to have occurred, the ALE annual release estimates would be reduced by approximately 35 million kg for both $CFCl_3$ and CF_2Cl_2. Thus year-to-year changes in the estimated release rates for nonreporting companies might be caused by variations in the rate of transport of material between the troposphere and stratosphere. On the basis of ALE release estimates shown in Tables 8 and 9, it would be interesting to see whether there is any meteorological evidence for a small transport change occurring in 1981–1982.

6. Effects of Release Uncertainties on Lifetime Estimates

The principal release uncertainty for $CFCl_3$ remains the rate at which $CFCl_3$ is emitted by closed-cell foams. As discussed by *Cunnold et al.* [1983*a*], these uncertainties contribute 0.005 $year^{-1}$ to the inventory inverse lifetime uncertainty and 0.004 $year^{-1}$ to the trend inverse lifetime uncertainty. For the trend inverse lifetime the combined uncertainty resulting from measurement and release errors is $(0.002^2 + 0.004^2)^{1/2} = 0.004$; it is clearly dominated by release uncertainties. The trend estimate of lifetime, including release uncertainties, is 74^{+31}_{-17} years. The inventory inverse lifetime uncertainty is obtained by combining the 2% uncertainty in absolute calibration with modeling uncertainties and is the same as it was in the 3-year data analysis [*Cunnold et al.*, 1983*a*]. The uncertainty is 0.008 $year^{-1}$ and gives upper and lower (1τ) limits on the 68-year inventory lifetime for January 1, 1981, of 149 and 44 years. Clearly, the trend estimate of the lifetime is more precise.

The principal release uncertainties for CF_2Cl_2 are the releases in Eastern Europe and the USSR and the rate of release from nonhermetically sealed containers. The annual release estimates obtained in this paper suggest that a 2σ uncertainty, corresponding to 3% and 18% growth in the releases in Eastern Europe since 1975, as was assumed by *Cunnold et al.* [1983*b*], is reasonable. Using the other release uncertainties described in that Cunnold et al.'s paper [1983*b*] (Table 9), the effect of release uncertainties on the trend inverse lifetime is ± 0.006 $year^{-1}$. This may be combined with measurement uncertainties of 0.002 $year^{-1}$ to give an uncertainty of $(0.002^2 + 0.006^2)^{1/2} = 0.006$ $year^{-}$. The trend estimate of lifetime is then 111^{+222}_{-44} years. Combining release uncertainties with uncertainties in absolute calibration and modeling gives an inventory inverse lifetime uncertainty of 0.005 $years^{-1}$. This corresponds to an uncertainty range for the inventory lifetime of 51 to 103 years (the 2σ upper limit being 212 years).

7. Conclusions

Five years of continuous global ALE data on the concentrations of $CFCl_3$ and CF_2Cl_2 in the lower atmosphere have been analyzed. For January 1, 1981, the mean latitudinally averaged mixing ratios of $CFCl_3$ and CF_2Cl_2 are 177.5 pptv and 300.4 pptv, respectively. Also, at that time the annually averaged rate of increase of the mixing ratios are 9.0 pptv per year and 15.3 pptv per year for $CFCl_3$ and CF_2Cl_2. The increases were 8.8 and 15.3 pptv per year, 1 year later.

The short-term variability (including imprecision) of the measurements is approximately 1%. However, from an analysis of the residuals with respect to a two-dimensional model of the atmosphere and, in particular, from a comparison of almost simultaneous measurements of $CFCl_3$ on two different columns of the same instruments, it has been shown that the spectrum of the noise in the measurements is dominated by periods longer than 1 year. Fortunately, for trend measurements, at such periods the noise spectrum is found to be approximately flat. The determinability of physically induced variations in the data is expected to be influenced by this noise. Thus for example, we suspect that interannual variability in transport is not large enough to be readily evident in the data.

The data is dominated by an almost linear increase in the fluorocarbon mixing ratios over the 5-year period. This feature has been used to determine the atmospheric lifetime of fluorocarbons using the year-by-year increase in the logarithm of the mixing ratios, which tends to eliminate absolute calibrations uncertainties. The trend lifetime for $CFCl_3$ is calculated to be 74^{+31}_{-17} years and 111^{+222}_{-44} years for CF_2Cl_2. The uncertainties in these lifetime estimates are dominated by uncertainties in the rate of release of fluorocarbons into the atmosphere.

The atmospheric content of fluorocarbons may be estimated from the data when combined with a model which provides an estimate of the stratospheric content of fluorocarbons. On January 1, 1981, we estimate that there were 3,960 million kg

of $CFCl_3$ and 6,000 million kg of CF_2Cl_2 in the atmosphere. Given the historical record of the releases of fluorocarbons into the atmosphere, these figures may be used to provide lifetime estimates by the inventory technique. These estimates are 68 years for each gas on January 1, 1981. Since the lifetime estimates for $CFCl_3$ by both the trend and inventory techniques are in excellent agreement with the calculated lifetime for $CFCl_3$ due to photodissociation in the stratosphere and since CF_2Cl_2 should be an even more stable species, errors in the CF_2Cl_2 release estimates are suspected. In fact, the CF_2Cl_2 releases are known to be particularly uncertain because of inadequate knowledge of the releases in the USSR and Eastern Europe.

The ALE data analysis has been inverted to yield estimates of the release of fluorocarbons into the atmosphere, year by year, during the 5-year period from mid-1978 to mid-1983. These calculations are based on the assumption that the only sink for fluorocarbons in the atmosphere is stratospheric photodissociation. It has been shown that annual release estimates may be obtained from the ALE data with an accuracy, based on measurement system noise, of approximately 8%. Release estimates averaged over 2 years may be estimated with an accuracy of approximately 4%. Biases in these estimates are expected to be in the range $\pm 5\%$. The annual release estimates for $CFCl_3$ exhibit excellent agreement with the estimates by the Chemical Manufacturers Association. For CF_2Cl_2, estimates of the release in Eastern Europe and the USSR have been obtained by subtracting release estimates from reporting companies by the CMA from the ALE estimates of the releases. Although the data suggests some year-to-year variability in the emissions, within the accuracy of the estimates the emissions in Eastern Europe and the USSR have been roughly constant since 1979 at a level of approximately 55 million kg/yr. This emission estimate is sensitive to modeling errors, absolute calibration uncertainties, and any error in the calculated atmospheric lifetime of CF_2Cl_2 as well as to the accuracy of the release estimates for reporting companies.

Acknowledgments. This research was supported by the Fluorocarbon Program of the Chemical Manufacturers Association and by the Upper Atmosphere Research Program of NASA.

REFERENCES

Borisenkov, Y. P., and Y. Y. Kazekov, Effect of freons and halocarbons on the ozone layer of the atmosphere and climate, report, U. N. Environ. Programme, New York, 1977.

Bullister, J. L., and R. F. Weiss, Anthropogenic chlorofluorocarbons in the Greenland and Norwegian seas, *Science*, *221*, 265–267, 1983.

Chatfield, C., *The Analysis of Time Series: Theory and Practice*, Chapman and Hall, London, 1975.

Chemical Manufacturers Association, World production and release of chlorofluorocarbons 11 and 12 through 1982, Report, Fluorocarbon Program Panel, Washington, D. C., 1983.

Chemical Manufacturers Association, Production, sales and calculated release of CFC 11 and 12 through 1983, Report, Fluorocarbon Program Panel, Washington, D. C., 1984.

Cunnold, D. M., R. G. Prinn, R. A. Rasmussen, P. G. Simmonds, F. N. Alyea, A. J. Crawford, P. J. Fraser, and R. D. Rosen, The Atmospheric Lifetime Experiment, 3, Lifetime methodology and application to 3 years of $CFCl_3$ data, *J. Geophys. Res.*, *88*, 8379–8400, 1983*a*.

Cunnold, D. M., R. G. Prinn, R. A. Rasmussen, P. G. Simmonds, F. N. Alyea, C. A. Cardelino, and A. J. Crawford, The Atmospheric Lifetime Experiment, 4, Results for CF_2Cl_2 based on 3 years data, *J. Geophys. Res.*, *88*, 8401–8414, 1983*b*.

Fraser, P. J., P. Hyson, I. G. Enting, and G. I. Peerman, Global distributions and southern hemisphere trends of atmospheric CCl_3F, *Nature*, *302*, 692–695, 1983.

Golombeck, A., and R. G. Prinn, A global three-dimensional model of the circulation and chemistry of $CFCl_3$, CF_2Cl_2, CH_3CCl_3, CCl_4, and N_2O, *J. Geophys. Res.*, *91*, 3985–4002, 1986.

Herman, J. R., and J. E. Mentall, O_2 absorption cross sections (187–225 nm) from stratospheric solar flux measurements, *J. Geophys. Res.*, *87*, 8967–9875, 1982.

Jackman, C. H., and P. D. Guthrie, Sensitivity of N_2O, $CFCl_3$, and CF_2Cl_2 two-dimensional distributions to O_2 absorption cross sections, *J. Geophys. Res.*, *90*, 3939–3923, 1985.

Ko, M. K. W., and N. D. Sze, A 2-D model calculation of atmospheric lifetimes for N_2O, CFC-11, and CFC-12, *Nature*, *297*, 317–319, 1982.

Owens, A. J., J. M. Steed, C. Miller, D. L. Filkin, and J. P. Jesson, The atmospheric lifetimes of CFC 11 and CFC 12, *Geophys. Res. Lett.*, *9*, 700–703, 1982.

Prather, M. J., Continental sources of halocarbons and nitrous oxide, *Nature*, *317*, 221–225, 1985.

Prinn, R. G., P. G. Simmonds, R. A. Rasmussen, R. D. Rosen, F. N. Alyea, C. A. Cardelino, A. J. Crawford, D. M. Cunnold, P. J. Fraser, and J. E. Lovelock, The Atmospheric Lifetime Experiment, 1, Introduction, instrumentation and overview, *J. Geophys. Res.*, *88*, 8353–8367, 1983*a*.

Prinn, R. G., R. A. Rasmussen, P. G. Simmonds, F. N. Alyea, D. M. Cunnold, B. Lane, A. J. Crawford, and C. Cardelino, The Atmospheric Lifetime Experiment, 5, Results for CH_3CCl_3 based on 3 years of data, *J. Geophys. Res.*, *88*, 8415–8426, 1983*b*.

Rasmussen, R. A., and J. E. Lovelock, The Atmospheric Lifetime Experiment, 2, Calibration, *J. Geophys. Res.*, *88*, 8369–8378, 1983.

Simmonds, P. G., F. N. Alyea, D. M. Cunnold, J. E. Lovelock, R. G. Prinn, R. A. Rasmussen, B. C. Lane, C. A. Cardelino, and A. J. Crawford, The Atmospheric Lifetime Experiment, 6, Results for CCl_4 based on 3 years of data, *J. Geophys. Res.*, *88*, 8427–8441, 1983.

Trenberth, K. E., Seasonal variations in global sea level pressure and the total mass of the atmosphere, *J. Geophys. Res.*, *86*, 5238–5246, 1981.

F. N. Alyea, C. A. Cardelino, and D. M. Cunnold, School of Geophysical Sciences, Georgia Institute of Technology, Atlanta, GA 30332.

A. J. Crawford and R. A. Rasmussen, Department of Environmental Science, Oregon Graduate Center, Beaverton, OR 97005.

P. J. Fraser, Division of Atmospheric Physics, Commonwealth Scientific and Industrial Research Organization, Aspendale, 3195 Victoria, Australia.

R. G. Prinn, Department of Earth, Atmospheric, and Planetary Sciences, Massachusetts Institute of Technology, Cambridge, MA 02130.

R. D. Rosen, Atmospheric and Environmental Research, Inc., 840 Memorial Drive, Cambridge, MA 02139.

P. G. Simmonds, Department of Geochemistry, University of Bristol, Bristol, BF8-1TS England.

(Received September 17, 1985;
revised April 28, 1986;
accepted May 27, 1986.)

JOURNAL OF GEOPHYSICAL RESEARCH, VOL. 98, NO. D8, PAGES 14,753–14,770, AUGUST 20, 1993

Atmospheric Methane at Cape Meares: Analysis of a High-Resolution Data Base and Its Environmental Implications

M. A. K. KHALIL, R. A. RASMUSSEN, AND F. MORAES

Global Change Research Center, Department of Environmental Science and Engineering, Oregon Graduate Institute of Science and Technology, Portland, Oregon

Between 1979 and 1992 we took some 120,000 measurements of atmospheric methane at Cape Meares on the Oregon coast. The site is representative of methane concentrations in the northern latitudes (from 30°N to 90°N). The average concentration during the experiment was 1698 parts per billion by volume (ppbv). Methane concentration increased by 190 ppbv (or 11.9%) during the 13-year span of the experiment. The rate of increase was about 20 ± 4 ppbv/yr in the first 2 years and 10 ± 2 ppbv/yr in the last 2 years of the experiment suggesting a substantial decline in the trend at northern middle and high latitudes (-1 ppbv/yr^2). Prominent seasonal cycles were observed. During the year, the concentration stays more or less constant until May and then starts falling, reaching lowest levels in July and August, then rises rapidly to nearly maximum concentrations in October. The average amplitude of this cycle is about 30 ± 7 ppbv and has increased during the course of the experiment. Interannual variations with small amplitudes of 2-3 ppbv occur with periods of 1.4 and 6.5 years. The residual concentrations, after accounting for the trends and cycles, have a standard deviation of 6 ppbv for monthly averaged data and 12 ppbv for the daily data. Mass balance calculations show that to explain the observed seasonality of concentrations, the emissions must peak in late summer and early fall (August-September). No increases in regional annual emissions are required over the last decade to explain the data. For further research, readers may obtain the complete and averaged data from the archives.

1. INTRODUCTION

Atmospheric methane is of considerable scientific interest because its concentration is increasing and it has an important role in global atmospheric chemistry and the greenhouse effect. In the troposphere, methane affects the oxidizing capacity of the atmosphere, it may create ozone in the presence of NOx, and it causes global warming. In the stratosphere, methane scavenges chlorine atoms preventing the destruction of the ozone layer from chlorofluorocarbons and other chlorine-containing gases. It also produces water vapor in the stratosphere, and possibly high clouds, which may have the opposite effect on ozone (for reviews see *World Meteorological Organization* [1985, 1988, 1989, 1991], *Intergovernmental Panel on Climate Change* [1990], and *Wuebbles and Tamaresis* [1993]).

More than a decade ago, automated measurements from Cape Meares established that methane was increasing in the atmosphere at a rapid rate [*Rasmussen and Khalil*, 1981]. The Cape Meares data have been used in many subsequent analyses of the trends and budgets of methane (see, for example, *Khalil and Rasmussen* [1983, 1990]). The subject of this paper is the present record, which spans the 13 years between 1979 and 1992 containing some 120,000 individual measurements linked to a single absolute calibration standard.

We will discuss the nature of the data in section 2. Section 3 is on the most significant patterns in the data set, namely the trends and seasonal cycles; both have been changing during the past decade. The validity of the measurements is discussed in section 4. The Cape Meares data provide information on the nature and seasonality of sources and sinks as discussed in section 5. We have tabulated the monthly data for use by the readers; the complete data are available from the archives as explained at the end.

2. MEASUREMENTS AND THE NATURE OF THE DATA

The measurements were taken using an automated sampling and measurement system. At the heart of the system is a gas chromatograph with a flame ionization detector (GC/FID). Air is drawn with a pump and dried to a dew point of -30°C by a Nafion® Dryer. The sample is injected into the gas chromatograph and the analysis cycle begins. Each analysis of an ambient air sample is followed by an analysis of a precisely calibrated laboratory standard. The chromatographic peaks representing methane (and CO and CO_2 in the early part of the experiment) are integrated using a electronic integrator.

At the start of the experiment a Carle 211-MS Gas Chromatograph was installed. In mid-1985 a Hewlett-Packard GC was also installed so that the Carle instrument could be replaced. The two instruments were operated simultaneously until the beginning of 1987, after which the Carle instrument was removed. The overlap period is used to adjust for the small difference between the instruments. The overlap also allowed time to fine tune the Hewlett-Packard GC to obtain a high degree of precision before the established instrument was discontinued. Details of the analytical system and experimental methodology are discussed by *Rasmussen and Khalil* [1981].

The ambient concentration C(t) is calculated as

$$C_{meas}(t) = A_a(t)C_s/\{1/2[A_s(t-\delta) + A_s(t+\delta)]\} \quad (1)$$

where C_s is the concentration in the standard, A_a is the peak area for methane in the ambient sample, and $A_s(t-\delta)$ and

Paper number 93JD01197.
0148-0227/93/93JD-01197 $0.5.00

$A_s(t+\delta)$ are the peak areas for the standard analyzed before and after the ambient sample.

The same primary calibration standard was used throughout the experiment. The precision relevant to the interpretation and use of these data is estimated from the variability of observed daily concentrations. It represents the overall precision including instrumental, atmospheric, and sampling variabilities. We represent the precision with two variables: the daily standard deviation (representing the variability of an individual measurement = sd) and the daily % standard error (representing the variability of the daily mean = sd 100%/(C$\sqrt{N}$)), where C is the mean concentration and N is the number of measurements taken during a day .

The results are shown in Figure 1. The daily standard deviations are about 10 parts per billion by volume (ppbv) with 90% of them between 4 and 21 ppbv. The daily % standard error is about 0.1% with 90% lying between 0.03% and 0.34%.

In the beginning of the experiment we took 72 ambient measurements per day. In May 1984 the sampling frequency was reduced to 24 samples/day, and in January 1986 the frequency was further reduced to 12 samples/day. More than 120,000 measurements were taken during this experiment. We will refer to this set as "continuous" data. After discarding data from periods when the instruments were found to be malfunctioning and a few extreme cases, the resulting data base consists of 118,762 points. This is about 70% of the maximum data that could have been collected under our sampling frequencies (during the rest of the time the instrument was not working).

We took daily and monthly averages of the data for further analysis. From the daily data we found that an average of 82% of the days between 2/1979 and 12/1992 were sampled. In the year of least number of daily measurements, 71% of the days were sampled and in the year of most daily

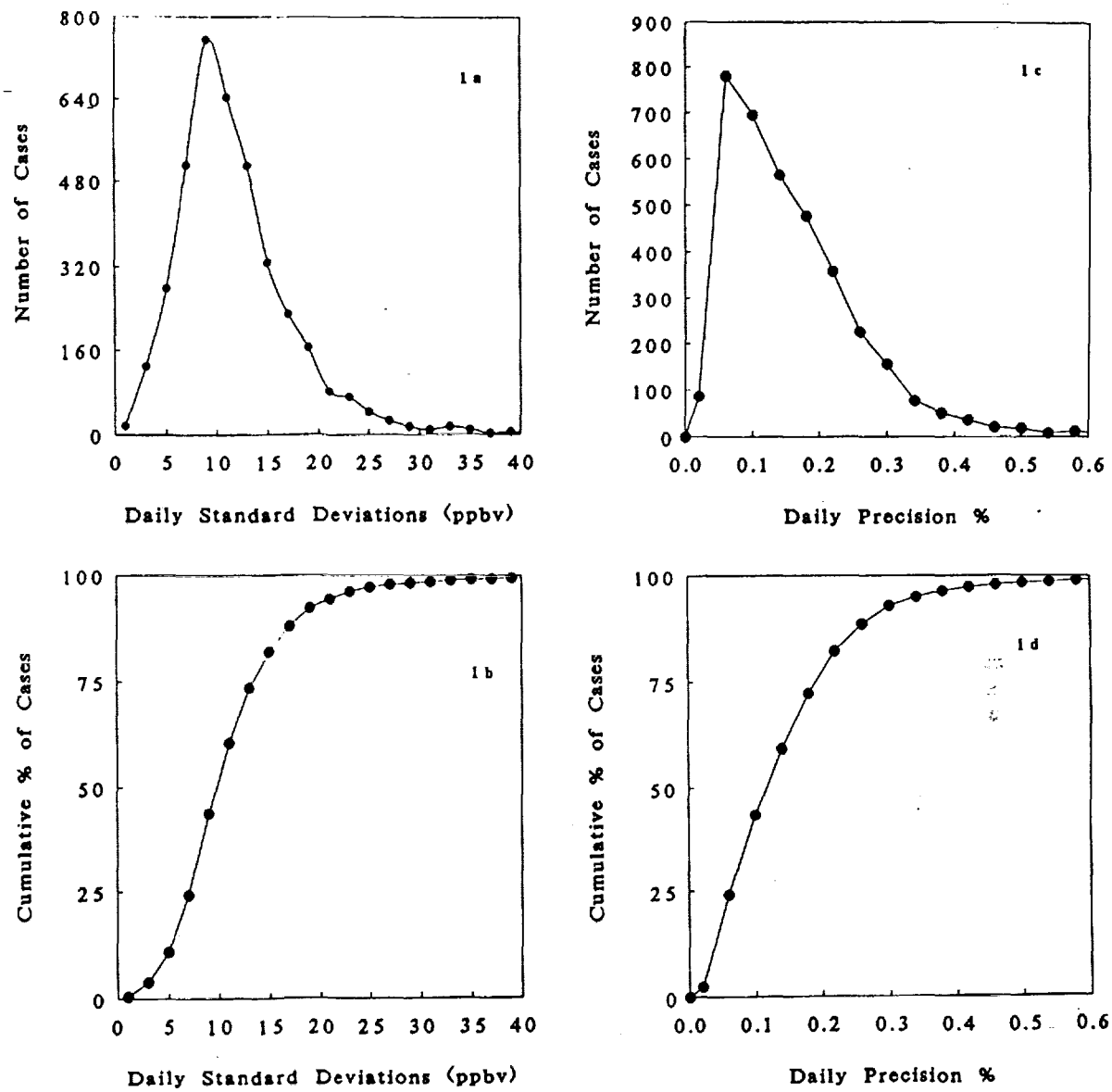

Fig. 1. The precision of daily concentrations of methane. (*a*) Frequency distribution of daily standard deviations. (*b*) Cumulative frequency distribution of daily standard deviations. (*c*) and (*d*) Analogous to Figures 1*a* and 1*b* but representing the percent variability, which is 100% standard deviation/mean/$\sqrt{N}$. These results show the extremely high daily precision of the measurements.

measurements, 91% of the days were sampled. There is a seasonal variation in the number of days sampled per month. For most months, 80 - 90% of the days were sampled. The lowest number of days sampled per month were for January months (73%) and highest for May months (90%). Generally between November and January, fewer days were sampled (per month) than during other months. This effect is due to the adverse weather conditions during the winters when storms cause power outages and make the station inaccessible for several weeks at a time. Sufficient data were available to form monthly averages for all the months of the experiment.

3. TRENDS, SEASONAL CYCLES AND INTERANNUAL VARIABILITY

3.1. *Representation of the Data*

The atmospheric concentrations are plotted in Figure 2. The continuous data are shown in Figure 2*a*, daily averages in Figure 2*b*, and monthly averages in Figure 2*c*. These data clearly show that there are significant seasonal variations, that the concentration is increasing, and that the present rates of increase are slower than in the earlier part of the data.

For most applications, daily or monthly average data are more appropriate than the continuous data. Using daily numbers, we have used three methods to obtain monthly concentrations and the variability of the means: arithmetic averages, nonparametric estimates of the middle value, and the medians. The different methods give very similar results, which are tabulated in *Khalil and Rasmussen* [1992] (see also *Snedecor and Cochran* [1980] and *Hollander and Wolfe* [1973]). The monthly averages are given in Table 1 (see section 2). All plus or minus values quoted in this paper are 90% confidence limits.

To discuss the patterns in these data, it is useful to state a parametric model so that each feature can be quantified according to the variables of this model. We chose the following model

$$C(t) = \text{Trend} + \text{Annual Cycle} + \text{Interannual Variability} + \epsilon = C_{T_r} + C_{cyc} + C_{IAV} + \epsilon \quad (2)$$

$$C_{T_r} = a + bt + ct^2 \quad (3)$$

$$C_{cyc} = g(t)\sum_{J=1}^{N} \alpha_J \sin(\omega_J t + \phi_J) = g(t)\langle C_{cyc}\rangle = [1 + \lambda(t - \frac{T}{2})]\langle C_{cyc}\rangle \quad (4)$$

$$\omega_J \le \frac{\pi}{6} \text{ months}$$

$$C_{IAV} = \sum_{J=N}^{M} \alpha_J \sin(\omega_J t + \phi_J) \; ; \quad \omega_J > \frac{\pi}{6} \text{ months} \quad (5)$$

$$\epsilon(t) \sim D(0, M_2, \ldots m_N) \quad (6)$$

In this model the trend is defined as a quadratic equation in time, which includes the decline in the accumulation rates that has been observed all over the world. The annual cycles have a duration ≤ 1 year and are here represented as sinusoidal functions. The function g(t) is included to represent the change of cycle amplitude, which is small in this case and can be approximated by the linear function as in (4). The time series $C_{des} = C - C_{cyc}$ is the deseasonalized data, $C_{det} = C - C_{T_r}$ is the detrended time series, and T is the time span of the experiment (155 months or 4715 days). The interannual variability includes variations, cyclic or not, that span times longer than a year and are not represented by polynomials such as used to describe the trend. Finally, $\epsilon(t)$ are residuals, presumed to be random and represented by some statistical distribution D with mean, m_1 = zero and described by canonical moments $m_2 \ldots m_N$. There are many approaches for decomposing the time series into the components described by (1). Here is how we did it.

Seasonal cycles. The first step is to evaluate the seasonal cycles. We subtract a 12-month running average of concentrations from the data. The end points of the running average time series are estimated by linearly extrapolating the trends of the closest year (calculated from the moving average time series). These running averages are a (digital) filter that remove cycles of 12 months or less. The original data minus the filter leave behind only cycles of 12 months or less.

In the second step, we evaluate the average seasonal cycle $\langle C_{cyc}\rangle$. We have used two approaches, which give almost the same results. One way to estimate the cycles is to search for sinusoidal periodicities of the form: $\alpha_i \sin(\omega_i t + \phi_i)$ where ω_i are the frequencies inherent in the data. The approach described by *Khalil and Moraes* [1993] produces a Fourier-type spectral analysis with the advantages that the algorithm does not require evenly spaced data and searches for true frequencies rather than the base frequencies and its harmonics. The spectral decomposition of the time series is shown in Figure 3.

The other way we estimate seasonal cycles is to calculate the average concentration, from the detrended data, on each of the 366 days of the year during the course of the experiment (365 are normal days and February 29 is the additional day for which there are data only during leap years, unless the instruments were not working on that day). The Fourier decomposition produces a parametric representation of the cycles in terms of a set of sinusoidal terms with frequencies ω_i (i = 1...n) and phases ϕ_i (i = 1...n) as in (4). The second method produces 366 seasonal indices rather than a parametric representation. The main content of these indices is almost the same as the Fourier decomposition. The procedures are the same when applied to the month-averaged concentrations except that there are 12 monthly indices instead of 366 daily indices and the Fourier frequencies are in radians/month instead of radians/day.

Long-term trends. The third step is to subtract the average seasonal cycle from the original data: $C - \langle C_{cyc}\rangle$. We then fit a polynomial trend to this deseasonalized data (in this case a quadratic function) to determine "a," "b," and "c" in (3).

In the present case there is an additional calculation at this point. Since the amplitude of the seasonal cycle is increasing (to be discussed later in more detail), we have assumed a simple model to describe the trend in cycle amplitude by (4); λ is estimated by linear regression through zero, between $C - C_{T_r} - \langle C_{cyc}\rangle$ and $(t - T/2) \times \langle C_{cyc}\rangle$. This turns out to be a small effect but worthy of documentation.

Next (fourth step) we subtract the polynomial trend from

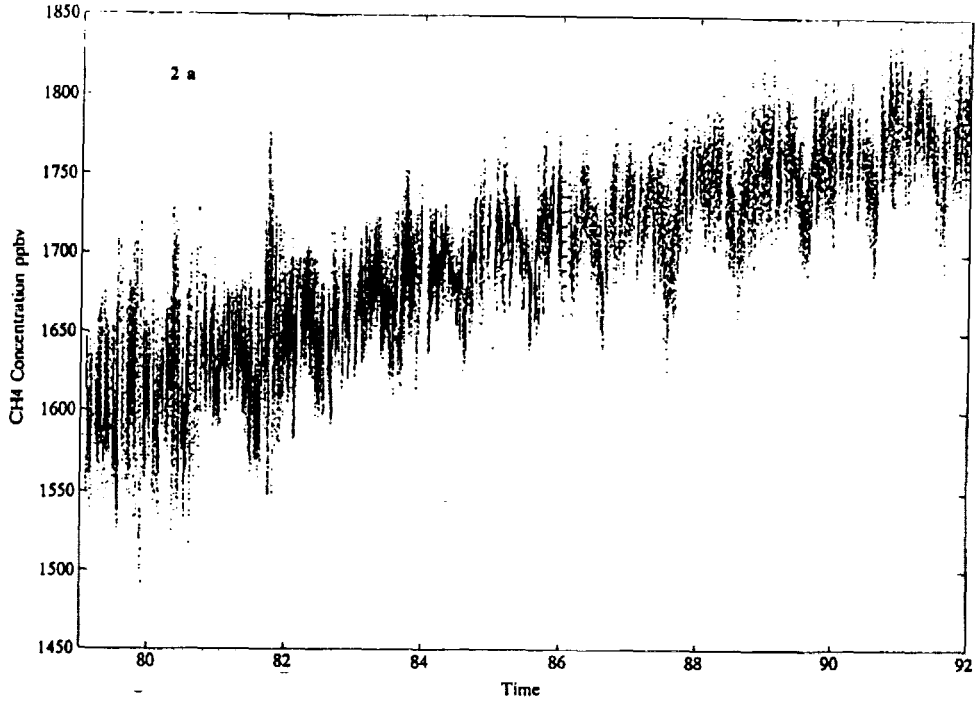
2 a
CH4 Concentration ppbv
1850
1800
1750
1700
1650
1600
1550
1500
1450
80
82
84
86
88
90
92
Time

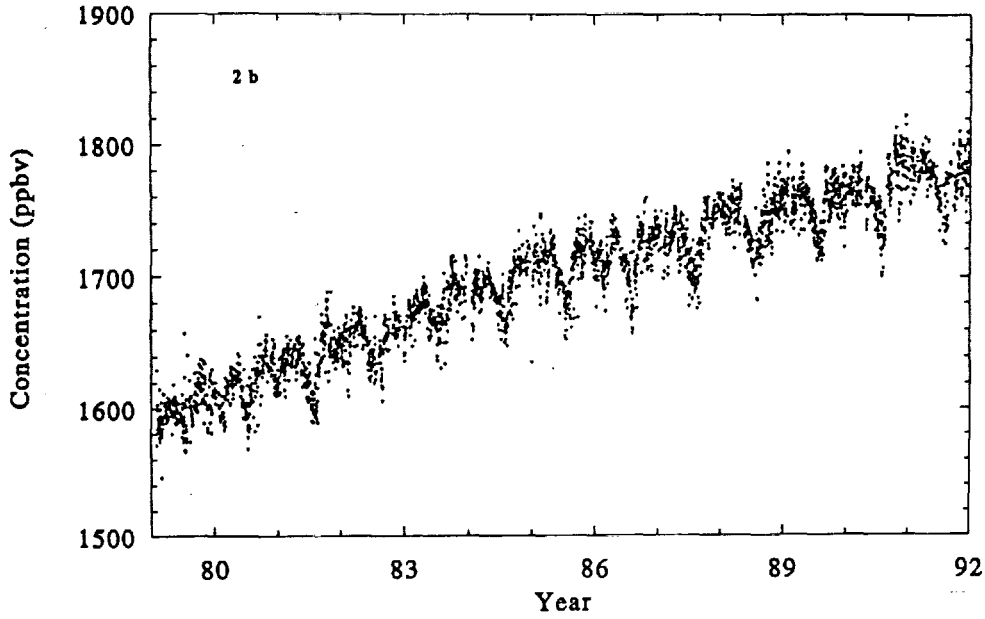
2 b
Concentration (ppbv)
1900
1800
1700
1600
1500
80
83
86
89
92
Year

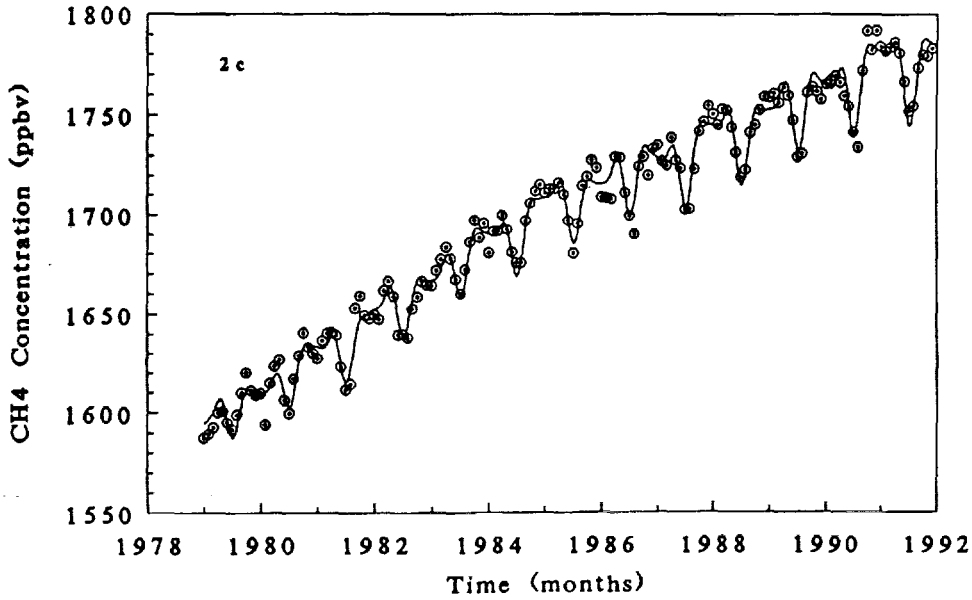
2 c
CH4 Concentration (ppbv)
1800
1750
1700
1650
1600
1550
1978
1980
1982
1984
1986
1988
1990
1992
Time (months)

TABLE 1. Monthly-Averaged Concentrations of Methane, in parts per billion by volume, at Cape Meares, Oregon

	1979	1980	1981	1982	1983	1984	1985
Jan.		1610 ± 3	1627 ± 3	1650 ± 3	1664 ± 5	1680 ± 8	1711 ± 7
Feb.	1589 ± 4	1594 ± 3	1637 ± 3	1648 ± 5	1672 ± 3	1692 ± 3	1713 ± 5
March	1593 ± 4	1615 ± 2	1640 ± 2	1662 ± 3	1677 ± 2	1691 ± 3	1713 ± 4
April	1600 ± 2	1624 ± 2	1641 ± 3	1666 ± 2	1683 ± 2	1700 ± 1	1716 ± 4
May	1601 ± 2	1627 ± 2	1640 ± 3	1659 ± 2	1677 ± 3	1692 ± 2	1710 ± 3
June	1595 ± 3	1606 ± 4	1623 ± 2	1640 ± 3	1667 ± 1	1681 ± 2	1697 ± 3
July	1592 ± 7	1600 ± 4	1612 ± 4	1640 ± 4	1660 ± 4	1675 ± 4	1680 ± 4
Aug.	1599 ± 4	1617 ± 6	1614 ± 6	1638 ± 4	1672 ± 5	1675 ± 5	1695 ± 6
Sept.	1610 ± 3	1629 ± 7	1653 ± 3	1653 ± 5	1686 ± 5	1697 ± 4	1715 ± 5
Oct.	1620 ± 3	1641 ± 3	1659 ± 6	1659 ± 2	1697 ± 3	1706 ± 4	1719 ± 3
Nov.	1611 ± 7	1633 ± 2	1649 ± 4	1666 ± 3	1688 ± 3	1712 ± 3	1728 ± 4
Dec.	1609 ± 5	1630 ± 5	1648 ± 2	1664 ± 2	1696 ± 5	1715 ± 4	1724 ± 3

	1986	1987	1988	1989	1990	1991
Jan.	1709 ± 4	1735 ± 3	1750 ± 2	1759 ± 3	1765 ± 2	1784 ± 5
Feb.	1708 ± 4	1727 ± 5	1745 ± 3	1761 ± 9	1767 ± 4	1782 ± 5
March	1708 ± 4	1725 ± 3	1753 ± 3	1756 ± 3	1769 ± 3	1783 ± 3
April	1729 ± 3	1739 ± 3	1752 ± 3	1764 ± 4	1766 ± 5	1786 ± 4
May	1729 ± 3	1727 ± 4	1744 ± 6	1760 ± 2	1759 ± 5	1781 ± 2
June	1711 ± 2	1723 ± 4	1731 ± 3	1747 ± 2	1754 ± 3	1766 ± 3
July	1699 ± 4	1703 ± 4	1719 ± 4	1729 ± 3	1741 ± 5	1751 ± 5
Aug.	1690 ± 6	1703 ± 4	1723 ± 5	1731 ± 4	1734 ± 6	1754 ± 6
Sept.	1724 ± 5	1723 ± 6	1741 ± 4	1761 ± 4	1772 ± 4	1773 ± 8
Oct.	1729 ± 5	1742 ± 4	1745 ± 5	1764 ± 3	1792 ± 4	1780 ± 5
Nov.	1720 ± 4	1747 ± 2	1752 ± 3	1762 ± 3	1782 ± 6	1779 ± 4
Dec.	1733 ± 2	1755 ± 2	1759 ± 3	1758 ± 4	1792 ± 6	1783 ± 5

Monthly averages and variability are calculated from daily-averaged concentrations. The plus and minus values are 90% confidence limits.

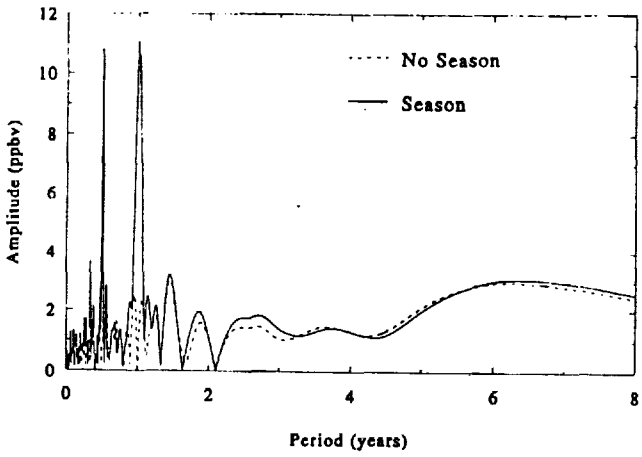

Fig. 3. The spectral decomposition of methane concentrations at Cape Meares.

the deseasonalized data: $C\text{-}C_{Tr}\text{-}C_{cyc}$. We are now left with a time series that has no seasonal variations (including increase of cycle amplitude) and no long-term trends. A Fourier spectrum of these data reveals long cycles (the interannual variability). When these are subtracted from the deseasonalized and detrended data, we are left with the residuals.

The fifth and final step is to analyze the residuals. We now look at the results of these calculations for various components of the time series.

3.2. *Seasonal Cycles and Changes in Cycle Amplitude and Cycle Length*

The first graphical view of the seasonal cycles, based on the continuous data, is shown in Figure 4*a*. It is obtained by subtracting the quadratic trend from the data and then plotting all data by the hour of the year on which it was taken regardless of which year.

The daily-averaged data were analyzed according to the two methods mentioned earlier. In Figure 4*b*, the results of both methods are shown. The solid circles are the daily seasonal index, and the line is from the Fourier decomposition using the three most prominent frequencies (see section 3.7). Days are sequentially numbered starting with January 1 as day 0 to December 31 (which is day 364 or 365). Between leap years, February 29 is treated as a missing value.

Finally the monthly-averaged data are used to obtain seasonal variations by the two methods as shown in Figure 4*c* and represented analogously to Figure 4*b*. Ninety percent confidence limits are added to the monthly indices.

The cycle essentially consists of two features, namely, the cycle amplitude and the cycle length. We analyzed the changes in these features during the experiment.

We defined the cycle length, using the detrended daily-averaged data, as the time between the day of minimum

Fig. 2. The atmospheric concentrations of methane at Cape Meares, Oregon, between 1979 and 1992. (*a*) Continuous data. Samples were collected and analyzed every 20 min. in the beginning of the record and at lower frequencies during later years (see text). These data show the detailed nature of the trends, slowdown in the trend in recent years and the seasonal variations. (*b*) Daily averages. (*c*) Monthly-averaged concentrations of methane. The line is the parametric statistical model based on quadratic trends, seasonal, and interannual variations (see text).

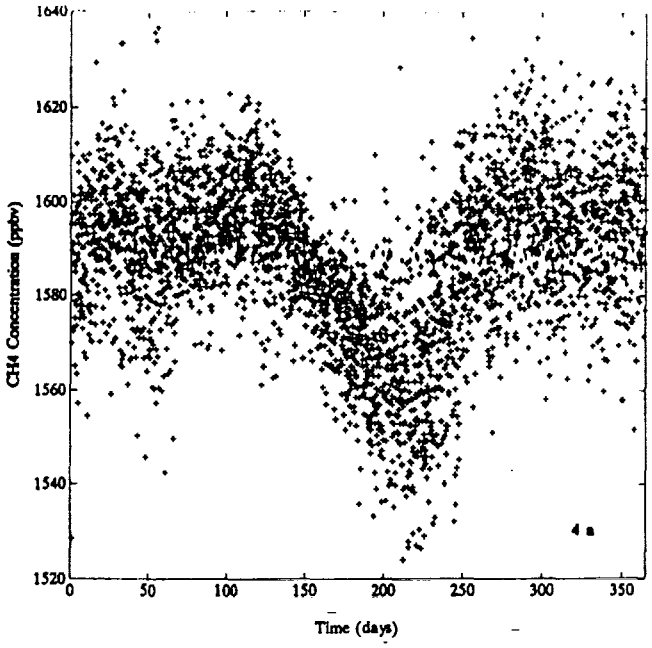

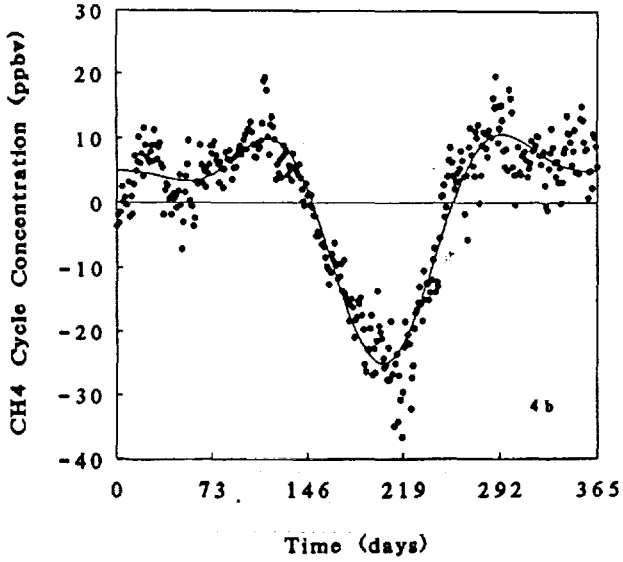

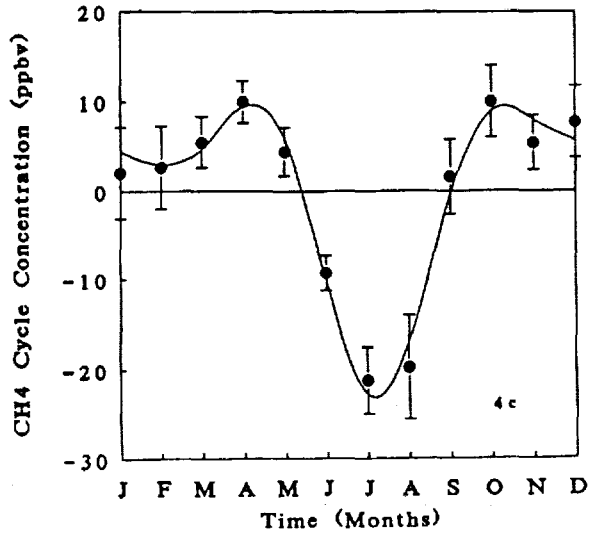

concentration in one year to the day of minimum concentration in the next year. The day on which minimum concentrations occur are very precisely defined in the data, while the maxima are not. The results show a remarkable stability of cycle length from year to year. The average cycle length is 365.6 days with a standard deviation of 19 days. The maximum cycle length was 397 days, and the minimum was 331 days. Both these occurred in the early part of the data. There is no trend in the cycle length (0.2 ± 2 days).

The cycle amplitude does have trends. We defined the cycle amplitude as the average difference of maximum and minimum concentrations during the year using the detrended data. For monthly data the cycle amplitude is defined as the average concentration during January to April and October to December minus the average concentration during July and August. For the daily averages the cycle amplitude is defined as the average concentrations during days 0-110 and 290-365 minus the average concentrations during days 190-250.

The calculations are shown in Figure 5. The amplitude of the average seasonal cycle is about 30 ± 7 ppbv by all methods considered. The relative cycle, the cycle divided by the average concentration for the year, is about 1.7% ± 0.4%. There is a trend in the cycle amplitude of 1.2 ± 0.9 ppbv/yr and varies somewhat by the method of calculating average concentrations. The trend of the relative cycle is less statistically significant at 0.05% ± 0.05% per year. The cycle amplitude during the first year is anomalously small and probably due to experimental errors rather than atmospheric behavior, it is therefore not included in the calculations or in Figure 5. In section 4 we will return to the possible causes of the changes in cycle amplitude.

3.3. *Rate of Long-Term Increase and Its Slowdown*

The long-term trends have one noteworthy feature, namely, that the rate of accumulation is slowing down. The slowdown of the methane trend has been reported earlier [see *Khalil and Rasmussen*, 1990, 1993; *Shearer and Khalil*, 1989; *Steele et al.*, 1992].

There are several methods for evaluating the change of trends; each method provides a unique perspective. The simplest calculation is the quadratic formula of (3). Another method is to calculate a time series of trends from the deseasonalized data using "running slopes." In this approach the slopes (or trends) of the concentration data from time T+j to T+j+δ are calculated by a linear regression model (where j = 0 to N-δ, N is the number of data, number of months or number of days in the data set as appropriate).

The results of these calculations for various assumed values of δ = 3, 5, 6, and 8 years are shown in Figure 6. The solid line is for the daily data, and the circles are for the monthly-averaged data. The decline of the trend is apparent. There are various other features that may represent atmospheric behavior or result from experimental errors.

A third analysis of the trends is to use the average data (without deseasonalization) and calculate the trends for each day or each month. For instance, the average concentrations

Fig. 4. The seasonal cycle of methane concentrations. (a) Continuous measurements. (*b*) Seasonal cycle based on daily measurements. The points are the 366 daily indices of the seasonal cycle and the line is the sum of three sinusoidal components from the Fourier decomposition (see text) with the highest amplitudes. (*c*) Same as Figure (*b*) but for monthly-averaged concentrations. The periods of these cycles are 12, 6, and 4 months.

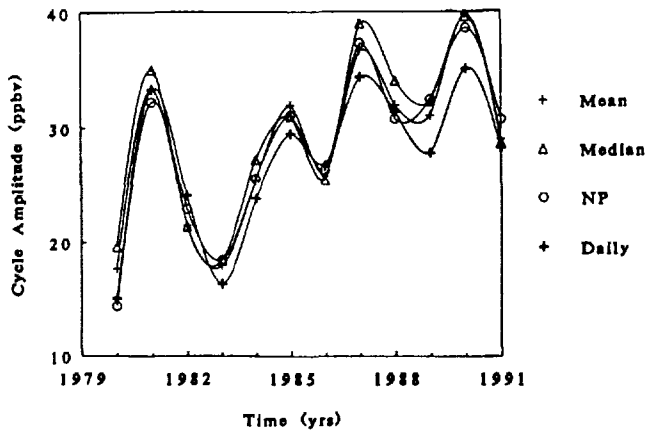

Fig. 5. Increase in the amplitude of the seasonal cycle of methane at Cape Meares. The legend at the right refers to the various averaging methods (see text for further details).

in January of each year between 1979 and 1991 constitute a time series from which a trend can be calculated for January, and similarly for each month of the year. For the daily data the same procedure is applied to each of the 365 days (February 29 is eliminated). For both these calculations we use the quadratic model:

$$C_J(t) = a_J + b_J t + c_J t^2 + \epsilon_J(t) \quad (7)$$

where C_J is the monthly (J = m) or daily average concentration (J = d), a_J, b_J, and c_J are constants determined from multiple linear regression, and $\epsilon_J(t)$ are the residuals. The average trend during the experiment is

$$\langle b_J \rangle = b_J + c_J T \quad (8)$$

where T is the length of the experiment (here 13 years).

For the monthly data, the average trend during each month is shown in Figure 7*a*, and the rate of decrease of trend, which is $2c_J$, is given in Figure 7*b*. Analogous results for the daily data are shown in Figure 8. The trends in the summer months are significantly lower than during the other months. The increase of cycle amplitude discussed earlier is implicit in this result. If the cycle amplitude increases, then trends in the months of highest concentrations have to be different from trends in months of lowest concentrations.

There is a curious anticorrelation between the b_J and the c_J coefficients of the calculations of the quadratic trend for each day of the year. It is shown in Figure 9. While the average trends are less in the summers compared to other times, they are also decreasing more slowly (or not at all) compared to other seasons.

The trend of methane was about 20 ± 4 ppbv/yr in the first 2 years and about 10 ± 2 ppbv/yr in the last 2 years of the experiment, representing a decline of about -1 ppbv/yr. The methods and an analysis of our global data set are given in more detail by *Khalil and Rasmussen* [1993]. In that paper we argue that most of the decrease in trend is likely caused by the slowdown in anthropogenic emissions, while a smaller effect may be caused by a possible increase of OH [*Prinn et al.*, 1992; *Madronich and Granier*, 1992].

3.4. *Interannual Variations*

The interannual variations are cycles over times greater than a year. There are two such cycles of periods 1.4 years and 6.5 years. Both are weak with amplitudes of only 2-3 ppbv, yet they are apparent to the eye in the detrended monthly data. The causes of these interannual cycles are unclear at present.

3.5. *Residuals*

The residuals are the concentrations left after all the known features (as in (2)) are subtracted from the data. The distribution of the residuals for daily averages is shown in Figure 10 along with a fit to a normal distribution for the same average and standard deviation. The mean is 0, and the standard deviation of the residuals is 12 ppbv for the daily data and 6 ppbv for the monthly data. The residuals are not quite normally distributed but exhibit both skewness, $g_1 = -0.16$, and kurtosis, $g_2 = 0.93$. A normal distribution would have g_1 and $g_2 = 0$ with standard deviations of about 0.04 and 0.08, respectively, so the observed skewness and kurtosis are 4 and 11 times higher than the standard deviations for a normal distribution. The skewness means that the model underestimates the measured concentrations more often than overestimating it, but the underestimates are usually smaller than the overestimates (since the mean is 0). The kurtosis means that the tails of the distribution have more cases than would be expected if the distribution was normal [see *Snedecor and Cochran*, 1980].

To further check whether the residuals are random or not, we applied the turning point test to the monthly data [*Kendall and Ord*, 1990]. In this test, we calculate the number of points that are either higher or lower than the two points immediately before and after, representing either peaks or troughs. If the data of 156 points were random, we would expect about 103 turning points with a variance of 24.4. In the Cape Meares time series of residuals, there are 96 turning points. This suggests that our residuals are indeed approximately random ($z = -1.27$). Nonetheless, there may be small signals that still have not been fully accounted for by our parametric representation.

3.6. *Other Cycles and Variabilities*

In addition to the patterns inherent in (2), other cycles and variabilities also exist in the data. First, there are submonthly variabilities that take the form of higher than average concentrations that are sustained for various number of days. The occurrence of sustained higher than average concentrations for a week or longer occur more frequently than may be expected from chance. These occurrences are probably related to long-distance transport of air from source regions.

Small diurnal variations are also seen in the continuous data. In most cases the concentrations during the day are higher than at night. We calculate the difference of concentrations between day and night for each day when appropriate data are available. Day concentrations are taken from 1000-1400 hours and night concentrations from 2200-0200 hours. We then calculate the average diurnal difference for each month during the course of the experiment. The results are shown in Figure 11. During late summer and part of fall (August - October) the day concentrations are significantly higher than night concentrations by about 2 ppbv. During other months there appears little or no difference between day and night concentrations. This cycle is likely related to local production of methane since diurnal changes are too fast to respond to distant processes. The exact mechanisms and sources that generate these cycles are not known.

Finally, using the daily data we can also calculate the variability of the monthly concentrations, which we estimate by the standard deviation. The monthly standard deviations of observed concentrations undergo a seasonal cycle but appear to have no other significant patterns such as trends or change of cycle length and amplitude.

3.7. *Summary of the Time Series Decomposition*

The standard deviation of the concentrations in the (raw) daily or monthly averaged time series is about 56 ppbv. When the trend is subtracted the standard deviation of the remaining data is reduced to about 17 ppbv for the daily data and 12 ppbv for the monthly data. As each feature is subtracted, the

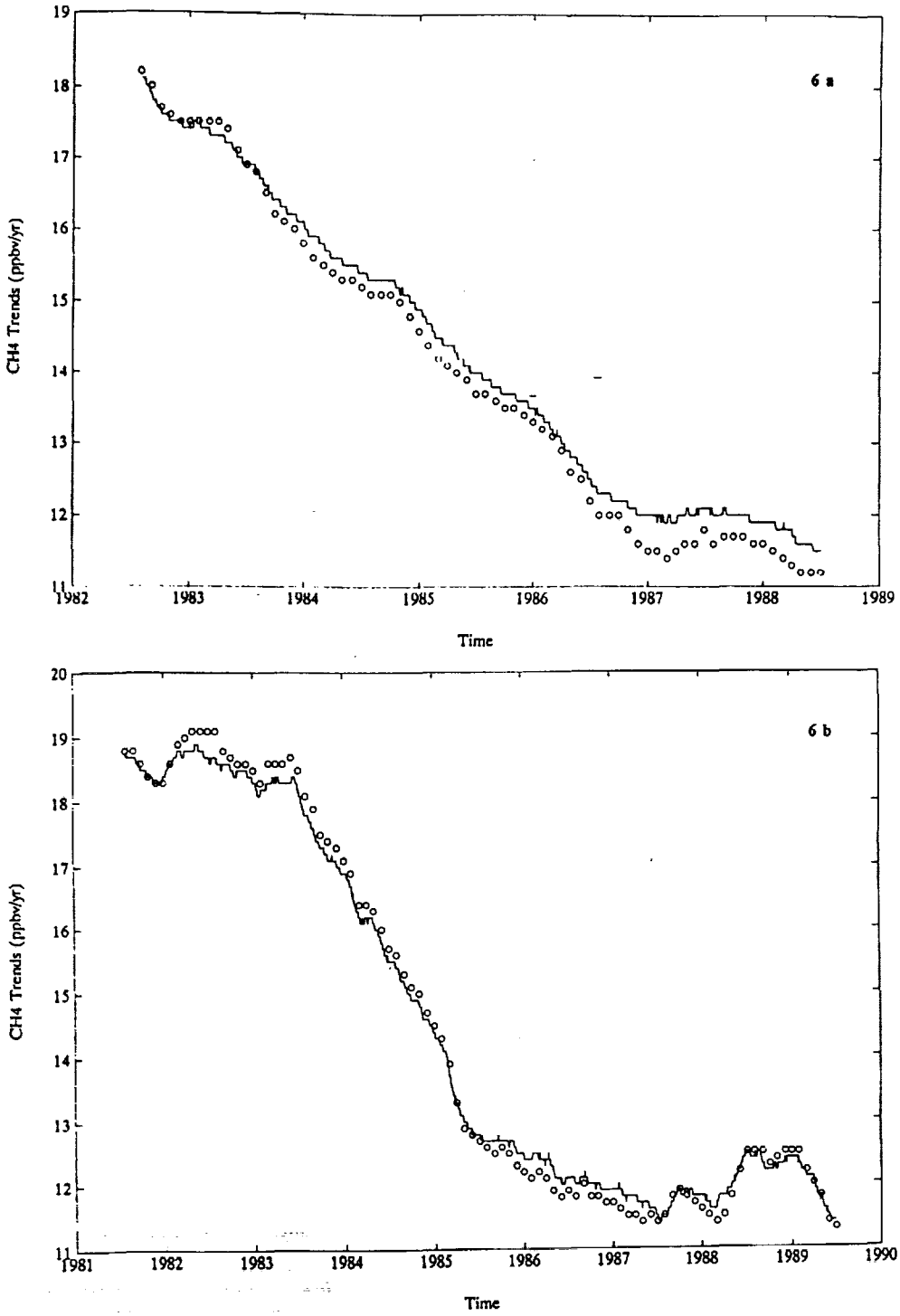

Fig. 6. The change of the trend of methane at Cape Meares. The moving trends are plotted for various "averaging" periods. The slopes of the concentration data from time T+j to T+j+δ are calculated by a linear regression model, where j = 0 to N-δ, N is the number of data, number of months, or number of days in the data set as appropriate. (*a*) The period over which the trends are calculated is 8 years, (*b*) the period is 6 years, (*c*) the period is 5 years, and (*d*) the period is 3 years. Solid lines are based on daily data; circles are from monthly-average data.

variance of the remaining time series is reduced until we come to the random residuals (ϵ). The reduction in variability from each feature of the parametric model of (2) is listed in Table 2. The parameters of the time series model are also given in Table 2.

The parametric formula is a compact representation of the daily-averaged data. If one accepts that the residuals between the observed concentrations and the sum of the factors isolated in (2), as evaluated here, contain no additional information except a measure of random variability (represented by the standard deviation), then the parametric model can be used to reconstitute the daily data by adding a normally distributed random $\epsilon(t)$ with mean 0 and standard deviation sd. This amounts to substituting a normal distribution N(0,sd) for the actual distribution of the residuals $D(0,sd,m_3,m_4)$. The reconstituted data should then be indistinguishable from the actual measurements and could therefore be used in any model requiring a methane database with a daily average measurement frequency. As discussed earlier, the residuals are not quite normally distributed, but we

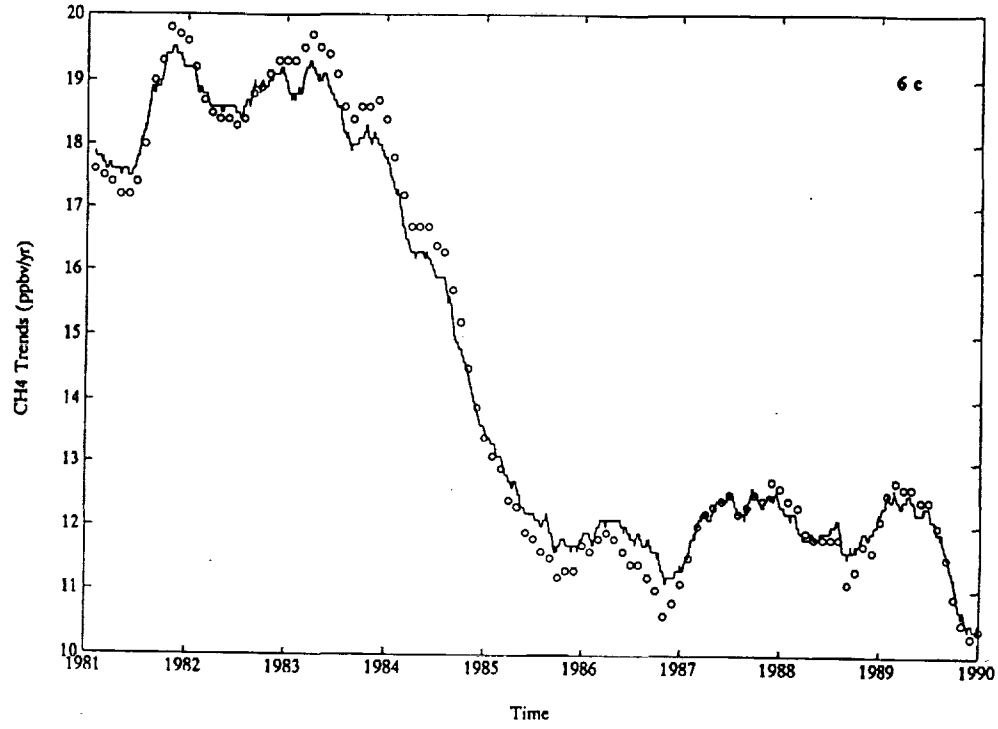

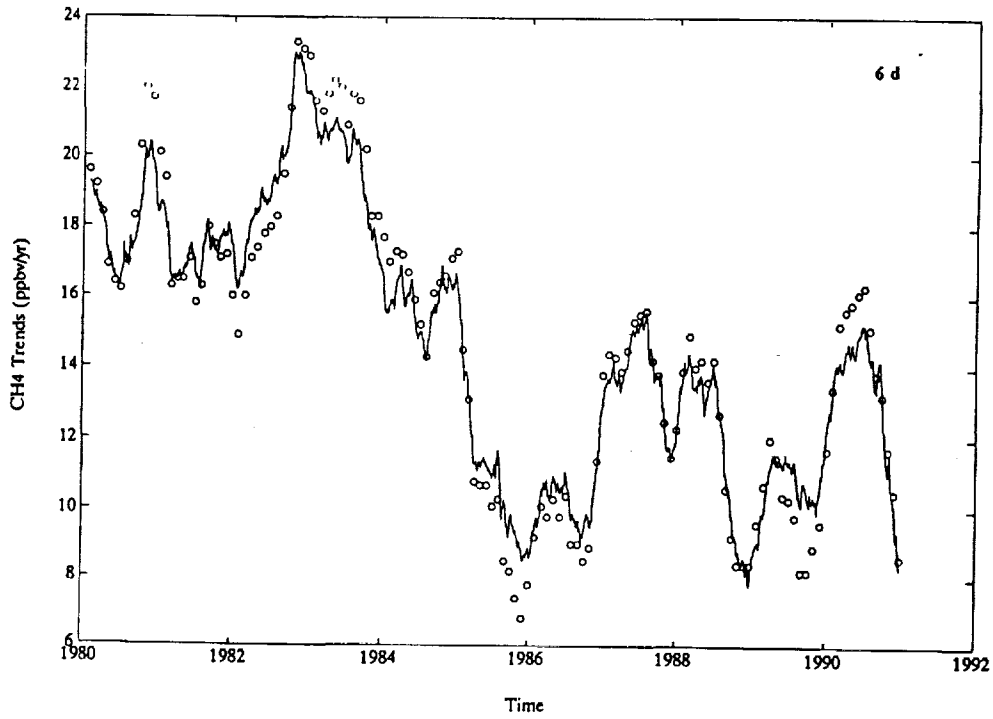

Fig. 6. (continued)

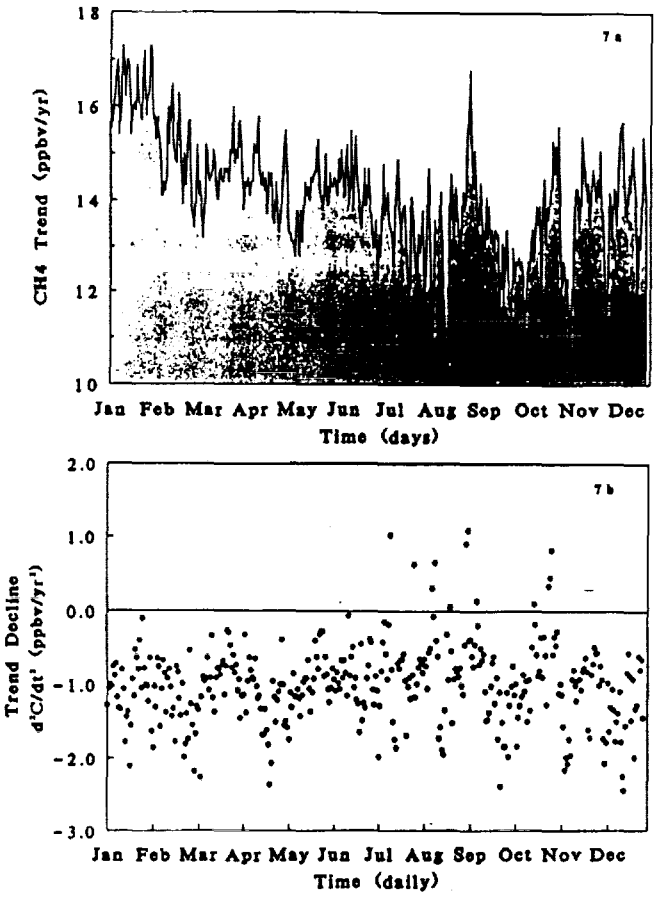

Fig. 7. The trends of methane during each day of the year. The concentrations on January 1 of every year during the experiment constitutes a 13-point time series. Similarly, every day of the year is a different time series. Each such time series is analyzed to determine the trends by a quadratic formula. (*a*) The average trend on each day of the year during the experiment. (*b*) The decline of trend for each day of the year ($d^2C_J/dt^2 = 2c$), where C_J is the coefficient of the quadratic formula for each day (designated by J).

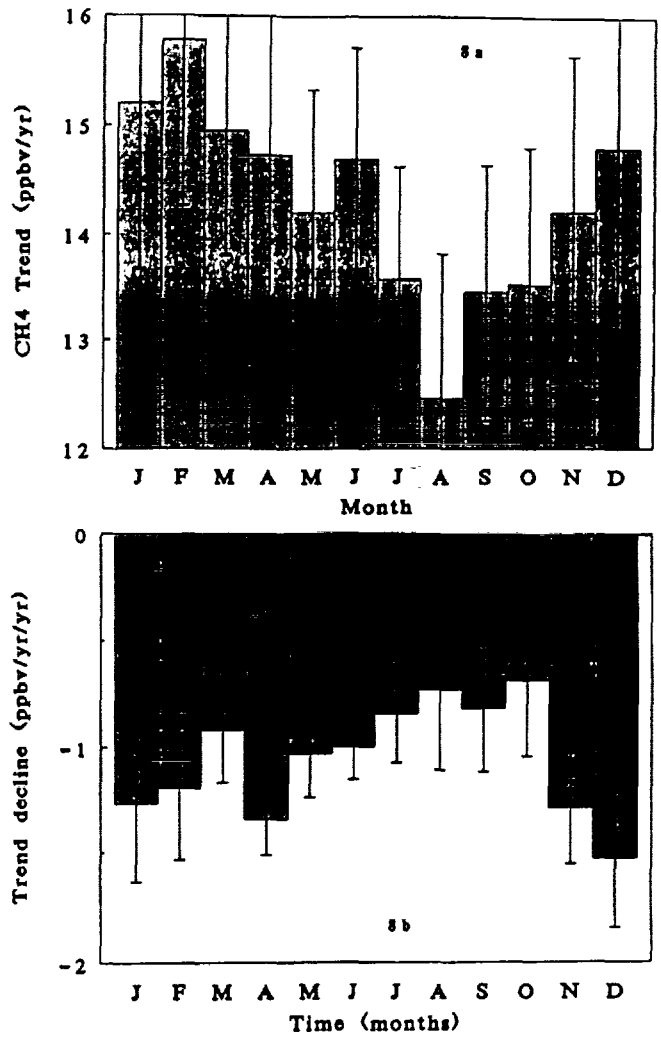

Fig. 8. The trends of methane for each month of the year. Same as Figure 7 except these results are for monthly-averaged concentrations instead of daily averages.

believe that this difference is of no practical importance for most applications.

There are five features of the data that have seasonal variations: the concentrations, the variability (standard deviations) of monthly concentrations, the diurnal patterns, the rate of change, and the cycle of emissions (which will be discussed in section 5). Of these, the sources, the standard deviations, and the diurnal variations have patterns of seasonal variation that are similar (correlated), all are at their highest during the summer and early fall. The correlation coefficients between the average seasonal cycles of these three factors are between 0.6 and 0.8. Taken together these features may mean that there are regional sources that are effective during the day and occur primarily in summer and early fall (July - October). Such emissions would then cause greater variability of atmospheric concentrations, would lead to larger emissions (per month), and would show diurnal variations during the late summer and early fall.

4. Calibration and Verification Issues

4.1. *Stability of Calibration Standards*

Measurements of methane are obtained by comparing the response of a GC/FID instrument to ambient samples and to

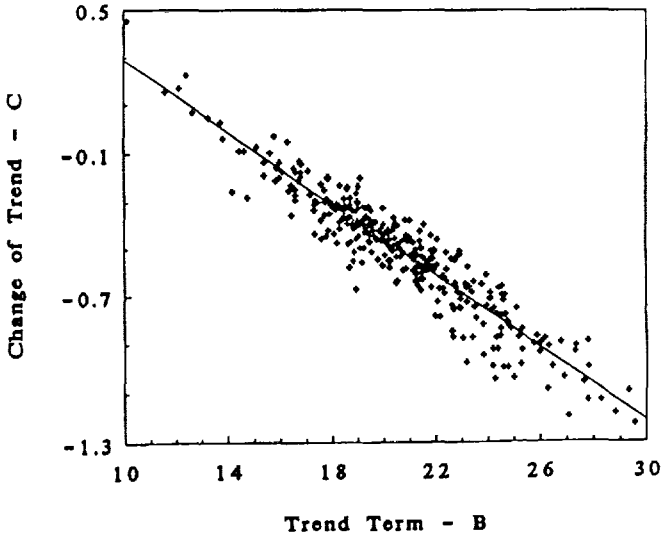

Fig. 9. The relationship between the initial rate of increase and the rate of decline in the trend based on the analysis daily-averaged data shown in Figure 7. These results show the relationship between b_J and c_J, where J indexes each day of the year and b_J and c_J are derived from the quadratic equation of the trend for each day.

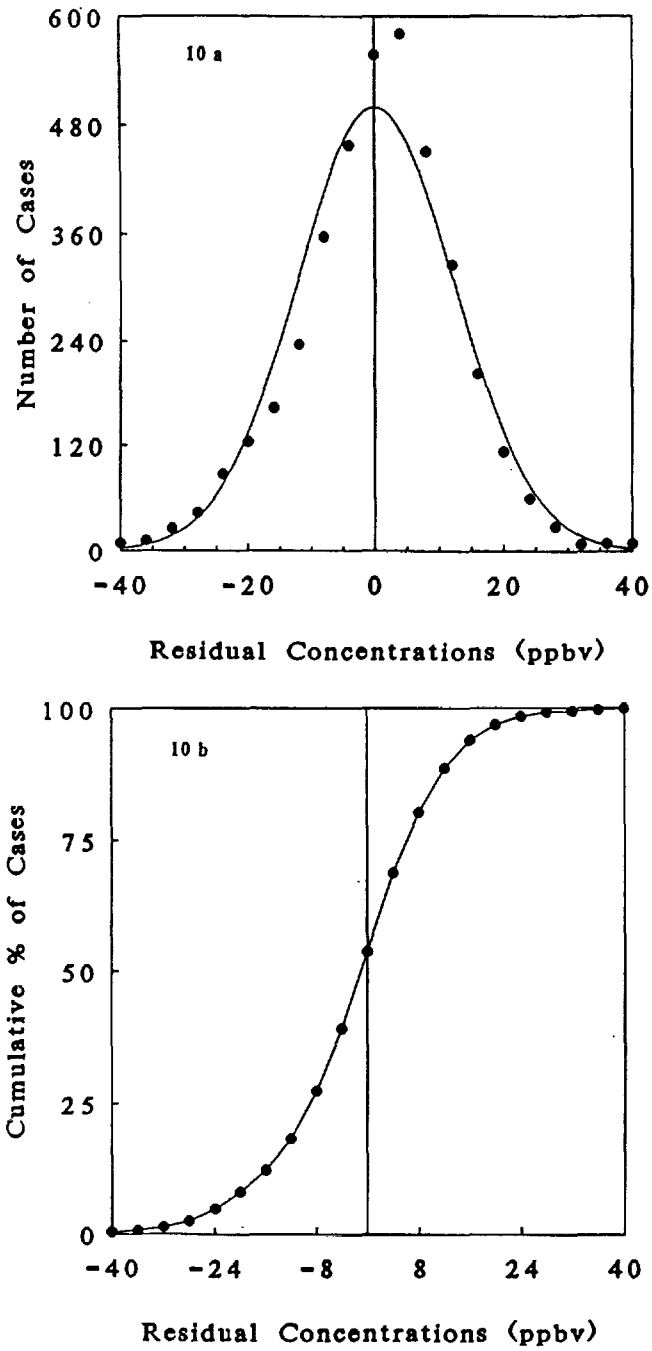

Fig. 10. Distribution of the residual daily average concentrations after trends, seasonal cycles, increase of cycle amplitude and interannual variabilities are subtracted from the data. (*a*) Frequency distribution. The solid line is the expected normal distribution with the same mean (= 0) and standard deviation (12 ppbv) as the distribution of observed residuals. The distribution of observed residuals has both skewness and kurtosis. (*b*) The cumulative frequency distribution of the daily-averaged residuals. From this graph, readers may estimate the spread of the residuals.

samples taken from precisely calibrated air stored in high pressure stainless steel (calibration) tanks as in (1). For long-term measurements it is crucial that the calibration not change over time (stability). If the calibration drifts, an apparent trend will appear in the measurements that does not represent increases or decreases in the atmospheric concentration. Furthermore, continuous measurements such as reported here depend also on secondary calibration standards that are used in the field and are calibrated against the standards kept in the laboratory. During the course of long experiments, several primary and many secondary calibration tanks are used, although all may be tied to the first or some intermediate single calibration standard.

During the course of this experiment, 11 primary calibration standards were used over periods of a year or more. The earliest tank is 0-002, derived from the dilution of a standard purchased from Scott Research Laboratories (933) (used between 1978 and August 1980). Tanks 0-111, 0-110, and 0-132 were made from another Scott standard (321) (used between August 1980 and July 1983). Tanks 0-213, 0-271, and 0-264 were derived from 0-132 and later tanks (used between July 1983 and December 1985). The remaining primary calibration tanks were derived from NBS-SRM 982 (National Bureau of Standards, now NIST, Standard Reference Material; used from January 1986 to the present). All data reported here are referenced to the original Rasmussen scale, which may be converted to the NBS (or NIST) scale by multiplying by 1.00927.

The primary calibration tanks mentioned above were measured periodically against the NBS standard (when it became available) or another standard that was later calibrated against the NBS-SRM 982. These measurements were to determine changes and drifts in concentration; none were found. The results of the periodic analyses are shown as percent differences from the originally measured concentrations for the 11 tanks used between 1979 and the present (Figure 12). The deviations appear to be random fluctuations of which 88% lie within ±0.5% of the originally measured values. For example, the original tank 0-002 changed by −0.3% between two measurements taken 11 years apart (August 1981 and August 1992). The trends of CH_4 concentrations in the calibration tanks, in percent per year, are

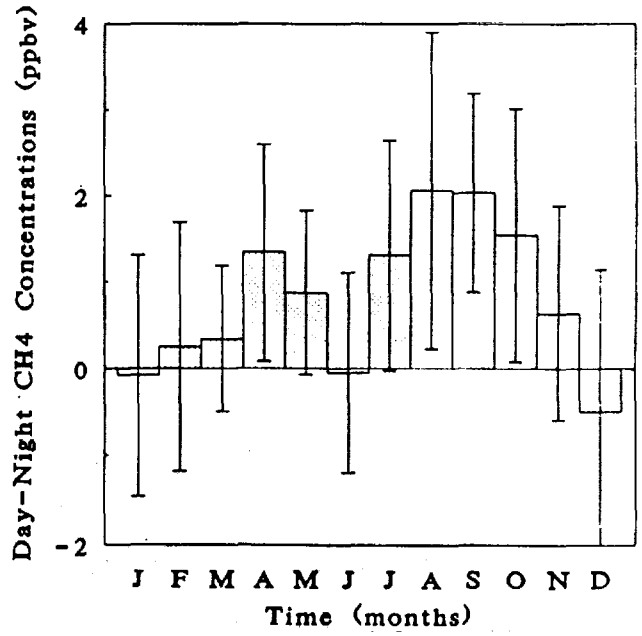

Fig. 11. Diurnal variations of methane concentrations at Cape Meares. The diurnal variations are small, with significant differences only during April, August-October. During this time day concentrations are higher than nighttime values.

TABLE 2. Parameters of the Statistical Model for Continuous Measurements of CH_4 at Cape Meares, Oregon

Trend	a	b	c	λ
Daily	1590 ± 28	0.057 ± 0.0014	-3.6E-06 ± 3.0E-07	9.6E-5 ± 2.3E-5
Monthly	1590 ± 11	1.77 ± 0.08	-0.0036 ± 0005	0.004 ± 0.002
Cycles	**α**	**ω**	**φ**	**T**
Daily	10.7	0.0172	1.24	365.2
	10.3	0.0344	3.95	182.6
	4.2	0.0516	0.5	121.4
Monthly	10.4	0.52	1.51	12
	9.6	1.05	4.42	6
	3.4	1.57	1.39	4
Interannual Variability	**α**	**ω**	**φ**	**T**
Daily	2.4	0.0119	6.15	527.6
	2.4	0.0027	2.39	2374
Monthly	2.6	0.08	2.31	78
	3.4	0.36	0.07	17.3

Variance	C	$C-C_{Tr}$	$C-C_{Tr}-\langle C_{cyc}\rangle$	$C-C_{Tr}-C_{cyc}$	Residual
Daily,					
ppbv,	56	17	12.8	12.7	12.4
%	3.3	1	0.75	0.75	0.73
Monthly,					
ppbv,	56	12.3	6.75	6.7	5.9
%	3.3	0.7	0.4	0.39	0.35

Units: The units of "a", "b", "c," and λ are ppbv, ppbv/day, ppbv/day^2, and ppbv/day for daily-averaged data and ppbv, ppbv/month, ppbv/month^2, and ppbv/month for monthly-averaged data. The units of α, ω, φ, and T are ppbv, radians/day, radians and days for daily-averaged data, ppbv, radians/month, radians and months for the monthly-averaged data.

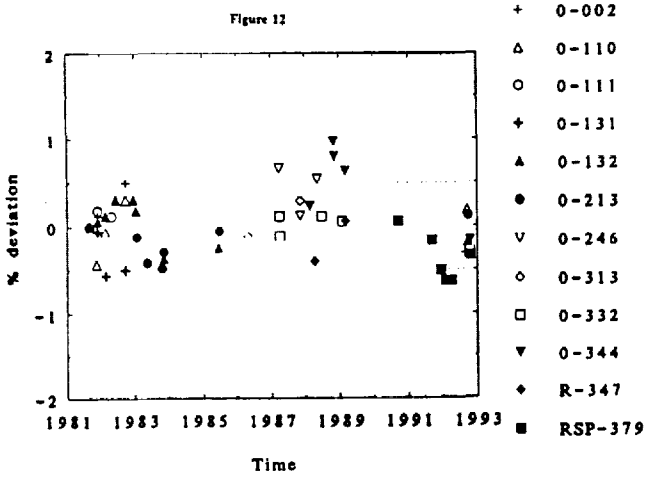

Fig. 12. Time course of concentration changes in primary calibration tanks. The dotted lines mark ±0.5% changes. Most fluctuations are within ±5%. Note that tanks were put together at different times.

shown in Figure 13. Most tanks have trends less than 0.1%/yr and are not statistically significant. For instance, the original tank 0-002 shows a CH_4 trend of −0.05% ± 0.09%/yr. For all practical purposes we can assume that the primary calibration tanks used in this study did not drift or fluctuate in concentrations enough to affect the methane measurements at Cape Meares. Further discussion of the calibrations is contained in the microfilm appendix of our earlier paper [*Rasmussen and Khalil*, 1981].

4.2. *Comparisons With an Independent Data Set*

Another way to unequivocally verify the accuracy of the trends is to compare the continuous data with an independent data set. We were able to construct such a data set of

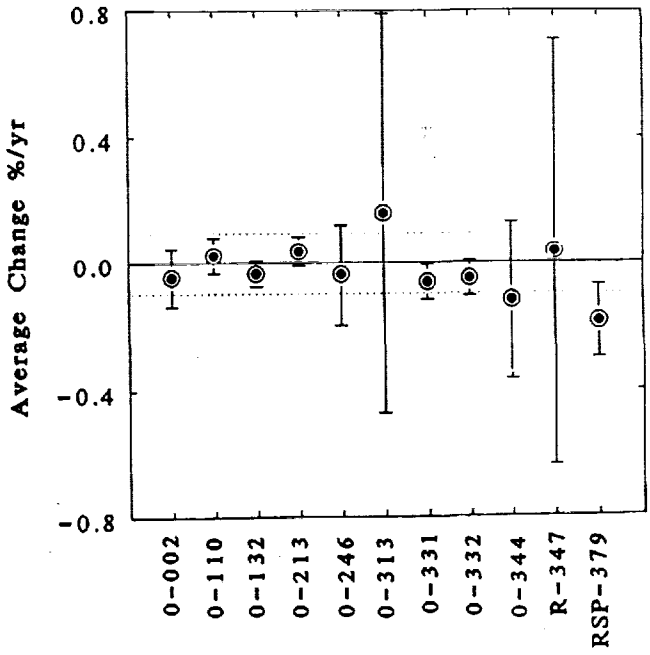

Fig. 13. Estimates of drifts (or trends) of methane in the primary calibration tanks. Most values are within ± 0.1%/yr and are not statistically significant.

methane concentrations at Cape Meares. It is, of course, not of comparable frequency or duration.

The independent time series consists of combining two data sets. The first is from the NOAA/CMDL network that includes Cape Meares, Oregon, and spans 1983-1989 (these data are publicly available (NOAA/CMDL, 1990). The samples are taken in glass flasks at Cape Meares and some 20 other locations and analyzed at NOAA/CMDL laboratories in Boulder, Colorado. In addition, we have been storing high-pressure samples of air from Cape Meares (and other locations) in 36-L stainless steel tanks similar to those used for the calibration standards. Numerous experiments (including the tests of calibration stability discussed in the previous section) have shown that such tanks can preserve methane concentrations over decadal time scales. We had 217 stored air samples from Cape Meares between 1978 and recent times. To support the present study, we measured the methane concentrations in these tanks. Methane in these tanks was measured against a single standard (referenced to NBS-982), and the whole experiment was done over a 6-week period. This method gives us a snapshot of the trends of methane (or any other gas) in tanks containing air collected over a long time. The results are not affected by changes or possible drifts of standards.

It happened that we had a good distribution of stored air before 1984 but a much lower number of samples afterwards. During some years crucial for the verification of the trends, particularly 1985-1989, we had almost no stored air. Therefore, the stored air tanks by themselves were not adequate for verifying the results of the continuous data. By combining these data with the NOAA/CMDL flask sample data, we obtained a composite data set that was suitable for validating the main features of the trends in the continuous data. We took monthly averages of both these data sets to construct the composite data. For the measurements on stored air we accepted a monthly average only if there were three samples collected during the month to make the monthly averages compatible with the NOAA/CMDL data. The two data sets were complementary, with the stored air representing the earlier and later concentrations (before 1984 and after 1989) and the NOAA data representing the intervening years. The results are shown in Figure 14. It is apparent that the independent data set constructed here agrees well with the continuous methane measurements as monthly averages.

We calculated the parameters of the model described by (2)-(6) using only the trend (quadratic), seasonal cycles, and residuals (no IAV or changes of cycle amplitude). We then interpolated the values for the missing months by substituting the values calculated from the model equations (2)-(6) including the addition of random fluctuations with mean 0 and standard deviation of ϵ = 10.6 ppbv, which, as expected, is much larger than for the continuous data. All of the numbers in these equations (trend, cycle, and residuals) were determined from the NOAA/CMDL+stored air composite data set and not from the continuous measurements. So the resulting interpolated data had no dependence on the continuous measurements or the effects of calibration standards used to obtain the continuous data. The results were as follows: a = 1591 ± 18 ppbv, b = 1.69 ± 0.23 ppbv/month, c = −0.0033 ± 0.0017 ppbv/month^2; (α in ppbv, ϕ in radians/month) for periods of 12, 6, and 4 months are (14.9, 1.35), (8, 4.61), and (3, 0.74), respectively. These values may be compared to results for the monthly averaged continuous data in Table 2.

Next we calculated the running slopes as discussed earlier but now applied to the interpolated composite data set. The results are shown in Figures 15*a* and 15*b*. It shows trends over 2- and 3-year overlapping periods of time. The agreement with the results from the continuous measurements is apparent. In particular, the somewhat abrupt decrease of trend between 1984 and 1986 is verified by the independent data set. Similarly, the magnitude of the large net change of trend between 1979 and the present is also verified to be from around 20 ppbv/yr down to about 10 ppbv/yr (actual results from the composite data are 21 ± 6 ppbv/yr for the first 3 years, from 1979 to 1982, and 11 ± 8 ppbv for the last 3

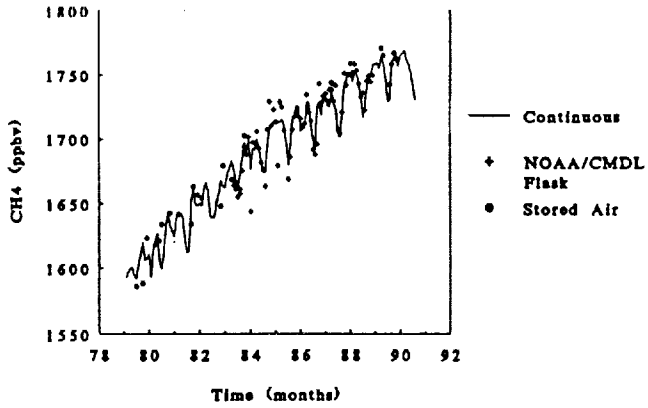

Fig. 14. Independent data from Cape Meares used to corroborate the main features of the continuous measurements.

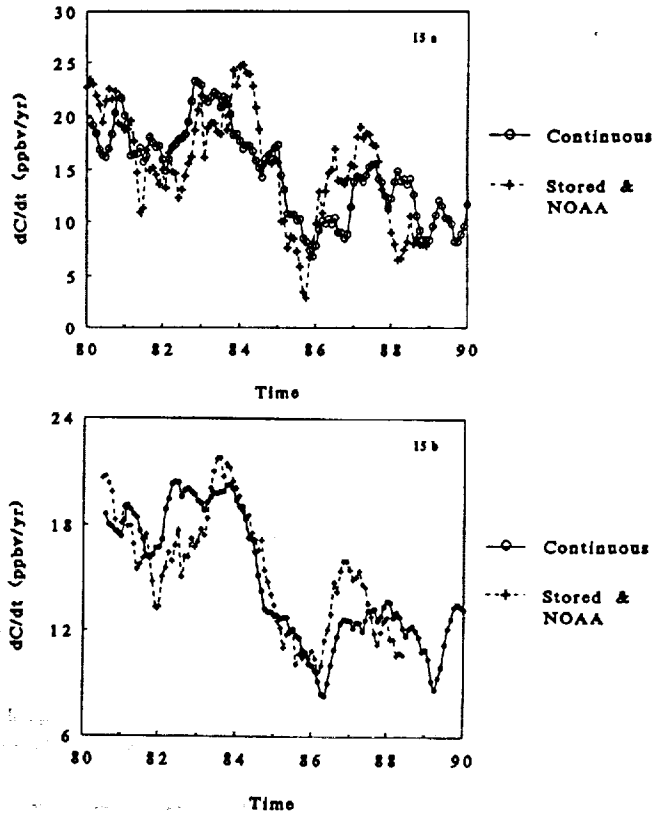

Fig. 15. Running slopes of methane concentrations at Cape Meares based on continuous data and compared to the independent data described in the text. (*a*) For 2-year periods and (*b*) for 3-year periods. Both data sets show somewhat abrupt changes of trend and a decline from around 20 ppbv/yr in the early part of the data to around 10 ppbv/yr in the later data.

years, from 1987 to 1990). The agreement between these independent data and the continuous measurements lends considerable support to the validity of the high-resolution data base.

We note for completeness that there is yet another data set on methane at Cape Meares based on our flask sampling program. These data come from weekly samples taken between 1981 and the present. We have not used these measurements here because they are not entirely independent of the continuous measurements. They are based on the same calibration standards and the changes of standards during the course of the experiment, as well as periodic cross calibrations with the continuous measurements.

5. Causes and Implications of Trends and Cycle Variations

5.1. *Estimates of Seasonal Emissions*

We consider next the emission and removal rates of methane and the possible reasons for the existence of the trends, seasonal cycles, and the increase of cycle amplitude. A local mass balance of methane in the middle- and high-latitude quadrant of the Earth's atmosphere (30°-90°N), represented by Cape Meares, may be written as

$$S = dC/dt + C/\tau(t) + (C - C_T)/\tau_T(t) \quad (9)$$

$$\tau(t) = [\tau_{OH}^{-1} + \tau_S^{-1}]^{-1} \quad (10)$$

where S are the emissions in ppbv/yr or Tg/yr, C is the concentration, $\tau_{OH}(t)$ is the atmospheric lifetime due to reactions with OH, $\tau_S(t)$ is the lifetime due to removal of methane by soils, and τ_T is the transport time between the middle latitude quadrant and the Northern tropical quadrant (where the concentration is C_T).

In (9), S is put on the left-hand side because data are most deficient for defining emissions, even though emission rates from many sources have been experimentally measured. For this reason, our aim will be to calculate the emissions from the knowledge of the other factors in this equation. The other quantities, on the right-hand side are at present, amenable to experimental and theoretical analysis and estimation. The concentrations (hence C, dC/dt and $(C-C_T) = \Delta$) are measured quantities, τ_T can be determined from observations of winds, turbulence and tracers, and $\tau(t)$, the atmospheric lifetime, can be calculated by using photochemical or other models for OH, recognizing that 80-90% of the methane is removed from the atmosphere by reacting with tropospheric OH radicals. The average concentrations of OH radicals are constrained by the budget of CH_3CCl_3. The possible effect of soils will be discussed later. Calculations based on (9) and (10) are highly constrained by observations (C, $\tau(t)$, and $\tau_T(t)$), particularly observations of methane concentrations at Cape Meares, and are easily reproducible, allowing readers to reevaluate our conclusions. The atmospheric lifetime of methane varies according to the seasonal and latitudinal variations of OH concentrations. The OH concentrations can be obtained from photochemical models such as the one described by *Lu and Khalil* [1991] or the results tabulated by *Spivakovski et al.* [1990]. From these calculations it appears that the average lifetime of methane in the northern quadrant (30°-90°) of the atmosphere is about 2.2 times longer than the lifetime in the equatorial quadrant (0°-30°). From the calculated average OH concentrations and the small effect of the soil sink, the global atmospheric lifetime of methane is between 10 and 12 years, so that the lifetime in the northern quadrant is between 16 and 19 years. This lifetime varies seasonally being shortest in the local summers (8-10 years) and longest (60-70 years) in the winters. The destruction rate, which is the inverse of the lifetime (1/yr), is 0.0167, 0.056, 0.012, and 0.06 in the four seasons from winter to fall in the northern quadrant [*Lu and Khalil*, 1991; *Spivakovski et al.*, 1990]. These are taken to represent the middle of the seasons and the rates for the rest of the months are obtained by linear interpolation.

The (intrahemispheric) transport time results from the motions of the winds and turbulent transport processes. While the average transport time is about 70-80 days, the seasonal variations are quite difficult to define precisely for the type of model in (9). Fortunately, the seasonal variations of transport do not have a large effect on the calculated emission rates (although it does effect the expected seasonal cycle of the concentration). The seasonal variations of the transport are discussed by *Cunnold et al.* [1983], *Newell et al.* [1969], and *Khalil and Rasmussen* [1983]. Here we take the seasonal transport times to be 61, 65, 113, and 80 days for winter to fall seasons. The transport times are linearly interpolated for the transition months between the middles of the seasons.

The other term in the transport part of (9); namely, $\Delta = C - C_T$ happens to be approximately constant at 37 ± 3 ppbv where the concentration for C_T are from measurements taken at Mauna Loa and Cape Kumukahi in Hawaii from 1981 to 1986. There are no trends or seasonal variations in Δ during this period. We chose to take this constant value of Δ rather than use the actual measured concentrations at Hawaii primarily because the certified data at Hawaii span a much shorter time (5 years) compared to the Cape Meares data base, which spans 13 years.

The effect of the "soil sink" is not explicitly included in the calculations because there are no data to assess its hemispherical-scale seasonal variation or even the magnitude of the effect. Globally, 10-50 Tg/yr are believed to be removed by soils. Since a large fraction of the land mass is in the region of our mass balance, the role of the soil sink may be important. We expect that the sink, which requires dry, active soil conditions, is most effective during summers and least effective during winters. In this case, the soil sink would reinforce the seasonal cycle of emissions found from the seasonality of OH.

Using the measured monthly-averaged concentrations at Cape Meares for C and dC/dt, we follow these steps in our analysis: We calculate the emissions from (9) based on the values of the remaining variables already described (seasonally varying OH and transport times are assumed throughout). This gives us a monthly time series of emissions that is analyzed by a model analogous to (2), or S = Trend + Seasonal Variation + Residuals, from which we estimate the seasonal variations of the emissions. We used several different time series for the concentrations in (9). We took just the trend represented by (3) to see what emission patterns would be needed to explain it (in this case $dC_{Tr}/dt = 2ct$). Then we took $C = C_{Tr} + \langle C_{cyc} \rangle$ to see the effect of adding the average seasonal cycle; next we took the concentration to be $C_{Tr} + C_{cyc} + C_{IAV}$, which represents the full model without the residuals. These calculations using the parametric model of the concentrations were carried out for a lifetime of 16

years (in this quadrant) and the dC/dt term was calculated explicitly by differentiating the appropriate formulae. The ability to explicitly calculate derivatives and integrate is an advantage of the parametric model. In the last two calculations, we used the full model $C = C_{Tr} + C_{cyc} + C_{IAV}$ but for average lifetimes of 12.8 and 19.2 years (representing global average lifetimes of 8 and 12 years).

From the calculations shown in Figure 16, it is evident that sizeable seasonal variations in the emissions of methane are required to explain the observed seasonal cycle of concentrations. Annual emission from this region add up to about 200 Tg/yr based on our model. Both the annual emissions and the seasonal variations of the emissions are close to our original estimates [*Khalil and Rasmussen*, 1983].

It is noteworthy that these calculations do not require the annual average emissions to be increasing during the last 13 years to explain the Cape Meares data. Apparently, methane emissions from this quadrant were substantially out of balance with ambient concentrations so that even though the emissions may not be increasing anymore, concentrations will continue to rise, asymptotically, approaching a new equilibrium value. The stable annual emission rates from this quadrant are probable, since large sources controlled by human activities such as cattle and rice agriculture have not increased during this time. Furthermore, the calculated seasonality of emissions is consistent with the current data on the seasonal emissions from wetlands and rice fields [*Aselman and Crutzen*, 1989; *Matthews*, 1993; *Khalil et al.*, 1991].

To further explore the role of seasonal emissions in determining the observed seasonality of methane at Cape Meares, we did the following calculations: We took the average emissions from the previous calculations just described (which are about 17 Tg/month for a global lifetime of 10 years or 16 Tg/yr for a lifetime of 12 years). Next we calculated the expected concentrations under several assumptions with a finite difference form of (9):

$$C(n+1) = [1+1/\tau(n)]C(n) + S(n) + [1/\tau_T(n)]\,\Delta C \quad (11)$$

First we assumed that the emissions were constant at the average rates $S(n) = S$ and $\tau_T(t)$ is constant, so that there are no seasonal cycles in transport or emissions (but the seasonal cycle of OH is always included). We then calculated the expected concentrations by (11) (base case). Next we included the seasonal variation of the transport times and calculated the expected concentrations (base case + transport). We then repeated the previous two calculations but we added an increase of OH (resulting in a decreasing lifetime of methane) at 1%/year. The results are shown in Figure 17.

The main conclusions are: First, the seasonal cycle calculated using the seasonal cycle of OH alone (no cycle for transport) is clearly out of phase with the observed seasonal cycle of concentrations. Curiously, the amplitude of the seasonal cycle of concentrations imposed by the cycle of OH is about the same as the observed seasonal cycle. The remaining observed cycle of concentrations must be driven by seasonal variations of emissions and transport.

Adding the seasonal cycle of transport does not substantially improve the agreement but reduces the amplitude of the calculated cycle, leaving a substantial role for the seasonal cycle of emissions in determining the observed seasonality of concentrations. The seasonal source cycle required to explain the observations is shown earlier in Figure 16.

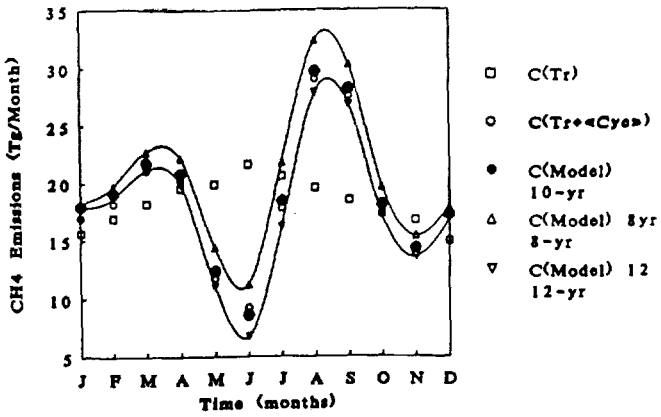

Fig. 16. The seasonal cycle of the emissions of methane from the region 30°-90°N. The estimate of emissions is derived using a mass balance model that is highly constrained by observations. Highest emissions occur during the late summer and early fall.

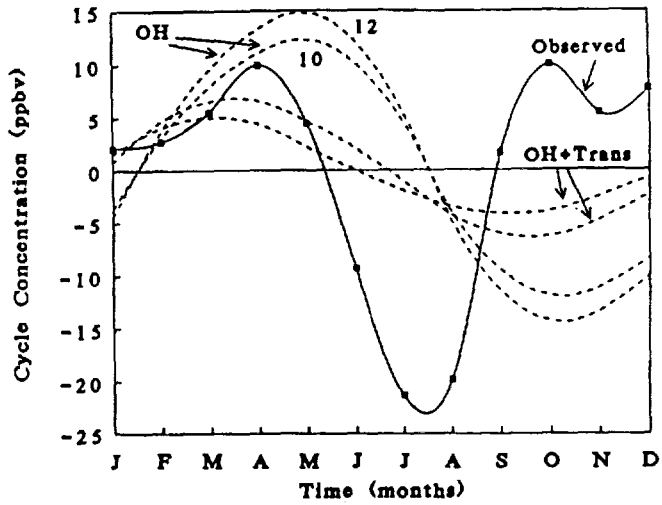

Fig. 17. The seasonal cycle of methane: expected and observed. The seasonal cycle of OH and transport does not explain the cycle of the source calculated by a mass balance model. A significant seasonal cycle of emissions is therefore required to explain the observed seasonal cycle of methane.

Adding a trend of OH at 1%/yr does not much affect the conclusions regarding the average seasonal cycle of observed concentrations. The addition of an increasing trend of OH requires that the emissions in this quadrant also must be increasing. Such increases are difficult to verify from the current knowledge of the sources.

These calculations also provide insights on the increase of cycle amplitude. The cycle amplitude is expected to increase as the concentration rises. This is so because the rate of removal of methane is $C/\tau_{OH} = -K[OH]C$ as in (9) and (10). As the concentration rises, more methane is removed during the peak of the OH concentration creating a larger dip in concentration each summer. According to our calculations described above, this effect amounts to about a 2 ppbv change in the cycle amplitude over the 13 years of the data. If we add increasing OH at 1%/yr, the change in cycle amplitude is about 5 ppbv during the last 13 years. The measured change of amplitude is about 10 ppbv over this time. Therefore only a small amount of the change of cycle amplitude is explained by the increasing concentration, and a little more is explained by

the dubious possibility of fast rising OH concentrations. It seems, then, that a large part of the increase in cycle amplitude is driven by seasonal changes in methane emissions in the northern quadrant of the Earth's atmosphere. The magnitude of the changes in emissions needed to explain the change of cycle amplitude are small and generally require some increase of emissions during late summers and small decreases during other seasons.

5.2. *Spatial Scales Associated with the Cape Meares Methane Time Series.*

We have discussed many features in the continuous methane data taken at Cape Meares. These features span time scales from diurnal variations to interannual variability. As usual, the temporal scales of variability are correlated with the spatial scales of the processes that produce the observed cycles. There is little doubt that the long-term increase, its recent declining rate and probably the interannual variations are representative of very large scale phenomena spanning this hemisphere and close even to global average trends. Similarly, diurnal variations and submonthly variability are probably representative of local and regional effects of undefined but relatively small spatial scales. This leaves seasonal cycles and their long-term variability, which is neither clearly representative of the northern semihemisphere nor of local or regional scales.

We have used the seasonal variation as a principal factor in the mass balance of the previous section and the claim of significant seasonal cycles in emissions deconvoluted from the measurements taken at Cape Meares. Cape Meares is far from populated areas and affected mostly by winds from over the Pacific Ocean. It is "upwind" of Portland, Oregon, and separated from it by the coast range. We therefore expect that Cape Meares is representative of concentrations over a very large spatial scale, but is the Cape Meares seasonal cycle representative of this semihemisphere?

To answer this question, we again used the independent methane data base from the NOAA/CMDL network. In this network there are eight stations between 30°N and 67°N representing the middle northern latitudes and three stations in the northern polar latitudes (we have added Sable Island, making 12 stations in all). These sites and their north latitudes and longitudes are Alert, NWT-Canada (82.45, 62.5), Azores-Terceria Is. (38.75, 27.08), Barrow, Alaska (71.32, 156.6), Cold Bay, Alaska (55.2, 162.7), Cape Meares, Oregon (45, 124), Mould Bay, NWT-Canada (76.23, 119.33), Niwot Ridge, Colorado (40.05, 105.63), Olympic Peninsula, Washington (48.25, 124.75), Shemya Is., Alaska (52.72, 185.9), Ocean Station M (66, 358), and Sable Island, Canada (44, 59.8), which is not a NOAA site but is in our long-term flask sampling network. Measurements are available between 1983 and 1989, but not all sites have measurements throughout this period.

We treated the data according to our general model described in (2)-(5) and determined the seasonal cycles. Then we took the average of the seasonal cycle at the middle latitudes and the average for the polar latitudes. Finally, we obtained the composite seasonal cycle for the northern semihemisphere as an area weighted average so that the semihemisphere cycle = 0.84 x middle latitude cycle + 0.16 x polar latitude cycle. In calculating this cycle we have not included the continuous data from Cape Meares, but we have included the NOAA Flask data from Cape Meares. The semihemisphere cycle according to these calculations is shown in Figure 18 along with the cycle from the continuous measurements at Cape Meares for the same period of time (1983-1989). The Cape Meares cycle is close to the semihemispherical average cycle. It differs in several details from the polar cycle, but the polar cycle makes only a small contribution to the semihemispherical average, so Cape Meares may be taken to represent this region. The only substantial differences between the Cape Meares cycle and the semihemispherical cycle arise in winter and early spring (December, January, February, and March). These differences do not greatly affect our conclusions on the seasonal emissions required to explain the seasonal cycle of concentrations at Cape Meares. The deconvoluted source is shown in Figure 19 in which we have used the semi-hemispherical average cycle to calculate seasonal emissions and compare it to the results of the previous section using continuous data only from Cape Meares.

6. CONCLUSIONS

The detailed methane data taken at Cape Meares during the last 13 years contain many prominent features as well as many details. The prominent features are the seasonal cycles and the increasing trend including the slowdown in the rate of accumulation. In addition to these features there are other

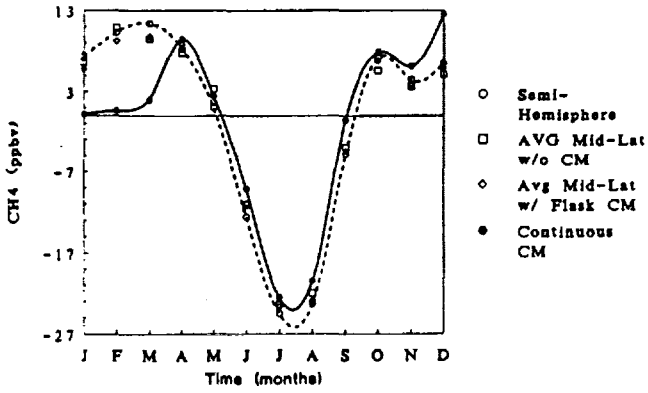

Fig. 18. The seasonal variation of methane at Cape Meares compared to the average seasonal cycle in the northern quadrant of the Earth's atmosphere (30°N-90°N). The average cycle is based on 12 stations and 5 years of measurements.

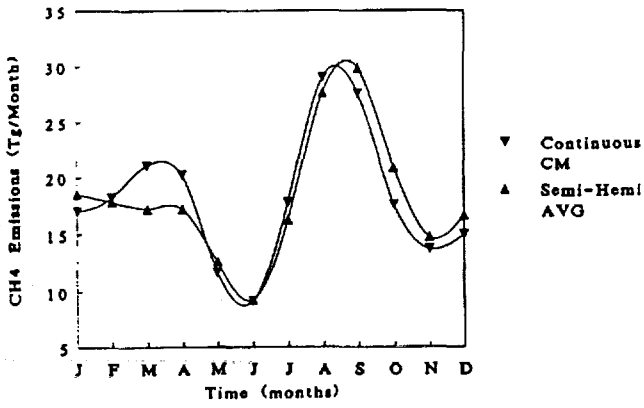

Fig. 19. The estimated seasonal source of methane in the northern quadrant (30°N-90°N) based on the seasonal cycle from the Cape Meares continuous data and the average cycle shown in Figure 18.

smaller effects. These are the increase of cycle amplitude, interannual variations, diurnal variations and its seasonal cycle and the seasonal cycles in the variability of concentrations. While these effects do not greatly influence the atmospheric concentrations, they provide unique information on the sources and sinks of methane from the middle northern latitudes which probably is the region of largest methane fluxes in the world because of the large land mass and population. Moreover, these features provide opportunities to test and tune detailed photochemical or transport models for methane and OH.

To explain the observations requires seasonally varying sources with highest emissions occurring in late summer and early fall. Annual emissions are not required to increase in order to explain the observed trends. These features quantitatively agree with assessments of the seasonality and trends in the emissions from sources such as cattle, rice agriculture, and the wetlands.

Cape Meares is the earliest station for continuous automated measurements of methane and other stable trace gases. While the experiment has provided much information on atmospheric methane, it has also provided valuable experience on implementing automated long-term measurements of trace gases in the Earth's atmosphere. The data discussed here are a prototype of the high-precision and high-frequency measurements that can be obtained from such experiments at various ground-based sites. The most important prerequisite to obtaining such measurements is producing calibration standards that are stable for decades and producing many reliable secondary standards that are used in the experiment over the years. A flask-sampling methodology is a direct competitor of the continuous automated measurements strategy that has distinct advantages that will be analyzed and discussed in subsequent papers.

The data are archived at the Carbon Dioxide Information and Assessment Center (CDIAC) and may be obtained by writing to the Carbon Dioxide Information and Analysis Center (CDIAC), Oak Ridge National Laboratory, Oak Ridge, TN 37831-9984. The data at CDIAC are in three tables that can be directly retrieved into the computer. Table 1 contains time and continuous data in ASCII format. Table 2 contains the time, daily average concentration, standard deviations (of daily concentrations), number of data during each day, and a column with interpolated data as described in section 3.6. The interpolation is used to fill gaps when samples were not collected. Table 3 contains monthly-averaged data and 90% confidence limits of the mean. Data based on the three averaging methods discussed earlier are included and are the same as Table 1 of this paper. The report by Khalil and Rasmussen [1992] and this paper are the primary reference for these data.

Acknowledgments. The Cape Meares station has been operating for about 15 years. During this time, many of our research staff have made valuable contributions to this experiment. In particular, we thank D. Pierotti, D. Joseph, S. Crawford, J. Mohan, D. Stearns, and R. Dalluge for experimental work and D. Joseph, P. Turner, and M. Shearer for data management. There has been no continuous or systematic financial support for this project. During some periods, grants have provided either full or partial financial support to the methane measurements program at Cape Meares Station. In particular, financial support was provided by the National Science Foundation (ATM-8109047), National Aeronautics and Space Administration (NAGW-1348, NAG-1-35, NAG-1-160), and the Department of Energy (DE-FG06-85ER6031). Some of the recent work was supported by the Environmental Protection Agency through a contract to Andarz Company for modeling and data analysis (contract 1D3216NASA). Additional support was provided by the resources of the Biospherics Research Corporation and the Andarz Co. The authors and not the sponsors are responsible for the contents, interpretations, and opinions expressed in this paper.

REFERENCES

Aselman, I., and P. J. Crutzen, Global distribution of natural freshwater wetlands and rice fields, their net primary productivity, seasonality and possible wetland emissions, *J. Atmos. Chem. 8*, 307-358, 1989.

Cunnold, D. M., R. G. Prinn, R. A. Rasmussen, P. G. Simmonds, F. N. Alyea, and G. A. Cardelino, The Atmospheric Lifetime Experiment, 4, Results from $CFCl_3$ based on three years of data, *J. Geophys. Res., 88*, 8401-8414, 1983.

Hollander, M., and D. A. Wolfe. *Nonparametric Statistical Methods*, John Wiley, 1973.

Intergovernmental Panel on Climate Change, *Climate Change*, edited by J. T. Houghton, G. J. Jenkins, and J. J. Ephraums, Cambridge University Press, New York, 1990.

Kendall, M., and J. K. Ord, *Time Series*, Edward Arnold, Kent, England, 1990.

Khalil, M. A. K., and F. Moraes, *Spectral analysis of time series*, Rep. 93-61, Oregon Graduate Institute, Portland, OR, 1993.

Khalil, M. A. K., and R. A. Rasmussen, Sources, sinks and seasonal cycles of atmospheric methane, *J. Geophys. Res., 88*, 5131-5144, 1983.

Khalil, M. A. K., and R. A. Rasmussen, The potential of soils as a sink of chlorofluorocarbons and other man-made chlorocarbons, *Geophys. Res. Lett., 16*, 679-682, 1989.

Khalil, M. A. K., and R. A. Rasmussen, Atmospheric methane: Recent global trends, *Environ. Sci Technol., 24*, 549-553, 1990.

Khalil, M. A. K., and R. A. Rasmussen, *Atmospheric methane at Cape Meares, Oregon*, Rep. 92-111, Oregon Graduate Institute, Beaverton, OR, 1992.

Khalil, M. A. K., and R. A. Rasmussen, Decreasing trend of methane: Unpredictability of future concentrations, *Chemosphere, 26*, 803-814, 1993.

Khalil, M. A. K., R. A. Rasmussen, M.-X. Wang, and L. Ren, Methane emissions from rice fields in China, *Environ. Sci Technol., 25*, 979-981, 1991.

Lu, Y., and M. A. K. Khalil, Tropospheric OH: Model calculations of spatial, temporal and secular variations, *Chemosphere, 23*, 397-444, 1991.

Madronich, S., C. Granier, Impact of recent total ozone changes on tropospheric ozone photodissociation, hydroxyl radicals and methane trends, *Geophys. Res. Lett., 19*, 465-467, 1992.

Matthews, E, Methane emissions from wetlands, in *Atmospheric Methane: Sources, Sinks and Role in Global Change*, edited by M. A. K. Khalil, Springer-Verlag, New York, 1993.

National Oceanic and Atmospheric Administration, Climate Monitoring and Diagnostics Laboratory Flask Sampling Program, in *Trends '90, a Compendium of Data on Global Change*, edited by T.A. Boden, P. Kanciruk, and M.P. Farrell, pp. 148-189, Carbon Dioxide Information Analysis Center, Oak Ridge, Tenn. ORNL/CDIAC-36, 1990.

Newell, R. E., D. G. Vincent, and J. W. Kidson, Interhemispheric mass exchange from meteorological and trace substance observations, *Tellus, 15*, 103-107, 1969.

Prinn, R. G., et al., Global average concentration and trend of hydroxyl radicals deduced from ALE/GAGE trichloroethane (methyl chloroform) data from 1978-1990, *J. Geophys. Res., 97*, 2445-2461, 1992.

Rasmussen, R. A., and M. A. K. Khalil, Atmospheric methane: Trends and seasonal cycles, *J. Geophys. Res., 86*, 9826-9832, 1981.

Shearer, M. J., and M. A. K. Khalil, The global emissions of methane over the last century, *EOS Trans., AGU 70*, Fall Meeting suppl.,

1017, 1989.

Snedecor, G. W., and W. G. Cochran. *Statistical Methods*, Iowa State University Press, Ames, 1980.

Spivakovski, C. M., R. Yevich, J. A. Logan, S. C. Wofsy, and M. B. McElroy, Tropospheric OH in a three-dimensional chemical tracer model: An assessment based on observations of CH_3CCl_3, *J. Geophys. Res.*, *95*, 18,441-18,471, 1990.

Steele, L. P., E. J. Dlugokensky, P. M. Lang, P. P. Tans, R. C. Martin, and K. A. Masarie, Slowing down of the global accumulation of atmospheric methane during the 1980s, *Nature*, *358*, 313-316, 1992.

Wuebbles, D., and J. Tamaresis, The environmental role of methane, in *Atmospheric Methane: Sources, Sinks and Role in Global Change*, edited by M. A. K. Khalil, Springer-Verlag, New York, 1993.

World Meteorological Organization, *Atmospheric Ozone, Rep. 16*, World Meteorol. Org., Geneva, Switzerland, 1985.

World Meteorological Organization, *Report of the International Ozone Trends Panel, Rep. 18*, World Meteorol. Org., Geneva, Switzerland, 1988.

World Meteorological Organization, *Scientific Assessment of Stratospheric Ozone, Rep. 20*, World Meteorol. Org., Geneva, Switzerland, 1989.

World Meteorological Organization, *Scientific Assessment of Ozone Depletion, Rep. 25*, World Meteorol. Org., Geneva, Switzerland, 1991.

M. A. K. Khalil, F. Moraes, and R. A. Rasmussen, Global Change Research Center, Department of Environmental Science and Engineering, Oregon Graduate Institute of Science and Technology, 20000 N. W. Walker Road, Portland, OR 97291-1000.

(Received December 10, 1992;
revised April 25, 1993;
accepted April 29, 1993.)

JOURNAL OF GEOPHYSICAL RESEARCH, VOL. 95, NO. D11, PAGES 18,369–18,385, OCTOBER 20, 1990

Atmospheric Emissions and Trends of Nitrous Oxide Deduced From 10 Years of ALE–GAGE Data

R. PRINN,[1] D. CUNNOLD,[2] R. RASMUSSEN,[3] P. SIMMONDS,[4]
F. ALYEA,[2] A. CRAWFORD,[3] P. FRASER,[5] AND R. ROSEN[6]

We present and interpret long-term measurements of the chemically and radiatively important trace gas nitrous oxide (N_2O) obtained during the Atmospheric Lifetime Experiment (ALE) and its successor the Global Atmospheric Gases Experiment (GAGE). The ALE/GAGE data for N_2O comprise over 110,000 individual calibrated real-time air analyses carried out over a 10-year (July 1978–June 1988) time period. These measurements indicate that the average concentration in the northern hemisphere is persistently 0.75 ± 0.16 ppbv higher than in the southern hemisphere and that the global average linear trend in N_2O lies in the range from 0.25 to 0.31% yr^{-1}, with the latter result contingent on certain assumptions about the long-term stability of the calibration gases used in the experiment. Interpretation of the data, using inverse theory and a 9-box (grid) model of the global atmosphere, indicates that the N_2O surface emissions into the 90°N–30°N, 30°N–0°, 0°–30°S, and 30°S–90°S semihemispheres account for about 22–34, 32–39, 20–29 and 11–15% of the global total emissions, respectively. The measured trends and latitudinal distributions are consistent with the hypothesis that stratospheric photodissociation is the major atmospheric sink for N_2O, but they do not support the hypothesis that the temporal N_2O increase is caused solely by increases in anthropogenic N_2O emissions associated with fossil fuel combustion. Instead, the cause for the N_2O trend appears to be a combination of a growing tropical source (probably resulting from tropical land disturbance) and a growing northern mid-latitude source (probably resulting from a combination of fertilizer use and fossil fuel combustion). The exact combination of these sources which best fits the data depends on the assumed tropospheric-stratospheric exchange rates for N_2O in the northern hemisphere relative to the southern hemisphere. Accepting a theoretically-calculated N_2O lifetime of 166 ± 16 years due to stratospheric destruction only, we deduce from the ALE/GAGE data a 10-year average global N_2O emission rate of $(20.5 \pm 2.4) \times 10^{12}$ g N_2O yr^{-1}, but with significant year-to-year variations in emissions associated perhaps with year-to-year variations in tropical land disturbance.

1. INTRODUCTION

Nitrous oxide (N_2O) is a very long-lived atmospheric species with both anthropogenic (e.g., combustion) and biogenic (e.g., soil microbes) sources whose only important recognized atmospheric sinks are stratospheric photodissociation and photooxidation. Its concentration has been observed currently to be increasing over the globe as first reported by Weiss [1981] and since confirmed by other observations [*Khalil and Rasmussen*, 1983; *Prinn et al.*, 1983; *Rasmussen and Khalil*, 1986; W. Komhyr et al., (unpublished manuscript, 1987)]. *Weiss* [1981] concluded that the observed rate of increase is consistent with combustion of fossil fuels and to a lesser extent agricultural activity as the cause of the increase. This trend in N_2O is a historically recent one since analyses of polar ice cores indicate that the N_2O mixing ratio over the preindustrial period 500 BC to 1800 AD was relatively constant at around 285–289 ppbv [*Pearman et al.*, 1986; *Khalil and Rasmussen*, 1988]. Using a simple mass balance model with an N_2O lifetime of 170 years, this rate of increase in modern times can be interpreted as indicating an approximately 40% current excess of the global N_2O annual source over its stratospheric annual sink and an approximately 50% growth in N_2O emissions from preindustrial times. The increase is of concern both because N_2O is the major stratospheric source of NO_X, which is important in catalytic destruction of stratospheric ozone [*Crutzen*, 1970; *McElroy and McConnell*, 1971], and because N_2O is one of the greenhouse gases that may contribute to future climatic change [*Wang et al.*, 1976; *Dickinson and Cicerone*, 1986].

Since 1978 we have carried out high-frequency (four to 12 measurements per day) real-time gas chromatographic measurements of N_2O at several globally distributed stations, first as a part of the Atmospheric Lifetime Experiment (ALE) and, subsequently (since late 1984), as a part of the Global Atmospheric Gases Experiment (GAGE) [*Prinn et al.*, 1983, 1987; *Cunnold et al.*, 1986; *Simmonds et al.*, 1988]. The surface measurement stations are located at coastal sites remote from industrial and urban areas and are designed to measure accurately the tropospheric trends of trace gases whose lifetimes are long compared to global tropospheric mixing times. The station locations are Cape Grim, Tasmania (41°S, 145°E), Point Matatula, American Samoa (14°S, 171°E), Ragged Point, Barbados (13°N, 59°W), Cape Meares, Oregon (45°N, 124°W), Adrigole, Ireland (52°N,

[1]Department of Earth, Atmospheric and Planetary Sciences, Massachusetts Institute of Technology, Cambridge, Massachusetts.
[2]School of Geophysical Sciences, Georgia Institute of Technology, Atlanta, Georgia.
[3]Institute of Atmospheric Sciences, Oregon Graduate Center, Beaverton, Oregon.
[4]Department of Geochemistry, University of Bristol, Bristol, United Kingdom.
[5]Division of Atmospheric Research, Commonwealth Scientific and Industrial Research Organization, Aspendale, Victoria, Australia.
[6]Atmospheric and Environmental Research, Inc., Cambridge, Massachusetts.

Paper number 90JD01439.
0148-0227/90JD-01439$05.00

10°W), and Mace Head, Ireland (53°N, 10°W). The Cape Meares station was opened in January 1980, the Mace Head station was opened in January 1987 and all other stations were opened in July 1978. The Adrigole station closed in December 1983 (the Mace Head station is a (belated) replacement).

We present in this paper the temporal and spatial variations in N_2O based on over 110,000 individual calibrated real-time ALE/GAGE air analyses carried out over a period of 10 years (July 1978 to June 1988). The ALE/GAGE data for this species are particularly useful because they are high-frequency measurements at fixed locations designed to be indicative of the four lower tropospheric semihemispheres of the globe. Using inverse methods, the observed persistent differences between N_2O concentrations and trends in each semihemisphere over this long time period are interpreted in terms of varying emissions in each semihemisphere, thus providing fundamental information on the magnitude and nature of the presently poorly quantified surface sources of N_2O. In particular, our analysis tests the hypotheses that fossil fuel combustion, which is highly concentrated in the 30°N–90°N semihemisphere, is a major source of N_2O [*Pierotti and Rasmussen*, 1976; *Weiss and Craig*, 1976] and that increases in fossil fuel combustion are the major cause of the observed global temporal N_2O increase [*Hao et al.*, 1987]. An application of the ALE/GAGE N_2O data, complementary to that presented here, involves analyzing the high-frequency variation of N_2O relative to several anthropogenic halocarbons ($CFCl_3$, CF_2Cl_2, CH_3CCl_3, CCl_4) also measured in ALE/GAGE to determine, for example, fundamental information on European sources using the Adrigole station data [*Prather*, 1985, 1988].

2. EXPERIMENT

Atmospheric N_2O is analyzed at each station by first drying the air sample with a Nafion dryer [*Fouiger and Simmonds*, 1979] and then using a microprocessor-controlled gas chromatograph equipped with an isothermal (50°C) 1.8-m column packed with 80–100 mesh Porasil D and an electron capture detector for the analysis [*Prinn et al.*, 1983]. In the initial phase of the experiment (ALE, 1978–1984) HP 5840 gas chromatographs taking four calibrated air measurements per day were used, whereas in the follow-on phase (GAGE, 1981 to present) the HP 5840 instruments were first run together with and then replaced by HP 5880 instruments taking 12 air measurements per day. Agreement between ALE and GAGE instruments for N_2O was excellent considering the fact that different calibration tanks were used for each instrument. In particular, the average magnitude of the difference between the monthly mean N_2O measurements on the two instruments was only 0.7 ± 0.4 ppbv for the 10-month overlap at Oregon, 0.6 ± 0.4 ppbv for the 9-month overlap at Barbados, 0.3 ± 0.2 ppbv for the 10-month overlap at Samoa, and 1.2 ± 0.9 ppbv for the 43-month overlap at Tasmania (1σ standard deviations). These differences are largely attributable to the finite accuracy with which individual calibration tanks are prepared in ALE/GAGE.

The combination of a Porasil D column packing, relatively low column temperature (50°C), and specially purified 95% Ar/5% CH_4 carrier gas enables N_2O to be reliably separated from other major electron-capturing atmospheric species. The separation is not optimal, since the N_2O chromatographic peak lies on the tail of the air (mainly O_2) peak (see *Prinn et al.* [1983] for a sample chromatogram). The precision of our N_2O analysis based on repeated analyses of calibration gas is about $\pm 0.35\%$ (1σ) for ALE and about $\pm 0.13\%$ (1σ) for GAGE. Co-elution of O_2 and CO_2 with N_2O, which is a problem with certain choices of column packings, column temperatures, and carrier gases (e.g., Porasil A, 75°C, and N_2 as used by W. Komhyr et al. (unpublished manuscript, 1987)) does not occur in our system. This was established by comparing gas chromatographic analyses of N_2O in a calibration tank with and without quantitative removal of CO_2 using a trap filled with Carbosorb (NaOH on asbestos). The ratio of successive N_2O analyses with and without CO_2 was 1.000 ± 0.005 (1σ) for 30 comparisons on a simulated GAGE system in the laboratory. Similar results were obtained using a Carbosorb trap with the Cape Grim GAGE instrument. This conclusion that CO_2 does not interfere with our N_2O analyses is corroborated by the lack of any evidence for the existence of the significant ($\approx 3\%$ amplitude) northern hemispheric annual CO_2 cycle [*Keeling and Bacastow*, 1977; *Fraser et al.*, 1983; *Komhyr et al.*, 1985] in the ALE/GAGE northern hemispheric N_2O data. Instead, as we will discuss later, the only statistically significant annual cycles in N_2O are in the southern hemisphere where in contrast CO_2 annual cycles have very low amplitudes [*Keeling and Bacastow*, 1977; *Fraser et al.*, 1983; *Komhyr et al.*, 1985].

Absolute calibration is achieved on site by comparing interspersed analyses of air and on-site (Nafion-dried) calibration gas. The on-site calibration gas tank is used for about 3–4 months and is analyzed relative to working secondary standards at the Oregon Graduate Center both before and after use at the site [*Rasmussen and Lovelock*, 1983]. This calibration procedure assumes a linear relation between instrument response R and mixing ratio χ (i.e., in the general expression $R \propto \chi^{(1-\varepsilon)}$, the nonlinearity parameter $\varepsilon = 1 - d\ln R/d\ln\chi = 0$). For small values of ε, $\Delta\ln R$ and $\Delta\ln\chi$, as in ALE/GAGE, the error in χ due to nonlinearity is therefore approximately $-\varepsilon\chi\Delta\ln R$. The linearities of the instruments at each of the five sites and of the instrument used to analyze the on-site calibration tanks relative to the secondary standards have been investigated using a suite of test tanks with mixing ratios ranging from 0.5 to 1.3 times present atmospheric concentrations. From these tests we find $\varepsilon = 0.055 \pm 0.081$. The largest difference between unknowns and standards in ALE/GAGE is 3% (i.e., $\Delta\ln R \leq 0.03$). Thus the largest error in χ due to nonlinearity is $\varepsilon \times 0.03 \times 100 = 0.17 \pm 0.24\%$ (or 0.5 ± 0.7 ppbv for $\chi \simeq 300$ ppbv), and this error would apply to 1988 atmospheric analyses in northern mid-latitudes calibrated against our original secondary standards. The above ε values could also reflect in part the finite accuracy with which the individual tanks for testing nonlinearity can be prepared. A recent reanalysis of the working secondary standards maintained by the Oregon Graduate Center relative to an original ALE secondary standard [*Rasmussen and Lovelock*, 1983] has necessitated corrections to the assigned values for these working secondary standards. These corrections are small for N_2O (the required changes to the on-site calibration tanks averaging only $0.18 \pm 0.5\%$; 1σ) but not for some of the other GAGE species.

Calibrations of the secondary standards are updated based on the best information currently available and the updated values are expressed in terms of the so-called ALE/GAGE calibration factor ξ which is the dimensionless factor by which the nominal values assigned to the standards at the beginning of ALE are to be multiplied. For N_2O our best current estimate for ξ is based on four calibration studies. First, the ALE/GAGE secondary standards have been compared to new primary standards prepared at the Oregon Graduate Center indicating $\xi = 0.91$ [*Rasmussen*

and Khalil, 1986]. Second, the ALE/GAGE standards have been compared to the primary standards from the National Bureau of Standards (NBS-SRM numbers 1631B and 1727B) yielding $\xi = 0.89$ [*Rasmussen and Khalil*, 1986]. Third, we have related our standards to the *Weiss* [1981] N_2O primary standard specifically by comparing our daily mean Samoa and Barbados data to shipboard measurements made by *Weiss* [1981] in the Pacific east of Samoa (24 measurements, August 1979 to May 20, 1980) and in the Atlantic east of Barbados (seven measurements, September–October 1978). Representative advective times between ship and ALE/GAGE stations of 2 days (Samoa) and 1 day (Barbados) due to the predominantly easterly winds are taken into account but the low variability in the ALE/GAGE data does not make this an important consideration. This comparison yields $\xi = 0.901 \pm 0.007$ (1σ). Finally, the ALE/GAGE standard has been compared to the National Oceanographic and Atmospheric Administration primary standard for N_2O (NOAA-GMCC Tank 3072) yielding $\xi = 0.904 \pm 0.006$ (1σ) (J. Elkins, private communication, 1989). For the results presented in this paper we have adopted the average $\xi = 0.90 \pm 0.01$ (1σ) from these four determinations with the standard deviation being used as an indicator of a possible systematic error in ξ of ± 0.01.

For determination of long-term trends in N_2O, the long-term stability of the ALE/GAGE secondary standards is clearly very important. These secondary standards are stored in internally electropolished stainless steel tanks which have been drained of water to minimize any possible aqueous phase production or removal of N_2O. The relative stability of N_2O in different tanks is checked using a suite of specially maintained tanks which are periodically analyzed relative to the original secondary tank 033 as described by *Rasmussen and Lovelock* [1983] (see their Table 1 for N_2O). For the six oldest surviving members of this suite (tank numbers 022, 028, 032, 036, 004 and 017) measured (relative to tank 033) 9 years apart (1978 and 1987) the 1987 N_2O values differed by -1.05 ± 1.32 ppbv or $-0.35 \pm 0.44\%$ (1σ) from the 1978 values which is not statistically different from zero. This result does not of course test whether tank 033 itself is drifting. If the drift in the six test tanks relative to tank 033 is indicative of the magnitude of the possible drift in 033 itself this implies the possibility of a linear downward drift in the secondary standards of -0.12 ± 0.15 ppbv yr^{-1} ($-0.039 \pm 0.049\%$ yr^{-1}) or, alternatively, a quadratic downward drift of -0.013 ± 0.016 ppbv yr^{-2} ($-0.0043 \pm 0.0054\%$ yr^{-2}), where all uncertainties are 1σ. Again these possible drifts are not statistically different from zero but we make the caveat that the long-term trends reported in this paper may be biased because they depend on explicit assumptions concerning the stability of N_2O in the above ALE/GAGE tanks.

3. ALE/GAGE Observations

Daily average N_2O mixing ratios and their standard deviations determined from the measurements at five ALE/GAGE sites during the middle year (January–December 1983) of the 10 years addressed in this paper are given in Figure 1. These results are illustrative of the data for this species. In this figure the times of calibration tank changes (and the calibration tank numbers) are indicated along the top of each graph. Objective and reliable techniques are used to recognize periods (typically less than a few days in duration) of local air pollution [*Prinn et al.*, 1983]. Episodes of obvious local nitrous oxide pollution occur from time to time at Adrigole/Mace Head but are much rarer at the other sites. For the analyses undertaken in this paper, each station is intended to be indicative of the air between the surface and a pressure of 500 mbar in the semihemisphere in which it lies, so periods of obvious local nitrous oxide pollution are removed. On the other hand, as noted earlier, the polluted periods can be used to deduce information on local sources [*Prather*, 1985, 1988].

It is evident from Figure 1 that the daily N_2O variability at the two 30°N–90°N sites (Ireland, Oregon) is generally greater than that at the other sites. This is evidence for large, spatially-discrete regional sources (e.g., industrial, agricultural) at the latitudes of these stations not present to the same degree at the other stations.

Figure 2 illustrates and Table 1 tabulates the monthly mean N_2O mixing ratios and their monthly standard deviations for the entire 10-year period, July 1978 to June 1988. Gradual upward trends are evident at all sites with superimposed annual and longer period oscillations evident at some stations. The first 6 months of data at each site represent a start-up phase for the field instrument and are generally less reliable than subsequent data. The first 4 months of data at Samoa, in which there exists a steady anomalously large increase from inception in July 1978, until a calibration tank change and an alteration of the sample loop size were made on November 10, 1978, are particularly suspect. The other species analyzed on the Porasil D column ($CFCl_3$, CF_2Cl_2) also showed anomalously large increases at Samoa in this same time period. This will be considered in our analysis. A large portion of data at Adrigole, Ireland (February 1979 to March 1980) unfortunately had to be discarded because of persistent instrumental problems evidenced by large variability in analyses of the calibration gas. There are also spuriously low values at Adrigole in April–June 1980 that are suspect but we have no obvious instrumental reason to discard them.

The long-term variability in the monthly mean mixing ratio χ_i at station i is described conveniently by an empirical model containing linear, quadratic, and cyclic (annual, quasi-biennial) temporal dependencies

$$\chi_i = a_i + b_i t + d_i t^2 + c_i \cos(2\pi t) + s_i \sin(2\pi t) + p_i \cos\left[(2\pi(t+5)/\tau)\right] + q_i \sin\left[(2\pi(t+5)/\tau)\right] \quad (1)$$

in which t is time (in years) measured from the "midpoint" of the record (July 1, 1983) and $\tau = 2.25$ years is the assumed period of the quasi-biennial oscillation. Maximum likelihood estimates of a_i, b_i, d_i, c_i, s_i, p_i, and q_i and their uncertainties are computed using an optimal estimation technique (see section 5) and the results are shown in Table 2. A statistically significant quasi-biennial oscillation is evident at Barbados (0.45 ppbv amplitude) and at Tasmania (0.28 ppbv amplitude) but otherwise both annual and quasi-biennial oscillations are weak or insignificant at all sites. Based on the first 16 months of ALE/GAGE data at Oregon and the first 3 years of data at Tasmania, *Khalil and Rasmussen* [1983] concluded that large seasonal cycles exist in N_2O but this conclusion is not supported by the subsequent data reported here. The 10-year averages of the mixing ratios (given by $a_i + 8.33d_i$) and the trends (given by b_i) at the Oregon, Barbados, Samoa, and Tasmania stations are 302.9 ppbv and 0.91 ± 0.03 ppbv yr^{-1} (1σ), respectively, implying a "global" trend in N_2O of $0.30 \pm 0.01\%$ yr^{-1} (1σ). Positive values for d_i at three of the five stations suggest that the N_2O increase is accelerating at a rate of about 0.03 ± 0.01 ppbv yr^{-2} (1σ) or about $0.01 \pm 0.003\%$ yr^{-2} (1σ) over the

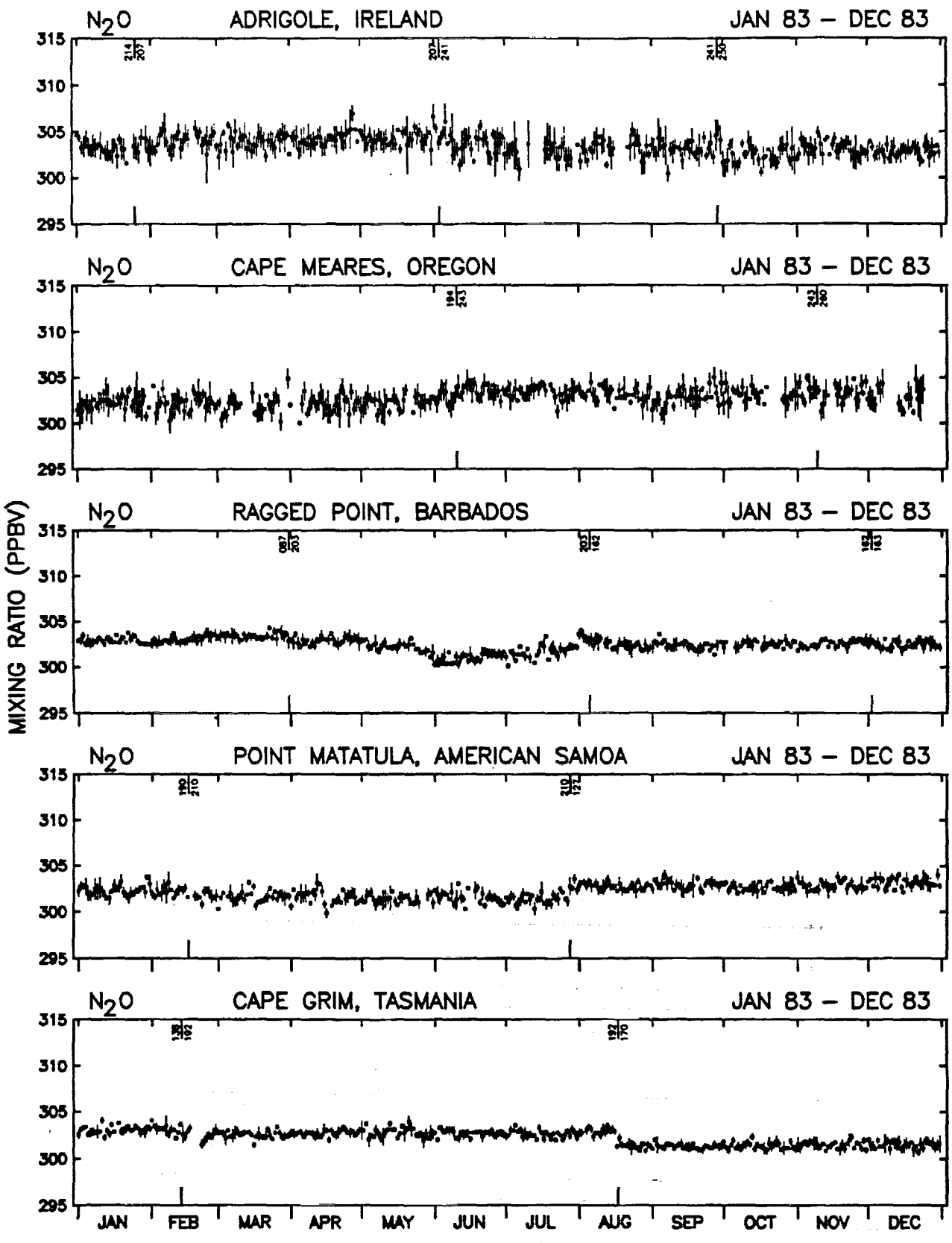

Fig. 1. Daily average N_2O mixing ratios (ppbv) and their standard deviations determined from high-frequency, real-time measurements using the ALE (HP 5840) gas chromatograph at the five ALE/GAGE sites during the middle year (1983) of the experiment. The available GAGE (HP 5880) data at Tasmania for 1983 are not shown here but are included in Table 1 and Figure 2. The random offsets, which occur occasionally at the times of the on-site calibration tank changes (tank numbers are indicated at the top of each panel), are due to the finite accuracy with which individual tanks are prepared in ALE/GAGE.

TABLE 1. Monthly Mean Mixing ratio χ (ppbv), Standard Deviations σ (ppbv), and Number of Measurements Each Month N at the ALE/GAGE sites over the period July 1978 to June 1988

		Ireland			Oregon			Barbados			Samoa			Tasmania		
Year	Month	χ	σ	N	χ	σ	N	χ	σ	N	χ	σ	N	χ	σ	N
1978	7	301.5	1.7	294		—		296.6	1.7	85	293.8	2.6	43	297.8	3.1	59
1978	8	299.2	2.6	241		—		298.8	1.7	102	292.7	1.6	77	298.5	2.4	84
1978	9	299.9	1.8	279		—		298.6	2.0	136	294.4	2.1	97	297.8	2.4	65
1978	10	301.4	2.0	275		—		298.9	1.3	84	294.8	2.7	70	298.2	1.7	49
1978	11	300.8	1.7	211		—		299.4	1.0	86	297.6	2.0	59	299.3	1.1	78
1978	12	301.0	1.6	93		—		298.3	1.2	106	300.1	1.5	48	297.2	1.4	92
1979	1	301.8	1.9	12		—		299.2	1.1	96	300.1	1.4	23	299.2	1.2	58
1979	2		—			—		300.8	1.3	94	300.1	1.5	96	299.0	0.8	104
1979	3		—			—		299.7	1.2	76	299.7	0.9	117	298.8	0.7	112
1979	4		—			—		301.0	0.9	4	299.6	0.8	111	298.6	0.7	120
1979	5		—			—		300.2	0.7	76	299.3	0.8	104	298.6	1.2	117
1979	6		—			—		300.1	0.8	42	299.0	0.7	114	299.5	0.5	112
1979	7		—			—		299.6	1.0	92	299.4	0.8	116	299.4	0.8	98
1979	8		—			—		299.3	0.9	103	299.5	0.9	112	299.1	0.5	118
1979	9		—			—		299.8	0.7	110	299.2	1.8	113	299.3	0.6	115
1979	10		—			—		300.2	0.8	107	299.5	1.1	115	299.0	0.6	114
1979	11		—			—		300.0	0.9	75	300.3	1.1	122	299.1	0.7	113
1979	12		—			—		300.0	0.9	112	299.7	1.5	116	299.1	0.6	85
1980	1		—			—		300.2	0.8	108	299.9	1.7	91	299.2	0.7	95
1980	2		—			—		299.4	0.8	90	300.3	1.1	111	299.3	0.6	73
1980	3		—		301.1	1.1	18	299.5	0.5	104	299.9	1.0	112	299.2	0.6	119
1980	4	297.1	3.2	41	301.0	1.5	72	299.8	0.7	96	299.9	0.8	92	299.3	0.8	79
1980	5	294.0	4.3	113	300.8	1.5	89	300.3	0.8	105	299.7	0.8	102	299.7	0.8	88
1980	6	295.3	4.7	107	301.0	1.4	104	300.9	0.8	106	299.8	1.0	82	299.5	0.7	83
1980	7	297.9	2.1	110	300.7	1.4	79	301.6	0.8	97	299.7	1.0	109	299.6	0.7	102
1980	8	298.1	1.7	115	300.5	1.5	78	300.9	1.3	56	299.3	1.1	91	299.7	0.6	100
1980	9	298.6	2.2	102	300.9	1.6	89	302.5	2.2	88	299.7	1.0	78	300.6	0.8	74
1980	10	300.6	1.4	99	300.6	1.7	99	302.9	1.2	63	299.5	0.6	13	300.1	0.7	49
1980	11	301.0	1.8	116	300.3	1.4	110	301.5	0.7	93	300.2	1.0	56	300.5	0.6	112
1980	12	299.9	2.4	117	300.4	1.3	105	300.6	1.0	80	300.0	0.9	94	301.0	0.6	88
1981	1	298.6	2.6	119	300.8	1.3	129	300.7	0.8	92	300.3	0.4	32	300.6	0.7	53
1981	2	298.6	2.6	109	300.6	1.5	104	300.6	0.8	81		—		299.3	0.5	39
1981	3	298.5	1.9	98	300.6	1.5	114	300.5	0.8	76		—		299.6	0.7	94
1981	4	300.9	2.3	114	300.9	1.3	114	301.0	1.0	83		—		299.7	0.8	67
1981	5	300.6	1.3	74	301.2	1.7	110	300.3	1.0	77	300.4	1.4	82	299.1	0.9	101
1981	6	300.2	1.9	61	300.8	1.1	110	300.2	0.7	84	300.3	1.1	104	298.7	0.7	66
1981	7	299.8	1.5	107	300.7	1.2	111	300.0	0.9	69	299.4	2.2	69	298.4	0.6	59
1981	8	300.7	1.5	97	301.3	1.2	110	300.3	0.7	89	300.4	1.7	103		—	
1981	9	301.1	1.9	89	301.4	1.1	114	300.7	0.9	89	300.2	1.3	65	299.4	0.7	80
1981	10	301.4	1.3	97	301.7	1.3	116	301.0	0.9	97	299.8	1.7	94	299.7	0.5	76
1981	11	301.8	1.3	117	301.7	1.4	85	301.3	0.9	87	300.4	1.1	58	300.2	0.5	106
1981	12	301.9	1.6	105	301.8	2.0	104	300.7	0.7	108	300.3	1.4	93	300.9	0.8	384
1982	1	303.2	1.3	113	302.0	1.4	100	300.6	0.5	99	301.2	1.3	68	300.9	0.7	360
1982	2	303.5	1.2	104	302.3	1.5	72	300.7	0.6	75	302.2	1.0	61	300.9	0.7	396
1982	3	303.8	1.1	97	302.5	1.6	111	301.0	0.9	95	302.1	1.1	68	301.0	0.7	368
1982	4	304.3	1.1	113	302.3	1.5	103	302.8	0.9	84		—		301.1	0.9	414
1982	5	303.7	1.7	40	302.5	1.7	60	303.7	0.8	95		—		301.6	0.6	417
1982	6	304.7	1.4	106	302.5	1.4	113	304.3	0.9	86	303.6	1.6	7	301.9	0.6	430
1982	7	304.1	1.7	117	302.4	1.2	112	303.9	1.4	52	302.0	1.7	90	302.0	0.5	447
1982	8	303.7	1.7	113	302.5	1.3	113	302.3	0.9	77	302.3	1.4	104	302.2	0.5	379
1982	9	303.3	1.8	109	302.8	1.2	100	302.9	0.8	97	302.1	0.7	107	302.3	1.1	421
1982	10	302.7	1.8	116	303.1	1.3	94	303.0	0.8	70	302.1	0.6	116	302.2	1.2	466
1982	11	303.1	1.2	100	302.8	1.1	89	303.2	0.8	104	302.2	0.8	110	302.2	1.2	411
1982	12	303.4	1.2	121	302.6	1.0	65	303.3	0.8	105	302.3	0.7	122	302.1	1.1	473
1983	1	303.3	1.2	102	302.3	1.4	118	302.9	0.5	101	302.3	0.8	121	302.3	1.2	470
1983	2	304.1	1.5	98	302.2	1.4	100	303.1	0.6	100	302.0	0.8	87	302.2	1.1	334
1983	3	304.0	1.3	121	302.0	1.3	91	303.5	0.6	103	301.7	0.7	95	302.3	0.9	473
1983	4	304.2	1.3	108	302.1	1.4	98	303.0	0.6	98	301.6	0.9	100	302.3	0.8	461
1983	5	304.2	1.3	115	302.3	1.2	97	302.2	0.7	91	301.5	0.7	106	302.4	1.0	462
1983	6	303.9	1.8	112	303.3	1.2	109	301.1	0.7	97	301.6	0.8	101	302.3	1.0	460

TABLE 1. (continued)

		Ireland			Oregon			Barbados			Samoa			Tasmania		
Year	Month	χ	σ	N	χ	σ	N	χ	σ	N	χ	σ	N	χ	σ	N
1983	7	302.9	1.8	74	303.4	1.1	104	301.7	0.8	85	301.6	0.9	121	302.3	0.9	439
1983	8	303.2	1.5	93	303.2	1.1	99	302.6	0.8	102	302.8	0.6	118	302.4	1.2	475
1983	9	303.3	1.5	114	302.0	1.3	444	302.4	0.6	82	302.9	0.7	114	302.2	1.4	439
1983	10	302.4	1.4	109	302.2	1.2	391	302.6	0.6	81	302.6	0.6	120	302.4	1.3	484
1983	11	303.2	1.2	112	302.5	1.3	351	302.6	0.5	94	302.9	0.7	116	302.5	1.4	389
1983	12	302.9	1.0	122	302.7	0.9	327	302.5	0.6	103	303.2	0.7	119	302.6	1.4	478
1984	1		—		302.6	0.5	24	302.5	0.6	102	303.4	0.7	123	302.5	1.5	404
1984	2		—		303.0	0.9	369	302.7	0.5	90	302.9	0.8	113	302.5	1.8	372
1984	3		—		302.7	0.8	445	302.8	0.5	74	302.4	0.7	116	302.2	1.5	440
1984	4		—		303.1	0.8	424	302.5	0.7	82	302.5	0.6	110	302.4	1.2	441
1984	5		—		303.6	0.9	354	302.9	0.6	96	302.2	0.8	119	303.8	0.9	461
1984	6		—		303.6	1.0	418	303.4	0.5	91	302.3	0.7	114	303.7	0.9	383
1984	7		—		303.5	1.0	328	303.3	0.6	80	302.3	0.7	115	303.8	0.9	382
1984	8		—		303.8	0.7	279	303.8	0.8	93	302.3	0.7	119	304.0	0.9	439
1984	9		—		303.7	0.5	329	304.6	0.7	109	302.6	0.7	119	304.1	1.0	442
1984	10		—		303.9	0.5	251	305.3	0.7	102	302.4	0.6	86	304.1	1.0	473
1984	11		—		304.2	0.5	245	305.8	0.7	106	302.5	0.9	104	304.0	0.8	445
1984	12		—		304.1	0.5	350	305.5	0.7	107	303.3	0.8	119	304.1	0.8	478
1985	1		—		304.3	0.5	300	305.3	0.7	107	303.4	1.0	119	304.5	0.6	383
1985	2		—		304.3	0.6	280	305.5	0.6	97	304.2	0.9	104	304.6	0.6	325
1985	3		—		304.4	0.6	304	305.5	0.8	114	304.0	0.9	109	304.4	0.6	491
1985	4		—		305.3	0.7	289	305.8	0.7	98	303.9	1.0	120	304.5	0.7	475
1985	5		—		305.2	0.8	246	306.3	0.6	109	304.0	1.1	113	304.6	0.7	481
1985	6		—		304.5	0.7	296	306.5	0.7	72	303.8	0.8	107	304.5	0.7	442
1985	7		—		305.6	1.0	225	305.8	0.5	19	304.3	0.9	221	304.9	0.6	353
1985	8		—		305.5	0.7	191	305.2	0.7	297	304.2	0.8	382	304.7	0.7	230
1985	9		—		305.5	0.7	241	305.5	0.6	269	304.3	0.8	277	304.5	0.5	299
1985	10		—		305.8	0.7	266	306.1	0.6	194	305.5	0.9	231	304.6	0.5	361
1985	11		—		305.8	0.7	226	305.5	0.5	422	304.9	0.7	512	304.6	0.6	252
1985	12		—		306.1	0.6	189	305.5	0.6	431	305.2	0.7	545	304.7	0.6	355
1986	1		—		305.9	0.6	214	306.0	0.8	400	305.2	0.9	451	304.8	0.7	359
1986	2		—		306.6	0.7	292	306.5	0.9	360	305.4	0.8	402	304.6	0.6	316
1986	3		—		307.0	0.8	232	306.6	1.1	401	305.6	1.2	340	304.5	0.7	364
1986	4		—		307.1	0.8	202	307.1	1.4	242	305.7	1.4	427	305.2	2.1	309
1986	5		—		306.2	0.8	210	305.9	0.7	230	305.5	1.3	265	305.4	2.4	299
1986	6		—		306.5	0.7	276	306.8	0.3	286	306.7	0.9	76	305.8	1.8	321
1986	7		—		306.9	0.7	300	306.9	0.7	303	306.1	0.7	69	306.1	1.7	344
1986	8		—		307.3	0.8	307	307.0	0.8	317	306.0	0.6	237	305.9	2.9	295
1986	9		—		307.4	1.0	185	307.1	0.7	303	306.4	0.8	245	306.2	1.9	323
1986	10		—		307.8	1.5	341	306.8	1.0	324	306.6	0.7	337	305.3	1.8	134
1986	11		—		307.1	1.3	269	306.8	0.7	326	306.4	0.8	285	305.9	2.4	180
1986	12		—		306.8	1.4	277	307.0	1.0	222	306.2	0.8	341	306.0	1.7	333
1987	1	305.8	0.6	105	307.3	1.1	191	307.3	1.0	320	306.2	0.8	220	306.0	1.7	336
1987	2	305.5	0.6	175	306.8	0.9	215	307.2	0.8	302	306.1	1.1	210	305.8	2.0	309
1987	3	305.2	0.7	280	307.5	1.0	275	307.0	0.5	290	306.3	0.8	244	306.0	1.4	340
1987	4	305.6	0.7	259	307.9	1.5	217	307.1	0.7	313	305.9	1.2	271	306.0	1.5	257
1987	5	305.5	0.4	309	308.0	2.0	268	307.1	0.7	264	306.3	1.1	307	306.0	1.3	334
1987	6	305.3	0.3	351	307.3	1.7	304	306.8	0.8	53	306.9	0.9	271	306.3	1.3	346
1987	7	305.2	0.4	343	307.1	1.7	316	306.4	0.6	294	306.9	0.9	358		—	
1987	8	305.2	0.4	326	307.4	1.6	336	306.6	0.7	333	306.8	1.4	369	305.9	1.1	199
1987	9	305.8	0.4	351	307.4	1.5	267	307.5	0.6	320	306.9	0.9	331	305.7	1.2	345
1987	10	305.9	0.5	278	308.1	1.4	302	307.8	0.7	336	306.5	1.0	89	306.0	1.1	303
1987	11	306.0	0.4	257	308.1	1.2	285	307.6	0.5	232	307.0	0.7	316	305.6	1.4	324
1987	12	306.2	0.4	170	308.0	1.3	145	307.5	0.6	368	307.3	1.3	338	305.8	1.6	345
1988	1	306.0	0.5	271	308.2	1.2	261	307.5	0.6	350	307.4	1.2	355	306.1	1.4	277
1988	2	305.8	0.5	297	308.4	1.2	262	307.4	0.7	321	306.3	1.5	316	305.4	2.0	338
1988	3	305.4	0.4	308	308.5	1.5	321	307.0	0.7	338	307.8	0.9	323	305.5	1.9	293
1988	4	305.9	0.7	318	308.7	1.9	339	307.1	0.6	317	308.2	1.0	312	305.5	1.5	60
1988	5	306.2	0.6	328	309.2	1.4	117	307.0	0.4	356	307.3	1.0	201	306.6	1.6	69
1988	6	306.3	0.5	335	309.2	1.6	315	307.2	0.6	342	307.7	1.1	341	306.3	1.6	304

For Oregon (beginning September 1983), Barbados (beginning August 1985), Samoa (beginning July 1985), and Tasmania (beginning July 1981), the ALE (HP 5840) and GAGE (HP 5880) monthly data are combined by weighting equally ALE and GAGE monthly means to determine χ and ALE and GAGE individual measurements to determine σ. The calibration factor $\xi = 0.90$ is included here.

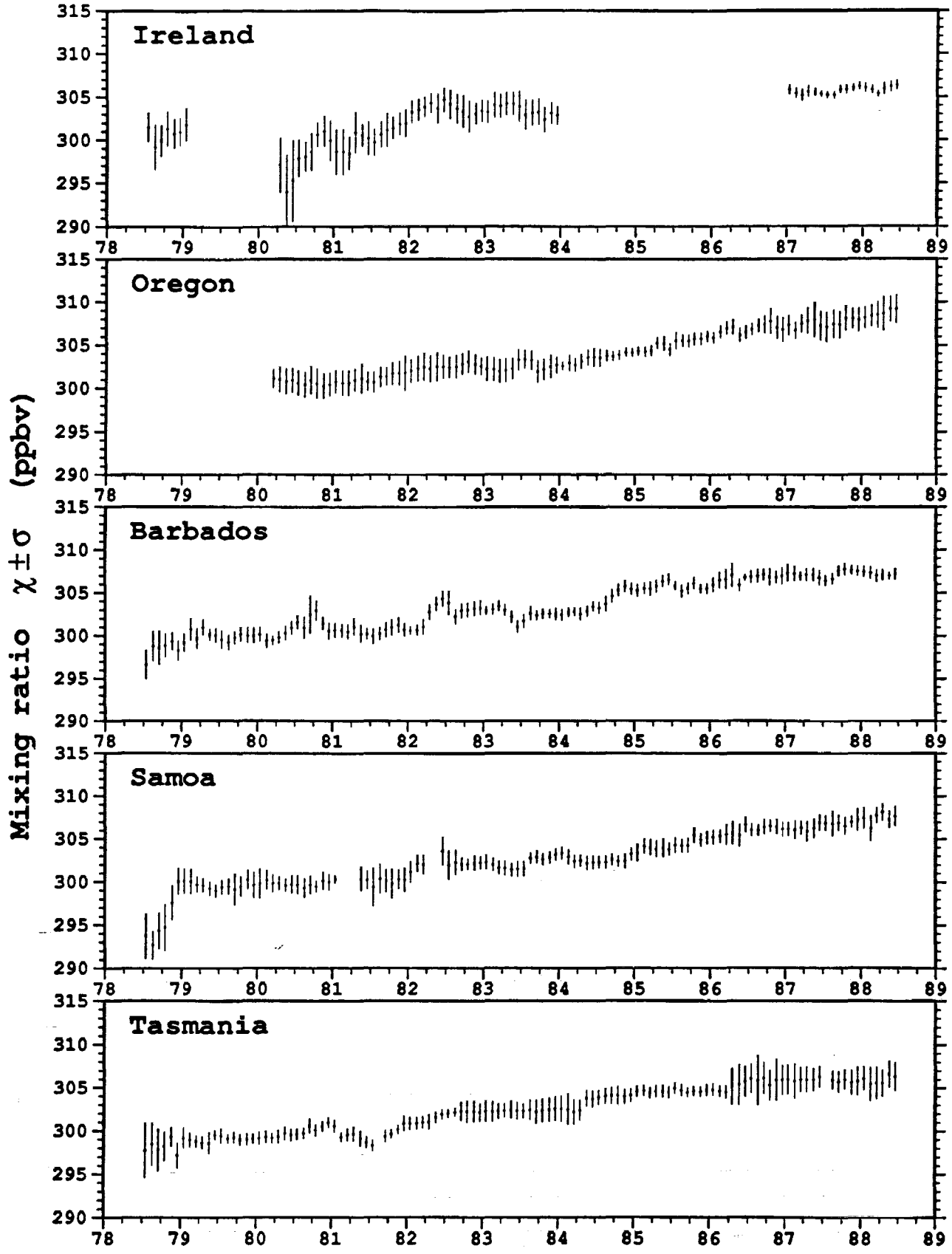

Fig. 2. Monthly mean N_2O mixing ratios (ppbv) and their standard deviations for the first 10 years of ALE/GAGE at the five ALE/GAGE sites. Data for the Adrigole, Ireland (1978–83) and MaceHead, Ireland (1987-88) sites are shown on the same graph. ALE (HP 5840) and GAGE (HP 5880) data combined where they overlap as described in Table 1.

TABLE 2. Optimally Determined Coefficients (±1σ Uncertainties) in Our Empirical Model for the 1978–1988 Monthly Mean N_2O Data in Table 1

Site	a_i ppbv	b_i ppbv yr^{-1}	d_i ppbv yr^{-2}	c_i ppbv	s_i ppbv	p_i ppbv	q_i ppbv
Adrigole/Mace Head, Ireland*	303.0±0.7	0.76±0.17	−0.02±0.06	−0.32±0.26	0.00±0.27		
Cape Meares, Oregon†	302.8±0.2	0.94±0.07	0.07±0.03	0.08±0.08	0.01±0.08	−0.10±0.15	−0.06±0.15
Ireland plus Oregon*	303.0±0.3	0.88±0.08	0.04±0.03	−0.10±0.12	0.08±0.12	−0.20±0.26	0.15±0.26
Ragged Point, Barbados*	303.1±0.3	0.94±0.06	0.01±0.02	−0.07±0.10	0.04±0.10	0.02±0.21	0.45±0.21
Point Matatula, Samoa‡	302.2±0.2	0.91±0.04	0.06±0.02	−0.16±0.16	−0.07±0.16	−0.02±0.16	0.09±0.16
Cape Grim, Tasmania*	302.4±0.2	0.90±0.05	−0.00±0.02	0.00±0.08	0.10±0.08	−0.08±0.15	−0.28±0.15

The calibration factor $\xi = 0.90$ is included here. The mean concentration is given by $a_i + 8.33d_i$ and the mean trend by b_i.
* July 1978 to June 1988.
† March 1980 to June 1988.
‡ January 1979 to June 1988.

1978–1988 time period. The stability of the secondary standards discussed in section 2 implies possible positive biases in these global trends (bi) and trend increase (di) of 0.04 ± 0.05% yr^{-1} (1σ) and 0.004 ± 0.005% yr^{-2} (1σ), respectively. Larger biases cannot be ruled out as discussed earlier.

The above mean linear trends bi can be compared to those measured by (1) *Weiss* [1981] in real-time at oceanic localities (45°N to 65°S), Barrow (Alaska), Mauna Loa (Hawaii), and South Pole (0.17 ± 0.04% yr^{-1} (2σ) or 0.52 ± 0.12 ppbv yr^{-1} (2σ) over the 1976–1980 time period); (2) *Khalil and Rasmussen* [1983] using the early data from two of the five ALE stations (Cape Grim from July 1978 to June 1981; Cape Meares from January 1980 to June 1981) (0.30 ± 0.1% yr^{-1} (90% confidence) or 0.8 ± 0.3 ppbv yr^{-1} (90% confidence)); (3) *Rasmussen and Khalil* [1986] using January flask collections in the Pacific Northwest and South Pole (0.34 ± 0.05% yr^{-1} (90% confidence) or 1.04 ± 0.14 ppbv yr^{-1} (90% confidence) over the 1975–1985 time period); (4) W. Komhyr et al. (unpublished manuscript, 1987) from periodic flask sampling in Colorado and at four globally distributed NOAA/GMCC stations (0.23 ± 0.07% yr^{-1} (2σ) or 0.68 ± 0.20 ppbv yr^{-1} (2σ) over the 1977–1984 time period). Taking into account the stated uncertainties and possible biases in the ALE/GAGE trends and the tentative evidence from the ALE/GAGE data for an accelerating rate of increase for N_2O, the ALE/GAGE trends do not contradict the smaller trends reported by *Weiss* [1981] and W. Komhyr et al. (unpublished manuscript, 1987). Because the same secondary standards are used, the surprisingly poor agreement at the 1σ level between ALE/GAGE and *Rasmussen and Khalil* [1986] may result simply from the fact that the *Rasmussen and Khalil* [1986] flask collections were infrequent and made at only two stations.

4. A Priori Emissions Estimates

While a wide variety of sources for atmospheric N_2O have been identified, the relative importance of these sources on a global scale and their temporal and spatial variations are in general neither well quantified nor well understood. Because of these inadequacies, it is not presently possible to provide sufficient constraints on N_2O emissions to enable accurate determinations of the N_2O atmospheric lifetime from the ALE/GAGE data. We can however answer the following questions: are present ideas on emissions consistent with the measurements at the ALE/GAGE sites and with present ideas on atmospheric sinks for N_2O?

For the latter purpose we have formulated an a priori model for emissions based on a number of recent papers which address the following individual N_2O sources: fossil fuel combustion, biomass burning and land clearing, fertilized soil, natural temperate soil, natural tropical soil, and oceans. The first and third of these sources are anthropogenic, the second is predominantly anthropogenic, and the last three are natural. For convenience the annual inputs I_i into each semihemisphere (see Figure 3) in the year Y are expressed in terms of the annual global emissions E_j associated with the above six surface source types using

$$I_i = \sum_{j=1}^{j=6} a_{ij}E_j \quad (i = 1, 3, 5, 7) \tag{2}$$

where a_{ij} is the fraction of E_j emitted into semihemisphere i.

Global N_2O annual emissions from fossil fuel combustion (designated here as E_1) have long been suggested as one of the major contributors to total N_2O emission [*Pierotti and Rasmussen*, 1976; *Weiss and Craig*, 1976]. Also, because E_1

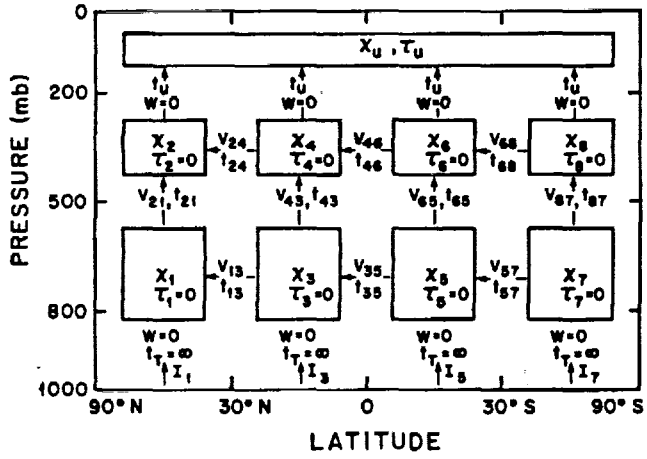

Fig. 3. Schematic of the nine-box two-dimensional model of the atmosphere used in the data inversion technique. Values of the eddy diffusion times (t_{ij}) and inverse advection times (V_{ij}, W) from *Cunnold et al.* [1983] but with certain adjustments as described in the text. Inputs I_i assumed to occur directly into boxes 1, 3, 5, and 7.

is generally increasing with time, this combustion is a possible major cause for the observed upward trend in atmospheric N_2O [*Hao et al.*, 1987]. We have specifically chosen values for E_1 in each year Y (see Table 3) consisting of a smooth fit (using exponential and linear functions of Y) to the estimates by *Hao et al.* [1987]. The fractions of E_1 assigned to each semihemisphere (see Table 4) are assumed proportional to 0.83 × (coal consumption) plus 0.17 × (oil consumption) in each semihemisphere. Coal and oil consumption data for relevant countries were taken from *Cleveland* [1987] and weights applied to coal and oil for N_2O production were taken from the experimental study by *Hao et al.* [1987] which demonstrated the dominant role of nitrogen in coal as a source of N_2O during combustion. Note from Table 4 that the fossil fuel combustion source for N_2O is strongly concentrated in the 30°N–90°N semihemisphere (and indeed *Prather* [1988] deduces an N_2O industrial source of about 1.3×10^{12} g N_2O yr^{-1} from Europe alone); this will be important in our subsequent analysis. The emissions from fossil fuel combustion estimated by *Hao et al.* [1987] have been questioned recently by *Muzio and Kramlich* [1988], who report formation of N_2O (apparently from NO, SO_2, and H_2O) in sampling containers of the type used by *Hao et al.* [1987] to collect combustion effluents. Therefore we explore in this paper the extent to which decreases in E_1 provide a better explanation for the ALE/GAGE data.

Global N_2O annual emissions from biomass burning are

TABLE 3. A Priori Estimates of Annual Global N_2O Emissions in Various Categories

Emission Source Emission Strength, 10^{12} g N_2O yr^{-1}		Reference
Fossil fuel combustion (E_1)		
2.5–4.8 (1978)		*Weiss* [1981]
1.0 (1910), 2.3 (1955), 5.0 (1982)		*Hao et al.* [1987]
$1.0 \times \exp([Y-1910]/20)$	(before 1910)	RUN A_{1M} [1,2]
$1.0 + 1.3 \times (Y-1910)/45$	(1910-1955)	RUN A_{1M} [1,2]
$2.3 + 2.7 \times (Y-1955)/27$	(1955-1988)	RUN A_{1M} [1,2]
$1/4 \times E_{tot}$		RUN B_{1M}
$0.5 \times E_1$ (RUN A_{1M})		RUN A_{2M}
$1/8 \times E_{tot}$		RUN B_{2M}
$0.25 \times E_1$ (RUN A_{1M})		RUN A_{3M}
$0.1 \times E_1$ (RUN A_{1M})		RUN A_{4M}
Fertilizer use (E_3)		
0.02–3.5		*Slemr et al.* [1984]
0.6–1.9		*Keller et al.* [1986]
0.0	(before 1946)	RUN A_{1M}, A_{2M}, A_{3M} [1,4]
$1.5 \times (Y-1946)/36$	(after 1946)	RUN A_{1M}, A_{2M}, A_{3M} [1,4]
$3/40 \times E_{tot}$		RUN B_{1M}, B_{2M}
$8/3 \times E_3$ (RUN A_{1M})		RUN A_{4M}
Natural tropical soil (E_5)		
4.7		*Slemr et al.* [1984]
4.9–14		*Keller et al.* [1986]
4.3[6]		*Livingston et al.* [1988]
5.2		*Matson and Vitousek* [1989], *Vitousek* [1989][8]
6.0		RUN A_{1M}, A_{2M}, A_{3M}
$1.25 \times E_5$ (RUN A_{1M})		RUN A_{4M}
$3/10 \times E_{tot}$		RUN B_{1M}, B_{2M}
Tropical land disturbance (E_2)		
0.8–7.5 (burning)		*Crutzen et al.* [1985]
0.2–0.9 (burning)		*Crutzen et al.* [1989]
1.3–2.0 (soil)		*Luizao et al.* [1989]
$2.5 \times \exp(-1)$	(before 1946)	RUN A_{1M} [3]
$2.5 \times \exp([Y-1982]/36)$	(after 1946)	RUN A_{1M} [1,3]
$1/8 \times E_{tot}$		RUN B_{1M}
$2 \times E_2$ (RUN A_{1M})		RUN A_{2M}
$1/4 \times E_{tot}$		RUN B_{2M}
$2.5 \times E_2$ (RUN A_{1M})		RUN A_{3M}
$1.2 \times E_2$ (RUN A_{1M})		RUN A_{4M}
Natural temperate soil (E_4)		
≤ 0.8[5]		*Keller et al.* [1983]
2.4		*Slemr et al.* [1984]
1.1–4.7		*Schmidt et al.* [1988]
1.0		RUN A_{1M}, A_{2M}, A_{3M}, A_{4M}
$1/20 \times E_{tot}$		RUN B_{1M}, B_{2M}
Ocean (E_6)		
11		*Elkins et al.* [1978]
6–16		*Cohen and Gordon* [1979]
$\ll$ atmospheric loss rate[7]		*Weiss* [1981]
4.0		RUN A_{1M}, A_{2M}, A_{3M}, A_{4M}
$1/5 \times E_{tot}$		RUN B_{1M}, B_{2M}

(1) Y = year (A.D.).

(2) Piecewise fit to *Hao et al.* [1987].

(3) Assumed to be constant, natural rate before 1946 and to increase exponentially after 1946 with an inverse e-folding time given by the sum of 0.68 × (inverse e-folding time for combined populations of Nigeria, Zaire, Tanzania, and Kenya), 0.22 × (inverse e-folding time for combined populations of Indonesia, Vietnam, and Thailand), and 0.10 × (inverse e-folding time for combined populations of Brazil and Mexico). The e-folding times are computed for the period 1950–1986 using population data from *Cleveland* [1987], and the weights given to the three regions are equated to the 1976 fractions of the total tropical population practicing shifting cultivation attributable to Africa, Southeast Asia, and Central and South America [*Logan et al.*, 1981].

(4) Assumed to increase linearly between 1950 and 1986 by the same factor as world chemical fertilizer use increased between 1950 and 1986 [*Brown et al.*, 1987].

(5) Obtained by multiplying maximum annual mean flux at Hubbard Brook NH [*Keller et al.*, 1986] by the global area of temperate forest and grassland, boreal forest, and woodland (33×10^6 km^2 [*Leith*, 1975]).

(6) Obtained by multiplying mean flux measured in certain Amazonian forest ecosystems [*Livingston et al.*, 1988] by the global area of tropical rain and raingreen forests (24.5×10^6 km^2 [*Leith*, 1975]).

(7) Atmospheric loss rate ~ (13-16) × 10^{12} g N_2O yr^{-1} for current atmospheric lifetime of 150–182 years.

(8) Obtained by adding *Matson and Vitousek's* [1990] estimate of 3.8×10^{12} g N_2O yr^{-1} from evergreen tropical forests and P. Vitousek's (private communication, 1989) estimate of 1.4×10^{12} g N_2O yr^{-1} from raingreen tropical forests.

TABLE 4. Fractions a_{ij} of Annual Global N_2O Emissions E_j Released in Semihemisphere i in All Model Runs

		$E_1^{(1)}$ (Fossil Fuel)	$E_2^{(2)}$ (Land Disturbance)	$E_3^{(3)}$ (Fertilized Soil)	$E_4^{(4)}$ (Temperate Soil)	$E_5^{(5)}$ (Tropical Soil)	$E_6^{(6)}$ (Ocean)
I_1	30°N–90°N	0.860	0	0.52	0.92	0	0.18
I_3	0°–30°N	0.089	0.57	0.37	0	0.55	0.25
I_5	30°S–0°	0.024	0.43	0.10	0	0.45	0.27
I_7	90°S–30°S	0.027	0	0.01	0.08	0	0.30

(1) Assumed proportional to 0.83 × (coal consumption) plus 0.17 × (oil consumption) in each semihemisphere. Coal and oil consumption data for relevant countries taken from *Cleveland* [1987] for the years 1984–1985 and weights applied to coal and oil for N_2O production taken from *Hao et al.* [1987].

(2) Assumed proportional to populations of principal countries practicing shifting cultivation in each tropical semihemisphere (see Table 3, footnote 3).

(3) Assumed proportional to population in each semihemisphere.

(4) Assumed proportional to unglaciated land area in each temperate semihemisphere.

(5) Assumed proportional to land area in each tropical semihemisphere.

(6) Assumed proportional to oceanic area in each semihemisphere.

dominated by the burning associated with the so-called "shifting" agriculture practiced in certain tropical and subtropical regions [*Seiler and Crutzen*, 1980] and are much more poorly quantified than those from fossil fuel burning. Estimates by *Crutzen et al.* [1985], which supersede the earlier larger estimates given by *Seiler and Crutzen* [1980], suggest global annual N_2O emission of 2.5×10^{12} g N_2O yr^{-1} with a large (factor of 3) uncertainty. Recent measurements of N_2O emissions in laboratory-scale biomass fires have lead *Crutzen et al.* [1989] to lower further their estimates of these latter emissions to $(0.2–0.9) \times 10^{12}$ g N_2O yr^{-1}; at the same time recent measurements [*Luizao et al.*, 1989; P. Vitousek, private communication, 1988; *Matson et al.*, 1987; *Anderson et al.*, 1988] indicate that N_2O emissions from the disturbed soil produced as a result of tropical land clearing and/or biomass burning may provide a global N_2O source of $(1.3–2) \times 10^{12}$ g N_2O yr^{-1}. We will adopt a value for the sum E_2 of the biomass burning and disturbed soil sources of 2.5×10^{12} g N_2O yr^{-1} for $Y = 1982$ in our a priori model. For the temporal variation of E_2 we take the fractional trend in the combined populations of (1) Nigeria, Zaire, Tanzania, and Kenya, (2) Indonesia, Vietnam, and Thailand, and (3) Brazil and Mexico as indicative, respectively, of the trends in (agriculturally related) land clearing and biomass burning in (1) equatorial Africa, (2) equatorial Southeast Asia, and (3) equatorial Central and South America. Specifically E_2 is assumed to vary exponentially with year Y (see Table 3) with an inverse e-folding time given by the sum of 0.68 × (inverse e-folding time for populations of the relevant African nations), 0.22 × (inverse e-folding time for populations of relevant Southeast Asian nations), and 0.10 × (inverse e-folding time for populations of relevant Central and South American nations). The e-folding times are computed for the period 1950–1986 using population data from *Cleveland* [1987], and the weights given to the three regions are equated to the 1976 fractions of the total tropical population practicing shifting (biomass burning) cultivation attributable to Africa, Southeast Asia and Central/South America as estimated by *Logan et al.* [1981]. In the absence of detailed information, the fraction of E_2 assigned to each of the two tropical semihemispheres is simply assumed to be proportional to the populations of the above nine principle countries practicing shifting agriculture in each semihemisphere (Table 4). Very similar fractions would result from assuming proportionality to the land areas in each tropical semihemisphere. Prior to 1946, E_2 is assumed to be constant representing "natural" biomass burning.

Nitrous oxide emission (E_3) due to microbial activity in fertilized agricultural soils is a third identifiable anthropogenic source. Recent measurements indicate that this emission is not as large a contributor to the global total as once proposed, but fertilization of certain tropical soils could make this source more important in the future (see [*Keller et al.*, 1988]). Based on experimental studies of fertilized soils, *Slemr et al.* [1984] deduce $E_3 = (1.74 \pm 1.72) \times 10^{12}$ g N_2O yr^{-1} while *Keller et al.* [1986] estimate $E_3 = (1.26 \pm 0.63) \times 10^{12}$ g N_2O yr^{-1}. We will adopt the average of these two values $E_3 = 1.5 \times 10^{12}$ g N_2O yr^{-1} for $Y = 1982$. For the temporal variation of fertilized soil emissions (Table 3) we will assume reasonably that E_3 increases linearly between 1950 and 1986 by the same factor as world chemical fertilizer use increased between 1950 and 1986 [*Brown et al.*, 1987] and that E_3 was negligible prior to 1946. The fractions of E_3 assigned to each semihemisphere (Table 4) are taken to be proportional to the total population in each semihemisphere.

Measurements of emission (E_4) due to microbial activity in natural temperate soils vary widely depending on location and time. If we multiply the maximum annual mean flux measured at Hubbard Brook [*Keller et al.*, 1986] by the combined global areas of temperate forest and grassland, boreal forest, and woodland (33×10^6 km^2 [*Leith*, 1975] we obtain $E_4 \leq 0.8 \times 10^{12}$ g N_2O yr^{-1}. In contrast, *Slemr et al.* [1984] estimate $E_4 = 2.4 \times 10^{12}$ g N_2O yr^{-1} and *Schmidt et al.* [1988] deduce $E_4 = (1.1–4.7) \times 10^{12}$ g N_2O yr^{-1} based on extrapolating measurements in German and Spanish soils to global scales. We will (somewhat arbitrarily) adopt a value for $E_4 = 1 \times 10^{12}$ g N_2O yr^{-1} (Table 3), but it is apparent that further field studies are needed to provide more reliable estimates for E_4. No significant global-average long-term temporal trends are expected in this natural source. The total emission E_4 is apportioned between the two temperate semihemispheres (Table 4) according to the unglaciated land area in each (i.e., most of E_4 is added to the 30°N–90°N region).

Following the prescient work by *Arnold* [1954], measurements made in the last few years by a number of independent groups have established emissions (E_5) due to microbial activity in natural tropical and subtropical soils as an important and perhaps the largest single contributor to the global total N_2O source. *Keller et al.* [1986] [see also *Keller et al.*, 1983] estimate $E_5 = (9.6 \pm 4.7) \times 10^{12}$ g N_2O yr^{-1} based on measurements in tropical forests in Brazil, Ecuador, and Puerto Rico. A somewhat lower value of $E_5 = 4.3 \times 10^{12}$ g N_2O yr^{-1} is

deduced if the mean flux measured by *Livingston et al.* [1988] in certain Amazonian forest ecosystems is multiplied by the global area of tropical rain and raingreen forests (24.5×10^6 km^2 [*Leith*, 1975]). *Slemr et al.* [1984] deduce $E_5 = 4.7 \times 10^{12}$ g N_2O yr^{-1} based on measurements for subtropical (Spanish) soils (Spain actually lies in our 30°N–90°N temperate semihemisphere). An arithmetic average of the *Keller et al.* [1986], *Livingston et al.* [1988], and *Slemr et al.* [1984] estimates yields $E_5 \simeq 6 \times 10^{12}$ g N_2O yr^{-1}, which is the value we will use (as such it is the largest single contributor to emissions in our nominal model). This is consistent with the value obtained by adding *Matson and Vitousek's* [1990] estimate of 3.8×10^{12} g N_2O yr^{-1} from evergreen tropical forests and P. Vitousek's (private communication, 1989) estimate of 1.4×10^{12} g N_2O yr^{-1} from raingreen tropical forests. We apportion E_5 between the two tropical semihemispheres according to the land area in each (Table 4) and (in the absence of any evidence otherwise) we assume E_5 does not vary with year Y.

The third recognized natural source is microbial activity in surface ocean water. The magnitude of the total emission (E_6) due to this source is controversial. From central Pacific measurements *Elkins et al.* [1978] deduce a total marine emission of 11×10^{12} g N_2O yr^{-1} between 20°N and 20°S. From North Atlantic and Pacific Ocean measurements *Cohen and Gordon* [1979] estimate a total marine N_2O production of $(11 \pm 5) \times 10^{12}$ g N_2O yr^{-1} and argue that most of this production is emitted to the atmosphere. However, *Weiss* [1981] reported that his extensive measurements of the global distribution of N_2O in ocean surface waters show that the mean oceanic source is small compared to the stratospheric destruction rate (which is (13–16) $\times 10^{12}$ g N_2O yr^{-1} for current atmospheric lifetimes of 150–182 years). Based on these conflicting results, we do not feel confident in estimating E_6 from the current oceanic measurements. Instead we note that the observed rate of increase of atmospheric N_2O of 0.2–0.3% yr^{-1} combined with a theoretical atmospheric lifetime of 150–182 years (see next section) implies that the total global N_2O source $E_{tot} = \sum_j E_j \approx 20 \times 10^{12}$ g N_2O yr^{-1}. Subtracting the sum of the 1982 values for E_1 through E_5 from this global total yields $E_6 \approx 4 \times 10^{12}$ g N_2O yr^{-1}, which is the value adopted here (Table 3). E_6 is assumed time invariant and is apportioned to the four semihemispheres of the globe according to the oceanic area in each (Table 4).

The 1982 values for emissions in our a priori model differ somewhat from those of *Keller et al.* [1986]; see also *McElroy and Wofsy* [1986] and *Seiler and Conrad* [1987]. However, taking into account the stated uncertainties, the only real disagreement with *Keller et al.* [1986] lies in the biomass combustion plus land clearing contribution E_2, where we have adopted a somewhat larger value and the only real disagreement with *Seiler and Conrad* [1987] is in the fossil fuel combustion term E_1, where we have adopted nominally the larger *Hao et al.* [1987] estimate. Note that because E_1 is largely confined to 30°N–90°N and E_2 is largely confined to 30°N–30°S their relative magnitudes effect the predicted latitudinal N_2O gradient and the comparison in the next section of predicted and observed gradients will provide a direct test of the accuracy of E_1 and E_2 in our a priori model.

5. INVERSE PROBLEMS

To interpret the N_2O measurements in terms of surface emissions, atmospheric circulation, and atmospheric destruction we utilize an optimal-estimation, inversion technique [*Cunnold et al.*, 1983, 1986]. The technique includes the use of a two-dimensional model of the global atmosphere consisting of eight tropospheric boxes (or grid points) and one upper atmospheric box (see Figure 3). The four lower tropospheric boxes (or grid points) are intended to provide predictions for comparing with the ALE/GAGE stations in the four semihemispheres. Mean inverse advective times (V_{ik}) and eddy diffusive times (t_{ik}) in the model vary seasonally and are specified from meteorological observations and an optimal fit to global ALE/GAGE data for $CFCl_3$, CF_2Cl_2 and CH_3CCl_3 [*Cunnold et al.*, 1986; *Prinn et al.*, 1987]. The only recognized atmospheric sink for N_2O is photochemical destruction in the stratosphere with a lifetime τ = 150 to 182 years according to computations in suitable global two-dimensional (2D) and three-dimensional (3D) chemical-dynamical models [*Johnston et al.*, 1979; *Ko and Sze*, 1982; *Levy et al.*, 1982; *Golombek and Prinn*, 1986]. To simulate this destruction in our 2D model, the N_2O destruction times τ_i (i = 1 to 8) for the eight tropospheric boxes are set equal to zero and the N_2O upper-atmospheric destruction time τ_u is adjusted to give the desired global atmospheric lifetime in the box model (the value for τ_u is sensitive to the specified upper troposphere-upper atmosphere mixing time t_u (= 4 years in the model)).

The 12-month running means for the lower tropospheric mixing ratios χ_1, χ_3, χ_5, and χ_7 predicted in this 2D model are compared with ALE/GAGE observations rather than the instantaneous predicted mixing ratios. This is because this 2D model is not capable of accurately simulating oscillations associated with the measurement technique (e.g., periodic renewal of on-site calibration tanks) or natural meteorological oscillations on interannual, seasonal, and shorter time scales which do exist (see Figures 1–2). To account in a statistical way for these unsimulated oscillations, the model output is augmented by two empirical statistical models that are designed to describe the spectrum of the differences (residuals) between the observations and the 12-month running mean model predictions [*Cunnold et al.*, 1986]. Lower frequencies in this spectrum were fit with a first-order, autoregressive model, common to all sites with a correlation of 0.5 after 1 month; higher frequencies were modeled by assuming that the spectra at each site were the same as those found in the residuals associated with the differences between the observations and the empirical model fit to the observations described earlier (section 3).

The optimal estimation scheme produces a best guess of the unknowns y_i (contained in vector $\mathbf{y}$) and their errors σ_i based on minimizing the squares of the deviations between the logarithms of the observed (vector $\mathbf{x}$) and model-calculated (vector $\mathbf{x}_c$) monthly mean mixing ratios at each ALE/GAGE site. The vector $\mathbf{y}$ is updated with each new month of data using

$$\Delta \mathbf{y} = \mathbf{C}\mathbf{P}' \left[\mathbf{P}\mathbf{C}\mathbf{P}' + \mathbf{N}\right]^{-1} (\mathbf{x} - \mathbf{x}_c) \qquad (3)$$

where $\mathbf{P}$ (transpose $\mathbf{P}'$) is a matrix of the partial derivatives of the elements of $\mathbf{x}_c$ (the model predictions) with respect to the elements of $\mathbf{y}$ (the unknowns), $\mathbf{N}$ is a diagonal matrix whose nonzero elements are the squares of the standard errors in the elements of $\mathbf{x}$ (the ALE/GAGE observations), and $\mathbf{C}$ is a matrix whose diagonal elements are the variance (i.e., σ_i^2) of the elements of $\mathbf{y}$ (the unknowns) based on an objective combination of a priori estimates of the uncertainties in the unknowns and the uncertainties in the measurements. The matrices $\mathbf{P}$ and $\mathbf{C}$ are updated during the inversion process as described by *Cunnold*

et al. [1983]. Estimates of unknowns y_i and errors σ_i can be obtained with each ALE/GAGE station data alone or all station data sets simultaneously.

We have interpreted the ALE/GAGE measurements in four distinct but not independent ways. First, using these measurements and our a priori emissions estimates (Tables 3, 4) we calculate the N_2O atmospheric lifetime τ. We also repeat this calculation after making adjustments to the a priori emissions and to the model transport rates in an attempt to fit better the observed N_2O latitudinal gradient. These calculations are labeled RUN A_{NM} where N and M are integers which identify the assumptions made concerning emissions and transport, respectively, in each run which are discussed below.

Second, we specify the lifetime $\tau = 166 \pm 16$ years based on the aforementioned theoretical 2D and 3D model studies for its photochemical destruction and then, using the measurements, we calculate instead the total annual global emission $E_{tot}(Y)$ for each ALE/GAGE year. In the latter case, the fractions f_i of $E_{tot}(Y)$ assumed emitted into each semihemisphere are equated to their fractions in our a priori emissions estimates (Tables 3, 4) for 1982, that is,

$$f_i = I_i(1982) \;/\; E_{tot}(1982) \qquad (i = 1, 3, 5, 7) \qquad (4)$$

(we label these calculations as RUN B_{NM} if f_i values from RUN A_{NM} are used).

Third and fourth, we specify both the lifetime $\tau = 166$ years and the global total emissions $E_{tot}(Y) = 20 \times 10^{12}$ g N_2O yr^{-1} and determine either the fractions f_i of emissions into each semihemisphere or the relative rates g_i of tropospheric-stratospheric exchange in each semihemisphere which provide the optimal fit to the observed ALE/GAGE N_2O latitudinal gradient. We label these runs as either RUN C_M or RUN D_N, where (as above) M and N are integers identifying the assumed rates of transport (M) or emissions (N) in the model.

5.1. *Global Lifetimes*

The lifetime deduced in RUN A_{11} by matching optimally the ALE/GAGE and box model fractional trends at all four stations is 185 ± 7 (1σ) years. The total atmospheric content calculated using the box model and ALE/GAGE data for the lower troposphere is 2330×10^{12} g N_2O on July 1, 1983; this result is sensitive to the choice of $t_u = 4$ years in the model with the content increasing to 2340×10^{12} g N_2O for $t_u = 3$ years. The lifetime deduced from an optimal match of the ALE/GAGE and RUN A_{11} global contents is 179 years, in good agreement with the value derived from the ALE/GAGE trends; the content-derived τ value is particularly sensitive to the absolute calibration factor ξ.

The agreement between the τ value computed in RUN A_{11} and the theoretical stratosphere-only destruction time (166 ± 16 years) results simply from the fact that E_{tot} in RUN A_{11} was chosen to ensure this approximate agreement. The primary purpose of RUN A_{11} is not to estimate τ (which is poorly determined due to the great a priori uncertainty in E_{tot}) but to test the relative importance of the individual emissions E_i to E_{tot}. Such a test is possible because each E_i has a different latitudinal and temporal dependence and therefore affects the latitudinal gradients and trends at each individual ALE/GAGE station in different ways.

In this respect, the RUN A_{11} emissions produce model predicted latitudinal gradients in N_2O that are significantly larger than those observed (see Table 5). In this table the "score" denotes the number of predictions in a particular run which lie within 1σ of the ALE/GAGE observations for the five quantities indicated. The sum "sigma" of the squares of the differences between the predictions and observations for the five quantities are also given as an alternative scoring method. One possible reason for the poor performance for RUN A_{11} involves the model troposphere to stratosphere transport rates. Since the upper tropospheric N_2O mixing ratio varies only slightly with latitude and we assume a single stratospheric box with a single mixing rate t_u^{-1} between this box and the four upper tropospheric boxes, the net tropospheric to stratospheric N_2O flux varies only slightly with latitude, which is unrealistic [*Mahlman et al.*, 1986; *Golombek and Prinn*, 1986]. To explore the sensitivity of our results to the above assumption, we therefore repeated RUN A_{11} after multiplying the constant t_u^{-1} value in RUN A_{11} by either 1.1, 1.1, 0.9, and 0.9 or 0.75, 1.25, 1.5, and 0.5 or 0.5, 1.5, 1.5, and 0.5 in the 90°N–30°N, 30°N–0°, 0°–30°S, and 30°S–90°S semihemispheres, respectively. This has the effect of changing the nearly equal semihemispheric atmospheric removal rates in RUN A_{11} to removal rates varying by semihemisphere in proportion to the above multipliers for t_u^{-1} (we made the rates symmetric or asymmetric about the equator to explore the effects of different meteorology in the two hemispheres). These three new runs were designated RUNs A_{12}, A_{13}, and A_{14}, respectively, and the results are given in Table 5. As expected, the larger the t_u^{-1} multiplier, the smaller the predicted mixing ratio in a particular semihemisphere relative to the global mean. Note however that the latitudinal gradients predicted in these latter three new runs are still larger than observed.

Another possible reason for the overprediction in RUN A_{11} is that the model transport rates in this run are derived by fitting the ALE/GAGE $CFCl_3$, CF_2Cl_2, and CH_3CCl_3 data. However, the latitudinal gradient for N_2O is much less than that for $CFCl_3$, CF_2Cl_2, and CH_3CCl_3 and its sources are much more globally dispersed. Numerical experiments with our model have demonstrated that, as a consequence of these gradient and source differences, species like N_2O are more sensitive than the above halocarbons to the assumed vertical eddy diffusion times (t_{21}, t_{43}, t_{65}, t_{87}) between the upper and lower tropospheric boxes in the model (see Figure 3). In particular, lowering the vertical eddy diffusion time decreases the N_2O latitudinal gradient by increasing meridional tracer advection in the upper troposphere in the model. Tropospheric vertical eddy diffusion coefficients typically assumed in atmospheric models are $(1 - 3) \times 10^5$ cm^2 s^{-1} with the larger values applying to the tropics. For the 6-km distance between the 750- and 350-mbar surfaces, these eddy diffusion coefficients correspond to t_{ik} values of 14–42 days. For the above halocarbons the assumption $t_{21} = t_{43} = t_{65} = t_{87} = 38$ days as used for N_2O in RUN A_{11} gave good agreement with observations [*Cunnold et al.*, 1986; *Prinn et al.*, 1987], but the sensitivity to these t_{ik} values is sufficiently small that satisfactory (but not optimal) agreement is also obtained if we take t_{ik} values of 14 days. To determine the maximum effect of our assumptions concerning vertical and horizontal diffusion times in the tropics, we therefore repeated RUN A_{11} with $t_{43} = t_{65} = 14$ days, $t_{21} = t_{87} = 42$ days, and also t_{35} and t_{46} equal to $\frac{8}{9}$ times their values in RUN A_{11}. The results of this run (designated A_{15}, i.e., M=5) are also given in Table 5, where we see that the latitudinal gradient is still overpredicted. Note that for $M = 5$ transport, the model still provides a good fit to the above ALE/GAGE $CFCl_3$ data.

TABLE 5. Differences Between the 10-year Mean Mixing Ratios (in ppbv) in the Four Semihemispheres and the Global Average of These Four Means, and the Difference Between the Northern and Southern Hemispheric Averages of these Means

	90°N – 30°N	30°N – 0°	0° – 30°S	30°S – 90°S	NH – SH	Score	Sigma†
Observed*	0.40	0.35	–0.25	–0.50	0.75	–	–
range	(0.18, 0.62)	(0.18, 0.52)	–(0.36, 0.14)	–(0.37, 0.63)	(0.59, 0.91)	–	–
A_{11}	0.72	0.52	–0.41	–0.83	1.24	0	0.51
A_{12}	0.61	0.46	–0.34	–0.73	1.07	3	0.22
A_{13}	0.73	0.49	–0.44	–0.78	1.22	1	0.46
A_{14}	0.78	0.49	–0.47	–0.80	1.27	1	0.57
A_{15}	0.80	0.42	–0.45	–0.77	1.22	1	0.50
A_{16}	0.39	0.37	–0.19	–0.57	0.76	5	0.009
A_{21}	0.38	0.51	–0.22	–0.67	0.89	4	0.075
A_{31}	0.22	0.49	–0.12	–0.59	0.71	4	0.079
A_{41}	0.34	0.53	–0.21	–0.66	0.87	3	0.078
A_{22}	0.28	0.44	–0.14	–0.58	0.72	5	0.042
A_{32}	0.11	0.42	–0.04	–0.49	0.53	2	0.18
A_{42}	0.23	0.46	–0.13	–0.56	0.69	4	0.063
A_{23}	0.40	0.47	–0.26	–0.61	0.87	5	0.041
A_{24}	0.45	0.47	–0.28	–0.64	0.92	4	0.066
A_{25}	0.46	0.40	–0.26	–0.60	0.86	5	0.028

* Observed values and (1σ) range are obtained from the ALE/GAGE data. Computed values in each RUN A_{NM} are from the four lower tropospheric boxes in the model.

† Units for sigma are (ppbv)^2.

The better performance of RUN A_{12} relative to RUNs A_{11}, A_{13}, A_{14}, and A_{15}, above is due to the greater troposphere-stratosphere exchange rates in the northern hemisphere relative to the southern hemisphere in RUN A_{12}. Indeed *Holton* [1990] has recently presented evidence that the downward stratosphere to troposphere mass flux in the northern hemisphere may be as large as twice that in the southern hemisphere. To apply the *Holton* [1990] estimates of total vertical mass fluxes at the 100-mbar level to the 200-mbar level in our box model we multiply them by 2 and use simple area weighting. This implies annual mean net vertical mass fluxes (in units of 10^8 kg s^{-1}) of –57.8, +30.6, +54.0, and –26.8 between the upper tropospheric boxes 2, 4, 6, and 8 and the stratosphere in our model (Figure 3). We therefore augment the diffusive troposphere-stratosphere exchanges in RUNs A_{14} with advective N_2O fluxes derived from the latter net vertical mass fluxes. For this purpose it is necessary also to divide the stratosphere into 4 boxes of equal mass. This run which is designed to simulate the *Holton* [1990] circulation is denoted A_{16} and it provides a very good fit to the latitudinal gradient (Table 5).

If we do not accept the RUN A_{16} transports, RUNs A_{11}, A_{12}, A_{13}, A_{14}, and A_{15} suggest that our a priori N_2O emissions are erroneously high in the northern hemisphere (i.e., that E_1 which is the major cause of the hemispheric emission differences is overestimated). To investigate this possibility, we performed six further runs designated A_{2M}, A_{3M} and A_{4M} (M = 1 or 2) in which the E_1 (fossil fuel combustion) values are respectively 0.5, 0.25, and 0.1 times those in RUN A_{1M}, the E_2 (land clearing and biomass burning) values are 2.0, 2.5, and 1.2 times those in RUN A_{1M}, the E_3 (fertilizer use) values are 1, 1, and $\frac{8}{5}$ times those in RUN A_{1M} and the E_5 (natural tropical soil) values are 1, 1, and 1.25 times those in RUN A_{1M}. Because E_1, E_2, and E_3 have similar (anthropogenic) trends RUNs A_{2M}, A_{3M}, and A_{4M} have almost the same global total emission magnitude and trend as in A_{1M} but have more of their emissions in the tropics than A_{1M} (Table 4). Run A_{2M} was also carried out for three other transport types (M = 3, 4, 5) to further elucidate the influence of the assumed transport scheme on the model predictions for the N = 2 scenario.

The results of these nine new runs are given in Table 5. Note that with the exception of RUN A_{32} these runs "score" much higher and have a much lower "sigma" relative to the ALE/GAGE observations than any of the A_{1M} runs except A_{16}. In other words, if we do not accept the transport in run A_{16}, a satisfactory fit to the ALE/GAGE data requires at least a factor of 2 decrease in our RUN A_{1M} emissions (E_1) due to fossil fuel combustion and a factor of 1.2–2.5 increase in our RUN A_{1M} emissions (E_2) associated with tropical land disturbance. Decreases in the fossil fuel combustion emissions by much greater than a factor of 2 are allowed if the emissions due to fertilizer use (E_3) are increased appropriately (e.g., as in RUNs A_{4M} in Table 5). The A_{2M} and A_{4M} emission scenarios provide a somewhat better fit to the ALE/GAGE data than the A_{3M} emission scenario. A decrease in the emissions estimates of *Hao et al.* [1987] by at least a factor of 2 is commensurate with the criticisms raised by *Muzio and Kramlich* [1988] discussed earlier. The feasibility of a large tropical land disturbance source is enhanced by the measurements of *Luizao et al.* [1989] and others discussed earlier. We note parenthetically that present emissions are 56% and 47% greater than preindustrial emissions for RUNs A_{2M} and A_{4M}, respectively, conversant with the need to explain preindustrial N_2O levels. The large fertilizer use source needed in RUN A_{4M} is speculative.

The lifetime results for RUNs A_{21}, A_{31} and A_{41} are shown in Table 6, where we give the N_2O lifetimes deduced using the trends in each station data alone and all station data sets simultaneously. The lifetime deduced by matching optimally the ALE/GAGE and model fractional trends at all four stations is

TABLE 6. Lifetimes τ for N_2O Optimally Estimated in RUNs A_{11}, A_{21}, A_{31} and A_{41} From Temporal Trends in ALE/GAGE Data at Each Site and All Sites Combined

Method	Value of τ, years				Weight in All-Sites Trend Estimate
	RUN A_{11}	RUN A_{21}	RUN A_{31}	RUN A_{41}	
Trend (Oregon/Ireland)	196	167	159	145	0.11*
Trend (Barbados)	179	152	145	133	0.15
Trend (Samoa)	182	159	149	137	0.45
Trend (Tasmania)	185	161	152	139	0.29
Trend (all sites)†	185 ± 7	159 ± 5	149 ± 5	137 ± 4	
Global content‡	179	172	167	164	

*The addition to the Oregon record of the more variable time series at Adrigole/Macehead produces an increase in the trend (and lifetime) uncertainty in the 30°–90°N semihemisphere, with the result that reduced weight is given to this record in the all-site estimate.

† Uncertainties are 1σ and do not include uncertainties in emissions. Weights are approximate.

‡ Lifetimes optimally estimated from the global atmospheric content derived from ALE/GAGE data. The first 6 months of Samoan ALE/GAGE data (July–December 1978) are not used.

159 ± 5 years (RUN A_{21}), 149 ± 5 years (RUN A_{31}) and 137 ± 4 years (RUN A_{41}). The lifetime deduced from an optimal match of the ALE/GAGE and box model global contents is 172 years in RUN A_{21}, 167 years in RUN A_{31} and 164 years in RUN A_{41}, in reasonable agreement with the value derived from the trends; the content-derived τ value is particularly sensitive to the absolute calibration factor ξ.

5.2. *Global Emissions*

Table 7 summarizes the N_2O annual emissions E_{tot} (Y) deduced for the nine successive calendar years beginning in 1979 in RUN B_{21}. Note that very similar results are obtained in all of the B_{NM} runs. While the uncertainties in the individual $E_{tot}(Y)$ values in Table 7 are large (due to the variability in the ALE/GAGE data), there is some evidence that total annual emissions vary significantly around the 10-year average of 20.5 × 10^{12} g N_2O yr^{-1}. Inspection of the ALE/GAGE data (Figure 2) indicates coherent oscillations in the trends in N_2O mixing ratios at Barbados, Samoa, and (to a lesser extent) Tasmania which, in the inversion process, are responsible for the predicted anomalously large 1982 and anomalously small 1983 emissions (a similar coherence with similar predictions for emissions occurs in 1984-1985). Curiously, in the 1982 time period the equatorial oceanic source for CO_2 [*Pearman et al.*, 1983] appears to have weakened associated putatively with decreased oceanic upwelling at the onset of the exceptionally strong El Niño-Southern Oscillation (ENSO) event of 1982-1983 [*Komhyr et al.*, 1985]. If we associate the oceanic N_2O emissions with nutrient-rich upwelling water, we would also expect a weakening of the N_2O tropical oceanic source (E_6, Tables 3, 4) with the onset of El Niño, contrary to the above conclusion from the ALE/GAGE data. This forces us to look at variations in E_2 (tropical land clearing and biomass burning) and E_5 (natural tropical soil emanations) as explanations for the interannual variations in N_2O emissions. For example, variability in tropical biomass burning due to wildfires (perhaps instigated by tropical climate changes associated with ENSO) leading to N_2O-producing soil disturbances would be a possible cause worth investigating.

TABLE 7. Nitrous Oxide Annual Emissions $E_{tot}(Y)$ Deduced in RUN B_{21} for Nine Successive Calendar Years

Period	$E_{tot}(Y)$, 10^{12} g N_2O yr^{-1})
1979	18.9 ± 1.7
1980	19.2 ± 1.7
1981	21.3 ± 1.9
1982	22.5 ± 2.0
1983	15.9 ± 2.0
1984	24.9 ± 2.3
1985	23.1 ± 2.1
1986	21.5 ± 1.6
1987	17.1 ± 1.6
Average	20.5 ± 1.0

Assumed lifetime τ is 166 years. The uncertainties are 1σ and are based on the smoothed standard deviations of the annual trends between the measurement sites during each year. An uncertainty of ±16 years in the lifetime corresponds to a potential bias in these estimates of ∓1.4 × 10^{12} g N_2O yr^{-1}.

5.3. *Semihemispheric Emissions*

The differences between the 10-year mean mixing ratios $\chi_i = a_i + 8.33d_i$ measured at the four ALE/GAGE "latitudes" (see Tables 2 and 5) are determined in part by the latitudinal distributions of emissions. Because the constant and quadratic terms in equation (1) are not orthogonal, the uncertainties in these 10-year means are obtained by fitting the data instead to the zeroth, first, and second order Legendre polynomials (P_0, P_1, P_2), in which case the uncertainty in the coefficient for P_0 is the required uncertainty. These uncertainties imply that the station to station differences are fairly well defined by the 10-year data set (see 1σ uncertainties given in Table 5) and due to the calibration procedures they are only marginally sensitive to a long-term drift in the calibration gases (major contributors to the error bars are, however, the offsets which occur sometimes as a result of calibration tank changes; see Figure 1).

To optimally determine the latitudinal distribution of emissions from the ALE/GAGE measurements, we have performed six runs of our inverse modeling procedure. They are designated

RUN C_1 through RUN C_6 and use the same transport parameters as RUNs A_{N1} through A_{N6}, respectively. The results are given in Table 8. The uncertainties in these optimally estimated percentage emissions in each semihemisphere are interdependent and are conveniently expressed in terms of the uncertainty with which the difference between the emissions in adjacent semihemispheres can be defined. Specifically for RUNs C_1 to C_6 in Table 8 the percentage differences in emissions between the 90°N–30°N and 30°N–0°, 30°N–0° and 0°–30°S, and 0°–30°S and 30°S–90°S semihemispheres have (1σ) absolute uncertainties of ± 9%, ± 3%, and ± 8%, respectively, (these uncertainties include consideration of the residuals between the model predictions and ALE/GAGE observations as well as the standard errors in the observations themselves).

Note that the optimally estimated hemispheric percentage emissions in RUNs C_1 through C_5 which are determined to ±3% do not agree with the prescribed A_{1M} emission scenario, while the estimated emissions in RUN C_6 do agree, which is the same conclusion reached in section 5.1. Another obvious difference between the optimally estimated and all the prescribed emission scenarios is the shift in emissions from the 0°–30°S to the 30°S–90°S semihemisphere implied by the optimal estimations but this shift lies within the absolute uncertainty of ±8% in the difference in emissions between these semihemispheres noted above.

TABLE 8. Percentage N_2O Emissions in Each Semihemisphere f_i in Designated Model Run

	90°N–30°N	30°N–0°	0°–30°S	30°S–90°S
A_{1M}	33.6	33.6	25.7	7.1
A_{2M}	22.8	39.7	30.7	6.8
A_{3M}	17.5	42.7	33.2	6.6
A_{4M}	20.8	41.8	30.8	6.6
C_1	28	32	25	15
C_2	29	34	24	13
C_3	26	34	28	12
C_4	24	34	29	13
C_5	22	39	28	11
C_6	34	34	20	12

Emissions are prescribed in A_{NM} runs and optimally estimated in C_M runs. Total 1982 emissions are 20×10^{12} g N_2O yr^{-1} in all runs. Lifetime for N_2O in C_M runs assumed to be 166 years.

The difference between the average of the observed 10-year-mean mixing ratios at our northern hemisphere ALE/GAGE stations (Ireland/Oregon, Barbados) and our southern hemisphere stations (Samoa, Tasmania) is 0.75 ± 0.16 ppbv. This is somewhat smaller than the 1 ppbv interhemispheric difference reported by *Butler et al.* [1989] based on Pacific and Indian Ocean cruise measurements. The ratios of the northern hemispheric to southern hemispheric emissions, in our emission scenarios A_{2M} and A_{4M}, are both 1.67 (compared to 2.05 in RUN A_{1M}). These latter ratios appear consistent with the values of 1.5 to 1.9 deduced using a simple two-box global model by *Cicerone* [1989] for an interhemispheric difference of 0.75 ppbv and no interhemispheric differences in stratospheric N_2O destruction.

5.4. *Semihemispheric Troposphere-Stratosphere Exchange*

To address further the issue raised earlier in section 5.1 concerning assumptions about tropospheric-stratospheric exchange in the model, we have carried out four further runs of our inverse modeling procedure. In these runs we optimally estimate the factors g_i by which we must multiply the troposphere-stratosphere exchange rate τ_u^{-1} in each semihemisphere in order to optimally fit the ALE/GAGE data. These runs are designated D_1, D_2, D_3, and D_4 and use the same emissions scenarios as in RUNs A_{1M}, A_{2M}, A_{3M}, and A_{4M}, respectively. The results for the g_i values are given in Table 9. The differences in the g_i values between the 90°N–30°N and 30°N–0°, 30°N–0° and 0°–30°S, and 0°–0°S and 30°S–90°S semihemispheres have (1σ) uncertainties of ±0.9, ±0.2, and ±0.8, respectively.

In RUNs D_1, D_2, D_3, and D_4 the tropospheric-stratospheric mixing rates are 1.9±0.2, 1.2±0.2, 1.0±0.2, and 1.2±0.2 times greater, respectively, in the northern hemisphere than the southern hemisphere. The required mixing rate asymmetry in D_1 is consistent with *Holton* [1990] but the fossil-fuel-driven emission scenario A_{1M} in D_1 is not consistent with the work of *Muzio and Kramlich* [1988]. Conversely, while emission scenarios A_{2M} (in D_2), A_{3M} (in D_3), and A_{4M} (in D_4) are consistent with the conclusions of *Muzio and Kramlich* [1988] the transport scenarios in runs D_2, D_3, and D_4 are not consistent with the *Holton* [1990] estimates for tropospheric-stratospheric exchange. Therefore, while we can conclude that both tropical and northern hemispheric mid-latitude nitrous oxide sources are significant, we cannot define precisely their relative importance at the present time. To resolve this issue, we need to determine stratospheric-tropospheric exchange rates with considerable accuracy.

TABLE 9. Optimally Estimated Multipliers g_i in D_N Runs for the Mixing Rate τ_u^{-1} Between the Upper Tropospheric and Stratospheric Box for the Indicated Semihemispheres and Prescribed Emission Scenarios

	90°N–30°N	30°N–0°	0°–30°S	30°S–90°S
D_1	1.28	1.32	0.75	0.65
D_2	0.73	1.46	1.23	0.58
D_3	0.49	1.51	1.43	0.57
D_4	0.65	1.50	1.24	0.61

Assumed N_2O lifetime is 166 years in all runs. The sum of the four g_i values is constrained to be 4.

6. CONCLUDING REMARKS

The ALE/GAGE data for N_2O comprise over 110,000 individual calibrated real-time air analyses carried out over a 10-year (July 1978 to June 1988) time period. These measurements indicate that the average N_2O concentration in the northern hemisphere is persistently 0.75 ±0.16 ppbv higher than in the southern hemisphere and that the global average linear trend in N_2O lies in the range 0.25–0.31% yr^{-1}. The latter trend result is contingent on certain assumptions about the long-term stability of the calibration gases used in the experiment. Interpretation of the data, using inverse theory and a nine-box (grid) model of the global atmosphere, indicates that the N_2O surface emissions into the 90°N–30°N, 30°N–0°, 0°–30°S, and 30°S–90°S semihemispheres account for about 22–34, 32–39, 20–29, and 11–15% of the global total emissions, respectively. This important new result depends primarily on

the ALE/GAGE determination of the N_2O latitudinal gradient rather than the N_2O temporal trend. The measured trends and latitudinal distributions are consistent with the hypothesis that stratospheric photodissociation is the major atmospheric sink for N_2O. However, they do not support the hypothesis that the temporal N_2O increase is caused solely by increases in anthropogenic N_2O emissions associated with fossil fuel combustion, contrary to some previous ideas. Instead, as first noted by *Prinn et al.* [1988], the cause for the N_2O trend appears to be a combination of a growing tropical source (probably resulting from tropical land disturbance) and a growing northern mid-latitude source (probably resulting from a combination of fertilizer use and fossil fuel combustion). The exact combination of these sources which best fits the data depends on the assumed tropospheric-stratospheric exchange rates for N_2O in the northern hemisphere relative to the southern hemisphere. Accepting a theoretically calculated N_2O lifetime of 166 ± 16 years due to stratospheric destruction only, we deduce from the ALE/GAGE data a 10-year average global N_2O emission rate of (20.5 ± 2.4) × 10^{12} g N_2O yr^{-1} but with significant year-to-year variations in emissions associated perhaps with year-to-year variations in tropical land emissions.

Acknowledgments. We thank Peter Vitousek and Pamela Matson for helpful advice on tropical nitrous oxide emissions, Michael McIntyre and James Holton for helpful advice on troposphere-stratosphere exchange, G. Rodriguez and R. Boldi for manuscript preparation, and D. Souza for drafting. This research was supported by NASA (grants NAGW-732 (R. Prinn), NAGW-729 (F. Alyea, D. Cunnold), NASW-4057 (R. Rosen), and NAGW-280 (A. Crawford, R. Rasmussen)); Chemical Manufacturers Association (contract FC-85-567 (P. Simmonds) and FC-87-640 (P. Fraser)); NOAA (contract NA85 – RACO5103 (P. Simmonds)); CSIRO, Aspendale, Victoria, Australia (P. Fraser); and Bureau of Meteorology, Melbourne, Victoria, Australia (P. Fraser).

REFERENCES

Anderson, I. C., J. S. Levine, M. A. Poth, and P. J. Riggan, Enhanced biogenic emissions of nitric oxide and nitrous oxide following surface biomass burning, *J. Geophys. Res., 93*, 3893–3898, 1988.

Arnold, P., Losses of nitrous oxide from soil, *J. Soil Sci., 5*, 116–128, 1954.

Brown, L., W. Chandler, C. Flavin, J. Jacobson, C. Pollock, S. Postel, L. Starke, and E. Wolf, *State of the World: 1987*, 268 pp., W.W. Norton, New York, 1987.

Butler, J., J. Elkins, T. Thompson, and K. Egan, Tropospheric and dissolved N_2O of the West Pacific and East Indian oceans during the El Niño Southern Oscillation event of 1987, *J. Geophys. Res., 94*, 14,865–14,877, 1989.

Cicerone, R., Analysis of sources and sinks of atmospheric nitrous oxide (N_2O), *J. Geophys. Res., 94*, 18,265–19,272, 1989.

Cleveland, W., 1987 Britannica World Data, in *1987 Britannica Book of the Year*, pp. 794–859, Encyclopedia Britannica, Inc., Chicago, Ill., 1987

Cohen, Y., and L. Gordon, Nitrous oxide production in the ocean, *J. Geophys. Res., 84*, 347–353, 1979.

Crutzen, P., The influence of nitrogen oxides on the atmospheric ozone content, *Q. J. R. Meteorol. Soc., 96*, 320–325, 1970.

Crutzen, P., A. Delany, J. Greenberg, P. Haagenson, L. Heidt, R. Lueb, W. Pollock, W. Seiler, A. Wartburg, and P. Zimmerman, Tropospheric chemical composition measurements in Brazil during the dry season, *J. Atmos. Chem., 2*, 233–256, 1985.

Crutzen, P., W. Hao, M. Liu, J. Lobert, and D. Scharffe, Emissions of CO_2 and other trace gases to the atmosphere from fires in the tropics, paper presented at the 28th Liege International Astrophysical Colloquium, Universite de Liege, Belgium, 1989.

Cunnold, D., R. Prinn, R. Rasmussen, P. Simmonds, F.Alyea, C.Cardelino, A. Crawford, P. Fraser, and R. Rosen, The atmospheric lifetime experiment, 3, Lifetime methodology and application to three years of $CFC\ell_3$ data, *J. Geophys. Res., 88*, 8379–8400, 1983.

Cunnold, D., R. Prinn, R. Rasmussen, P. Simmonds, F.Alyea, C.Cardelino, A. Crawford, P. Fraser, and R. Rosen, The atmospheric lifetime and annual release estimates for $CFC\ell_3$ and $CF_2C\ell_2$ from 5 years of ALE data, *J. Geophys. Res., 91*, 10,797–10,817, 1983.

Dickinson, R., and R. Cicerone, Future global warming from atmospheric trace gases, *Nature, 319*, 109–115, 1986.

Elkins, J., S. Wofsy, M. McElroy, C. Kolb, and W. Kaplan, Aquatic sources and sinks for nitrous oxide, *Nature, 275*, 602–606, 1978.

Foulger, B., and P. Simmonds, Drier for field use in the determination of trace atmospheric gases, *Anal. Chem., 51*, 1089–1090, 1979.

Fraser, P., G. Pearman and P. Hyson, The global distribution of atmospheric carbon dioxide, II, A review of provisional background observations, 1978–1980, *J. Geophys. Res., 88*, 3591–3598, 1983.

Golombek, A., and R. Prinn, A global three-dimensional model of the circulation and chemistry of $CFC\ell_3$, $CF_2C\ell_2$, $CH_3CC\ell_3$, $CC\ell_4$, and N_2O, *J. Geophys. Res., 91*, 3985–4001, 1986.

Hao, W., S. Wofsy, M. McElroy, J. Beer, and M. Toqan, Sources of atmospheric nitrous oxide from combustion, *J. Geophys. Res., 92*, 3098–3104, 1987.

Holton, J., On the exchange of mass between the stratosphere and troposphere, *J. Atmos. Sci., 47*, 392–395, 1990.

Johnston, H., O. Serange, and J. Podolske, Instantaneous global nitrous oxide photochemical rates, *J. Geophys. Res., 84*, 5077–5082, 1979.

Keeling, C. D., and R. B. Bacastow, *Energy and Climate: Studies in Geophysics*, pp. 110–160, National Academy Press, Washington D. C., 1977.

Keller, M., T. Goreau, S. Wofsy, W. Kaplan, and M. McElroy, Production of nitrous oxide and consumption of methane by forest soils, *Geophys. Res. Lett., 10*, 1156–1159, 1983.

Keller, M., W. Kaplan, and S. Wofsy, Emissions of N_2O, CH_4, and CO_2 from tropical forest soils, *J. Geophys. Res., 91*, 11,791–11,802, 1986.

Keller, M., W. Kaplan, S. Wofsy, and J. Da Costa, Emissions of N_2O from tropical soils: Response to fertilization with NH_4^+, NO_3^-, and PO_4^{3-}, *J. Geophys. Res., 93*, 1600–1604, 1988.

Khalil, M., and R. Rasmussen, Increase and seasonal cycles of nitrous oxide in the Earth's atmosphere, *Tellus, 35B*, 161–169, 1983.

Khalil, M., and R. Rasmussen, Nitrous oxide: Trends and global mass balance over the past 3000 years, *Ann. Glaciol., 10*, 73–79, 1988.

Ko, M., and D. Sze, A 2-D model calculation of atmospheric lifetimes for N_2O, CFC-11, and CFC-12, *Nature, 297*, 317–319, 1982.

Komhyr, W., R. Gammon, T. Harris, L. Waterman, T. Conway, W. Taylor, and K. Thoning, Global atmospheric CO_2 distribution and variations from 1968–1982 NOAA/GMCC CO_2 flask sample data, *J. Geophys. Res., 90*, 5567–5596, 1985.

Levy, H., J. Mahlman, and W. Moxim, Tropospheric N_2O variability, *J. Geophys. Res., 87*, 3061–3080, 1982.

Lieth, H., Primary Production of the major vegetation units of the world, in *Primary Productivity of the Biosphere*, edited by H. Lieth and R. Whittaker, pp. 203–215, Springer-Verlag, New York, 1975.

Livingston, G., P. Vitousek, and P. Matson, Nitrous oxide flux and nitrogen transformations across a landscape gradient in Amazonia, *J. Geophys. Res., 93*, 1593–1599, 1988.

Logan, J., M. Prather, S. Wofsy, and M. McElroy, Tropospheric chemistry: A global perspective, *J. Geophys. Res., 86*, 7210–7254, 1981.

Luizao, F., P. Matson, G. Livingston, R. Luizao, and P. Vitousek, Nitrous oxide flux following tropical land clearing, *Global Biogeochem. Cycles*, *3*, 281–285, 1989.

Mahlman, J., H. Levy, and W. Moxim, Three-dimensional simulations of stratospheric N_2O: Predictions for other trace constituents, *J. Geophys. Res.*, *91*, 2687–2707, 1986.

Matson, P., and P. Vitousek, Ecosystem approaches for the development of a global nitrous oxide budget, *Bioscience*, in press, 1990.

Matson, P., P. Vitousek, J. Ewel, M. Mazzarino, and G. Robertson, Nitrogen transformations following tropical forest felling and burning on a volcanic soil, *Ecology*, *68*, 491–502, 1987.

McElroy, M., and J. McConnell, Nitrous oxide: A natural source of stratospheric NO, *J. Atmos. Sci.*, *28*, 1095–1098, 1971.

McElroy, M., and S. Wofsy, Tropical forests: Interactions with the atmosphere, in *Tropical Rainforests and the World Atmosphere*, edited by G. Prance, Westview Press, Boulder, Colo., 1986.

Muzio, L., and J. Kramlich, An artifact in the measurement of N_2O from combustion sources, *Geophys. Res. Lett.*, *15*, 1369–1372, 1988.

Pearman, G., P. Hyson, and P. Fraser, The global distribution of carbon dioxide, 1, Aspects of observations and modelling, *J. Geophys. Res.*, *88*, 3581–3590, 1983.

Pearman, G., D. Etheridge, F. de Silva, and P. Fraser, Evidence of changing concentrations of atmospheric CO_2, N_2O, and CH_4 from air bubbles in Antarctic ice, *Nature*, *320*, 248–250, 1986.

Pierotti, D., and R. Rasmussen, Combustion as a source of nitrous oxide in the atmosphere, *Geophys. Res. Lett.*, *3*, 265–267, 1976.

Prather, M., Continental sources of halocarbons and nitrous oxide, *Nature*, *317*, 221–225, 1985.

Prather, M., European sources of halocarbons and nitrous oxide, *J. Atmos. Chem.*, *6*, 375–406, 1988.

Prinn, R., P. Simmonds, R. Rasmussen, R. Rosen, F. Alyea, C. Cardelino, A. Crawford, D. Cunnold, P. Fraser, and J. Lovelock, The atmospheric lifetime experiment, 1, Introduction, Instrumentation, and overview, *J. Geophys. Res.*, *88*, 8352–8367, 1983.

Prinn, R., D. Cunnold, R. Rasmussen, P. Simmonds, F. Alyea, A. Crawford, P. Fraser, and R. Rosen, Atmospheric trends in methylchloroform and the global average for the hydroxyl radical, *Science*, *238*, 945–950, 1987.

Prinn, R., D. Cunnold, R. Rasmussen, P. Simmonds, F. Alyea, A. Crawford, P. Fraser, and R. Rosen, Atmospheric trends and emissions of nitrous oxide deduced from nine years of ALE/GAGE data, in *The Scientific Application of Baseline Observations of Atmospheric Composition: Extended Abstracts*, p. 55, CSIRO, Aspendale, Australia, 1988.

Rasmussen, R., and A. Khalil, Atmospheric trace gases: Trends and distributions over the last decade, *Science*, *232*, 1623–1624, 1986.

Rasmussen, R., and J. Lovelock, The atmospheric lifetime experiment, 2, Calibration, *J. Geophys. Res.*, *88*, 8369–8378, 1983.

Schmidt, J., W. Seiler, and R. Conrad, Emission of nitrous oxide from temperate forest soils into the atmosphere, *J. Atmos. Chem.*, *6*, 95–115, 1988.

Seiler, W., and R. Conrad, Contribution of tropical ecosystems to the global budgets of trace gases especially CH_4, H_2, CO, and N_2O, in *The Geophysiology of Amazonia*, edited by R. Dickinson, pp. 133–160, J. Wiley, New York, 1987.

Seiler, W., and P. Crutzen, Estimates of gross and net fluxes of carbon between the biosphere and atmosphere from biomass burning, *Climatic Change*, *2*, 207–248, 1980.

Simmonds, P., D. Cunnold, F. Alyea, C. Cardelino, A. Crawford, R. Prinn, P. Fraser, R. Rasmussen, and R. Rosen, Carbon tetrachloride lifetimes and emissions determined from daily global measurements during 1978–1985, *J. Atmos. Chem.*, *7*, 35–58, 1988.

Slemr, F., R. Conrad, and W. Seiler, Nitrous oxide emissions from fertilized and unfertilized soils in a subtropical region (Andalusia, Spain), *J. Atmos. Chem.*, *1*, 159–169, 1984.

Wang, W., Y. Yung, A. Lacis, T. Mo, and J. Hansen, Greenhouse effects due to man-made perturbations of trace gases, *Science*, *194*, 685–690, 1976.

Weiss, R., The temporal and spatial distribution of tropospheric nitrous oxide, *J. Geophys. Res.*, *86*, 7185–7195, 1981.

Weiss, R., and H. Craig, Production of atmospheric nitrous oxide by combustion, *Geophys. Res. Lett.*, *3*, 751–753, 1976.

F. Alyea, D. Cunnold, School of Geophysical Sciences, Georgia Institute of Technology, Atlanta GA 30332.

A. Crawford, R. Rasmussen, Institute of Atmospheric Sciences, Oregon Graduate Center, Beaverton OR 97005.

P. Fraser, Division of Atmospheric Research, Commonwealth Scientific and Industrial Research Organization, Aspendale, Victoria, Australia.

R. Prinn, Department of Earth, Atmospheric and Planetary Sciences, Massachusetts Institute of Technology, Cambridge MA 02139.

R. Rosen, Atmospheric and Environmental Research, Inc., 840 Memorial Drive, Cambridge MA 02139

P. Simmonds, Department of Geochemistry, University of Bristol, Bristol, United Kingdom.

(Received September 6, 1989;
revised May 25, 1990;
accepted July 2, 1990.)